IMMOBILIZATION OF CHIRAL BRØNSTED ACIDS AND LEWIS BASES FOR BATCH AND FLOW ENANTIOSELECTIVE CATALYSIS

Lidia Clot Almenara

UNIVERSITAT ROVIRA I VIRGILI
IMMOBILIZATION OF CHIRAL BRØNSTED ACIDS AND LEWIS BASES FOR BATCH AND FLOW ENANTIOSELECTIVE CATALYSIS
Lidia Clot Almenara

UNIVERSITAT ROVIRA I VIRGILI
IMMOBILIZATION OF CHIRAL BRØNSTED ACIDS AND LEWIS BASES FOR BATCH AND FLOW ENANTIOSELECTIVE CATALYSIS
Lidia Clot Almenara

Immobilization of Chiral Brønsted Acids and Lewis Bases for Batch and Flow Enantioselective Catalysis

Doctoral Thesis by
Lidia Clot Almenara

Developed under the supervision of:
Prof. Miquel A. Pericàs and Dr. Carles Rodríguez Escrich

UNIVERSITAT ROVIRA i VIRGILI

ICIQ Institut Català d'Investigació Química

Departament de Química Analítica i Química Orgànica (URV)
Institut Català d'Investigació Química (ICIQ)

Tarragona
2018

UNIVERSITAT ROVIRA I VIRGILI
IMMOBILIZATION OF CHIRAL BRØNSTED ACIDS AND LEWIS BASES FOR BATCH AND FLOW ENANTIOSELECTIVE CATALYSIS
Lidia Clot Almenara

UNIVERSITAT ROVIRA i VIRGILI

ICIQ Institut Català d'Investigació Química

Prof. Miquel A. Pericàs Brondo, Group Leader and Director of the Institute of Chemical Research of Catalonia (ICIQ) and,

Dr. Carles Rodríguez Escrich, Researcher and Group Coordinator in the Pericàs Research Group (ICIQ),

STATE, that the present Doctoral Thesis entitled: "**Immobilization of Chiral Brønsted Acids and Lewis Bases for Batch and Flow Enantioselective Catalysis**", presented by Lidia Clot Almenara to receive the degree of Doctor, has been carried out under our supervision at the Institute of Chemical Research of Catalonia (ICIQ).

Tarragona, March 2018

PhD Thesis Supervisor

Miquel A. Pericàs Brondo

PhD Thesis Co-supervisor

Carles Rodríguez Escrich

UNIVERSITAT ROVIRA I VIRGILI
IMMOBILIZATION OF CHIRAL BRØNSTED ACIDS AND LEWIS BASES FOR BATCH AND FLOW ENANTIOSELECTIVE CATALYSIS
Lidia Clot Almenara

Acknowledgments

Amb la presentació d'aquesta tesis tanco un capítol de la meva vida. Ara, després de 4 anys i mig, miro enrere i veig un període de la meva vida ple de vivències, experiències i coneixements que la tesi m'ha brindat la oportunitat de viure. Ha sigut un camí que és difícil de descriure, però molt positiu, on moltes persones han format part d'ell. I és per això que en aquest espai m'agradaria agrair a totes aquelles persones, que d'una manera o d'una altra, han estat partícips al llarg d'aquests anys.

En primer lloc, vull agrair al Miquel Pericàs, per confiar en mi a l`hora de desenvolupar aquest treball en el seu grup d'investigació, per totes les oportunitats durant el doctorat. Però sobretot, pel seu suport i positivisme, pels seus grans consells i guiar-me quan l'he necessitat.

M'agradaria agrair als coordinadors del grup, Sonia i Carles, que sempre han estat disposats a donar-me un cop de mà. En particular al Carles, per tots els seus consells, per la paciència que el caracteritza i per compartir tots els teus coneixements. També m'agradaria destacar a la Sara García, sempre disposada a solucionar-nos els problemes amb els papers i pel somriure que et tranquil·litza quan comences a estar estressada.

I would like to thank specially each and every one of all the past and present members of the Pericàs group, for all the funny moments that we have enjoyed together. In particular, I will always remember the deep conversations with my mates, Sara and Francesca, with whom I shared desk during these years.

I would like also to thank Ruben Martín, where I developed my master project and where I started my experience in the ICIQ. I am grateful to all the members of his

group. But I would like to emphasize the support from Alvaro who helped in the project master. We spent a really good time during my stay in that group.

I am also grateful to Prof. Corey Stephenson for all the knowledge fulfill during my stay in the University of Michigan. I want to give particular thanks to all the members of Stephenson group for their hospitality and all the activities that they organized to have a nice stay and for all the support in chemistry aspects.

No quiero olvidarme de todas las personas que formen parte del departamento de Soporte a la Investigación en el ICIQ, sus conocimientos facilitan encontrar las soluciones adecuadas a los problemas que nos encontramos diariamente.

Vull agrair a totes aquelles persones fora del àmbit de la recerca, però que han sigut un pilar fonamental durant tots aquets anys, en especial a: Raquel, Silvia, Maria, Lati, Joan Soler, Gerard, Pol, Jordi, Joan Civit, Ferran, Ramon, Gloria, Oscar, Josep, David y Marc. També, a mi profesor de Capoeira, Armand, por sus lecciones sobre la capoeira i la vida. I a todo el grupo Os Bambas da Capoeira, un espacio donde he desconectado de las duras tardes del laboratorio "El arte de luchar sonriendo".

Han sido muchos años de dedicación a la química desde el primer año de carrera, y no hubieran sido los mismos sin la amistad i el compañerismo incondicional de Marta, Patri y Cris, con vosotras empecé este camino y solo puedo deciros que gracias por ser como sois.

A mi Familia por todo su apoyo, ellos hacen que la vida sea especial, por todos los valores que me han dado. Mis padres, ellos son mi pilar, hacen que siga luchando día tras día, siempre tienen la respuesta que necesitas, gracias porque me habéis enseñado el verdadero valor de la vida. En especial i con todo mi cariño a mi prima Sandra,

gracias, has sido la mejor i porque esta tesis la he escrito pensado en ti cada día, me has dado la fuerza para continuar luchando, siempre te querré.

Finalment, vull acabar amb el meu company de viatge, la meva parella, i a qui li dedico aquesta tesi. Marcel, ets la persona que en cada pas sempre has estat al meu costat. Sempre m'has recolzat en cada una de les meves decisions, cada pas hem estat junts. Per això et dec les gràcies. Gràcies per ser com ets, per ensenyar-me cada dia, ets una persona que fas les coses de tot cor i sempre saps com treure un somriure, no canviïs mai. Ets la persona que sempre he admirat.

Gràcies a tothom – Gracias a todos – Thank you!!

UNIVERSITAT ROVIRA I VIRGILI
IMMOBILIZATION OF CHIRAL BRØNSTED ACIDS AND LEWIS BASES FOR BATCH AND FLOW ENANTIOSELECTIVE CATALYSIS
Lidia Clot Almenara

Financial sources

The present doctoral thesis has been possible thanks to the funding received from Institute of Chemical Research of Catalonia (ICIQ) foundation.

The works have been developed within the following projects founded by: CERCA Programme/Generalitat de Catalunya, especially to MINECO (FPI predoctoral Grant CTQ2012-38594-C02-01 and CTQ2015- 69136-R) and AGAUR (Grant 2014SGR827). We also thank Severo Ochoa Excellence Accreditation 2014−2018 (SEV-2013-0319).

UNIVERSITAT ROVIRA I VIRGILI
IMMOBILIZATION OF CHIRAL BRØNSTED ACIDS AND LEWIS BASES FOR BATCH AND FLOW ENANTIOSELECTIVE CATALYSIS
Lidia Clot Almenara

Abbreviations

In this document the abbreviations and acronyms most commonly used in organic chemistry have been used, according to the recommendations of the ACS "*Guidelines for authors*":

http://pubs.acs.org/paragonplus/submission/joceah/joceah_authguide.

UNIVERSITAT ROVIRA I VIRGILI
IMMOBILIZATION OF CHIRAL BRØNSTED ACIDS AND LEWIS BASES FOR BATCH AND FLOW ENANTIOSELECTIVE CATALYSIS
Lidia Clot Almenara

Que quan siguis lluny una cançó et torni a casa.
Alguer Miquel

Vive como si fueras a morir mañana.
Aprende como si fueras a vivir para siempre.
Gandhi

UNIVERSITAT ROVIRA I VIRGILI
IMMOBILIZATION OF CHIRAL BRØNSTED ACIDS AND LEWIS BASES FOR BATCH AND FLOW ENANTIOSELECTIVE CATALYSIS
Lidia Clot Almenara

To My Family.

UNIVERSITAT ROVIRA I VIRGILI
IMMOBILIZATION OF CHIRAL BRØNSTED ACIDS AND LEWIS BASES FOR BATCH AND FLOW ENANTIOSELECTIVE CATALYSIS
Lidia Clot Almenara

List of Publications

The following publications are the results from the present thesis:

- Lidia Clot-Almenara, Carles Rodríguez-Escrich, Laura Osorio-Planes, and Miquel A. Pericàs

Polystyrene-Supported TRIP: A Highly Recyclable Catalyst for Batch and Flow Enantioselective Allylation of Aldehydes

ACS Catal. **2016**, *6*, 7647−7651

- Lidia Clot-Almenara, Carles Rodríguez-Escrich and Miquel A. Pericàs

Desymmetrisation of *meso*-diones promoted by a highly recyclable polymer-supported chiral phosphoric acid catalyst

RSC Adv. **2018**, *8*, 6910 – 6914

UNIVERSITAT ROVIRA I VIRGILI
IMMOBILIZATION OF CHIRAL BRØNSTED ACIDS AND LEWIS BASES FOR BATCH AND FLOW ENANTIOSELECTIVE CATALYSIS
Lidia Clot Almenara

Table of Contents

OVERALL GOALS

UNIVERSITAT ROVIRA I VIRGILI
IMMOBILIZATION OF CHIRAL BRØNSTED ACIDS AND LEWIS BASES FOR BATCH AND FLOW ENANTIOSELECTIVE CATALYSIS
Lidia Clot Almenara

Overall Goals

In order to develop the present thesis, our main goal was focused on the design of different approaches for the immobilization of chiral units to create new catalytic materials for applications in enantioselective transformations.

Our interest for the synthesis of supported chiral homogeneous catalysts is due to the fact that they are easily recoverable, which makes them easily reusable. These features convert these catalysts in perfect candidates to be applied in continuous flow applications.

In order to reach these goals, the guidelines to follow are: (i) explored different routes for the functionalization of the related homogeneous counterpart catalysts (ii) immobilize onto polystyrene of the desired chiral organocatalysts, (iii) explore their potential in asymmetric catalysis and (iv) implement enantioselective continuous flow processes with the supported organocatalysts prepared.

With this aim in mind, different aspects will be taken into consideration for an improvement on sustainability. The efficiency of the resulting polymers will be elucidated in terms of activity, selectivity as well as the possibility to recover and reuse them.

In particular, we will focus on Brønsted acids and Lewis bases catalysts.

UNIVERSITAT ROVIRA I VIRGILI
IMMOBILIZATION OF CHIRAL BRØNSTED ACIDS AND LEWIS BASES FOR BATCH AND FLOW ENANTIOSELECTIVE CATALYSIS
Lidia Clot Almenara

CHAPTER I

UNIVERSITAT ROVIRA I VIRGILI
IMMOBILIZATION OF CHIRAL BRØNSTED ACIDS AND LEWIS BASES FOR BATCH AND FLOW ENANTIOSELECTIVE CATALYSIS
Lidia Clot Almenara

Chapter I

General Introduction: Organocatalysis

Chemistry plays a central role in the technological development of society to move forward towards the creation of a better standard of life. In this task, it is the role of chemists to produce new materials or compounds, which requires the development of new methods and reactions in order to achieve the target compound in an efficient way. Catalysis, which is the discipline of science that deals with the acceleration of chemical reactions by species not consumed in the processes, holds a great potential to contribute to the improvement of quality of life. A catalyst is the material that can convert the reagents into the final compound under milder conditions than without its participation. This is possible providing an alternative reaction pathway of less energy. However, this is not always trivial and, since its discovery, researchers always try to find the answer to the question *"how does the catalyst act?"*.

In particular, asymmetric catalysis[1] is the branch of science that studies the preferential formation of one enantiomer over the other, aiming for the highest level of selectivity in chemical reactions.[2] Consequently, it introduces the possibility of controlling the three-dimensional structure of the molecular architecture. The importance of this strategy lies in the fact that, while one enantiomer may be responsible for the activity of interest, its mirror image can be either inactive, an antagonist or have a separate activity that may be desirable or undesirable.

Louis Pasteur introduced the concept of chemical chirality dissymmetry after he resolved in 1848 the racemic sodium ammonium(±)-tartrate. The term

chirality originates from the word *Kheir*, which means 'hand' in Greek. It is the property of an object that exits in two distinguishable forms, which are mirror images but they are not superimposable; the most representative example of chirality in life is given by the human hands, hence the name.[3] Chirality is present in the central molecules of life as DNA, RNA, amino acids, peptides, proteins, carbohydrates and enzymes, among others. We are in contact with chiral molecules daily, for instance, the limonene enantiomers, both are natural products and smells differently. While the enantiomer (*S*)-limonene smells of lemon, its mirror image (*R*)-limonene smells of orange. The fact that our nasal receptors are also made up of chiral molecules, allows us to recognize the different smells (Figure 1.1).

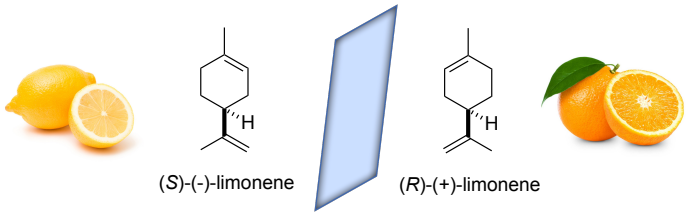

Figure 1.1: Smell of limonene enantiomers.

The direct production of enantiomerically pure compounds has had a high impact in industry, as it avoids the tedious process to separate the desired enantiomer and simplifying the treatment for wasteful undesirable products. Every year, new concepts and methods emerge with an increased selectivity profile, economically more appealing and environmentally friendlier. Nevertheless, asymmetric catalysis represents still one of the major challenges in modern organic chemistry, due to the inherent difficulty in distinguishing between two species as similar as enantiomers.[4]

Until recently, enantioselective catalysis was dominated by two general categories: namely enzymatic methods and metal catalysis. The importance of

transition metal complexes in asymmetric catalysis was made evident in 2001, when the Nobel Prize in Chemistry was awarded to William R. Knowles, Ryoji Noyori and K. Barry Sharpless for the development of metal-catalyzed enantioselective transformations. On the other hand, enzymatic methods represent a more limited strategy due to the high specificity shown between enzymes and substrates. Thus, asymmetric organocatalysis has risen in popularity as it complements the gap left by these fields.

1.1. Historical Evolution

Nature has been a source of inspiration for synthetic chemists, a clear example being enzymatic catalysis.[5] The efficient manner to engage the enzymes with the substrate has often been the inspiration for the evolution of organocatalysis, paving the way for the design of new small molecule catalysts. Chemists are continually trying to emulate the enzyme's behaviour. This is how the field 'biomimetic chemistry' emerged, as Ronald Breslow[6] said: "*In biomimetic chemistry, we take what we have observed in nature and apply its principles to the invention of novel synthetic compounds that can achieve the same goals... as an analogy, we did not simply make larger versions of birds when we invented airplanes, but we did take the idea of the wing from nature, and then used the aerodynamic principles in our own way to build a jumbo jet.''*

Indeed, early stage of organocatalysis can be traced back to much earlier, but usually the origins of this is located in 1998-2000.[7] Nowadays, it has become one of the major branches of catalysis. Organocatalysis[7a, 8] implies the use of catalytically active molecules consisting mostly of carbon, hydrogen, and other nonmetallic elements, nitrogen being the most common. In the same way that metal complexes and enzymes, this strategy significantly accelerates chemical reactions. However, the main feature of organocatalysts is the use of organic

molecules without the aid of metallic elements to mediate organic transformations. Despite the widespread availability of organic chemicals in enantiopure form and the economic benefits that this approach entails for academy and industry, it has not been since last decade that chemists have started to appreciate the value of organocatalysis. Organometallic complexes have been the center of attention in the vast majority of reactions in asymmetric catalysis. This may be due to the fact that, in the beginning, asymmetric organocatalysis was considered to be inefficient and limited in scope.

Organocatalysts present some distinctive advantages when compared to the organometallic compounds in terms of simple processes involving non-anhydrous or inert conditions, and use of starting materials that are often inexpensive and readily available. This emerging field led to many nearly simultaneous publications by various research groups who wanted to be the first in discovering new enantioselective organocatalyzed versions of classical reactions.

Organocatalysts present inherent benefits:[9] in the first place, the small organic molecules used as catalyst are generally very stable since they tend to be insensitive to moisture and air as well as oxidation and hydrolysis, which greatly simplifies their design and synthesis, making them generally inexpensive. Moreover, on many occasions, they are derivatives of biological compounds, such as carbohydrates, peptides or amino acids, or can even be found readily available from nature, such as proline and quinine acetate which are inexpensive and bio-renewable. Finally, the most important characteristic, they are generally non-toxic and they do not contain traces of heavy metals, which often represent a real challenge in the production process in the chemical and pharmaceutical industry. Avoiding the high cost of purchase and disposal of metal derivatives is an appealing feature for chemists.[10]

The origins of organocatalysis can be attributed to Justus von Liebig's work, who accidentally found in 1860 that dicyan is transformed into oxamide in the presence of an aqueous solution of acetaldehyde (Scheme 1.1).

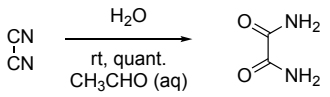

Scheme 1.1: Justus von Liebig's oxamide synthesis.

The early use of organic catalysis in enantioselective synthesis dates back in 1971, two industrial research groups independently at Hoffmann-La Roche and Schering reported the first enantioselective intramolecular aldol reaction of *meso*-diones catalyzed by chiral (*S*)-proline (Scheme 2.2). The triketone starting material requires just 3 mol% of catalyst to furnish the product in 93% enantiomeric excess. These landmark works showed that a metal-free system could give rise to very high enantioselectivities and represents the dawn of a new era in asymmetric catalysis.[11] This transformation, known as the Hajos-Parrish-Eder-Sauer-Wiechert reaction,[12] will be discussed in more detail in chapter IV.

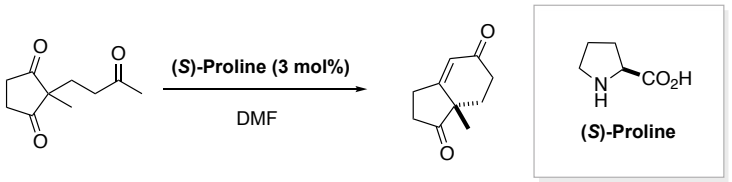

Scheme 2.2: Hajos-Parrish ketone synthesis.

1.2. Classes of Organocatalysts

Today, the field organocatalysis encompasses a wide range of complex catalytic systems, which have been designed to target new natural products and with the purpose of achieving chemical efficiency.[13] One way of achieving this is through the multiple formation of new bonds and stereocenters in one-pot procedures, which has a direct impact in speeding up time-consuming processes and avoiding purifications of intermediate. [14]

It is difficult to establish one rigorous criteria of classification. However, in order to give a logical understanding, List categorized the organocatalysts according to their acid/base reactivity in four main groups. In his work, we can distinguish the following groups: Lewis base, Lewis acid, Brønsted base and Brønsted acid.[15]

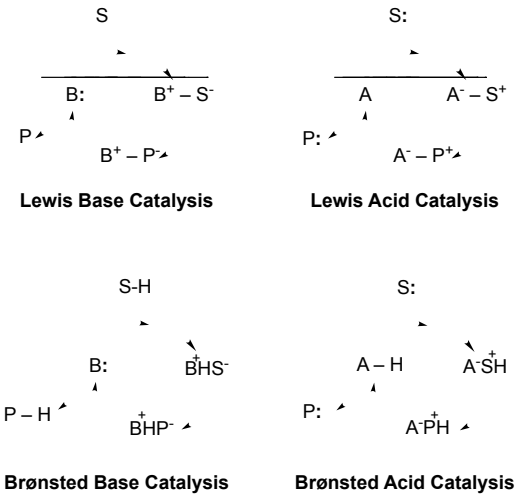

Scheme 2.3: The four categories of organocatalysts according to their acid-base properties.

In this sense, while Lewis bases and Lewis acids initiate the catalytic cycle via electrophilic or nucleophilic addition to substrates (S), Brønsted base and acid catalytic cycles are initiated via a (partial) deprotonation or protonation, respectively, as illustrated in Scheme 2.3.

Another distinction can be formulated if we pay attention to the strength of the interaction between the catalyst and the substrates: the ones that involve the formation of covalent interactions between the catalyst and the substrate in the catalytic cycle, and those which rely on non-covalent interactions (Scheme 2.4).[16]

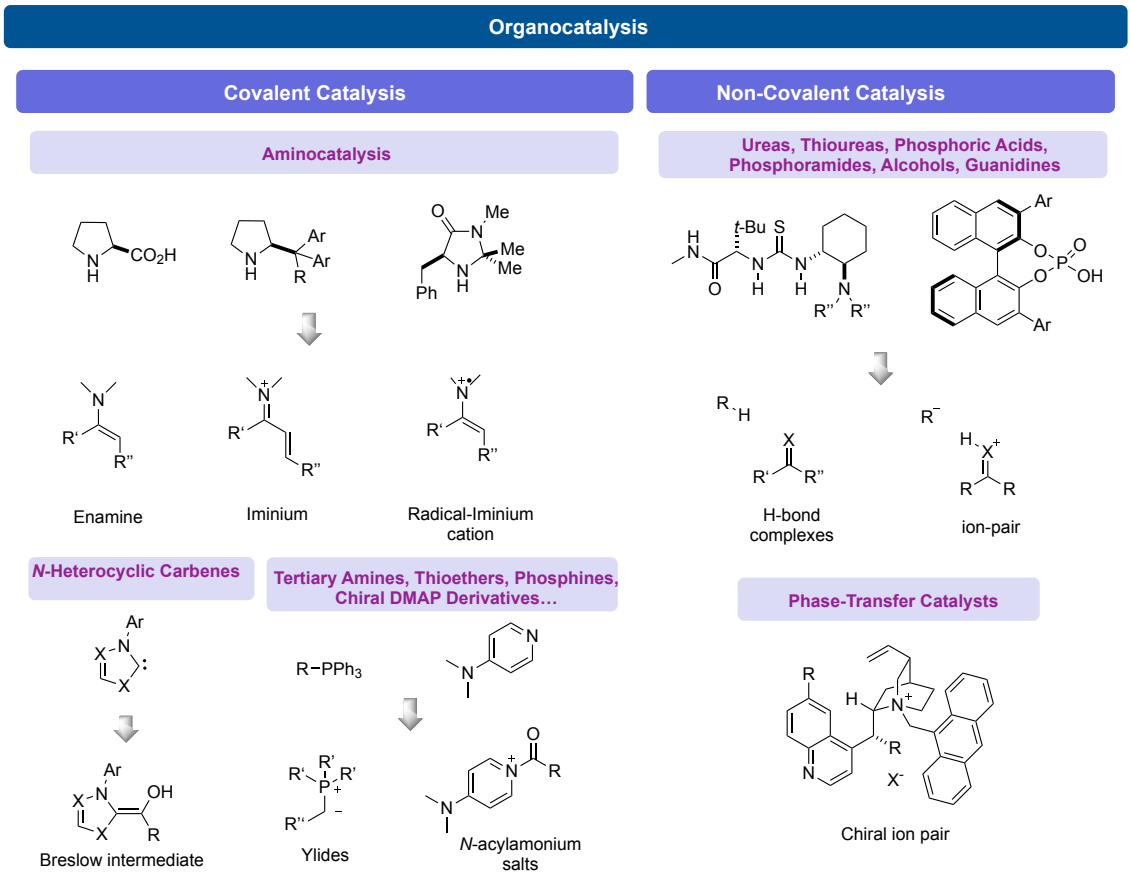

Scheme 2.4: Classification of catalyst by covalent or non-covalent catalysis and the corresponding reactive intermediate.

1.2.1. Covalent Catalysis

Aminocatalysts represent the most classical example of organocatalysts able to form covalent bonds with the substrate;[8a, 17] this group includes chiral amine-based species as peptides, alkaloids and synthetic nitrogen-containing molecules. The well-stablished strategy of aminocatalysis involve condensation

of the organic catalyst with the substrate to generate enamine, iminium and radical-iminium cation intermediates, which are considerably more reactive than the starting material.[18] Another example of covalent catalysis, but not less important, are *N*-heterocyclic carbenes,[19] where the reaction pathway entail the formation of an enaminol-like structure (Breslow intermediate) that leads to *umpolung* transformations. Finally, we also find catalysts as tertiary amines, thioethers, chiral DMAP derivatives, etc. In these cases, the most common intermediates are the corresponding ylides and *N*-acylammonium salts. The strong nature of the covalent bond formed in substrate-catalyst interaction allows an efficient spatial arrangement of the molecules in the stereodetermining event.

- **Proline**

We can say that proline is one of the most remarkable molecules in asymmetric catalysis,[20] the historical development of which is ligated to this amino acid. Proline is considered a universal asymmetric catalyst for several reasons;[21] firstly, it is an abundant chiral molecule that is inexpensive and available in both enantiomeric forms. Its unique structure, containing a carboxylic acid moiety (that can act as a Brønsted acid cocatalyst) and a secondary amine, makes them an ideal bifunctional catalyst for a broad range of applications, simulating enzymatic catalysis. It is worth stressing that proline can act as a bidentate ligand in asymmetric transition-metal catalysis, but it can also be an organocatalyst in several reactions owing to the ease of formation of enamine intermediates.[22] These transformations include aldol, Mannich, and Michael reactions, among many others (Figure 2.2).[22-23] Moreover, its cyclic, conformationally rigid structure has a beneficial effect in the process of chirality transfer and it is also displays increased pK_a values compared with primary amino acids.

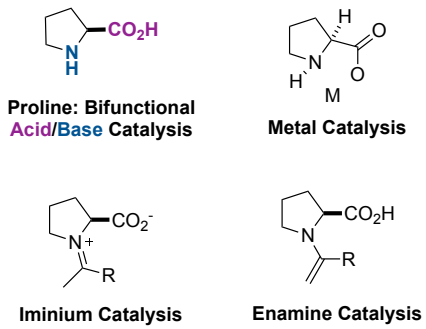

Figure 2.2: Possible intermediates in proline catalysis.

- ***N*-Heterocyclic Carbenes**

A significant contribution to the organocatalysis field is related to the use of stable *N*-heterocyclic carbenes (NHCs) in catalysis. Its roots can be traced back to the beginning of organic synthesis.[24] NHCs are heterocyclic rings that contain a carbene carbon and at least one nitrogen atom. Initially, due to the incomplete electron octet and coordinative unsaturation, they were considered just as highly reactive intermediates. Later, in 1988, Bertrand and co-workers isolated the first stabilized carbene.[25] The success of NHCs as ligands is associated to strong σ-electron withdrawing and π-electron-donating nitrogen ability, their high nucleophilicity,[26] which allow for a highly covalent contribution in metal complex formation. The stability arises from π-electron-donation by the ion pairs of the *N* atoms into the empty p_π orbital of the carbene. These properties make NHCs suitable to perform the role of organocatalyst or transition metal ligand by coordinating with low valent and high valent transition metals, alkaline earth metals, and lanthanides (Yt and Sc) for organometallic reactions.[27]

NHC organocatalysts have been extensively used to activate aldehydes; the reaction proceeds through nucleophilic attack followed by a proton transfer from the former carbonyl carbon to oxygen atom bonded to it, to generate an enamine-like 'Breslow intermediate' (Figure 2.3). During the course of the reaction, the nature of the aldehyde is indeed inverted; this means that the

usually electrophilic carbonyl carbon is acting as a nucleophile, which is called *umpolung*.[28] NHCs have proven very versatile, promoting several reactions, such as cyclization, polymerization, Stetter reaction, kinetic resolution, transesterification, Diels-Alder reaction, etc.

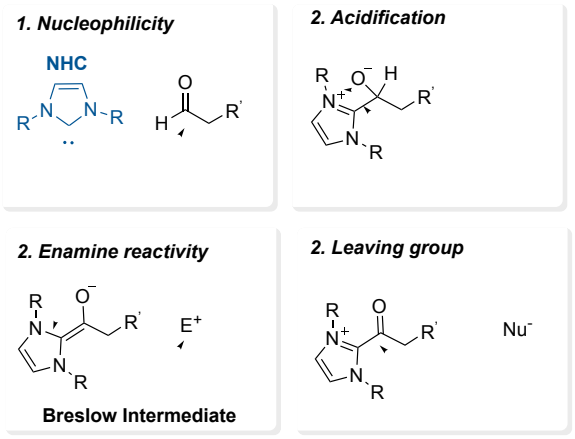

Figure 2.3: Modes of action from *N*-heterocyclic carbenes.

1.2.2. Non-Covalent Organocatalysis

Non-covalent catalysis takes place when the catalyst interacts with the substrates by means of weaker interactions, including neutral substrate-catalyst complex or acid-base reactions. The most important activation mechanism in this block is focused on hydrogens bonds. Catalysts able to interact with reagents in this manner include ureas, thioureas, phosphoramides, among others. In addition, other activation modes not less important are chiral ion pairing using phase-transfer catalysts, or the use of bases as tertiary amines in the activation of nucleophiles by deprotonation forming chiral ammonium salts. Finally, host-guest complexation should be as well included in this group of organocatalysts.

- **Hydrogen-Bonded Complexes**

Despite their importance in modern enantioselective organic chemistry, it was in the field of biocatalysis where reactions accelerated by hydrogen bonding interactions gained importance.[29] In the early days, it was considered that H-bonds were not strong enough for the assembly of complex molecules in an enantioselective manner.

Pioneering study by Hine and co-workers disclosed the use of 1,8-biphenylenediol to promote epoxide-opening reaction.[30] Representative H-bond catalysts as Brønsted acids, ureas and thioureas are depicted in Figure 1.4. These classes of catalysts operate via simultaneous donation of two H-bonds in order to facilitate the attack of nucleophiles.[31]

Consequently, electrophiles that are likely to be activated include aldehydes, ketones, esters, β-dicarbonylic compounds, a variety of imine derivatives, *N*-acyliminium ions and nitro compounds.[32]

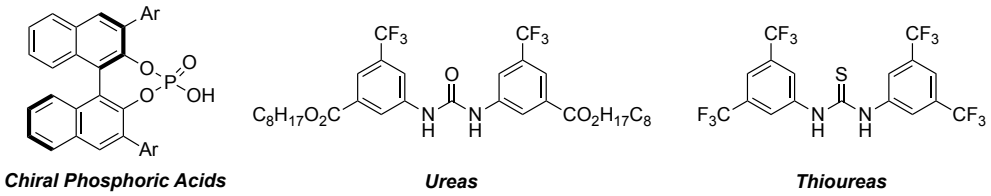

Chiral Phosphoric Acids ***Ureas*** ***Thioureas***

Figure 1.4: Representative H-bond complexes.

- **Phase-Transfer Catalysts**

Since Starks, together with Makosza, coined the term "phase transfer catalysis (PTC)"[33] this field has gained tremendous progress.[34] The most distinctive catalysts of this family are the quaternary chiral ammonium catalysts,[35] the most common of which are depicted in Figure 1.5.

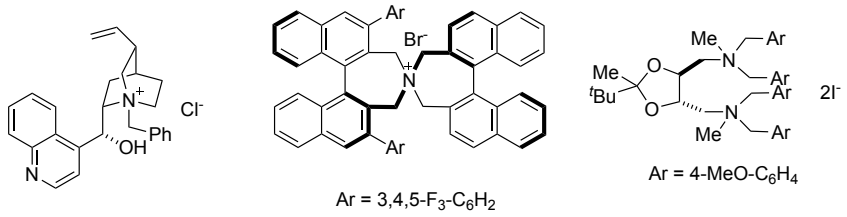

Figure 1.5: Chiral ammonium phase-transfer catalysts.

Toste and co-workers[36] reported a new concept of chiral anionic PTC. The conjugate base of chiral phosphoric **1** acts as chiral anionic phase-trasnfer catalyst for the enantioselective fluorination of enamides using Selectfluor in non-polar solvents. Catalyst **1** underges anion exchange with Selectfluor, which presents low solubility in non-polar solvents, in order to bring this into the solution and facilitate the fluorination of alkenes.

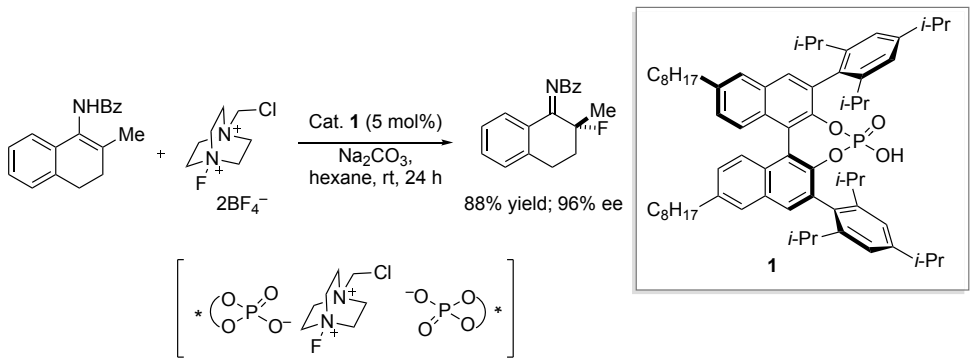

Scheme 1.5: Enamide fluorination reaction catalyzed by anionic chiral phase-transfer catalyst.

1.3. Activation Mode and Chiral Induction

One of the most important keys for the development of organocatalysis has been the identification of the different types of interaction between the catalyst and the substrate,[37] which gives a general overview of the catalytic cycle. Understanding the catalyst mode of substrate activation has allowed to establish a platform for designing new enantioselective reactions. In fact, most of the organocatalytic reactions reported since 1998 are based on five or six activation modes. It is astonishing to think how a broad range of reactions has

been developed with only a few activation modes, but this is what makes organocatalysis so versatile. In addition, it is much easier to develop new reactions with a known activation mode than to invent a new one.

- **Enamine Catalysis**

The referent work of enamine catalysis was reported by two industrial groups independently: on the one hand Zoltan Hajos and David Parrish,[12b] and on the other Rudolf Weichert, Gerhard Sauer and Ulrich Eder.[12a] They reported the proline-mediated enantioselective version of the Robinson annulation in 1971 (Scheme 2.2). However, the underlying activation mode was not understood and exploited until almost 30 years later than the first report. Thus, it was not until the year 2000 that Barbas, Lerner and List published the ingenious work dealing with the proline-catalyzed direct enantioselective intermolecular aldol reaction (Scheme 1.6),[38] where they proposed that the mechanism takes place via a transient enamine intermediate.[39]

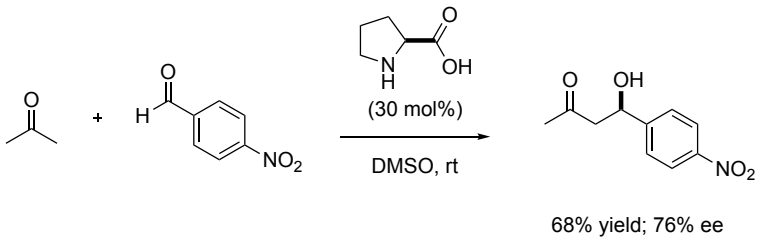

Scheme 1.6: Asymmetric proline-catalyzed intermolecular aldol reaction.

Proline has sometimes been described as a bifunctional catalyst; the amino group forms an enamine intermediate upon condensation with the carbonyl group, while simultaneously the acid moiety engages with the electrophilic partner through hydrogen bonding, as shown in the intermediate **2** (Figure 1.6).[40] This mechanism proceeds increasing the energy of the HOMO orbital and is explained with a Zimmerman-Traxler type transition state. The

interaction between proline and electrophile was rationalized in the work of List, Houk *et al.*[41] using quantum mechanical predictions.

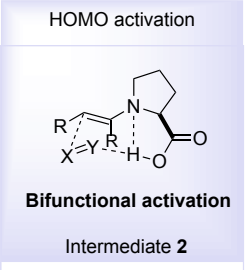

Figure 1.6: Houk-List model for the transition state of enamine catalysis.

Examples of reactions that procced via enamine catalysis are the aldehyde-aldehyde cross aldol coupling, intramolecular α-alkylation, Mannich reaction or Michael reaction.

- **Hydrogen-Bonding Catalysis**

In the early 1980s, some studies demonstrated that the catalyst could interact with the substrate via hydrogen-bonding interaction, even though these examples were considered to be exceptions to the idea that this kind of interaction alone was insufficient to be generally applied in catalysis.[34a, 42] This conception was superseded with the work of Jacobsen[43] and Corey,[44] who reported an asymmetric variant of the Strecker reaction catalysed by Schiff base and guanidine respectively, that used well-defined hydrogen bonding catalysts to activate imine electrophiles. Hydrogen bonding catalysis activates the counterpart electrophile via noncovalent interactions.[45] Rate acceleration results from the decrease in energy of the electrophile's lowest unoccupied molecular orbital (LUMO), making it more susceptible to the attack of a nucleophile (Figure 1.7, **3**).[31] The list of enantioselective reactions that can be promoted by hydrogen-bonding catalysts includes the Strecker, Mannich or Pictet-Spengler reactions, among many others.

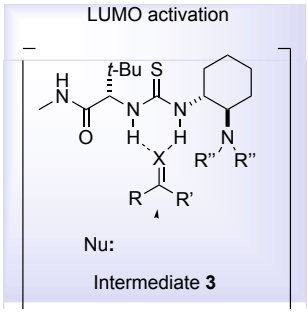

Figure 1.7: Proposed mode of action in hydrogen-bonding catalysis.

- **Iminium catalysis**

Nowadays, it is considered that the earliest report in iminium catalysis is the Knoevenagel condensation introduced in 1894,[46] but the real mechanism associated to this activation mode was not rationalized and applied to asymmetric catalysis until much later.[47] MacMillan and co-workers[48] were the first to do so and give a name to this concept and to the entire organocatalysis field. In 2000, they published the first highly enantioselective organocatalytic Diels-Alder reaction between cinnamaldehyde and cyclopentadiene,[48] paving the road for a general strategy for asymmetric catalysis (Scheme 1.7).

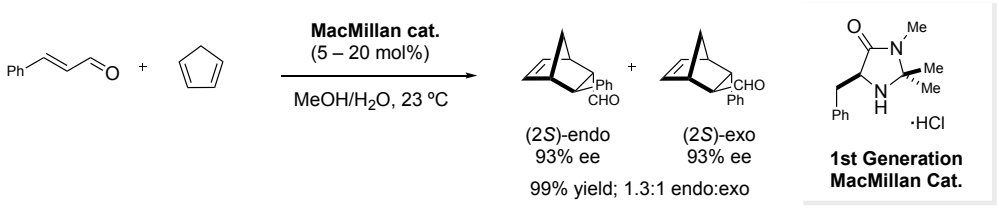

Scheme 1.7: Asymmetric Diels-Alder cycloadditon via iminium catalysis.

MacMillan *et al.* described the reversible condensation between a chiral amine (1st generation MacMillan catalyst) and an α,β-unsaturated aldehyde to generate an iminium ion. Note that they designed this new platform for organocatalytic processes envisioning that iminium ion might generate a situation comparable to the complex formed in metal-based, Lewis acid catalysis (Figure 1.8). The general feature is the existence of a rapid

equilibrium between an electron-deficient and an electron-rich state (iminium-enamine equilibrium). This is an example of the so-called "LUMO-lowering catalysis", where the electrophilicity is enhanced by formation of a covalent intermediate (**4**). Iminium ion catalysis has been successfully applied in cycloadditions, conjugate additions, Friedel-Crafts alkylations, Mukaiyama-Michael additions, transfer hydrogenations, and enantioselective organocatalytic cascade reactions, to name the most significant.

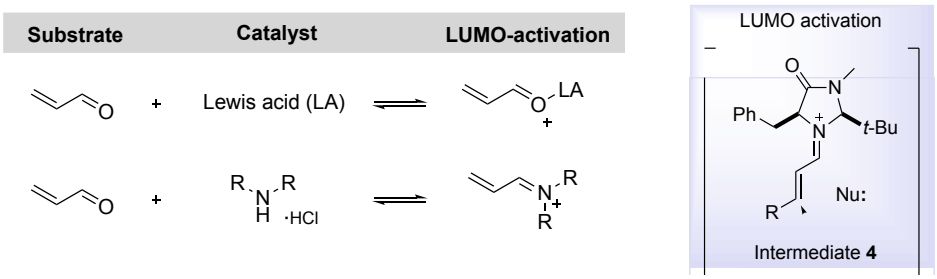

Figure 1.8: Comparative LUMO-lowering via Lewis acid and amine catalyst and iminium intermediate **4**.

- **SOMO catalysis**

The activation via SOMO catalysis, is one of the most recently discovered activation modes and it was introduced by the MacMillan group.[49] However, its use has been quickly spread to include: α-allylation, α-enolation, α-vinylation and α-heteroarylation in an efficient manner. This activation mode increases the electrophilicity by generating a singly occupied molecular orbital (SOMO)[50] upon single-electron oxidation of an electron-rich enamine. [51] The intermediate produced in this manner is a very reactive radical cation with three π-electrons (Figure 1.9, **5**).

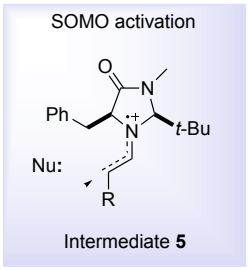

Figure 1.9: Radical cation intermediate of SOMO catalysis.

- **Counterion-Directed Catalysis**

Counterion-directed catalysis includes all chemical reactions involving chiral ionic species as catalysts.[52] We can appreciate four different classes, which can be encompassed in two big groups: (1) interaction via ion-pairing of charged catalysts with ionic species and (2) chiral neutral catalysts that interact via noncovalent binding to the intermediate ion pair (Figure 1.10).[53] Jacobsen *et al.* described this concept in their work on the enantioselective Pictet-Spengler-type cyclization.[54] They proposed evidences of the formation of a chiral *N*-acyliminium chloride-thiourea complex (Intermediate **6**) proving the well-established anion-binding properties of ureas and thioureas.

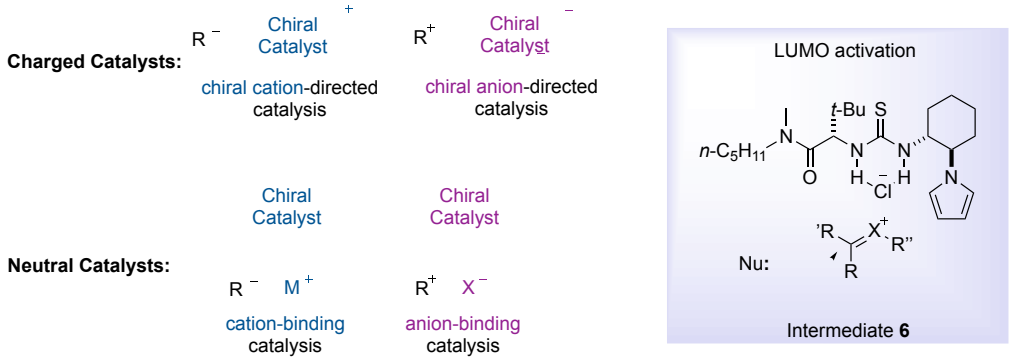

Figure 1.10: Types of asymmetric ion-pairing catalysis and an example of counterion-directed catalysis.

1.4. Recoverable Catalytic Systems

Synthetic organic chemistry evolves continuously for the development of improved catalytic processes. The global awareness of the limits of natural resources and the environmental impact of waste materials puts chemical industries under pressure to discover, develop and utilise more efficient protocols.[55] The most affected areas in industry are pharmaceuticals and agrochemicals due to the fact that traditional approaches are both expensive and time consuming. Therefore, the challenge is to find more efficient and cost-effective methods for the synthesis of valuable compounds. A possible solution proposed has been the use of supported catalysts, which combine both homogeneous and heterogeneous characteristics, as the catalysts are dispersed on a second material.[56] As a consequence, they possess the advantages of solid phase chemistry (the recyclability and their use in flow processes), as well as the versatility of the synthetic homogeneous processes known so far. Thereby, new families of immobilized catalysts have been developed during the past years.[57]

A significant breakthrough dates back to 1963, with the seminal work of Robert Bruce Merrifield where he pioneered the synthesis of polypeptides in solid phase.[58] Twenty years later, he received the Nobel Prize "*for his development of methodology for chemical synthesis on a solid matrix*". This important application for peptides was later adapted for the immobilization of reagents and catalysts. This opened a new branch of research in catalysis and remains an active field in modern chemistry and chemical industries. The immobilization of homogeneous chiral catalysts onto different solid supports has spread in recent years due to an increase in environmental concerns in the practice of organic synthesis.[59]

1.4.1. Homogeneous vs Heterogeneous Catalysis

Over the years, polymer supported catalysts have been an attractive field for chemists due to their inherent advantages over their homogeneous counterparts. In general, supported catalysts are simple to handle and store but, as can be expected, every synthetic methodology has associated drawbacks (Table 1.1).[60]

The main problem related to homogeneous catalysts is that in some cases their synthesis is not precisely simple; indeed, it can require multi-step sequences or problems can arise in the scale-up. If the catalyst cannot be reused, the synthesis becomes very expensive, which emphasizes the necessity to recover the catalyst. A simple way to perform this catalyst recovery is the immobilization of the homogeneous catalyst onto a proper support. Sometimes, more complex catalysts have high molecular weight, which entails using a higher mass of catalyst, even when working in a small scale. Although with heterogeneous catalysts the increase of catalyst mass also occurs, in the ideal cases this can be recovered and reused several times. Furthermore, the commercially available resins that are used to anchor the catalytic monomer tend to be expensive. This effect can be less relevant if the catalytic material generated turns out to be highly recyclable.[59-60]

In homogeneous catalysis, the fact of working in the same phase facilitates the mechanistic understanding, which ultimately lead to fine-tuning of the steric and electronic properties of the catalyst. Moreover, the improved diffusivity under proper stirring ensures good mass transfer. Conversely, in heterogeneous catalysis the fine-tuning may be influenced by the steric hindrance imparted by the solid matrix and the heterogeneous phase can affect the diffusivity.[61]

On the other hand, working in biphasic systems drastically improves the separation of the catalyst, providing a straightforward way for recycling of the catalyst, even though sometimes requires further treatment.

One of the most important applications of immobilized catalysts is their use in continuous flow processes, which present remarkable advantages over batch processes, as it is discuss in the next section.

Table 1.1: Advantages and drawbacks of homogeneous and heterogeneous catalysis.

	Homogeneous	**Heterogeneous**
Advantages	Preparation High diffusion Easier fine-tuning	Separation Recovery Recycling Stability
Drawbacks	Handling stability Separation Expensive recycling	Characterization Synthesis Resin cost Diffusivity can be an issue Fine-tuning

Since the first examples of reagent and catalyst immobilization on a polymeric matrix,[62][63] different methods and materials have been used to generate more active catalysts. The appropriate choice of the support material, the linker and the anchoring strategy might have an impact on the catalytic activity.[64] The appropriate scaffold to anchor should be chemically inert, cost-effective, and

display favorable swelling properties or the perfect pore size or permeability to ensure that reagent reach the active site of the catalyst. Examples of reported inorganic supports are silica,[65] zeolite, alumina, mesoporous materials,[64a, 66] among others. On the other hand, representative organic supports are polystyrene (PS),[67] poly(ethylene glycol) (PEG), polymethacrylate, polysaccharides, dendrimers or monolith.[68] More recently, researchers turned their attention to magnetic nanoparticles,[69] in this case the catalyst is recovered by an external magnetic field.

In general, in order to prepare a polymer-supported catalyst, in general, chemical modification of the homogeneous catalyst is developed to allow for subsequent anchoring on the resin.

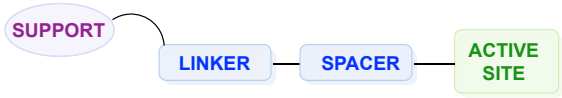

Figure 1.11: Representation of covalently supported catalyst.

To this end, several approaches can be formulated. For instance, the interactions between catalyst and support can be either covalent or non-covalent.[70] The linker is the functional unit that covalently connects the resin with the catalytically active moiety. In some cases, the activity is not as good as expected, which can be attributed to the proximity between the active site of the catalyst and the polymeric matrix. A possible solution involves the use of a spacer,[71] that can be a functional group, or a carbon chain (Figure 1.11). In our group, a long standing interest in the design of new families of solid supported catalysts[72] has led to a new catalytic materials which, in some cases, can be applied to asymmetric continuous flow systems (Figure 2.12).

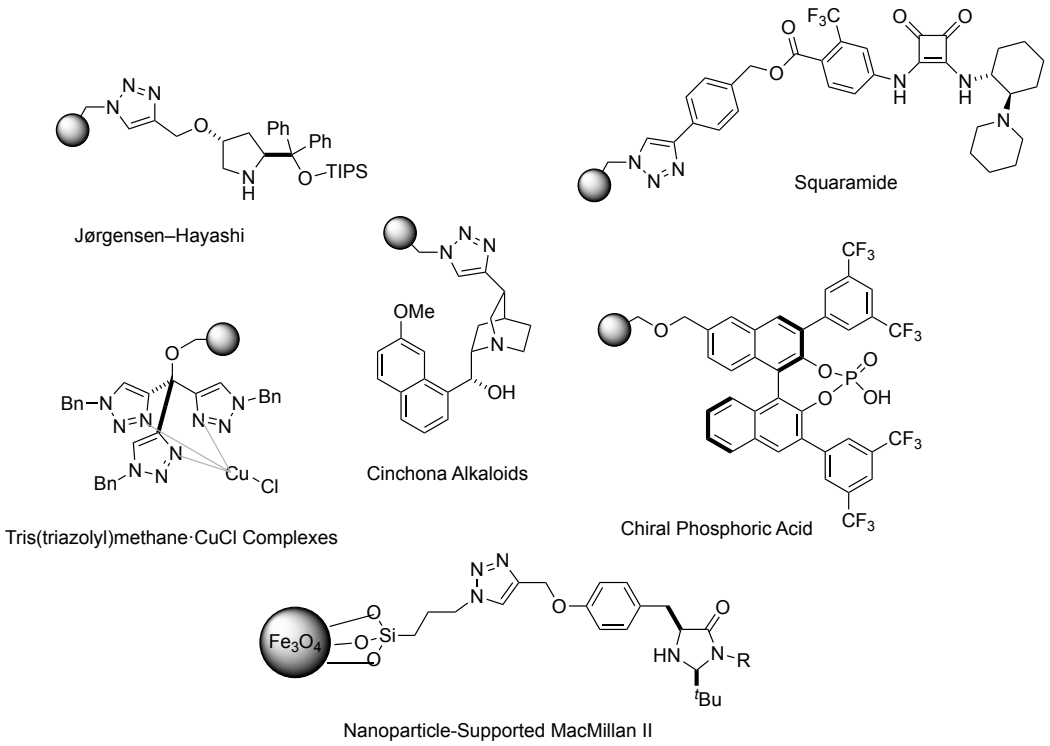

Figure 2.12: Previous supported organocatalysts developed in our group.[73]

1.4.2. Continuous Flow Systems

The traditional setup of organic reactions, which entails using round-bottom flasks, test tubes, or closed vessels has been lately complemented with continuous flow methodologies. Such flow processes have enhanced efficiency, cost and reaction optimization, among others features, in comparison with batch transformations.[74]

In some processes, batch reactions require harsh conditions, as high temperatures, high concentrations, use of hazardous or unstable intermediates, etc. In these cases, the implementation of continuous flow techniques has proven to be a safer alternative on both laboratory and production scale, thus facilitating the scale up processes.[75] This is undoubtedly one of the driving forces behind the adaptation from batch to flow conditions. There are principal differences that need to be considered between batch and flow processes.

Production reaction time under batch conditions is calculated by how long a vessel is held at a given temperature. In contrast, in continuous processes the reactor volume and the flow rate determine the production rate.[74b] Important points to consider are the facile automation, work up, reproducibility and process reliability due to the constant, easy to control parameters, efficient mixing, temperature, time, amount of reagent and solvents (pump).[76]

Multistep reaction sequences can also be conducted in a completely different fashion in flow,[77] by designing a system with different flow reactors coupled in line, an approach that decreases the production time and greatly simplifies work up. Reagents can be added into the stream of reactants anywhere in the flow system at any precise time that is required for the reaction.[78]

In the last years, the development and applications of continuous flow processing have arisen as efficient methods in several research areas.[74c, 79] We could say that flow systems are going to acquire more relevance in industrial environment, in particular for pharmaceutical[78b] and agrochemical compounds synthesis, etc.[80] The benefits of the implementation of flow processes has motivated investigation in new designs, techniques and concepts, which has generated a range of tools to be applied in flow.[81] For instance, we can find in the market from inexpensive syringe pumps to complex HPLC pumps, that are connected to some appropriate reactor which can be a simple coil made of inert material. If hazardous substances are employed, sealed systems that provide safer handling are the most convenient choice, as the parameters can be accurately controlled via computer.[73, 82]

1.5. References

[1] P. J. Walsh, M. C. Kozlowski, in: *Fundamentals of Asymmetric Catalysis*, University Science Books, **2009**.

[2] Morrison, R.T. and Boyd, R.N., **1987**. Organic Chemistry, 5th ed. Allyn & Bacon Inc. p.157

[3] L. D. Barron, *Space Sci. Rev*. **2008**, *135*, 187-201.

[4] R. Noyori, *Angew. Chem. Int. Ed.* **2002**, *41*, 2008-2022.

[5] a) A. Berkessel, H. Gröger, Asymmetric Organocatalysis: from *Biomimetic Concepts to Applications in Asymmetric Synthesis*, Wiley VCH, Weinheim, **2005**; b) P. I. Dalko, *Enantioselective Organocatalysis*, Wiley VCH, Weinheim, **2007**.

[6] R. Breslow, *Acc. Chem. Res*. **1995**, *28*, 146-153.

[7] (a) B. List, *Chem. Rev*. **2007**, *107*, 5413-5415; (b) C. F. Barbas, *Angew. Chem. Int. Ed.* **2008**, *47*, 42-47.

[8] (a) S. Bertelsen, K. A. Jørgensen, *Chem. Soc. Rev*. **2009**, *38*, 2178-2189; (b) P. I. Dalko, L. Moisan, *Angew. Chem. Int. Ed.* **2004**, *43*, 5138-5175.

[9] P. I. Dalko, L. Moisan, *Angew. Chem. Int. Ed.* **2001**, *40*, 3726-3748.

[10] M. North, *Sustainable Catalysis: With Non-endangered Metals*, Royal Society of Chemistry, **2015**.

[11] P. R. Schreiner, *Chem. Soc. Rev*. **2003**, *32*, 289-296.

[12] (a) U. Eder, G. Sauer, R. Wiechert, *Angew. Chem. Int. Ed.* **1971**, *10*, 496-497; (b) Z. G. Hajos, D. R. Parrish, *J. Org. Chem.* **1974**, *39*, 1615-1621.

[13] (a) E. Marques-Lopez, R. P. Herrera, M. Christmann, *Nat. Prod. Rep*. **2010**, *27*, 1138-1167; (b) K. C. Nicolaou, S. A. Snyder, *Classics in Total Synthesis II: More Targets, Strategies, Methods*, Wiley, **2003**.

[14] A. Dondoni, A. Massi, *Angew. Chem. Int. Ed.* **2008**, *47*, 4638-4660.

[15] J. Seayad, B. List, *Org. Biomol. Chem.* **2005**, *3*, 719-724.

[16] T. P. Yoon, E. N. Jacobsen, *Science* **2003**, *299*, 1691-1693.

[17] (a) M. C. Holland, R. Gilmour, *Angew. Chem. Int. Ed.* **2015**, *54*, 3862-3871; (b) D. Enders, O. Niemeier, A. Henseler, *Chem. Rev*. **2007**, *107*, 5606-5655.

[18] (a) P. Melchiorre, M. Marigo, A. Carlone, G. Bartoli, *Angew. Chem. Int. Ed.* **2008**, *47*, 6138-6171; (b) M. J. Gaunt, C. C. C. Johansson, *Chem. Rev*. **2007**, *107*, 5596-5605; (c) F. Giacalone, M. Gruttadauria, P. Agrigento, R. Noto, *Chem. Soc. Rev*. **2012**, *41*, 2406-2447.

[19] N. Marion, S. Díez-González, S. P. Nolan, *Angew. Chem. Int. Ed.* **2007**, *46*, 2988-3000.

[20] (a) A. Mielgo, C. Palomo, *Chem. Asian J*. **2008**, *3*, 922-948; (b) C. Agami, C. Puchot, H. Sevestre, *Tetrahedron Lett*. **1986**, *27*, 1501-1504.

[21] B. List, *Chem. Commun*. **2006**, 819-824.

[22] B. List, *Tetrahedron* **2002**, *58*, 5573-5590.

[23] R. C. Wende, P. R. Schreiner, *Green Chem.* **2012**, *14*, 1821-1849.
[24] D. Enders, U. Kallfass, *Angew. Chem. Int. Ed.* **2002**, *41*, 1743-1745.
[25] A. Igau, H. Grutzmacher, A. Baceiredo, G. Bertrand, *J. Am. Chem. Soc.* **1988**, *110*, 6463-6466.
[26] R. W. Alder, P. R. Allen, S. J. Williams, *J. Chem. Soc., Chem. Commun.* **1995**, 1267-1268.
[27] M. N. Hopkinson, C. Richter, M. Schedler, F. Glorius, *Nature* **2014**, *510*, 485.
[28] X. Bugaut, F. Glorius, *Chem. Soc. Rev.* **2012**, *41*, 3511-3522.
[29] (a) R. Dutzler, E. B. Campbell, M. Cadene, B. T. Chait, R. MacKinnon, *Nature* **2002**, *415*, 287; (b) L. Hedstrom, *Chem. Rev.* **2002**, *102*, 4501-4524.
[30] (a) J. Hine, K. Ahn, J. C. Gallucci, S. M. Linden, *J. Am. Chem. Soc.* **1984**, *106*, 7980-7981; (b) J. Hine, S. M. Linden, V. M. Kanagasabapathy, *J. Am. Chem. Soc.* **1985**, *107*, 1082-1083.
[31] M. S. Taylor, E. N. Jacobsen, *Angew. Chem. Int. Ed.* **2006**, *45*, 1520-1543.
[32] A. G. Doyle, E. N. Jacobsen, *Chem. Rev.* **2007**, *107*, 5713-5743.
[33] (a) M. Makosza, *Tetrahedron Lett.* **1966**, *7*, 4621-4624; (b) M. Mkosza, *Tetrahedron Lett.* **1969**, *10*, 677-678.
[34] (a) U. H. Dolling, P. Davis, E. J. J. Grabowski, *J. Am. Chem. Soc.* **1984**, *106*, 446-447; (b) K. Maruoka, T. Ooi, *Chem. Rev.* **2003**, *103*, 3013-3028; (c) M. J. O'Donnell, *Acc. Chem. Res.* **2004**, *37*, 506-517; (d) T. Ooi, K. Maruoka, *Angew. Chem. Int. Ed.* **2007**, *46*, 4222-4266; (e) S. Shirakawa, K. Maruoka, *Angew. Chem. Int. Ed.* **2013**, *52*, 4312-4348.
[35] (a) B. Lygo, B. I. Andrews, *Acc. Chem. Res.* **2004**, *37*, 518-525; (b) T. Ooi, K. Maruoka, *Acc. Chem. Res.* **2004**, *37*, 526-533; (c) T. Hashimoto, K. Maruoka, *Chem. Rev.* **2007**, *107*, 5656-5682; (d) K. Maruoka, *Chem. Rec.* **2010**, *10*, 254-259.
[36] (a) V. Rauniyar, A. D. Lackner, G. L. Hamilton, F. D. Toste, *Science* **2011**, *334*, 1681-1684; (b) R. J. Phipps, K. Hiramatsu, F. D. Toste, *J. Am. Chem. Soc.* **2012**, *134*, 8376-8379.
[37] D. W. C. MacMillan, *Nature* **2008**, *455*, 304-308.
[38] B. List, R. A. Lerner, C. F. Barbas, *J. Am. Chem. Soc.* **2000**, *122*, 2395-2396.
[39] S. Mukherjee, J. W. Yang, S. Hoffmann, B. List, *Chem. Rev.* **2007**, *107*, 5471-5569.
[40] S. Bahmanyar, K. N. Houk, H. J. Martin, B. List, *J. Am. Chem. Soc.* **2003**, *125*, 2475-2479.
[41] R. Marcia de Figueiredo, M. Christmann, *Eur. J. Org. Chem.* **2007**, 2575-2600.
[42] (a) H. Hiemstra, H. Wynberg, *J. Am. Chem. Soc.* **1981**, *103*, 417-430; (b) J.-i. Oku, S. Inoue, *J. Chem. Soc., Chem. Commun.* **1981**, 229-230.

[43] (a) M. S. Sigman, E. N. Jacobsen, *J. Am. Chem. Soc.* **1998**, *120*, 4901-4902; (b) P. Vachal, E. N. Jacobsen, *J. Am. Chem. Soc.* **2002**, *124*, 10012-10014.
[44] E. J. Corey, M. J. Grogan, *Org. Lett.* **1999**, *1*, 157-160.
[45] G. Jakab, C. Tancon, Z. Zhang, K. M. Lippert, P. R. Schreiner, *Org. Lett.* **2012**, *14*, 1724-1727.
[46] E. Knoevenagel, *Ber. Dtsch. Chem. Ges.* **1894**, *27*, 2345-2346.
[47] A. Erkkilä, I. Majander, P. M. Pihko, *Chem. Rev.* **2007**, *107*, 5416-5470.
[48] K. A. Ahrendt, C. J. Borths, D. W. C. MacMillan, *J. Am. Chem. Soc.* **2000**, *122*, 4243-4244.
[49] (a) T. D. Beeson, A. Mastracchio, J.-B. Hong, K. Ashton, D. W. C. MacMillan, *Science* **2007**, *316*, 582-585; (b) A. Mastracchio, A. A. Warkentin, A. M. Walji, D. W. C. MacMillan, *Proc. Natl. Acad. Sci. USA.* **2010**, *107*, 20648-20651.
[50] R. Beel, S. Kobialka, M. L. Schmidt, M. Engeser, *Chem. Commun.* **2011**, *47*, 3293-3295.
[51] J. J. Devery, J. C. Conrad, D. W. C. MacMillan, R. A. Flowers, *Angew. Chem. Int. Ed.* **2010**, *49*, 6106-6110.
[52] (a) S. Mayer, B. List, *Angew. Chem. Int. Ed.* **2006**, *45*, 4193-4195; (b) G. L. Hamilton, E. J. Kang, M. Mba, F. D. Toste, *Science* **2007**, *317*, 496-499; (c) K. Brak, E. N. Jacobsen, *Angew. Chem. Int. Ed.* **2013**, *52*, 534-561.
[53] K. Brak, E. N. Jacobsen, *Angew. Chem. Int. Ed.* **2013**, *52*, 534-561.
[54] (a) I. T. Raheem, P. S. Thiara, E. A. Peterson, E. N. Jacobsen, *J. Am. Chem. Soc.* **2007**, *129*, 13404-13405; (b) S. E. Reisman, A. G. Doyle, E. N. Jacobsen, *J. Am. Chem. Soc.* **2008**, *130*, 7198-7199.
[55] J. A. Gladysz, *Chem. Rev.* **2002**, *102*, 3215-3216.
[56] S. Ceylan, A. Kirschning, in: *Recoverable and Recyclable Catalysts,* (Ed.: M. Benaglia), John Wiley & Sons Ltd., **2009**, Chapter 13, p 379
[57] For reviews, see: a) D. E. De Vos, I. F. J. Van-kelecom, P. A. Jacobs, *Chiral Catalyst Immobilization and Recycling*, Wiley-VCH, Weinheim, **2000**; b) R. A. Sheldon, H. Bekkum, *Fine Chemicals Through Heterogeneous Catalysis,* Wiley-VCH, Weinheim, **2001**; c) J. A. Gladysz, *Chem. Rev.* Special Issue: Recoverable Catalysts and Reagents **2002**, *102*, 3215; d) P. McMorn, G. Hutchings, *Chem. Soc. Rev.* **2004**, *33*, 108; e) K. Ding, Y. Uozumi, Handbook of *Asymmetric Heterogeneous Catalysis*, Wiley-VCH, Weinheim, **2008**; f) M. Benaglia, R*ecoverable and Recyclable Catalysts*, John Wiley & Sons, Chichester, **2009**; g) P. Barbaro, F. Liguari, *Heterogenized Homogeneous Catalysts for Fine Chemicals Production Catalysis by Metal Complexes*, Springer, Heidelberg, Vol. 33, **2010**; h) R. Iebesta, *Enantioselective Homogeneous Supported Catalysts*, RCS Publishing, Cambridge, **2012**.
[58] R. B. Merrifield, *J. Am. Chem. Soc.* **1963**, *85*, 2149-2154.

[59] I. F. J. Vankelecom, P. A. Jacobs, in *Chiral Catalyst Immobilization and Recycling*, Wiley-VCH Verlag GmbH, **2007**, pp. 19-42.
[60] J. Lu, P. H. Toy, *Chem. Rev.* **2009**, *109*, 815-838.
[61] P. Munnik, P. E. de Jongh, K. P. de Jong, *Chem. Rev.* **2015**, *115*, 6687-6718.
[62] M. Benaglia, A. Puglisi, F. Cozzi, *Chem. Rev.* **2003**, *103*, 3401-3430.
[63] a) R. Haag, S. Roller, Immobilized Catalysts, in: A. Kirsching (editor), Topics in Current Chemistry, Springer, Heidelberg, 2004; b) B. M. L. Dioos, I. F. J. Vankelecom, P. A. Jacobs, *Adv. Synth. Catal.* **2006**, *348*, 1413; c) S. Itsuno, N. Haraguchi, Heterogeneous Enantioselective Catalysis Using Organic Polymeric Supports, in: K. Ding, Y. Uozumi (editors), Handbook of *Asymmetric Heterogeneous Catalysis*, Wiley-VCH, Weinheim, **2008**.
[64] (a) B. F. G. Johnson, S. A. Raynor, D. S. Shephard, T. Mashmeyer, T. Mashmeyer, J. Meurig Thomas, G. Sankar, S. Bromley, R. Oldroyd, L. Gladden, M. D. Mantle, *Chem. Commun.* **1999**, 1167-1168; (b) T. E. Kristensen, K. Vestli, M. G. Jakobsen, F. K. Hansen, T. Hansen, *J. Org. Chem.* **2010**, *75*, 1620-1629; (c) P. McMorn, G. J. Hutchings, *Chem. Soc. Rev.* **2004**, *33*, 108-122.
[65] J. M. Fraile, J. I. García, J. A. Mayoral, *Coord. Chem. Rev.* **2008**, *252*, 624-646.
[66] A. H. Lu, F. Schüth, *Adv. Mater.* **2006**, *18*, 1793-1805.
[67] D. Font, C. Jimeno, M. A. Pericàs, *Org. Lett.* **2006**, *8*, 4653-4655.
[68] (a) Y. Meng, D. Gu, F. Zhang, Y. Shi, H. Yang, Z. Li, C. Yu, B. Tu, D. Zhao, *Angew. Chem. Int. Ed.* **2005**, *44*, 7053-7059; (b) T. E. Kristensen, T. Hansen, *Eur. J. Org. Chem.* **2010**, *2010*, 3179-3204.
[69] (a) M. A. Newton, *Chem. Soc. Rev.* **2008**, *37*, 2644-2657; (b) R. J. White, R. Luque, V. L. Budarin, J. H. Clark, D. J. Macquarrie, *Chem. Soc. Rev.* **2009**, *38*, 481-494.
[70] D. Font, S. Sayalero, A. Bastero, C. Jimeno, M. A. Pericàs, *Org. Lett.* **2008**, *10*, 337-340.
[71] (a) P. L. Anelli, B. Czech, F. Montanari, S. Quici, *J. Am. Chem. Soc.* **1984**, *106*, 861-869; (b) P. Hodge, *Chem. Soc. Rev.* **1997**, *26*, 417-424.
[72] (a) J. Izquierdo, C. Ayats, A. H. Henseler, M. A. Pericàs, *Org. Biomol. Chem.* **2015**, *13*, 4204-4209; (b) P. Kasaplar, E. Ozkal, C. Rodriguez-Escrich, M. A. Pericàs, *Green Chem.* **2015**, *17*, 3122-3129; (c) I. Sagamanova, C. Rodríguez-Escrich, I. G. Molnár, S. Sayalero, R. Gilmour, M. A. Pericàs, *ACS Catal.* **2015**, *5*, 6241-6248; (d) J. Izquierdo, M. A. Pericàs, *ACS Catal.* **2016**, *6*, 348-356; (e) P. Llanes, S. Sayalero, C. Rodriguez-Escrich, M. A. Pericàs, *Green Chem.* **2016**, *18*, 3507-3512; (f) E. Ozkal, S. Ozcubukcu, C. Jimeno, M. A. Pericas, *Catal. Sci. Technol.* **2012**, *2*, 195-200; (g) E. Alza, X. C. Cambeiro, C. Jimeno, M. A. Pericàs,

Org. Lett. **2007**, *9*, 3717-3720; (h) C. Ayats, A. H. Henseler, M. A. Pericàs, *ChemSusChem* **2012**, *5*, 320-325; (i) P. Riente, J. Yadav, M. A. Pericàs, *Org. Lett.* **2012**, *14*, 3668-3671.

[73] C. Rodríguez-Escrich, M. A. Pericàs, *Eur. J. Org. Chem.* **2015**, *2015*, 1173-1188.

[74] (a) A. Puglisi, M. Benaglia, V. Chiroli, *Green Chem.* **2013**, *15*, 1790-1813; (b) I. Atodiresei, C. Vila, M. Rueping, *ACS Catal.* **2015**, *5*, 1972-1985; (c) D. Zhao, K. Ding, *ACS Catal.* **2013**, *3*, 928-944; (d) B. Gutmann, D. Cantillo, C. O. Kappe, *Angew. Chem. Int. Ed.* **2015**, *54*, 6688-6728.

[75] (a) J. C. Pastre, D. L. Browne, S. V. Ley, *Chem. Soc. Rev.* **2013**, *42*, 8849-8869; (b) J. C. Pastre, D. L. Browne, M. O'Brien, S. V. Ley, *Org. Process Res. Dev.* **2013**, *17*, 1183-1191; (c) P. Poechlauer, W. Skranc, in *Sustainable Flow Chemistry*, Wiley-VCH Verlag GmbH & Co. KGaA, **2017**, pp. 73-102.

[76] (a) G. Müller, T. Gaupp, F. Wahl, G. Wille, *CHIMIA International Journal for Chemistry* **2006**, *60*, 618-622; (b) Z. J. Garlets, J. D. Nguyen, C. R. J. Stephenson, *Isr. J. Chem.* **2014**, *54*, 351-360.

[77] J. Britton, C. L. Raston, *Chem. Soc. Rev.* **2017**, *46*, 1250-1271.

[78] (a) R. Munirathinam, J. Huskens, W. Verboom, *Adv. Synth. Catal.* **2015**, *357*, 1093-1123; (b) R. Porta, M. Benaglia, A. Puglisi, *Org. Process Res. Dev.* **2016**, *20*, 2-25; (c) J. Wegner, S. Ceylan, A. Kirschning, *Adv. Synth. Catal.* **2012**, *354*, 17-57; (d) V. Hessel, D. Kralisch, N. Kockmann, T. Noël, Q. Wang, *ChemSusChem* **2013**, *6*, 746-789.

[79] F. Mastronardi, B. Gutmann, C. O. Kappe, *Org. Lett.* **2013**, *15*, 5590-5593.

[80] S. Hübner, J. G. de Vries, V. Farina, *Adv. Synth. Catal.* **2016**, *358*, 3-25.

[81] I. R. Baxendale, *J. Chem. Technol. Biotechnol.* **2013**, *88*, 519-552.

[82] I. R. Baxendale, J. Deeley, C. M. Griffiths-Jones, S. V. Ley, S. Saaby, G. K. Tranmer, *Chem. Commun.* **2006**, 2566-2568.

CHAPTER II

UNIVERSITAT ROVIRA I VIRGILI
IMMOBILIZATION OF CHIRAL BRØNSTED ACIDS AND LEWIS BASES FOR BATCH AND FLOW ENANTIOSELECTIVE CATALYSIS
Lidia Clot Almenara

Chapter II

Immobilization of Chiral Phosphoric Acids (CPA)

2.1. Introduction

Within the field of organocatalysis, chiral Brønsted acids (BA) have gained increasing significance due to their application in many asymmetric transformations involving carbonyl and imine activation, a field traditionally restricted to metal-based Lewis acid catalysts. Lewis acid catalysis relies in the activation of C=X bond (X = O, NR, CR_2) by coordination, which decrease the energy of the LUMO, thus promoting nucleophilic addition to C=X.[1] Chiral Lewis acid catalysts are achieved by the combination of a metal-centered Lewis acid and a chiral ligand.[2] Later, Brønsted acid catalysts attracted much attention due to their for its ability to activate substrates through hydrogen bonding.[3] Initially, they were mainly employed to cleave C-O bonds, such as in hydrolysis reactions and formation of esters, acetals, etc. Afterwards, it was found that they are able to activate carbonyl, imine, alkene, alkyne and hydroxyl groups, This is due to the fact that Brønsted acids activate the electrophiles via protonation, which lowers the energy of the LUMO.[4] From that moment on, the use of Brønsted acids has experienced a tremendous growth, expanding the list of synthetic transformations mediated by organocatalysts. Brønsted acids are easy to handle, since given that they are usually stable toward oxygen and moisture, environmentally friendly and can be stored for a long period of time. All these combined features make them a very convenient choice for enantioselective catalysis.[5]

The term Brønsted acids actually encompasses very different species. In addition to the common achiral Brønsted acids[6] as HCl, H_2SO_4, acetic acid, and trifluoromethanesulfonic acid (TfOH),[7] more appealing hydrogen-bond donor chiral organic molecules such as chiral thiourea, TADDOL and squaramide derivatives have been reported so far. Furthermore, a range of BINOL-derivatives are also included in this group, for instance, binaphtols, dicarboxylic acids, disulfonic acids, and disulfonimides.

Table 2.1: Brønsted acid derivatives and their acidities.

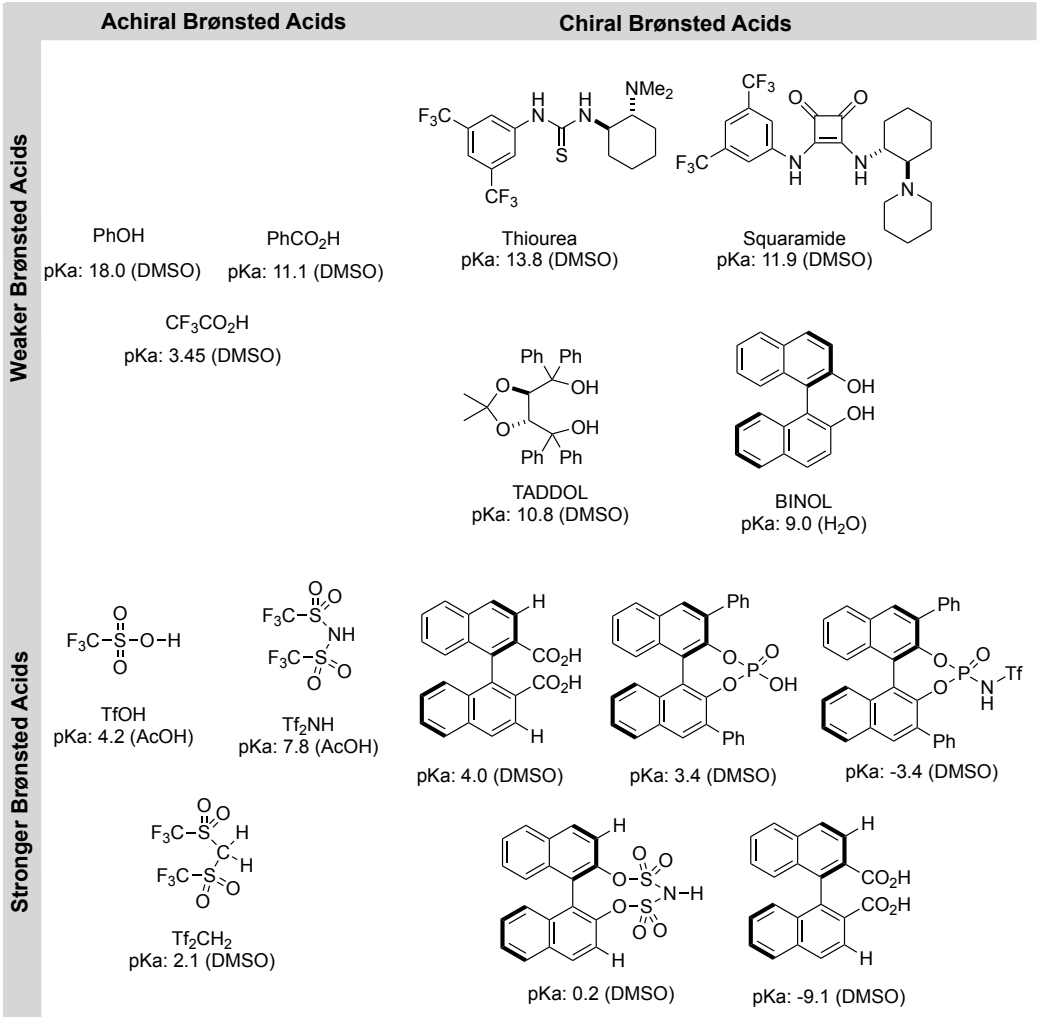

Chiral Brønsted acids can be divided in two main groups according to the strength of interaction with the substrate (Table 2.1):[6a, 8]

(I) Neutral Brønsted acids, herein we can include BINOL,[9] thiourea and TADDOL derivatives.[10]

(II) Stronger, readily ionizing, Brønsted acids, where we can find BINOL derivatives including the phosphoric acids. The latter group will be discussed in more detail.[11]

Nowadays, the field of enantioselective Brønsted acid catalysis is dominated by BINOL-derived chiral phosphoric acids, whose potential started to unravel with the pioneering works of Akiyama[12] and Terada[13] in 2004, who independently introduced their use in asymmetric catalysis. In particular, they reported that *N*-protected imines could be activated by phosphoric acids, demonstrating this premise in highly enantioselective Mannich-reactions. Akiyama *et al*. reported the reaction of silyl enol ethers with aldimines to give chiral β-amino carbonyl compounds (Scheme 2.1). The methodology provided excellent yields and high diastereo- and enantioselectivity for all the substrates. They observed that the 3,3'-groups directly influence the asymmetric induction. Catalyst **7**, bearing a 4-nitrophenyl group, turned out to be the best in terms of both reactivity and enantioselectivity. Even though the mechanism of action was not elucidated, Akiyama postulated the importance of the 2-hydroxy group in the imine to carry out this transformation.[14] Later, in 2007[14] he published a theoretical study with calculations involving the mechanism, where he concluded that double activation of the catalyst was operative: On the one hand, the acidic proton activates the imine by protonation whereas on the other hand, an additional interaction takes place between the phenolic proton and the phosphoryl Lewis basic site.

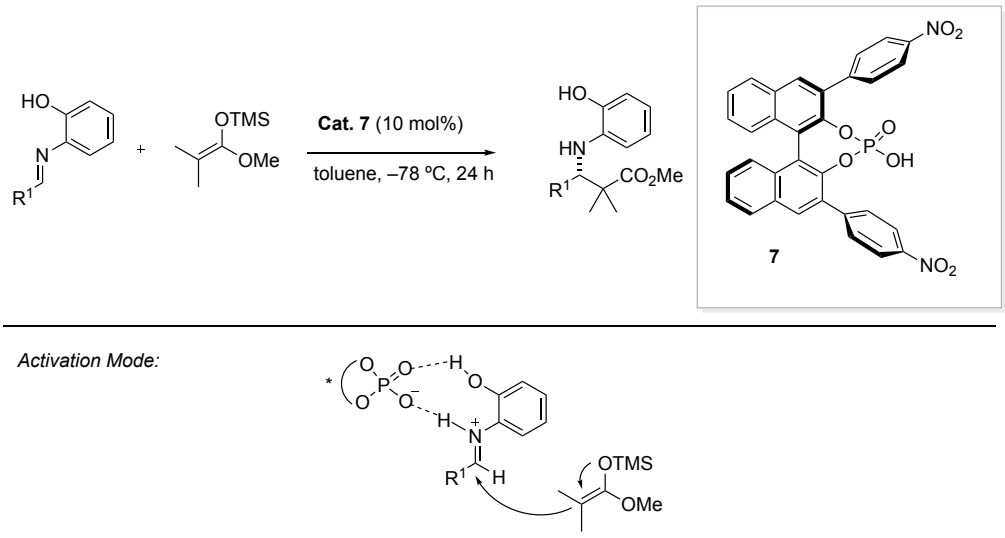

Scheme 2.1: Enantioselective Mannich-type reaction and the proposed dual activation mode.

More or less at the same time, the group of Terada described the synthesis of β-aminoketones arising from the reaction of *N*-Boc-protected imines with acetylacetone (Scheme 2.2).[15] The tendency they appreciated was that yield and enantioselectivity were proportional to the bulk of the substituents in the 3,3'-positions of the BINOL scaffold. The mechanism was corroborated with the work of Goodman, who claims that the catalyst plays a bifunctional role, activating both the imine and the nucleophile through its tautomeric enol form.

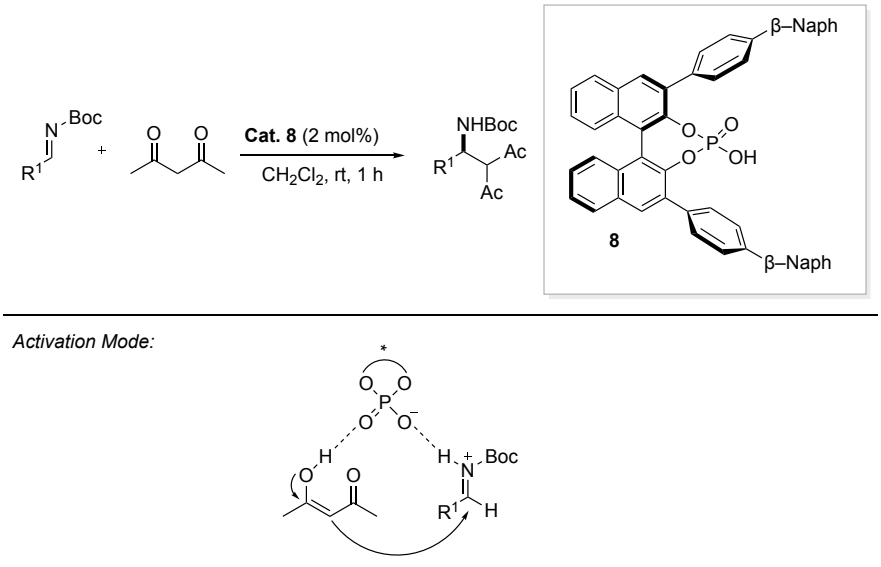

Scheme 2.2: Mannich reaction catalyzed by CPA and the proposed dual activation mode.

These were the first examples of enantioselective Mannich-type reaction in which the carbon–nitrogen double bond is activated by a strong, metal-free, chiral Brønsted acid. After these findings, chiral phosphoric acids (CPAs) were acknowledged as novel chiral catalysts and attracted the attention of synthetic organic chemists.[16] These methods can potentially be extended to a variety of enantioselective nucleophilic addition reactions to carbon–nitrogen double bonds.

Inspired by these pioneering works, novel chiral phosphoric acids have been designed according to the following points.[17] The core scaffold is usually derived from BINOL, which has been chosen as a readily available chiral source, as it guarantees high rigidity and presents a C_2 symmetry axis. Later, in order to achieve the suitable acidity to promote the reaction, Akiyama relied in the acid $(EtO)_2P(O)OH$ because of its high acidity with a pK_a = 1.3. Finally, the introduction of substituents in the 3,3'-positions allowed to create a perfect cavity for the substrates. These catalysts are considered as bifunctional activators, because they bear both a Brønsted-acid and a Lewis-base. The appropriate choice of substituents at 3,3'-positions is crucial to induce high stereoselectivity (Figure 2.1).

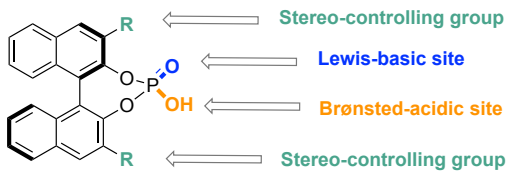

Figure 2.1: Chiral Brønsted acid.

The versatile nature of these species is due to the fact that they are quite acidic and therefore able to activate a broad range of substrates. Most of the reactions initially developed were in the fields of transfer hydrogenation and nucleophilic addition to basic imines. Promising results could be obtained if phosphoric acids could activate more challenging and less basic carbonyls compounds.[18]

Thereby, the modification of the catalytic site with the idea of increasing acidity was carried out by different research groups.[19] Rueping *et al.* reported a study about the correlation between the pK_a and the reactivity, with the aim of choosing the best phosphoric acid for each reaction. They measured the pK_a in acetonitrile of different derivatives of the following three types of Brønsted acids: phosphoric acids (PA), *N*-triflylphosphoramides (NTPA) and bis(sulfuryl)imides (JINGLE).[20] According to their results, the strongest influence is mainly exerted by the nature of the acidic center. Consequently, the less acidic type is PA, which pK_a value oscillates approximately around 14-12, followed by NTPA (assigned 6-7), and finally JINGLE, which has a reported pK_a value of around 5. Factors such as the electronic properties of substituents on the 3,3'-positions and the aromatic or aliphatic nature of the outer binaphtalene ring have less influence on the pK_a value (Figure 2.2). Later, they calculated the rate constant of the reaction in the Nazarov cyclization, observing that a higher acidity correlated with a higher ability to activate and accelerate the reaction, whereas the enantioselectivity was determined by the architecture of the catalyst.

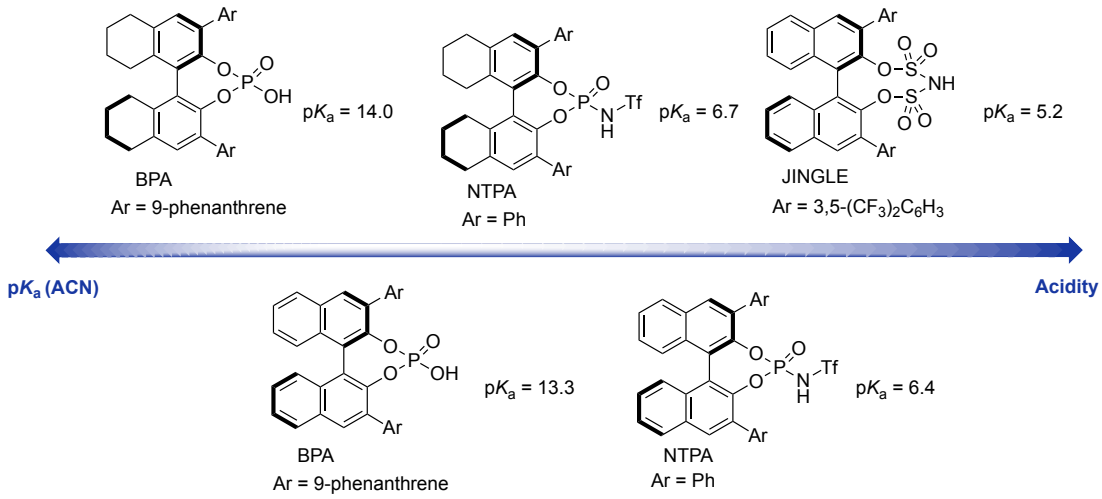

Figure 2.2: pK_a of selected BINOL-derived Brønsted acids.

2.1.1. General Outlook of BINOL-Derived Catalysts

Solid evidences show how alterations in the structural scaffold of the catalytic center, the acidity of the catalysts, or the influence of different substituents have a direct impact on the enantiomeric excess and yield of a given transformation. Since a common solution has been, so far, elusive, research has focused on determining the best catalyst structure for a particular reaction.[20-21] In this section, we have tried to summarize the most remarkable catalysts developed so far (Figure **2.3**). Among all chiral phosphoric acid derivatives synthesized to date, the most popular scaffold is still the BINOL backbone. The simplest phosphoric acid employed in asymmetric catalysis is **9** bearing hydrogen as the R groups in 3,3'-positions. Then, more complex compounds, containing bulkier substituents such as adamantyl, or phenanthryl have also been prepared and tested in asymmetric transformations.[22] The most frequent alternative to the use of BINOL is the related [H8]-BINOL scaffold,[23] which possesses the same key features of its fully aromatic counterpart but different solubility and acidity. Silicon-based groups are less common, but in some cases, they have improved the results obtained with aryl substituents **10** (R=Ph_3; or (4-*t*-$BuC_6H_4)_3$).[24] The presence of a trisubstituted aryl ring **11** in 3,3'-position increases dramatically the steric hindrance, and thus catalysts as **12**, bearing 4-substituents or **13**, with 3,5-substituents, are also seen in the literature. Substituents on the backbone are introduced to control other parameters of the catalyst such as electronic properties or solubility **14**.[25] Other particular catalysts, which have been employed in specific reactions, are derivatives of biphenyl core as **15** or the relatively new class of chiral phosphoric acids derived from spiro-diols (*R*)–VANOL **16**, (*R*)–VAPOL **17** or (*S*)–SPINOL **18**.[26] The use of ammonium salts **19** and **20** has allowed to develop asymmetric counteranion-directed catalysis.[27] This strategy has been

widely used for reactions involving iminium ion-catalysis and ring-opening of epoxides.

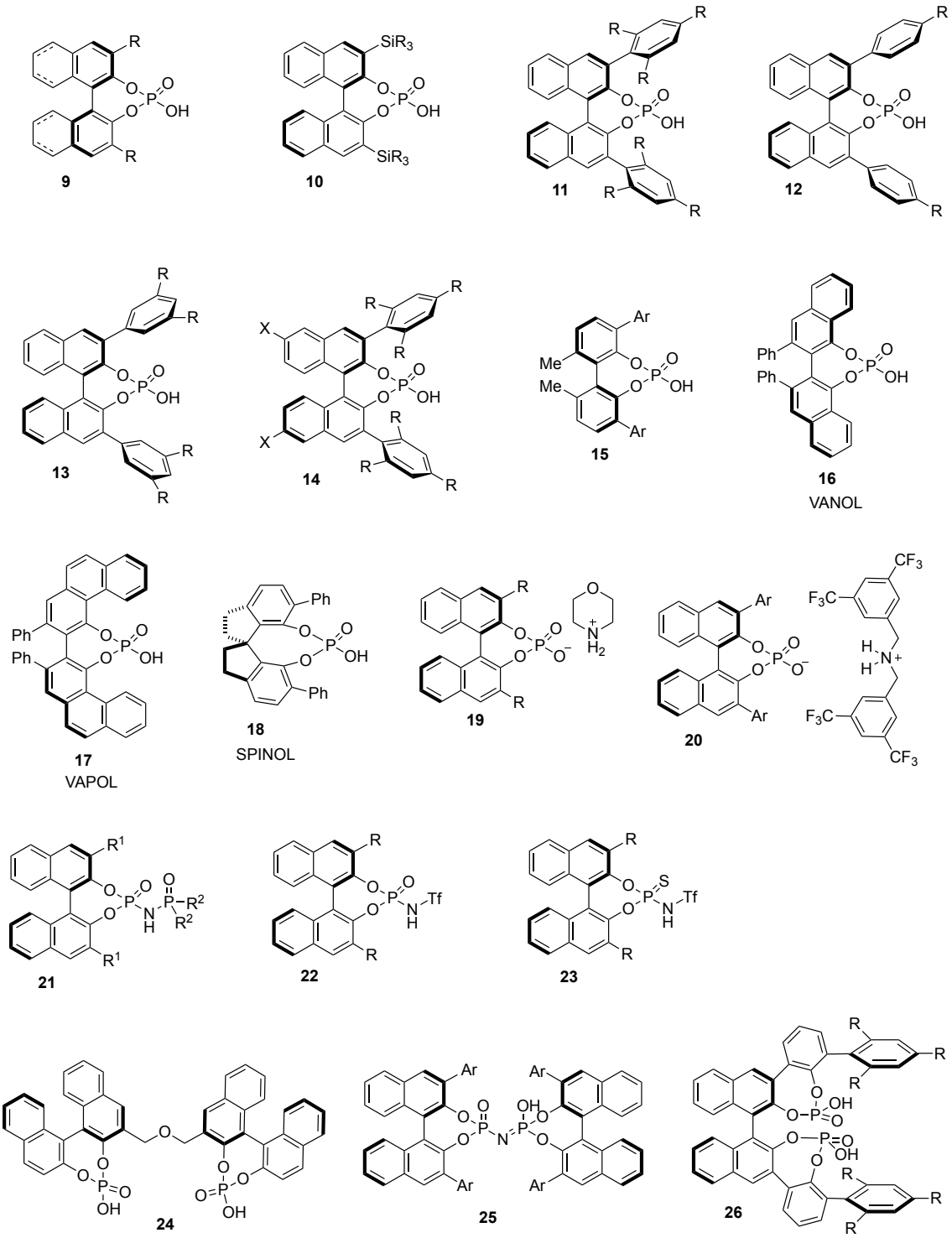

Figure 2.3: Overview of the most relevant CPAs reported in the literature.

As mentioned in the previous section, modification of the phosphate group has also been studied in order to enhance the Brønsted acidity of BINOL-based catalysts; *N*-phosphoramide catalysts **21** and **22**[28] are a good example of this class. Another subclass within this category are *N*-thiophosphoramide catalysts (NTA) **23**,[29] which are stronger Brønsted acids, albeit they have been applied just in a few transformations. Finally, an under-developed area would cover the category of catalysts containing multiple chiral axes as **24**,[30] **25**,[31] and **26**. The acidity of these latter catalysts can be increased upon intramolecular hydrogen bonding between two acidic functionalities. Furthermore, it is worth mentioning that a novel chiral scaffold has been created having extra axial chirality.

2.1.2. Modes of Activation and their Applications

Given the versatility of chiral phosphoric acids, which have shown high activity in numerous transformations (Figure 2.4),[25a, 32] showing high activity, their mechanism of action has caught the eye of many research groups.

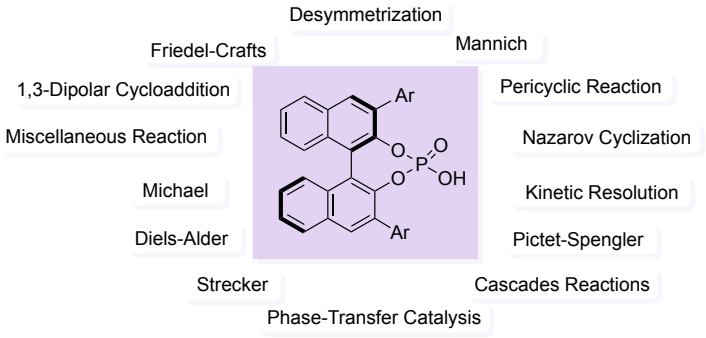

Figure 2.4: Versatility of chiral phosphoric acid catalysts.[32a, 33]

However, it is hard to establish a general model for all substrates, due to the fact that the activation mode depends on many factors,[34] mainly, the nature of the substrates and how the catalysts will interact with the corresponding functional groups present in the different starting materials. In this section, we have tried to summarize the main approaches that have been postulated.[17a]

- **Single Activation**

Understanding the interaction between the catalyst and the substrate has been key to explore the versatility of chiral phosphoric acids.[35] At the beginning, it was assumed that full protonation of the imine resulted in the formation of an ion pair. However, it was later corroborated through NMR spectroscopy that a large number of possible interactions can happen and ascertaining exactly how the catalyst acts is not a trivial issue. Rueping and Gschwind carried out NMR experiments to determine the activation mode in imines. They concluded that the actual mechanism depends on the sum of many factors as the imine structure, the temperature, the concentration, the solvent and the nature of the Brønsted acid. But above all, the electronic properties of substituents are ultimately responsible to determine if the interaction is considered a H-bond or an ion pair. While electron-rich imines usually work via ion-pair activation mode, electron-deficient imines tend to form H-bonds (Figure 2.5). However, in the case of carbonyl activation, the interaction between the catalyst and the carbonyl group becomes more challenging due to its low basicity. For this reason, H-bonding is more probable in carbonyl activation than ion-pairing. Nevertheless, the difference of pK_a between the Brønsted-acid catalysts and the carbonyl compound will influence if hydrogen bonding or contact ion pair are operative in the mechanism.

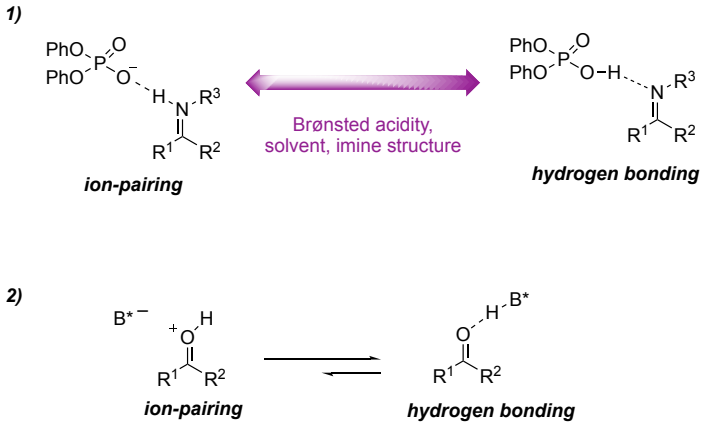

Figure 2.5: Monoactivation of carbonyl (1) and imines (2) with Brønsted acids.

- **Dual Activation:**

This activation mode takes place when a substrate is able to coordinate to the catalyst by making two specific contacts. Two different possibilities for this are depicted in Figure 2.6. On the one hand, bidentate hydrogen bonding interaction is generated in the case that another hydrogen bonding acceptor is close to the carbonyl group, in a manner that the substrate can chelate the acidic Brønsted acid proton during the activation. On the other hand, double H-bonding interaction is possible when besides the acidic proton on the catalyst, the phosphoryl oxygen also interacts with a second H-bond donor, thus forming a double hydrogen bonding motif. Dual activation has a major impact on carbonyl activation because the activation of the carbon-oxygen double bond via one hydrogen bond may be not enough to engage them in a reaction. These bonding modes have improved the nucleophilic attack to carbonyl compounds.

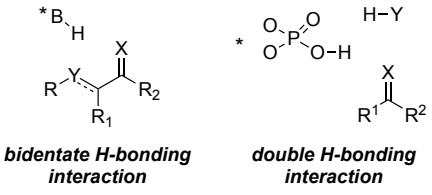

Figure 2.6: Main activation mode features under dual-activation.

- **Bifunctional Activation:**

The Rueping and Hoffman groups have reported in their respective works in transfer hydrogenation, the possibility of a stepwise mechanism. This would consist of the activation of imines by protonation with the acid catalyst, which is later regenerated by recovering the proton from the protonated nucleophile.[33e, 33f, 36] However, chiral phosphoric acids can act simultaneously as Brønsted acids and Lewis bases, enabling them to activate the substrates simultaneously.[33a, 37] Bifunctional activation covers most of the reaction catalyzed by CPAs. Although, Akiyama and other groups had already reported a concerted mechanism,[38] it was Goodman in his publication in 2011, who conducted a comprehensive mechanistic study in the reduction of imines by DFT calculations.[39] Goodman explained that the stereochemical outcome of many reactions in based on two transition states named Type I and Type II (Figure 2.7). In the proposed Type I and Type II transition state the phosphoric acid oxygens are on different side from the bulky substituents. They predicted for both models that nucleophiles containing an acidic proton will be interacting by H-bonding to the catalyst. The difference between the two prototypes remains in the steric impact of R^2 and R^3. The calculated energy transition state resulted to be lower in the case of Type I, when R^3 is larger than R^2 and consequently, R^3 is placed in the empty space. On the other hand, higher energy was shown in the case of R^2 is larger than R^3, where R^2 is positioned in the empty space.

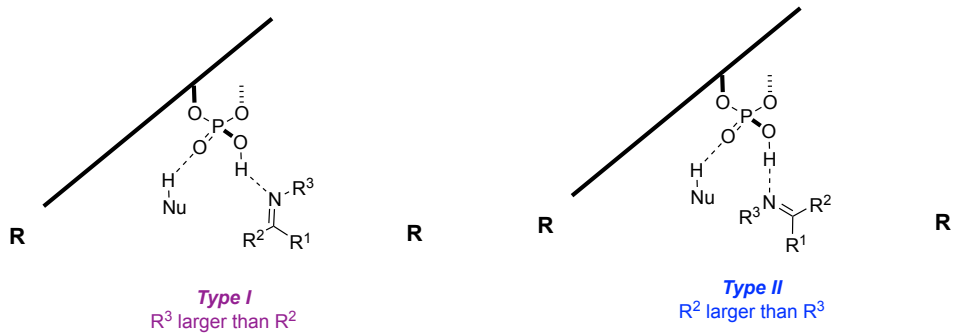

Figure 2.7: Models proposed from Goodman to explain the stereochemical outcome.

- **Counterion Catalysis**

This section can be considered the least explored, and involve the use of catalyst such as **19** and **20** depicted in Figure 2.3.[40] The conjugate bases of chiral phosphoric acids can be used as chiral anion in asymmetric transfomations.[41] This transformation involves the use of charged intermediates, where the proton is covalently linked between both the catalyst and the substrate (Figure 2.8).

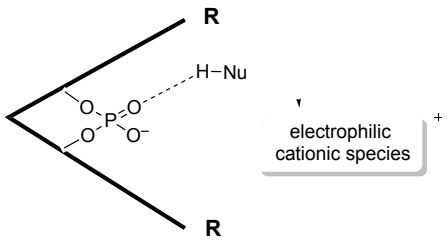

Figure 2.8: Representation of chiral phosphate catalysis.

2.1.3. TRIP: The Ideal Chiral Environment

In the asymmetric transformations catalyzed by CPAs the stereocontrol relies in the proper choice of sterically demanding substituents in the 3,3'-positions, in order to create a perfect chiral environment. This fact has led to the study of different scaffolds in search for the highest ee (Figure 2.9); among them, it is worth highlighting the work of Benjamin List *et al*. who were the first in describing phosphoric acid **33**, which they initially applied to the asymmetric hydrogenation of imines with a Hantzsch ester (Scheme 2.3). The CPA protonates the imines forming an iminium ion that subsequently reacts with the Hantzsch ester to provide enantioenriched amines.[33e, 42] List made an exhaustive analysis of the synthesis of **35** due to the fact that differences in the reactivity were observed between different batches,[42] even if the signals from ^{1}H NMR showed to be desired TRIP catalyst, the signals corresponding to isopropyl groups in ^{1}H NMR were shifted depending on the batch. They treated the different batches of catalyst with bases and acids and these experiments revealed that the catalyst contained inorganic salts impurities. Then, analysis by ICP-OES confirmed the presence of silicon mostly although other metals impurities were also found. The presence of these metals can be attributed to the purification process by column chromatography.[43] After solving this synthetic issue, the CPA bearing 2,4,6-*i*Pr-phenyl substituents, namely TRIP, has been present in numerous works giving rise to higher ee in comparison with other scaffolds. Some examples are illustrated in Scheme 2.3.[42, 44]

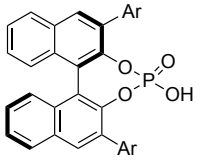

27: Ar = H
28: Ar = C_6H_5
29: Ar = 4-NO_2-C_6H_4
30: Ar = 2-naphthyl
31: Ar = 9-anthracenyl
32: Ar = 4-biphenyl
33: Ar = 2,4,6-(*i*-Pr)$_3$$C_6H_2$
34: Ar = 2-thienyl
35: Ar = 2,4,6-$F_3C_6H_2$

Figure 2.9: Brief summary of BINOL-derived CPAs.

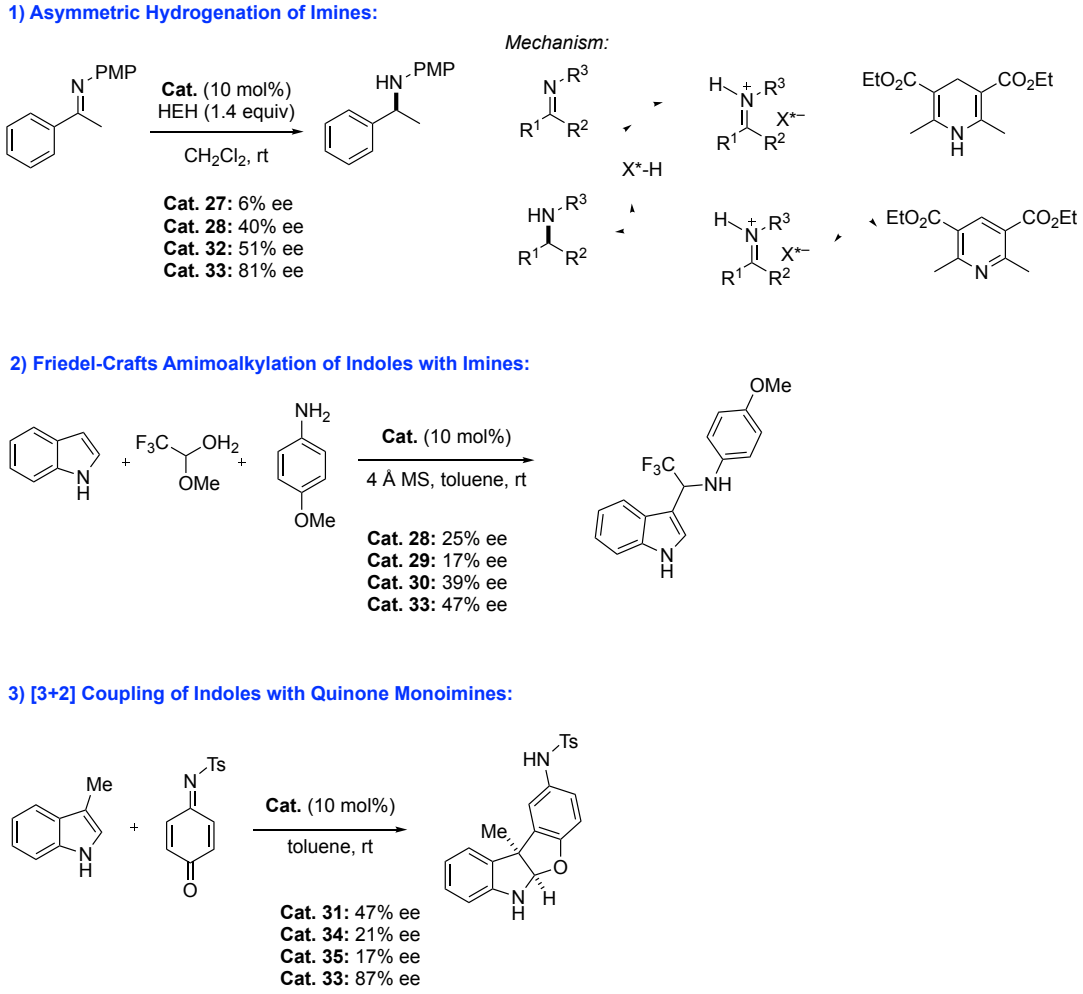

Scheme 2.3: Representative asymmetric transformations catalyzed by TRIP.

2.1.4. Procedures for Heterogenization of CPAs

Chiral BINOL-derived phosphoric acid catalysts have shown to be highly efficient in a broad range of enantioselective reactions, and these transformations remain an active area of research nowadays.

However, these homogeneous catalysts present some drawbacks: their synthesis is not particularly simple, they are very expensive and have high molecular weights, which leads to the use of high catalyst to substrate mass ratios. It can be postulated that the synthesis of a heterogenized version of phosphoric acid catalysts could overcome some of these main problems, as the

resulting catalysts immobilized on polymeric support are expected to be easily recoverable, allowing separation and isolation by filtration. Furthermore, their use can be extended to flow applications. However, one must bear in mind that in order to compensate the increase in cost, they will have to prove robust enough to allow recycling.[45]

With this idea in mind, several research groups, including our own, have studied the immobilization of CPAs to assess the impact of this approach on the activity and recyclability of the resulting catalytic materials.[46]

The Beller and Köckritz groups were the first in developing a supported CPA in 2008.[47] In an attempt to recover the catalyst, they incorporated a vinyl group in 3,3'-position for further polymerization. In such a way, they obtained a solid material which was insoluble in organic solvents (Scheme 2.4).

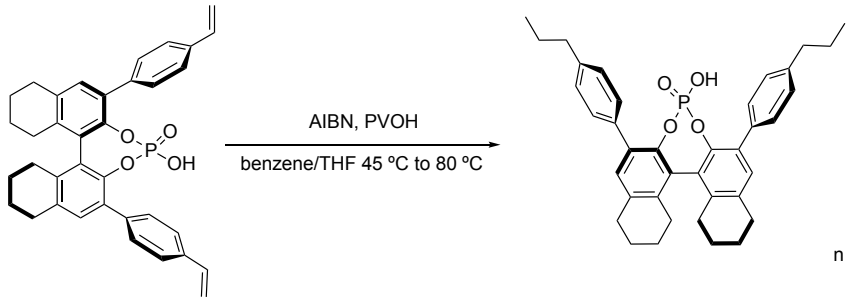

Scheme 2.4: Heterogeneous CPA via polymerization of vinyl group in 3,3'-position.

Nevertheless, it was not until 2010 when Rueping *et al.* showed significant advances in supported CPAs applying them to asymmetric transfer hydrogenation. After incorporating a styrene group in the BINOL scaffold, they achieved the heterogenization of CPA by radical co-polymerization with styrene, DVB as cross-linker and AIBN as radical initiator. Contrary to the typical heterogeneous catalysts, which tend to be microporous or macroporous resins, they formed a polymer-stick. First, they synthesized catalyst **36**, which

gratifyingly was used over 10 reaction cycles in the asymmetric transfer hydrogenation of quinolone obtaining from 60% up to 67% ee of **38** in the recyclability test (Scheme 2.5). Afterwards, they decided to introduced a 9-phenantryl group in 3,3'-position to fine tune the steric hindrance. In this approach, they carried out the cross-linking copolymerization by introducing a styrene group in the 6,6'-positions thus giving catalyst **37**. Next, catalyst **37** was used in the asymmetric hydrogenation, providing **39** in 97% yield and 96% ee. This catalyst was reused for 12 runs maintaining high yields and the ee remained 94% in all these experiments.[48]

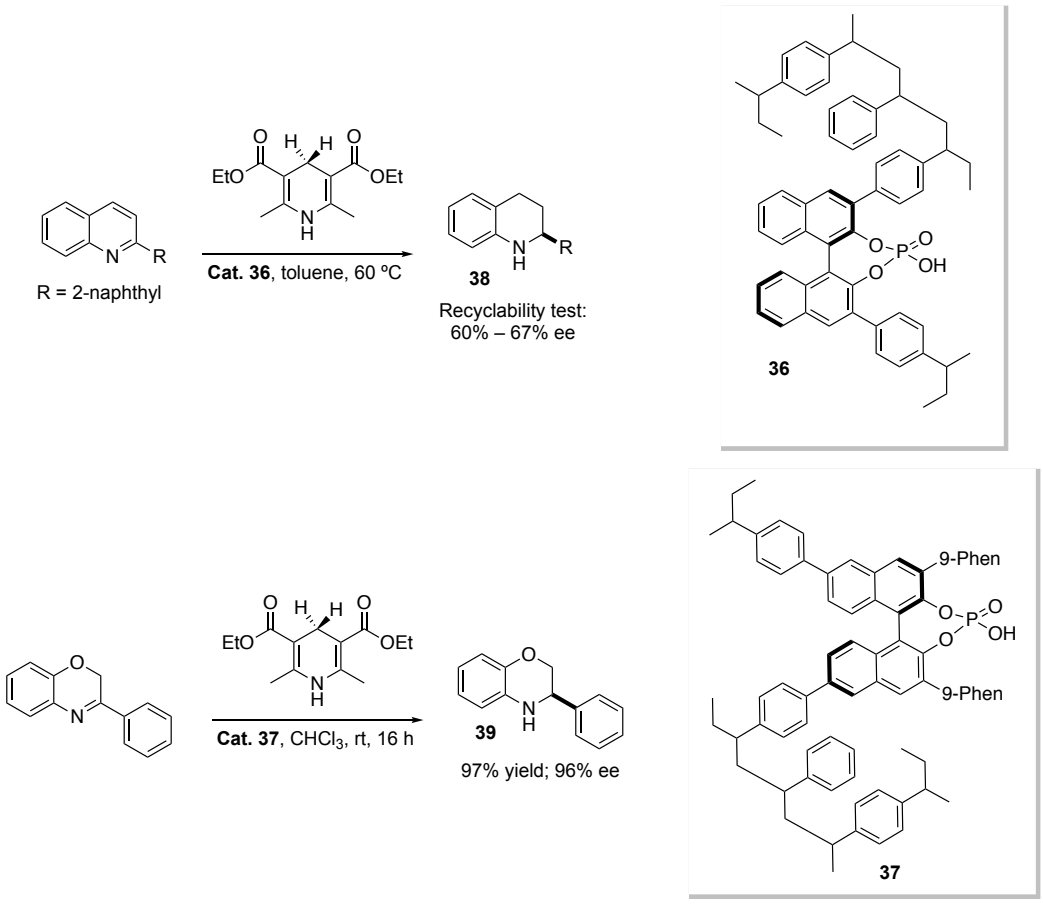

Scheme 2.5: Asymmetric transfer hydrogenation of quinolone **38** and benzoxazines **39**.

More recently, the Blechert group followed a strategy based on a microporous polymer network to obtain immobilized CPAs.[49] They reported the novel BINOL derivatives as a new structure-directing monomer for the generation of micropores in polymer networks. This strategy established that the polymer is built up through the repetition of monomers of the CPA which contain a polymerizable group (Scheme 2.6). With this idea in mind, they incorporated in the BINOL scaffold thiophene groups as reactive sites for a further oxidative coupling reaction. In doing so, they achieved cross-linking between BINOLs, making them at the same time insoluble networked structures while increasing the steric hindrance, which was expected to have a positive influence in the selectivity of the catalyst.

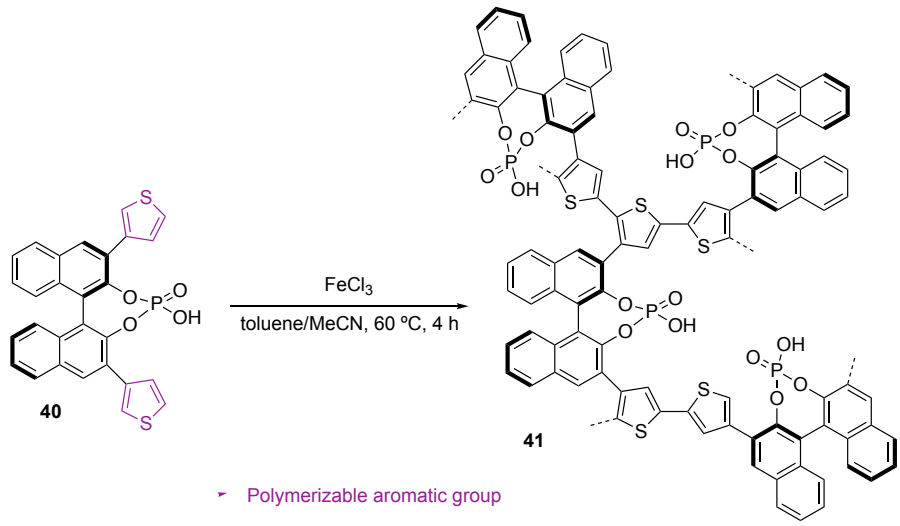

Scheme 2.6: Microporous polymer network via oxidative coupling between thiophenes.

Afterwards, they decided to apply polymer **41** to an asymmetric transfer hydrogenation of benzoxazines (Table 2.2). Gratifyingly, an increase of enantiomeric excess was observed in comparison with its homogeneous counterpart (entry 2). Strikingly, the major isomer obtained when **40** was used as catalyst had the opposite absolute configuration, despite the fact that both catalysts, **40** and **41**, had the same chirality. It is worth mentioning that the

catalyst was re-used three more times showing even higher ee (entry 3-5). This may be due to the presence of traces of acid remaining from the acidic work-up carried ou after polymerization.

Tableb 2.2: Catalytic asymmetric transfer hydrogenation of benzoxazines.

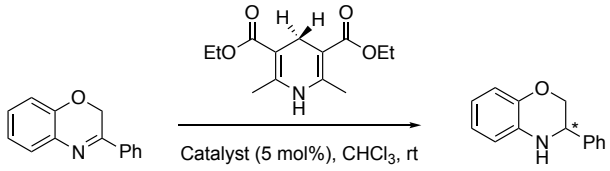

Entry	Catalyst	Cycle	Conv. [%][a]	ee [%][b]
1	**40**		99	34 [c]
2	**41**		99	47
3	**41**	2nd run	99	54
4	**41**	3rd run	99	55
5	**41**	4th run	97	56

[a]Determined by ^{1}H NMR analysis. [b]Determined by HPLC analysis. [c]Opposite stereochemistry.

It is worth noting that Kobayashi *et al.* reported on a very similar co-polymerization based immobilization strategy very similar to ours, which gave rise to a hybrid material that combined supported TRIP and Au/Pd nanoparticles (**42**).[50] The bifunctional catalyst was constructed through a pseudo-suspension co-polymerization method, from a TRIP derivative bearing two moieties of styrene in 6,6'-position. The chiral bifunctional heterogeneous material was able to facilitate a sequential aerobic oxidation-asymmetric aza-Friedel-Crafts (FC) reaction (Scheme 2.7). Chiral piperazines were furnished after sequential oxidation of benzyl alcohol and asymmetric aza-Friedel-Crafts reaction with *N*-aminoethylpyrrole.

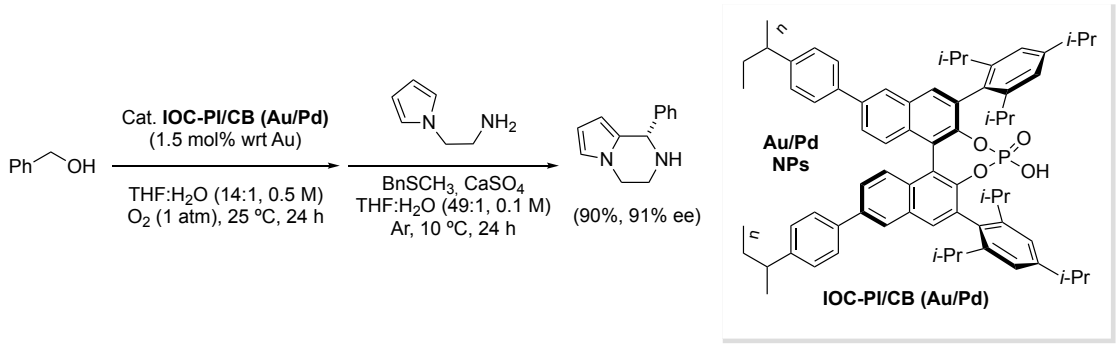

Scheme 2.7: (a) Synthesis of bifunctional supported material and (b) sequential aerobic oxidation and aza-Friedel-Crafts reactions.

Previously, in our group, Laura Osorio studied the synthesis of supported CPAs. In catalyst **43** the presence of CF_3 groups in the aromatic rings facilitates the determination of the functionalization of the resin by elemental analysis of fluorine. After preparing catalyst **43**, it was applied in the enantioselective Friedel-Crafts reaction of indoles and sulfonylimines (Scheme 2.8).[51]

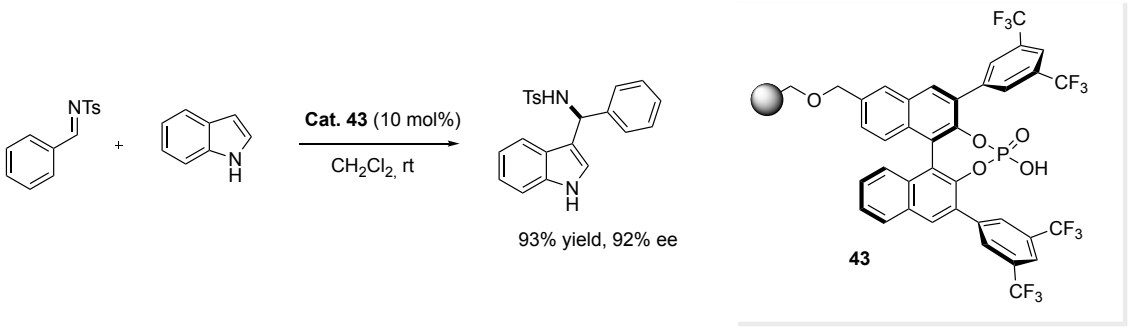

Scheme 2.8: Enantioselective Friedel-Crafts reaction of indoles and sulfonylimines.

The immobilized catalyst was subjected to several consecutive reaction runs to test the recyclability. Remarkably, the resin showed to be highly recyclable during six cycles, after that, the activity slightly dropped. However, treatment of **43** with HCl in EtOAc resulted in the recovery of the catalytic activity. The supported catalyst remained operative up to the fourteenth cycle showing no significant sign of diminishing in yield and enantioselectivity. Finally,

considering the high activity, the supported catalyst was studied in continuous flow processes giving high productivities (4.3 – 5.0 mmol h^{-1} $gresin^{-1}$).

2.2. Aims

Chiral phosphoric acids have proven to be versatile catalysts in a wide array of asymmetric reactions. Nevertheless, the main drawback associated to CPAs is the long and tedious sequences requires for their preparation.

For this reason, we became interested in the immobilization of CPAs. Furthermore, after the successful results obtained previously in our group for the supported CPA-catalyzed Friedel-Crafts alkylation of indoles (Scheme 2.8), we were encouraged to design a new synthetic route that could be applicable to the immobilization of the vast majority of CPA derivatives.

The TRIP catalyst, introduced by List *et al.*, has usually proven to be the best alternative among CPAs in terms of activity and enantioselectivity. For this reason, it was important to go a step further and find a new synthetic design for the supported TRIP catalyst (Figure 2.10). Even if it might entail a longer reaction sequence, a reduction in the cost can take place upon would be appreciated due to the recovery and reuse of the catalyst. Moreover, chromatographic purification would no longer be necessary.

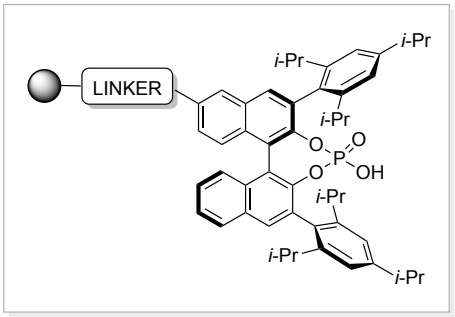

Figure 2.10: Immobilization of CPA.

Our main aim in this research was to anchor the resin via a linker containing a nitrogen atom, which was expected to facilitate the characterization of the resin. In contrast, our previous supported CPA **43**, had been anchored via nucleophilic substitution giving an ether. Our goal was then to find a synthetic sequence that introduced a nitrogen in the linker and that was able to include any BINOL derivative to facilitate the characterization of the material by elemental analysis.

2.3. Results and Discussion

With this aim in mind, we designed several synthetic alternatives. Thus, we thought about what would be the ideal resin to anchor the homogenous catalyst, and we postulated that the amine group could be introduced by nucleophilic addition to a commercially available sulfonyl chloride polystyrene resin.

From the outset, our first thought was trying to functionalize the BINOL structure in the 6-position with bromine, a versatile atom which is involved in many reactions. From a practical point of view, we deemed necessary to transform the bromine into an amine precursor before the introduction of the corresponding bulky substituents in 3,3'-positions. In Scheme 2.9 is depicted the general strategy devised to obtain the supported CPA via 6-amination in order to have a sulfonamide as a linker, starting from (*R*)-BINOL as a commercially available chiral precursor.

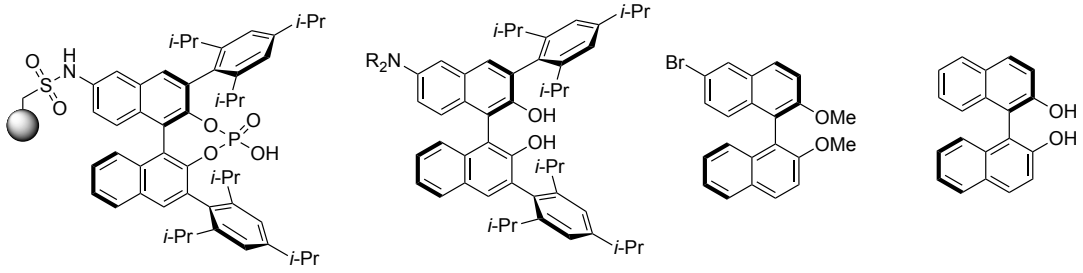

Scheme 2.9: Strategy to anchor the homogeneous catalyst to the resin via sulfonamide formation.

Our first attempt involved the transformation of the bromide into a cyano group, that would later be reduced to the amine. Thus, as shown in Scheme 2.10, our synthetic sequence began with the mono-protection of BINOL with pivaloyl chloride, followed by regioselective bromination in 6-position and deprotection in basic media. After that, protection of both hydroxy groups as

methyl ethers was carried out, bearing in mind the introduction of substituents in the 3,3'-position to be performed later.

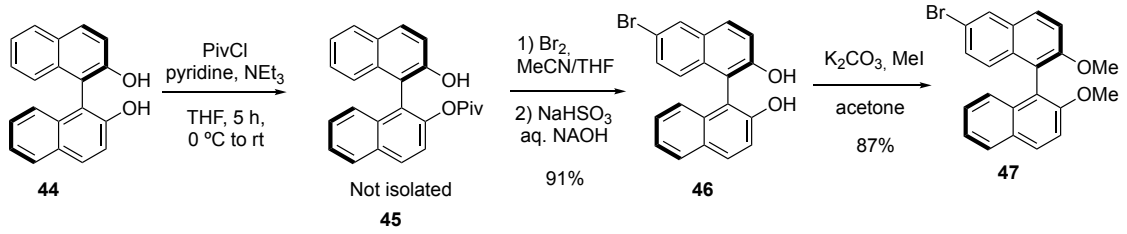

Scheme 2.10: Synthesis of brominated BINOL **47**.

The next step was the cyanation of BINOL-derived bromide **48**, which took place with CuCN. However, functionalization in the 3,3'-positions proved unsuccessful; even if we tried both bromination and iodination, we could not obtain the desired product. Two different conditions were tested for the bromination, and in both cases starting material was recovered. In the case of iodination, traces of mono-iodination product were found (Scheme 2.11).

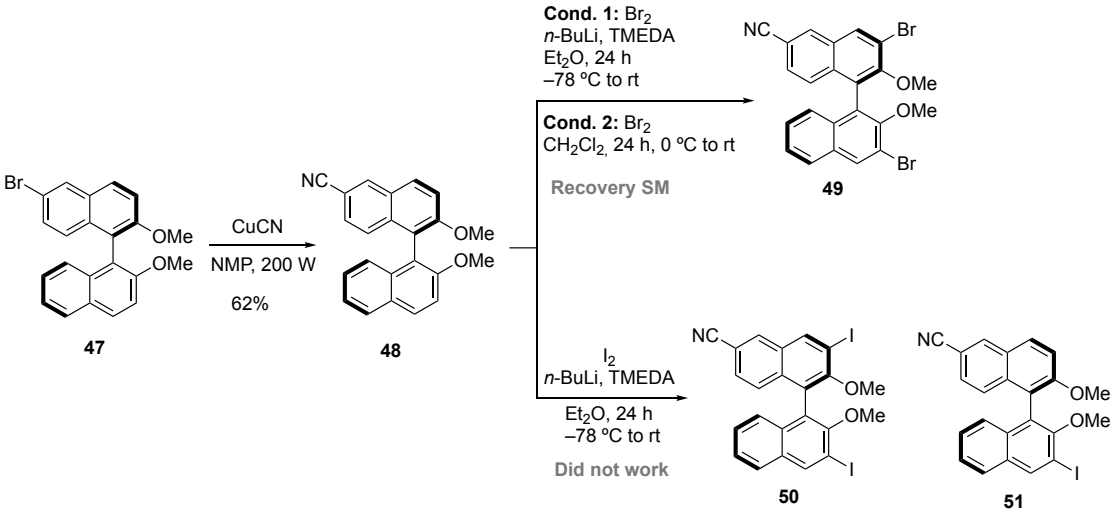

Scheme 2.11: Conditions attempted in the bromination and iodination of **48**.

After these results, we decided to reduce first the cyano group to the amine and then carry out the bromination step (Scheme 2.12). Unfortunately, it was not possible to identify the desired product **52** in the NMR spectra of the reaction crude the resulting aromatic signals being inconclusive.

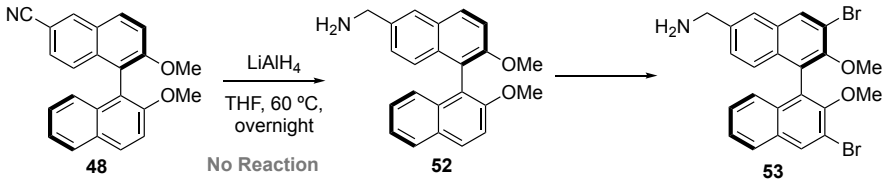

Scheme 2.12: Strategy for 3,3'-bromination via reduction of the cyano group.

Next, we turned our attention to an alternative functional group to replace the nitrile, but keeping in mind the incorporation of a nitrogenated group in order to anchor to the resin (Scheme 2.13). An interesting approach was based on the work of Trost, where imidazolidinones were efficiently converted to diamines in two sequential steps: treatment with $LiAlH_4$, followed by the addition of $H_2NOH{\cdot}HCl$. The introduction of the imidazolidinone group took place in 60% yield **54**, but the attempted bromination resulted in the recovery of starting material (Scheme 2.13, eq. 1). Then, we tried the direct amination of the bromoarene catalyzed by nickel (Scheme 2.13, eq. 2), but starting material was recovered. An alternative approach to introduce a nitrogen atom was the direct nitration of the brominated BINOL **47**, which resulted in no reactivity (Scheme 2.13, eq. 3).

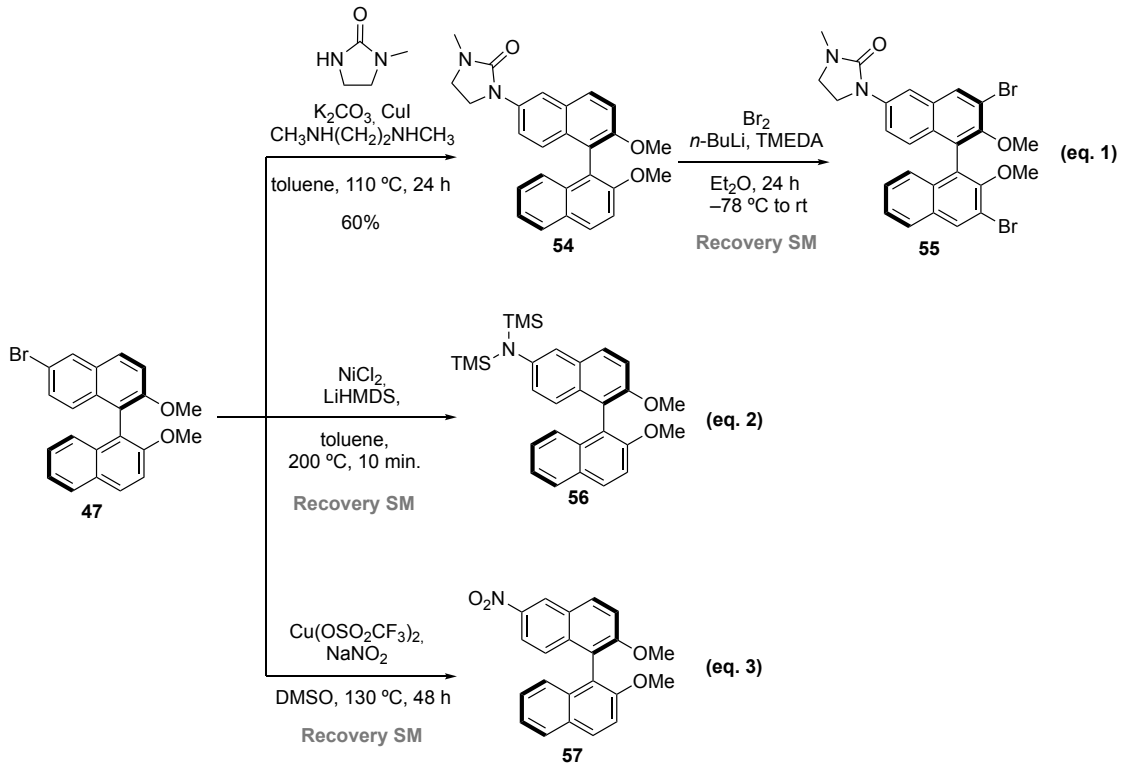

Scheme 2.13: Attempted amination of bromide **47**.

At that point, we postulated that 6-nitration of the BINOL moiety can be achieved without the previous bromination step (**47**). With that idea in mind, we focused our attention in the pathway depicted in Scheme 2.14.

This strategy started with the monoprotection of BINOL as a bulky pivalate ester. Treatment with conc. HNO_3 and H_2SO_4 acids resulted in the desired nitration product **58** in 85% overall yield. The deprotection of the pivalate was carried out under basic conditions, followed by double methylation of the hydroxyl groups to furnish **57**. Unfortunately, the selective bromination in 3,3'-positions was difficult and the formation of compound **60** did not proceed as we expected. A complex mixture was obtained according to NMR, where the desired product was not appreciated.

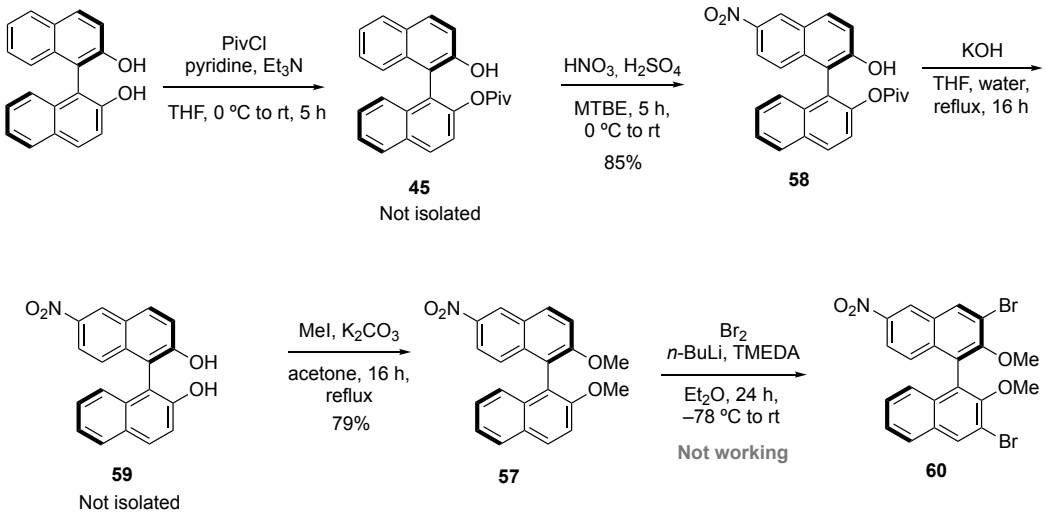

Scheme 2.14: Nitration in BINOL's 6-position.

Remarkably, the main problem associated to the previous syntheses took place in the bromination step after the 6-functionalization. This led us to conclude that it might be worth inverting the order of the steps. In short, we decided to proceed first with the 3,3'-bromination, which would allow to convert the bromo into the desired bulky group (in our case the *tri*-isopropylphenyl group) through a Ni-catalyzed Kumada cross-coupling to obtain **63**. Hopefully, 6-amino functionalization can be accomplished to provide target precursor (**62**) to execute the immobilization onto sulfonyl chloride resin. Then, the desired heterogeneous catalyst **61** would be obtained via phosphorylation of the resulting polymer, previously formed through a sulfonamide linker through the 6-amino group in the BINOL (Scheme 2.15).

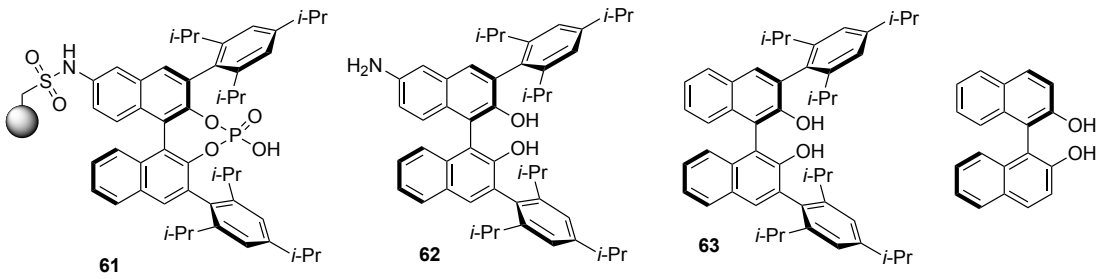

Scheme 2.15: Alternative strategy for anchoring via sulfonamide.

The steps followed for the target (*R*)-BINOL TRIP **63**, are summarized in Scheme 2.16. This approach began with the commercially available (*R*)-BINOL, that was protected by methylation with MeI to obtain **64** in 96% yield. Bromination of **64** afforded **65** brominated in the 3,3'-positions, in moderate yield. In order to install the desired bulky substituents, Kumada cross-coupling between **65** and the corresponding Grignard reagent (generated *in situ*) followed by deprotection of the hydroxy groups with BBr_3 was carried out to afford **63**. This sequence is the same previously described by List *et al*. for the preparation of homogeneous TRIP.[42]

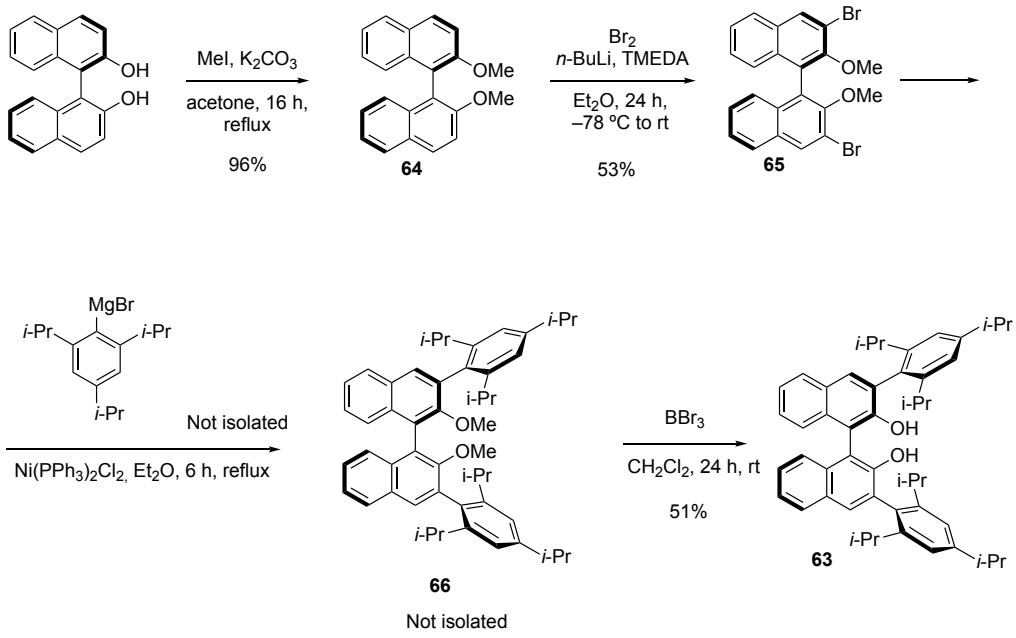

Scheme 2.16: Synthesis of (*R*)-BINOL TRIP.

Different possible pathways were explored in order to find the appropriate linker between the BINOL scaffold and the resin. In line with our previous strategy to introduce a cyano group in the 6-position, we proceeded with the synthesis shown in the Scheme 2.17. Dibromination of **63** gave **64** in moderate yield. The next step was the double cyanation under the conditions established in the previous syntheses, which furnished **65** in low yield. Unexpectedly, the treatment of **65** with $LiAlH_4$ resulted mainly in the recovery of the starting

material, however, we could appreciate traces of the final product. Then, we decided to increase the scale in order to facilitate purification of the desired product by recrystallization. Even if the starting material could be identified by NMR, another unidentified product was also present. We purified the product by column chromatography, and the NMR of the isolated product was unclear. Analysis by MS and IR showed that the desired product was not formed. Then, we moved to an alternative reduction procedure using Ni-Raney/H_2 in MeOH. Unfortunately, the NMR was quite complex showing mostly recovered **65**, whereas no peak related with the desired methylene groups was detected.

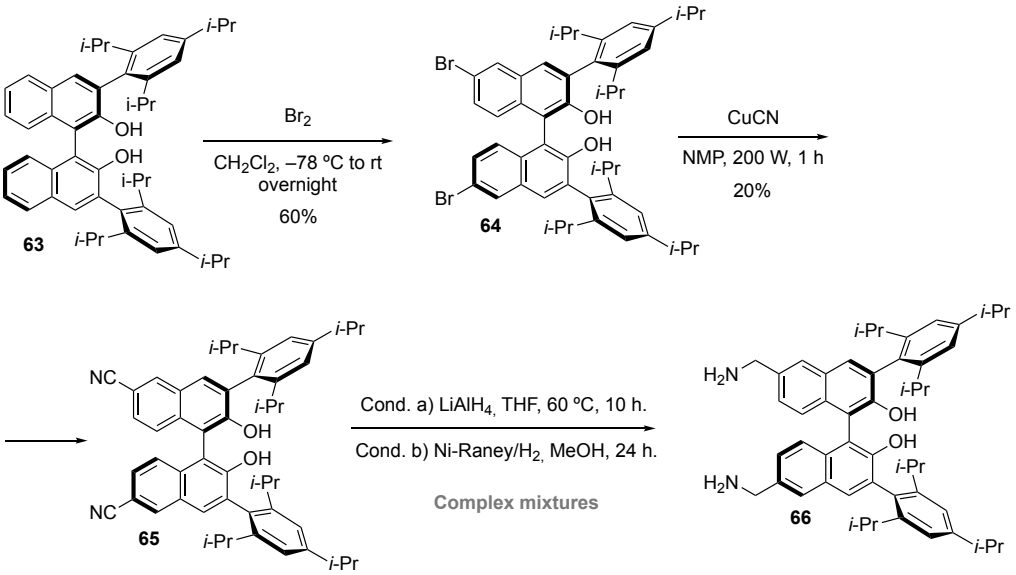

Scheme 2.17: Double aminomethylation of the BINOL **63** via dicyanide.

At this point, we envisioned that dibrominated BINOL derivative **64** could also undergo cross-coupling with alkynes, alkyl groups or aryl amines. The conditions tested along these lines are summarized in Table 2.3. We firstly considered the Sonogashira coupling of **64** with a propargylic amine, but this resulted in recovery of starting material (Table 2.3, entry 1). We postulated that benzylamines might also be interesting substrates, so different conditions based on Cu catalysis were tried (Table 2.3, entry 2-4). While under copper at

100 ºC (Table 2.3, entry 2) we observed mostly starting material, more reactivity was observed using CuI and CuO under the conditions in entries 3 and 4 of Table 2.3. In both cases, we could isolate a product in which the integration of NMR spectra seemed to match our desired product, but the product isolated for each reaction was not the same.

Table 2.3: Cross-coupling between **64** and alkyl or aryl amines.

Starting Material	Entry	Substrate	Conditions	Expected Compound
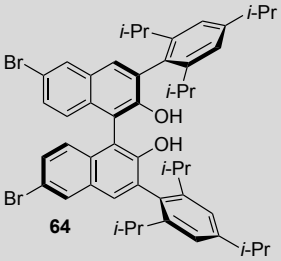 **64**	1	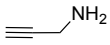	CuI, Et_3N $PdCl_2(PPh_3)_2$ 50 ºC, 24 h	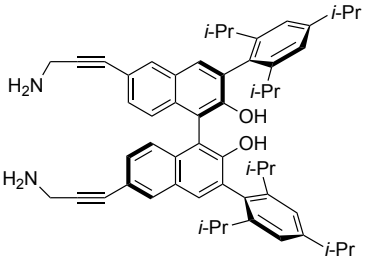
	2	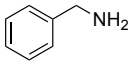	Cu, 100 ºC	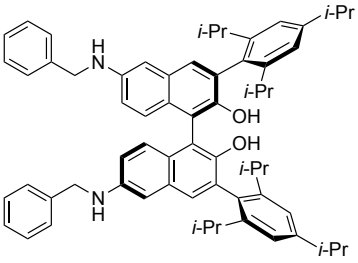
	3	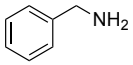	proline, Cs_2CO_3, CuI, MeCN, reflux, 24 h	
	4	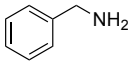	Cu_2O, NMP, 80 ºC, 24 h	
	5	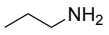	Cu_2O, NMP, 200 ºC, 24 h	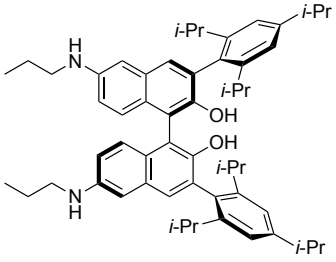
	6	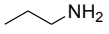	proline, Cs_2CO_3, CuI, MeCN, reflux, 24 h	

In both cases, MS analysis was carried out and the results corroborated that the final compound had not been obtained. Next, using the same conditions with which we had obtained reactivity, we tested more nucleophilic aliphatic amines (Table 2.3, entry 5-6), but starting material was recovered in all cases.

Given our previous success in the nitration of BINOL (Scheme 2.14), we were encouraged to pursue another nitration-based strategy (Scheme 2.18, 1st strategy). Therefore, we proceeded with the mono-protection of **63** with pivaloyl chloride. Treatment of **67** with HNO_3 and H_2SO_4, resulted in nitration at the BINOL 6-position but, unexpectedly, the deprotection of **68** in strong basic media (KOH, MeLi, or *t*-BuOK) was not achieved.

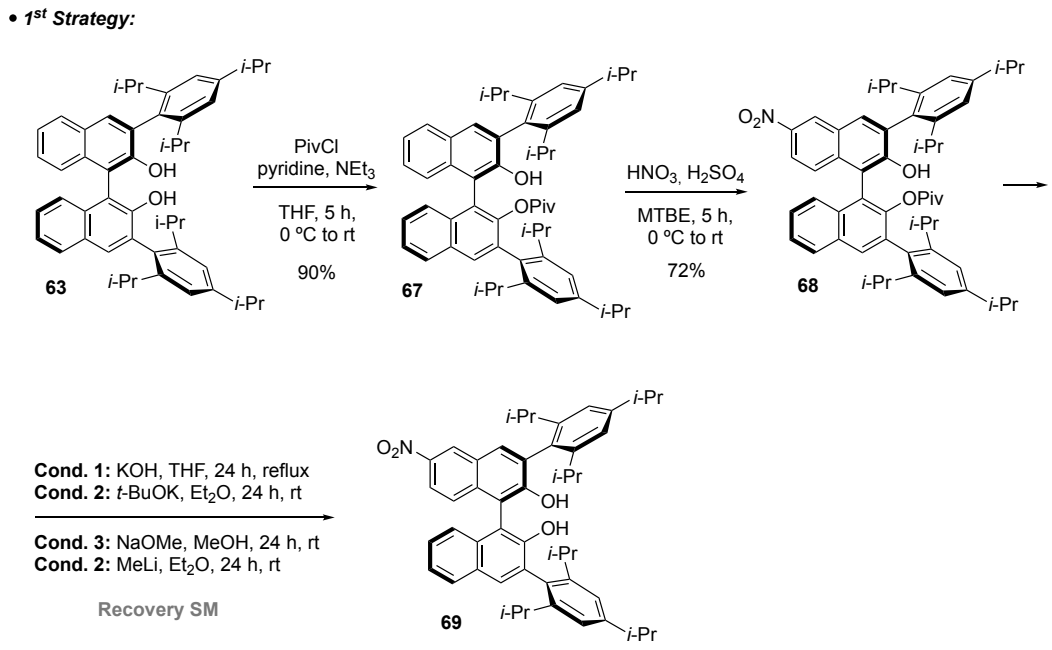

Scheme 2.18: Sequence of reactions for 6-nitration employing pivalate ester as mono protecting group.

At this point, in an attempt to employ a less hindered protecting group, we decided to introduce an acetate group (Scheme 2.19, 2nd strategy). Compound **70** was obtained in 80% yield. Subsequently, nitration of **70,** followed by deprotection under basic media resulted in the desired **62** bearing a nitro group in C_6. After a survey of conditions for the reduction of the nitro to

amine, we found that $SnCl_2 \cdot H_2O$ gave the final product with a 60% yield. Previous experiments involved attempts to reduce the nitro with: Pd/C, H_2, 3.5 bar 5 h; Pd/C with formic acid; Mg with formic acid and hydrazine; Zn with formic acid and finally we also tested $NaBH_4$, in MeOH or EtOH. With **62** in hand, we proceeded to anchor the monomer onto the resin via nucleophilic substitution of **62** with commercially available sulfonyl chloride cross-linked polystyrene resin. In order to ensure maximum functionalization of the final resin, we treated the resin with 2 equivalents of monomer and the reaction was kept for 24 h. Then, the resin was washed with HCl, water and CH_2Cl_2. Finally, the resulting supported catalyst was analysed by IR (paying special attention to the characteristic absorption of the S=O bond from sulfonamide formation) as well as elemental analysis. Regarding the IR, we could appreciate the appearance of peaks at 1362 and 1153 cm^{-1}. On the other hand, elemental analysis of nitrogen displayed the maximum functionalization: while the calculated $f_{(Max)}$ had a value of nitrogen equal to 0.8 $mmol/g_{resin}$ we found that the values obtained from elemental analysis were $f_{(N)}$: 0.76 $mmol/g_{resin}$. However, we also analyzed the presence of remaining chlorine by elemental analysis. Unexpectedly, the results showed 0.7% of Cl. On the basis of these results, we concluded that the connection between resin and monomer had taken place. To complete the synthesis, we proceeded to phosphorylate **73** using the same conditions than homogeneous CPA to generate the desired resin **74**. The result from elemental analysis of nitrogen of catalyst **74** was $f_{(N)}$: 0.78 $mmol/g_{resin}$, being the same than precursor **73**. However, the functionalization of P was considerably low ($f_{(P)}$: 0.48 $mmol/g_{resin}$). Even if longer reaction times (24 h or 48 h) and an increase of the amounts of $POCl_3$ equivalent (3 or 10 equivalents) were evaluated, we could not obtain a better functionalization. This fact was also observed in the previous supported CPA developed in our group,[51] so we decided to test in catalysis.

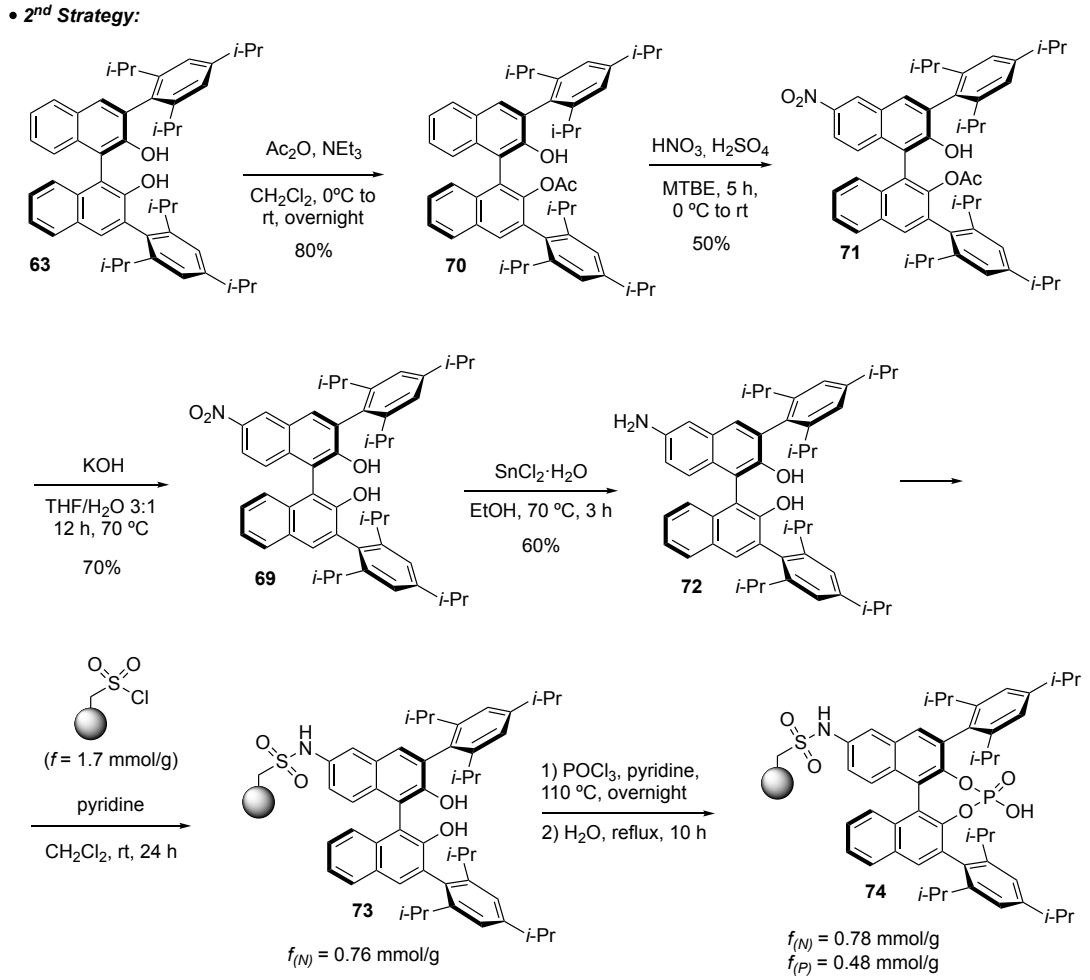

Scheme 2.19: Strategy for PS-TRIP synthesis via sulfonamide linker toward 6-amino functionalization from compound **63** and employing acetate ester as mono protecting group.

After searching the literature, we found the semipinacol rearrangement, reported by the group of Tu in 2009,[44g] an ideal transformation to test our supported TRIP due to the spiroethers generated. The homogeneous TRIP reported in the literature showed high activity and selectivity. Furthermore, the intermediates generated are versatile structural motifs present in a variety of biologically significant natural products. In the Scheme 2.20, we compared the results of heterogeneous catalyst **(*R*)-PS-74** with its counterpart homogeneous catalyst **(*R*)-33**. Unfortunately, despite achieving full conversion of the desired product in the semipinacol rearrangement catalyzed by our **PS-TRIP 74**, the reaction was not enantioselective, thus giving the product in a racemic manner.

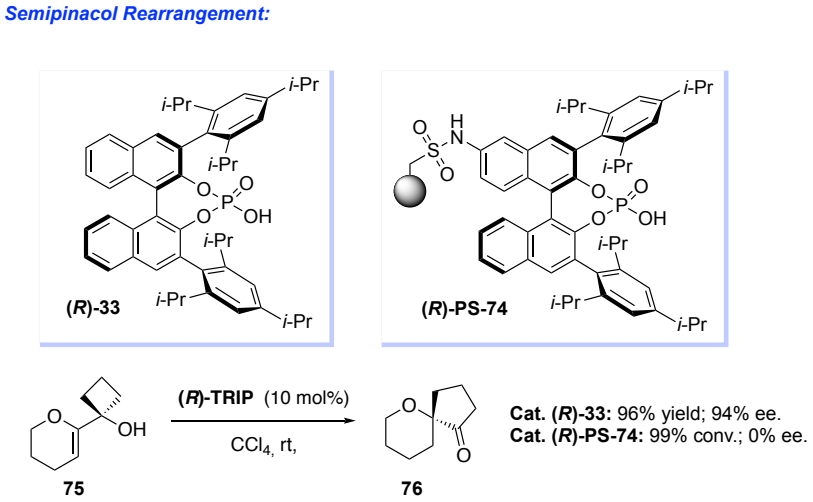

Scheme 2.20: Semipinacol rearrangement catalyzed by homogeneous TRIP and supported TRIP via sulfonamide linker.

After these disappointing results, we considered that the synthesis via sulfonamide was not a viable strategy. The fact that not even low ee was identified led us to abandon this strategy. At this moment, we decided to turn our attention to an alternative strategy for immobilization of CPAs. Previously in our group, appealing strategies have been described where homogeneous organocatalysts were immobilized via co-polymerization from styrene moieties providing excellent results.[52] In this perspective, compound **64** (Scheme 2.21) can undergo Suzuki coupling to introduce a styrene moiety in the BINOL scaffold. Indeed, precursor **77**, containing two styrene groups, was isolated in 70% yield. Then, it was submitted to the conditions optimized in our group for the co-polymerization[52b] (Scheme 2.21, 1st Strategy). Gratifyingly, the established conditions also worked with this BINOL derivative, thus forming **78**. Finally, we phosphorylated the supported BINOL to build the target **79**. However, we encountered some reproducibility issues that led to poor ee when **(*R*)-PS-TRIP 79** catalyzed the semipinacol rearrangement (Scheme 2.22).

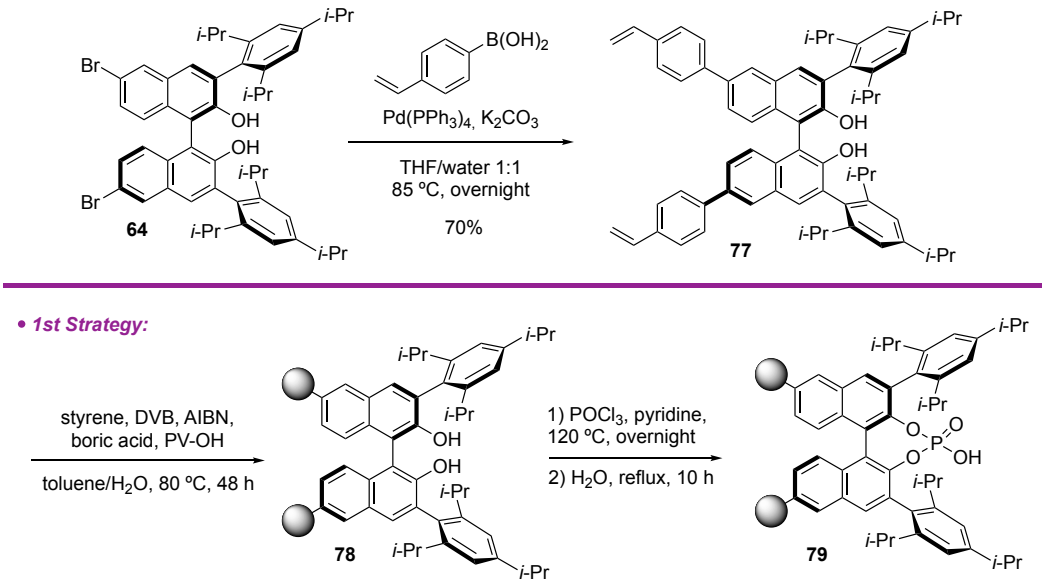

Scheme 2.21: Synthetic strategy: 1) co-polymerization of styrene moiety in 6,6'-position and 2) phosphorylation.

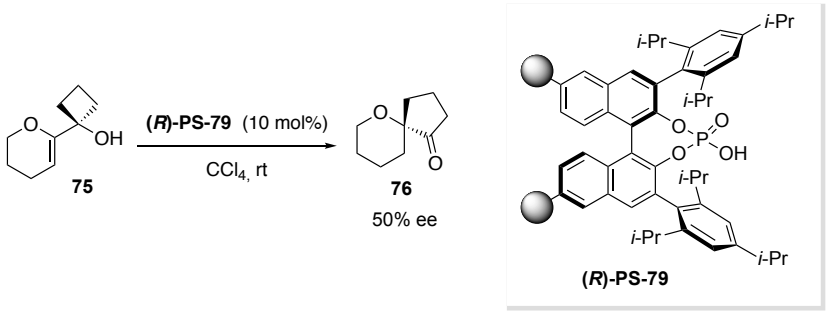

Scheme 2.22: Semipinacol rearrangement catalyzed by **(*R*)-PS-TRIP**.

We decided to carry out further exploration in the conditions for polymerization. To our delight, the Schrock group reported a new polymer-supported chiral Mo-based complex for enantioselective olefin methatesis,[53] the asymmetric induction is possible owing to the presence of a chiral binaphtyl. In order to develop their catalyst, they polymerized our common precursor **77** using benzoyl peroxide as radical initiator and styrene and DVB as cross linker, but in comparison, the hydroxy groups were protected as methyl ethers. We thought it would be interesting to avoid post-polymerization reactions, so we moved to the 2nd strategy depicted in Scheme 2.23, reversing the steps of the 1st strategy. Initial phosphorylation first of **77**

would allow to control the complete formation of the phosphoric acid and not have the hydroxy groups free. To our satisfaction, target **80** was isolated in 75% yield and this proceeded to the final supported **(*R*)-PS-TRIP 79**. The heterogeneous catalyst **(*R*)-PS-TRIP 79** obtained following the second strategy was tested in catalysis.

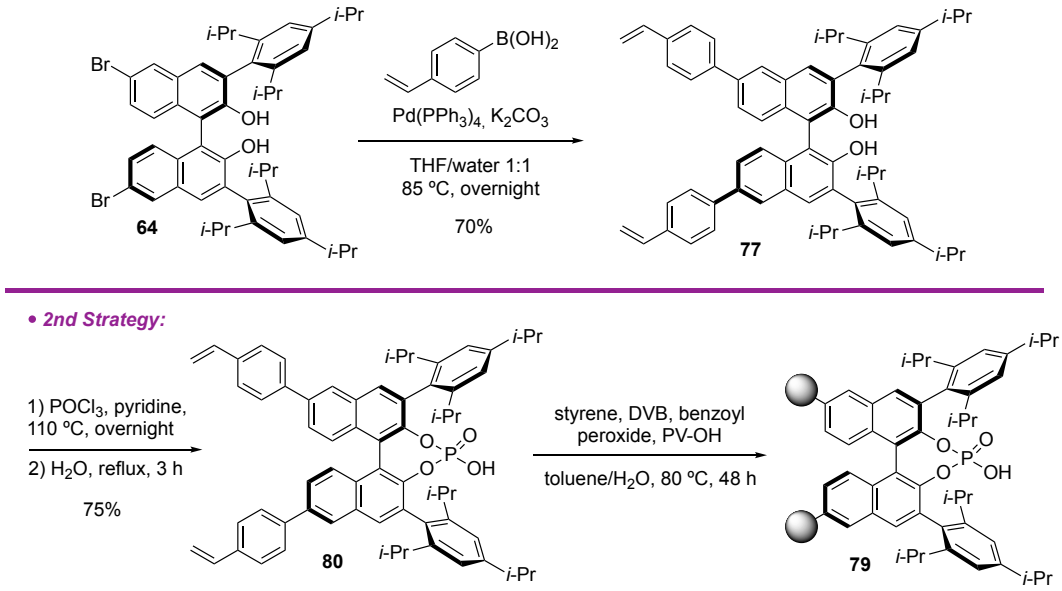

Scheme 2.23: Synthetic strategy: 1) phosphorylation of **77** and 2) co-polymerization of styrene moiety in 6,6'-position.

Then, we postulated that maybe we can test the activity of our supported catalysts from both batches 1st strategy and 2nd strategy (Scheme 2.22 and 2.3), in alternative reactions. Therefore, we decided to test **(*R*)-PS-79** in the allylation of aldehydes reported by Antilla *et al.*[54] We achieved to apply our **(*R*)-PS-79** in this asymmetric transformation giving excellent results and proving high activity (Scheme 2.24). This transformation will be discussed in more detail in the next Chapter III.

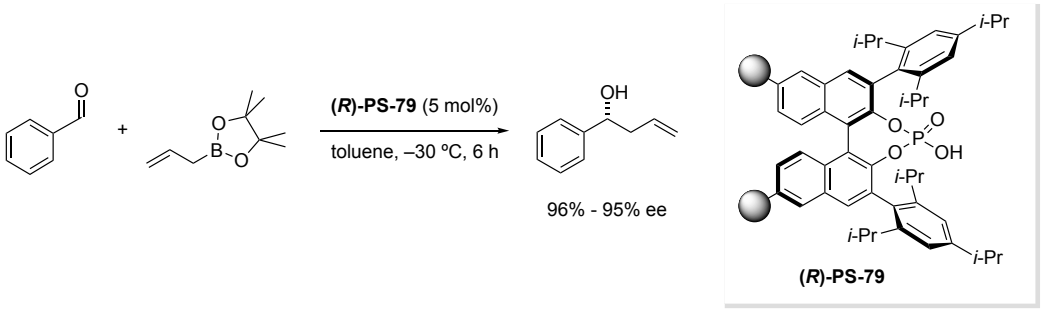

Scheme 2.24: Allylation of benzaldehyde catalyzed by **(*R*)-PS-79**.

2.4. Conclusions

To sum up, in this chapter, we have described a method for the immobilization onto polystyrene of the widely applicable TRIP phosphoric acid catalyst using a copolymerization-based strategy.

Note that the described synthetic route, which involves the copolymerization of a vinylated analogue of the TRIP diol, only requires three more steps than that of the homogeneous counterpart. We have developed a simple and effective strategy without compromising the excellent catalytic activity and enantioselectivity displayed by the monomer. Furthermore, it can be scaled up to multigram production.

Despite our initial interest in the incorporation of a nitrogen atom to determine the functionalization, the current strategy is even more effective, as it involves less steps, and the polymerization process increases considerable the mass in the last step (Scheme 2.25). Finally, the polymer-supported phosphoric acid has been applied to the enantioselective allylation of aldehydes.

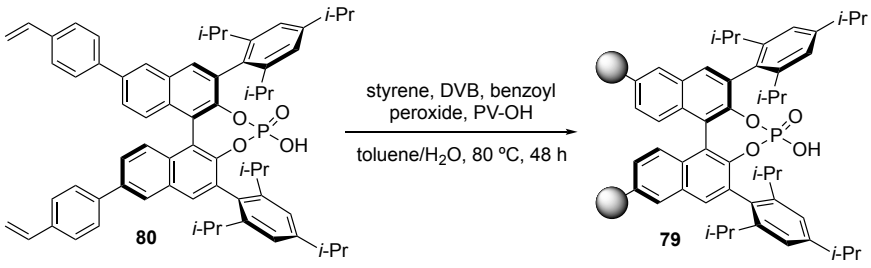

Scheme 2.25: Final strategy for immobilization of TRIP derivative.

2.5. Experimental Procedures and Characterization of Compounds

2.5.1. General Remarks

Thin layer chromatography was performed on Merck TLC Silicagel 60 F254 aluminum sheets. Components were visualized by UV light (λ = 254 nm) and stained with *p*-anisaldehyde or phosphomolybdic dip. Flash column chromatography was carried out using Sigma-Aldrich 60 mesh silica gel and dry-packed columns. ^{1}H NMR and ^{13}C NMR spectra were recorded at 298 K on a Bruker Avance 500 or 400 Ultrashield apparatus. ^{1}H NMR spectroscopy chemical shifts are quoted in ppm relative to tetramethylsilane (TMS). $CDCl_3$ was used as internal standard for ^{13}C NMR spectra. Chemical shifts are given in δ and coupling constants in Hz. IR spectra were recorded on a Bruker Tensor 27 FT-IR spectrometer and are reported in wavenumbers (cm^{-1}). Elemental analyses were performed by MEDAC Ltd. (Surrey, UK) on a LECO CHNS 932 micro-analyzer. High performance liquid chromatography (HPLC) was performed on Agilent Technologies chromatographs (1100 and 1200 Series). High resolution mass spectrometry analyses were performed in a Waters LCD Premier™ instrument operating in ESI (Electro-Spray Ionization) mode or APCI (Atmospheric-Pressure Chemical Ionization) mode. Specific optical rotation measurements were carried out on a Jasco P-1030 polarimeter.

2.5.2. Characterization of the Intermediates Generated for the Synthesis of PS-CPA

6-Bromo-[1,1'-binaphthalene]-2,2'-diol (46)[55]

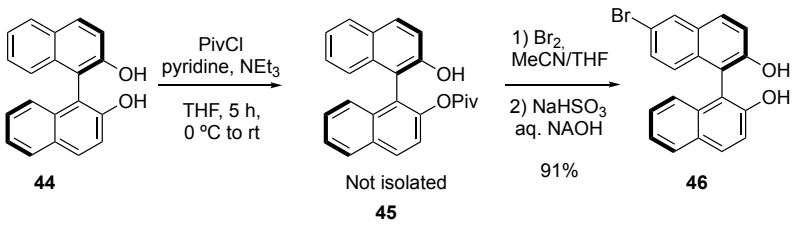

44 Not isolated **45** **46**

A 500 mL round-bottom flask was charged with a solution of (*R*)-BINOL (25 g, 87 mmol) in THF (218 mL). The solution was cooled to 0 ºC, and trimethylamine (17.04 mL, 122 mmol), pyridine (0.176 mL, 2.183 mmol) and pivaloyl chloride (11.83 mL, 96 mmol) were added dropwise. The solution was allowed to warm to rt and stirred for 5 hours. The resulting mixture was diluted with ether and washed with aqueous 1 N HCl, sat. $NaHCO_3$ and brine. The organic layer was dried over Na_2SO_4 and concentrated under reduced pressure. BINOL derivative **45** was used without further purification.

To a solution of **45** (32 g, 87 mmol) in MeCN (174 mL) and toluene (174 mL) was added bromine at 0 ºC dropwise via addition funnel. Then the reaction mixture was allowed to warm to rt. After 6 hours under stirring, $NaHSO_3$ and NaOH (150 mL, 6 N) was added to the solution and left under stirring for a further 16 hours. The reaction mixture was acidified with 3 N HCl until pH = 1, then extracted with EtOAc. The organic layer was washed with brine, separated and concentrated under reduced pressure. The crude was dissolved in DCM and washed with Na_2CO_3 (×3). The combined organic layers were dried over anhydrous $MgSO_4$ and concentrated under reduced pressure. The crude product was purified by flash column chromatography on silica gel using cyclohexane/EtOAc (70:30) as the eluent to give the diol **46** (29 g, 0.79 mmol)

in 91% overall yield as a slightly yellow solid. **^{1}H NMR** (500 MHz, $CDCl_3$) δ 8.05 (d, *J* = 2.0 Hz, 1H), 7.98 (d, *J* = 8.9 Hz, 1H), 7.89 (t, *J* = 8.5 Hz, 2H), 7.42 – 7.35 (m, 4H), 7.32 (ddd, *J* = 8.3, 6.8, 1.4 Hz, 1H), 7.10 (d, *J* = 8.3 Hz, 1H), 7.02 (d, *J* = 8.8 Hz, 1H), 5.09 (s, 1H), 4.99 (s, 1H). **^{13}C NMR** (126 MHz, $CDCl_3$) δ 153.2, 152.9, 133.4, 132.2, 131.9, 130.8, 130.7, 130.6, 130.5, 129.6, 128.6, 127.8, 126.3, 124.3, 124.2, 119.1, 118.0, 117.9, 111.4, 110.4.

6-Bromo-2,2'-dimethoxy-1,1'-binaphthalene (47)[56]

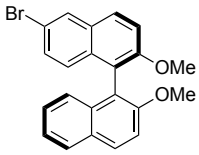

A three-necked round-bottom flask containing **46** (12.6 g, 34.4 mmol) was equipped with a magnetic stirring bar, an addition funnel, a reflux condenser and a glass stopper. The system was evacuated and flushed with argon. Subsequently, the vessel was charged with dry acetonitrile (316 mL) and potassium carbonate (15.68 g, 113 mmol). Then iodomethane (8.56 mL, 138 mmol) was added dropwise. The resulting mixture was heated to reflux in an oil bath for 24 h. After that time, the reaction was cooled to rt and the volatile compounds were removed under reduced pressure. The resulting slurry was re-dissolved in water and stirred for a further 2 h. The resulting solid was collected on a funnel, washed with water and dried under vacuum. The crude was subjected to flash column chromatography with hexane/CH_2Cl_2 (3:2) to isolate **47** in 87% yield. **^{1}H NMR** (500 MHz, $CDCl_3$) δ 8.02 (d, *J* = 2.0 Hz, 1H), 7.98 (dd, *J* = 9.1, 0.8 Hz, 1H), 7.90 – 7.85 (m, 2H), 7.46 (m, 2H), 7.32 (ddd, *J* = 8.1, 6.7, 1.2 Hz, 1H), 7.28 – 7.20 (m, 2H), 7.06 (d, *J* = 8.5 Hz, 1H), 6.98 (d, *J* = 9.1 Hz, 1H), 3.76 (d, *J* = 2.7 Hz, 6H). **^{13}C NMR** (126 MHz, $CDCl_3$) δ 155.4, 155.1, 134.0, 132.7, 130.4, 130.0, 129.8, 129.7, 129.3, 128.6, 128.2, 127.3, 126.6, 125.1, 123.8, 120.0, 119.0, 117.5, 115.3, 114.2, 57.0, 57.0. **$[\alpha]_D$**: +38.2.

2,2'-Dimethoxy-[1,1'-binaphthalene]-6-carbonitrile (48)

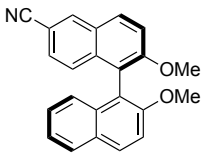

A mixture of **47** (500 mg, 1.27 mmol), CuCN (148 mg, 1.65 mmol), and NMP (1271 μL) as solvent was subjected to microwave irradiation (200 W). After 30 min. of irradiation, the mixture was cooled to room temperature and diluted with water. The precipitates were collected by filtration and treated with aqueous ammonia. After removal of the solvents, the product was further purified by recrystallization from aqueous ethanol to obtain **48** in 62% yield. **^{1}H NMR** (300 MHz, $CDCl_3$) δ 8.26 (d, *J* = 1.7 Hz, 1H), 8.07 – 7.98 (m, 2H), 7.88 (d, *J* = 8.2 Hz, 1H), 7.56 (d, *J* = 9.1 Hz, 1H), 7.46 (d, *J* = 9.1 Hz, 1H), 7.38 – 7.29 (m, 2H), 7.25 – 7.20 (m, 1H), 7.20 – 7.14 (m, 1H), 7.05 – 6.98 (m, 1H), 3.81 (s, 3H), 3.77 (s, 3H). **^{13}C NMR** (126 MHz, $CDCl_3$) δ 157.5, 155.0, 135.7, 134.5, 133.8, 130.3, 130.1, 129.3, 128.3, 128.0, 126.8, 126.8, 126.6, 124.8, 123.8, 120.0, 119.8, 118.1, 115.4, 114.0, 106.8, 56.8, 56.7. **IR** (ATR): v 2932, 2224, 1739, 1617, 1590, 1462, 1347, 1250, 1094, 1060, 1044, 805, 780. cm^{-1}. **HRMS** (ESI+): *m/z* calcd. for $C_{23}H_{17}NNaO_2$ $[M+Na]^+$: 362.1151, found: 362.1166. **mp**: 220 – 225 °C. **$[\alpha]_D$**: +53.0 (*c* 1.00, CH_2Cl_2).

1-(2,2'-Dimethoxy-[1,1'-binaphthalen]-6-yl)-3-methylimidazolidin-2-one (54)

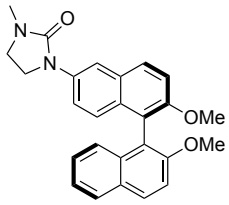

A Schlenk tube was charged with **48** (300 mg, 0.76 mmol), 1-methylimidazolidin-2-one[57] (99 mg, 0.99 mmol), K_2CO_3 (211 mg, 1.53 mmol) and CuI (14.53 mg, 0.08 mmol). To the mixture was added toluene (509 μL) and *N,N'*-dimethylethylenediamine (16.0 μL, 0.15 mmol). The mixture was sealed and heated at 110 ºC for 24 h. After cooling to room temperature, the mixture was diluted with EtOAc and washed with water and brine. The organic fraction was

dried over Na_2SO_4 and concentrated under reduced pressure. The crude was subjected to flash column chromatography with hexane/CH_2Cl_2 (60:40) to afford **54** in 60% yield. **^{1}H NMR** (500 MHz, $CDCl_3$) δ 7.97 (d, *J* = 9.0 Hz, 1H), 7.89 (d, *J* = 9.1 Hz, 1H), 7.86 (d, *J* = 8.2 Hz, 1H), 7.77 (d, *J* = 2.3 Hz, 1H), 7.69 (dd, *J* = 9.3, 2.3 Hz, 1H), 7.44 (dd, *J* = 12.1, 9.0 Hz, 2H), 7.31 (ddd, *J* = 8.1, 6.7, 1.2 Hz, 1H), 7.21 (ddd, *J* = 8.2, 6.7, 1.3 Hz, 1H), 7.13 – 7.10 (m, 1H), 7.08 (d, *J* = 9.3 Hz, 1H), 3.85 (t, *J* = 8.0 Hz, 2H), 3.76 (s, 3H), 3.73 (s, 3H), 3.45 (t, *J* = 7.3 Hz, 2H), 2.89 (s, 3H). **^{13}C NMR** (126 MHz, $CDCl_3$) δ 158.5, 155.1, 154.2, 136.7, 134.2, 130.3, 129.7, 129.5, 129.3, 128.8, 128.0, 126.4, 126.1, 125.4, 123.6, 119.8, 119.7, 119.2, 115.2, 114.4, 113.8, 57.2, 57.0, 44.4, 42.8, 31.4. **HRMS** (ESI+): *m/z* calcd. for $C_{26}H_{25}N_2O_3$ $[M+H]^+$: 413.1860, found: 413.1855. **mp**: > 200 °C decompose.

2'-Hydroxy-6'-nitro-[1,1'-binaphthalen]-2-yl pivalate (58)[58]

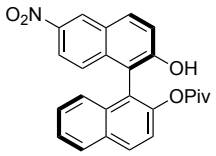

A solution of **45** (12 g, 32.4 mmol) in MTBE (45 ml) was added dropwise to a mixture of conc. HNO_3 (25 mL, 40 mmol), MTBE (45 mL) and conc. H_2SO_4 (10 mL, 40 mmol) at 0 °C. The color of the reaction mixture turned yellow and then green. The reaction mixture was warmed to rt and stirred for 5 h at rt. Once the reaction was finished, diethyl ether was added and the organic phase was washed with 100 ml of water (×4). The crude was purified by recrystallization in cyclohexane to obtain 85% yield of **58**. **^{1}H NMR** (400 MHz, $CDCl_3$) δ 8.81 (d, *J* = 2.4 Hz, 1H), 8.13 (d, *J* = 8.6 Hz, 1H), 8.08 (d, *J* = 8.8 Hz, 1H), 8.04 – 7.99 (m, 2H), 7.55 (ddd, *J* = 8.2, 6.8, 1.2 Hz, 1H), 7.47 (d, *J* = 9.0 Hz, 1H), 7.43 – 7.35 (m, 2H), 7.25 – 7.21 (m, 1H), 7.17 (dt, *J* = 9.3, 0.7 Hz, 1H), 5.52 (s, 1H), 0.81 (s, 9H).

2,2'-Dimethoxy-6-nitro-1,1'-binaphthalene (57)[59]

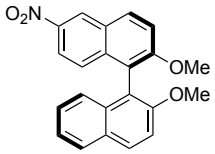

A two-necked round-bottom flask with a magnetic stirring bar, an addition funnel and a reflux condenser with argon inlet and a glass stopper was charged with **59** (10.4 g, 31.4 mmol) and dry acetone (288 mL). Subsequently, upon complete solution of the prior compound, K_2CO_3 (14.3 g, 104 mmol) was added, followed by MeI (7.82 mL, 126 mmol). The resulting mixture was heated to reflux in an oil bath overnight. After that time, the volatile compounds were removed under reduced pressure. The resulting slurry was redissolved in water and stirred for 2 h. The resulting solid was collected on a funnel, washed with water and dried in vacuum. The crude was purified by recrystallization in cyclohexane to obtain **57** as a brownish solid in 79% yield. **^{1}H NMR** (500 MHz, $CDCl_3$) δ 8.85 (d, *J* = 2.4 Hz, 1H), 8.17 (d, *J* = 8.8 Hz, 1H), 8.02 (d, *J* = 8.3 Hz, 1H), 7.96 (dd, *J* = 9.3, 2.4 Hz, 1H), 7.90 (d, *J* = 8.2 Hz, 1H), 7.59 (d, *J* = 9.1 Hz, 1H), 7.47 (d, *J* = 9.0 Hz, 1H), 7.35 (ddd, *J* = 8.1, 6.7, 1.2 Hz, 1H), 7.26 – 7.18 (m, 2H), 7.06 – 7.01 (m, 1H), 3.83 (s, 3H), 3.78 (s, 3H). **^{13}C NMR** (126 MHz, $CDCl_3$) δ 158.2, 155.0, 143.8, 137.0, 133.8, 132.0, 130.2, 129.3, 128.3, 127.3, 126.9 (×2), 126.8 (×2), 125.3, 124.7, 123.8, 119.8, 115.6, 114.0, 56.8, 56.7.

2,2'-Dimethoxy-1,1'-binaphthalene (64)[42]

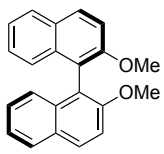

A two-necked round-bottom flask containing (*R*)-BINOL (15 g, 52.4 mmol) is equipped with a magnetic stirring bar, an addition funnel, and a reflux condenser with argon inlet and a glass stopper. The flask was evacuated and flushed with argon three times. Subsequently, the vessel was charged with dry acetone (481 mL). Upon complete dissolution of the prior compound, K_2CO_3 (23.9 g, 173 mmol) was added followed by MeI (13.1 mL, 210 mmol). The resulting mixture was

heated to reflux in an oil bath overnight. After that time, the volatile compounds were removed under reduced pressure. The resulting slurry was redissolved in water and stirred for a further 2 h. The resulting solid was collected on a funnel, washed with water and dried in vacuum (95 ºC, $3.0 \cdot 10^{-2}$ mbar) furnishing **64** in 96% yield as a slight yellow solid. **^{1}H NMR** (400 MHz, $CDCl_3$) δ 7.99 – 7.96 (m, 1H), 7.90 – 7.83 (m, 2H), 7.46 (d, *J* = 9.0 Hz, 2H), 7.31 (ddd, *J* = 8.1, 6.7, 1.3 Hz, 2H), 7.21 (ddd, *J* = 8.2, 6.7, 1.4 Hz, 2H), 7.11 (ddt, *J* = 8.5, 1.4, 0.8 Hz, 2H), 3.77 (s, 6H). **^{13}C NMR** (101 MHz, $CDCl_3$) δ 155.1 (×2), 134.2 (×2), 129.5 (×2), 129.4 (×2), 128.1 (×2), 126.4 (×2), 125.4 (×2), 123.7 (×2), 119.8 (×2), 114.4 (×2), 57.1 (×2).

3,3'-Dibromo-2,2'-dimethoxy-1,1'-binaphthalene (65)[42]

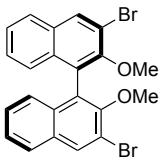

A two-necked round-bottom flask equipped with a magnetic stirring bar, an addition funnel, an argon inlet and a glass stopper was evacuated and flushed with argon. Subsequently, diethyl ether (350 mL) was added, followed by TMEDA (7.39 mL, 49.0 mmol). To the resulting solution, *n*-BuLi (31.2 mL, 78 mmol) was added slowly at rt via syringe and the mixture was allowed to stir 1 h. Then, **64** (7 g, 22.27 mmol) was added as a solid at rt and the resulting solution was stirred for a further 3.5 h. After this time, the reaction was cooled to –78 ºC and Br_2 (5.73 mL, 111 mmol) was added dropwise via the addition funnel. After addition was completed, the cooling bath was removed and the yellowish-brown reaction mixture was allowed to stir for 20 h at rt. The reaction was quenched with $NaSO_3$ sat. and stirred for 1 h. The mixture was extracted with Et_2O (×3), the organic phases were combined, washed with brine and dried over $MgSO_4$. After filtration, the solvents were removed in vacuum and the crude mixture was subjected to column chromatography eluting with hexane/EtOAc (99:1). Compound **65** was obtained in 53% yield as a slightly yellow solid.

^{1}H NMR (400 MHz, $CDCl_3$) δ 8.27 (s, 2H), 7.86 – 7.80 (m, 2H), 7.42 (ddd, *J* = 8.2, 6.8, 1.2 Hz, 2H), 7.31 – 7.23 (m, 2H), 7.12 – 7.04 (m, 2H), 3.51 (s, 6H). **^{13}C NMR** (101 MHz, $CDCl_3$) δ 152.7 (×2), 133.3 (×2), 133.2 (×2), 131.6 (×2), 127.3 (×2), 127.0 (×2), 126.7 (×2), 126.0 (×2), 125.9 (×2), 117.7 (×2), 61.3 (×2).

(3*S*)-3,3'-Bis(2,4,6-triisopropylphenyl)-[1,1'-binaphthalene]-2,2'-diol (63)[42]

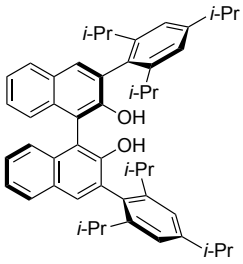

In a two-necked flask with magnetic stirrer, Ar-inlet and an addition funel, was added **65** (4 g, 5.56 mmol) and dry CH_2Cl_2 (132 mL). Subsequently, the solution was cooled with an ice bath to add slowly BBr_3 (1.0 M in methylene chloride, 38.9 mL, 38.9 mmol). After complete addition, the resulting solution was allowed to stir for 24 h at rt. After that, water was carefully added to quench the reaction. The aqueous layer was extracted with CH_2Cl_2 (×3). Then, the combined organic layers were dried over $MgSO_4$ and the solvent was evaporated under reduced pressure. The crude mixture was subjected to column chromatography eluting with hexane/EtOAc (99:1). BINOL derivative **63** was obtained in 51% yield as a slightly yellow solid. **^{1}H NMR** (400 MHz, $CDCl_3$) δ 7.90 – 7.86 (m, 2H), 7.79 (s, 2H), 7.40 (s, 2H), 7.37 – 7.29 (m, 4H), 7.18 – 7.12 (m, 4H), 3.03 – 2.94 (m, 2H), 2.92 – 2.82 (m, 2H), 2.76 – 2.66 (m, 2H), 1.34 (d, *J* = 6.9 Hz, 12H), 1.22 (d, *J* = 6.8 Hz, 6H), 1.12 (dd, *J* = 9.5, 6.9 Hz, 12H), 1.05 (d, *J* = 6.9 Hz, 6H). **^{13}C NMR** (101 MHz, $CDCl_3$) δ 150.8 (×2), 149.3 (×2), 148.0 (×2), 147.9 (×2), 133.6 (×2), 130.8 (×2), 130.5 (×2), 129.3 (×2), 129.2 (×2), 128.4 (×2), 126.8 (×2), 124.7 (×2), 123.9 (×2), 121.4 (×2), 121.3 (×2), 113.3 (×2), 34.5, 31.0 (×2), 31.0 (×2), 27.1 (×2), 24.5 (×2), 24.4 (×2), 24.2 (×2), 24.2 (×2), 24.1 (×2), 23.9.

(*R*)-6,6'-Dibromo-3,3'-bis(2,4,6-triisopropylphenyl)-[1,1'-binaphthalene]-2,2'-diol (64)

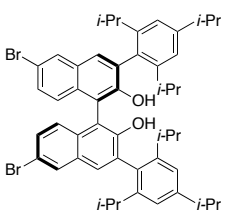

A solution of (*R*)-3,3'-bis(2,4,6-triisopropylphenyl)-[1,1'-binaphthalene]-2,2'-diol (**63**) (2.60 g, 3.76 mmol) in CH_2Cl_2 (19 mL) was cooled to –78 °C and a solution of Br_2 (1.32 g, 8.28 mmol) in CH_2Cl_2 (19 mL) was added dropwise. After being stirred at –78 °C for 2.5 h the reaction mixture was warmed to room temperature and stirred for a further 2.5 h. The reaction mixture was quenched by addition of sat. aqueous solution of Na_2SO_3. The biphasic system was extracted with CH_2Cl_2, and the combined organic layers were washed with Na_2SO_3, brine, dried over $MgSO_4$ and concentrated *in vacuo*. The crude product was purified by flash column chromatography on silica gel using cyclohexane/CH_2Cl_2 (90:10) as the eluent to give dibrominated compound **64** (1.9 g, 2.26 mmol) in 60% yield as a slightly yellow solid. **^{1}H NMR** (500 MHz, $CDCl_3$) δ 8.04 (d, *J* = 2.0 Hz, 2H), 7.7 (s, 2H), 7.14 (dd, *J* = 9.0, 2.0 Hz, 2H), 7.17 – 7.11 (m, 6H), 4.92 (s, 2H), 3.0 (sept, *J* = 6.8 Hz, 2H), 2.81 (sept, *J* = 6.8 Hz, 2H), 2.66 (sept, *J* = 6.8 Hz, 2H), 1.35 (d, *J* = 6.9 Hz, 12H), 1.23 (d, *J* = 6.8 Hz, 6H), 1.14 (d, *J* = 6.9 Hz, 6H), 1.11 (d, *J* = 6.9 Hz, 6H), 1.06 (d, *J* = 6.8 Hz, 6H). **^{13}C NMR** (126 MHz, $CDCl_3$) δ 150.7 (×2), 149.7 (×2), 148.0 (×2), 147.8 (×2), 132.0 (×2), 130.2 (×2), 130.1 (×2), 130.1 (×2), 129.9 (×2), 129.4 (×2), 129.2 (×2), 126.2 (×2), 121.5 (×2), 121.4 (×2), 117.6 (×2), 113.5 (×2), 34.4 (×2), 30.9 (×2), 30.8 (×2), 24.3 (×2), 24.3 (×2), 24.0 (×2), 234.0 (×2), 23.9 (×2), 23.7 (×2). **IR** (ATR): v 3518, 2958, 2926, 2868, 1593, 1433, 1258, 1226, 933, 899 cm^{-1}. **HRMS** (ESI-): *m/z* calcd. for $C_{50}H_{55}Br_2O_2$ $[M-H]^-$: 845.2574, found: 845.2556. **mp**: 165–172 °C. **$[\alpha]_D$**: +75.2 (*c* 1.00, CH_2Cl_2).

(3*S*)-2,2'-Dihydroxy-3,3'-bis(2,4,6-triisopropylphenyl)-[1,1'-binaphthalene]-6,6'-dicarbonitrile (65)

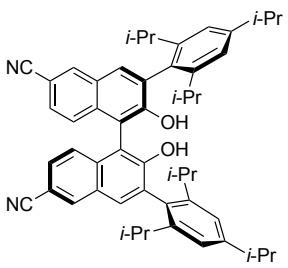

A mixture of **64** (1 g, 1.18 mmol), CuCN (0.42 g, 4.71 mmol), and NMP (1.70 ml) as solvent was subjected to microwave irradiation (200 W) for 1 h. After irradiation, the mixture was cooled to room temperature and diluted with water. The precipitate was collected by filtration and treated with aqueous ammonia. After removal of the solvents, the product was further purified by recrystallization from aqueous ethanol. Dinitrile **65** was obtained in 20% yield as a yellow solid. **^{1}H NMR** (300 MHz, $CDCl_3$) δ 8.25 (d, *J* = 1.6 Hz, 2H), 7.81 (s, 2H), 7.45 (dd, *J* = 8.8, 1.7 Hz, 2H), 7.31 (d, *J* = 8.8 Hz, 2H), 7.20 – 7.14 (m, 4H), 5.11 (br s, 2H), 3.06 – 2.88 (m, 2H), 2.80 – 2.66 (m, 2H), 2.66 – 2.51 (m, 2H), 1.31 (d, *J* = 6.9 Hz, 12H), 1.22 (d, *J* = 6.8 Hz, 6H), 1.10 (t, *J* = 7.3 Hz, 12H), 1.02 (d, *J* = 6.8 Hz, 6H). **^{13}C NMR** (126 MHz, $CDCl_3$) δ 153.0 (×2), 150.6 (×2), 148.4 (×2), 148.2 (×2), 135.4 (×2), 134.6 (×2), 131.1 (×2), 130.8 (×2), 128.0 (×2), 127.4 (×2), 125.6 (×2), 122.0 (×2), 121.9 (×2), 121.0 (×2), 119.6 (×2), 114.1 (×2), 107.3 (×2), 43.6, 34.6, 32.2, 31.2, 31.0, 30.3, 29.8, 27.7, 27.0, 24.4 (×2), 24.1, 24.1, 24.1, 23.8, 23.7, 22.5, 20.9. **IR** (ATR): v 3506, 3421, 2958, 2926, 2867, 2225, 2170, 1617, 1459, 1171, 1151, 999, 978, 957 cm^{-1}. **HRMS** (ESI-): *m/z* calcd. for $C_{52}H_{55}O_2$ $[M-H]^-$: 739.4269, found: 739.4271. **mp**: 215–221 °C. **$[\alpha]_D$**: +63.8 (*c* 1.00, CH_2Cl_2).

(3*S*)-2'-Hydroxy-3,3'-bis(2,4,6-triisopropylphenyl)-[1,1'-binaphthalen]-2-yl pivalate (67)

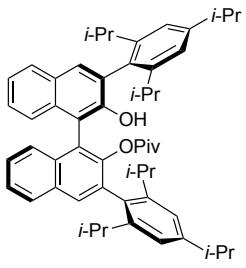

To a solution of (*R*)-BINOL (128 mg, 0.19 mmol) in THF (0.5 mL) at 0 ºC was added Et_3N (36.1 μL, 0.26 mmol) and pyridine (4 μL, 0.5 mmol), followed by PivCl (25.1 mL, 0.2 mmol). The solution was allowed to warm to rt and stirred for 5 hours. The resulting mixture was quenched with water and conc. HCl and extracted with diethyl ether (×3). The combined organic layers were washed with brine, dried over $MgSO_4$ and concentrated under reduced pressure. The crude was subjected to column chromatography eluting with hexane/CH_2Cl_2 (95:5). Monoprotected BINOL derivative **67** was obtained in 90% yield as a slightly yellow solid. ^{1}**H NMR** (500 MHz, $CDCl_3$) δ 8.00 – 7.92 (m, 2H), 7.84 – 7.80 (m, 1H), 7.74 (s, 1H), 7.55 – 7.47 (m, 2H), 7.40 – 7.29 (m, 4H), 7.15 (s, 2H), 7.12 – 7.05 (m, 42), 5.43 – 5.35 (br s, 1H), 3.03 – 2.91 (m, 2H), 2.90 – 2.79 (m, 2H), 2.77 – 2.65 (m, 2H), 1.34 (d, J = 6.9 Hz, 10H), 1.29 (d, J = 6.7 Hz, 8H), 1.22 (d, J = 6.8 Hz, 6H), 1.20 (d, J = 6.8 Hz, 6H), 1.13 (d, J = 6.9 Hz, 6H), 0.38 (s, 9H). ^{13}**C NMR** (126 MHz, $CDCl_3$) δ 175.6, 148.9 (×2), 147.5 (×2), 133.8, 133.1, 132.1 (×2), 131.5 (×2), 131.0, 130.8, 128.9 (×2), 128.4 (×2), 128.0 (×2), 126.7 (×2), 126.2 (×2), 125.7, 125.0, 124.5 (×2), 123.6 (×2), 121.0 (×2), 120.6, 115.2, 38.2, 34.6 (×2), 34.5 (×2), 31.3, 31.0, 30.9, 30.7, 27.1 (×2), 25.9 (×2), 25.1, 24.4 (×2), 24.3, 24.3, 24.2, 23.9, 23.5, 23.0. **HRMS** (ESI-): *m/z* calcd. for $C_{55}H_{65}O_3$ $[M-H]^-$: 773.4939, found: 773.4947. **mp**: 118–122 °C. **[α]$_D$**: +120.1 (*c* 1.00, CH_2Cl_2).

(3*S*)-2'-Hydroxy-6'-nitro-3,3'-bis(2,4,6-triisopropylphenyl)-[1,1'-binaphthalen]-2-yl pivalate (68)

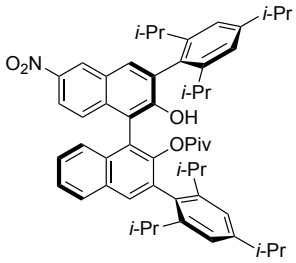

To a mixture of conc. HNO_3 (564 μL, 0.90 mmol), conc. H_2SO_4 (226 μL, 0.90 mmol), and MTBE (0.90 mL) in a 25 mL round-bottom flask was added dropwise at 0 ºC a solution of **67** (700 mg, 0.90 mmol) in MTBE (0.9 mL). The yellow color of the reaction mixture turned green. The solution was warmed to rt and stirred overnight. Once the reaction was completed, EtOAc was added and washed (×4) with water. The crude was subjected to column chromatography eluting with cyclohexane/EtOAc (80:20). Nitro derivative **68** was obtained in 72% yield as a slightly yellow solid. **^{1}H NMR** (500 MHz, $CDCl_3$) δ 8.77 (s, 1H), 8.07 (d, *J* = 9.3, 1.9 Hz, 1H), 7.99 – 7.95 (m, 2H), 7.91 (s, 1H), 7.55 (t, *J* = 7.7 Hz, 1H), 7.44 – 7.32 (m, 3H), 7.15 (s, 2H), 7.11 – 7.05 (m, 2H), 3.02 – 2.88 (m, 2H), 2.83 – 2.69 (m, 2H), 2.67 – 2.55 (m, 2H), 1.33 (dd, *J* = 6.9, 1.2 Hz, 9H), 1.27 (d, *J* = 6.8 Hz, 9H), 1.23 – 1.15 (m, 13H), 1.11 (d, *J* = 5.6 Hz, 5H), 0.37 (s, 9H). **^{13}C NMR** (126 MHz, $CDCl_3$) δ 175.6, 149.2, 147.4, 143.9, 136.1, 134.0, 132.1, 131.7, 131.0, 128.7, 128.4, 127.2, 127.1, 126.6, 125.0, 123.6, 121.3, 121.0, 120.8, 119.7, 115.9, 38.3, 34.6, 34.5, 31.2, 31.1, 30.8, 25.9, 25.0, 24.3, 24.2, 24.2, 24.2, 23.9, 23.5, 22.9. **HRMS** (ESI-): *m/z* calcd. for $C_{55}H_{64}O_5$ $[M-H]^-$: 818.4790, found: 818.4782. **mp:** 152–159 °C. **$[\alpha]_D$**: +178.8 (*c* 1.00, CH_2Cl_2).

(3*S*)-2'-Hydroxy-3,3'-bis(2,4,6-triisopropylphenyl)-[1,1'-binaphthalen]-2-yl acetate (70)

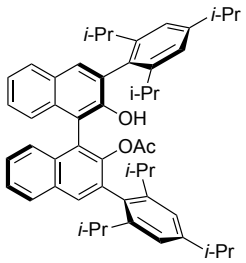

In a test tube containing a solution of **63** (515 mg, 0.75 mmol), DMAP (2.73 mg, 0.02 mmol) and Et_3N (312 μL, 2.24 mmol) in CH_2Cl_2 (2.50 mL) was added Ac_2O (77 μL, 2.24 mmol) dropwise at 0 °C. The solution was allowed to warm to rt and stirred for 6 houfrs. Once the reaction was completed, the resulting mixture was diluted with CH_2Cl_2 and washed with water, followed by aqueous 1 N HCl, saturated $NaHCO_3$ and brine successively. The organic phase was dried over Na_2SO_4 and the solvent was evaporated. The crude was subjected to column chromatography eluting with hexane/CH_2Cl_2 (95:5). Monoacetylated BINOL derivative **70** was obtained in 80% yield as a slightly yellow solid. **^{1}H NMR** (500 MHz, $CDCl_3$) δ 7.95 (d, *J* = 8.2 Hz, 1H), 7.91 (s, 1H), 7.86 – 7.83 (m, 1H), 7.75 (s, 1H), 7.53 (ddd, *J* = 8.1, 6.4, 1.7 Hz, 1H), 7.39 – 7.34 (m, 3H), 7.33 – 7.28 (m, 1H), 7.15 – 7.12 (m, 2H), 7.09 (dd, *J* = 7.2, 1.9 Hz, 2H), 3.00 – 2.92 (m, 2H), 2.89 – 2.79 (m, 2H), 2.72 – 2.63 (m, 2H), 1.38 (s, 3H), 1.35 – 1.30 (m, 13H) 1.25 – 1.19 (m, 8H), 1.15 – 1.10 (m, 12H), 1.07 (d, *J* = 6.7 Hz, 3H). **^{13}C NMR** (126 MHz, $CDCl_3$) δ 169.1, 148.8, 147.7, 147.6, 147.4, 133.6, 133.4 (×2), 133.1 (×2), 132.1, 131.5, 131.3, 131.1, 130.8, 128.9, 128.4 (×2), 128.0, 127.8, 126.9, 126.3 (×2), 126.0, 125.8, 125.1, 123.7 (×2), 122.0, 121.0 (×2), 120.6, 115.1, 34.5 (×2), 31.3, 31.1, 30.9, 30.8, 27.9, 24.6, 24.4, 24.3 (×2), 24.2, 24.2, 24.1, 23.9, 23.7, 23.6, 23.4, 19.6. **HRMS** (ESI-): *m/z* calcd. for $C_{52}H_{59}O_3$ $[M-H]^-$: 731.4470, found: 731.4479. **mp**: 120–125 °C. **$[\alpha]_D$**: +107.0 (*c* 1.00, CH_2Cl_2).

(3*S*)-2'-Hydroxy-6'-nitro-3,3'-bis(2,4,6-triisopropylphenyl)-[1,1'-binaphthalen]-2-yl acetate (71)

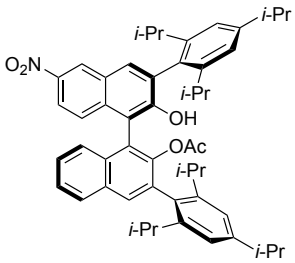

To a mixture of conc. HNO_3 (419 μL, 0.67 mmol), conc. H_2SO_4 (168 μL, 0.67 mmol), and MTBE (0.6 mL) in a 25 mL round-bottom flask was added dropwise at 0 °C a solution of **70** (492 mg, 0.967 mmol) in MTBE (0.6 mL). The yellow color of the reaction mixture turned green. The solution was warmed to rt and stirred overnight. Once the reaction was completed, EtOAc was added and washed (×4) with water. The crude was subjected to column chromatography eluting with hexane/EtOAc (90:10). Compound **71** was obtained in 50% yield as a slightly yellow solid. **^{1}H NMR** (500 MHz, $CDCl_3$) δ 8.79 (d, *J* = 2.3 Hz, 1H), 8.05 (dd, *J* = 9.3, 2.4 Hz, 1H), 7.97 (d, *J* = 8.4 Hz, 1H), 7.94 (s, 1H), 7.91 (s, 1H), 7.55 (ddd, *J* = 8.1, 6.8, 1.2 Hz, 1H), 7.39 (ddd, *J* = 8.3, 6.8, 1.3 Hz, 1H), 7.33 – 7.27 (m, 1H), 7.25 – 7.22 (m, 1H), 7.15 – 7.12 (m, 2H), 7.09 – 7.05 (m, 2H), 3.01 – 2.90 (m, 2H), 2.78 – 2.70 (m, 2H), 2.64 – 2.53 (m, 2H), 1.32 (d, *J* = 6.9 Hz 8H), 1.29 (d, *J* = 6.9 Hz, 8H), 1.20 (dd, *J* = 6.9, 2.2 Hz, 8H), 1.13 – 1.08 (m, 12H). **^{13}C NMR** (126 MHz, $CDCl_3$) δ 168.8, 149.1, 147.7 (×2), 147.6, 147.5, 144.1 (×2), 139.8, 136.4, 133.8, 132.7, 132.6 (×2), 132.2, 131.9, 130.7, 128.7 (×2), 127.3 (×2), 127.2, 126.6, 125.2, 125.0, 123.7, 122.0, 121.3 (×2), 121.0, 120.8, 119.9 (×2), 115.7, 34.5, 34.5, 31.3, 31.3, 31.1, 30.9, 24.6, 24.4, 24.3(×2), 24.2 (×3), 24.1, 24.0, 23.8, 23.7, 23.4, 19.5. **mp**: 212–216 °C. **HRMS** (ESI-): *m/z* calcd. for $C_{52}H_{58}O_5$ $[M-H]^-$: 776.4320, found: 776.4326. **$[\alpha]_D$**: +110.0 (*c* 1.00, CH_2Cl_2).

(3'*S*)-6-Nitro-3,3'-bis(2,4,6-triisopropylphenyl)-[1,1'-binaphthalene]-2,2'-diol (69)

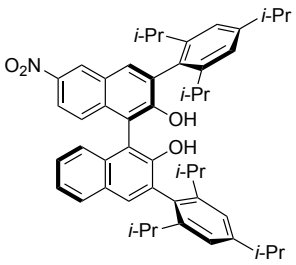

A 50 mL round-bottom flask was charged with **71**, KOH (2.5 mg, 3.21 mmol), THF (34.4 mL), and water (11.5 mL) and the reaction mixture was refluxed for 12 h. After that time, it was cooled to room temperature. Then, the mixture was acidified with 1 N HCl and extracted with EtOAc (×3). The combined organic phases were washed with aqueous $NaHCO_3$, brine and dried over Na_2SO_4. The crude obtained after evaporation was subjected to column chromatography eluting with hexane/CH_2Cl_2 (90:10). BINOL derivative **69** was obtained in 70% yield as a slightly yellow solid. **^{1}H NMR** (500 MHz, $CDCl_3$) δ 8.83 (d, *J* = 2.3 Hz, 1H), 8.06 (dd, *J* = 9.3, 2.3 Hz, 1H), 7.93 (s, 1H), 7.81 (s, 1H), 7.45 – 7.32 (m, 5H), 7.20 – 7.17 (m, 2H), 7.16 (s, 2H), 7.11 – 7.05 (m, 1H), 5.24 (s, 1H), 4.89 (s, 1H), 3.02 – 2.91 (m, 2H), 2.87 – 2.74 (m, 2H), 2.71 – 2.60 (s, 2H), 1.33 (dd, *J* = 7.0, 3.4 Hz, 12H), 1.23 (dd, *J* = 6.9, 2.0 Hz, 6H), 1.15 – 1.09 (m, 12H), 1.04 (dd, *J* = 6.9, 4.1 Hz, 6H). **^{13}C NMR** (126 MHz, $CDCl_3$) δ 153.8, 150.7, 150.2, 149.9, 148.5, 148.4, 147.9, 147.7, 144.1, 136.8, 133.5, 132.2, 131.7, 131.0, 129.3, 129.2, 129.1, 128.9, 128.6, 127.5, 127.2, 126.2, 125.3, 124.2, 124.2, 121.8, 121.6, 121.5, 119.9, 115.6, 112.2, 34.6, 34.5, 34.5, 31.2, 31.1, 31.0, 31.0, 24.5, 24.4, 24.3, 24.2, 24.2, 24.1, 24.0, 23.9, 23.8, 23.6, 22.9. **HRMS** (ESI-): *m/z* calcd. for $C_{50}H_{56}O_4$ $[M-H]^-$: 734.4215, found: 734.4213. **mp**: 135–141 °C. **$[\alpha]_D$**: +36.8 (*c* 1.00, CH_2Cl_2).

(3'*S*)-6-Amino-3,3'-bis(2,4,6-triisopropylphenyl)-[1,1'-binaphthalene]-2,2'-diol (72)

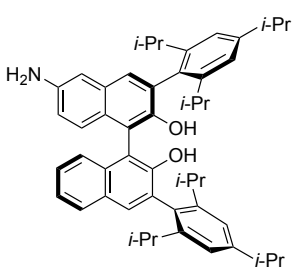

A solution containing **69** (400 mg, 0.54 mmol) and $SnCl_2 \cdot H_2O$ (491 mg, 2.17 mmol) in EtOH (1359 μL) was stirred at 70 ºC during 3 h. After that time, the reaction mixture was diluted with water and neutralized with sat. aq. $NaHCO_3$. After that, it was extracted with EtOAc and washed with brine. The combined organic layers were dried over $MgSO_4$ anhydrous and the solvent was evaporated to furnish the desired amino derivative. The crude was subjected to column chromatography eluting with hexane/EtOAc (90:10). Compound **72** was obtained in 60% yield as a red-brownish solid. **^{1}H NMR** (400 MHz, $CDCl_3$) δ 7.88 (d, *J* = 8.4 Hz, 1H), 7.77 (s, 1H), 7.55 (s, 1H), 7.42 – 7.31 (m, 3H), 7.18 – 7.05 (m, 6H), 6.83 (dd, *J* = 8.9, 2.4 Hz, 1H), 4.98 (s, 1H), 4.70 (s, 1H), 3.78 (br s, 2H), 3.03 – 2.92 (m, 2H), 2.92 – 2.80 (m, 2H), 2.78 – 2.65 (m, 2H), 1.33 (dd, *J* = 6.9, 2.9 Hz, 12H), 1.22 (dd, *J* = 6.8, 1.5 Hz, 6H), 1.12 (dd, *J* = , 6.9, 1.4 Hz, 12H), 1.05 (dd, *J* = 6.9, 0.8 Hz, 6H). **^{13}C NMR** (126 MHz, $CDCl_3$) δ 150.7, 149.1, 149.0, 148.4, 147.8 (×2), 147.8, 147.7, 142.7, 133.6, 131.0, 130.9, 130.7, 130.5, 129.7, 129.3, 129.1, 128.8, 128.3, 127.7, 126.7, 125.9, 124.8, 123.8, 121.3, 121.3 (×2), 121.2, 119.2, 113.6, 113.0, 109.6, 34.5, 34.4, 31.0, 31.0, 24.6, 24.5, 24.4, 24.4, 24.3, 24.2, 24.1, 24.1, 24.1, 23.9, 23.9, 23.7, 23.4, 19.6. **HRMS** (ESI-): *m/z* calcd. for $C_{50}H_{58}O_2$ $[M-H]^-$: 704.4473, found: 704.4474. **mp**: 168–175 °C. **$[\alpha]_D$**: +81.5 (*c* 1.00, CH_2Cl_2).

Polystyrene Sulfonamide Supported (*R*)-BINOL (73)

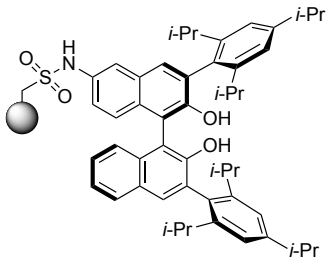

To a suspension of sulfonyl chloride polystyrene ($f_{(N)}$ = 1.73 mmol g^{-1}, 241 mg, 0.42 mmol) in anhydrous CH_2Cl_2 (11 mL) were added pyridine (0.09 mL, 1.06 mmol) and monomer **72** (500 mg, 0.71 mmol) subsequently. Then, the reaction mixture was stirred in a stirrer Shaker Orbital under nitrogen at rt during 24 h. After that time, the resin was filtered and washed with 1 M HCl, water and DCM. Then, the resin was dried overnight in a 40 °C vacuum oven to afford a red-dark resin (418 mg). **IR** (ATR): v 571, 697, 748, 1095, 1153, 1362, 1382, 1602, 2869, 2927, 2959, 3515 cm^{-1}. **N elemental analysis** (%): 1.06. $f_{(Max.\ N)}$: 0.8 $mmol/g_{resin.}$ $f_{(N)}$: 0.76 $mmol/g_{resin.}$

Polystyrene Sulfonamide Supported (*R*)-BINOL (74)

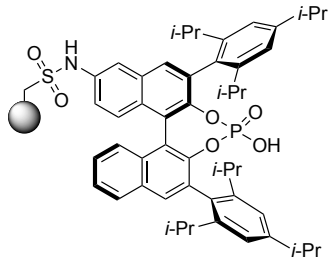

In a flame dried Schlenk tube, **PS-Sulfonamide (*R*)-BINOL (73)** (400 mg, 0.3 mmol) was suspended in pyridine (1 mL) under Ar. Then, $POCl_3$ (0.1 mL, 0.95 mmol) was added and the reaction mixture was heated in the closed Schlenk tube at 120 ºC. After 24 h, it was cooled to rt and 4 mL of water were added. Then, the system was closed again and heated at 100 ºC overnight. The resin was filtered and washed with water, THF/water, THF, 2 M HCl/EtOAc, EtOAC/DCM, and DCM and dried overnight in a 40 °C vacuum oven to afford a yellow resin (390 mg). **P elemental analysis** (%): 1.48. **N elemental analysis** (%): 1.10. $f_{(P)}$: 0.48 $mmol/g_{resin.}$ $f_{(N)}$: 0.78 $mmol/g_{resin.}$

(*R*)-3,3'-Bis(2,4,6-triisopropylphenyl)-6,6'-bis(4-vinylphenyl)-[1,1'-binaphthalene]- 2,2'-diol (77)

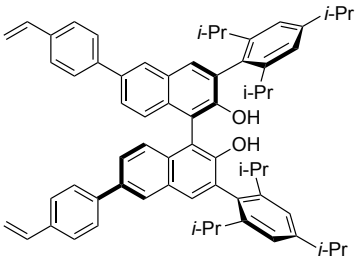

A flame-dried 50 mL round-bottom flask with Ar-inlet, magnetic stirring bar and reflux condenser was charged with dibromide **64** (1.20 g, 1.41 mmol), 4-vinylphenylboronic acid (0.46 g, 3.11 mmol) and K_2CO_3 (0.59 g, 4.24 mmol) and purged with Ar. Then, it was dissolved with THF (10 mL) and a solution of $Pd(PPh_3)_4$ (82 mg, 0.07 mmol, 5 mol%) in THF (5 mL) was added, followed by water (15 mL). The mixture was vigorously stirred at 85 °C overnight, and then it was cooled to room temperature and extracted with CH_2Cl_2 (×3). The combined organic layers were dried over $MgSO_4$ and concentrated under reduced pressure. The crude product was purified by flash column chromatography on silica gel using cyclohexane/CH_2Cl_2 (90:10) as the eluent to give compound **77** (0.88 g, 0.98 mmol) in 70% yield as a slightly yellow solid. **^{1}H NMR** (500 MHz, $CDCl_3$) δ 8.12 (s, 2H), 7.87 (s, 2H), 7.71(d, *J* = 8.2 Hz, 4H), 7.67 – 7.63 (m, 2H), 7.54 (d, *J* = 7.9 Hz, 4H), 7.45 (d, *J* = 8.8 Hz, 2H), 7.22 – 7.17 (m, 4H), 6.80 (dd, *J* = 11.0, 17.6 Hz, 2H), 5.83 (d, *J* = 17.6 Hz, 2H), 5.30 (d, *J* = 10.9 Hz, 2H), 5.01 (s, 2H), 3.01 (sept, *J* = 6.8 Hz, 2H), 2.94 (sept, *J* = 6.8 Hz, 2H), 2.78 (sept, *J* = 6.8 Hz, 2H), 1.36 (d, *J* = 6.9 Hz, 12H), 1.27 (d, *J* = 6.9 Hz, 6H), 1.19 (d, *J* = 6.9 Hz, 6H), 1.15 (d, *J* = 6.8 Hz, 6H), 1.10 (d, *J* = 6.9 Hz, 6H). **^{13}C NMR** (126 MHz, $CDCl_3$) δ 150.9 (×2), 149.5 (×2), 148.0 (×2), 148.0 (×2), 140.6 (×2), 136.6 (×2), 136.6 (×2), 136.3 (×2), 132.9 (×2), 131.0 (×2), 130.2 (×2), 129.8 (×2), 129.4 (×2), 127.5 (×4), 126.9 (×4), 126.3 (×2), 126.2 (×2), 125.3 (×2), 121.5 (×2), 121.4 (×2), 114.0 (×2), 113.4 (×2), 34.5 (×2), 31.1 (×2), 31.0 (×2), 24.5 (×2), 24.5 (×2), 24.2 (×2), 24.2 (×2), 24.1 (×2), 23.9 (×2). **IR** (ATR): v 3519, 2958, 2926, 2867, 1604, 1437, 1254, 820

cm^{-1}. **HRMS** (ESI-): *m/z* calcd. for $C_{66}H_{69}O_2$ $[M-H]^-$: 893.5310, found: 893.5303. **mp**: 195–210 °C. $[\alpha]_D$: +61.3 (*c* 1.00, CH_2Cl_2).

Polystyrene Supported (*R*)-TRIP BINOL (78)

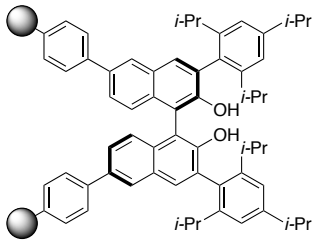

A 100 mL reactor was charged with a suspension of polyvinyl alcohol (PV-OH) (52 mg, 0.50 μmol, 0.002 equiv.) in 37 mL of deionized and degassed water. The solution was heated at 90 °C until PV-OH was dissolved. Then, it was cooled to rt and a solution of boric acid (235 mg, 3.8 mmol) in 10 mL of deionized and degassed water was transferred to the reactor. Later, a degassed solution containing divinylbenzene (DVB, filtered on a short pad o silica immediately before use, 80%, 62 μL, 0.36 mmol, 1.3 equiv.), diol **77** (250 mg, 0.279 mmol), styrene (1.5 mL, 13.33 mmol, 47.75 equiv.) and AIBN (16.05 mg, 0.09 mmol, 0.35 equiv.) in toluene (1.27 mL) was transferred to the reactor. After that, the system was heated at 80 °C and mechanically stirred at 440 rpm. After two days, the aqueous solution was decanted off and the resin was washed with water (50 °C) several times, followed by MeOH and CH_2Cl_2. Finally, it was dried overnight in a 40 °C vacuum oven to afford a yellow resin (630 mg).

Polystyrene Supported (*R*)-TRIP (79)

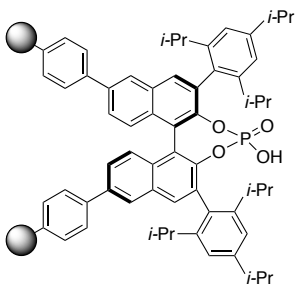

In a flame dried Schlenk tube, PS-(*R*)-TRIP BINOL **78** (779 mg, 0.13 mmol) was suspended in pyridine (4 mL) under Ar. Then, $POCl_3$ (35 mL, 0.37 mmol) was added and the reaction mixture was heated in the closed Schlenk tube at 120 °C. After 2 days, it was cooled to rt and 5 mL of water were added. Then, the system was closed again

and heated at 100 °C overnight. The resin was filtered and washed with water, THF/water, THF, 2 M HCl/EtOAc, EtOAC/DCM, and DCM and dried overnight in a 40 °C vacuum oven to afford a yellow resin (754 mg). **P elemental analysis** (%): 0.69. $f_{(P)}$: 0.22 mmol/$g_{resin.}$

(*R*)-TRIP Phosphoric acid (80)[50]

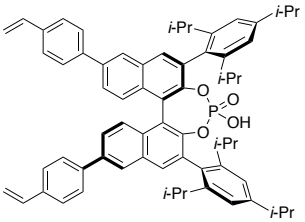

A flame-dried Schlenk tube was charged with a solution of BINOL derivative **77** (1 g, 1.12 mmol) in pyridine (2.3 mL) under Ar. Then, $POCl_3$ (0.31 mL, 3.35 mmol) was added and the reaction mixture was heated in the closed Schlenk tube for 14 h at 120 °C. After this time, the reaction was allowed to reach rt, followed by addition of water (2.3 mL). The resulting brownish slurry was heated to reflux for 3 h. Once the reaction was completed, the solution was cooled to rt, 10 mL of CH_2Cl_2 were added and the resulting organic phase was thoroughly washed with 1 M HCl (3×5 mL). The resulting organic layers were dried over $MgSO_4$ and recrystallized from MeCN to give compound **80** in 70% yield as a slightly yellow solid. The aqueous solution should have a pH = 1 – 2 to ensure the compound in its free acid from. ^{1}**H NMR** (400 MHz, $CDCl_3$) δ 8.07 (d, *J* = 1.9 Hz, 2H), 7.87 (s, 2H), 7.70 (d, *J* = 8.3 Hz, 4H), 7.62 (dd, *J* = 8.9, 1.9 Hz, 2H), 7.54 (d, *J* = 8.3 Hz, 4H), 7.45 (d, *J* = 8.9 Hz, 2H), 6.95 (s, 4H), 6.78 (dd, *J* = 17.6, 10.9 Hz, 2H), 5.82 (dd, *J* = 17.6, 0.9 Hz, 2H), 5.30 (dd, *J* = 10.9, 0.9 Hz, 2H), 2.91 – 2.78 (m, 2H), 2.67 – 2.54 (m, 4H), 1.23 (dd, *J* = 6.9, 4.8 Hz, 12H), 1.08 (d, *J* = 6.7 Hz, 6H), 1.01 (d, *J* = 6.8 Hz, 6H), 0.93 (d, *J* = 6.8 Hz, 6H), 0.80 (d, *J* = 6.7 Hz, 6H). ^{13}**C NMR** (126 MHz, $CDCl_3$) δ 148.6 (×2), 148.1 (×2), 147.6 (×2), 140.1 (×2), 138.2 (×2), 137.1 (×2), 136.5 (×2), 133.0 (×2), 132.9 (×2), 131.7 (×2), 131.5 (×2), 131.4 (×2), 128.1 (×2), 127.6 (×4), 127.0 (×4), 126.0 (×2), 125.8 (×2), 122.1 (×2), 122.1 (×2), 121.3 (×2), 120.4 (×2),

114.3 (×2), 34.4 (×2), 31.1 (×2), 30.8 (×2), 26.5 (×2), 25.2 (×2), 24.3 (×2), 24.0 (×2), 23.4 (×2), 22.9 (×2). $[\alpha]_D$: –1.4 (*c* 1.00, CH_2Cl_2).

Polystyrene Supported (*R*)-TRIP (79)

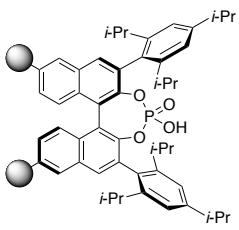

A 100 mL reactor was charged with a suspension of polyvinyl alcohol (PV-OH) (38 mg, 0.37 μmol) in 38 mL of deionized and degassed water. The solution was heated at 90 ºC until PV-OH was dissolved. Then, it was cooled to rt and a solution under N_2, containing divinylbenzene (DVB; 80%, 111 μL, 0.62 mmol) filtered on a short pad of silica immediately before use, phosphoric acid **80** (350 mg, 0.37 mmol), styrene (3.0 mL, 25.9 mmol) and benzoyl peroxide (75%, 39 mg, 0.12 mmol) in toluene (1.27 mL) was transferred to the reactor. After that, the system was heated at 80 ºC and mechanically stirred at 440 rpm. After two days, the aqueous solution was decanted off and the resin was washed with water (50 °C) several times, followed by THF, EtOAc, 2 M HCl/EtOAc, and CH_2Cl_2. Finally, it was dried overnight in a vacuum oven at 40 °C to afford a brownish resin (1.0 g). **P elemental analysis** (%): 0.39. $f_{(P)}$: 0.13 $mmol/g_{resin.}$

(*R*)-6-Oxaspiro[4.5]decan-1-one (76)[44g]

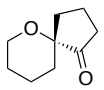

A vial was charged with 4 Å (200 mg) molecular sieves, catalyst (10 mol%) and CCl_4 (1 mL). The mixture was stirred for 10 min. at rt. Then, a solution of **75**[44g] in CCl_4 (1 mL) was added to the reaction mixture. After 24 h, the crude reaction mixture was directly purified by flash column chromatography on silica gel using penatne/Et_2O (5:1) as the eluent to give compound **76** as a colourless oil. **^{1}H NMR (**400 MHz, Chloroform-*d*) δ 3.94 – 3.83 (m, 1H), 3.70 – 3.58 (m, 1H), 2.43 – 2.18 (m, 2H), 2.09 – 1.87 (m, 4H),

1.83 – 1.69 (m, 1H), 1.69 – 1.46 (m, 5H). **^{13}C NMR** (101 MHz, $CDCl_3$) δ 217.15, 79.26, 63.99, 36.12, 35.04, 29.07, 25.61, 19.12, 17.64. **HPLC** (Daicel Chiralpak AD-H column, hexane/*i*-PrOH 99:1, flow rate 1.0 mL/min, λ = 210 nm): t_{major} = 7.9 min; t_{minor} = 6.9 min.

2.6. References

[1] S. Kobayashi, M. Sugiura, H. Kitagawa, W. W. L. Lam, *Chem. Rev.* **2002**, *102*, 2227-2302.

[2] (a) J. S. Johnson, D. A. Evans, *Acc. Chem. Res.* **2000**, *33*, 325-335; (b) S. Kobayashi, H. Ishitani, *Chem. Rev.* **1999**, *99*, 1069-1094; (c) M. Shibasaki, M. Kanai, K. Funabashi, *Chem. Commun.* **2002**, 1989-1999; (d) T. Mukaiyama, S. Kobayashi, in *Organic Reactions*, John Wiley & Sons, Inc., **2004**.

[3] J. Merad, C. Lalli, G. Bernadat, J. Maury, G. Masson, *Chem. Eur. J.*, n/a-n/a.

[4] T. Akiyama, K. Mori, *Chem. Rev.* **2015**, *115*, 9277-9306.

[5] T. Akiyama, J. Itoh, K. Fuchibe, *Adv. Synth. Catal.* **2006**, *348*, 999-1010.

[6] (a) J. Foropoulos, D. D. DesMarteau, *Inorg. Chem.* **1984**, *23*, 3720-3723; (b) F. G. Bordwell, *Acc. Chem. Res.* **1988**, *21*, 456-463.

[7] A. Kütt, I. Leito, I. Kaljurand, L. Sooväli, V. M. Vlasov, L. M. Yagupolskii, I. A. Koppel, *J. Org. Chem.* **2006**, *71*, 2829-2838.

[8] C. Bolm, T. Rantanen, I. Schiffers, L. Zani, *Angew. Chem. Int. Ed.* **2005**, *44*, 1758-1763.

[9] S. Lou, S. E. Schaus, *J. Am. Chem. Soc.* **2008**, *130*, 6922-6923.

[10] S. J. Connon, *Angew. Chem. Int. Ed.* **2006**, *45*, 3909-3912.

[11] T. Akiyama, *Chem. Rev.* **2007**, *107*, 5744-5758.

[12] T. Akiyama, J. Itoh, K. Yokota, K. Fuchibe, *Angew. Chem. Int. Ed.* **2004**, *43*, 1566-1568.

[13] D. Uraguchi, M. Terada, *J. Am. Chem. Soc.* **2004**, *126*, 5356-5357.

[14] M. Yamanaka, J. Itoh, K. Fuchibe, T. Akiyama, *J. Am. Chem. Soc.* **2007**, *129*, 6756-6764.

[15] I. D. Gridnev, M. Kouchi, K. Sorimachi, M. Terada, *Tetrahedron Lett.* **2007**, *48*, 497-500.

[16] A. Zamfir, S. Schenker, M. Freund, S. B. Tsogoeva, *Org. Biomol. Chem.* **2010**, *8*, 5262-5276.

[17] (a) D. Parmar, E. Sugiono, S. Raja, M. Rueping, *Chem. Rev.* **2014**, *114*, 9047-9153; (b) R. Maji, S. C. Mallojjala, S. E. Wheeler, *Chem. Soc. Rev.* **2018**.

[18] P. M. Pihko, *Angew. Chem. Int. Ed.* **2004**, *43*, 2062-2064.

[19] (a) P. Christ, A. G. Lindsay, S. S. Vormittag, J.-M. Neudörfl, A. Berkessel, A. C. O'Donoghue, *Chem. Eur. J.* **2011**, *17*, 8524-8528; (b) K. Kaupmees, N. Tolstoluzhsky, S. Raja, M. Rueping, I. Leito, *Angew. Chem. Int. Ed.* **2013**, *52*, 11569-11572; (c) C. Yang, X.-S. Xue, X. Li, J.-P. Cheng, *J. Org. Chem.* **2014**, *79*, 4340-4351; (d) C. Yang, X. S. Xue, J. L. Jin, X. Li, J. P. Cheng, *J. Org. Chem.* **2013**, *78*, 7076-7085.

[20] (a) P. García-García, F. Lay, P. García-García, C. Rabalakos, B. List, *Angew. Chem. Int. Ed.* **2009**, *48*, 4363-4366; (b) A. Berkessel, P. Christ, N. Leconte, J.-M. Neudörfl, M. Schäfer, *Eur. J. Org. Chem.* **2010**, *2010*, 5165-5170.

[21] M. Treskow, J. Neudörfl, R. Giernoth, *Eur. J. Org. Chem.* **2009**, *2009*, 3693-3697.

[22] K. Mori, M. Kobayashi, T. Itakura, T. Akiyama, *Adv. Synth. Catal.* **2015**, *357*, 35-40.

[23] J.-H. Tay, A. J. Arguelles, P. Nagorny, *Org. Lett.* **2015**, *17*, 3774-3777.

[24] (a) R. I. Storer, D. E. Carrera, Y. Ni, D. W. C. MacMillan, *J. Am. Chem. Soc.* **2006**, *128*, 84-86; (b) T. Akiyama, T. Suzuki, K. Mori, *Org. Lett.* **2009**, *11*, 2445-2447; (c) A. Sakakura, M. Sakuma, K. Ishihara, *Org. Lett.* **2011**, *13*, 3130-3133.

[25] (a) S. Harada, S. Kuwano, Y. Yamaoka, K.-i. Yamada, K. Takasu, *Angew. Chem. Int. Ed.* **2013**, *52*, 10227-10230; (b) Y. Kuroda, S. Harada, A. Oonishi, H. Kiyama, Y. Yamaoka, K.-i. Yamada, K. Takasu, *Angew. Chem. Int. Ed.* **2016**, *55*, 13137-13141; (c) T. Akiyama, Y. Honma, J. Itoh, K. Fuchibe, *Adv. Synth. Catal.* **2008**, *350*, 399-402.

[26] F. Xu, D. Huang, C. Han, W. Shen, X. Lin, Y. Wang, *J. Org. Chem.* **2010**, *75*, 8677-8680.

[27] (a) E. P. Ávila, G. W. Amarante, *ChemCatChem* **2012**, *4*, 1713-1721; (b) M. Mahlau, B. List, *Isr. J. Chem.* **2012**, *52*, 630-638; (c) M. Mahlau, B. List, *Angew. Chem. Int. Ed.* **2013**, *52*, 518-533.

[28] D. Nakashima, H. Yamamoto, *J. Am. Chem. Soc.* **2006**, *128*, 9626-9627.

[29] (a) M. Rueping, B. J. Nachtsheim, R. M. Koenigs, W. Ieawsuwan, *Chem. Eur. J.* **2010**, *16*, 13116-13126; (b) M. Rueping, B. J. Nachtsheim, W. Ieawsuwan, I. Atodiresei, *Angew. Chem. Int. Ed.* **2011**, *50*, 6706-6720.

[30] N. Momiyama, T. Konno, Y. Furiya, T. Iwamoto, M. Terada, *J. Am. Chem. Soc.* **2011**, *133*, 19294-19297.

[31] Y. Wang, Q. Wang, J. Zhu, *Angew. Chem. Int. Ed.* **2017**, *56*, 5612-5615.

[32] (a) D. Banerjee, K. Junge, M. Beller, *Angew. Chem. Int. Ed.* **2014**, *53*, 13049-13053; (b) A. Chatupheeraphat, H.-H. Liao, S. Mader, M. Sako, H. Sasai, I. Atodiresei, M. Rueping, *Angew. Chem. Int. Ed.* **2016**, *55*, 4803-4807; (c) O. El-Sepelgy, S. Haseloff, S. K. Alamsetti, C. Schneider, *Angew. Chem. Int. Ed.* **2014**, *53*, 7923-7927; (d) J.-B. Gualtierotti, D. Pasche, Q. Wang, J. Zhu, *Angew. Chem. Int. Ed.* **2014**, *53*, 9926-9930; (e) P. Jain, P. Verma, G. Xia, J.-Q. Yu, *Nature Chem.* **2016**, *advance online publication*; (f) J.-S. Lin, P. Yu, L. Huang, P. Zhang, B. Tan, X.-Y. Liu, *Angew. Chem. Int. Ed.* **2015**, *54*, 7847-7851; (g) E. Mensah, N. Camasso, W. Kaplan, P. Nagorny, *Angew. Chem. Int. Ed.* **2013**, *52*, 12932-12936; (h) C. Romano, M. Jia, M. Monari, E. Manoni, M. Bandini, *Angew. Chem. Int. Ed.* **2014**, *53*, 13854-13857; (i) M. Vlatković, B. L. Feringa, S. J.

Wezenberg, *Angew. Chem. Int. Ed.* **2016**, *55*, 1001-1004; (j) S.-G. Wang, Q. Yin, C.-X. Zhuo, S.-L. You, *Angew. Chem. Int. Ed.* **2015**, *54*, 647-650; (k) W. Yang, J. Sun, *Angew. Chem. Int. Ed.* **2016**, *55*, 1868-1871; (l) J.-J. Zhao, S.-B. Sun, S.-H. He, Q. Wu, F. Shi, *Angew. Chem. Int. Ed.* **2015**, *54*, 5460-5464; (m) F. Zhou, H. Yamamoto, *Angew. Chem. Int. Ed.* **2016**, *55*, 8970-8974; (n) T. Miura, J. Nakahashi, M. Murakami, *Angew. Chem. Int. Ed.* **2017**, *56*, 6989-6993.

[33] (a) T. Akiyama, H. Morita, J. Itoh, K. Fuchibe, *Org. Lett.* **2005**, *7*, 2583-2585; (b) S. K. Nimmagadda, S. C. Mallojjala, L. Woztas, S. E. Wheeler, J. C. Antilla, *Angew. Chem. Int. Ed.* **2017**, *56*, 2454-2458; (c) Q.-X. Guo, H. Liu, C. Guo, S.-W. Luo, Y. Gu, L.-Z. Gong, *J. Am. Chem. Soc.* **2007**, *129*, 3790-3791; (d) M. Hatano, T. Ikeno, T. Matsumura, S. Torii, K. Ishihara, *Adv. Synth. Catal.* **2008**, *350*, 1776-1780; (e) S. Hoffmann, A. M. Seayad, B. List, *Angew. Chem. Int. Ed.* **2005**, *44*, 7424-7427; (f) M. Rueping, E. Sugiono, C. Azap, T. Theissmann, M. Bolte, *Org. Lett.* **2005**, *7*, 3781-3783; (g) R.-R. Liu, S.-C. Ye, C.-J. Lu, G.-L. Zhuang, J.-R. Gao, Y.-X. Jia, *Angew. Chem. Int. Ed.* **2015**, *54*, 11205-11208.

[34] M. Rueping, A. Kuenkel, I. Atodiresei, *Chem. Soc. Rev.* **2011**, *40*, 4539-4549.

[35] (a) M. Fleischmann, D. Drettwan, E. Sugiono, M. Rueping, R. M. Gschwind, *Angew. Chem. Int. Ed.* **2011**, *50*, 6364-6369; (b) R. Appel, S. Chelli, T. Tokuyasu, K. Troshin, H. Mayr, *J. Am. Chem. Soc.* **2013**, *135*, 6579-6587.

[36] (a) M. Rueping, A. P. Antonchick, T. Theissmann, *Angew. Chem. Int. Ed.* **2006**, *45*, 3683-3686; (b) M. Rueping, A. P. Antonchick, T. Theissmann, *Angew. Chem. Int. Ed.* **2006**, *45*, 6751-6755; (c) M. Terada, K. Machioka, K. Sorimachi, *Angew. Chem. Int. Ed.* **2006**, *45*, 2254-2257; (d) Y.-X. Jia, J. Zhong, S.-F. Zhu, C.-M. Zhang, Q.-L. Zhou, *Angew. Chem. Int. Ed.* **2007**, *46*, 5565-5567.

[37] (a) T. Marcelli, P. Hammar, F. Himo, *Chem. Eur. J.* **2008**, *14*, 8562-8571; (b) T. Akiyama, H. Morita, P. Bachu, K. Mori, M. Yamanaka, T. Hirata, *Tetrahedron* **2009**, *65*, 4950-4956.

[38] (a) M. Yamanaka, T. Hirata, *J. Org. Chem.* **2009**, *74*, 3266-3271; (b) F.-Q. Shi, B.-A. Song, *Org. Biomol. Chem.* **2009**, *7*, 1292-1298; (c) T. Marcelli, P. Hammar, F. Himo, *Adv. Synth. Catal.* **2009**, *351*, 525-529.

[39] (a) L. Simón, J. M. Goodman, *J. Org. Chem.* **2011**, *76*, 1775-1788; (b) L. Simón, J. M. Goodman, *J. Org. Chem.* **2010**, *75*, 589-597; (c) L. Simón, J. M. Goodman, *J. Am. Chem. Soc.* **2009**, *131*, 4070-4077; (d) L. Simón, J. M. Goodman, *J. Am. Chem. Soc.* **2008**, *130*, 8741-8747.

[40] (a) K. Brak, E. N. Jacobsen, *Angew. Chem. Int. Ed.* **2013**, *52*, 534-561; (b) S. Mayer, B. List, *Angew. Chem. Int. Ed.* **2006**, *45*, 4193-4195.

[41] (a) R. J. Phipps, K. Hiramatsu, F. D. Toste, *J. Am. Chem. Soc.* **2012**, *134*, 8376-8379; (b) V. Rauniyar, A. D. Lackner, G. L. Hamilton, F. D. Toste, *Science* **2011**, *334*, 1681-1684.

[42] M. Klussmann, L. Ratjen, S. Hoffmann, V. Wakchaure, R. Goddard, B. List, *Synlett* **2010**, *2010*, 2189-2192.

[43] M. Rueping, T. Theissmann, A. Kuenkel, R. M. Koenigs, *Angew. Chem. Int. Ed.* **2008**, *47*, 6798-6801.

[44] (a) W.-J. Liu, X.-H. Chen, L.-Z. Gong, *Org. Lett.* **2008**, *10*, 5357-5360; (b) G.-W. Zhang, L. Wang, J. Nie, J.-A. Ma, *Adv. Synth. Catal.* **2008**, *350*, 1457-1463; (c) K. Mori, T. Katoh, T. Suzuki, T. Noji, M. Yamanaka, T. Akiyama, *Angew. Chem. Int. Ed.* **2009**, *48*, 9652-9654; (d) J. Nie, G.-W. Zhang, L. Wang, A. Fu, Y. Zheng, J.-A. Ma, *Chem. Commun.* **2009**, 2356-2358; (e) J. Nie, G.-W. Zhang, L. Wang, D.-H. Zheng, Y. Zheng, J.-A. Ma, *Eur. J. Org. Chem.* **2009**, *2009*, 3145-3149; (f) M. Rueping, A. P. Antonchick, E. Sugiono, K. Grenader, *Angew. Chem. Int. Ed.* **2009**, *48*, 908-910; (g) Q.-W. Zhang, C.-A. Fan, H.-J. Zhang, Y.-Q. Tu, Y.-M. Zhao, P. Gu, Z.-M. Chen, *Angew. Chem. Int. Ed.* **2009**, *48*, 8572-8574; (h) S. Duce, F. Pesciaioli, L. Gramigna, L. Bernardi, A. Mazzanti, A. Ricci, G. Bartoli, G. Bencivenni, *Adv. Synth. Catal.* **2011**, *353*, 860-864; (i) Y. Xie, Y. Zhao, B. Qian, L. Yang, C. Xia, H. Huang, *Angew. Chem. Int. Ed.* **2011**, *50*, 5682-5686; (j) K. Saito, T. Akiyama, *Chem. Commun.* **2012**, *48*, 4573-4575; (k) Z. Sun, G. A. Winschel, A. Borovika, P. Nagorny, *J. Am. Chem. Soc.* **2012**, *134*, 8074-8077; (l) Z. Zhang, J. C. Antilla, *Angew. Chem. Int. Ed.* **2012**, *51*, 11778-11782; (m) I. Coric, J. H. Kim, T. Vlaar, M. Patil, W. Thiel, B. List, *Angew. Chem.* **2013**, *52*, 3490-3493; (n) M. Fuchs, M. Schober, A. Orthaber, K. Faber, *Adv. Synth. Catal.* **2013**, *355*, 2499-2505; (o) S. Jia, D. Xing, D. Zhang, W. Hu, *Angew. Chem. Int. Ed.* **2014**, *53*, 13098-13101; (p) L. Liao, C. Shu, M. Zhang, Y. Liao, X. Hu, Y. Zhang, Z. Wu, W. Yuan, X. Zhang, *Angew. Chem. Int. Ed.* **2014**, *53*, 10471-10475; (q) Z. Sun, G. A. Winschel, P. M. Zimmerman, P. Nagorny, *Angew. Chem. Int. Ed.* **2014**, *53*, 11194-11198; (r) P.-S. Wang, H.-C. Lin, Y.-J. Zhai, Z.-Y. Han, L.-Z. Gong, *Angew. Chem. Int. Ed.* **2014**, *53*, 12218-12221; (s) Y.-C. Zhang, J.-J. Zhao, F. Jiang, S.-B. Sun, F. Shi, *Angew. Chem. Int. Ed.* **2014**, *53*, 13912-13915; (t) A. R. Burns, A. G. E. Madec, D. W. Low, I. D. Roy, H. W. Lam, *Chem. Sci.* **2015**, *6*, 3550-3555; (u) Y. Wang, L. Jiang, L. Li, J. Dai, D. Xiong, Z. Shao, *Angew. Chem. Int. Ed.* **2016**, n/a-n/a; (v) Z. Yang, Y. He, F. D. Toste, *J. Am. Chem. Soc.* **2016**, *138*, 9775-9778; (w) M. Chen, J. Sun, *Angew. Chem. Int. Ed.* **2017**, *56*, 11966-11970.

[45] (a) H. Sellner, C. Faber, P. B. Rheiner, D. Seebach, *Chem. Eur. J.* **2000**, *6*, 3692-3705; (b) H. Hocke, Y. Uozumi, *Tetrahedron* **2003**, *59*, 619-630; (c) J. Bunzen, U. Kiehne, C. Benkhäuser-Schunk, A. Lützen, *Org. Lett.* **2009**,

11, 4786-4789; (d) Y. K. Lee, K. S. Tay, V. S. Lee, N. A. Rahman, *Applied Catalysis A: General* **2015**, *502*, 246-253; (e) E. M. Schuster, P. Wipf, *Isr. J. Chem.* **2014**, *54*, 361-370; (f) F. G. Finelli, L. S. M. Miranda, R. O. M. A. de Souza, *Chem. Commun.* **2015**, *51*, 3708-3722.

[46] (a) I. P. Beletskaya, L. S. Patrikeeva, F. Lamaty, *Russ. Chem. Bull.* **2011**, *60*, 2370-2374; (b) A. K. Mutyala, N. T. Patil, *Org. Chem. Front.* **2014**, *1*, 582-586; (c) Y. Huangfu, Q. Sun, S. Pan, X. Meng, F.-S. Xiao, *ACS Catal.* **2015**, *5*, 1556-1559; (d) T. Mayer-Gall, J.-W. Lee, K. Opwis, B. List, J. S. Gutmann, *ChemCatChem* **2016**, *8*, 1428-1436.

[47] M. Bartoszek, M. Beller, J. Deutsch, M. Klawonn, A. Köckritz, N. Nemati, A. Pews-Davtyan, *Tetrahedron* **2008**, *64*, 1316-1322.

[48] M. Rueping, E. Sugiono, A. Steck, T. Theissmann, *Adv. Synth. Catal.* **2010**, *352*, 281-287.

[49] (a) D. S. Kundu, J. Schmidt, C. Bleschke, A. Thomas, S. Blechert, *Angew. Chem. Int. Ed.* **2012**, *51*, 5456-5459; (b) C. Bleschke, J. Schmidt, D. S. Kundu, S. Blechert, A. Thomas, *Adv. Synth. Catal.* **2011**, *353*, 3101-3106.

[50] H.-G. Cheng, J. Miguelez, H. Miyamura, W.-J. Yoo, S. Kobayashi, *Chem. Sci.* **2017**, *8*, 1356-1359.

[51] L. Osorio-Planes, C. Rodríguez-Escrich, M. A. Pericàs *Chem. Eur. J.* **2014**, *20*, 2367-2372.

[52] (a) I. Sagamanova, C. Rodríguez-Escrich, I. G. Molnár, S. Sayalero, R. Gilmour, M. A. Pericàs, *ACS Catal.* **2015**, *5*, 6241-6248; (b) P. Llanes, C. Rodríguez-Escrich, S. Sayalero, M. A. Pericàs, *Org. Lett.* **2016**, *18*, 6292-6295.

[53] S. J. Dolman, K. C. Hultzsch, F. Pezet, X. Teng, A. H. Hoveyda, R. R. Schrock, *J. Am. Chem. Soc.* **2004**, *126*, 10945-10953.

[54] P. Jain, J. C. Antilla, *J. Am. Chem. Soc.* **2010**, *132*, 11884-11886.

[55] Y. Li, Q. Li, *Org. Lett.* **2012**, *14*, 4362-4365.

[56] A. P. Bhatt, K. Pathak, R. V. Jasra, R. I. Kureshy, N.-u. H. Khan, S. H. R. Abdi, *J. Mol. Catal. A: Chem.* **2006**, *244*, 110-117.

[57] C.-C. Lee, P.-S. Wang, M. B. Viswanath, M.-k. Leung, *Synthesis* **2008**, *2008*, 1359-1366.

[58] M. Thoß, R. W. Seidel, I. M. Oppel, M. Feigel, *J. Mol. Struct.* **2010**, *980*, 245-249.

[59] K. Kazuhiro, O. Munetosi, K. Atsushi, O. Hideaki, N. Keiichi, Y. Noriyuki, *Chem. Lett.* **2008**, *37*, 660-661.

2.7. ^{1}H and ^{13}C NMR Spectra

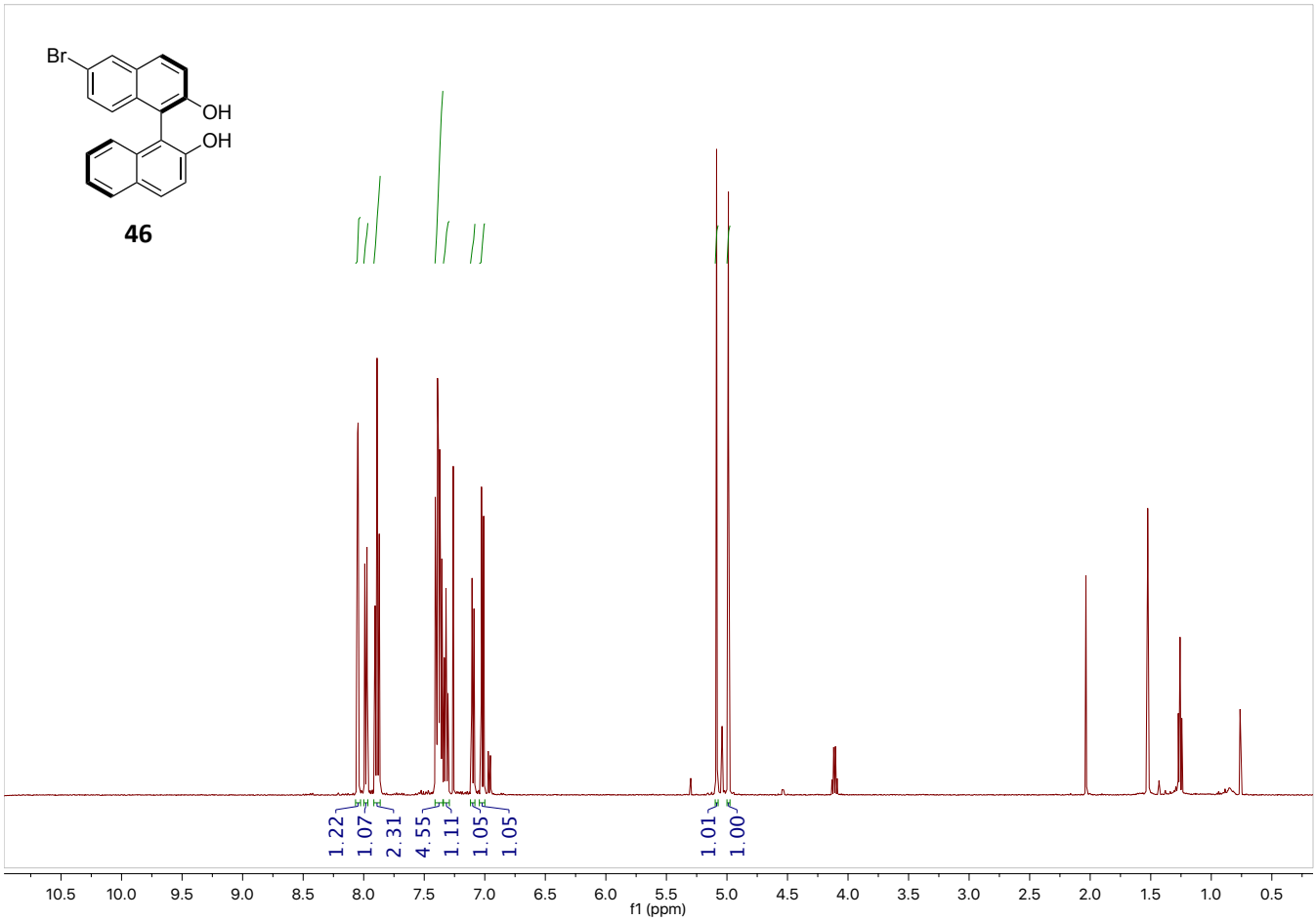

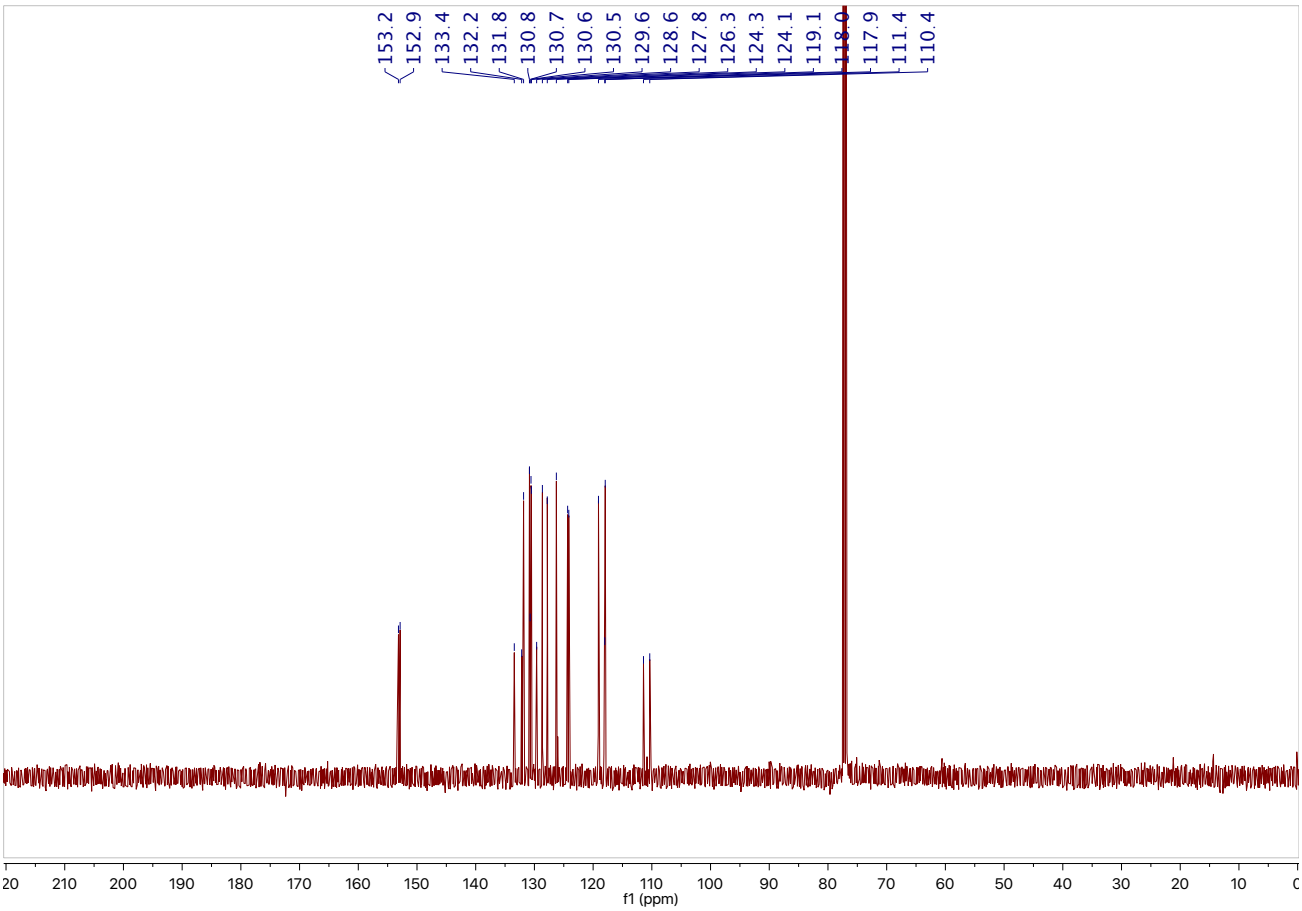

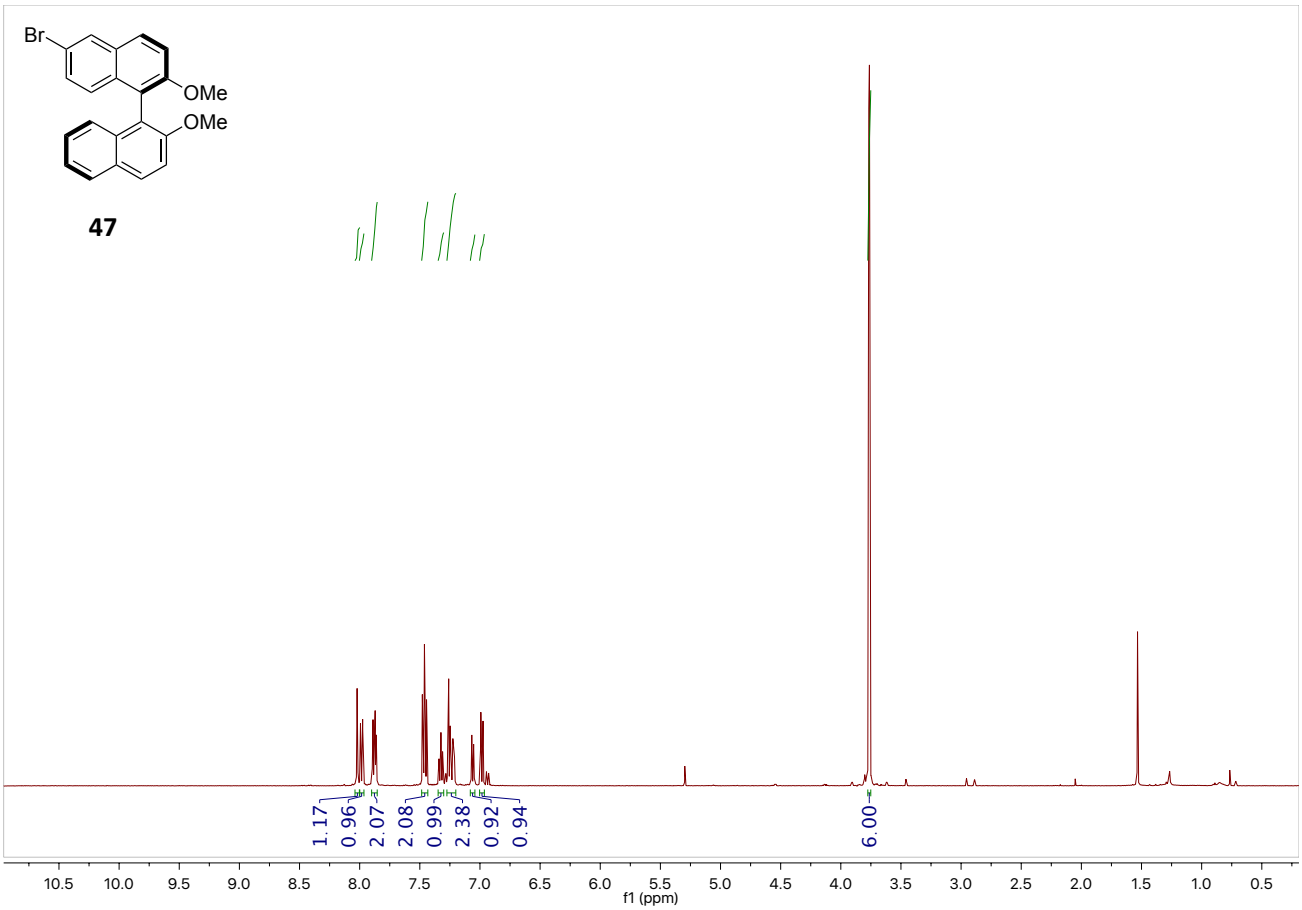
Br
OMe
OMe
47
1.17
0.96
2.07
2.08
0.99
2.38
0.92
0.94
6.00
f1 (ppm)

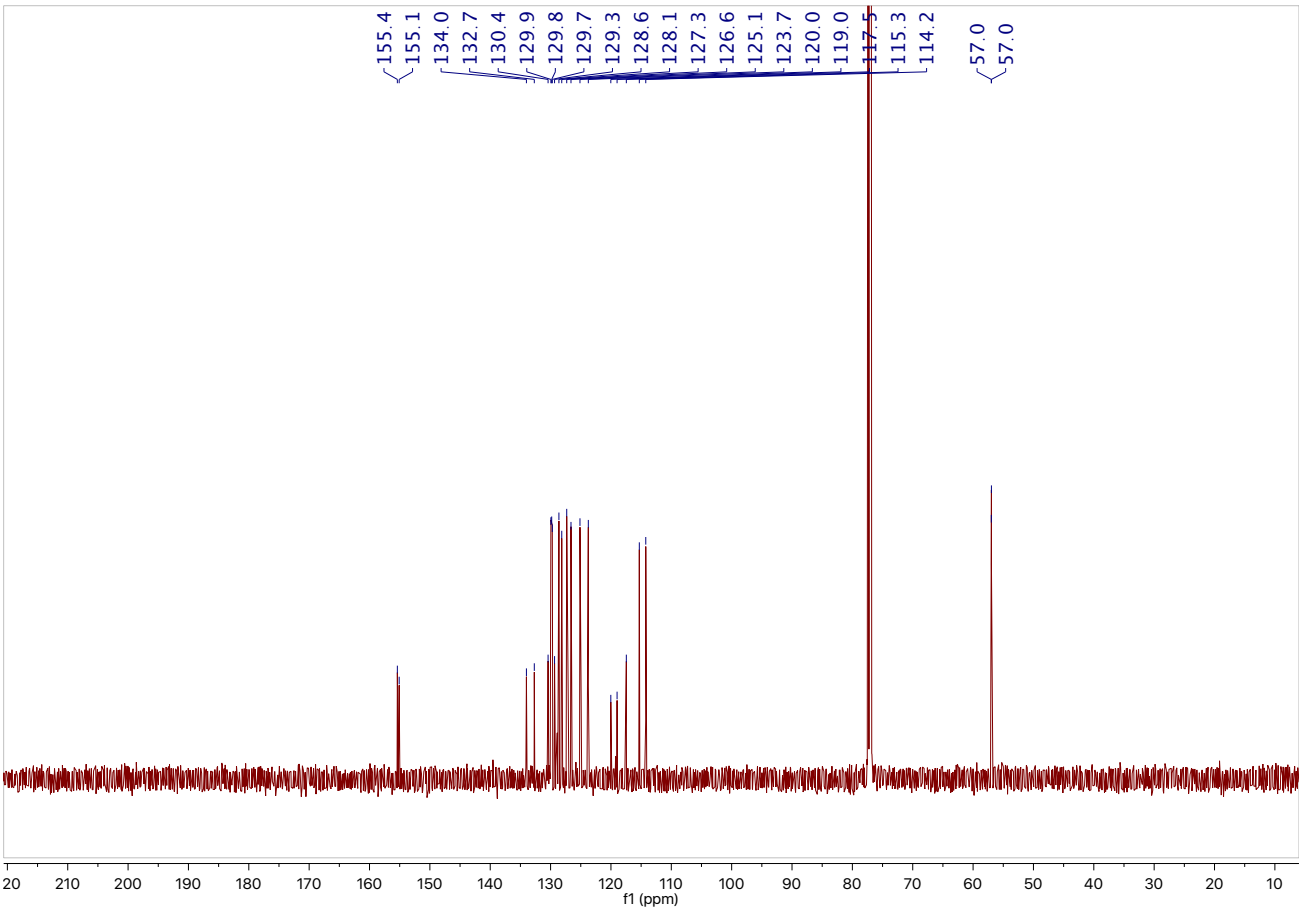
155.4
155.1
134.0
132.7
130.4
129.9
129.8
129.7
129.3
128.6
128.1
127.3
126.6
125.1
123.7
120.0
119.0
117.5
115.3
114.2
57.0
57.0
f1 (ppm)

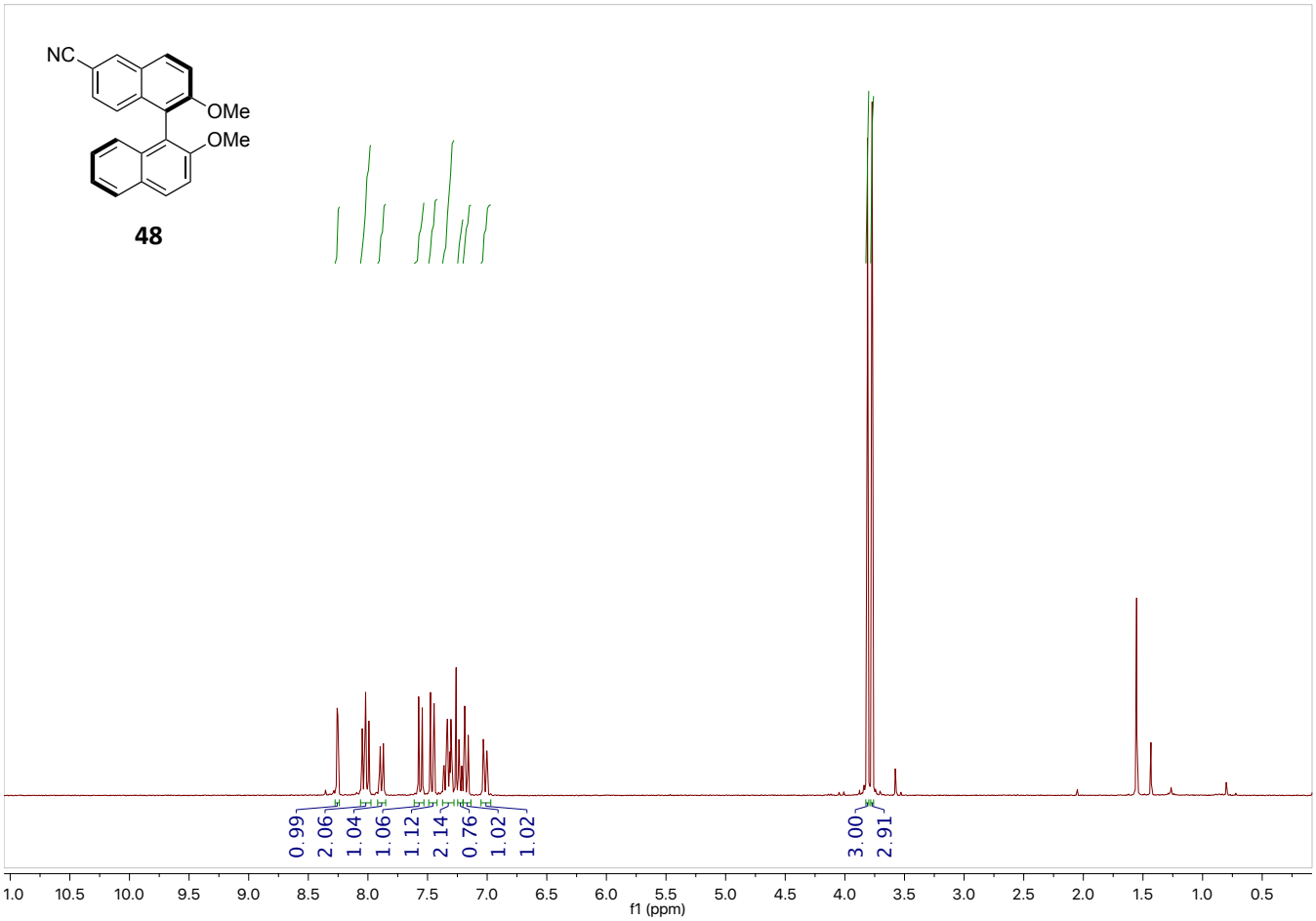
NC
OMe
OMe
48
0.99
2.06
1.04
1.06
1.12
2.14
0.76
1.02
1.02
3.00
2.91
f1 (ppm)

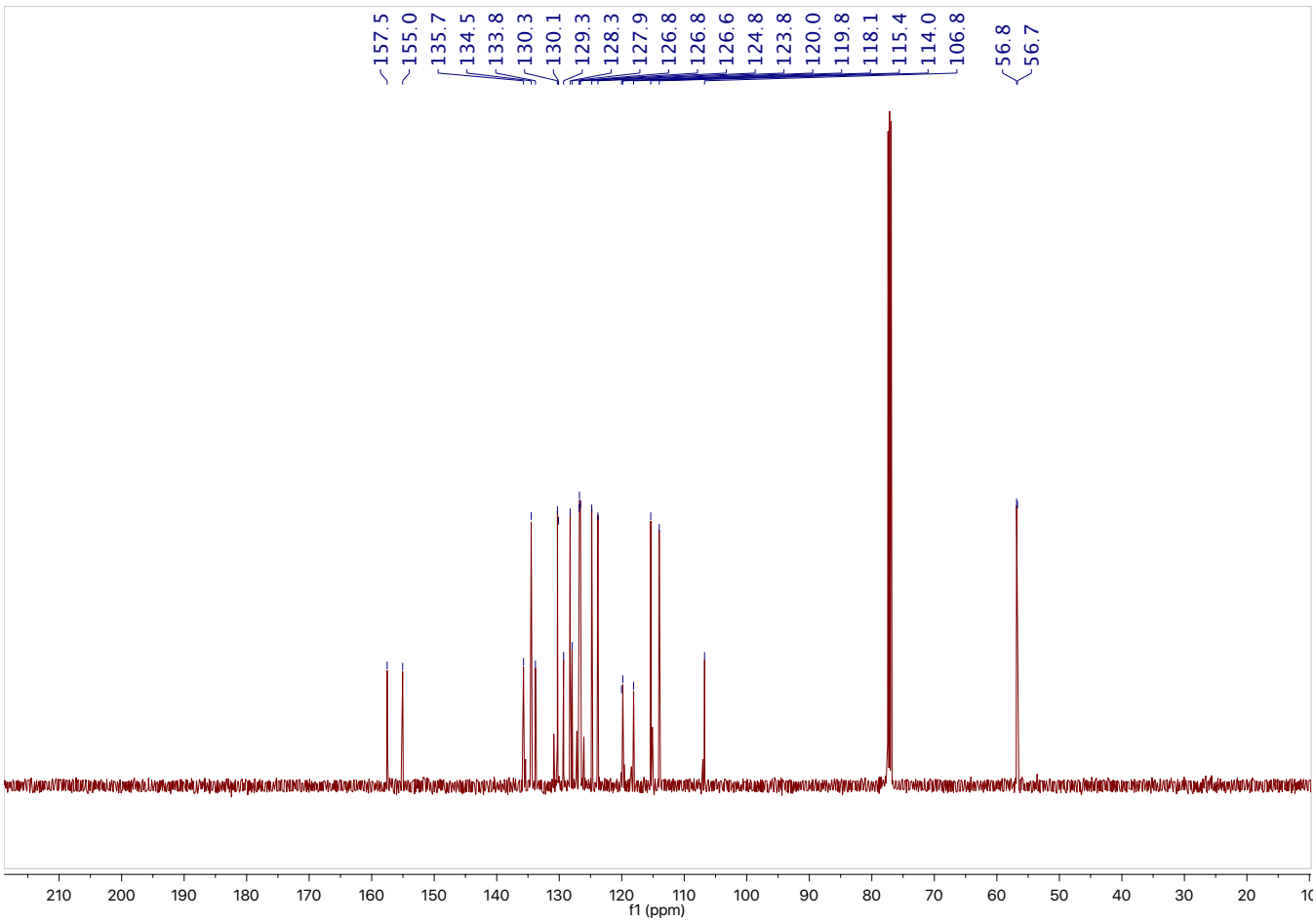
157.5
155.0
135.7
134.5
133.8
130.3
130.1
129.3
128.3
127.9
126.8
126.8
126.6
124.8
123.8
120.0
119.8
118.1
115.4
114.0
106.8
56.8
56.7
f1 (ppm)

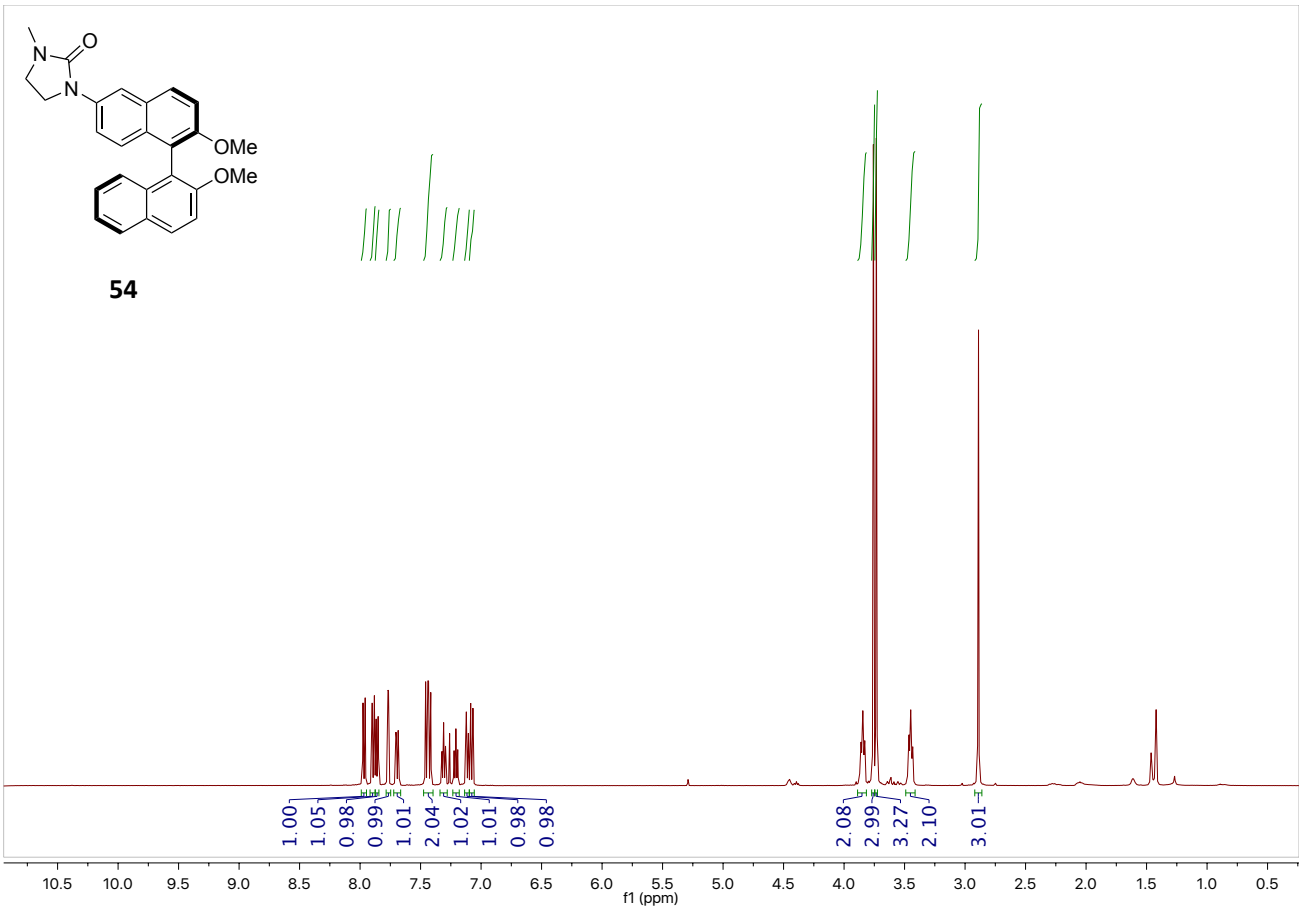
OMe
OMe
54
1.00
1.05
0.98
0.99
1.01
2.04
1.02
1.01
0.98
0.98
2.08
2.99
3.27
2.10
3.01
f1 (ppm)

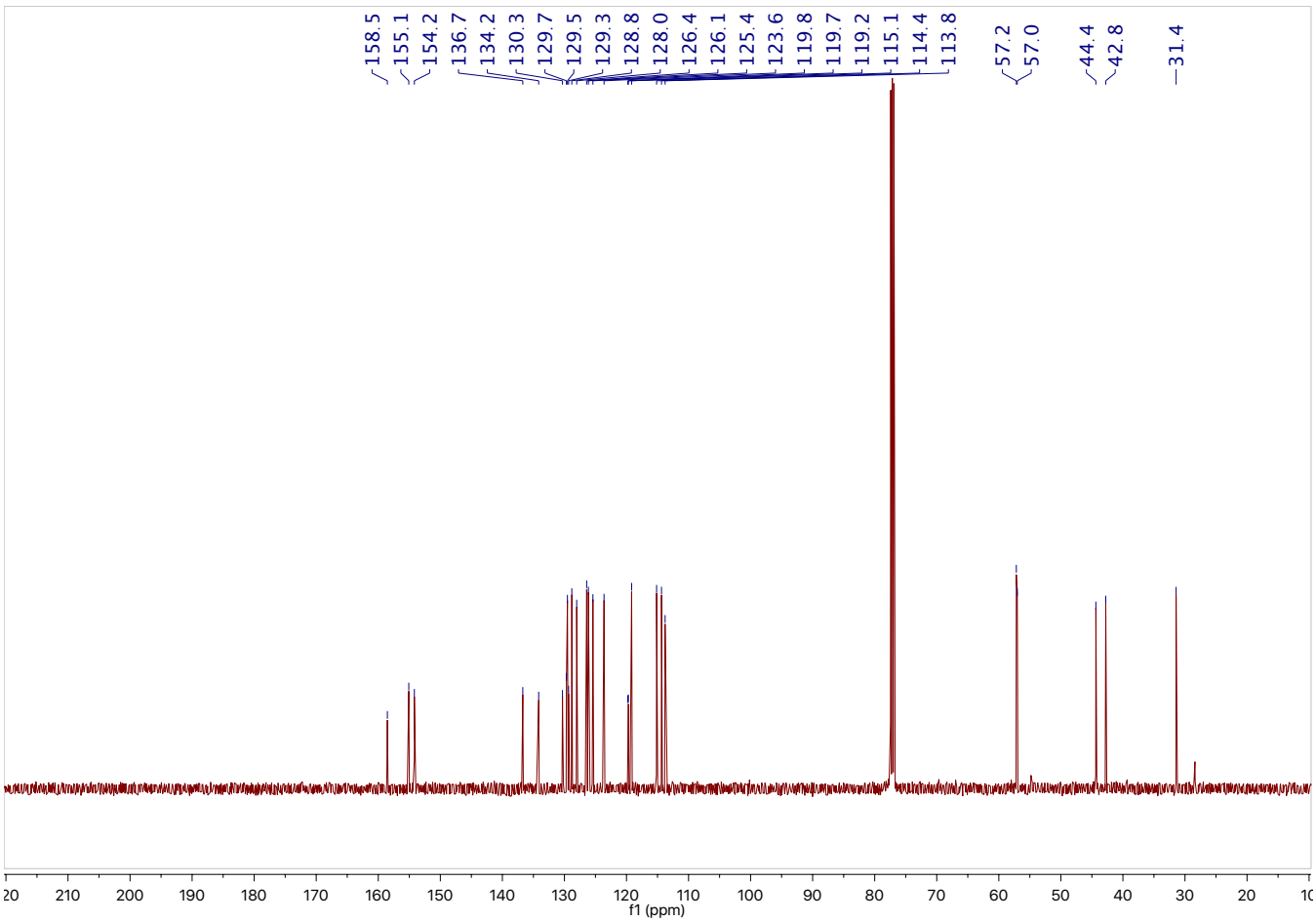
158.5
155.1
154.2
136.7
134.2
130.3
129.7
129.5
129.3
128.8
128.0
126.4
126.1
125.4
123.6
119.8
119.7
119.2
115.1
114.4
113.8
57.2
57.0
44.4
42.8
31.4
f1 (ppm)

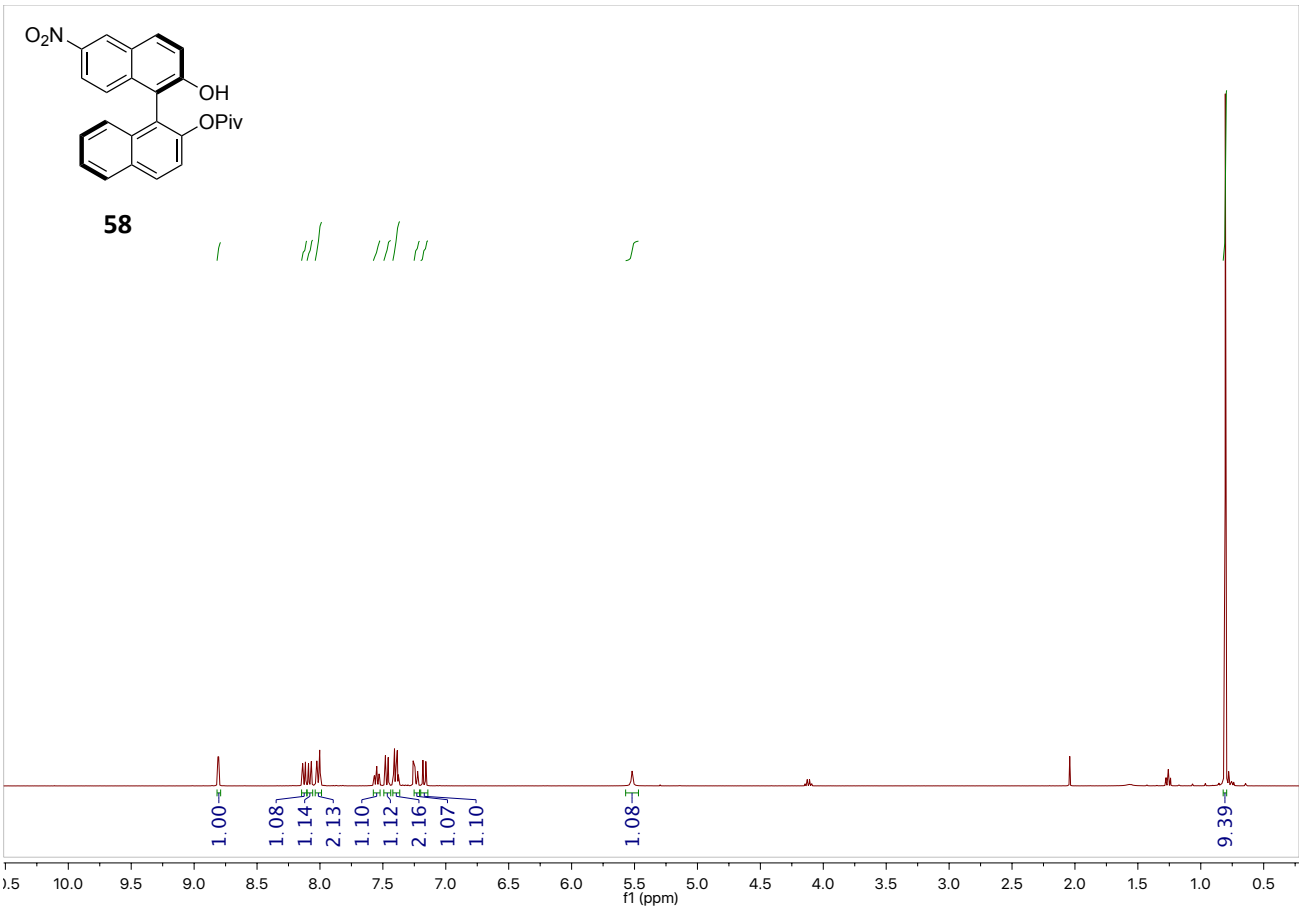
O2N
OH
OPiv
58
1.00
1.08
1.14
2.13
1.10
1.12
2.16
1.07
1.10
1.08
9.39
f1 (ppm)

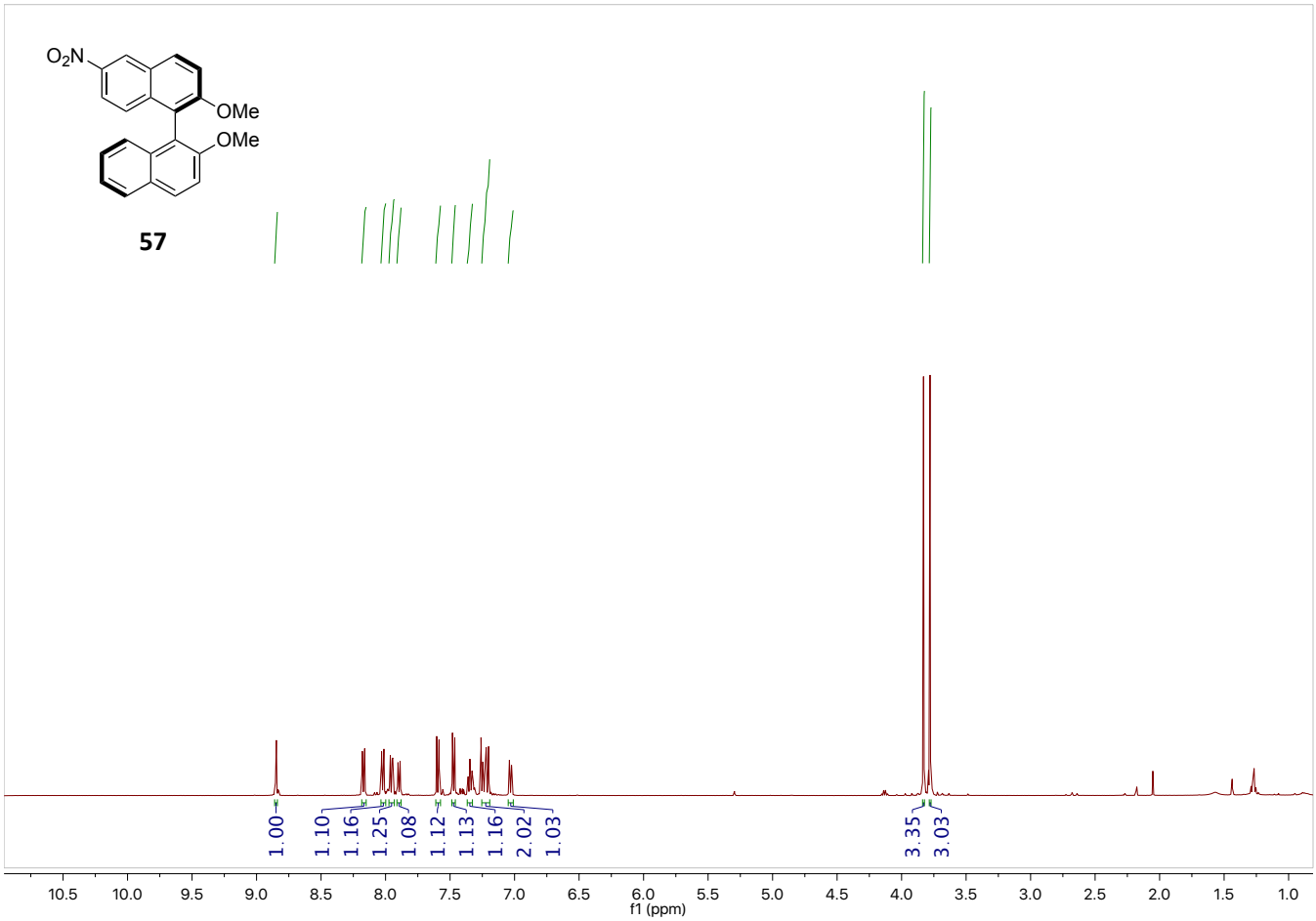
O2N
OMe
OMe
57
1.00
1.10
1.16
1.25
1.08
1.12
1.13
1.16
2.02
1.03
3.35
3.03
f1 (ppm)

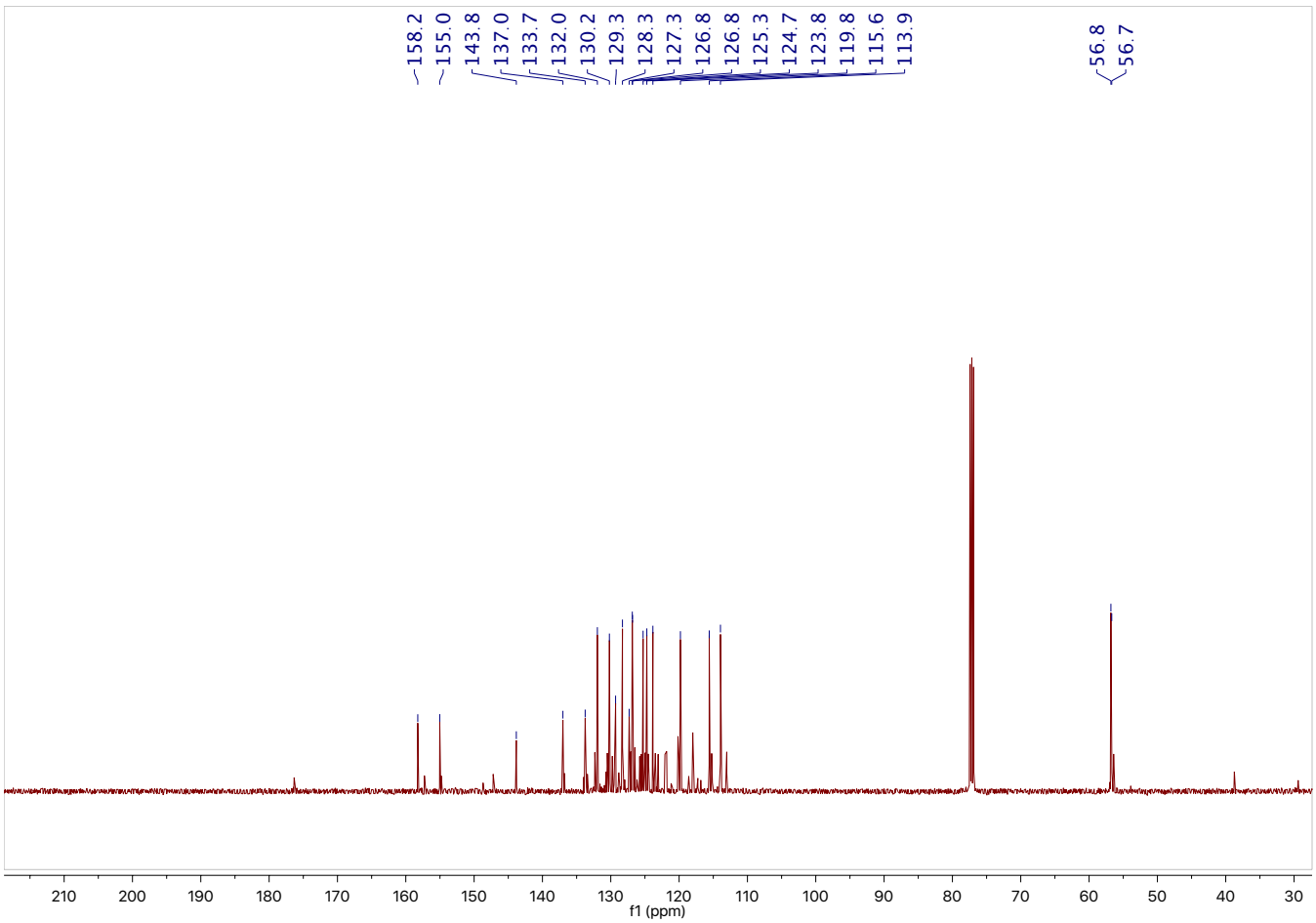
158.2
155.0
143.8
137.0
133.7
132.0
130.2
129.3
128.3
127.3
126.8
126.8
125.3
124.7
123.8
119.8
115.6
113.9
56.8
56.7
f1 (ppm)

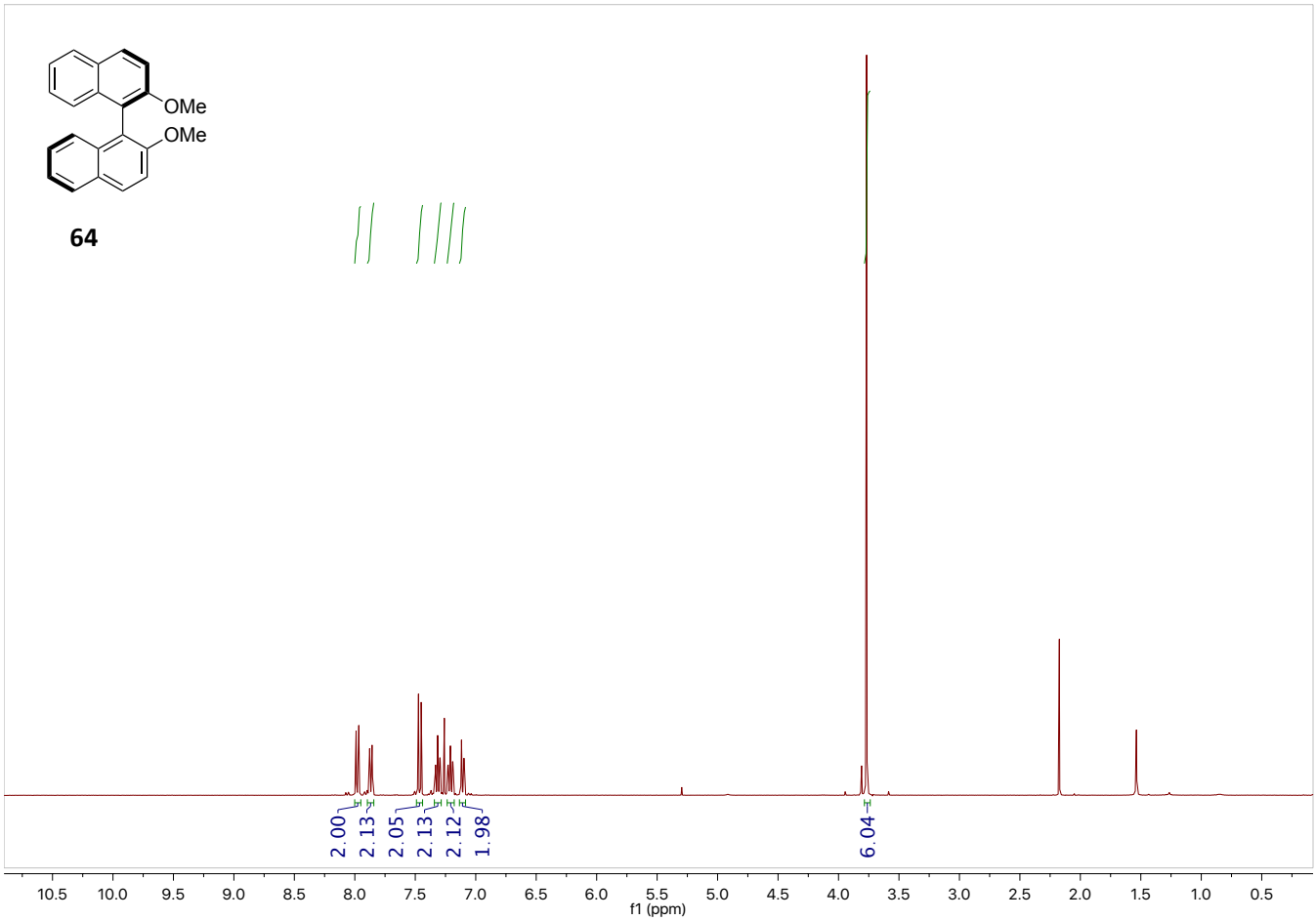
OMe
OMe
64
2.00
2.13
2.05
2.13
2.12
1.98
6.04
f1 (ppm)

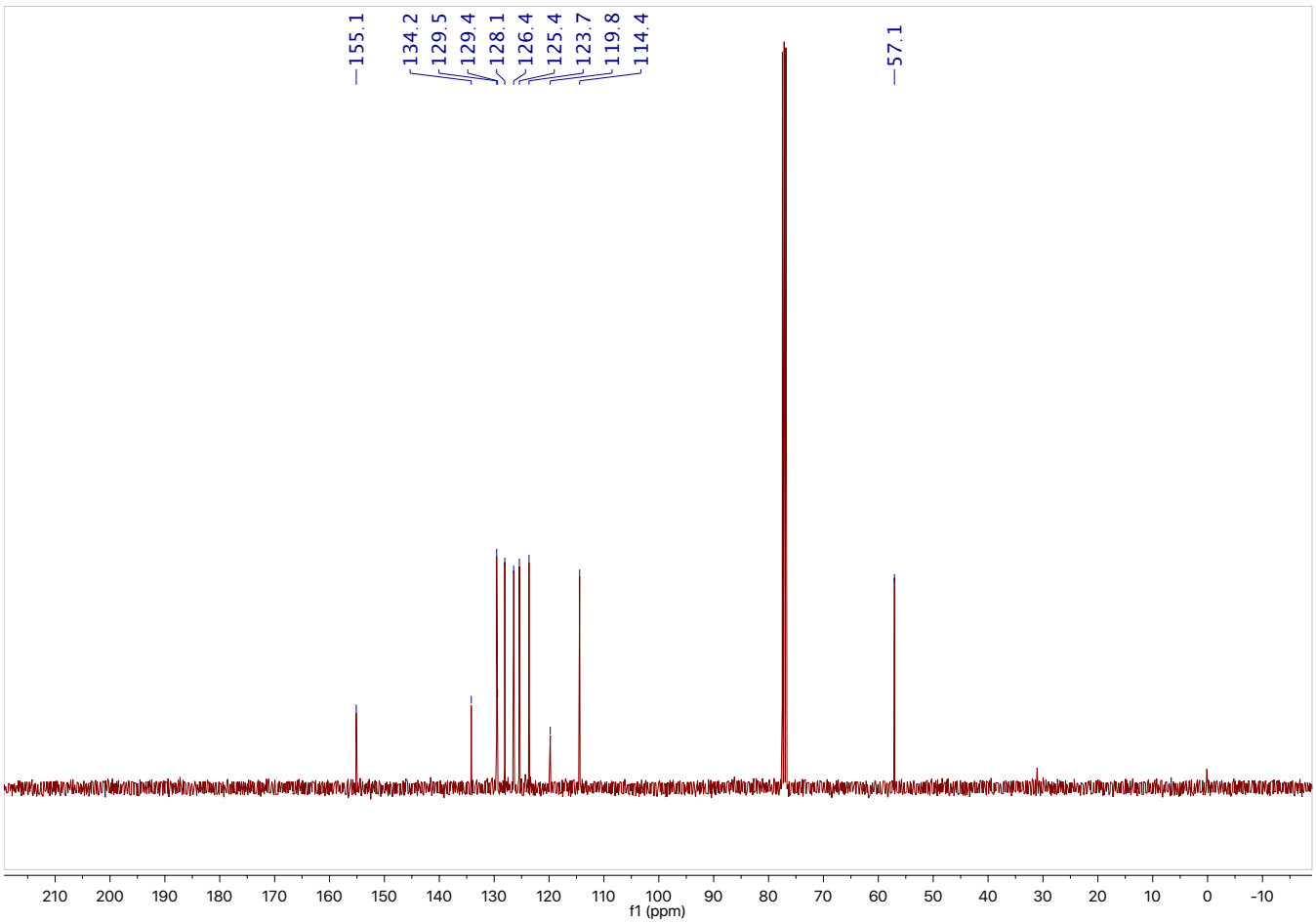
155.1
134.2
129.5
129.4
128.1
126.4
125.4
123.7
119.8
114.4
57.1
f1 (ppm)

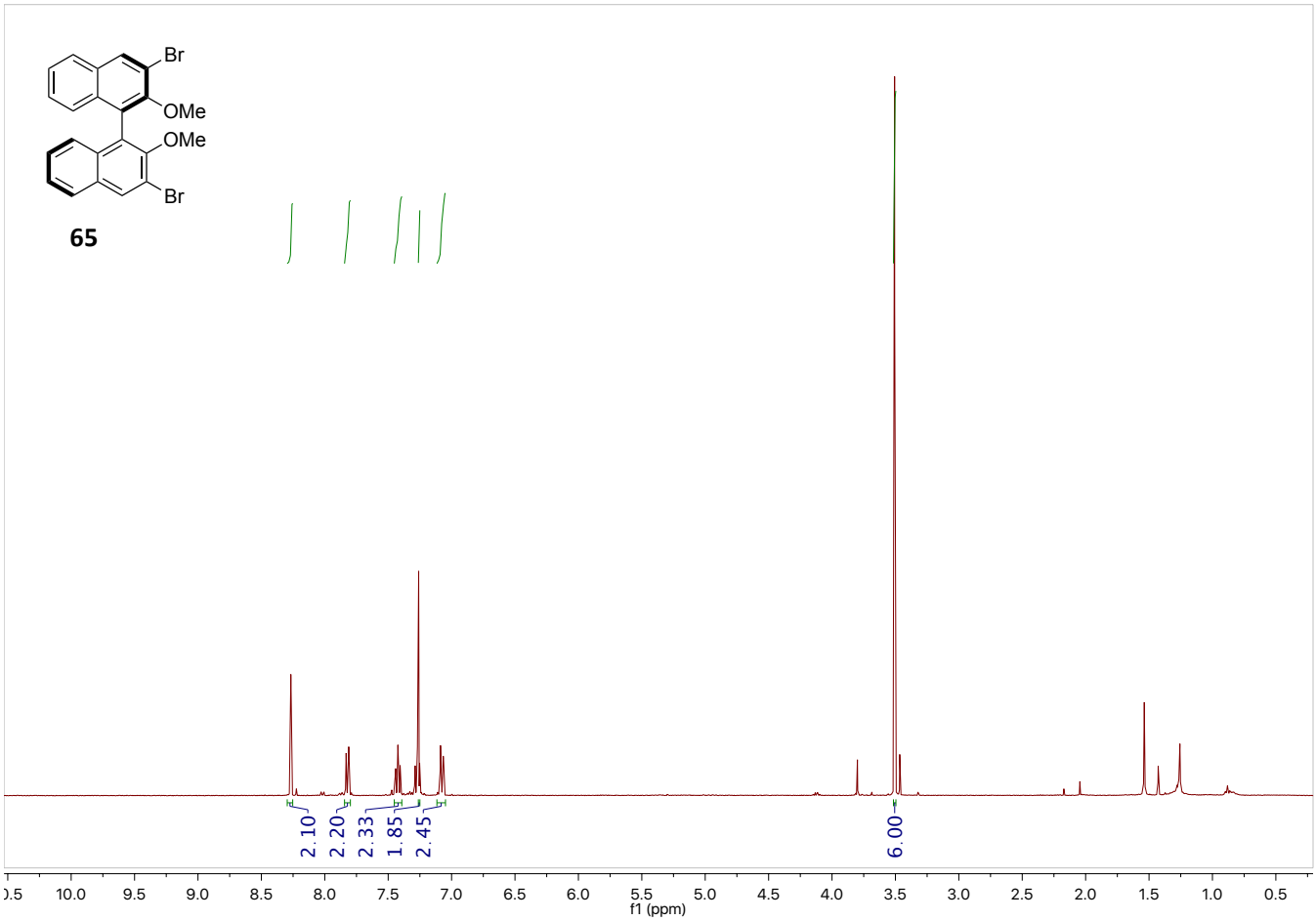
Br
OMe
OMe
Br
65
2.10
2.20
2.33
1.85
2.45
6.00
f1 (ppm)

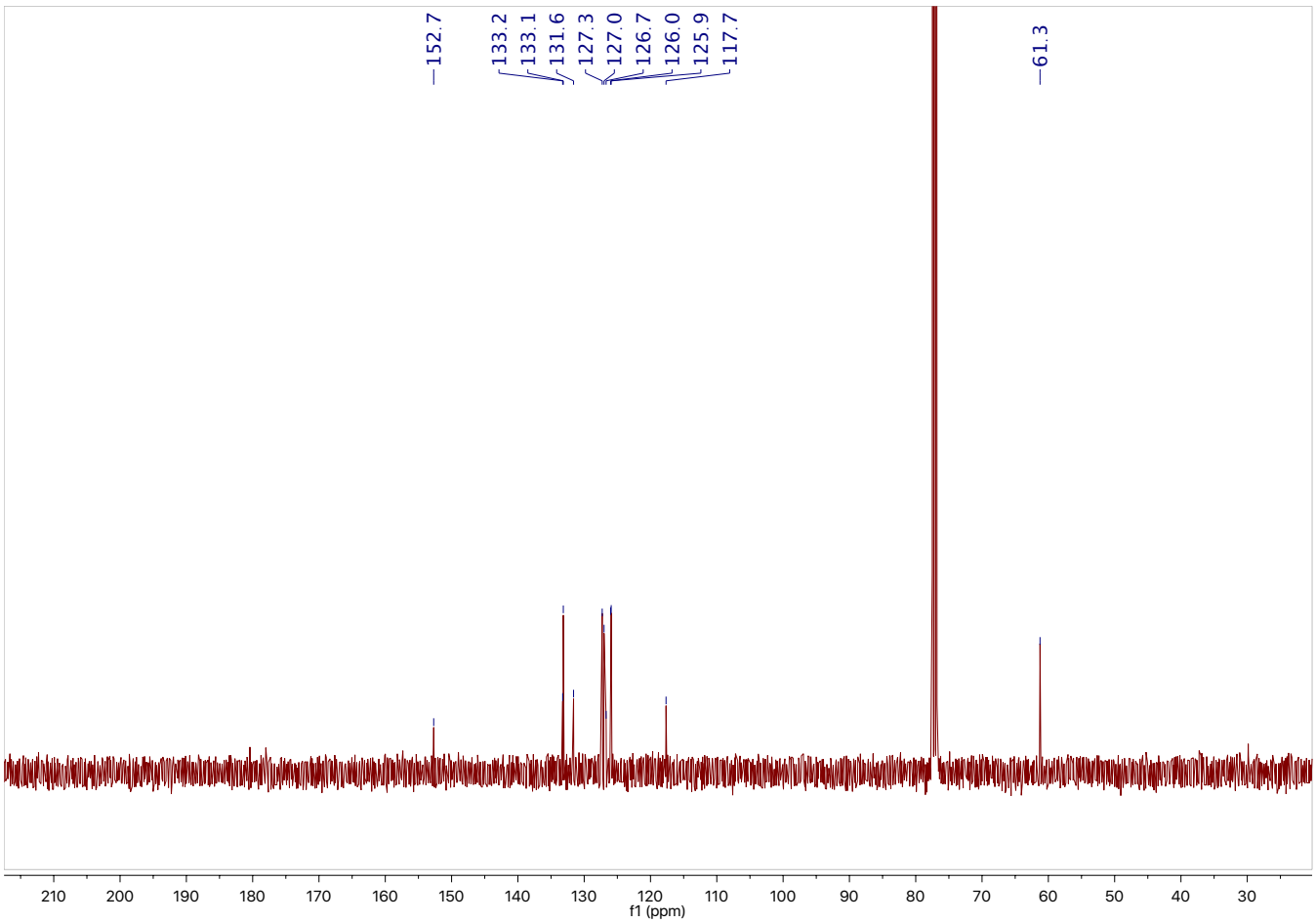
152.7
133.2
133.1
131.6
127.3
127.0
126.7
126.0
125.9
117.7
61.3
f1 (ppm)

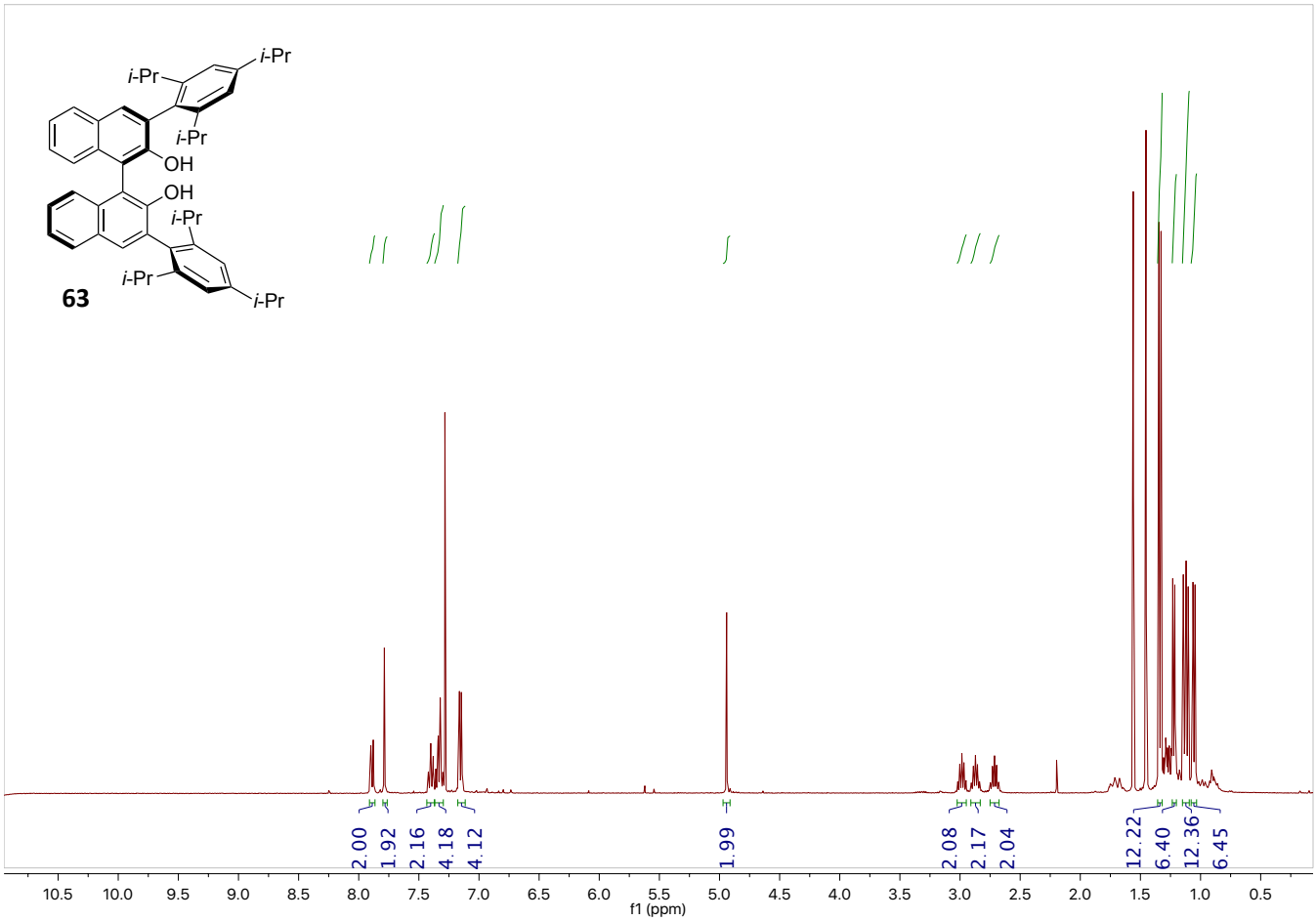
i-Pr
i-Pr
i-Pr
OH
OH
i-Pr
i-Pr
i-Pr
63
2.00
1.92
2.16
4.18
4.12
1.99
2.08
2.17
2.04
12.22
6.40
12.36
6.45
f1 (ppm)

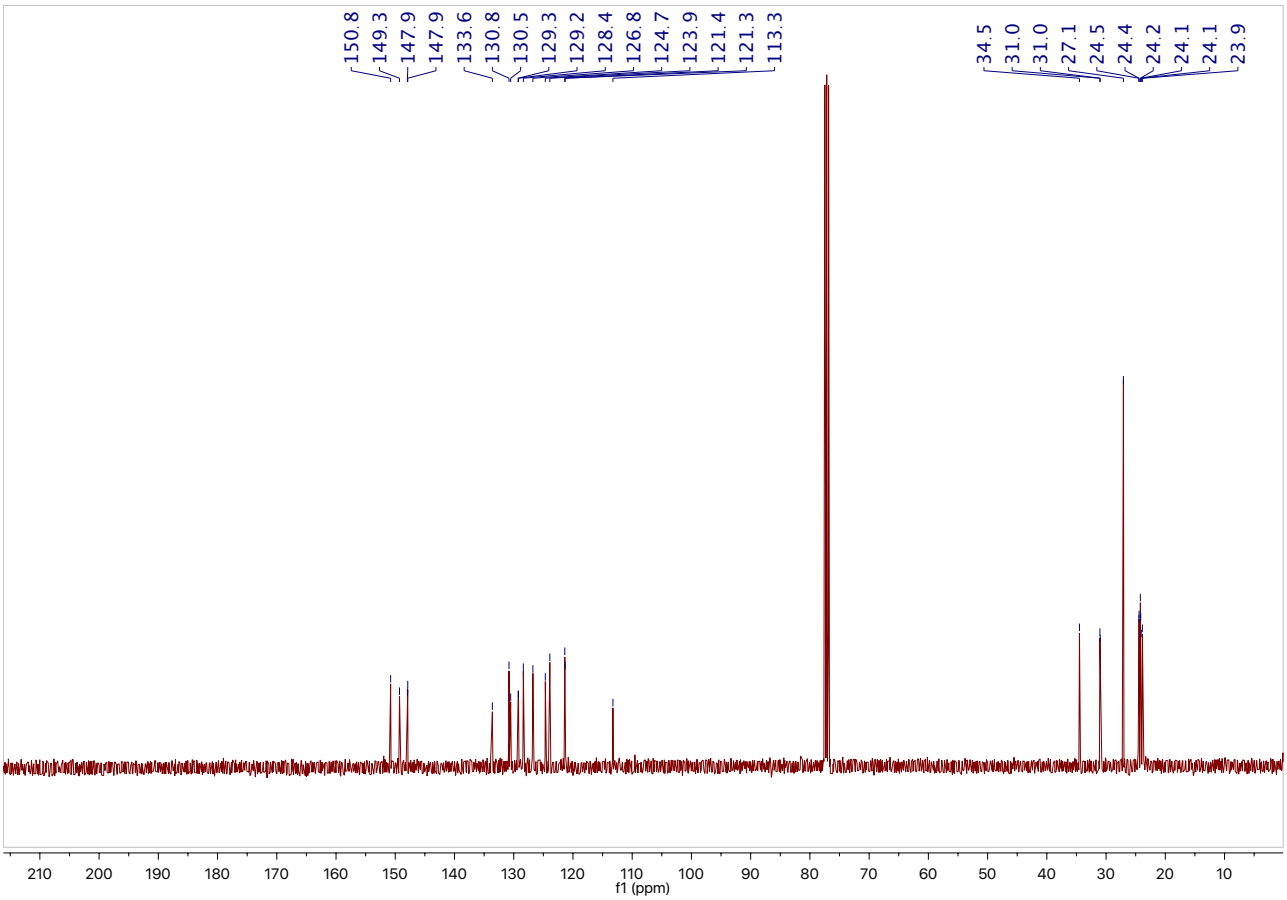
150.8
149.3
147.9
147.9
133.6
130.8
130.5
129.3
129.2
128.4
126.8
124.7
123.9
121.4
121.3
113.3
34.5
31.0
31.0
27.1
24.5
24.4
24.2
24.1
24.1
23.9
f1 (ppm)

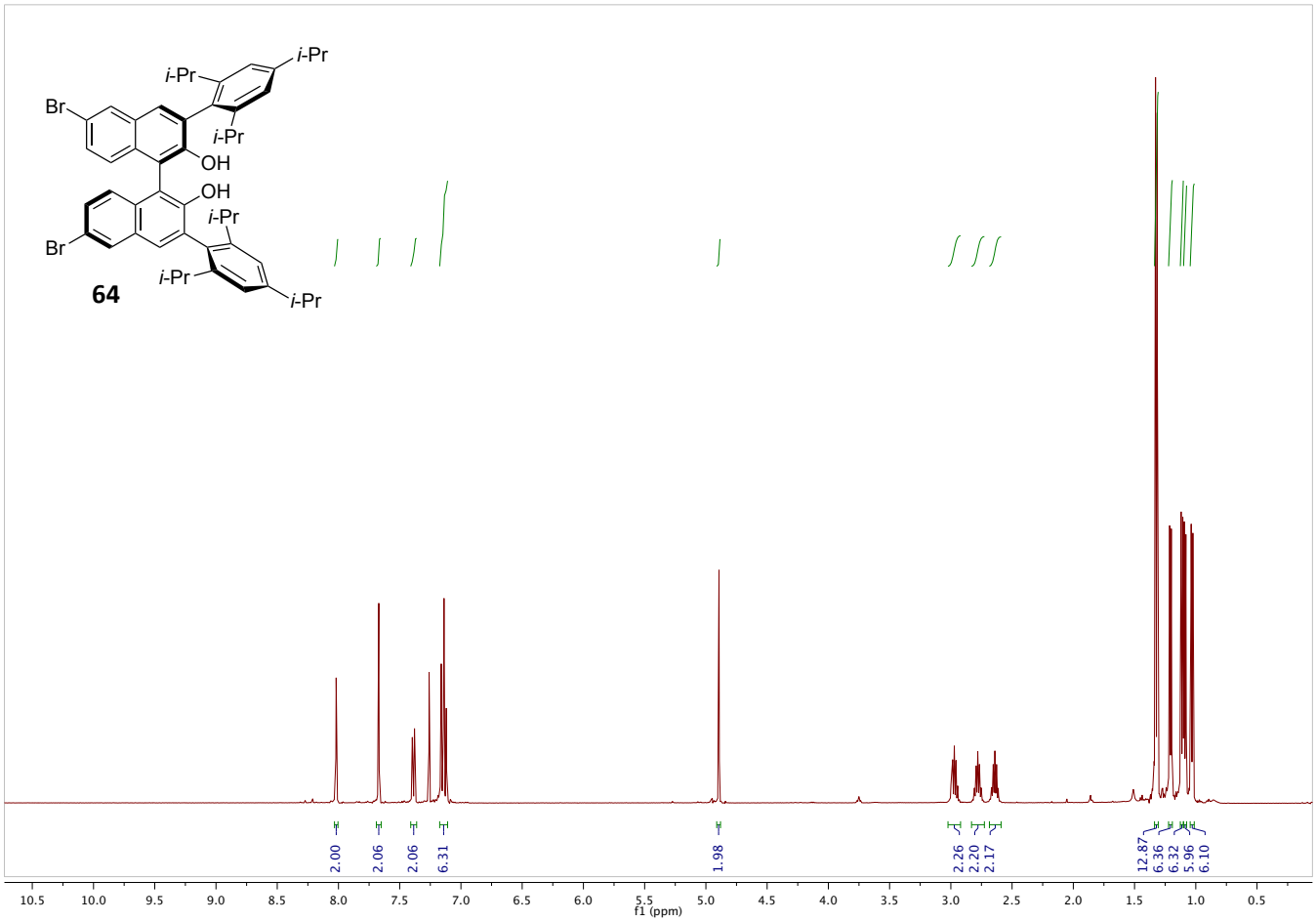
i-Pr
i-Pr
Br
i-Pr
OH
OH
i-Pr
Br
i-Pr
i-Pr
64
2.00
2.06
2.06
6.31
1.98
2.26
2.20
2.17
12.87
6.36
6.32
5.96
6.10
f1 (ppm)

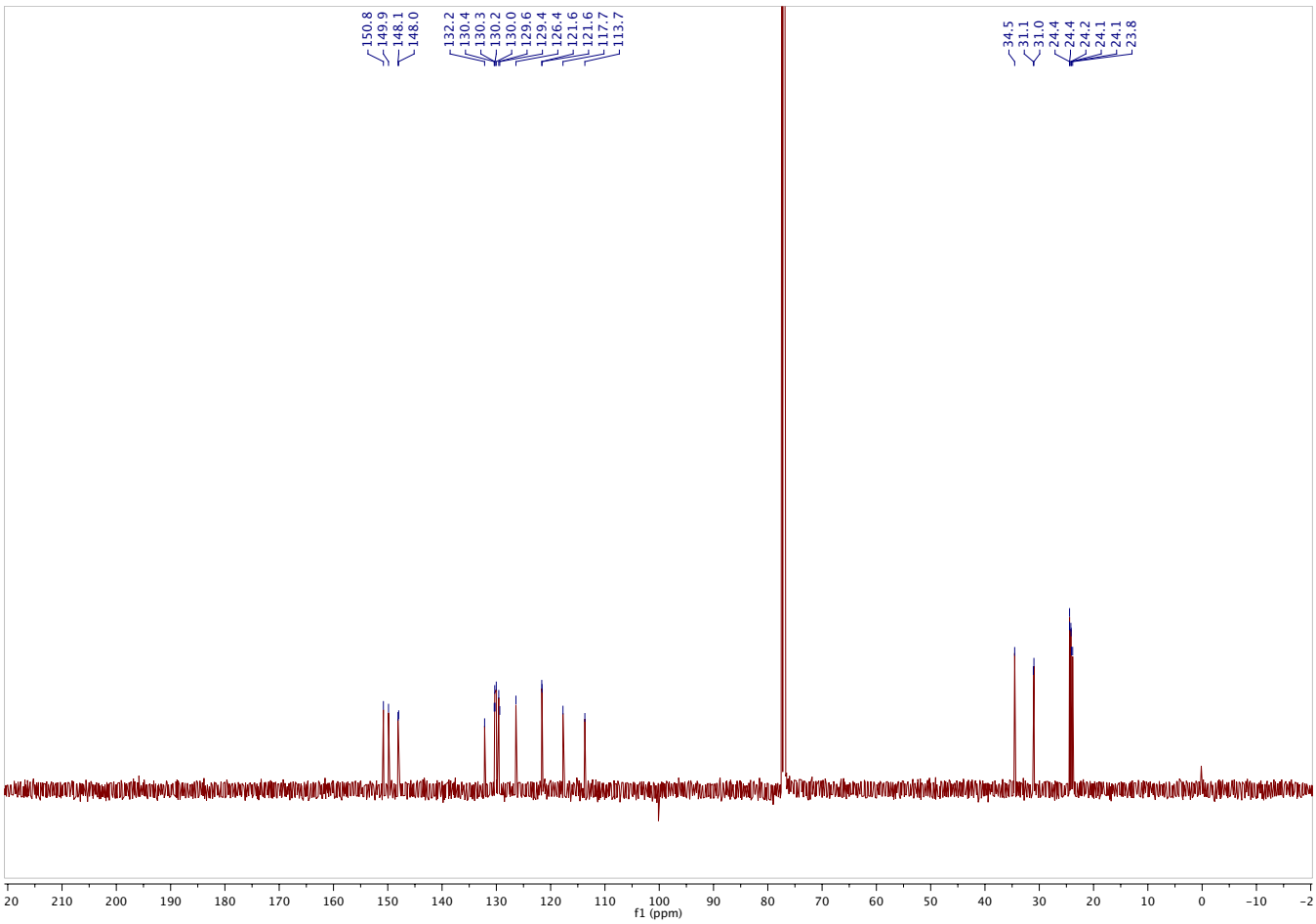
150.8
149.9
148.1
148.0
132.2
130.4
130.3
130.2
130.0
129.6
129.4
126.4
121.6
121.6
117.7
113.7
34.5
31.1
31.0
24.4
24.4
24.2
24.1
24.1
23.8
f1 (ppm)

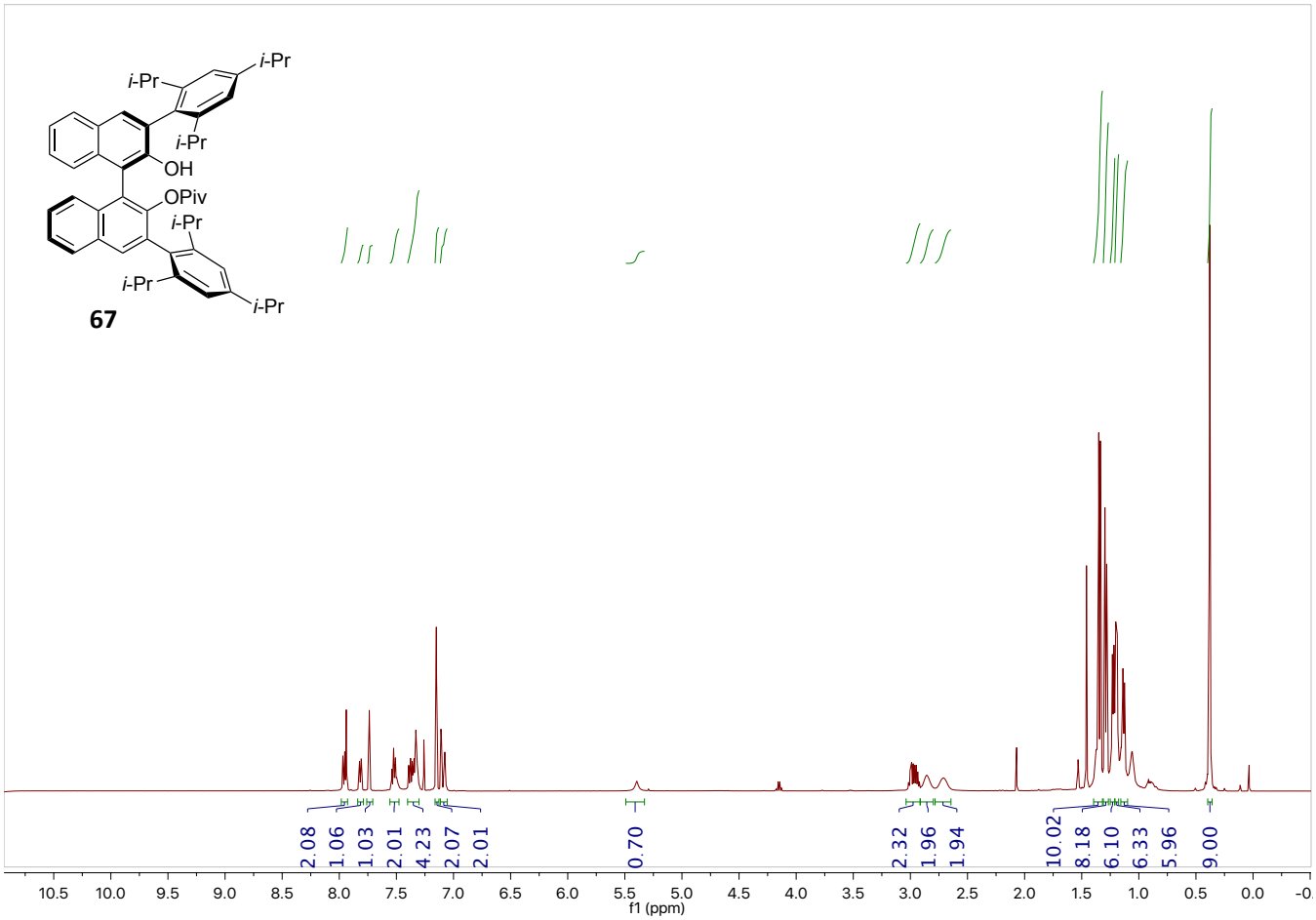
i-Pr
i-Pr
i-Pr
OH
OPiv
i-Pr
i-Pr
i-Pr
67
2.08
1.06
1.03
2.01
4.23
2.07
2.01
0.70
2.32
1.96
1.94
10.02
8.18
6.10
6.33
5.96
9.00
f1 (ppm)

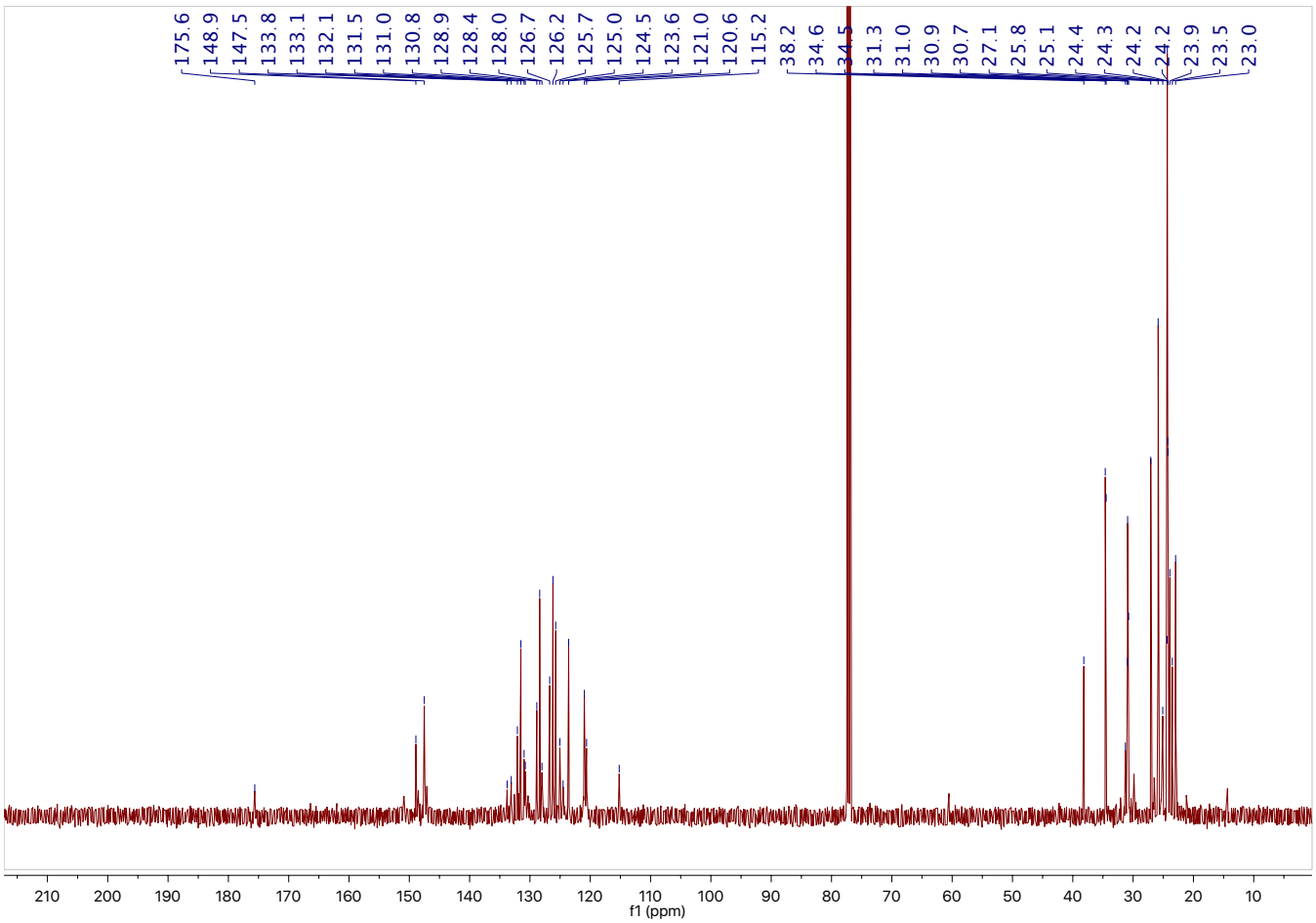
175.6
148.9
147.5
133.8
133.1
132.1
131.5
131.0
130.8
128.9
128.4
128.0
126.7
126.2
125.7
125.0
124.5
123.6
121.0
120.6
115.2
38.2
34.6
34.5
31.3
31.0
30.9
30.7
27.1
25.8
25.1
24.4
24.3
24.2
24.2
23.9
23.5
23.0
f1 (ppm)

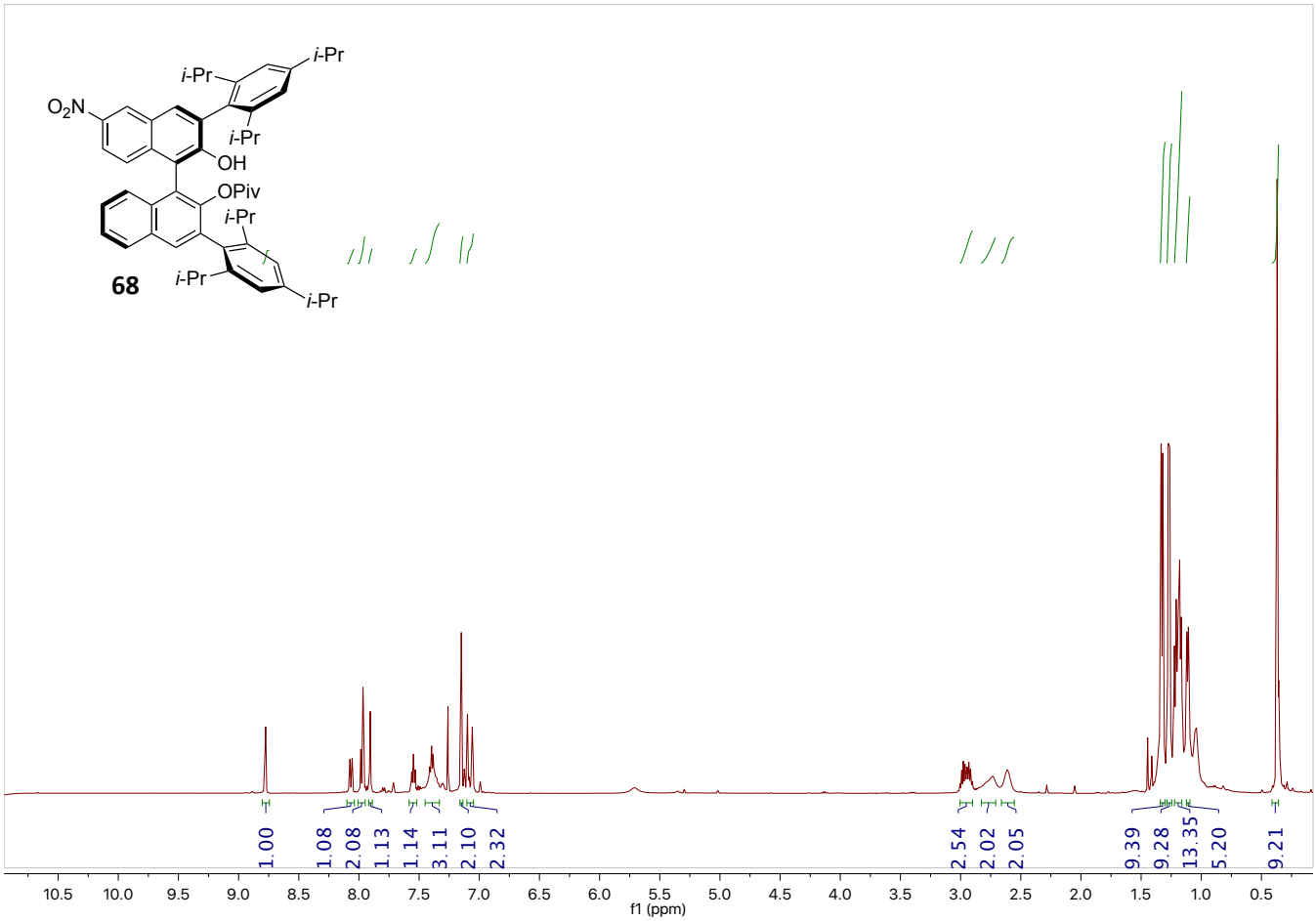
i-Pr
i-Pr
O2N
i-Pr
OH
OPiv
i-Pr
i-Pr
i-Pr
68
1.00
1.08
2.08
1.13
1.14
3.11
2.10
2.32
2.54
2.02
2.05
9.39
9.28
13.35
5.20
9.21
f1 (ppm)

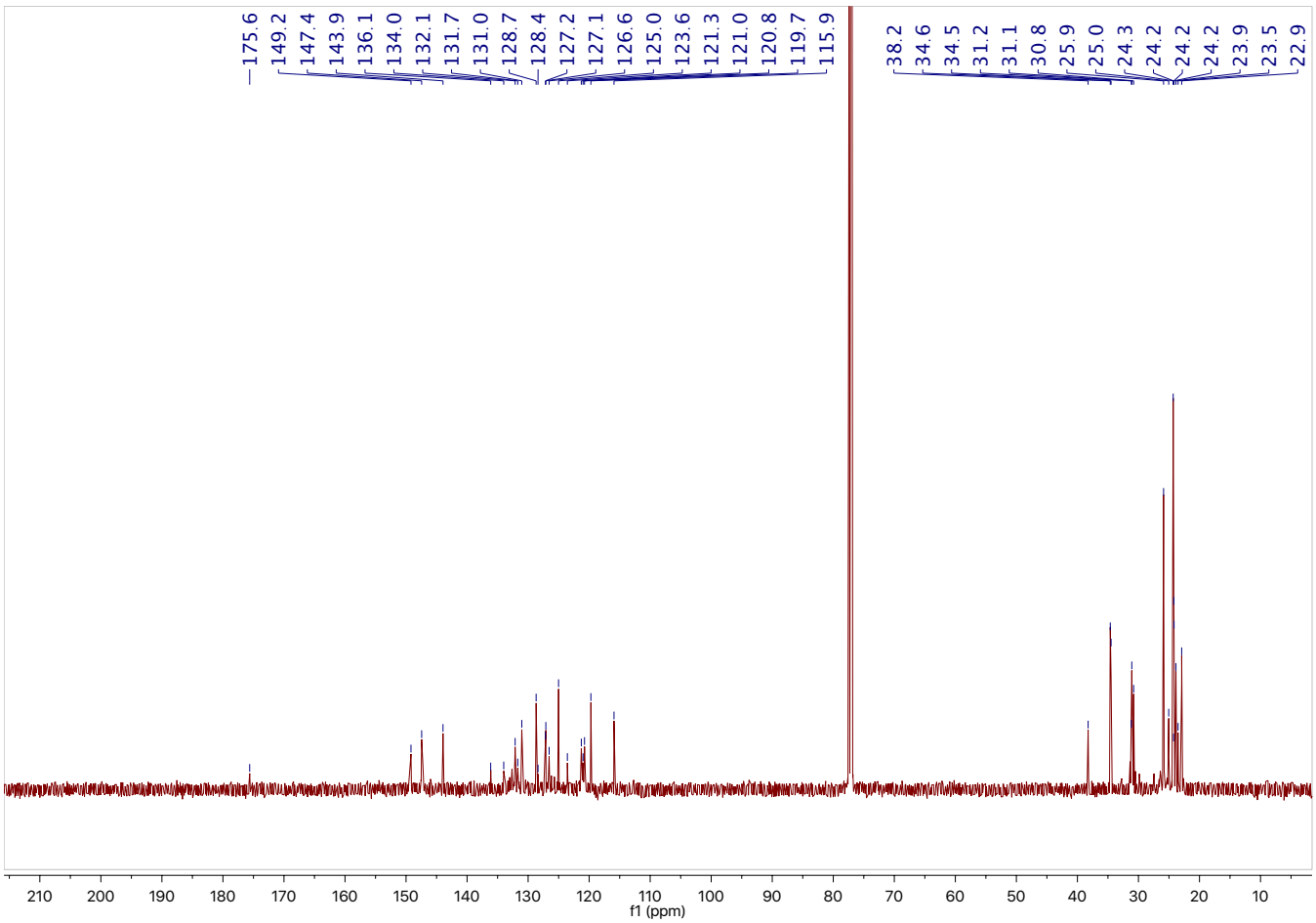
175.6
149.2
147.4
143.9
136.1
134.0
132.1
131.7
131.0
128.7
128.4
127.2
127.1
126.6
125.0
123.6
121.3
121.0
120.8
119.7
115.9
38.2
34.6
34.5
31.2
31.1
30.8
25.9
25.0
24.3
24.2
24.2
24.2
23.9
23.5
22.9
f1 (ppm)

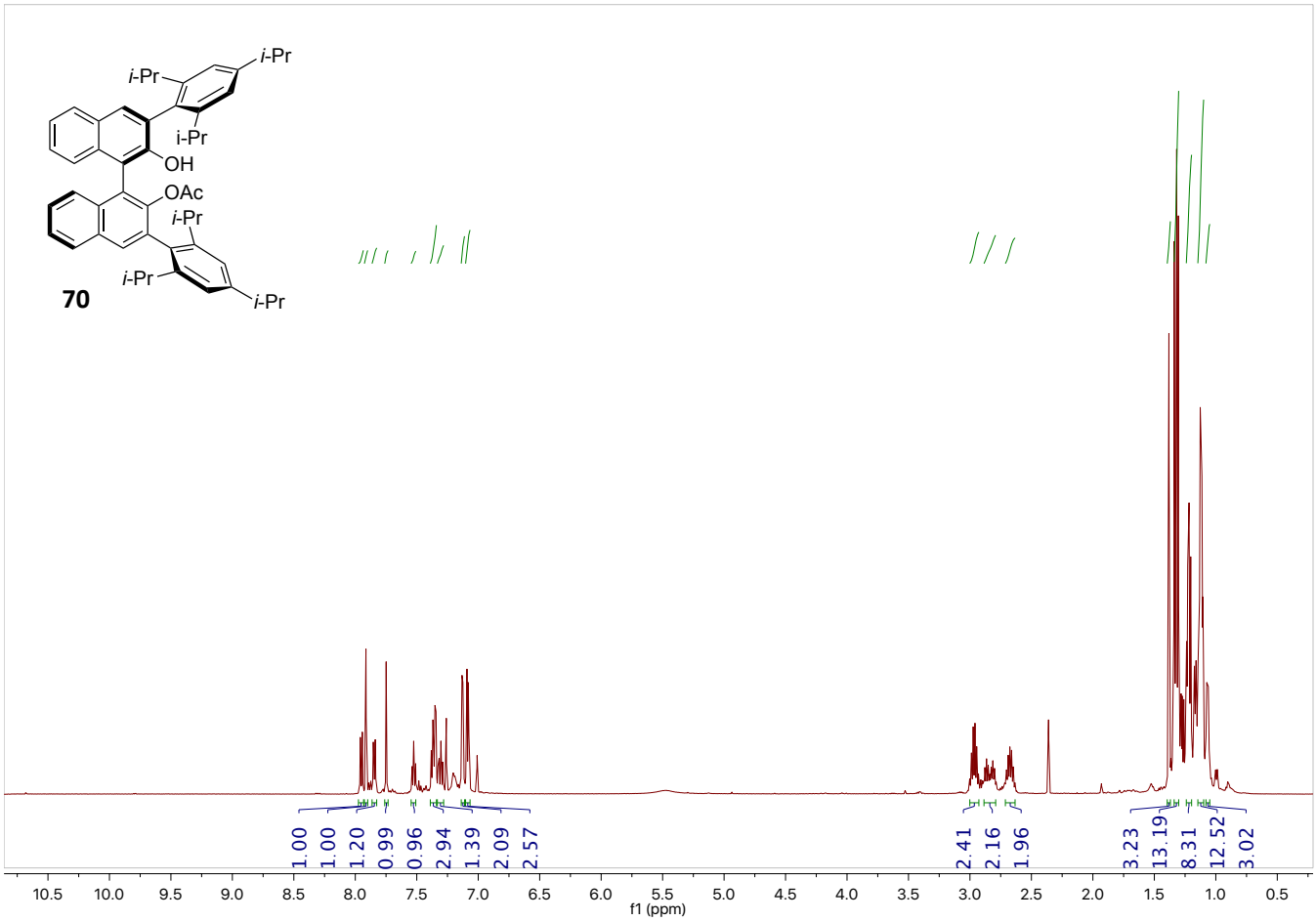
i-Pr
i-Pr
i-Pr
OH
OAc
i-Pr
i-Pr
i-Pr
70
1.00 1.00 1.20 0.99 0.96 2.94 1.39 2.09 2.57
2.41 2.16 1.96
3.23 13.19 8.31 12.52 3.02
f1 (ppm)

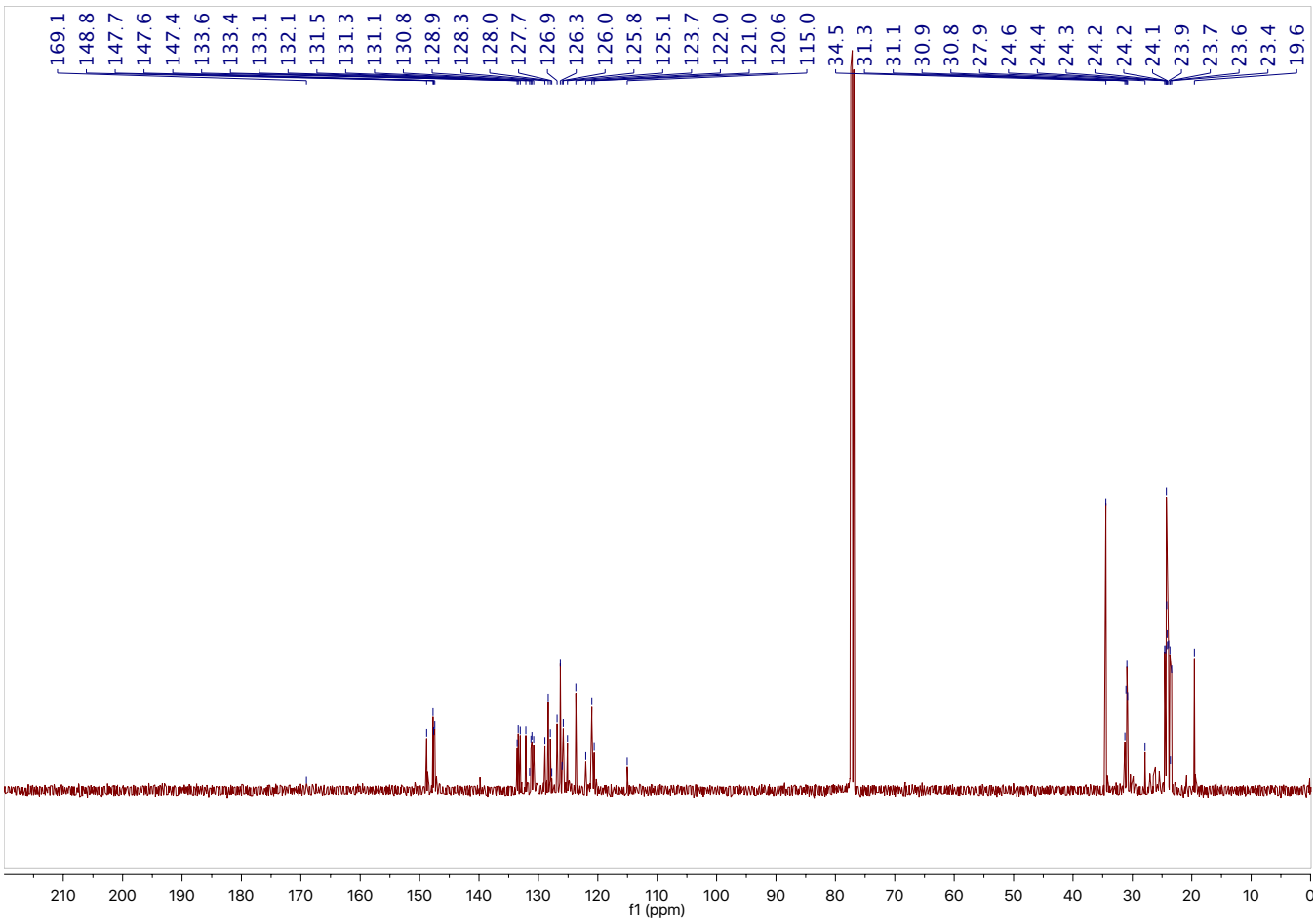
169.1 148.8 147.7 147.6 147.4 133.6 133.4 133.1 132.1 131.5 131.3 131.1 130.8 128.9 128.3 128.0 127.7 126.9 126.3 126.0 125.8 125.1 123.7 122.0 121.0 120.6 115.0
34.5 31.3 31.1 30.9 30.8 27.9 24.6 24.4 24.3 24.2 24.2 24.1 23.9 23.7 23.6 23.4 19.6
f1 (ppm)

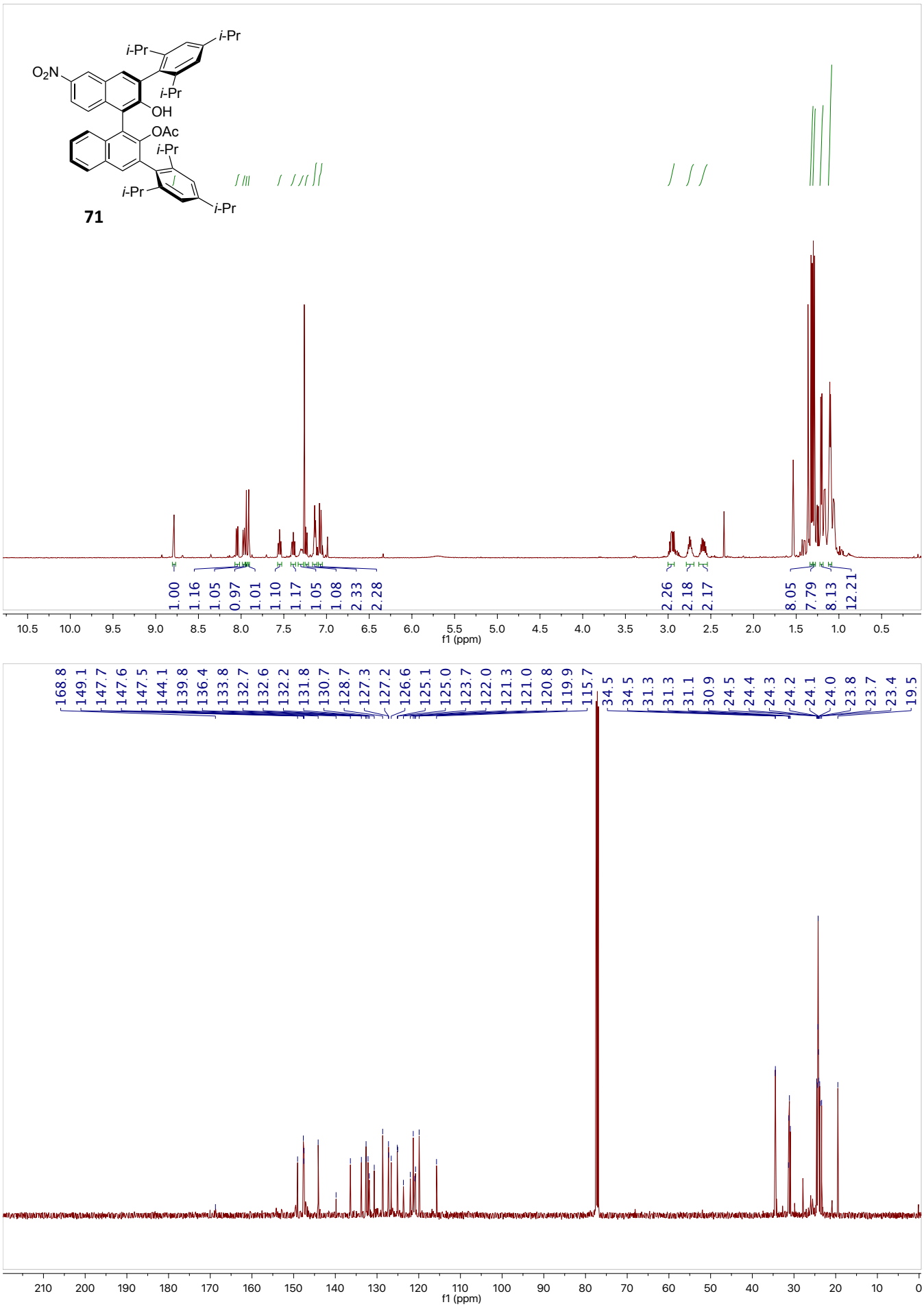
i-Pr
i-Pr
O2N
i-Pr
OH
OAc
i-Pr
i-Pr
i-Pr
71
1.00 1.16 1.05 0.97 1.01 1.10 1.17 1.05 1.08 2.33 2.28
2.26 2.18 2.17
8.05 7.79 8.13 12.21
f1 (ppm)
168.8 149.1 147.7 147.6 147.5 144.1 139.8 136.4 133.8 132.7 132.6 132.2 131.8 130.7 128.7 127.3 127.2 126.6 125.1 125.0 123.7 122.0 121.3 121.0 120.8 119.9 115.7
34.5 34.5 31.3 31.3 31.1 30.9 24.5 24.4 24.3 24.2 24.1 24.0 23.8 23.7 23.4 19.5
f1 (ppm)

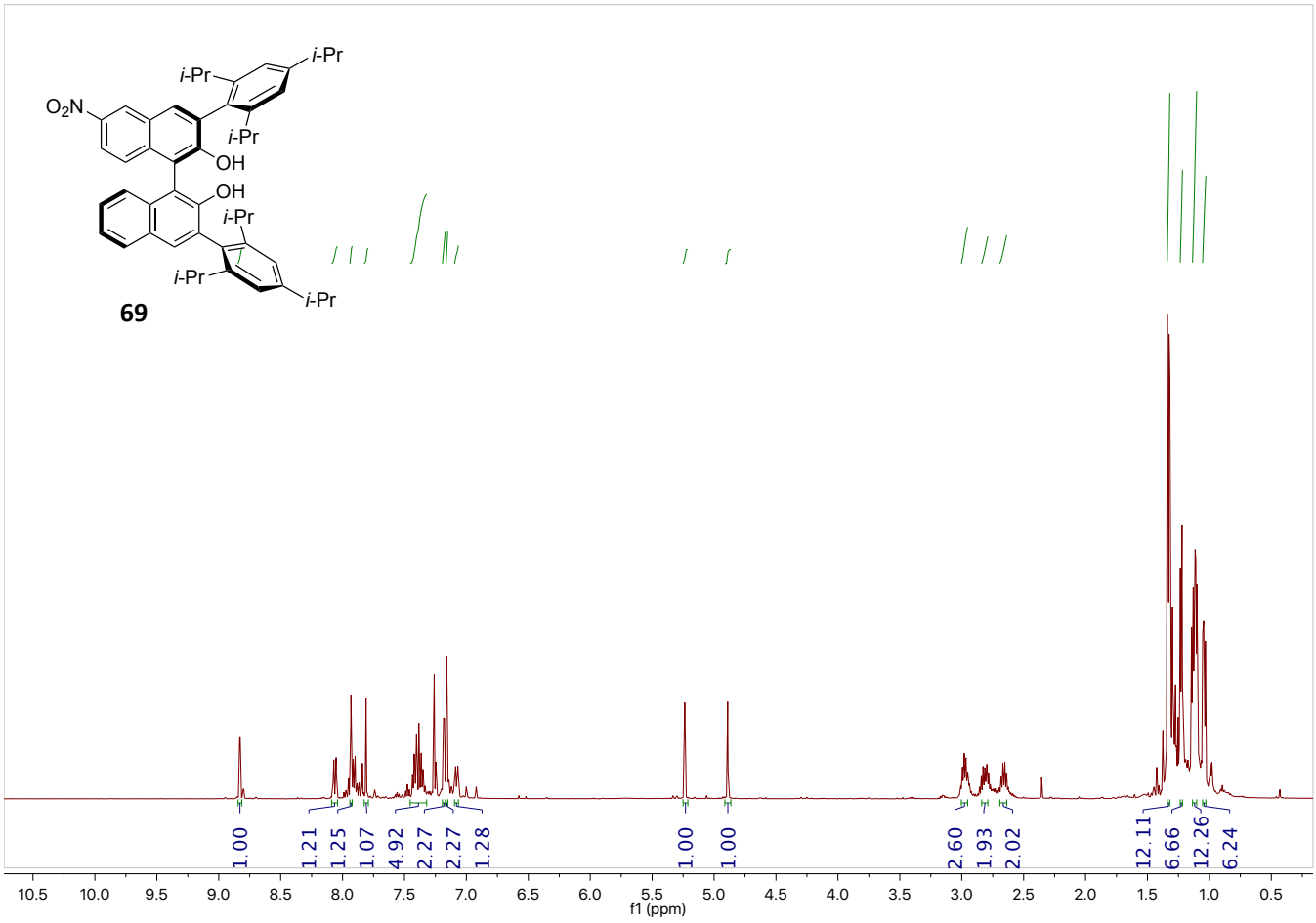
i-Pr
i-Pr
O2N
i-Pr
OH
OH
i-Pr
i-Pr
i-Pr
69
1.00
1.21
1.25
1.07
4.92
2.27
2.27
1.28
1.00
1.00
2.60
1.93
2.02
12.11
6.66
12.26
6.24
f1 (ppm)

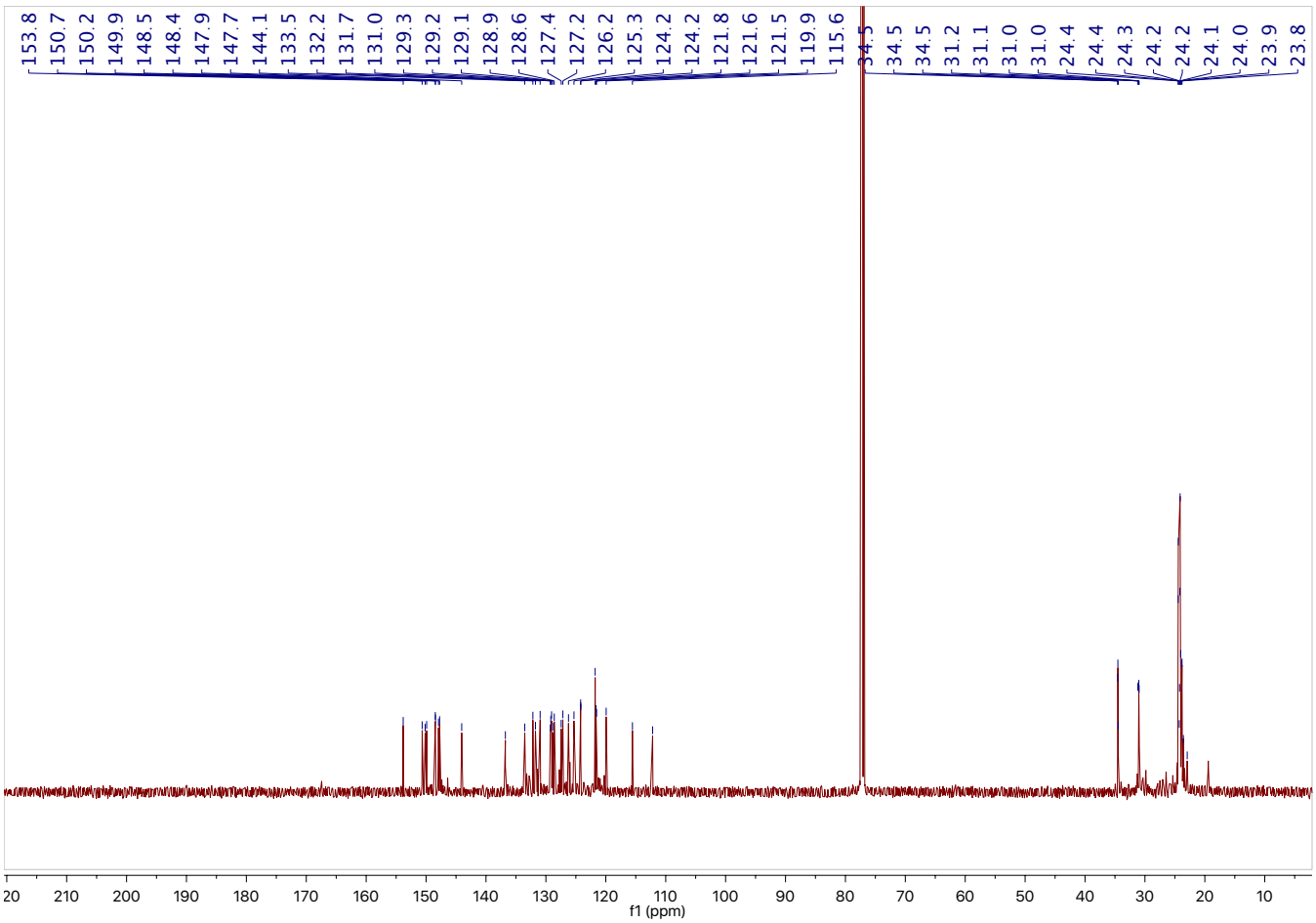
153.8
150.7
150.2
149.9
148.5
148.4
147.9
147.7
144.1
133.5
132.2
131.7
131.0
129.3
129.2
129.1
128.9
128.6
127.4
127.2
126.2
125.3
124.2
124.2
121.8
121.6
121.5
119.9
115.6
34.5
34.5
34.5
31.2
31.1
31.0
31.0
24.4
24.4
24.3
24.2
24.2
24.1
24.0
23.9
23.8
f1 (ppm)

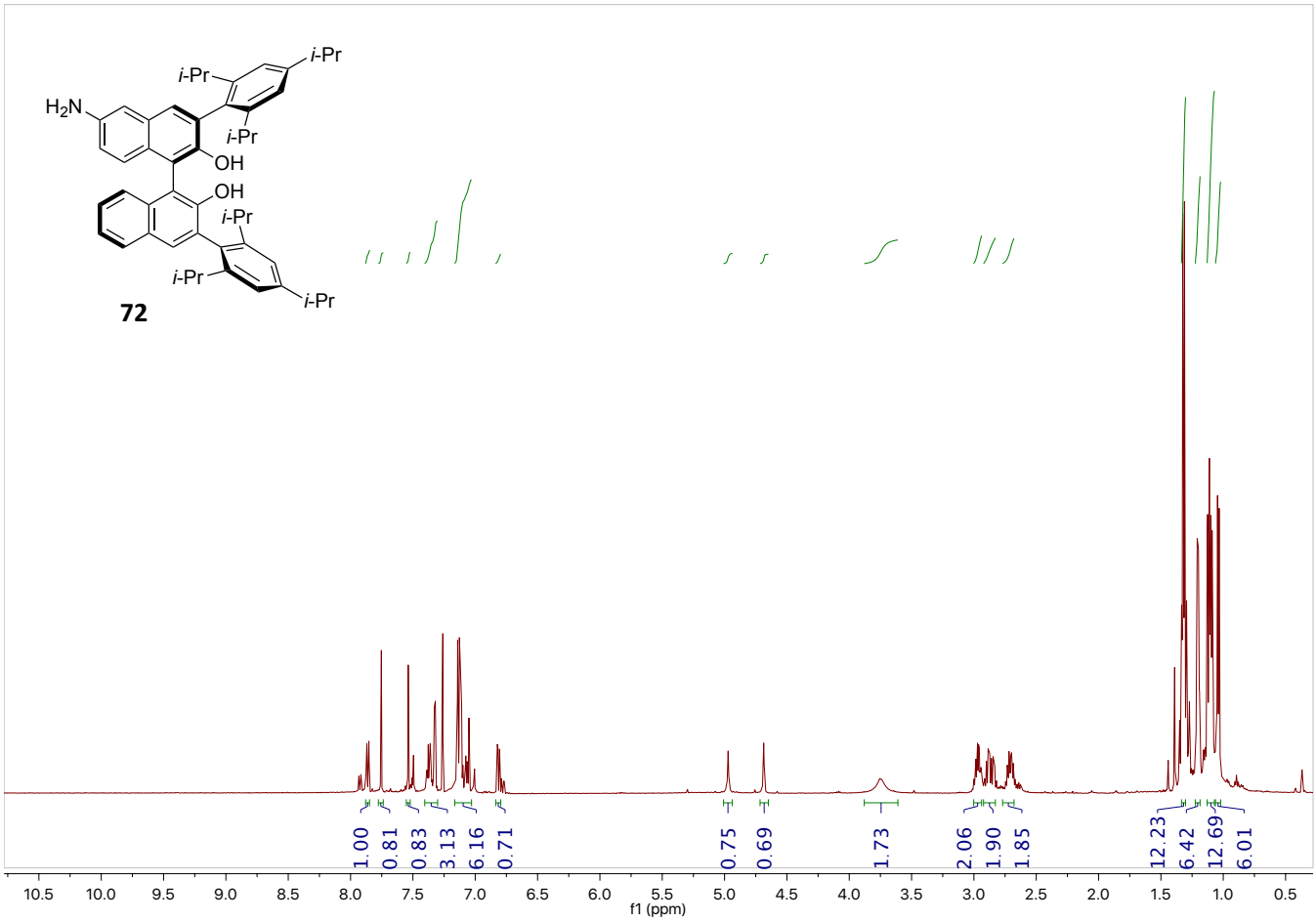
i-Pr
i-Pr
i-Pr
H2N
OH
OH
i-Pr
i-Pr
i-Pr
72
1.00
0.81
0.83
3.13
6.16
0.71
0.75
0.69
1.73
2.06
1.90
1.85
12.23
6.42
12.69
6.01
f1 (ppm)

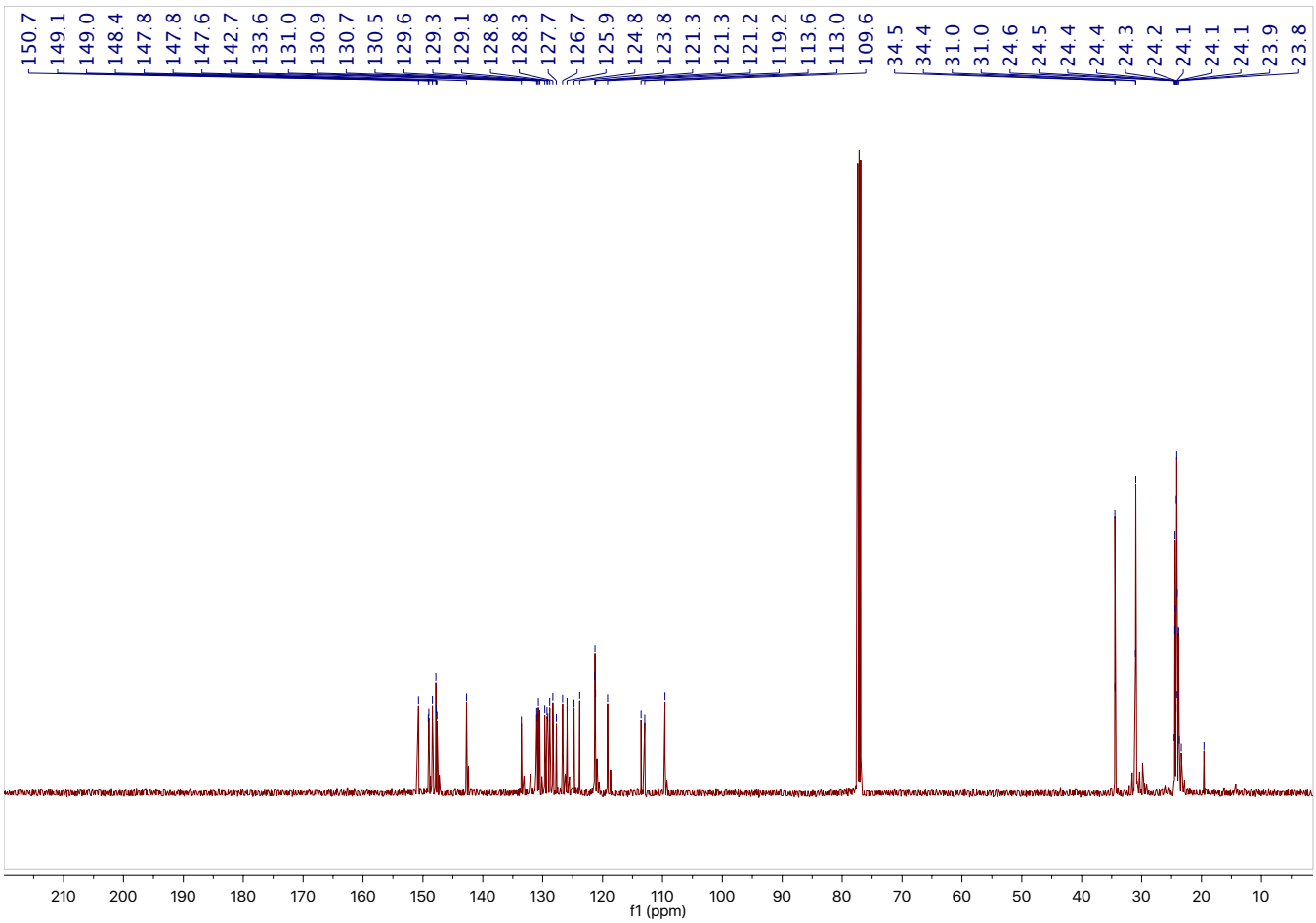
150.7
149.1
149.0
148.4
147.8
147.8
147.6
142.7
133.6
131.0
130.9
130.7
130.5
129.6
129.3
129.1
128.8
128.3
127.7
126.7
125.9
124.8
123.8
121.3
121.3
121.2
119.2
113.6
113.0
109.6
34.5
34.4
31.0
31.0
24.6
24.5
24.4
24.4
24.3
24.2
24.1
24.1
24.1
23.9
23.8
f1 (ppm)

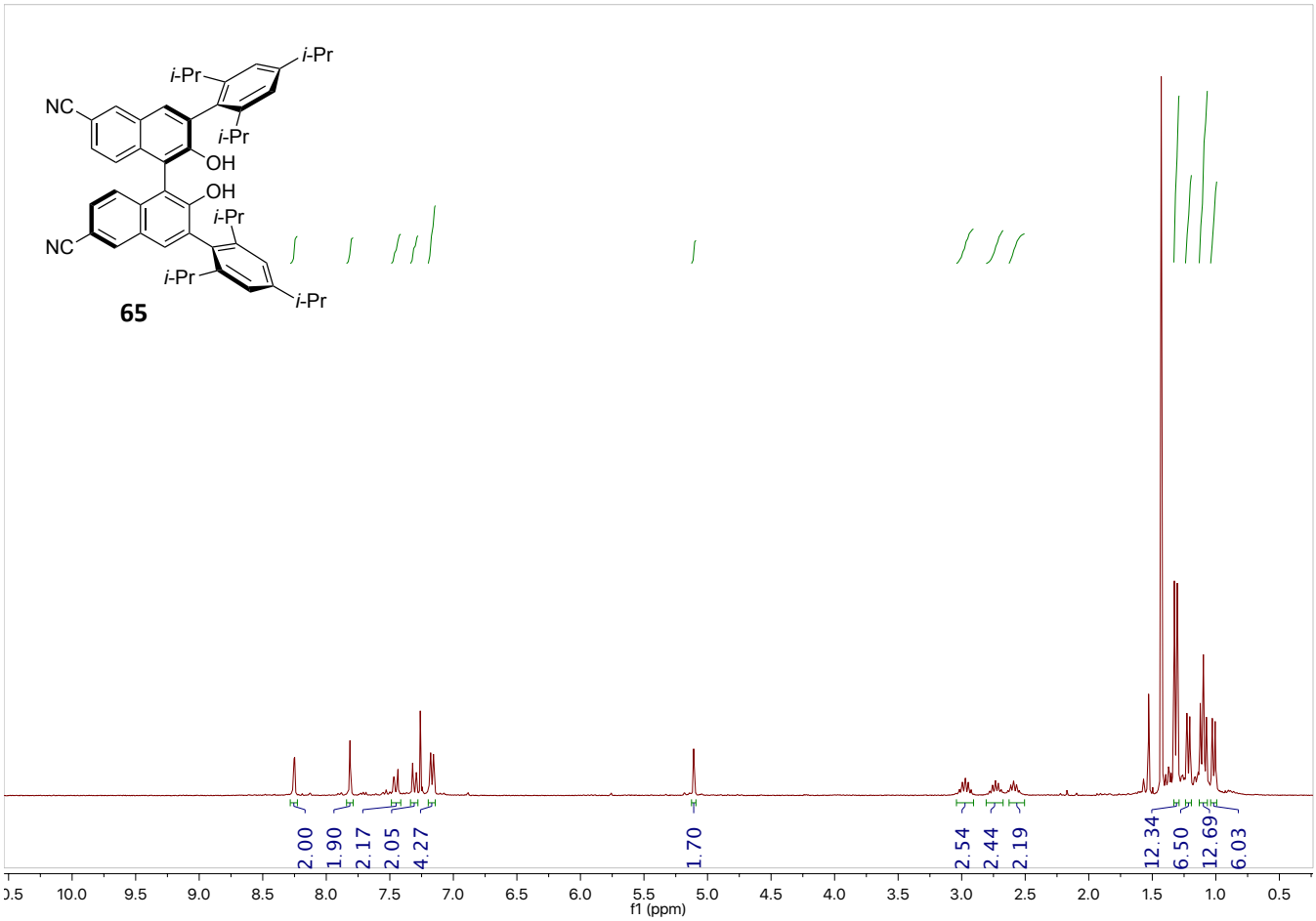
i-Pr
i-Pr
NC
i-Pr
OH
OH
i-Pr
NC
i-Pr
i-Pr
65
2.00
1.90
2.17
2.05
4.27
1.70
2.54
2.44
2.19
12.34
6.50
12.69
6.03
f1 (ppm)

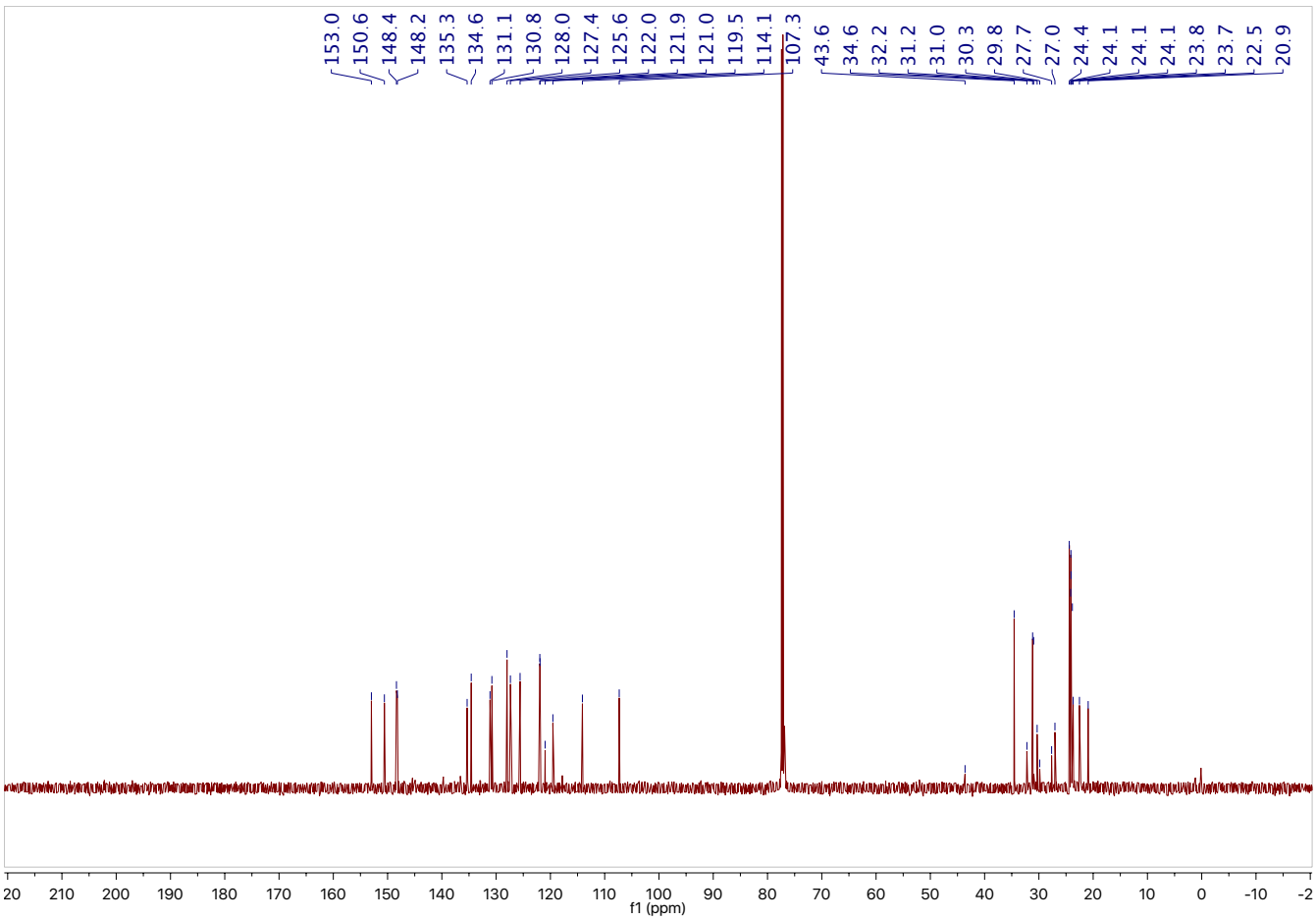
153.0
150.6
148.4
148.2
135.3
134.6
131.1
130.8
128.0
127.4
125.6
122.0
121.9
121.0
119.5
114.1
107.3
43.6
34.6
32.2
31.2
31.0
30.3
29.8
27.7
27.0
24.4
24.1
24.1
24.1
23.8
23.7
22.5
20.9
f1 (ppm)

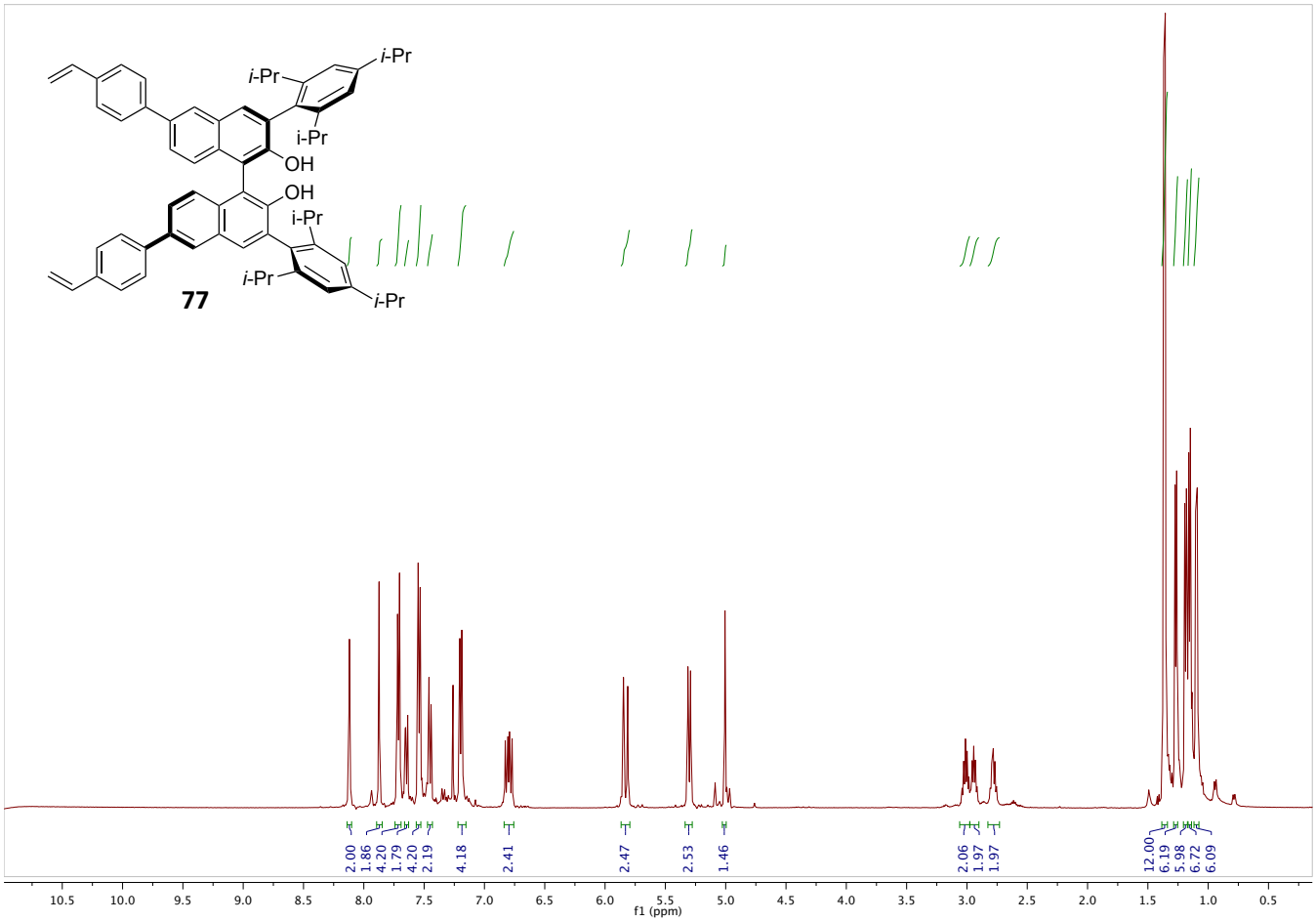
i-Pr
i-Pr
i-Pr
OH
OH
i-Pr
i-Pr
i-Pr
77
2.00
1.86
4.20
1.79
4.20
2.19
4.18
2.41
2.47
2.53
1.46
2.06
1.97
1.97
12.00
6.19
5.98
6.72
6.09
f1 (ppm)

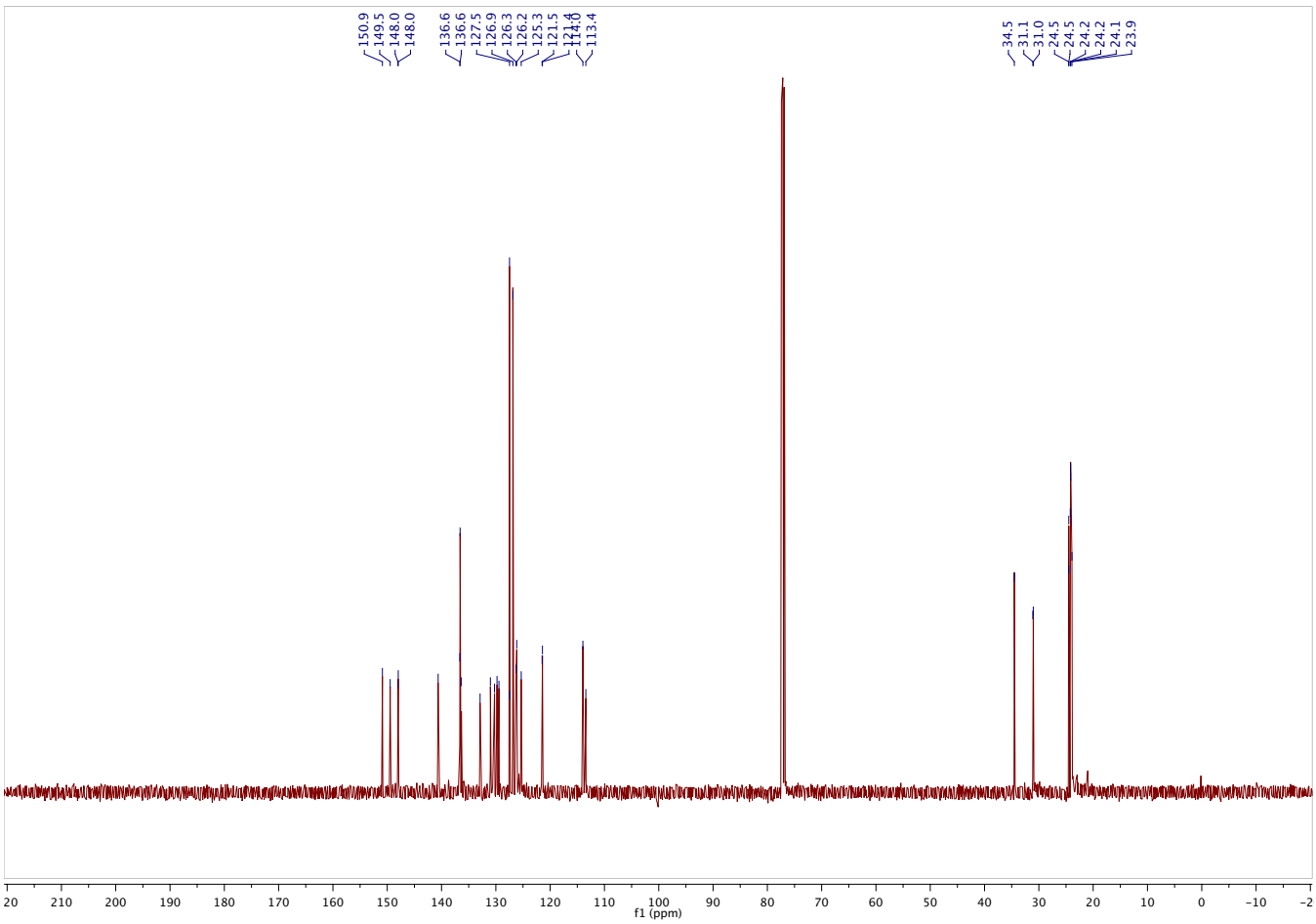
150.9
149.5
148.0
148.0
136.6
136.6
127.5
126.9
126.3
126.2
125.3
121.5
113.4
34.5
31.1
31.0
24.5
24.5
24.2
24.2
24.1
23.9
f1 (ppm)

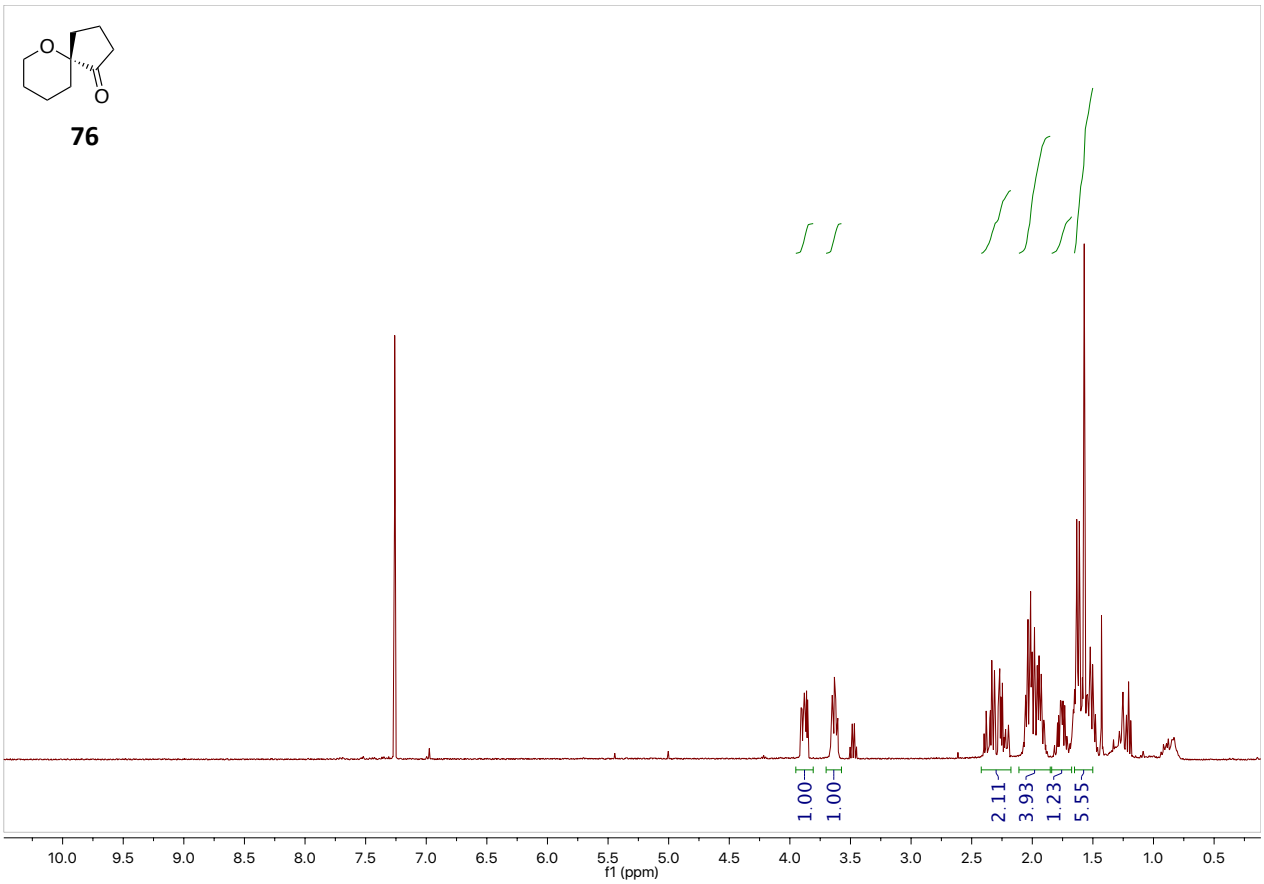
76
1.00
1.00
2.11
3.93
1.23
5.55
f1 (ppm)

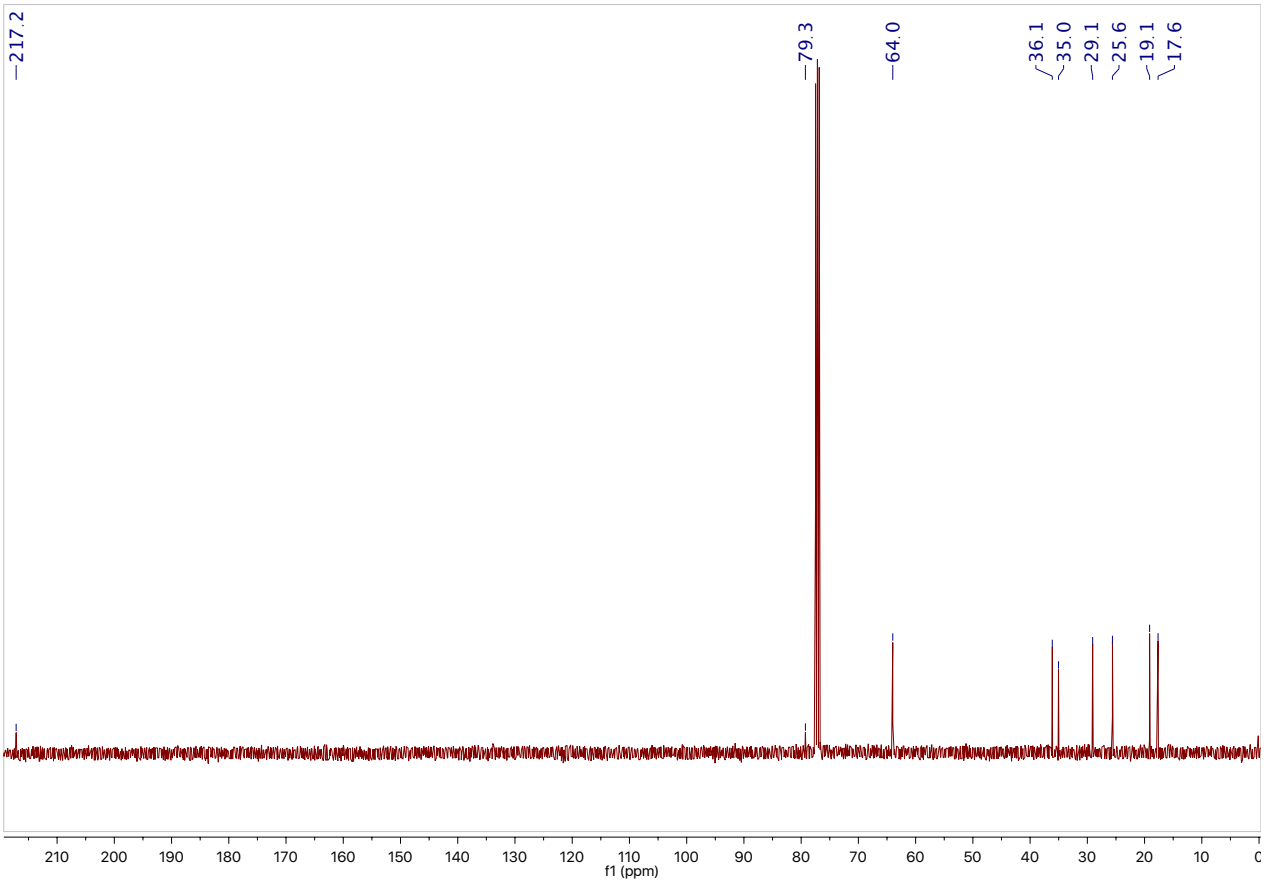
217.2
79.3
64.0
36.1
35.0
29.1
25.6
19.1
17.6
f1 (ppm)

UNIVERSITAT ROVIRA I VIRGILI
IMMOBILIZATION OF CHIRAL BRØNSTED ACIDS AND LEWIS BASES FOR BATCH AND FLOW ENANTIOSELECTIVE CATALYSIS
Lidia Clot Almenara

CHAPTER III

UNIVERSITAT ROVIRA I VIRGILI
IMMOBILIZATION OF CHIRAL BRØNSTED ACIDS AND LEWIS BASES FOR BATCH AND FLOW ENANTIOSELECTIVE CATALYSIS
Lidia Clot Almenara

Chapter III

Catalytic Enantioselective Allylation of Aldehydes with PS-TRIP

3.1. Background on Asymmetric Allylation of Aldehydes

The discovery of new synthetic routes for the synthesis of natural and unnatural products or bioactive compounds remains a challenge in organic chemistry.[1] The asymmetric allylation of carbonyl compounds has proven to be one of the most straightforward ways for the construction of C-C bonds forming valuable chiral substances.[2] Allylation of carbonyls is a well-known reaction that gives rise to optically active homoallylic alcohols,[3] which are simple but versatile intermediates employed in the synthesis of optically active complex molecules of great importance (Figure 3.1).[4]

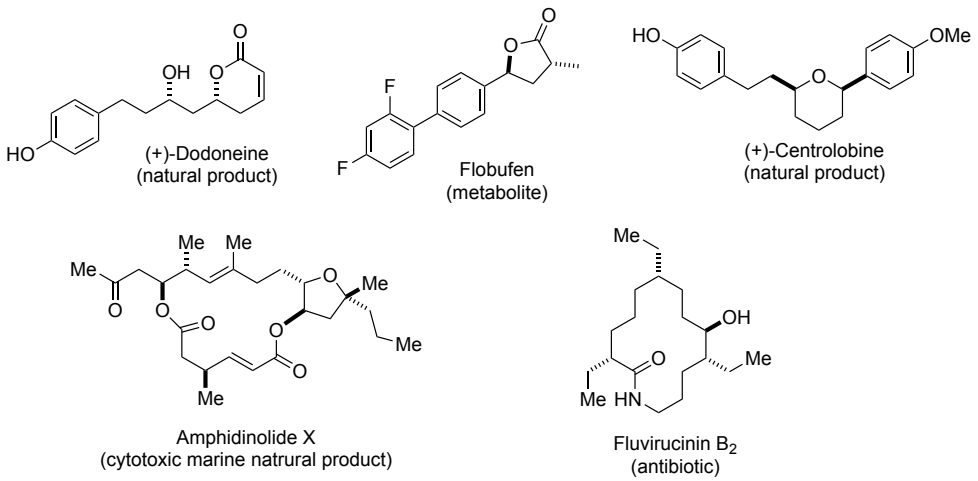

Figure 3.1: The synthesis of these natural products includes an allylation of aldehydes step.

Remarkable progress has been achieved since the pioneering work of Hoffman in the diastereoselective synthesis of homoallylic alcohols employing (*E*)- and (*Z*)-crotylboronates.[5] Over the years, different alternative pathways for the asymmetric allylation of aldehydes have been developed.[6] Within this area, Brown[7] (scheme 3.1, eq. 1) and Roush[8] (scheme 3.1, eq. 2) made the most significant breakthroughs. Initial studies from Brown reported the formation of chiral homoallylic alcohols from allylboranes and aldehydes. Brown described that the boron coordination to the oxygen of the aldehyde followed a Zimmerman-Traxler transition state model, where the allylic double bond attacks the electrophilic carbon of the aldehyde forming a new C-C bond. In the case of starting with crotyl reagents, the chiral transition state blocks the stereochemistry, thus the *Z*-isomer gives the *syn* adduct, and the *E*-isomer gives the *anti*. Later, Roush[9] studied the use of more stable allylboronates,[10] which are advantageous because they can stabilize the transition state through interaction between the tartrate ester carbonyl group and the aldehyde carbonyl. However, under these conditions there is a decrease in ee and yield.

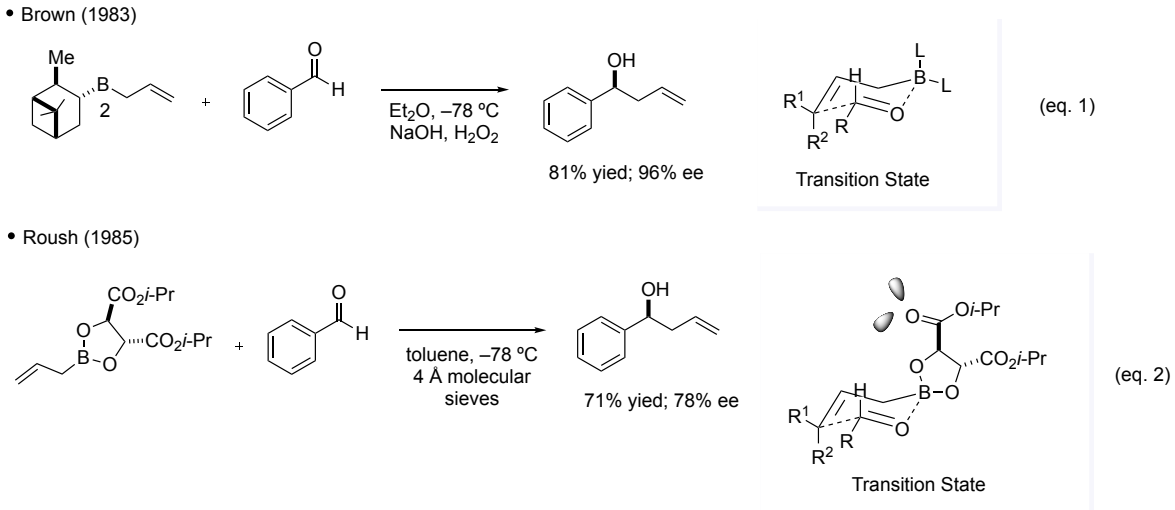

Scheme 3.1: Brown and Roush allylation of aldehydes with boron reagents.

Alternatives methodologies for the production of chiral homoallylic alcohols based on stoichiometric chiral allylating reagents[3e, 11] involve the works by Masamune,[12] Corey,[13] Riediker,[14] Leighton,[15] Chong,[16] Soderquist,[17] and Aggarwal[18] (Figure 3.2).

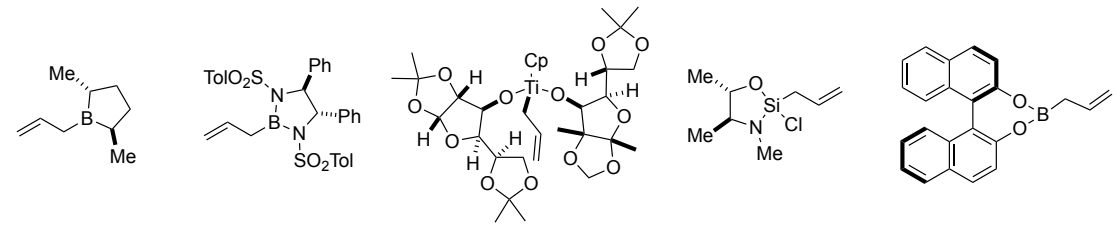

Figure 3.2: Representative chiral allylating reagents.

Recent publications detailing the preparation of homoallylic alcohols in a stereocontrolled manner are led by the works of Buse and Heathcock, Hoffman and Zeiss, and Yamamoto *et al.* Allylating agents containing elements such as boron,[7a, 18-19] silicon[11a, 20] and tin[21] have been popularized due to their stability and the ability to predict the relative and absolute configuration of the products. Common strategies have been based on the use of allylic organometallic reagents,[22] in which the metal is ligated by chiral modifiers.[23] In this category, allylic borane and allylic titanium reagents showed excellent diastereocontrol because the organizational features of the metal center allow the chiral modifier to be in a proximal position to the reacting nucleophile (Scheme 3.3). The main drawback associated to these compounds is the requirement of stoichiometric amounts of the chiral ligand.[24] On the other hand, the related allylic reagents derived from lithium,[25] magnesium or zinc turn out to be more unstable and, consequently, the resulting crotyl compounds are obtained as a mixture of *E*- and *Z*-isomers even at low temperature.[26] In order to solve the main problem with the relative stereoselection in allylation of aldehydes,[23b] groups as Knochel's employed the

use of masked allylic zinc reagents,[27] which can be generated *in situ* in two sequential steps.[22d, 28] Allylic zinc bromides are obtained after treatment of the corresponding tertiary homoallylic alcohol with *n*-Buli, aldehyde and $ZnCl_2$.

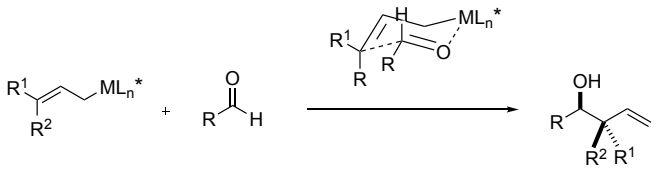

Scheme 3.3: Transition state proposed to account for the stereochemical outcome.

Several routes can be followed for the chiral induction in carbonyl allylation reactions.[2b, 29] We can differentiate two main approaches: inducing the enantioselectivity by one of the starting materials (either a chiral group on the organometallic reagent or the allylating reagent), or by an external element such as a chiral catalyst.

In this chapter, we will be more focused on allylboration using achiral allylboron derivatives in the presence of an external source of chirality.

Early reports employed highly toxic allyl reagents such as allyltin compounds.[2a] In recent publications, less toxic allyltrichlorosilanes[30] and allylboron reagents have emerged as a versatile choice showing wide scope and mild conditions. In particular, pinacol allylboronates[31] have given the most promising results due to the fact that they are air- and water-stable, non-toxic and give rise to high levels of diastereoselectivity.

In 1991, Yamamoto *et al*. were the first to develop a catalytic asymmetric allylation of aldehydes with allylsilanes promoted by chiral (acyloxy)borane.[20e] They achieved high selectivity, albeit the yield were only moderate (Scheme 3.4).

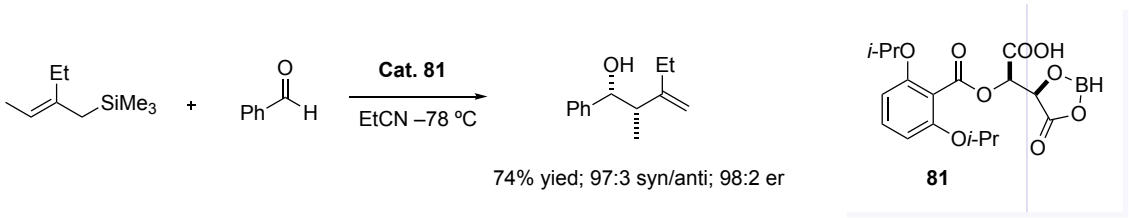

Scheme 3.4: Addition of allylsilanes to aldehydes catalyzed by Lewis acid.

Despite the wide range of synthetic methods for the preparation of homoallylic alcohols, chiral Brønsted acid catalysts have attracted much attention because of the high levels of enantiomeric excess, wide substrate scope, mild conditions and functional group compatibility. This strategy avoids expensive transition-metal catalysts as in the case of Lewis acids or the use of chromium salts.

3.2. Enantioselective Addition of Allylboronate to Aldehydes

3.2.1. Chiral Lewis Acid-Catalyzed Reaction (LA)

Pioneering works in the Lewis acid-mediated synthesis of homoallylic alcohols via addition of allylboronates to aldehydes have been carried out by the groups of Hall and [6e, 32] Ishiyama[33] (Scheme 3.5).

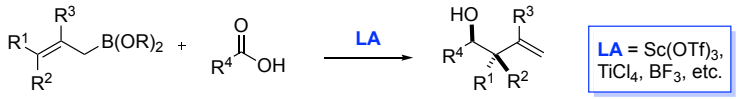

Figure 3.5: General transformation for allyboration of aldehydes catalyzed by LA.

Two possible transition states (TS) have been postulated to account for the mechanism of aldehyde allylation under Lewis acid catalysis (Scheme 3.6). Hall *et al.*[29b] and other groups have been interested in the mechanistic pathway. Their research concludes that: (I) allylboranes and boronates (ML_n = BR_2 and $B(OR)_2$) involve a closed six-membered chair transition state due to the

coordination of the boron center with the aldehyde. Here, the Lewis acid can be coordinated to one oxygen of the boronate or also form a double complexation on the aldehyde and (II) allylstannane[34] and allylsilane analogues[35] ($M'L_n$ = SiR_3, SnR_3) involve an "open" transition structure, where the Lewis acid activates the carbonyl, which generally results in lower diastereoselectivity levels.

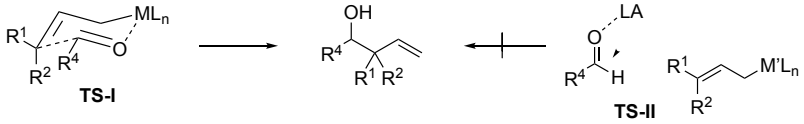

Scheme 3.6: Proposed mechanisms for the allylation of aldehydes catalyzed by Lewis acid.

3.2.2. Lewis Acid-Assisted Brønsted Acid (LBA) Catalyzed Reaction

This concept was introduced by Yamamoto and Ishihara and results from the combination of chiral BINOL as a Brønsted acid with a Lewis acid, which enhance the strength of the Brønsted acid.[36] The generated LBA, formed *in situ* from (*R*)-BINOL and $SnCl_4$, proved to be robust in the enantioselective protonation of silyl enol ethers (Scheme 3.7).

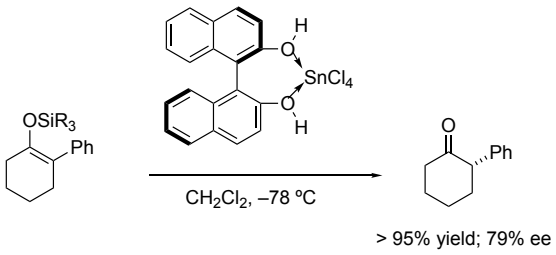

Scheme 3.7: LBA for enantioselective protonation of silyl enol ether.

Since then, this methodology has opened the doors toward enantioselective addition of allyl- and crotylboronates to aldehydes.[37] Hall and co-workers extended the application of LBA toward the allylation of aldehydes giving rise to high levels of enantioselctivity not achieved before.[4b] In their research, they

noticed that after 4-5 h slow background (uncatalyzed) reaction took place. In order to avoid this background reaction, they employed a highly acidic diol (**82**) bearing electron-withdrawing substituents in the aromatic scaffold. This catalyst accelerated the catalyzed reaction, which achieved high levels of activity. In contrast, the scope remains limited and just a few examples of aldehydes were reported (Scheme 3.8).

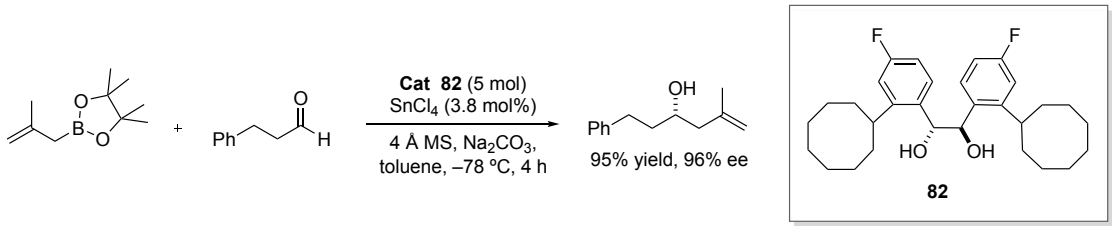

Figure 3.8: Allylboration of aldehydes catalyzed by LBA.

3.2.3. Brønsted Acid Catalyzed Reaction

More recently, Brønsted acids[38] have been shown to facilitate the allylboration of aldehydes in the synthesis of homoallylic alcohols have been highlighted to facilitate the allylboration of aldehydes.[10, 16, 20f, 31, 37a, 39]

Antilla *et al.* reported for the first time an effective catalytic enantioselective addition of allylboronic acid pinacol ester to aldehydes catalyzed by the chiral phosphoric acid (*R*)-**TRIP** (Scheme 3.9).[40] A broad range of aldehydes were examined under the optimized conditions (5 mol% of catalyst, toluene and –30 ºC), giving rise to the desired products in high ee and yield; crotylboronates were also competent allylating reagents under these consitions.

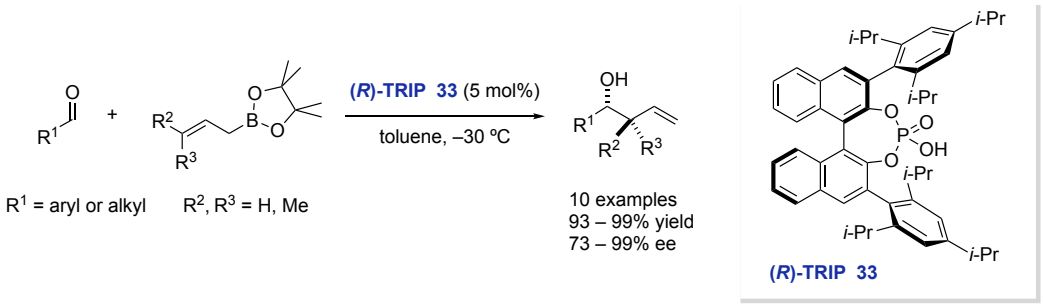

Scheme 3.9: Allylation of aldehydes catalyzed by CPA.

Based on the diastereoselectivity observed in the crotylation products the authors proposed the transition state depicted in Figure 3.3, which involves a chair-like six-membered cyclic transition state. The mechanism is initiated by the activation of the pseudoequatorial oxygen of the cyclic boronate via protonation through the Brønsted acid of the CPA.

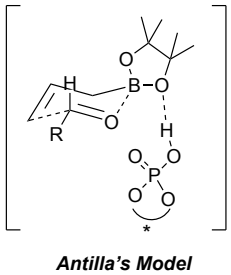

Figure 3.3: Possible assembly for the enantioselective allylation of aldehydes proposed by Antilla.

Goodman *et al.*[39e] envisioned that the mechanism involving only the Brønsted acidic site cannot explain the high enantiomeric ratio observed in the allylation of aldehydes due to the flexible system formed via monocoordination activation. They carried out computational studies in depth in order to gain mechanistic insight to justify the enantioselectivity, concluding that a more rigid transition state is taking place. In this manner, two hydrogen-bonding interaction occurs: the Brønsted acid site interacts with the pseudoaxial oxygen of the cyclic boronate and the phosphoryl oxygen Lewis base site stabilizes the

system via H-bond with the proton from the aldehyde (Figure 3.4).

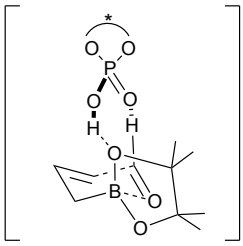

Figure 3.4: Transition state involving double two hydrogen-bonding interactions.

3.2. Aims

In the previous chapter, we optimized the synthesis of a polystyrene-immobilized chiral phosphoric acid catalyst. Now, we want to set our sights in finding a benchmark reaction to put the new catalytic resin PS-TRIP to the test. Our main goal is exploring the potential in catalysis of these supported CPAs, as well as their recyclability.

We envisaged that the asymmetric allylboration of aldehydes reported by Antilla *et al.* (Scheme 3.9)[40] might be an interesting choice, given the versatility of chiral homoallylic alcohols as building blocks in synthesis and the simplicity of the reaction protocol (Scheme 3.10).

If the catalytic material succeeds in displaying in promising results, the long-term goal involves the implementation of continuous flow applications for extended periods of times.

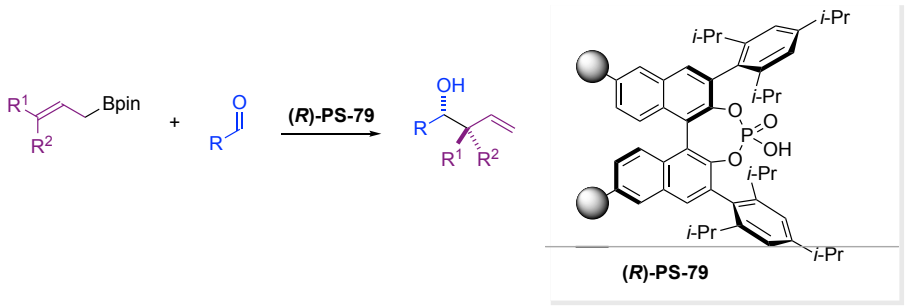

Scheme 3.10: Allylboration of aldehydes catalyzed by PS-TRIP.

3.3. Results and Discussion

Nowadays, the catalytic enantioselective allylation of aldehydes remains an open field of research considering that previous stereoselective methods present some drawbacks. These limitations are related with the use of stoichiometric chiral inductors, the difficulty in preparing the allyl reagent, their air/moisture-sensitivity, and the presence of undesirable metal species as tin.[41]

Herein, we present our results by virtue of searching a more sustainable pathway for the catalytic allylboration of aldehydes, using non-toxic reagents, that are stable and commercially available, as allylboronic acid pinacol ester, and a reusable polystyrene-supported chiral phosphoric acid catalyst.

3.3.1 Optimization and Scope of the Allylation of Aldehydes

We started our investigation regarding the allylation of aldehydes, using commercially available benzaldehyde and allylboronic acid pinacol ester as the allylating agent. To our delight, working with 10 mol% PS-TRIP (with a $f_{(P)}$ = 0.22 mmol/g_{resin}) in toluene at 0 °C, the reaction between these gave **85a** in excellent yield and enantioselectivity (Table 3.1, entry 1). Lowering the catalyst loading to 5 mol% did not have a significant impact (entry 2). Next, we moved to evaluate the influence of solvents to more polar ones, which are still able to swell the resin, but this resulted in lower ee's (entries 3-5). When the reaction was cooled to −30 °C, the result with benzaldehyde was affected minimally (entry 6), but more electrophilic aldehydes gave better ee's. We attribute this to a non-catalyzed background reaction, and thus, in order to minimize this unwanted process, we decided to carry out the rest of the scope at −30 °C. Lastly, when concentration was increased to 0.1 M, the reaction turned out to

be much faster while maintaining yield and ee (entry 7). However, increasing the concentration up 0.2 M the yield and ee decreased considerably (entry 8).

Table 3.1: Screening of reaction conditions.[a]

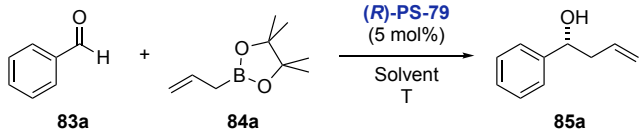

83a **84a** **85a**

Entry	Solvent	T [°C]	*t* [h]	yield [%][e]	ee [%][f]
1[b]	toluene	0	16	89	96
2	toluene	0	16	92	94
3	THF	0	48	Traces	n.d.
4	DCM	0	16	90	88
5	EtOAc	0	48	67	52
6	toluene	–30	16	97	95
7[c]	**toluene**	**–30**	**6**	**96**	**95**
8[d]	toluene	–30	7	90	90

[a]Reactions carried out at a concentration of 0.06 M with 5 mol% (R)-PS-**79** and 1.2 equiv. of **84a**. [b]Using 10 mol% PS-TRIP. [c]Concentration: 0.1 M. [d]Concentration: 0.2 M. [e]Yield of isolated product after column chromatography. [f]Determined by HPLC analysis.

Once the optimal conditions for the allylation of aldehydes had been established (entry 7, 5 mol% PS-TRIP, 0.1 M in toluene, −30 °C, 6 h), we moved to explore the scope of the reaction. Our secondary goal during the study of the scope was to demonstrate the recyclability of our supported TRIP. Consequently, we used the same sample of (PS)-TRIP for all the examples in Table 3.2, where we studied a panel of model aldehydes. Interestingly, electron-poor and electron-rich aromatic aldehydes (products **85a-o**) are generally well-tolerated, giving rise to outstanding yields and enantioselectivities (up to 96% ee). Notwithstanding, a decrease in ee was appreciated in the case of *ortho*-halogenated derivatives (products **85e** and **j**).

However, *o*-tolualaldehyde, which contains a methyl in *ortho* position gave rise to product **85** in 95% ee, which seems to indicate that electronic factors are responsible for the low ee's recorded with *o*-halobenzaldehydes. Even though 3-pyridine (**85k**) gave high yield, the product resulted to be completely racemic. This effect can be attributed to the basicity of pyridine moiety which presumably interacts with the phosphoric acid. In fact, the supported CPA was not active in the next run. However, the catalytic activity of the catalyst could be regenerated by washing the catalyst in acidic media. On the other hand, we decided to test other heteroaromatic rings like 3-furyl (product **85l**) which gave very good results. Further interesting substrates besides benzaldehydes were also tested such as an α,β-unsaturated aldehyde (product **85p**), that reached 84% ee. Aliphatic aldehydes resulted in a decrease in yield and ee (product **85q)**, whereas isophthalaldehyde, could undergo double allylation, providing the C_2-symmetric product **85r**.

Table 3.2: Scope of the reaction for the allylboration of aldehydes (and concomitant recyclability study)[a].

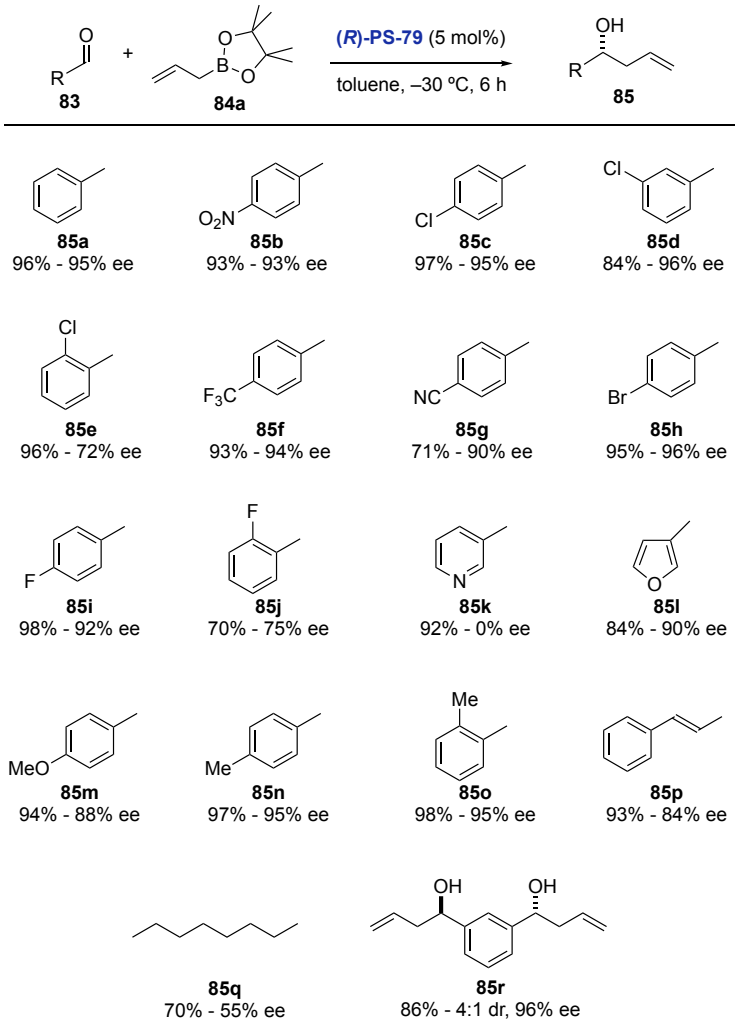

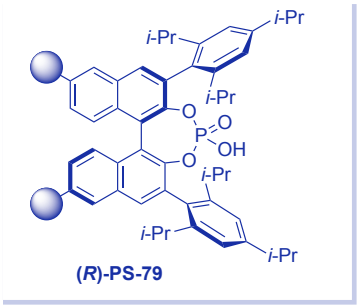

18 examples with the same sample of PS-TRIP

[a]All reactions were carried out with the same sample of PS-TRIP (recycled after each run). Reactions carried out at a concentration of 0.1 M with 5 mol% PS-TRIP **79** and 1.2 equiv. of **84a**.

To our satisfaction, PS-TRIP showed to be extensively reusable without decay in activity. This remarkable feature has been demonstrated by the fact that the same sample of catalyst has been used for all the examples shown in Table 3.2: a total of 18 enantioenriched homoallylic alcohols have been prepared with excellent results. In fact, as mentioned above, the catalyst did lose activity a couple of times (e.g., after running the test with 3-pyridinecarboxaldehyde), but the catalytic activity was recovered by simply washing the resin with a

solution of 2 M HCl in EtOAc. Moreover, we verified the catalytic activity at the end of the scope for further experiments. To this end, benzaldehyde was allylated again and the results replicated those obtained at the beginning. Consequently, an accumulated TON was quantified giving rise to a value of 321, which shows the inherent robustness of PS-TRIP.

To develop a more appealing and general method, we moved to study the allylating partner scope. The use of *trans*- and *cis*-crotylboronates made possible the creation of a new stereogenic center (products **85s** and **85t**, Table 3.3) giving excellent results. However, longer reaction times were necessary for **85t**, which was isolated in a moderate 83% ee, perhaps due to a competitive background reaction. Finally, dimethylallylation of benzaldehyde to provide **85u** was successfully achieved.

Table 3.3: Scope of the allylating partner [a].

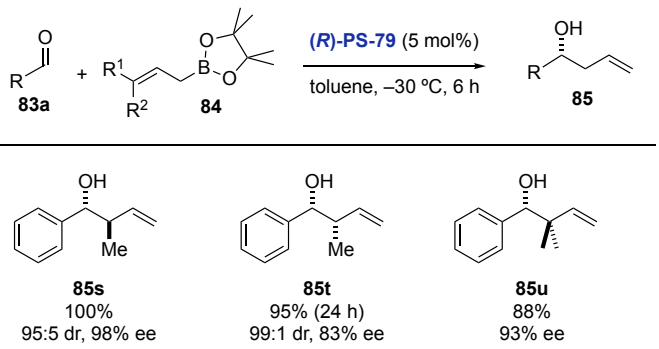

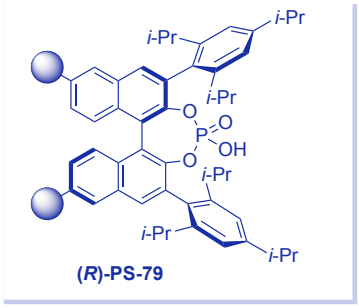

[a]Reactions carried out at a concentration of 0.1 M with 5 mol% PS-TRIP **79** and 1.2 equiv. of **84a**.

3.3.2. Implementation of a Continuous Flow Asymmetric Allylation

Encouraged by the high robustness displayed by the PS-TRIP in the asymmetric allylation of aldehydes, we set our sights on the study of the related flow process.

Our initial thoughts were to reproduce in flow the previously optimized conditions in batch; however, we decided to carry out this flow experiment at 25 °C instead of –30 °C for the sake of simplicity due to the similar behavior of benzaldehyde at rt and –30 °C, as shown in the preliminary batch tests using **85a**. Thus, parameters as the flow rate and the amount of catalyst packed in the column were studied (Table 3.4). Preliminary attempts in a two-pump system, with a packed bed reactor containing 400 mg of resin did not show full conversion by HPLC, whereas the ee was of 93% (entry 1). In seek of full conversion, the flow rate was decreased to 0.1 mL/min (entry 2) but benzaldehyde was still observed by NMR and the ee was even lower. Later, we decided to study the activity using more resin instead of decreasing the flow. In that case, higher ee (up to 94%) was recorded, but full conversion was still not achieved. In an effort to reach full conversion, we decided to use more equivalents of allylboronic acid. Unfortunately, even if full conversion of the aldehyde was observed, the ee decreased to 88% (entry 4) presumably because the excess allylboronate accelerated the background reaction. Note that, to study the parameters for the flow process, an aliquot after 1 h of circulating the reagents was taken.

Table 3.4: Screening for flow conditions.

Entry	Flow [mL/min.]	Cat. Loading [mg]	Equiv.84a	ee [%]
1	0.20	400	1.2	93
2	0.10	400	1.2	92
3	0.20	500	1.2	94
4	0.20	500	1.4	88

[a]Flow experiments were carried out at a concentration of 0.1 M, and at room temperature.

After these results, we proceeded to purify the product collected from the experiment in entry 3 (Table 3.4) which showed somewhat diminished ee's when comparing the aliquot with the isolated product. This observation was attributed to a background reaction which can take place in the collecting flask between the excess allylboronic ester and the small amounts of aldehyde remaining in the outstream. In order to rule out this undesired process, a work-up after the column would be required to remove any unreacted aldehyde. Determined to find a solution to this problem, we proceeded to treat a solution with the desired homoallylic alcohol (4 equiv.), aldehyde **83a** (1 equiv.) and allylboronic acid pinacol ester (2 equiv.) in toluene (0.02 M) with 20 mL of a 0.5 M sodium hydrogen sulfite aqueous solution (Scheme 3.11). Gratifyingly, we observed the consumption of the aldehyde without the appearance of any precipitate, which could complicate the flow process in the case of obstructing the channels. The homoallylic alcohol was totally recovered after washing the aqueous phase with dichloromethane.

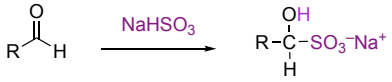

Scheme 3.11: Addition of sodium hydrogen sulphite to aldehydes.

Finally, we proceeded to set up our flow system. As depicted in Figure 3.5, a three-pump system was assembled: two pumps to circulate each solution of starting material (aldehyde and allylboronic ester) separately, in order to avoid background reaction. The reaction took place in a packed bed reactor containing 500 mg of PS-TRIP. Finally, downstream of the column, an aqueous solution of $NaHSO_3$ was pumped to scavenge any unreacted aldehyde. Under these conditions, the flow experiment was operated for 28 h leading to the isolation of 4.60 g of **85a** (92% yield) in 91% ee. An overall TON of 282 was achieved, which corresponds to a productivity of 2.22 mmol h^{-1} g_{resin}^{-1}. It is worth noting that the ee was constant during the 28 h experiment, as no detectable decrease in the catalytic selectivity of the resin was observed. The easy-to-assemble flow set-up can indeed be regarded as a micropilot plant which, due to the robustness of the catalyst can function for extended periods of time with reduced costs due to the lack of cooling material.

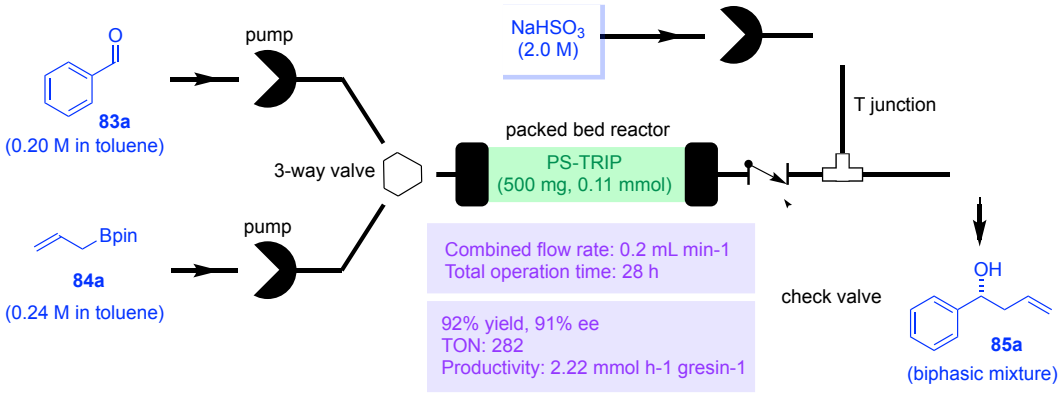

Figure 3.5: Experimental setup for the continuous flow catalytic enantioselective allylation.

3.4. Conclusions

In summary, the polystyrene-supported TRIP catalyst prepared by co-polymerization has proven to be highly active and enantioselective in the asymmetric allylboration of aldehydes.

The reaction protocol tolerates aryl, heteroaryl, unsaturated and aliphatic aldehydes, which are transformed, in mild conditions, into a broad range of homoallylic alcohols in a highly enantioenriched manner. Further experiments have also shown that the reaction is effective for the catalytic enantioselective *cis* and *trans* crotylation of aldehydes.

The high recyclability of PS-TRIP has been demonstrated in the scope, which has reached accumulated TONs in batch of 321. Remarkably, the catalyst was still active after 18 runs. These results exceedingly compensate the slightly longer synthesis shown in Chapter II.

Lastly, we have been able to further test the catalytic resin by means of a continuous flow experiment spanning 28 h, in which 4.60 g of allylated product were obtained (TON of 282, productivity of 2.22 mmol h^{-1} $gresin^{-1}$) without decrease in activity. We conclude that the recyclability and robustness of PS-TRIP make it an interesting alternative to the already successful homogeneous version.

3.5. Experimental Procedures and Characterization of Compounds

3.5.1. General Remarks

Unless otherwise noted, all reactions were performed in oven-dried screw-cap test tubes and were allowed to proceed under a dry argon atmosphere. All solvents used in the reactions were dried using an SPS (Solvent Purification System) unless otherwise stated. All reagents were purchased from commercial sources and used as received except the liquid aldehydes that were distilled prior to use. Thin layer chromatography was performed on Merck TLC Silicagel 60 F254 aluminum sheets. Components were visualized by UV light (λ = 254 nm) and stained with *p*-anisaldehyde or phosphomolybdic dip. Flash column chromatography was carried out using Sigma-Aldrich 60 mesh silica gel and dry-packed columns. ^{1}H NMR and ^{13}C NMR spectra were recorded at 298 K on a Bruker Avance 500 or 400 Ultrashield apparatus. ^{1}H NMR spectroscopy chemical shifts are quoted in ppm relative to tetramethylsilane (TMS). $CDCl_3$ was used as internal standard for ^{13}C NMR spectra. Chemical shifts are given in δ and coupling constants in Hz. IR spectra were recorded on a Bruker Tensor 27 FT-IR spectrometer and are reported in wavenumbers (cm^{-1}). Elemental analyses were performed by MEDAC Ltd. (Surrey, UK) on a LECO CHNS 932 micro-analyzer. High performance liquid chromatography (HPLC) was performed on Agilent Technologies chromatographs (1100 and 1200 Series), using Chiralcel or Chiralpak columns and guard column. UltraPerformance Convergence Chromatography was performed on Aquity UPC^2 of Waters, PDA detector. Racemic standard products were prepared according to the reported procedure.[1] The column employed in each case is indicated. High resolution mass spectrometry analyses were performed in a Waters LCD Premier™ instrument operating in ESI (Electro-Spray Ionization) mode or APCI

(Atmospheric-Pressure Chemical Ionization) mode. Specific optical rotation measurements were carried out on a Jasco P-1030 polarimeter.

3.5.2. General Procedure for the Allylation/Crotylation of Aldehydes

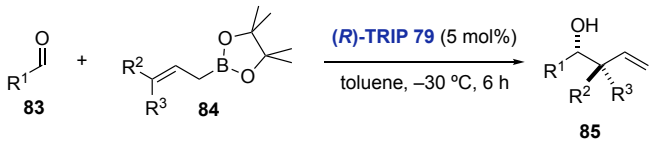

A screw-cap reaction tube containing the supported **(*R*)-PS-79** (5 mol%) was evacuated and flushed with Argon. Subsequently, the tube was charged with toluene (4.4 mL) and the freshly distilled aldehyde (0.44 mmol). The reaction mixture was then cooled to –30 °C followed by the addition of allylboronic acid pinacol ester (0.52 mmol, 1.2 equiv.) or crotyl derivative, dropwise over 30 seconds. The mixture was stirred for 6 h (unless otherwise noted) at this temperature and then the resin was filtered and rinsed with toluene. The filtrate was directly loaded on a silica gel column and the crude product was purified by flash chromatography using cyclohexane/EtOAc (90:10).

3.5.3. Characterization of the Allyl- and Crotylboration Products

(*R*)-1-Phenylbut-3-en-1-ol (85a)[42]

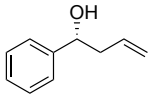

Compound **85a** was obtained in 96% yield and 95% ee as a colourless oil. **^{1}H NMR** (500 MHz, $CDCl_3$): δ 7.43-7.32 (m, 4H), 7.33-7.23 (m, 1H), 5.90-5.72 (m, 1H), 5.22-5.10 (m, 2H), 4.74 (dd, *J* = 5.4, 7.6 Hz, 1H), 2.61-2.41 (m, 2H), 2.01 (br s, 1H). **^{13}C NMR** (126 MHz, $CDCl_3$): δ 144.0, 134.6, 128.6 (×2), 127.7, 126.0 (×2), 118.6, 73.4, 44.0. **HPLC** (Daicel Chiralpak IB column, hexane/*i*-PrOH 98:2, flow rate 1.0 mL/min, λ = 210 nm): t_{major} = 12.1 min; t_{minor} = 12.8 min.

(*R*)-1-(4-Nitrophenyl)but-3-en-1-ol (85b)[42]

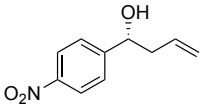

Compound **85b** was obtained in 93% yield and 93% ee as a colourless oil. **^{1}H NMR** (500 MHz, $CDCl_3$): δ 7.28 (d, *J* = 8,9 Hz, 2H), 6.89 (d, *J* = 8.7, 2H), 5.82-5.69 (m, 1H), 5.19-5.10 (m, 2H), 4.68 (t, *J* = 6.5, Hz 1H), 3.81 (s, 3H), 2.50 (tt, *J* = 1.3, 6.8 Hz, 2H), 2.15 (br s, 1H). **^{13}C NMR** (126 MHz, $CDCl_3$): δ 151.3, 147.2, 133.3, 126.6 (×2), 123.6 (×2), 119.5, 72.2, 43.8. **HPLC** (Daicel Chiralpak AS-H column, hexane/*i*-PrOH 97:3, flow rate 1.0 mL/min, λ = 210 nm): t_{major} = 44.8 min; t_{minor} = 48.4 min.

(*R*)-1-(4-Chlorophenyl)but-3-en-1-ol (85c)[42]

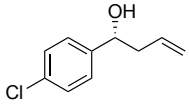

Compound **85c** was obtained in 97% yield and 95% ee as a colourless oil. **^{1}H NMR** (500 MHz, $CDCl_3$): δ 7.39-7.19 (m, 4H), 5.92-5.64 (m, 1H), 5.2-5.08 (m, 2H), 4.71 (dd, *J* = 5.1, 7.7 Hz, 1H), 2.60-2.34 (m, 2H), 2.16 (br s, 1H). **^{13}C NMR** (126 MHz, $CDCl_3$): δ 142.4, 134.1, 133.3, 128.7 (×2), 127.3 (×2), 119.0, 72.7, 44.0. **HPLC** (Daicel Chiralpak AD-

H column, hexane/*i*-PrOH 99:1, flow rate 1.0 mL/min, λ = 210 nm): t_{major} = 26.4 min; t_{minor} = 27.9 min.

(*R*)-1-(3-Chlorophenyl)but-3-en-1-ol (85d)[24]

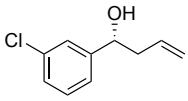

Compound **85d** was obtained in 84% yield and 96% ee as a colourless oil. **^{1}H NMR** (500 MHz, $CDCl_3$): δ 7.35 (s, 1H), 7.28-7.18 (m, 3H), 5.93-5.56 (m, 1H), 5.26-5.06 (m, 2H), 4.68 (dd, *J* = 5.1, 7.7 Hz, 1H), 2.57-2.38 (m, 2H), 2.32 (br s, 1H). **^{13}C NMR** (126 MHz, $CDCl_3$): δ 146.0, 134.4, 134.0, 129.8, 127.7, 126.1, 124.1, 119.0, 72.7, 43.9. **HPLC** (Daicel Chiralpak AD-H column, hexane/*i*-PrOH 98:2, flow rate 1.0 mL/min, λ = 210 nm): t_{major} = 17.7 min; t_{minor} = 19.1 min.

(*R*)-1-(2-Chlorophenyl)but-3-en-1-ol (85e)[24]

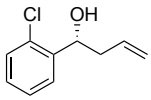

Compound **85e** was obtained in 96% yield and 72% ee as a colourless oil. **^{1}H NMR** (500 MHz, $CDCl_3$): δ 7.56 (dd, *J* = 1.8, 7.7 Hz, 1H), 7.39-6.96 (m, 3H), 5.95-5.75 (m, 1H), 5.30-4.97 (m, 3H), 2.72-2.55 (m, 1H), 2.48-2.34 (m, 1H), 2.31 (br s, 1H). **^{13}C NMR** (126 MHz, $CDCl_3$): δ 141.3, 134.4, 131.8, 129.5, 128.6, 127.2, 127.2, 118.9, 69.8, 42.2. **HPLC** (Daicel Chiralpak AD-H column, hexane/*i*-PrOH 98:2, flow rate 1.0 mL/min, λ = 210 nm): t_{major} = 16.0 min; t_{minor} = 17.3 min.

(*R*)-1-(4-(Trifluoromethyl)phenyl)but-3-en-1-ol (85f)[16]

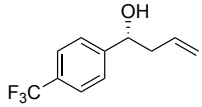

Compound **85f** was obtained in 93% yield and 94% ee as a colourless oil. **^{1}H NMR** (500 MHz, $CDCl_3$): δ 7.60 (d, *J* = 8.1 Hz, 2H), 7.45 (d, *J* = 8.1 Hz, 2H), 5.88-5.65 (m, 1H), 5.22-5.07 (m, 1H), 4.77 (t, *J* = 4.9, 1H), 2.56-2.46 (m, 2H), 2.44 (s, 1H). **^{13}C NMR** (126 MHz, $CDCl_3$): δ 147.9 (q, *J* = 1.5 Hz), 133.8, 129.8 (q, *J* = 32.3 Hz), 126.2 (×2), 125.4 (q, *J* = 3.8 Hz, ×2), 124.3 (q, *J* = 271.1 Hz), 119.2, 72.7,

44.0. **HPLC** (Daicel Chiralpak AD-H column, hexane/*i*-PrOH 99:1, flow rate 1.0 mL/min, λ = 210 nm): t_{major} = 21.4 min; t_{minor} = 22.8 min.

(*R*)-4-(1-Hydroxybut-3-en-1-yl)benzonitrile (85g)[24]

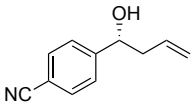

Compound **85g** was obtained in 71% yield and 90% ee as a colourless oil. **^{1}H NMR** (500 MHz, $CDCl_3$): δ 7.61 (d, *J* = 8.2 Hz, 2H), 7.45 (d, *J* = 8.2 Hz, 2H), 5.84-5.68 (m, 1H), 5.19-5.10 (m, 1H), 4.78 (dd, *J* = 4.8, 8.0, 1H), 2.57-2.33 (m, 3H). **^{13}C NMR** (126 MHz, $CDCl_3$): δ 149.3, 133.5, 132.3 (×2), 126.6 (×2), 119.4, 118.9, 111.1, 72.5, 43.9. **HPLC** (Daicel Chiralpak AD-H column, hexane/*i*-PrOH 97:3, flow rate 1.0 mL/min, λ = 210 nm): t_{major} = 34.1 min; t_{minor} = 36.4 min.

(*R*)-1-(4-Bromophenyl)but-3-en-1-ol (85h)[42]

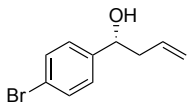

Compound **85h** was obtained in 95% yield and 96% ee as a colourless oil. **^{1}H NMR** (500 MHz, $CDCl_3$): δ 7.46 (d, *J* = 8.4 Hz, 2H), 7.21 (d, *J* = 8.4 Hz, 2H), 5.84-5.68 (m, 1H), 5.22-5.08 (m, 2H), 4.67 (dd, *J* = 5.1, 7.7 Hz, 1H), 2.56-2.35 (m, 2H), 2.26 (br s, 1H). **^{13}C NMR** (126 MHz, $CDCl_3$): δ 142.9, 134.0, 131.6 (×2), 127.7 (×2), 121.4, 118.9, 72.7, 43.9. **HPLC** (Daicel Chiralpak AD-H column, hexane/*i*-PrOH 99:1, flow rate 1.0 mL/min, λ = 210 nm): t_{major} = 29.8 min; t_{minor} = 31.4 min.

(*R*)-1-(4-Fluorophenyl)but-3-en-1-ol (85i)[20c]

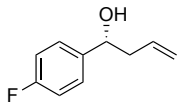

Compound **85i** was obtained in 98% yield and 92% ee as a colourless oil. **^{1}H NMR** (500 MHz, $CDCl_3$): δ 7.39-7.27 (m, 2H), 7.12-7.96 (m, 2H), 5.94-5.67 (m, 1H), 5.24-5.06 (m, 2H), 4.72 (dd, *J* = 5.3, 7.67 Hz, 1H), 2.65-2.35 (m, 2H), 2.09 (br s, 1H). **^{13}C NMR** (126 MHz, $CDCl_3$): δ 162.2 (d, *J* = 245.2 Hz), 139.7 (d, *J* = 3.1 Hz), 134.3, 127.6 (d, *J* = 8.1 Hz, ×2), 118.7, 115.3 (d, *J* = 21.4 Hz, ×2), 72.8, 44.0. **HPLC** (Daicel

Chiralpak AD-H column, hexane/*i*-PrOH 98:2, flow rate 1.0 mL/min, λ = 210 nm): t_{major} = 22.9 min; t_{minor} = 24.1 min.

(*R*)-1-(2-Fluorophenyl)but-3-en-1-ol (85j)[31]

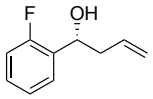

Compound **85j** was obtained in 70% yield and 75% ee as a colourless oil. **^{1}H NMR** (500 MHz, $CDCl_3$): δ 7.47 (td, *J* = 1.9, 7.6 Hz, 1H), 7.33-7.21 (m, 1H), 7.15 (td, *J* = 1.4, 7.5 Hz, 1H), 7.06-6.97 (m, 1H), 5.97-5.69 (m, 1H), 5.23-4.98 (m, 2H), 5.06 (dd, *J* = 4.8, 7.9 Hz, 1H), 2.63-2.39 (m, 2H), 2.14 (br s, 1H). **^{13}C NMR** (126 MHz, $CDCl_3$): δ 159.8 (d, *J* = 245.4 Hz), 134.2, 130.9 (d, *J* = 13.2 Hz), 128.9 (d, *J* = 8.3 Hz), 127.3 (d, *J* = 4.6 Hz), 124.3 (d, *J* = 3.5 Hz), 118.8, 115.3 (d, *J* = 21.8 Hz), 67.4, 42.7. **HPLC** (Daicel Chiralpak AD-H column, hexane/*i*-PrOH 98:2, flow rate 1.0 mL/min, λ = 210 nm): t_{major} = 17.7 min; t_{minor} = 19.1 min.

(*R*)-1-(Pyridin-3-yl)but-3-en-1-ol (85k)[43]

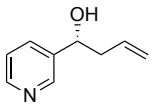

Compound **85k** was obtained <u>in racemic form</u> in 92% yield as a colourless oil. **^{1}H NMR** (500 MHz, $CDCl_3$): δ 8.55-8.40 (m, 2H), 7.73 (dt, *J* = 7.8, 2.0 Hz, 1H), 7.30-7.24 (m, 1H), 5.86-5.74 (m, 1H), 5.19-5.16 (m, 1H), 5.16-5.11 (m, 1H), 4.78 (t, *J* = 6.3 Hz, 1H), 3.75-3.35 (br s, 1H), 2.53 (t, *J* = 6.7 Hz, 2H). **^{13}C NMR** (126 MHz, $CDCl_3$): δ 148.6, 147.7, 139.5, 133.8, 133.7, 123.4, 118.9, 70.9, 43.7.

(*R*)-1-(Furan-3-yl)but-3-en-1-ol (85l)[24]

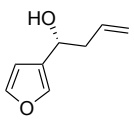

Compound **85l** was obtained in 84% yield and 90% ee as a colourless oil. **^{1}H NMR** (500 MHz, $CDCl_3$): δ 7.40-3.37 (m, 2H), 6.40 (dd, *J* = 1.0, 1.8 Hz, 1H), 5.94-5.63 (m, 1H), 5.26-5.08 (m, 2H), 4.71 (dd, *J* = 5.4, 7.4, 1H), 2.26-2.40 (m, 2H), 1.95 (br s, 1H). **^{13}C NMR** (126 MHz, $CDCl_3$): δ 143.5, 139.2, 134.2, 128.6, 118.8, 108.7, 66.3, 42.6. **HPLC** (Daicel

Chiralpak AD-H column, hexane/*i*-PrOH 95:5, flow rate 1.0 mL/min, λ = 210 nm): t_{major} = 10.4 min; t_{minor} = 11.7 min.

(R)-1-(4-Methoxyphenyl)but-3-en-1-ol (85m)[42]

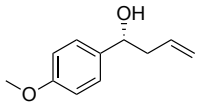

Compound **85m** was obtained in 94% yield and 88% ee as a colourless oil. **^{1}H NMR** (500 MHz, $CDCl_3$): δ 8.15 (d, *J* = 8,7 Hz, 2H), 7.50 (d, *J* = 8.6, 2H), 5.91-5.72 (m, 1H), 5.25-5.06 (m, 2H), 4.84 (dd, *J* = 4.6, 7.9 Hz, 1H), 2.55 (br s, 1H), 2.56-2.44 (m, 2H). **^{13}C NMR** (126 MHz, $CDCl_3$): δ 159.2, 136.2, 134.7, 127.2 (×2), 118.3, 114.0 (×2), 73.1, 55.4, 43.9. **HPLC** (Daicel Chiralpak IC column, hexane/*i*-PrOH 98:8, flow rate 1.0 mL/min, λ = 230 nm): t_{major} = 24.2 min; t_{minor} = 26.4 min.

(*R*)-1-(*p*-Tolyl)but-3-en-1-ol (85n)[20c]

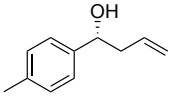

Compound **85n** was obtained in 97% yield and 95% ee as a colourless oil. **^{1}H NMR** (500 MHz, $CDCl_3$): δ 7.28-7.13 (m, 4H), 5.94-5.67 (m, 1H), 5.25-5.09 (m, 2H), 4.71 (dd, *J* = 5.9, 7.0 Hz, 1H), 2.51 (tt, *J* = 1.0, 6.4 Hz, 2H), 2.35 (s, 3H), 1.97 (br s, 1H). **^{13}C NMR** (126 MHz, $CDCl_3$): δ 141.0, 137.2, 134.7, 129.2 (×2), 125.9 (×2), 118.2, 73.3, 43.8, 21.2. **HPLC** (Daicel Chiralpak AD-H column, Hexane/*i*-PrOH 95:5, flow rate 1.0 mL/min, λ = 210 nm): t_{major} = 9.5 min; t_{minor} = 10.6 min.

(*R*)-1-(*o*-Tolyl)but-3-en-1-ol (85o)[42]

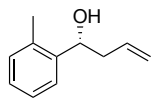

Compound **85o** was obtained in 98% yield and 95% ee as a colourless oil. **^{1}H NMR** (500 MHz, $CDCl_3$): δ 7.57-7.48 (m, 1H), 7.25 (td, *J* = 1.7, 7.4 Hz, 1H), 7.19 (td, *J* = 1.4, 7.4 Hz, 1H), 7.19-7.15 (m, 1H), 5.96-5.82 (m, 1H), 5.27-5.16 (m, 2H), 4.97 (dd, *J* = 4.5, 8.3 Hz, 1H), 2.59-2.43 (m, 2H), 2.35 (s, 3H), 2.07 (br s, 1H). **^{13}C NMR** (126 MHz, $CDCl_3$): δ 142.0, 134.8, 134.4, 130.4, 127.2, 126.3, 125.2, 118.2, 69.7, 42.6, 19.1.

HPLC (Daicel Chiralpak AD-H column, hexane/*i*-PrOH 98:2, flow rate 1.0 mL/min, λ = 210 nm): t_{major} = 14.0 min; t_{minor} = 17.0 min.

(*R*,*E*)-1-Phenylhexa-1,5-dien-3-ol (85p)[16]

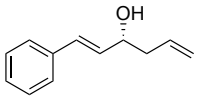

Compound **85p** was obtained in 93% yield and 84% ee as a colourless oil. **^{1}H NMR** (500 MHz, $CDCl_3$): δ 7.53-7.15 (m, 5H), 6.61 (dd, *J* = 1.4, 16.0 Hz, 1H), 5.90-5.74 (m, 1H), 5.25-5.10 (m, 2H), 4.36 (tdd, *J* = 1.3, 5.6, 6.9, 1H), 2.14-2.10 (m, 2H), 2.1 (br s, 1H). **^{13}C NMR** (126 MHz, $CDCl_3$): δ 136.8, 134.2, 132.4, 131.7, 130.5, 128.7, 127.8, 126.6 (×2), 118.7, 71.9, 42.2. **HPLC** (Daicel Chiralpak AS-H column, hexane/*i*-PrOH 95:5, flow rate 1.0 mL/min, λ = 210 nm): t_{major} = 9.3 min; t_{minor} = 10.4 min.

(*S*)-Undec-1-en-4-ol (85q)[44]

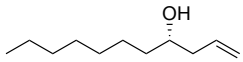

Compound **85q** was obtained in 70% yield and 55% ee as a colourless oil. **^{1}H NMR** (500 MHz, $CDCl_3$): δ 5.90-5.76 (m, 1H), 5.21-5.06 (m, 2H), 3.68-3.59 (m, 1H), 2.35-2.23 (m, 1H), 2.13 (dtt, *J* = 13.9, 7.9, 1.1 Hz, 1H), 1.65 (br s, 1H), 1.53-1.36 (m, 2H), 1.37-1.18 (m, 9H), 0.91-0.82 (m, 3H). **^{13}C NMR** (126 MHz, $CDCl_3$): δ ^{13}C NMR (126 MHz, $CDCl_3$) δ 135.1, 118.2, 70.8, 42.1, 37.0, 32.0, 29.8, 29.43, 25.8, 22.8, 14.2. Chiral **GC** (β-DEX™ 120 [30 m length x 0.25 mm internal diameter x 0.25 μm film], isotherm 100 °C): t_{major} = 41.9 min; t_{minor} = 43.1 min.

(1*R*,1'*R*)-1,1'-(1,3-Phenylene)bis(but-3-en-1-ol) (85r)

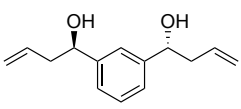

Compound **85r** was obtained in 86% yield, 55% ee and 4:1 dr as a colourless oil. **^{1}H NMR** (500 MHz, $CDCl_3$): δ 7.38-7.19 (m, 4H), 5.92-5.67 (m, 2H), 5.28-5.03 (m, 4H), 4.81-4.64 (m, 2H), 2.61-2.37 (m, 4H), 2.16 (br s, 2H). **^{13}C NMR** (126 MHz, $CDCl_3$): δ 144.2, 134.5 (×2), 128.6, 125.1 (×2), 123.4 (×2), 118.6 (×2), 73.4 (×2), 44.0 (×2). **SFC**

(ID column, isocratic CO_2/ACN 80:20, λ = 210 nm): t_{major} = 1.7 min; t_{minor} = 2.7 min. **[α]$_D$**: +36.8 (*c* 1.00, CH_2Cl_2).

(1*R*,2*R*)-2-Methyl-1-phenylbut-3-en-1-ol (85s)[19b]

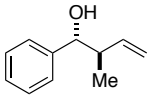

Compound **85s** was obtained in quantitative yield, 95:5 dr and 98% ee as a colourless oil. **^{1}H NMR** (500 MHz, $CDCl_3$): δ 7.37-7.27 (m, 5H), 5.82 (ddd, *J* = 17.2, 10.3, 8.2 Hz, 1H), 5.21 (ddd, *J* = 13.7, 1.8, 1.0 Hz, 1H), 5.18 (ddd, *J* = 6.7, 1.8, 0.9 Hz, 1H), 4.37 (d, *J* = 7.9 Hz, 1H), 2.49 (sext, *J* = 6.9 Hz, 1H), 2.15 (br s, 1H), 0.88 (d, *J* = 6.8 Hz, 3H). **^{13}C NMR** (126 MHz, $CDCl_3$): δ 142.6, 140.8, 128.4 (×2), 127.8, 127.0 (×2), 117.0, 78.0, 46.4, 16.7. **SFC** (Daicel IC column, CO_2/MTBE 95:5, flow rate 1.0 mL/min, λ = 210 nm): t_{major} = 2.68 min; t_{minor} = 2.51 min.

(1*R*,2*S*)-2-Methyl-1-phenylbut-3-en-1-ol (85t)[19b]

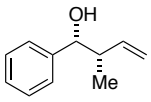

Compound **85t** was obtained in 95% yield dr > 99:1 and 83% ee as colourless oil. **^{1}H NMR** (500 MHz, $CDCl_3$): δ 7.37-7.23 (m, 5H), 5.83-5.70 (m, 1H), 5.10-5.06 (m, 1H), 5.05-5.01 (m, 1H), 4.62 (d, *J* = 5.5 Hz, 1H) 2.59 (tdt, *J* = 6.9, 5.5, 1.2 Hz, 1H), 1.85 (br s, 1H), 1.02 (d, *J* = 6.8 Hz, 3H). **^{13}C NMR** (126 MHz, $CDCl_3$): δ 142.7, 140.5, 128.2 (×2), 127.5, 126.7 (×2), 115.7, 77.4, 44.8, 14.1. **HPLC** (OD-H column, hexane/*i*-PrOH 99:1, flow rate 1.0 mL/min, λ = 210 nm): t_{major} = 19.3 min; t_{minor} = 16.8 min.

(*R*)-2,2-Dimethyl-1-phenylbut-3-en-1-ol (85u)[45]

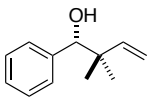

Compound **85u** was obtained in 88% yield and 93% ee as a colourless oil. **^{1}H NMR** (500 MHz, $CDCl_3$): δ 7.34-7.26 (m, 5H), 5.92 (dd, *J* = 17.5, 10.8 Hz, 1H), 5.15 (dd, *J* = 10.8, 1.3 Hz, 1H), 5.08 (dd, *J* = 17.5, 1.3 Hz, 1H), 4.44 (br s, 1H), 2.00 (br s, 1H), 1.02 (s, 3H), 0.97 (s, 3H). **^{13}C NMR** (126 MHz, $CDCl_3$): δ 145.3, 140.9, 128.0 (×2), 127.7 (×2), 127.6,

114.0, 80.8, 42.4, 24.6, 21.2. **HPLC** (Daicel IB column, hexane/*i*-PrOH 98:2, flow rate 1.0 mL/min, λ = 210 nm): t_{major} = 10.9 min; t_{minor} = 8.3 min.

3.5.4. Description of the Continuous Flow Experiment

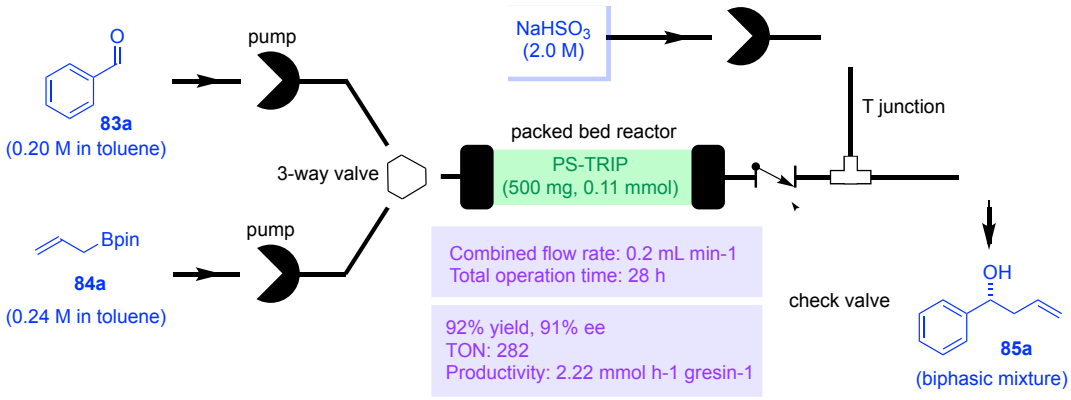

A cylindrical glass column (1 cm diameter) was filled with 500 mg of **PS-TRIP (79)** and the resin was swollen by circulating toluene at 200 μL min^{-1}. After that, the feed was changed for a combination of two streams (a 0.20 M solution of benzaldehyde in toluene and a 0.24 M solution of **83a** in the same solvent), each with its own pump (100 μL min^{-1}), that were combined right before the column (combined flow rate: 200 μL min^{-1}).

Downstream of the column was placed a check valve and the outstream was combined with a stream of $NaHSO_3$ (at 400 μL min^{-1}) to scavenge unreacted aldehyde and avoid a background reaction that would otherwise lower the ee. The biphasic mixture thus obtained was collected in an open flask at room temperature and maintained under vigorous stirring.

The flow experiment was running for 28 h, and afterwards toluene was circulated through the system at 200 μL min^{-1} to rinse away all the organic materials.

At the end, the collected mixture was poured into an extraction funnel and the two phases were separated. The aqueous layer was washed with EtOAc and the combined organic extracts were dried over $MgSO_4$ and concentrated *in vacuo*. The resulting residue was purified by flash column chromatography to give 4.60 g of **85a** as a colourless oil (91% ee).

TON: 282.; Productivity: 2.22 mmol h^{-1} g_{resin}^{-1}.

3.6. References

[1] E. Rodriguez, M. N. Grayson, A. Asensio, P. Barrio, K. N. Houk, S. Fustero, *ACS Catal.* **2016**, *6*, 2506-2514.

[2] (a) S. E. Denmark, J. Fu, *Chem. Rev.* **2003**, *103*, 2763-2794; (b) I. Marek, G. Sklute, *Chem. Commun.* **2007**, 1683-1691.

[3] (a) M. Yus, J. C. González-Gómez, F. Foubelo, *Chem. Rev.* **2011**, *111*, 7774-7854; (b) M. Yus, J. C. González-Gómez, F. Foubelo, *Chem. Rev.* **2013**, *113*, 5595-5698; (c) H.-X. Huo, J. R. Duvall, M.-Y. Huang, R. Hong, *Org. Chem. Front.* **2014**, *1*, 303-320; (d) V. De Sio, A. Massa, A. Scettri, *Org. Biomol. Chem.* **2010**, *8*, 3055-3059; (e) S. Tabassum, M. A. Gilani, K. Ayub, R. Wilhelm, *J. Iran. Chem. Soc.* **2015**, *12*, 1199-1205; (f) J.-S. Poh, S.-H. Lau, I. G. Dykes, D. N. Tran, C. Battilocchio, S. V. Ley, *Chem. Sci.* **2016**, *7*, 6803-6807; (g) D. G. Hall, *Synlett* **2007**, *2007*, 1644-1655; (h) A. S. Tsai, M. Chen, W. R. Roush, *Org. Lett.* **2013**, *15*, 1568-1571; (i) U. Bhakta, E. Sullivan, D. G. Hall, *Tetrahedron* **2014**, *70*, 678-683; (j) E. J. Corey, C. M. Yu, D. H. Lee, *J. Am. Chem. Soc.* **1990**, *112*, 878-879.

[4] (a) S. R. Chemler, W. R. Roush, in *Modern Carbonyl Chemistry*, Wiley-VCH Verlag GmbH, **2007**, pp. 403-490; (b) V. Rauniyar, D. G. Hall, *J. Org. Chem.* **2009**, *74*, 4236-4241; (c) F. Hessler, A. Korotvička, D. Nečas, I. Valterová, M. Kotora, *Eur. J. Org. Chem.* **2014**, *2014*, 2543-2548.

[5] (a) R. W. Hoffmann, W. Ladner, *Tetrahedron Lett.* **1979**, *20*, 4653-4656; (b) R. W. Hoffmann, H.-J. Zeiss, *Angew. Chem. Int. Ed.* **1979**, *18*, 306-307.

[6] (a) S. E. Denmark, D. M. Coe, N. E. Pratt, B. D. Griedel, *J. Org. Chem.* **1994**, *59*, 6161-6163; (b) S. Kobayashi, K. Nishio, *J. Org. Chem.* **1994**, *59*, 6620-6628; (c) Y. Li, K. N. Houk, *J. Am. Chem. Soc.* **1989**, *111*, 1236-1240; (d) J. S. Panek, M. Yang, *J. Am. Chem. Soc.* **1991**, *113*, 6594-6600; (e) J. W. J. Kennedy, D. G. Hall, *J. Am. Chem. Soc.* **2002**, *124*, 11586-11587.

[7] (a) H. C. Brown, P. K. Jadhav, *J. Am. Chem. Soc.* **1983**, *105*, 2092-2093; (b) H. C. Brown, P. K. Jadhav, P. T. Perumal, *Tetrahedron Lett.* **1984**, *25*, 5111-5114; (c) H. C. Brown, K. S. Bhat, *J. Am. Chem. Soc.* **1986**, *108*, 293-294; (d) H. C. Brown, K. S. Bhat, R. S. Randad, *J. Org. Chem.* **1987**, *52*, 319-320; (e) H. C. Brown, P. K. Jadhav, K. S. Bhat, *J. Am. Chem. Soc.* **1988**, *110*, 1535-1538; (f) H. C. Brown, K. S. Bhat, R. S. Randad, *J. Org. Chem.* **1989**, *54*, 1570-1576; (g) H. C. Brown, B. Singaram, *J. Org. Chem.* **1984**, *49*, 945-947; (h) H. C. Brown, U. S. Racherla, P. J. Pellechia, *J. Org. Chem.* **1990**, *55*, 1868-1874; (i) N. Miralles, R. Alam, K. J. Szabó, E. Fernández, *Angew. Chem. Int. Ed.* **2016**, *55*, 4303-4307.

[8] W. R. Roush, A. D. Palkowitz, K. Ando, *J. Am. Chem. Soc.* **1990**, *112*, 6348-6359.

[9] (a) W. R. Roush, A. E. Walts, L. K. Hoong, *J. Am. Chem. Soc.* **1985**, *107*, 8186-8190; (b) M. Chen, M. Handa, W. R. Roush, *J. Am. Chem. Soc.* **2009**, *131*, 14602-14603.

[10] C.-H. Xing, Y.-X. Liao, Y. Zhang, D. Sabarova, M. Bassous, Q.-S. Hu, *Eur. J. Org. Chem.* **2012**, *2012*, 1115-1118.

[11] (a) S. E. Denmark, J. Fu, *J. Am. Chem. Soc.* **2001**, *123*, 9488-9489; (b) A. V. Malkov, M. Orsini, D. Pernazza, K. W. Muir, V. Langer, P. Meghani, P. Kočovský, *Org. Lett.* **2002**, *4*, 1047-1049; (c) S. E. Denmark, J. Fu, *J. Am. Chem. Soc.* **2003**, *125*, 2208-2216; (d) A. V. Malkov, P. Ramírez-López, L. Biedermannová, L. Rulísek, L. Dufková, M. Kotora, F. Zhu, P. Kocosky, *J. Am. Chem. Soc.* **2008**, *130*, 5341-5348.

[12] R. P. Short, S. Masamune, *J. Am. Chem. Soc.* **1989**, *111*, 1892-1894.

[13] E. J. Corey, C. M. Yu, S. S. Kim, *J. Am. Chem. Soc.* **1989**, *111*, 5495-5496.

[14] M. Riediker, R. O. Duthaler, *Angew. Chem. Int. Ed.* **1989**, *28*, 494-495.

[15] (a) J. W. A. Kinnaird, P. Y. Ng, K. Kubota, X. Wang, J. L. Leighton, *J. Am. Chem. Soc.* **2002**, *124*, 7920-7921; (b) B. M. Hackman, P. J. Lombardi, J. L. Leighton, *Org. Lett.* **2004**, *6*, 4375-4377.

[16] T. R. Wu, L. Shen, J. M. Chong, *Org. Lett.* **2004**, *6*, 2701-2704.

[17] (a) C. H. Burgos, E. Canales, K. Matos, J. A. Soderquist, *J. Am. Chem. Soc.* **2005**, *127*, 8044-8049; (b) A. Z. González, J. G. Román, E. Alicea, E. Canales, J. A. Soderquist, *J. Am. Chem. Soc.* **2009**, *131*, 1269-1273.

[18] M. Althaus, A. Mahmood, J. R. Suárez, S. P. Thomas, V. K. Aggarwal, *J. Am. Chem. Soc.* **2010**, *132*, 4025-4028.

[19] (a) H. C. Brown, M. C. Desai, P. K. Jadhav, *J. Org. Chem.* **1982**, *47*, 5065-5069; (b) H. C. Brown, K. S. Bhat, *J. Am. Chem. Soc.* **1986**, *108*, 5919-5923; (c) P. K. Jadhav, K. S. Bhat, P. T. Perumal, H. C. Brown, *J. Org. Chem.* **1986**, *51*, 432-439.

[20] (a) J. W. J. Kennedy, D. G. Hall, *Angew. Chem. Int. Ed.* **2003**, *42*, 4732-4739; (b) T. Naicker, P. I. Arvidsson, H. G. Kruger, G. E. M. Maguire, T. Govender, *Eur. J. Org. Chem.* **2011**, *2011*, 6923-6932; (c) Y. Deng, W. Pan, Y.-N. Pei, J.-L. Li, B. Bai, H.-J. Zhu, *Tetrahedron* **2013**, *69*, 10431-10437; (d) S. Kobayashi, K. Nishio, *Tetrahedron Lett.* **1993**, *34*, 3453-3456; (e) K. Furuta, M. Mouri, H. Yamamoto, *Synlett* **1991**, 561-562; (f) K. Cheng, T. Fan, J. Sun, *Chin. J. Chem* . **2011**, *29*, 1669-1671.

[21] Y. Yamamoto, H. Yatagai, Y. Naruta, K. Maruyama, *J. Am. Chem. Soc.* **1980**, *102*, 7107-7109.

[22] (a) G. Courtois, L. Miginiac, *J. Organomet. Chem.* **1974**, *69*, 1-44; (b) H. Felkin, Y. Gault, G. Roussi, *Tetrahedron* **1970**, *26*, 3761-3778; (c) G. Fraenkel, W. R. Winchester, *J. Am. Chem. Soc.* **1989**, *111*, 3794-3797; (d) P. Jones, P. Knochel, *Chem. Commun.* **1998**, 2407-2408.

[23] (a) B. M. Trost, M. L. Crawley, *Chem. Rev.* **2003**, *103*, 2921-2944; (b) S. E. Denmark, N. G. Almstead, in *Modern Carbonyl Chemistry*, Wiley-VCH Verlag GmbH, **2007**, pp. 299-401.
[24] R.-Y. Chen, A. P. Dhondge, G.-H. Lee, C. Chen, *Adv. Synth. Catal.* **2015**, *357*, 961-966.
[25] R. W. Hoffmann, H. J. Zeiss, *J. Org. Chem.* **1981**, *46*, 1309-1314.
[26] W. R. Roush, R. L. Halterman, *J. Am. Chem. Soc.* **1986**, *108*, 294-296.
[27] P. Jones, P. Knochel, *J. Org. Chem.* **1999**, *64*, 186-195.
[28] P. Jones, N. Millot, P. Knochel, *Chem. Commun.* **1998**, 2405-2406.
[29] (a) B. W. Gung, X. Xue, W. R. Roush, *J. Am. Chem. Soc.* **2002**, *124*, 10692-10697; (b) V. Rauniyar, D. G. Hall, *J. Am. Chem. Soc.* **2004**, *126*, 4518-4519; (c) K. Sakata, H. Fujimoto, *J. Am. Chem. Soc.* **2008**, *130*, 12519-12526.
[30] M. Mahlau, P. García-García, B. List, *Chem. Eur. J.* **2012**, *18*, 16283-16287.
[31] V. Rauniyar, H. Zhai, D. G. Hall, *J. Am. Chem. Soc.* **2008**, *130*, 8481-8490.
[32] H. Lachance, X. Lu, M. Gravel, D. G. Hall, *J. Am. Chem. Soc.* **2003**, *125*, 10160-10161.
[33] T. Ishiyama, T.-a. Ahiko, N. Miyaura, *J. Am. Chem. Soc.* **2002**, *124*, 12414-12415.
[34] G. E. Keck, K. H. Tarbet, L. S. Geraci, *J. Am. Chem. Soc.* **1993**, *115*, 8467-8468.
[35] (a) A. V. Malkov, M. Bell, F. Castelluzzo, P. Kocovsky, *Org. Lett.* **2005**, *7*, 3219-3222; (b) S. E. Denmark, J. Fu, D. M. Coe, X. Su, N. E. Pratt, B. D. Griedel, *J. Org. Chem.* **2006**, *71*, 1513-1522.
[36] (a) H. Yamamoto, K. Futatsugi, *Angew. Chem. Int. Ed.* **2005**, *44*, 1924-1942; (b) K. Ishihara, M. Kaneeda, H. Yamamoto, *J. Am. Chem. Soc.* **1994**, *116*, 11179-11180; (c) S. Nakamura, M. Kaneeda, K. Ishihara, H. Yamamoto, *J. Am. Chem. Soc.* **2000**, *122*, 8120-8130; (d) H. Ishibashi, K. Ishihara, H. Yamamoto, *Chem. Rec.* **2002**, *2*, 177-188; (e) K. Ishihara, D. Nakashima, Y. Hiraiwa, H. Yamamoto, *J. Am. Chem. Soc.* **2003**, *125*, 24-25.
[37] (a) V. Rauniyar, D. G. Hall, *Angew. Chem. Int. Ed.* **2006**, *45*, 2426-2428; (b) V. Rauniyar, D. G. Hall, *Synthesis* **2007**, *2007*, 3421-3426; (c) I. S. Kim, M.-Y. Ngai, M. J. Krische, *J. Am. Chem. Soc.* **2008**, *130*, 14891-14899; (d) V. Rauniyar, H. Zhai, D. G. Hall, *J. Am. Chem. Soc.* **2008**, *130*, 8481-8490.
[38] (a) S. Lou, P. N. Moquist, S. E. Schaus, *J. Am. Chem. Soc.* **2007**, *129*, 15398-15404; (b) S. Lou, S. E. Schaus, *J. Am. Chem. Soc.* **2008**, *130*, 6922-6923.
[39] (a) S. H. Yu, M. J. Ferguson, R. McDonald, D. G. Hall, *J. Am. Chem. Soc.* **2005**, *127*, 12808-12809; (b) M. Fuchs, M. Schober, A. Orthaber, K.

Faber, *Adv. Synth. Catal.* **2013**, *355*, 2499-2505; (c) D. S. Barnett, P. N. Moquist, S. E. Schaus, *Angew. Chem. Int. Ed.* **2009**, *48*, 8679-8682; (d) V. Rauniyar, D. G. Hall, *J. Org. Chem.* **2009**, *74*, 4236-4241; (e) M. N. Grayson, S. C. Pellegrinet, J. M. Goodman, *J. Am. Chem. Soc.* **2012**, *134*, 2716-2722.

[40] P. Jain, J. C. Antilla, *J. Am. Chem. Soc.* **2010**, *132*, 11884-11886.

[41] Y. Yamamoto, N. Asao, *Chem. Rev.* **1993**, *93*, 2207-2293.

[42] P. Jain, J. C. Antilla, *J. Am. Chem. Soc.* **2010**, *132*, 11884-11886.

[43] U. S. Racherla, Y. Liao, H. C. Brown, *J. Org. Chem.* **1992**, *57*, 6614-6617.

[44] H. Nemoto, W. Zhong, T. Kawamura, M. Kamiya, Y. Nakano, K. Sakamoto, *Synlett* **2007**, 2343-2346.

[45] M. Nakajima, M. Saito, M. Shiro, S.-i. Hashimoto, *J. Am. Chem. Soc.* **1998**, *120*, 6419-6420.

3.7. ^{1}H and ^{13}C NMR Spectra

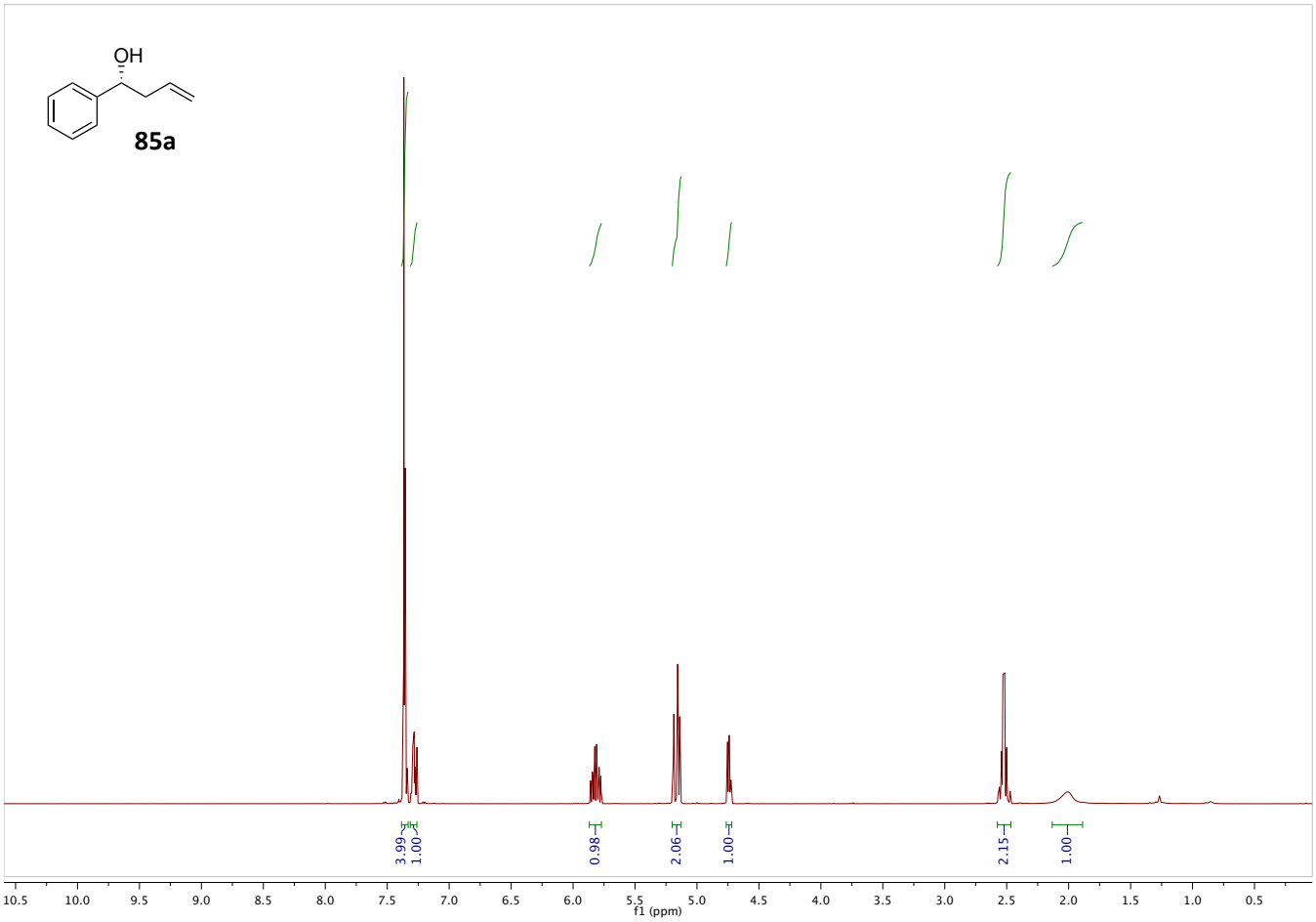

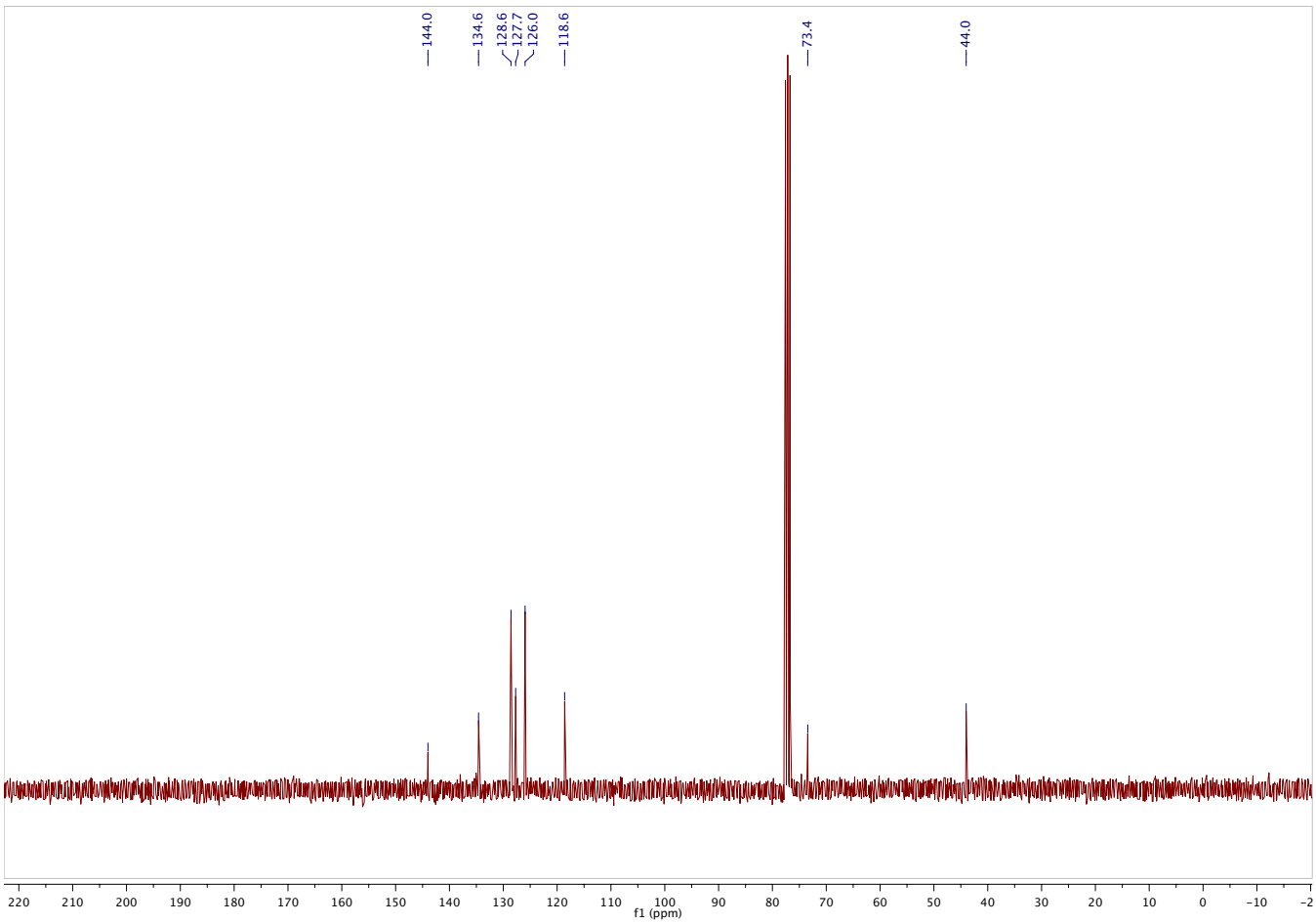

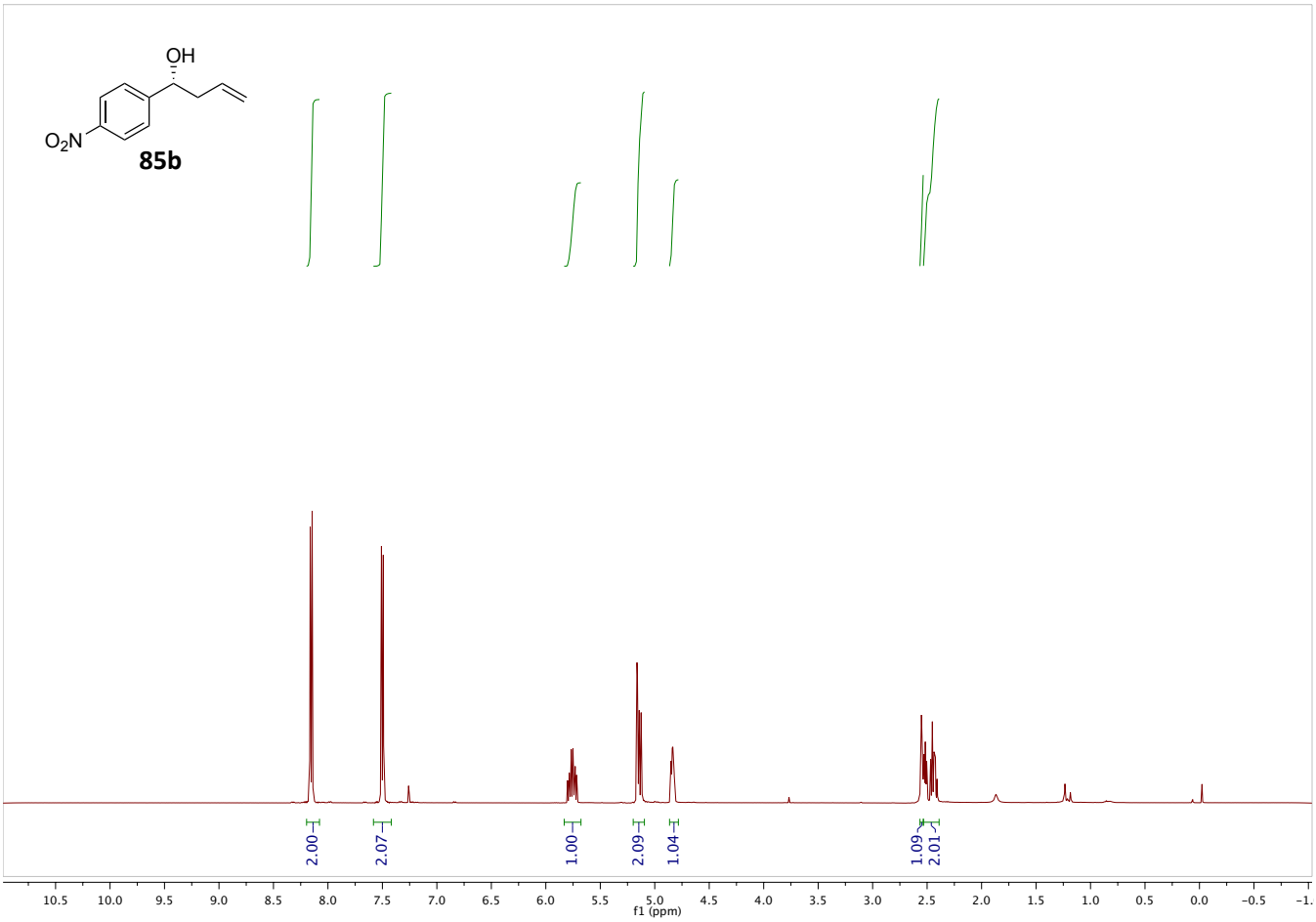
OH
O2N
85b
2.00
2.07
1.00
2.09
1.04
1.09
2.01
f1 (ppm)

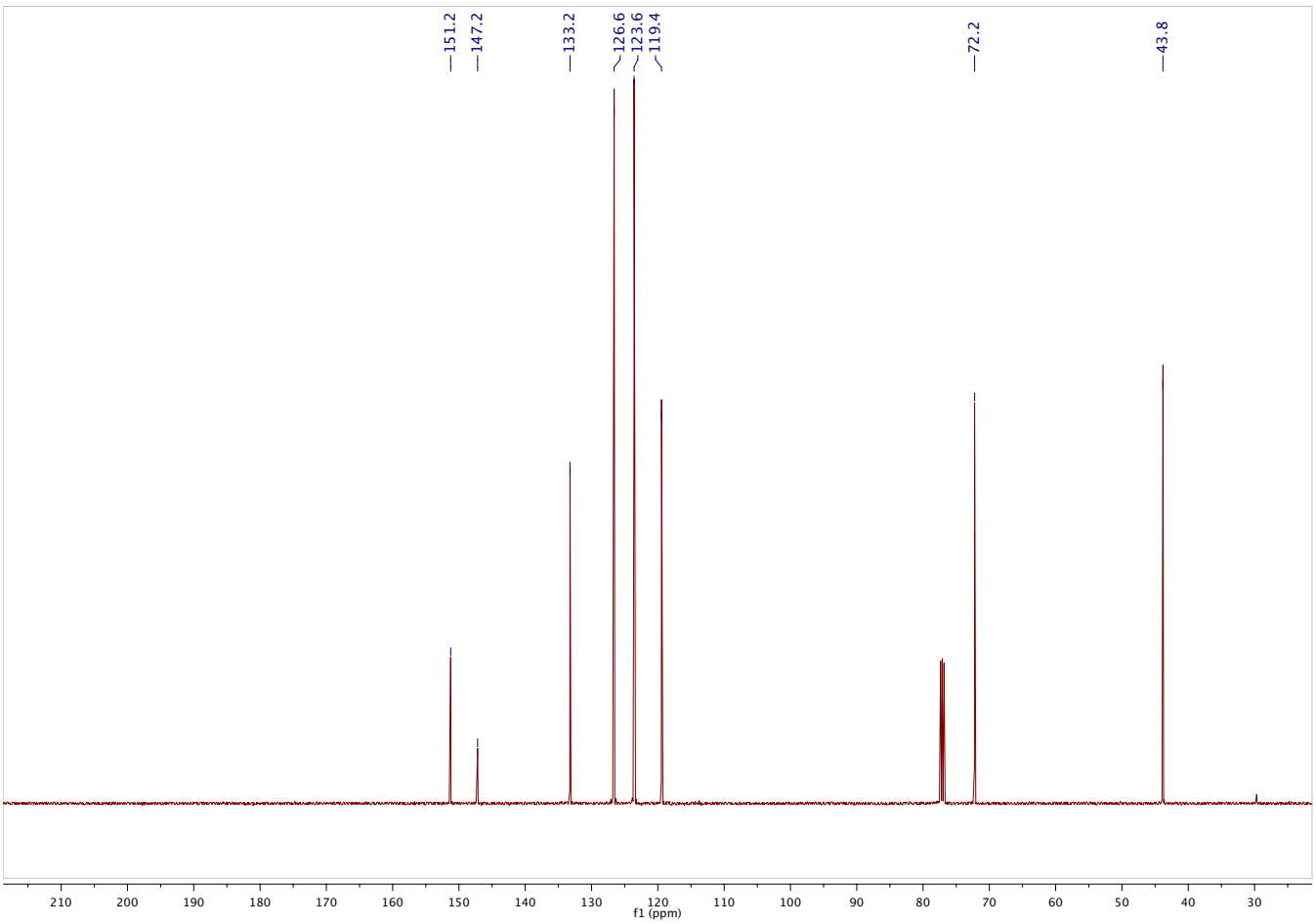
151.2
147.2
133.2
126.6
123.6
119.4
72.2
43.8
f1 (ppm)

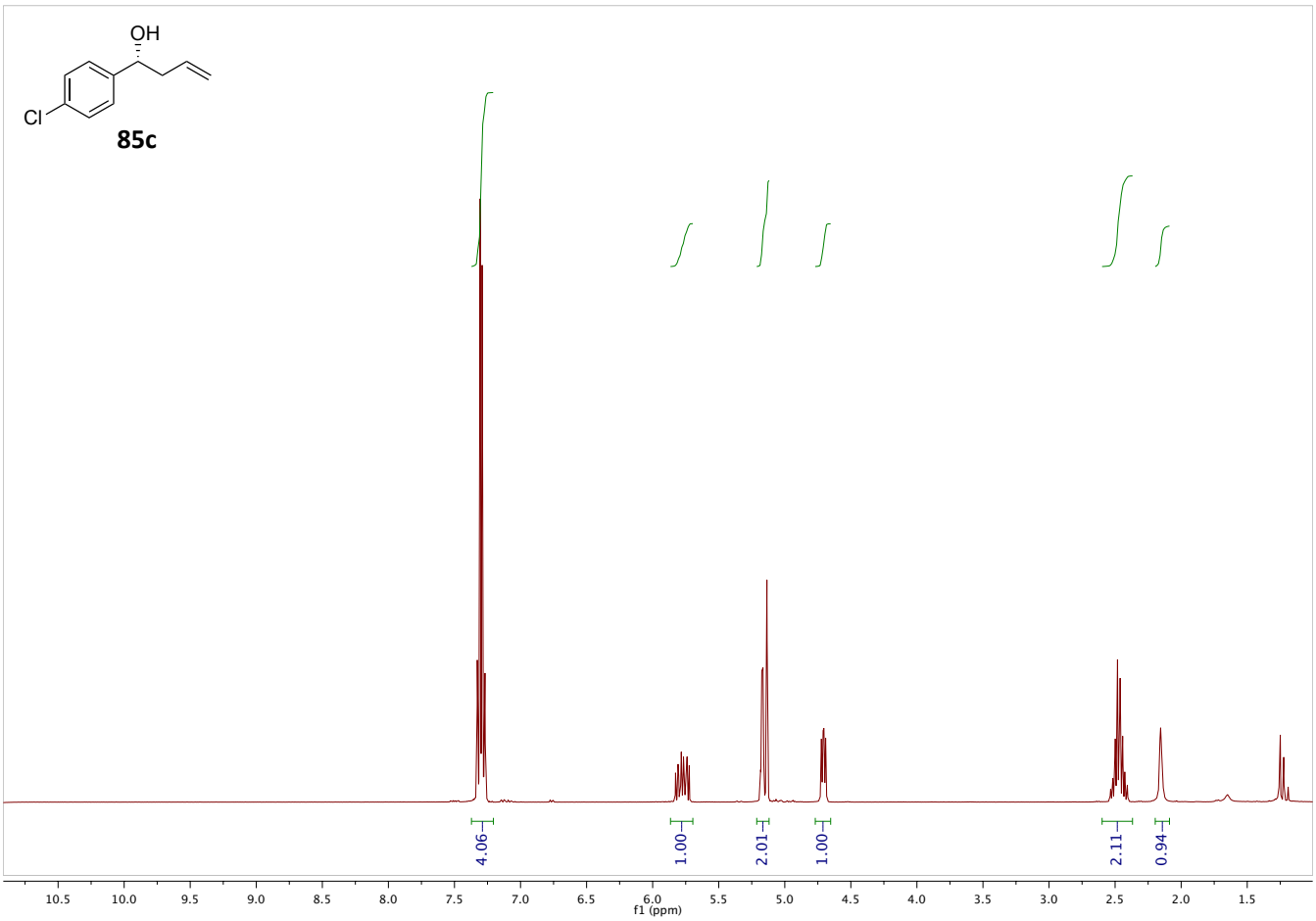
OH
Cl
85c
4.06
1.00
2.01
1.00
2.11
0.94
f1 (ppm)

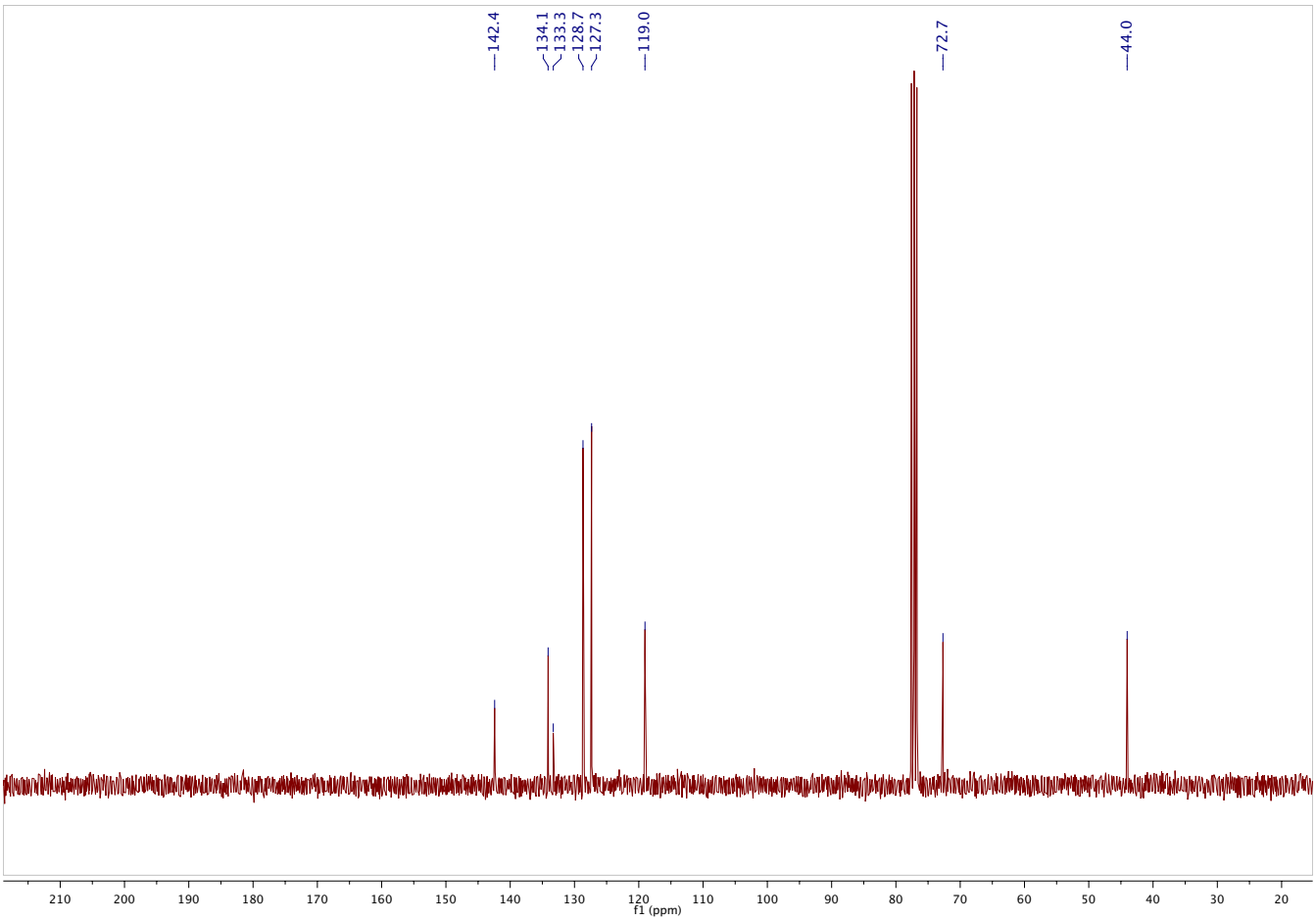
142.4
134.1
133.3
128.7
127.3
119.0
72.7
44.0
f1 (ppm)

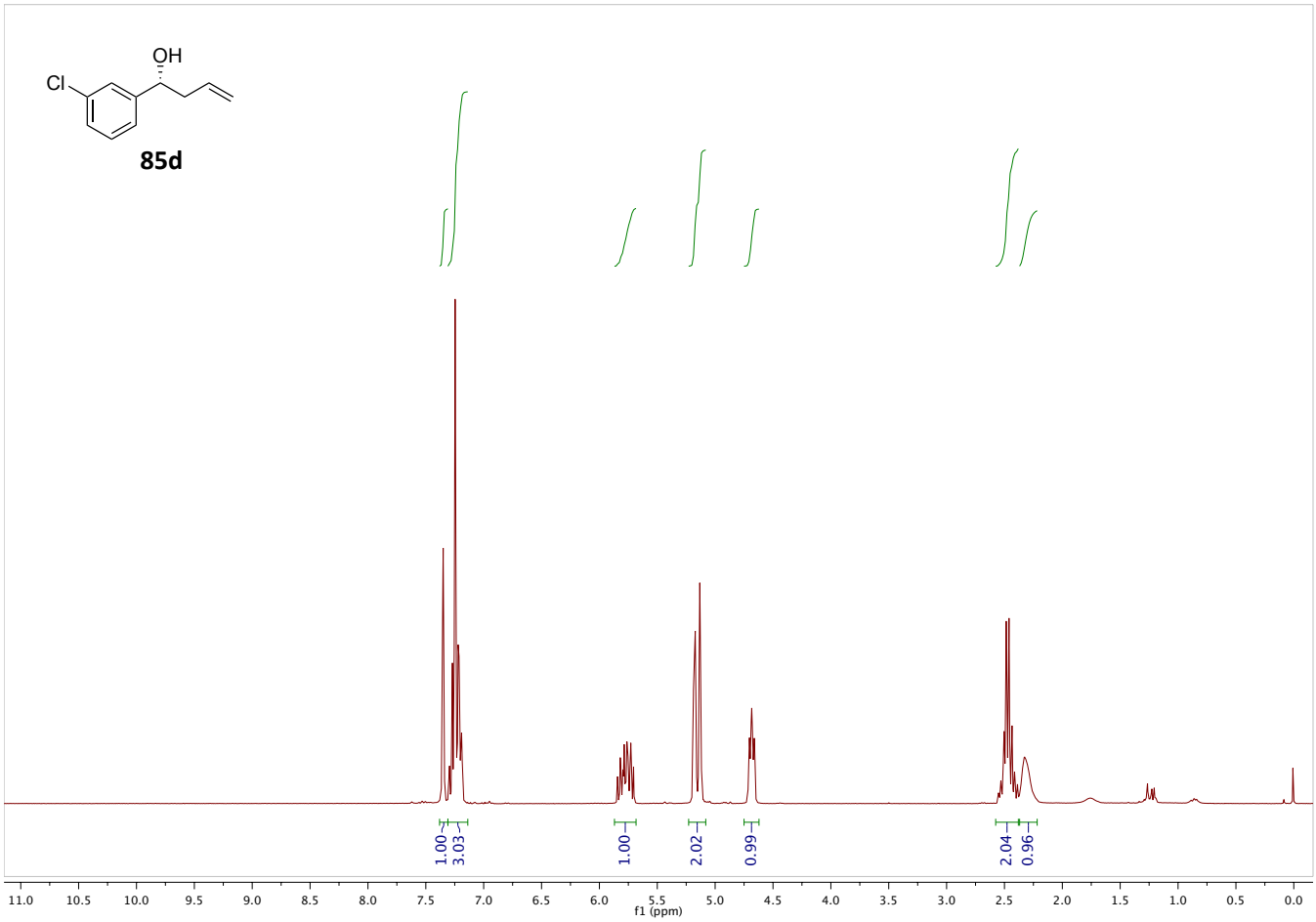
OH
Cl
85d
1.00
3.03
1.00
2.02
0.99
2.04
0.96
f1 (ppm)

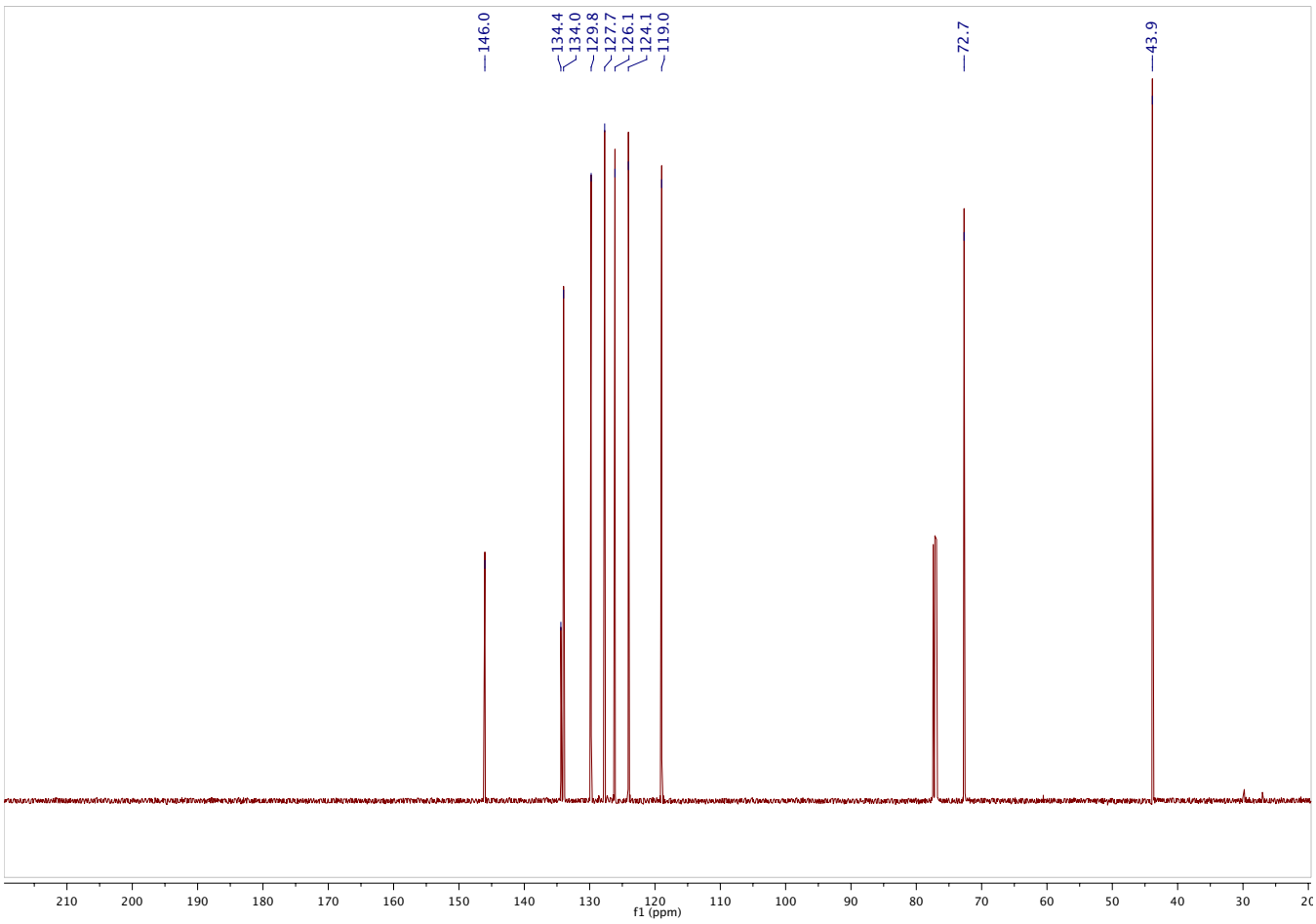
146.0
134.4
134.0
129.8
127.7
126.1
124.1
119.0
72.7
43.9
f1 (ppm)

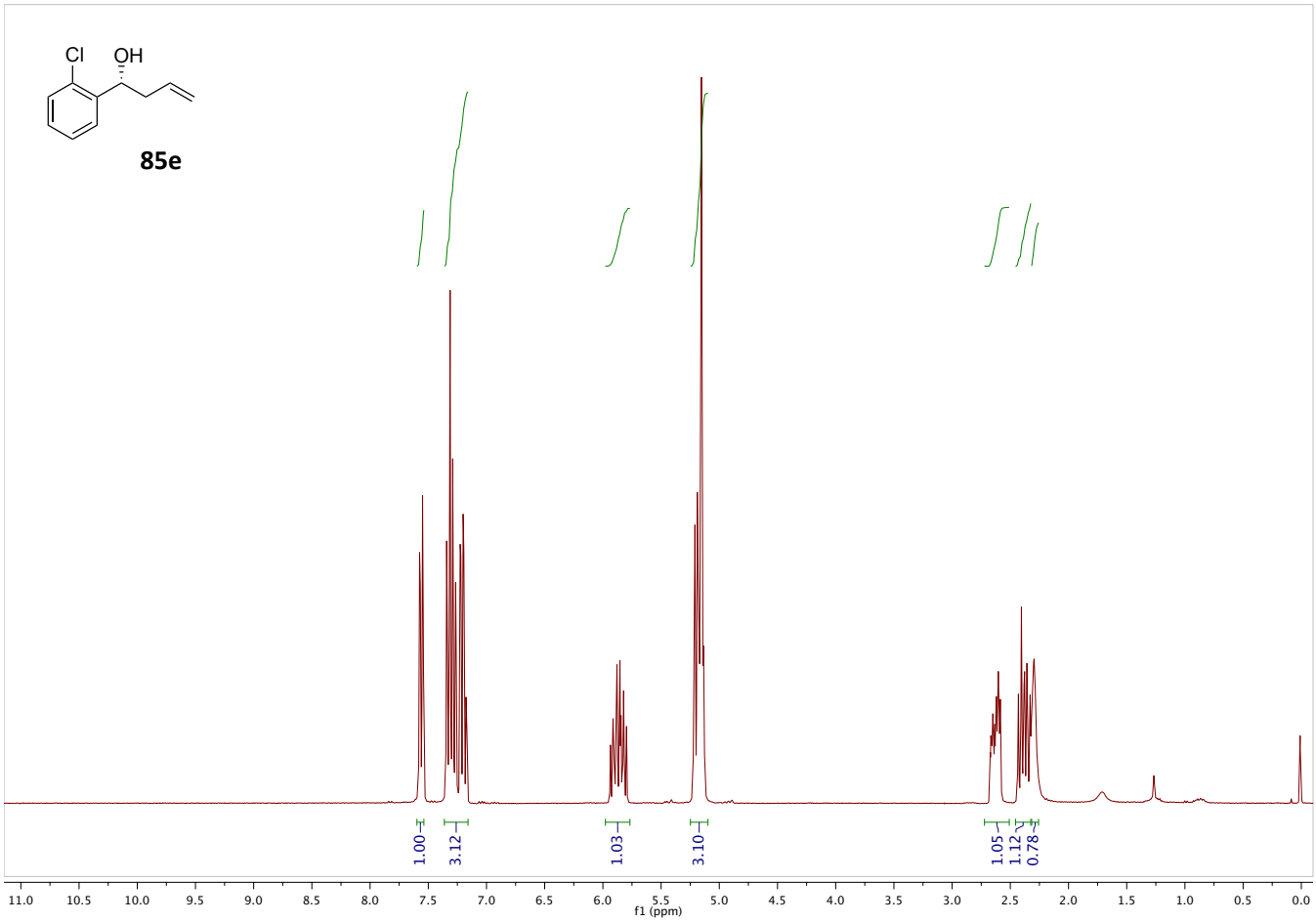
Cl
OH
85e
1.00
3.12
1.03
3.10
1.05
1.12
0.78
f1 (ppm)

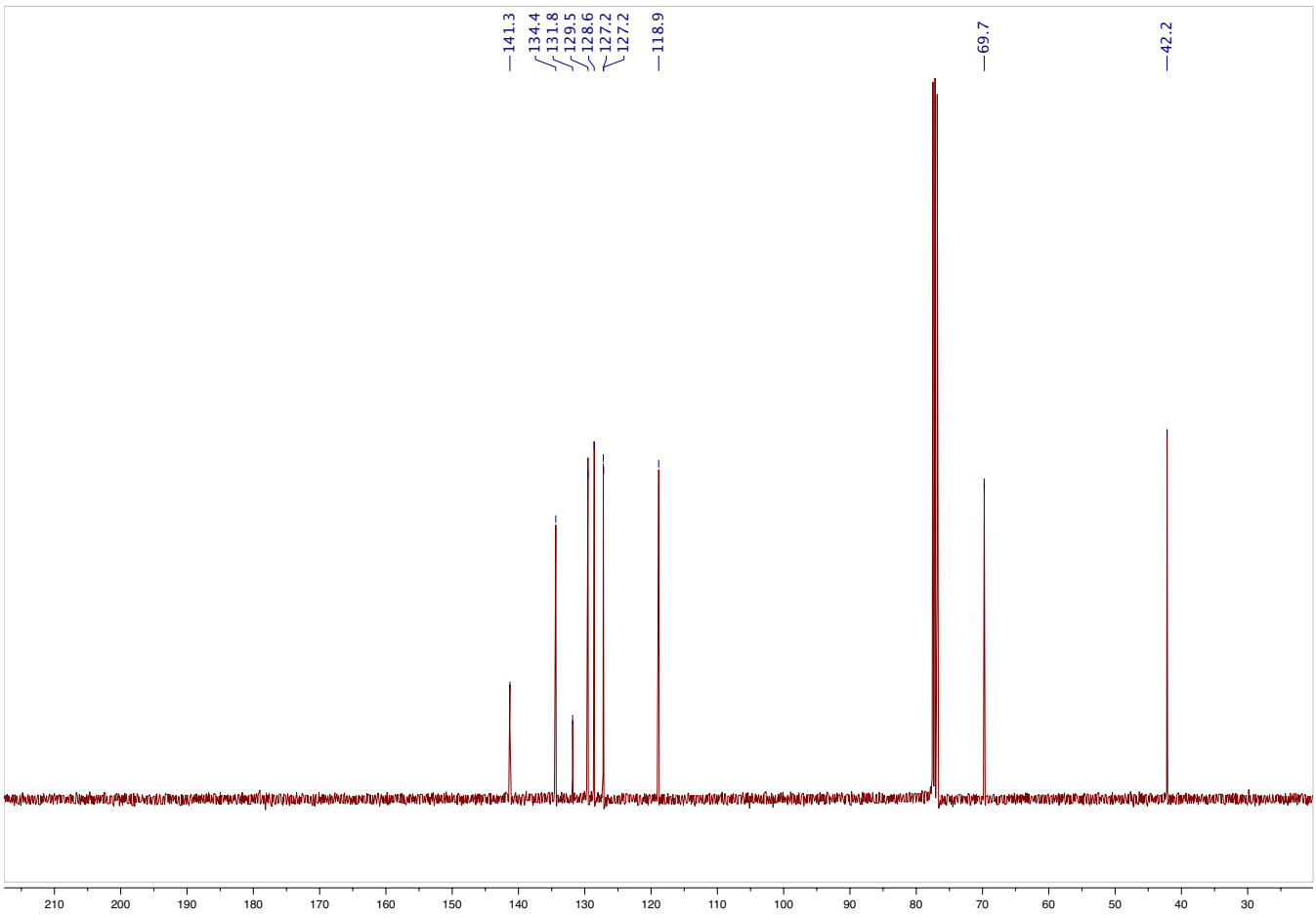
141.3
134.4
131.8
129.5
128.6
127.2
127.2
118.9
69.7
42.2

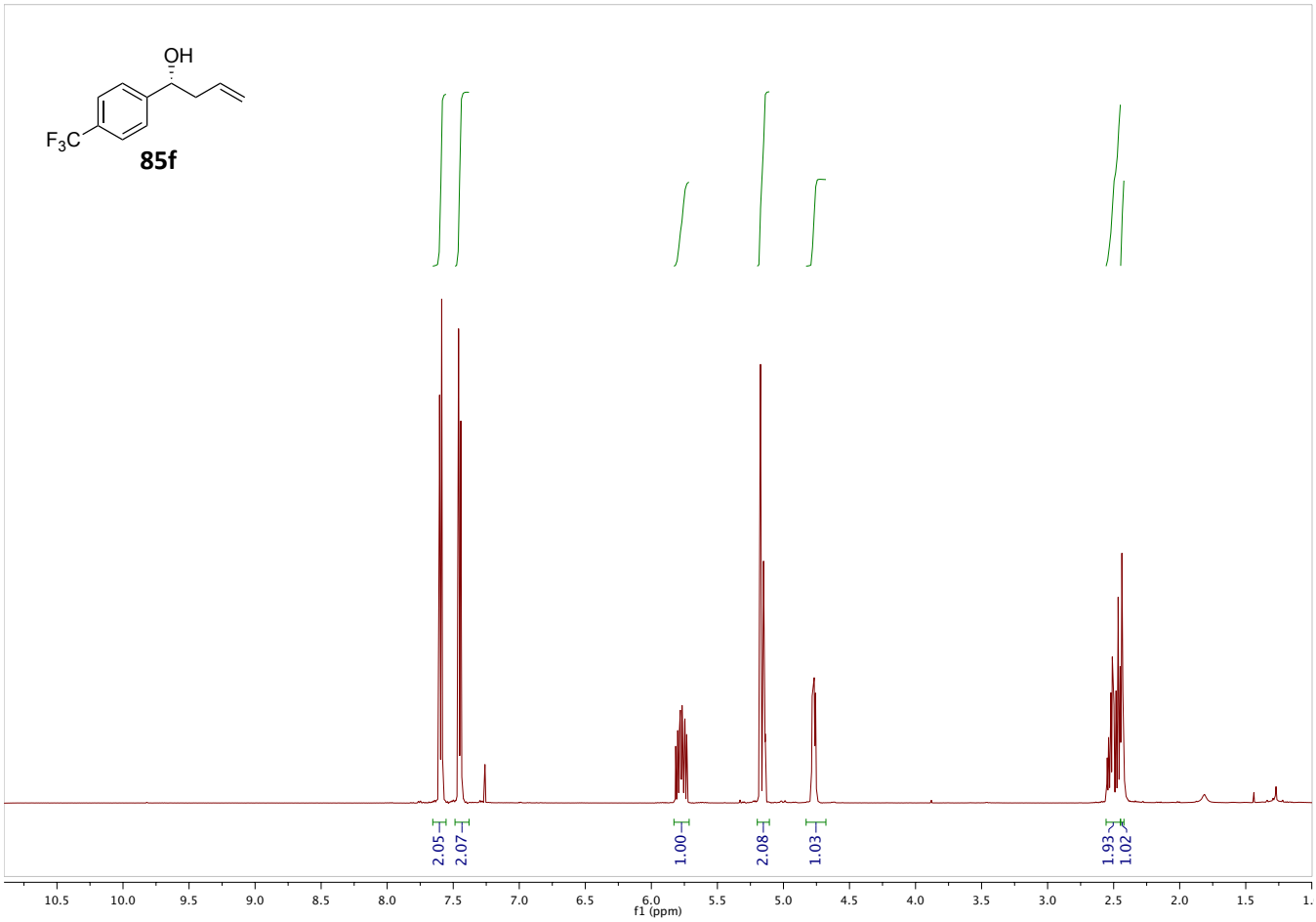
OH
F3C
85f
2.05
2.07
1.00
2.08
1.03
1.93
1.02
f1 (ppm)

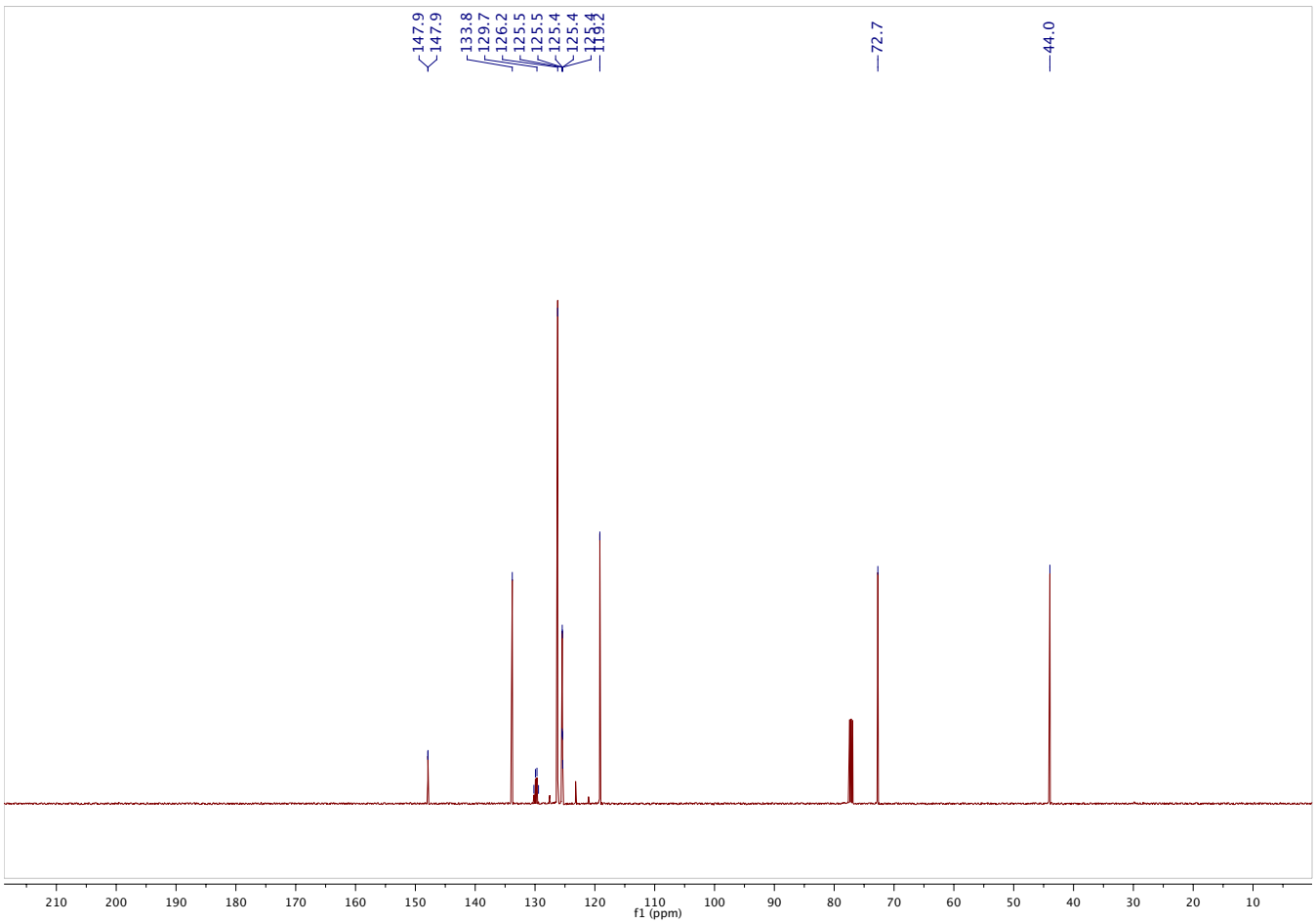
147.9
147.9
133.8
129.7
126.2
125.5
125.5
125.4
125.4
72.7
44.0
f1 (ppm)

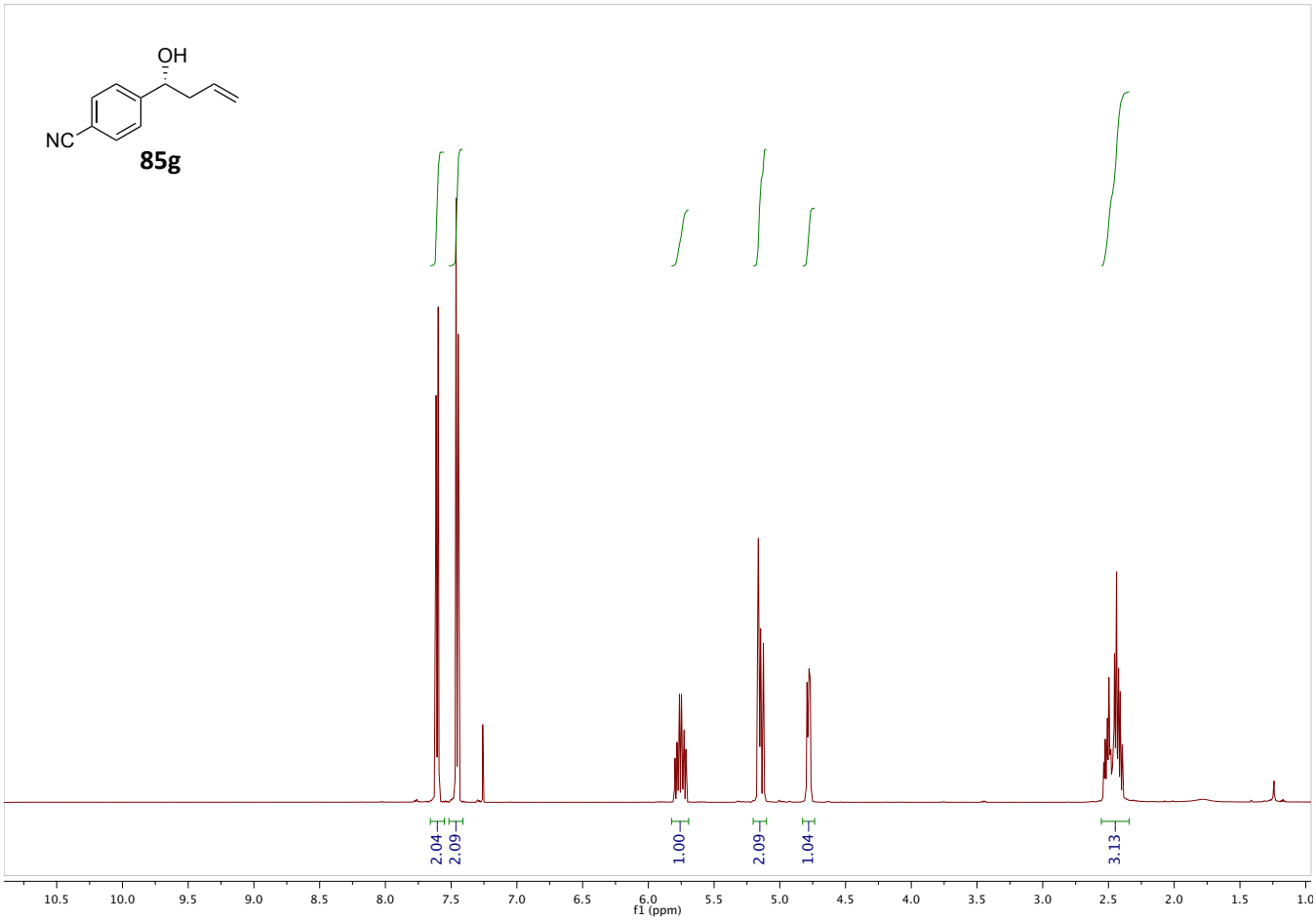
OH
NC
85g
2.04
2.09
1.00
2.09
1.04
3.13
f1 (ppm)

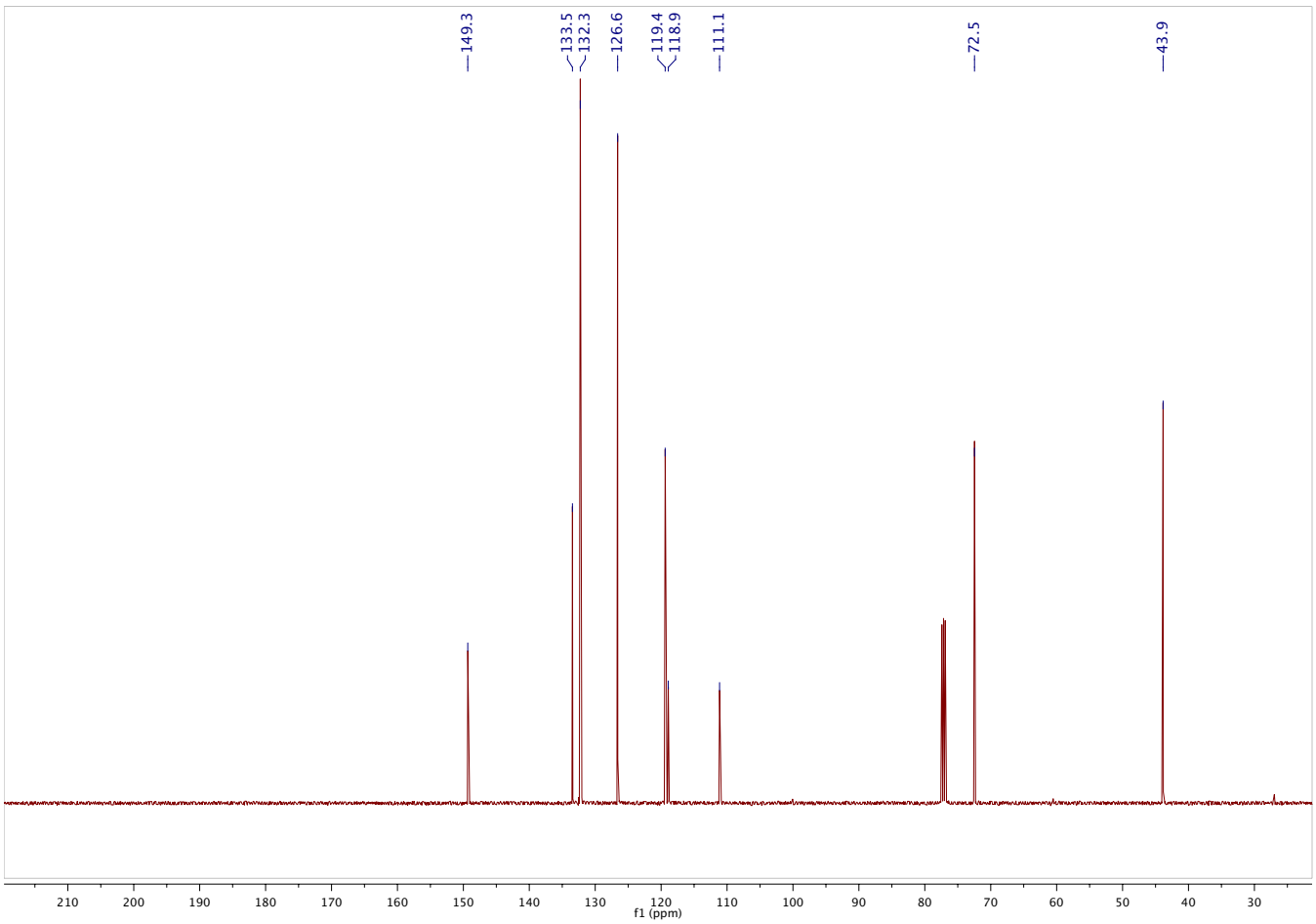
149.3
133.5
132.3
126.6
119.4
118.9
111.1
72.5
43.9
f1 (ppm)

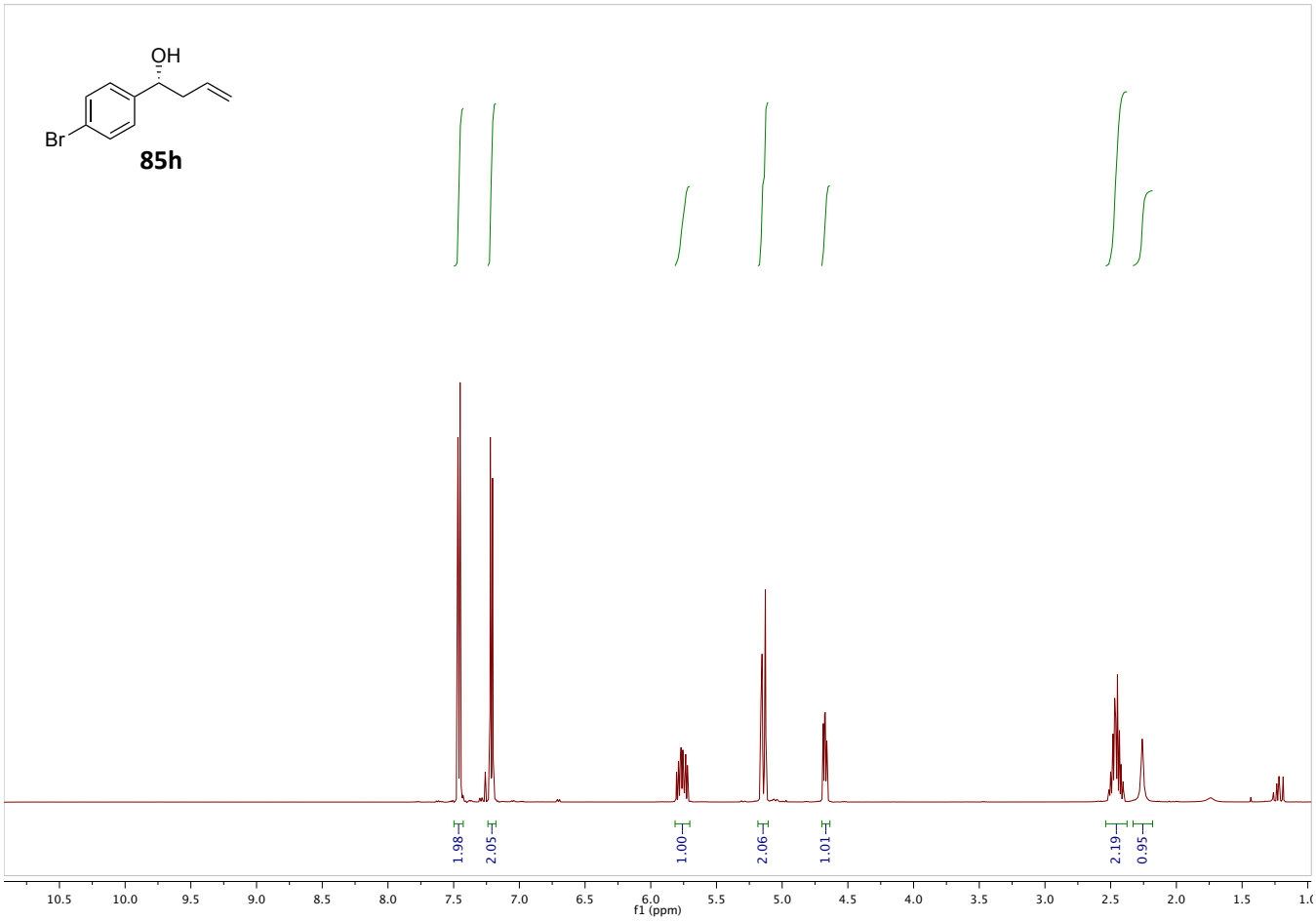
OH
Br
85h
1.98
2.05
1.00
2.06
1.01
2.19
0.95
f1 (ppm)

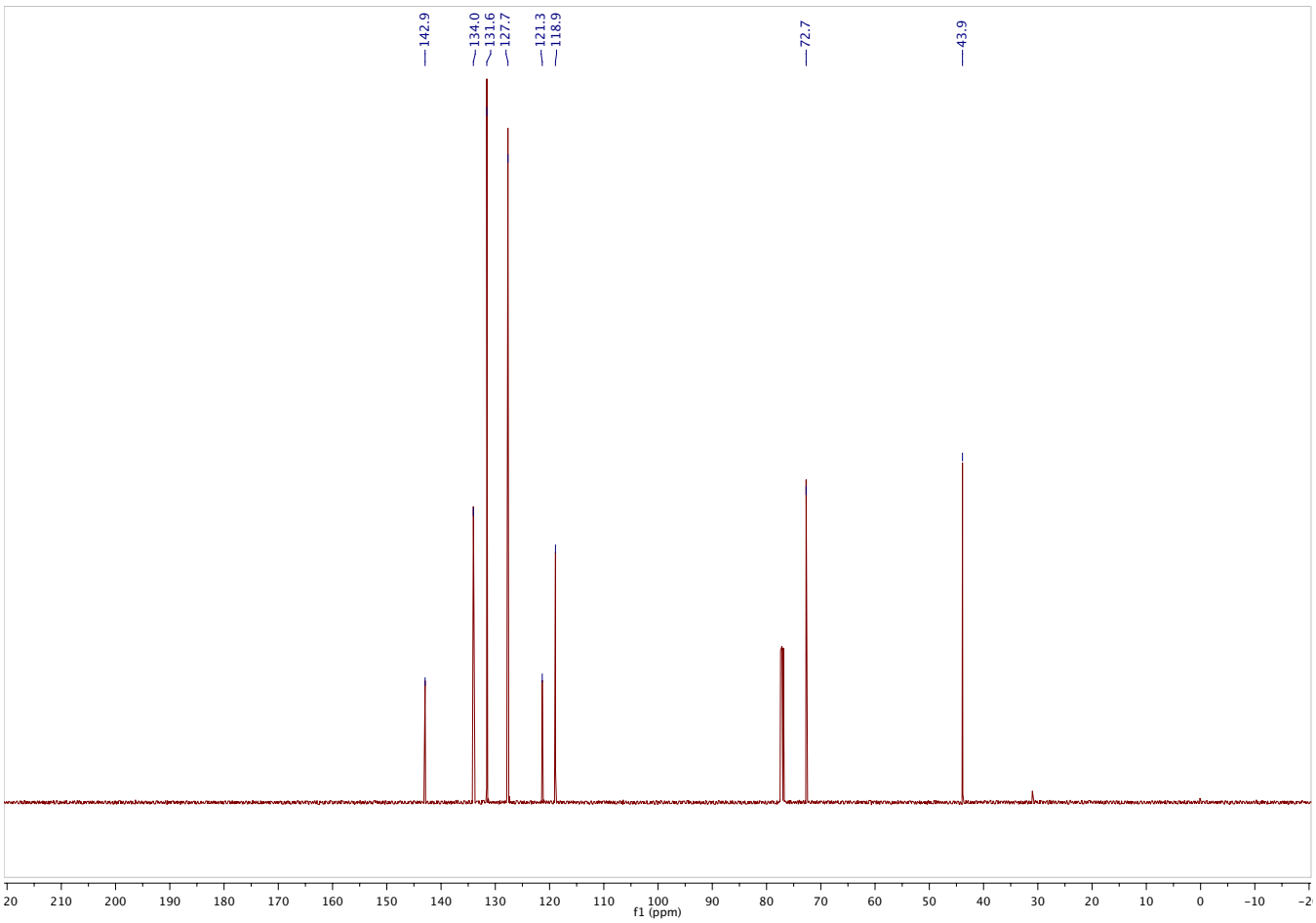
142.9
134.0
131.6
127.7
121.3
118.9
72.7
43.9
f1 (ppm)

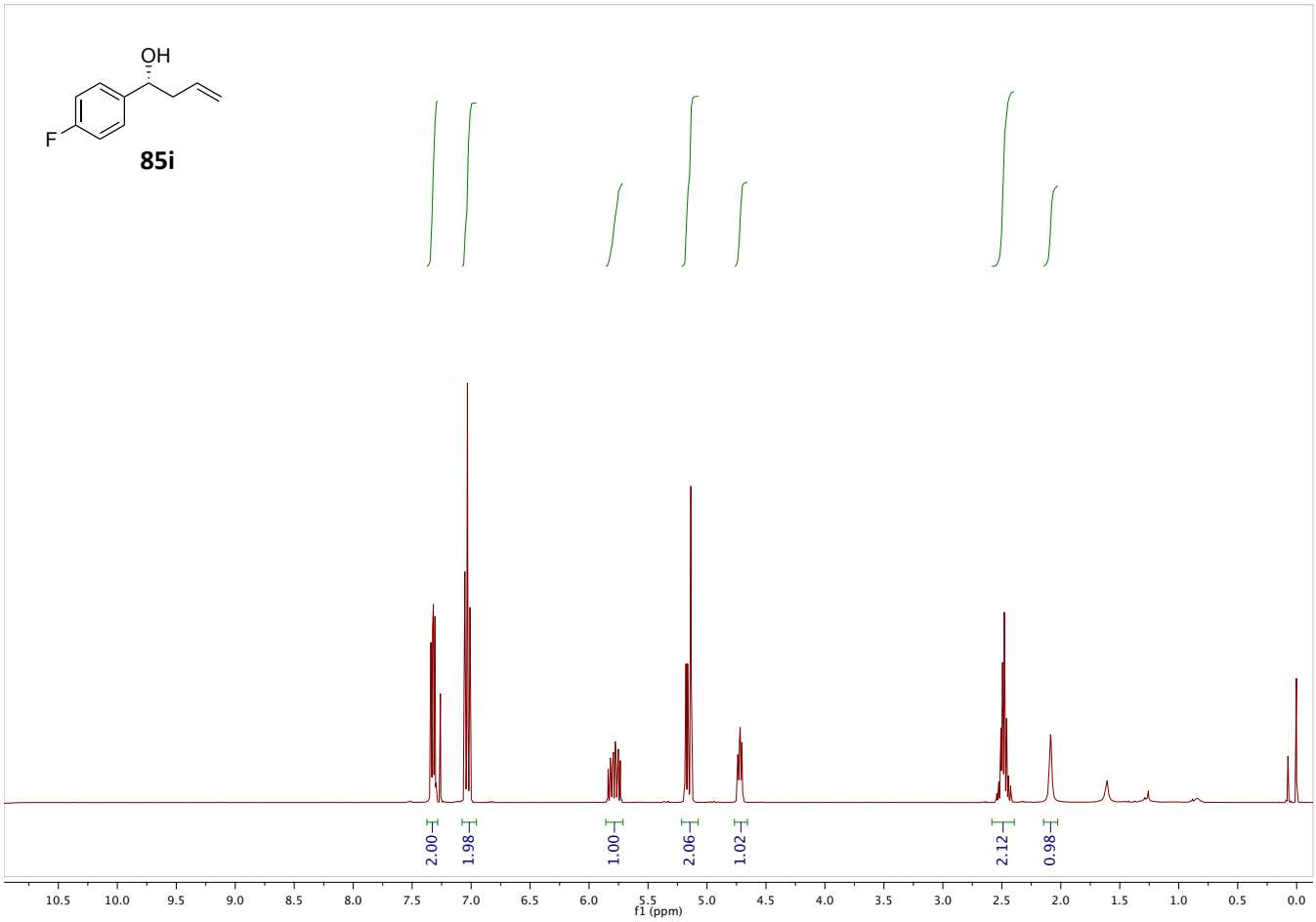
OH
F
85i
2.00
1.98
1.00
2.06
1.02
2.12
0.98
f1 (ppm)

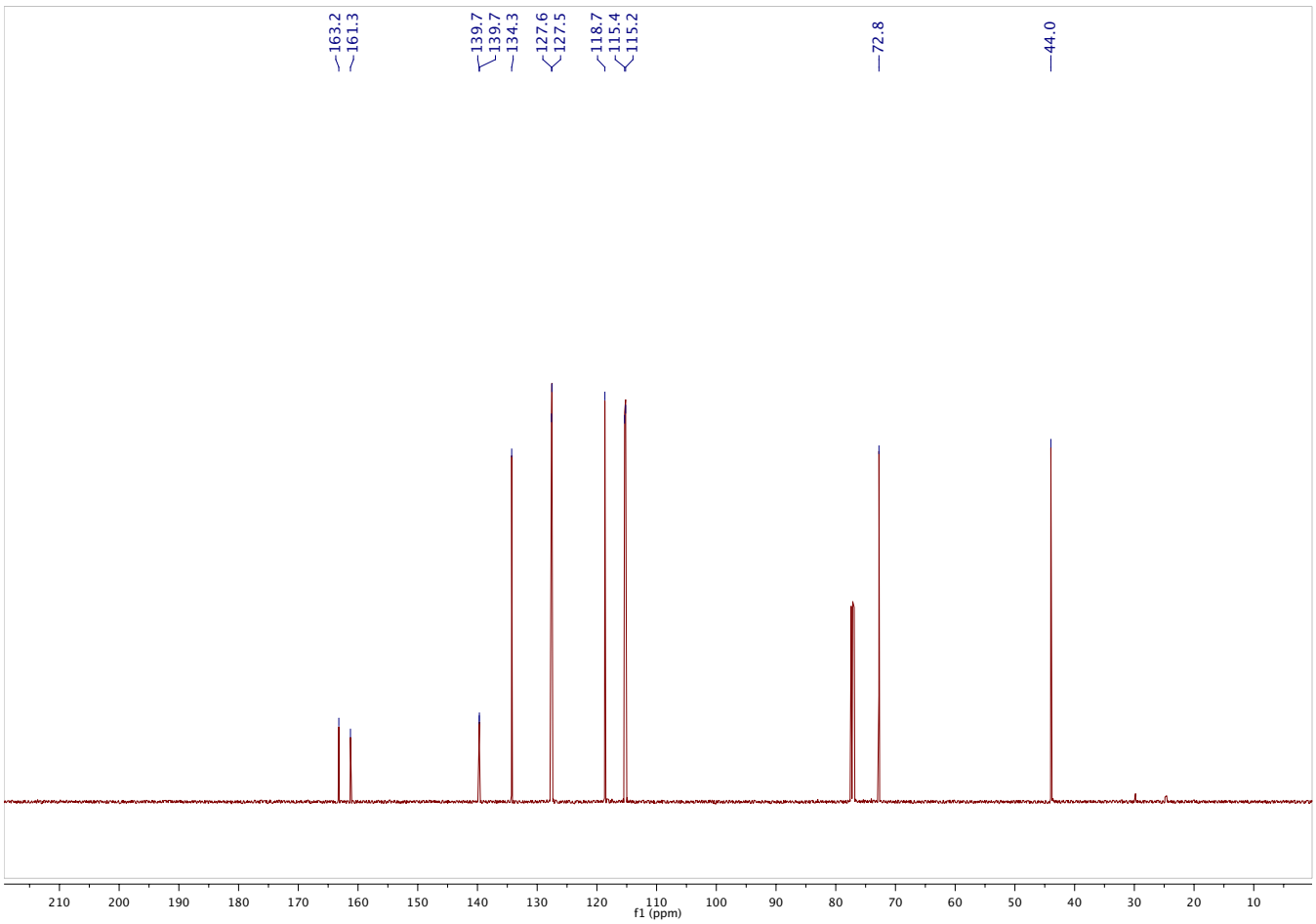
163.2
161.3
139.7
139.7
134.3
127.6
127.5
118.7
115.4
115.2
72.8
44.0
f1 (ppm)

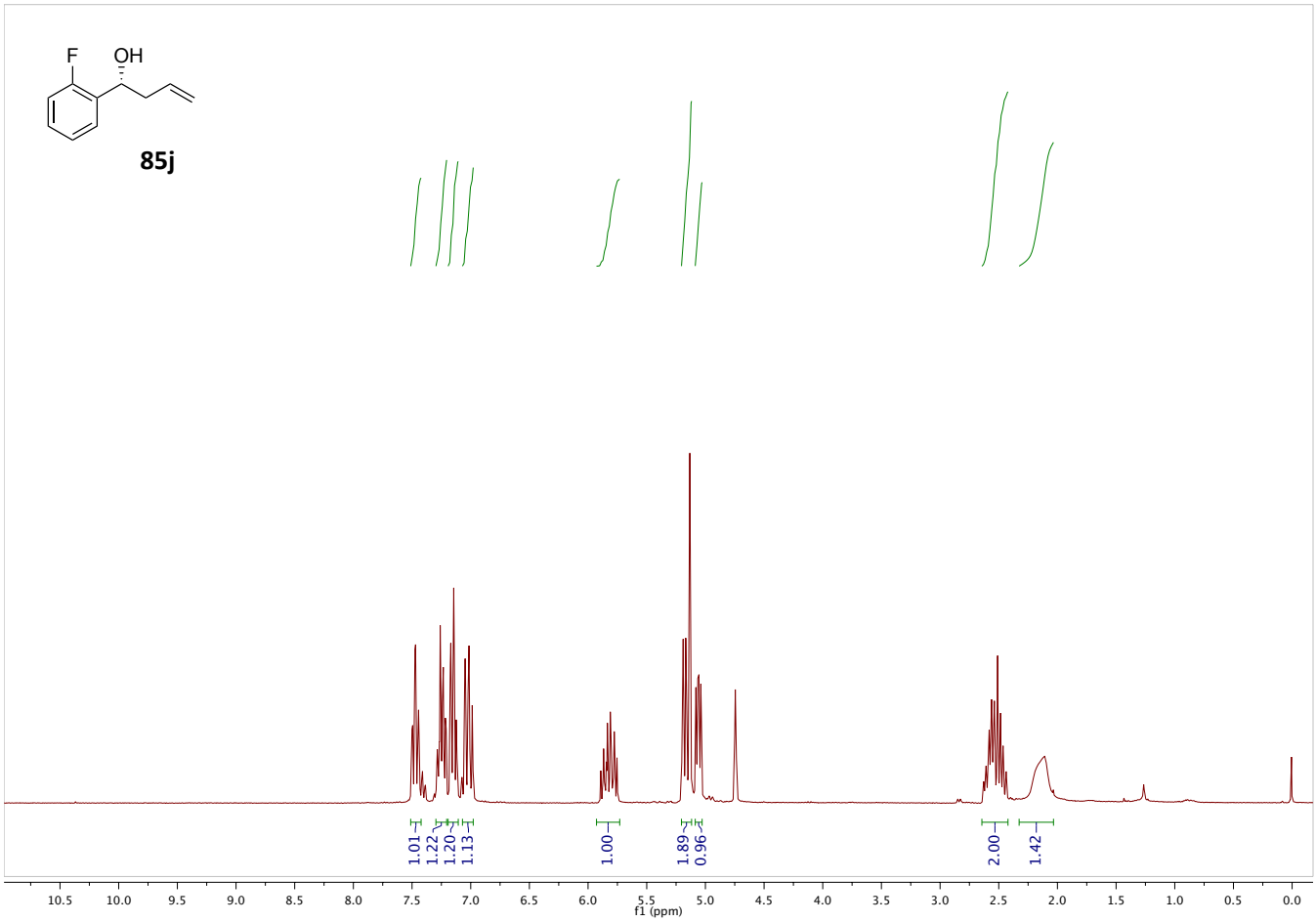
F
OH
85j
1.01
1.22
1.20
1.13
1.00
1.89
0.96
2.00
1.42
f1 (ppm)

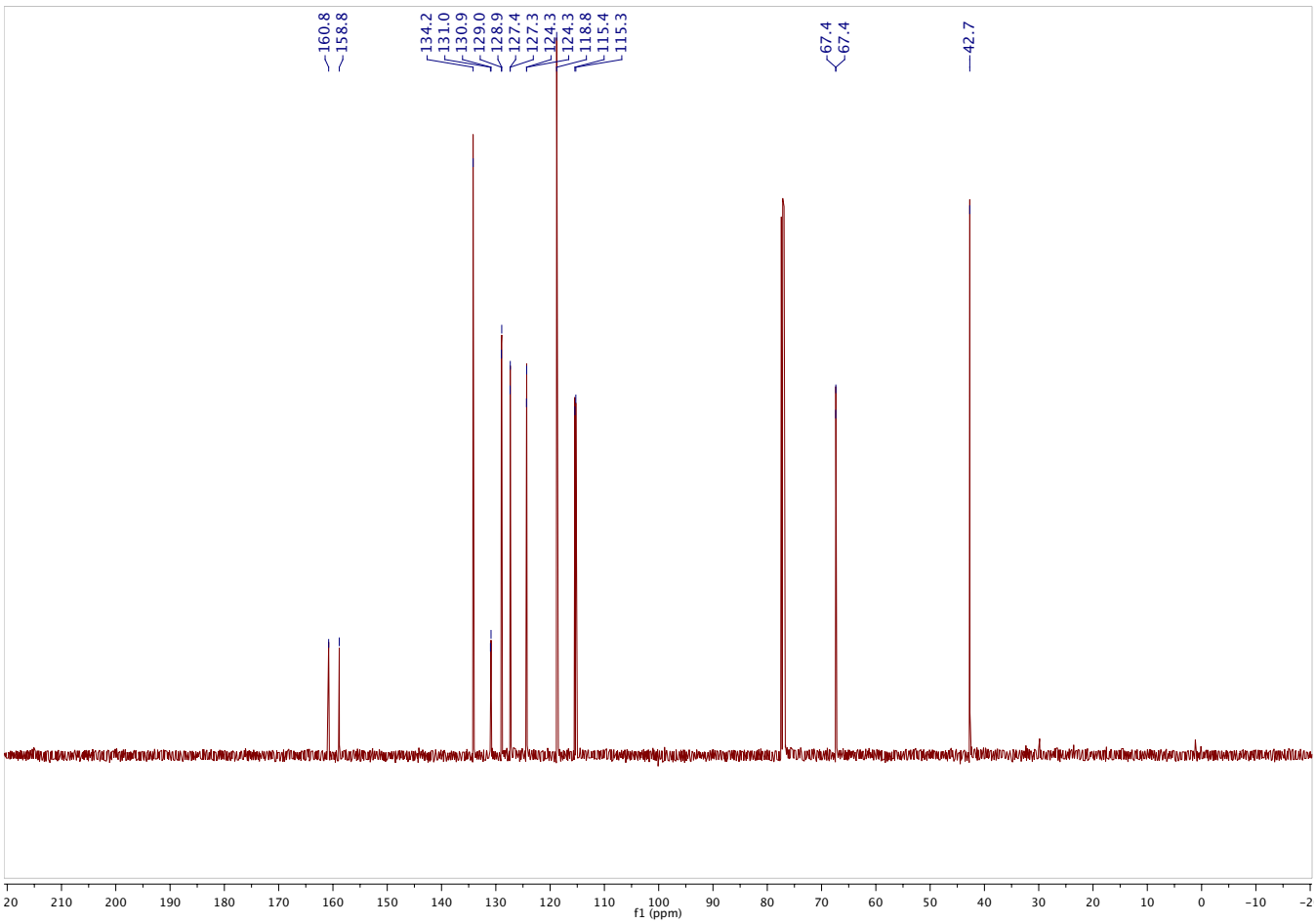
160.8
158.8
134.2
131.0
130.9
129.0
128.9
127.4
127.3
124.3
124.3
118.8
115.4
115.3
67.4
67.4
42.7
f1 (ppm)

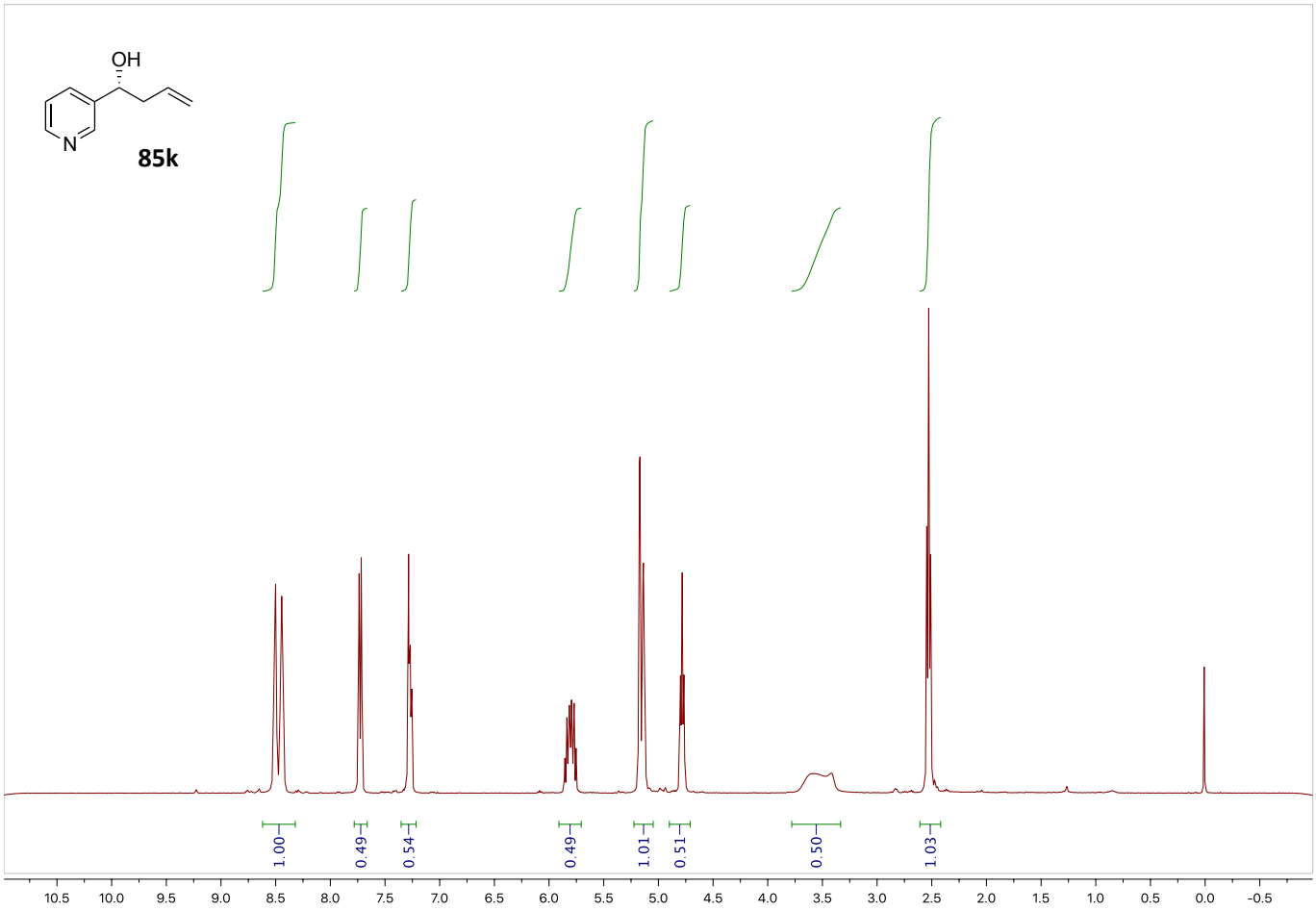
OH
N
85k
1.00
0.49
0.54
0.49
1.01
0.51
0.50
1.03
10.5 10.0 9.5 9.0 8.5 8.0 7.5 7.0 6.5 6.0 5.5 5.0 4.5 4.0 3.5 3.0 2.5 2.0 1.5 1.0 0.5 0.0 -0.5

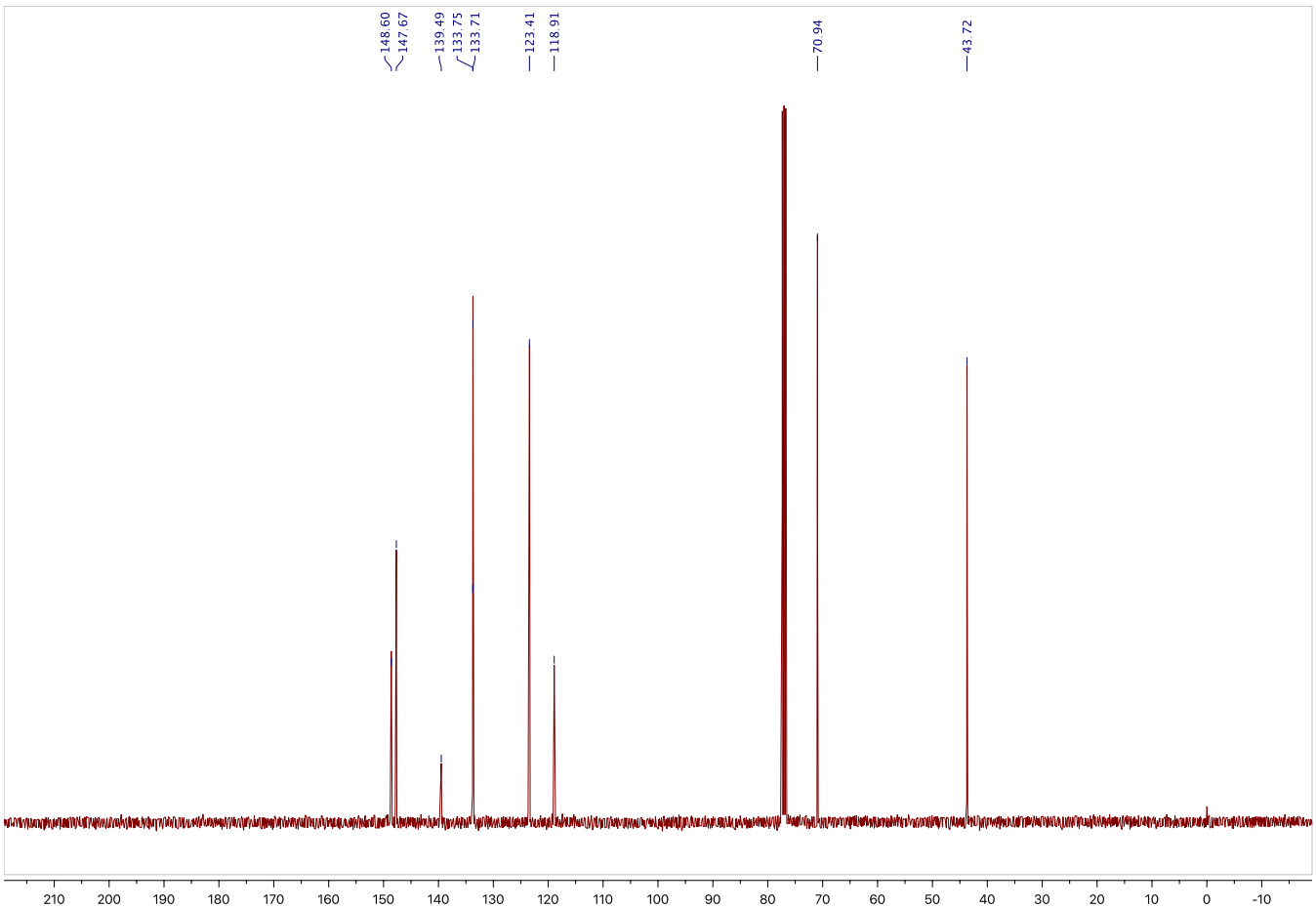
148.60
147.67
139.49
133.75
133.71
123.41
118.91
70.94
43.72
210 200 190 180 170 160 150 140 130 120 110 100 90 80 70 60 50 40 30 20 10 0 -10

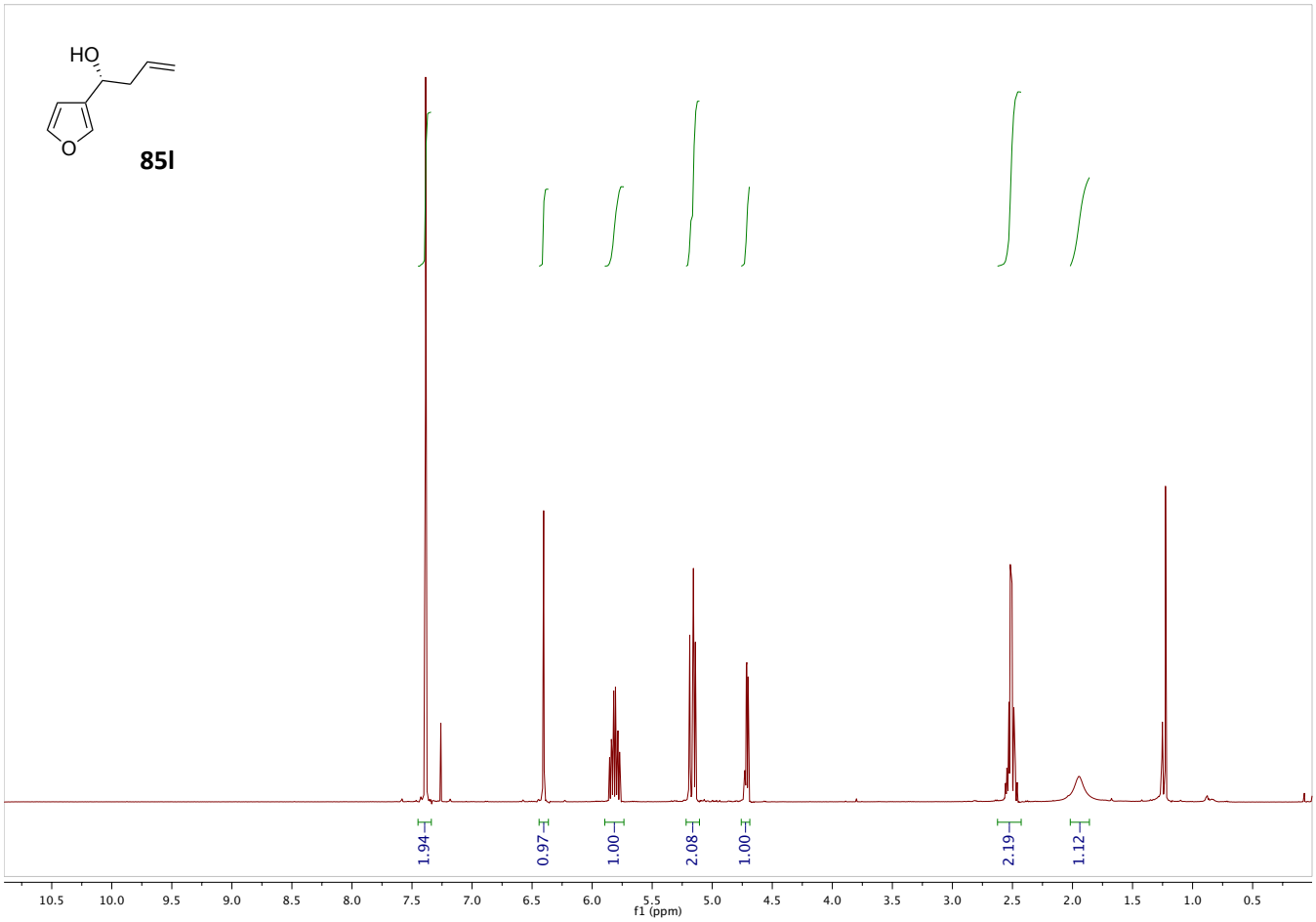
HO
O
85l
1.94
0.97
1.00
2.08
1.00
2.19
1.12
f1 (ppm)

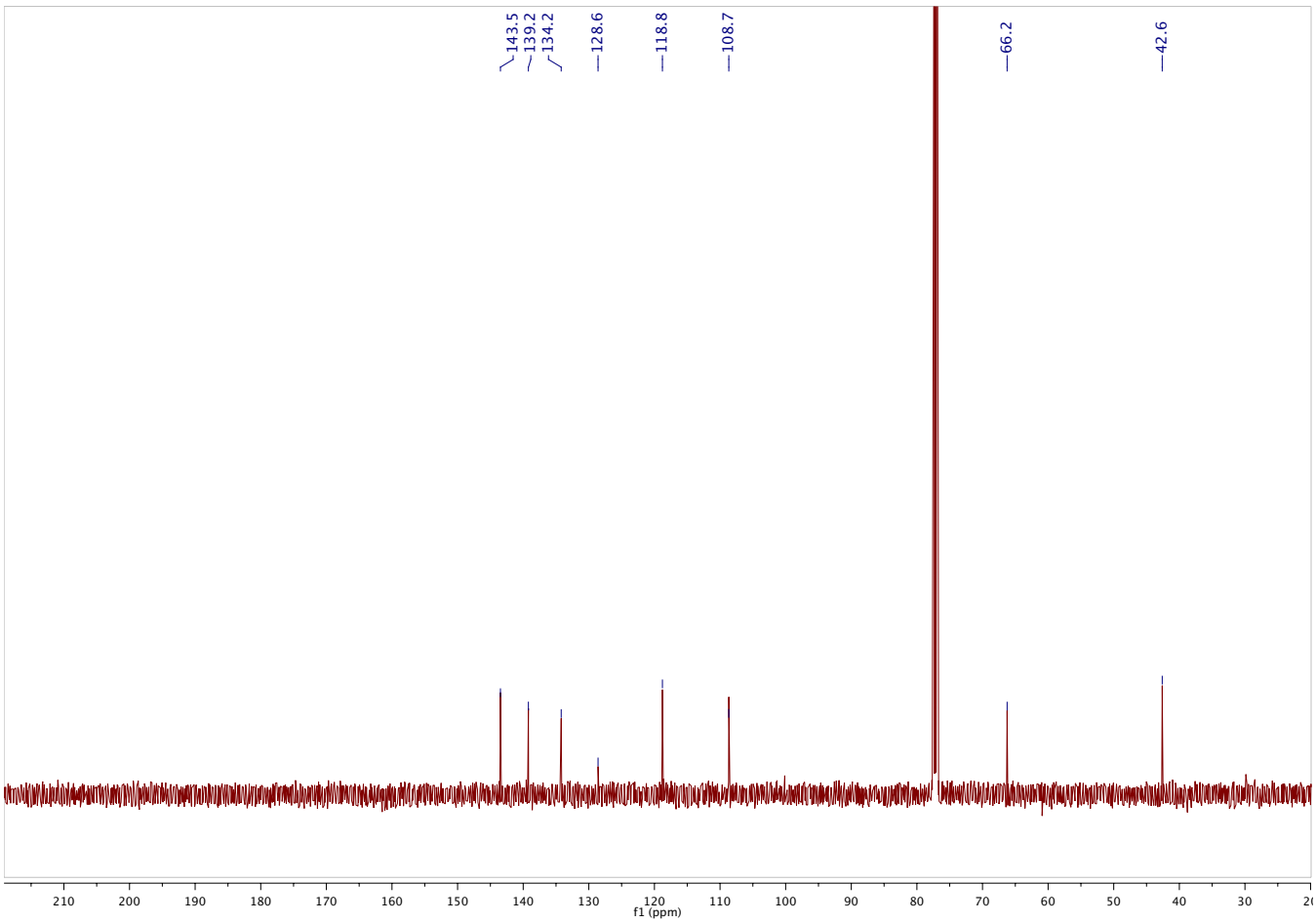
143.5
139.2
134.2
128.6
118.8
108.7
66.2
42.6
f1 (ppm)

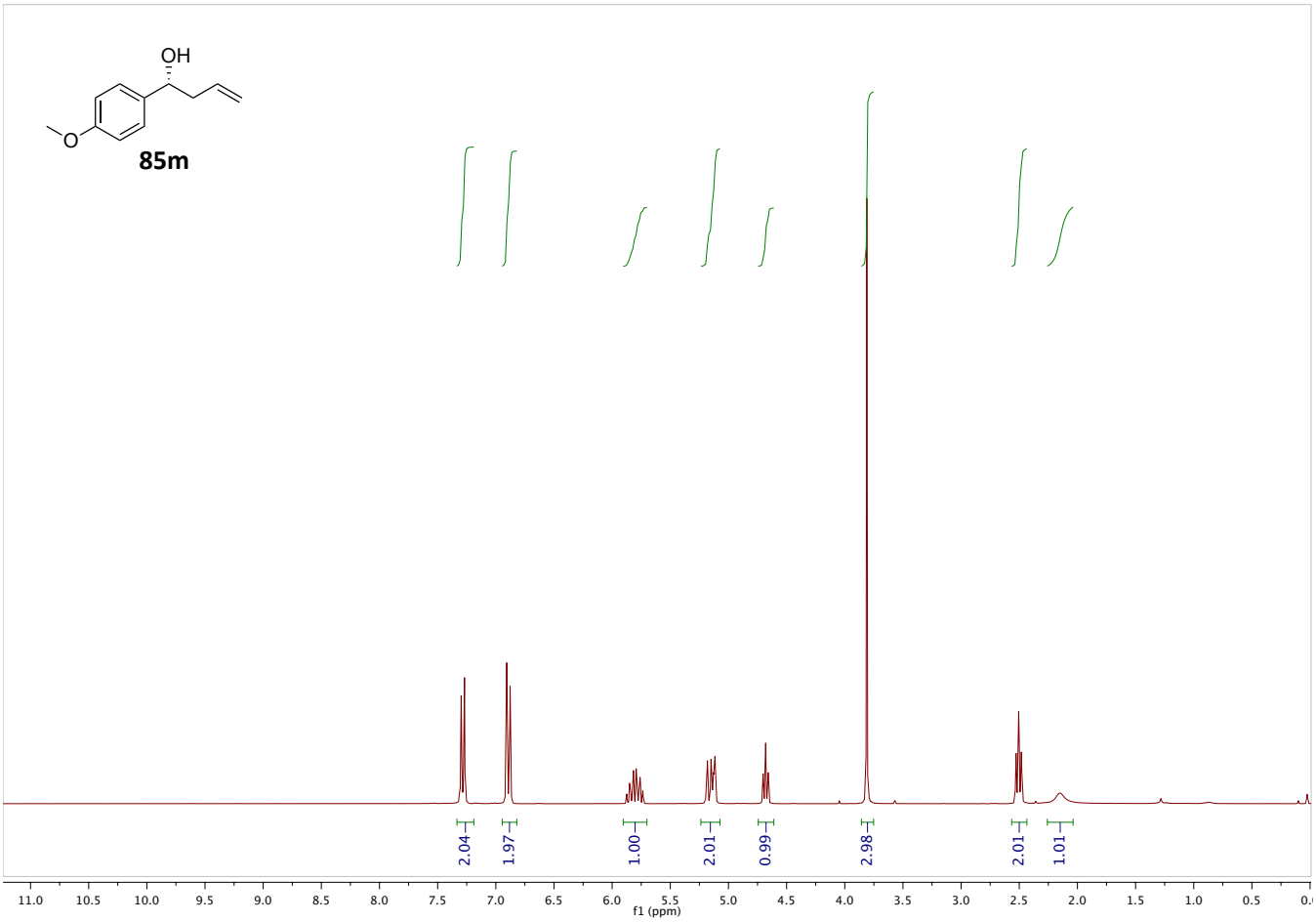
OH
O
85m
2.04
1.97
1.00
2.01
0.99
2.98
2.01
1.01
f1 (ppm)

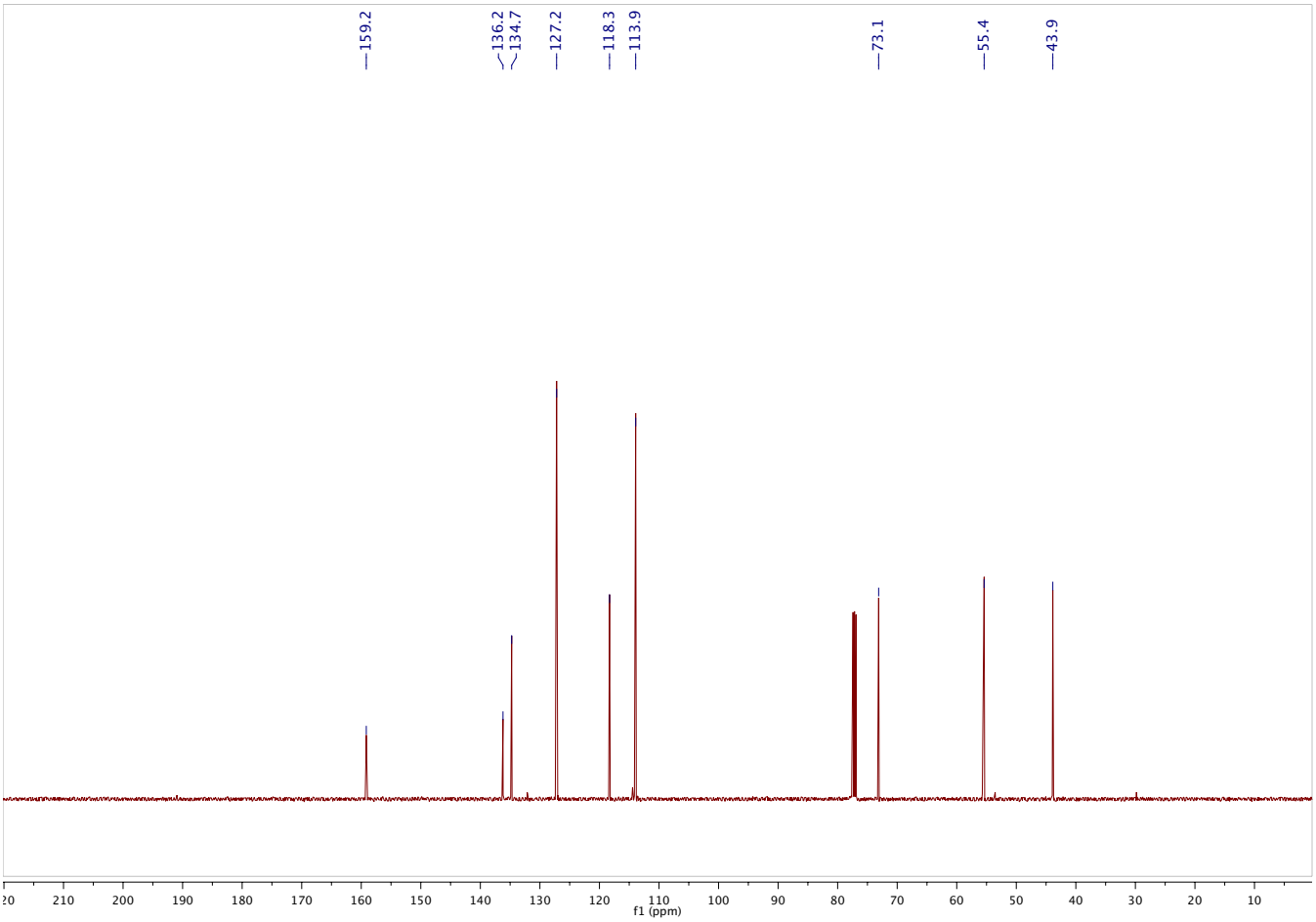
159.2
136.2
134.7
127.2
118.3
113.9
73.1
55.4
43.9
f1 (ppm)

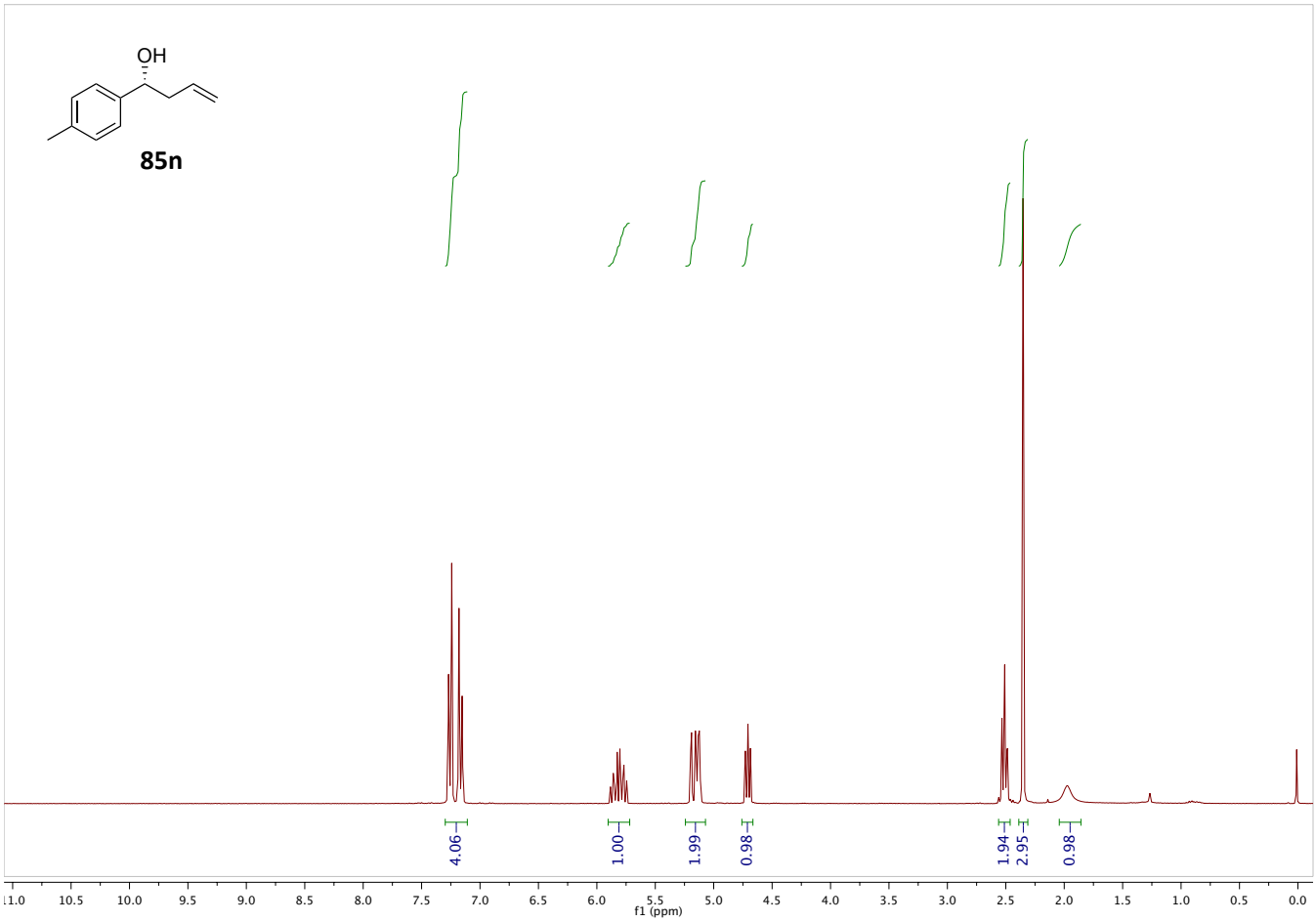
OH
85n
4.06
1.00
1.99
0.98
1.94
2.95
0.98
f1 (ppm)

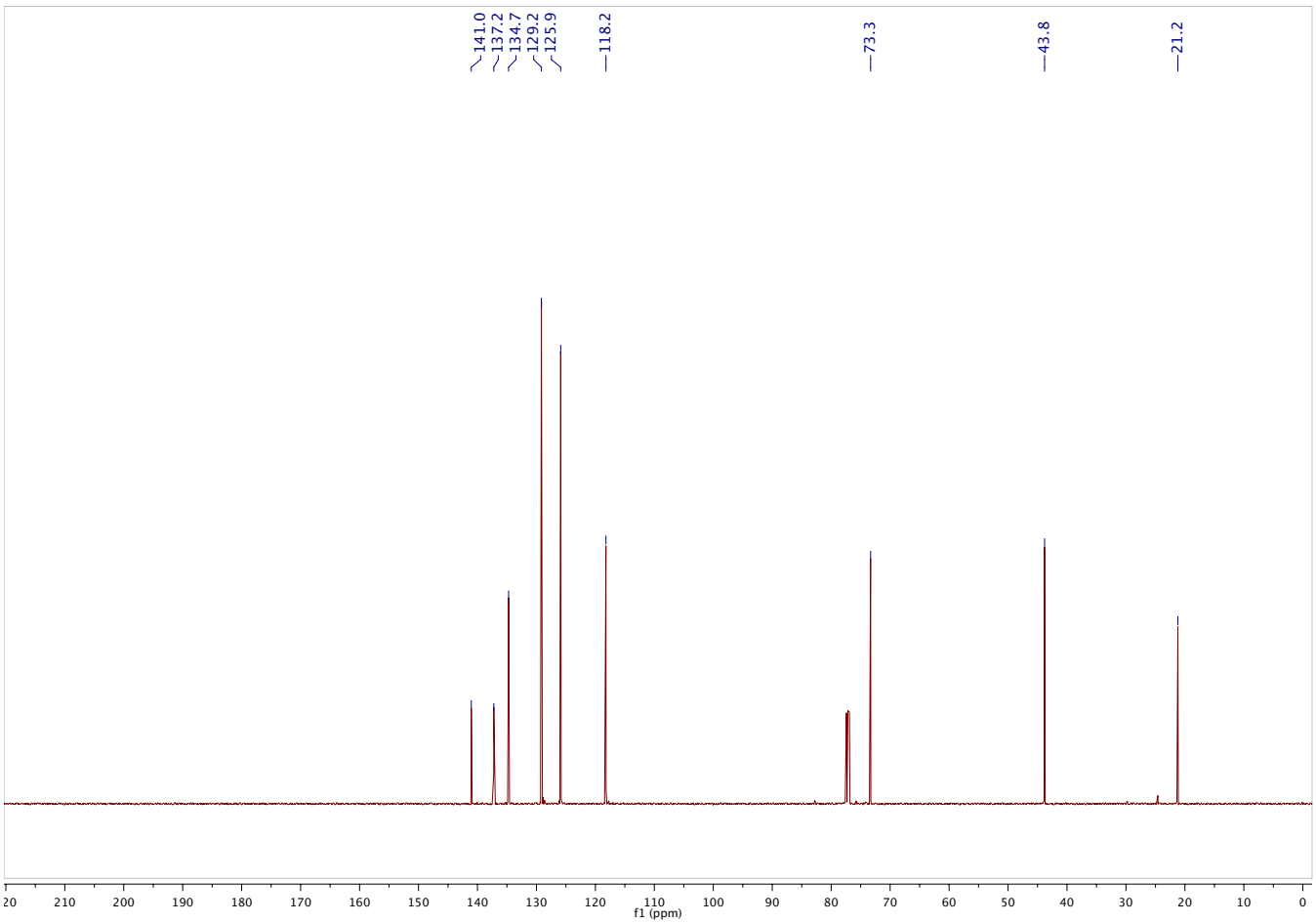
141.0
137.2
134.7
129.2
125.9
118.2
73.3
43.8
21.2
f1 (ppm)

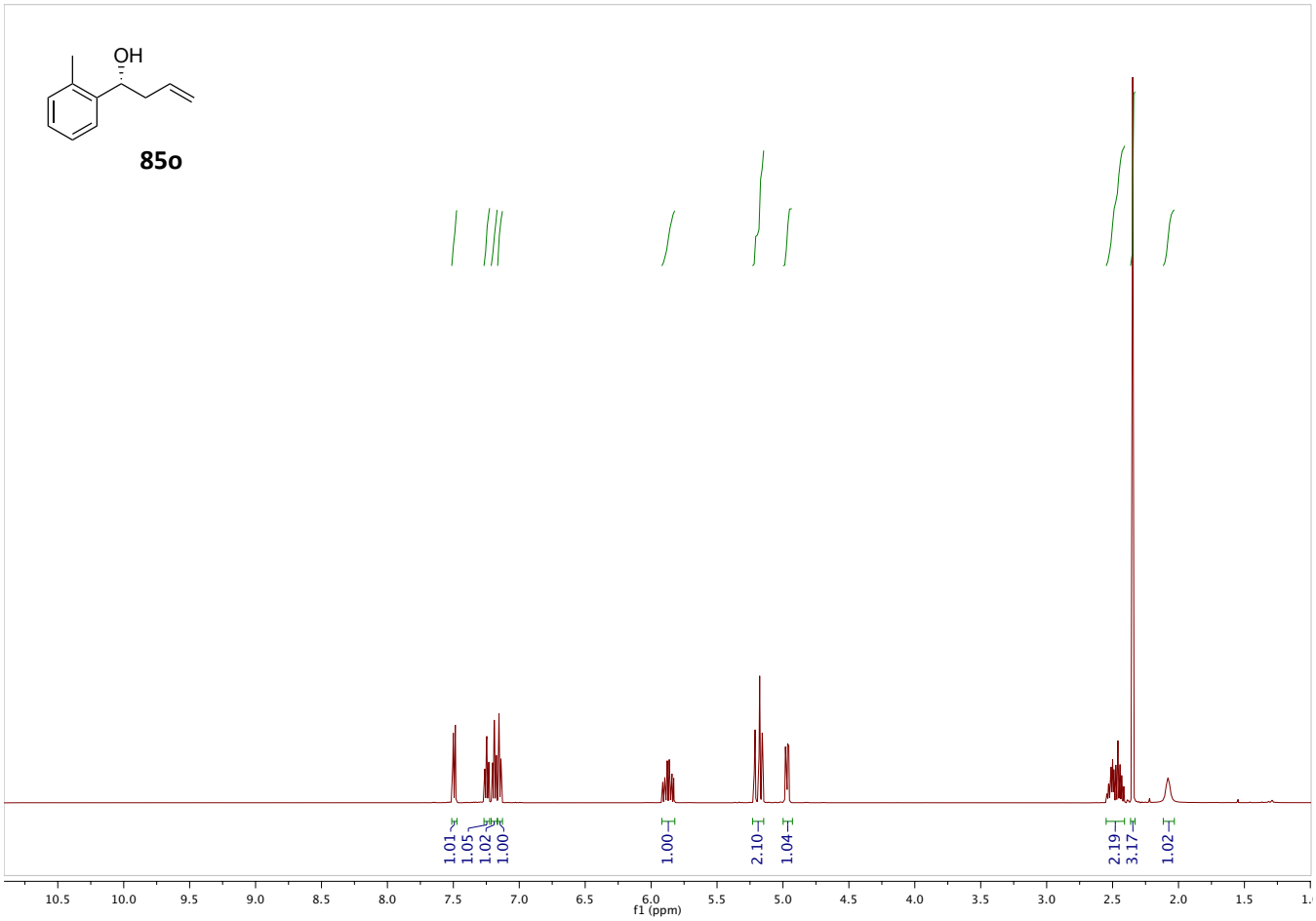
OH
85o
1.01
1.05
1.02
1.00
1.00
2.10
1.04
2.19
3.17
1.02
f1 (ppm)

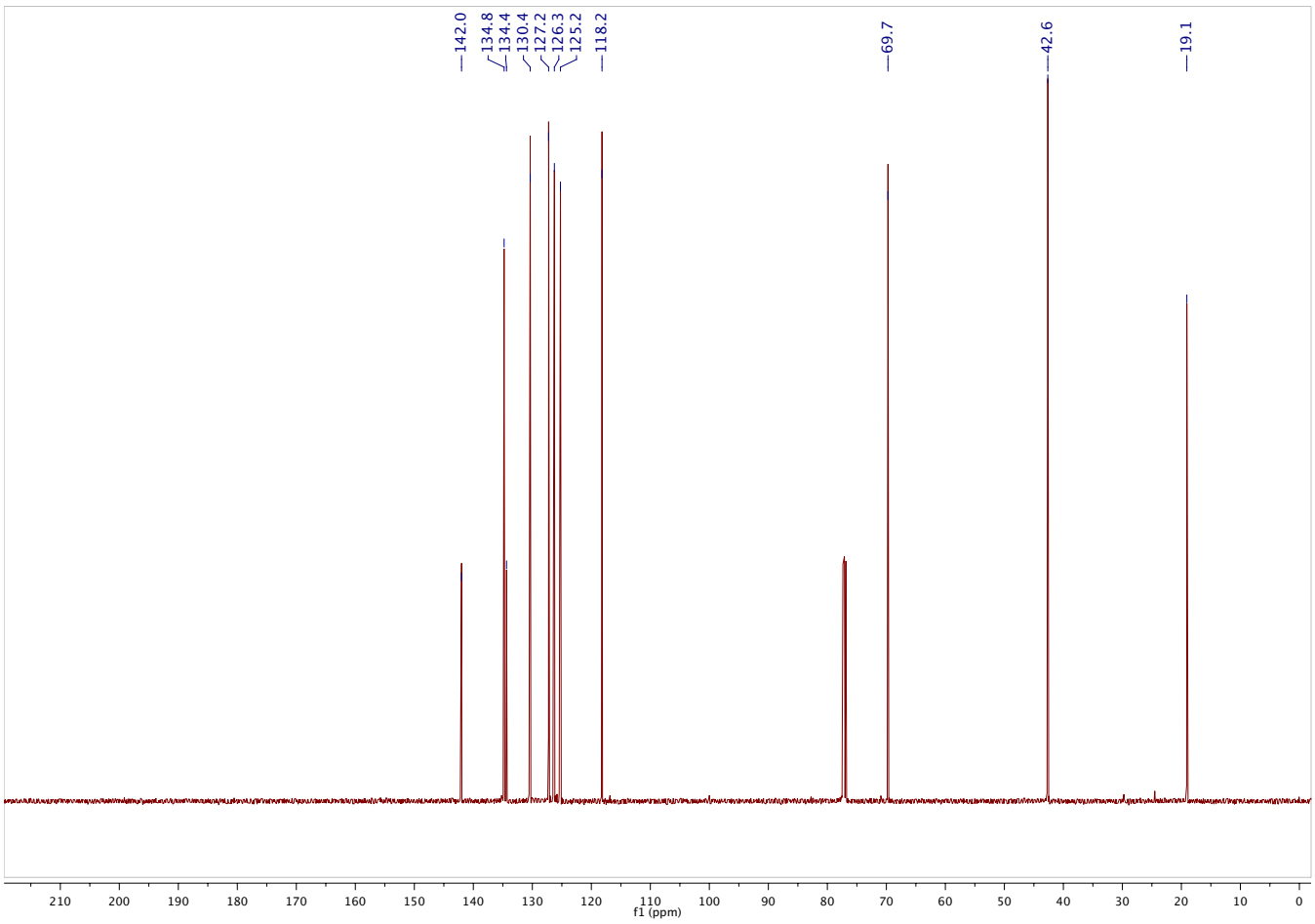
142.0
134.8
134.4
130.4
127.2
126.3
125.2
118.2
69.7
42.6
19.1
f1 (ppm)

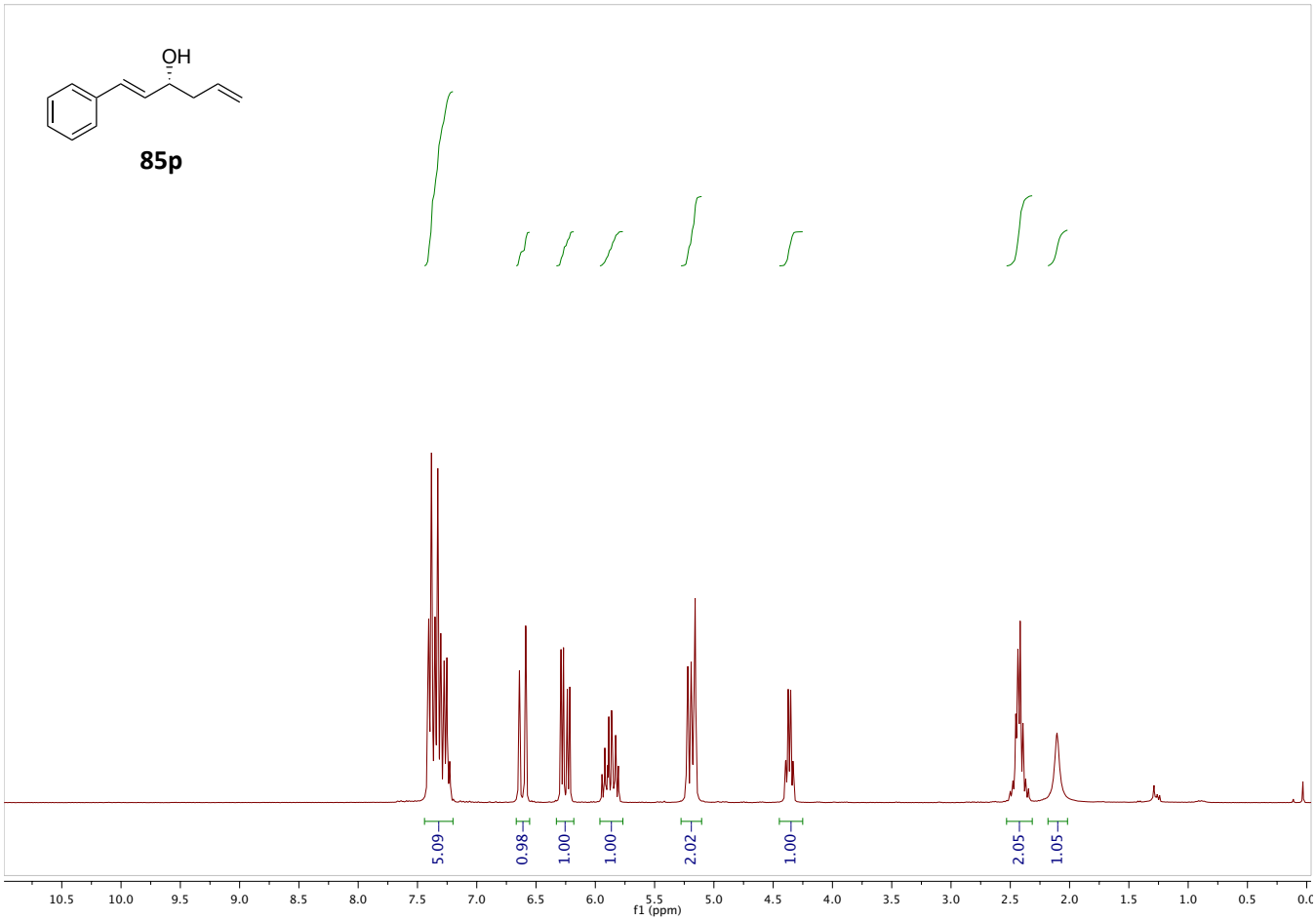
OH
85p
5.09
0.98
1.00
1.00
2.02
1.00
2.05
1.05
f1 (ppm)

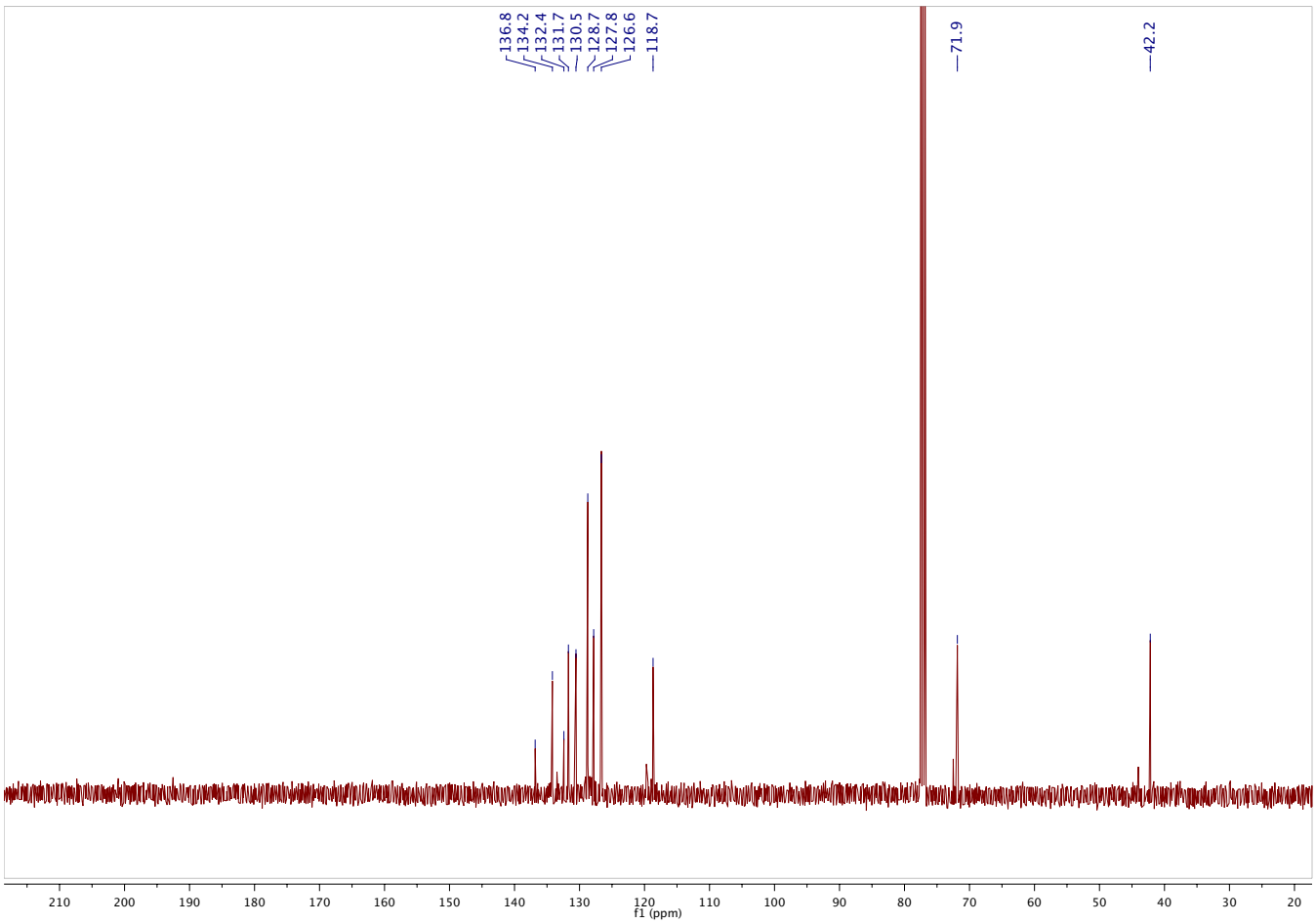
136.8
134.2
132.4
131.7
130.5
128.7
127.8
126.6
118.7
71.9
42.2
f1 (ppm)

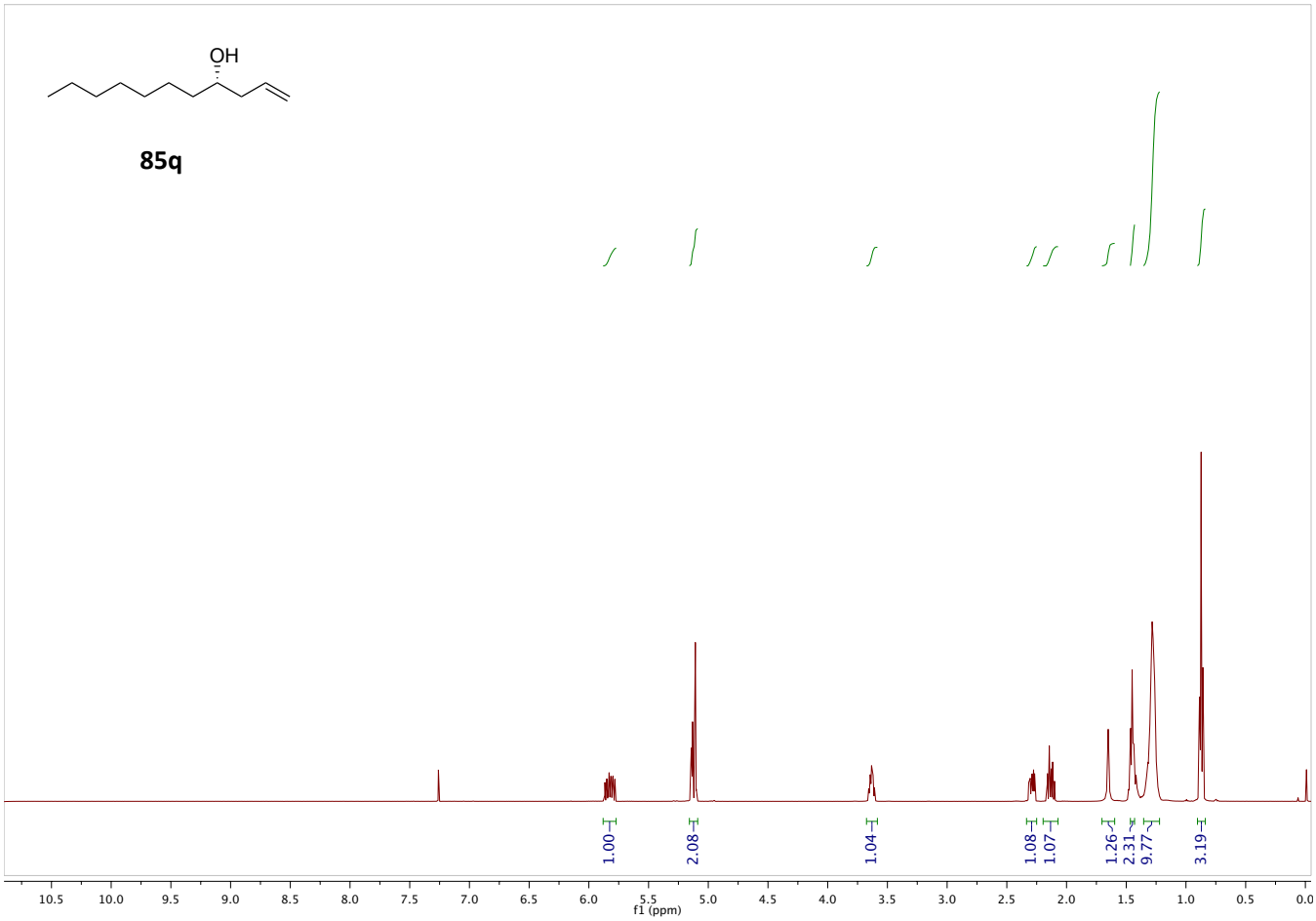
OH
85q
1.00
2.08
1.04
1.08
1.07
1.26
2.31
9.77
3.19
f1 (ppm)

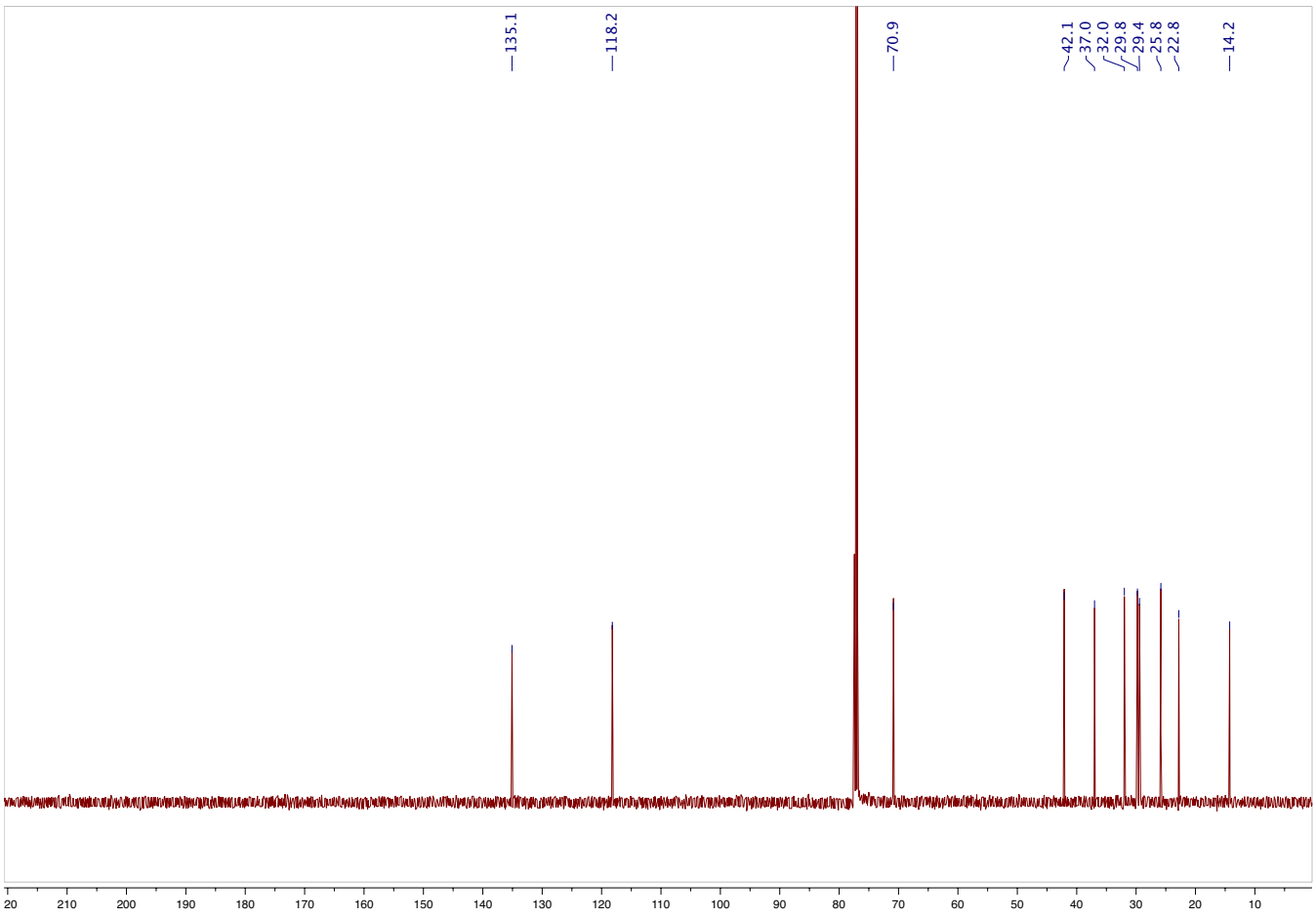
135.1
118.2
70.9
42.1
37.0
32.0
29.8
29.4
25.8
22.8
14.2

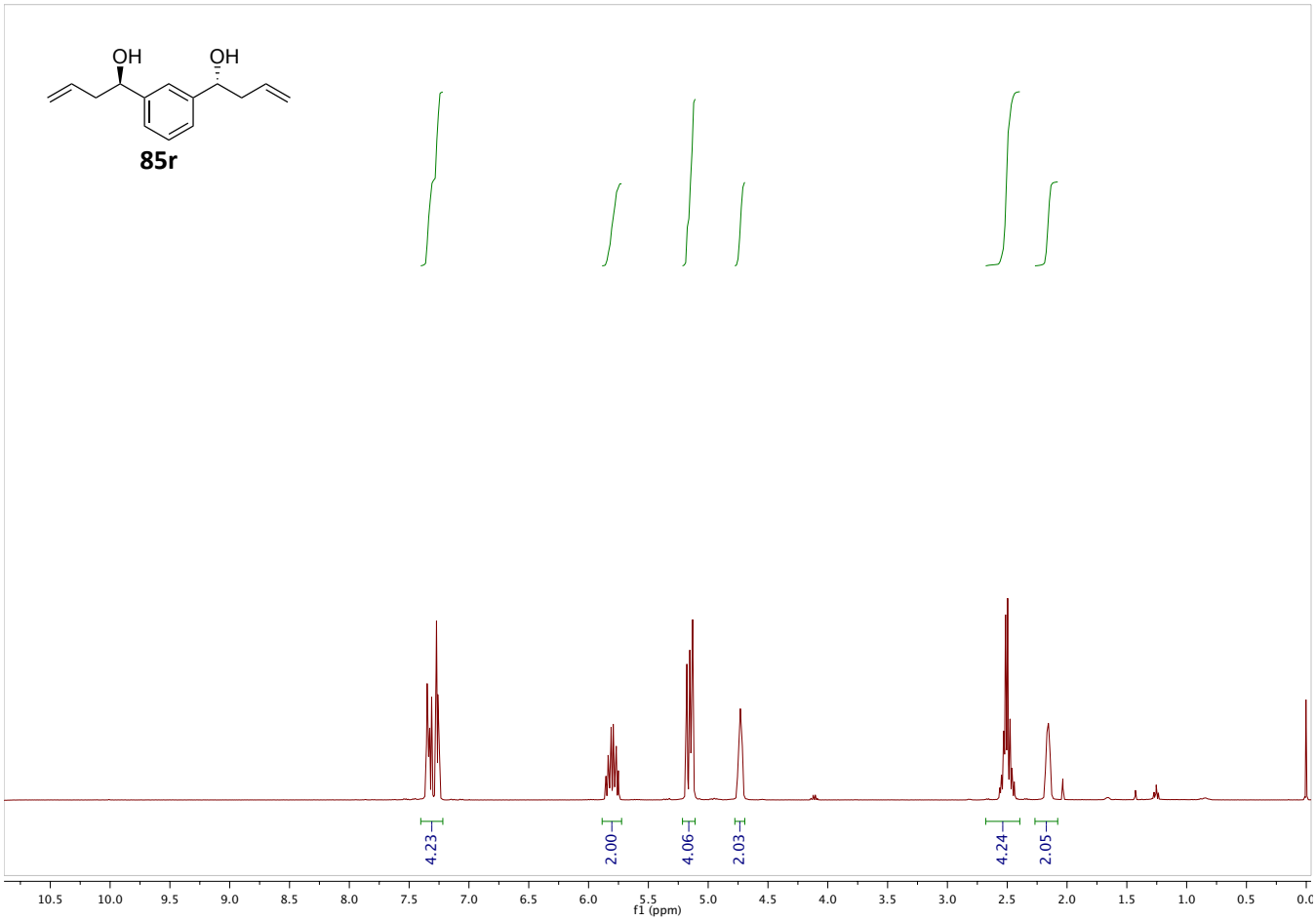
OH
OH
85r
4.23
2.00
4.06
2.03
4.24
2.05
f1 (ppm)

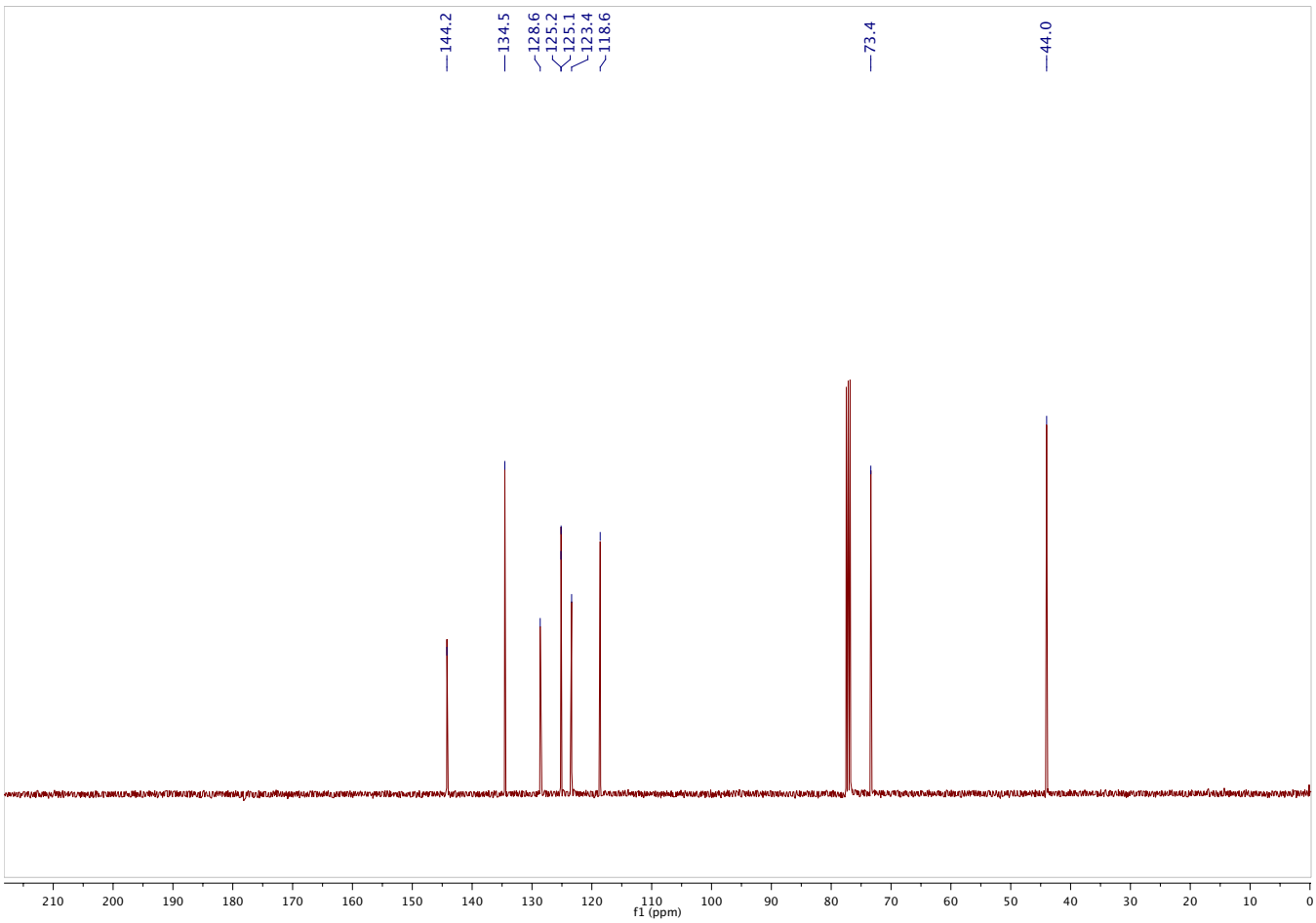
144.2
134.5
128.6
125.2
125.1
123.4
118.6
73.4
44.0
f1 (ppm)

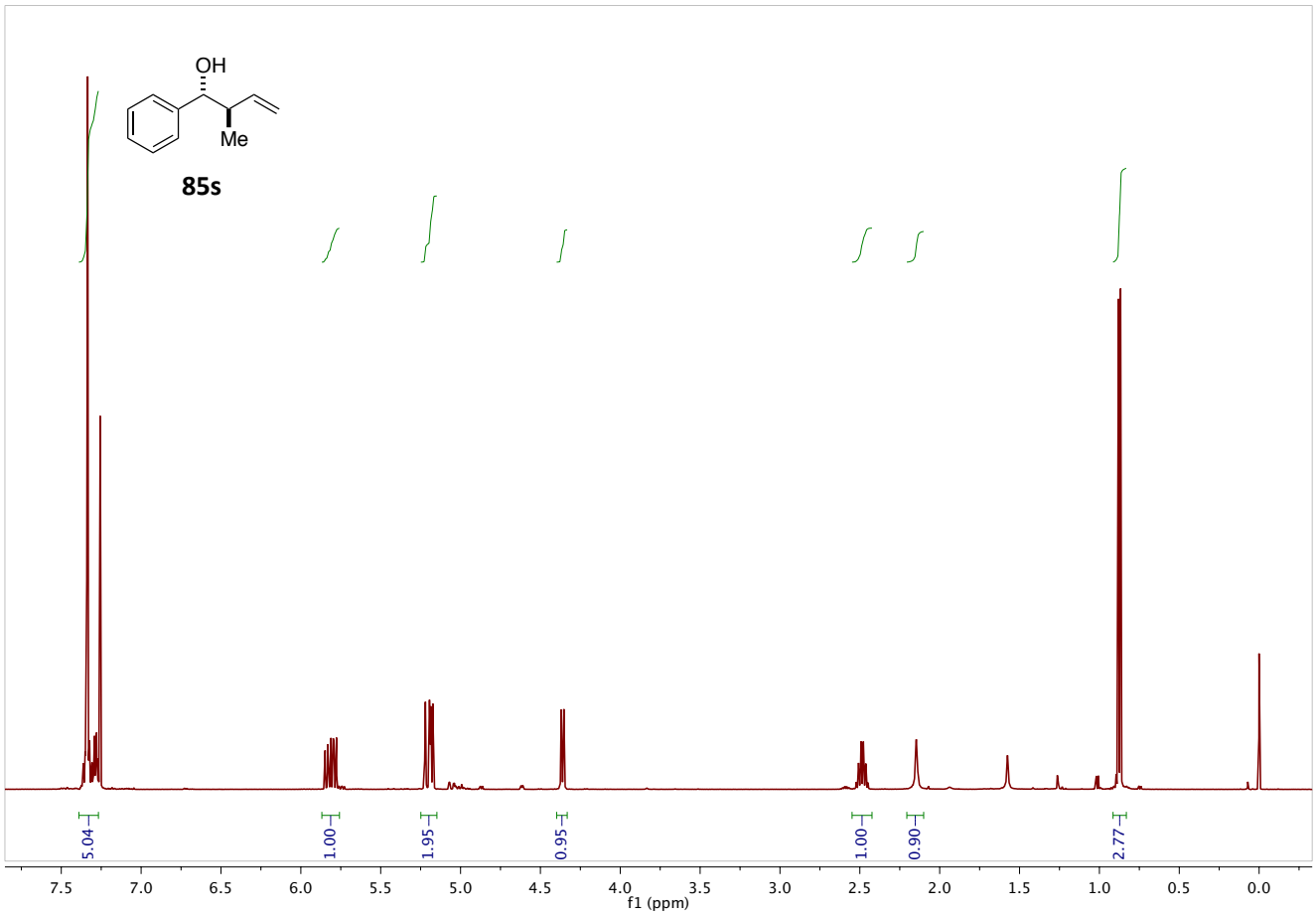
OH
Me
85s
5.04
1.00
1.95
0.95
1.00
0.90
2.77
f1 (ppm)

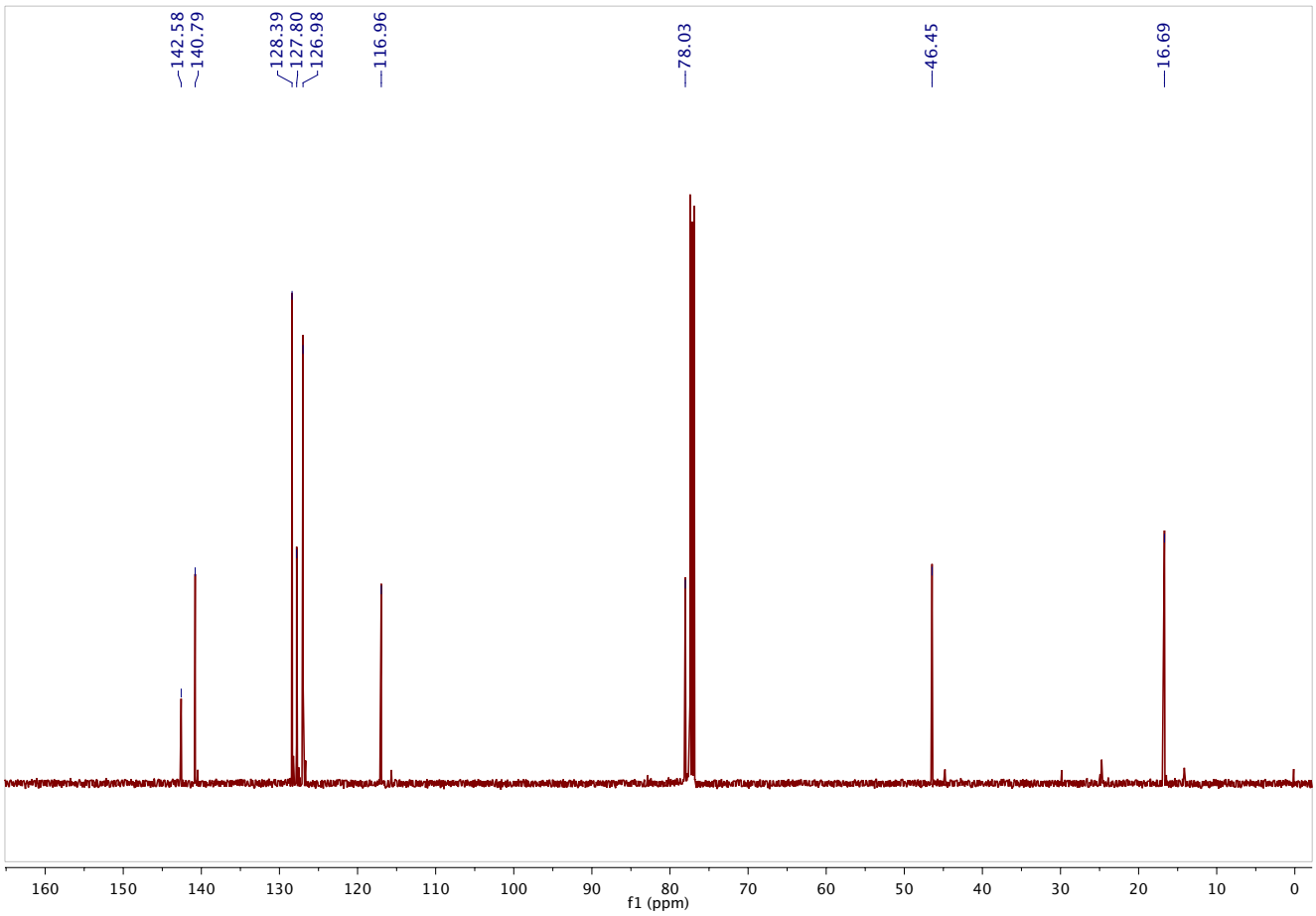
142.58
140.79
128.39
127.80
126.98
116.96
78.03
46.45
16.69
f1 (ppm)

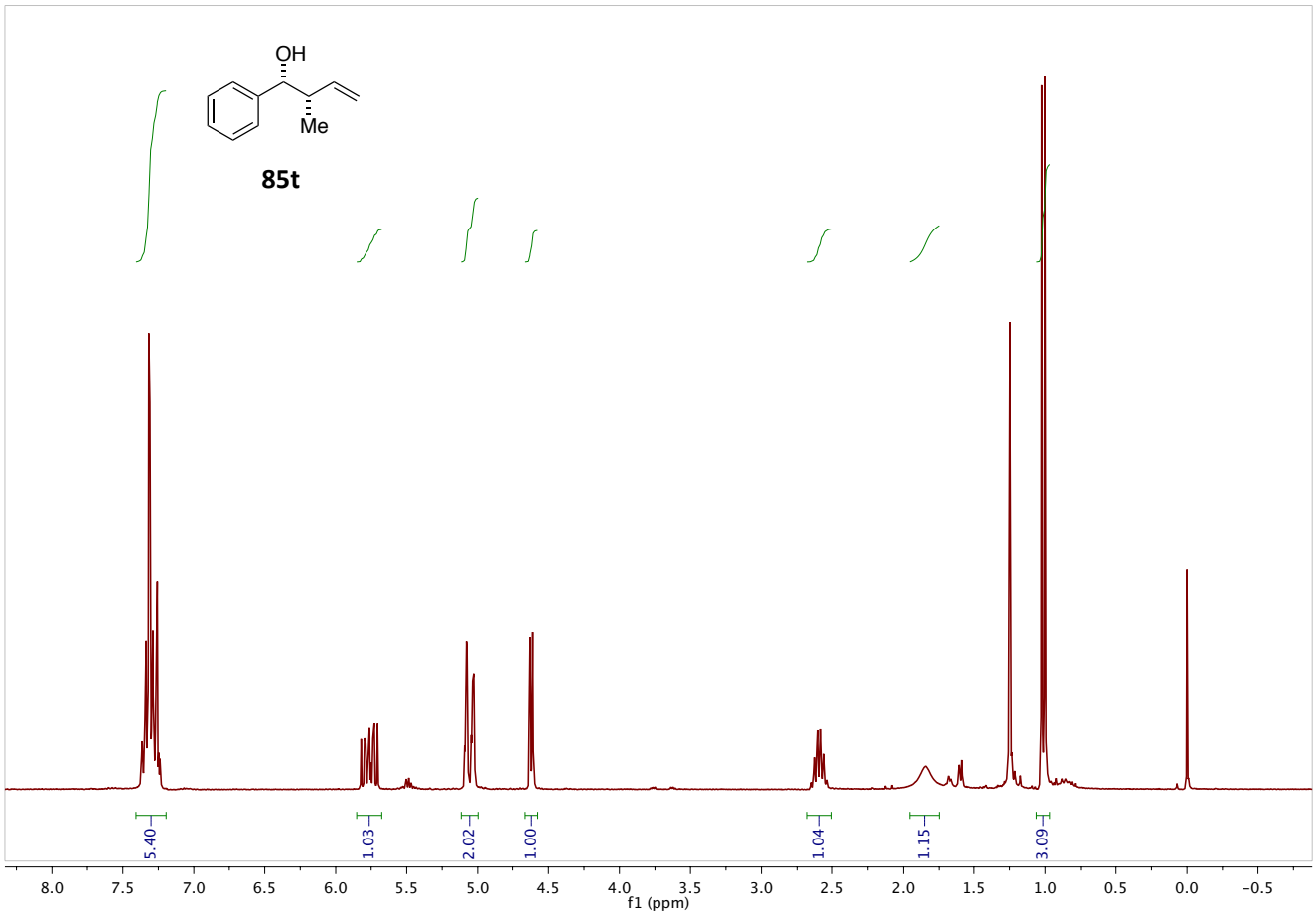
OH
Me
85t
5.40
1.03
2.02
1.00
1.04
1.15
3.09
f1 (ppm)

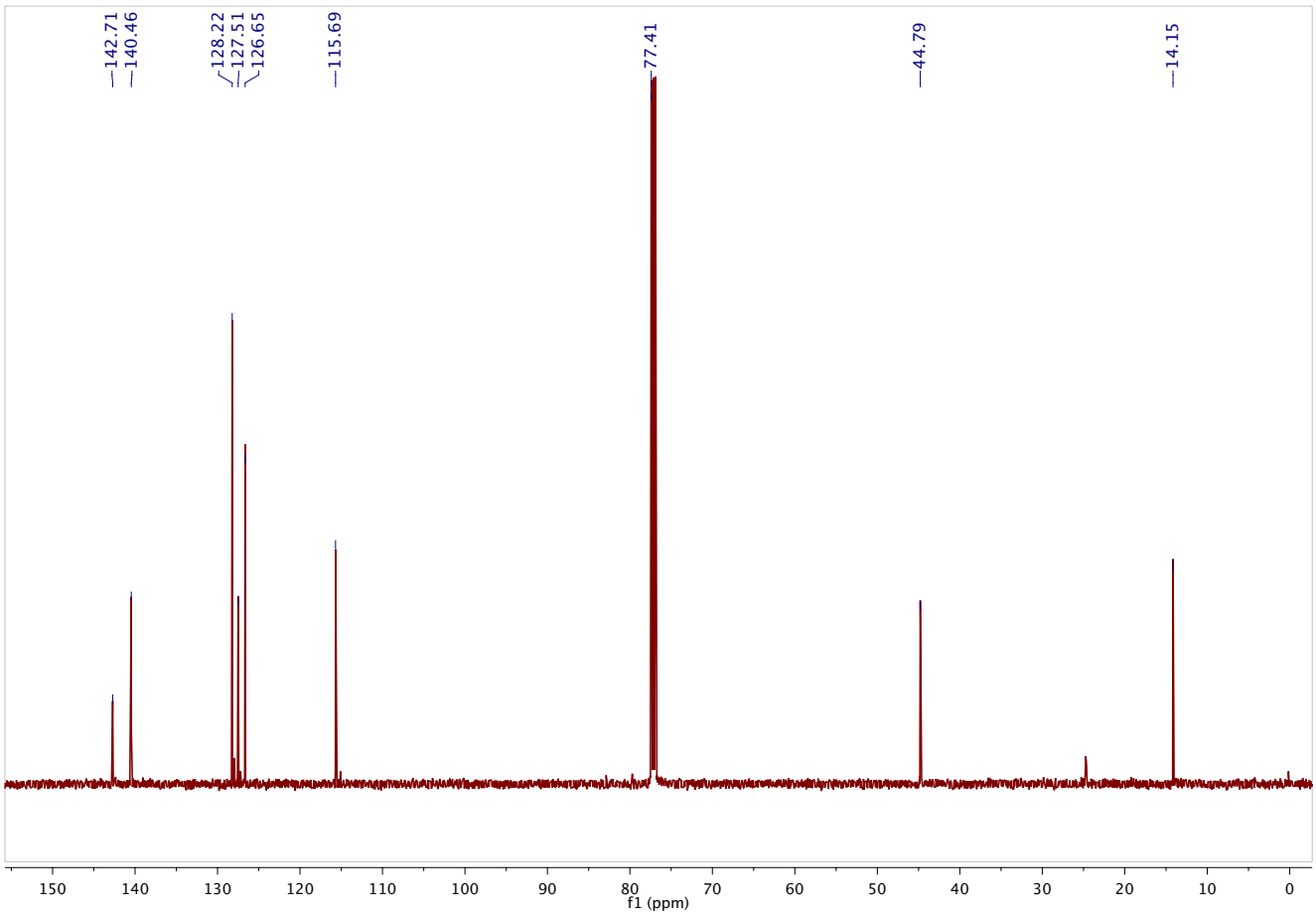
142.71
140.46
128.22
127.51
126.65
115.69
77.41
44.79
14.15
f1 (ppm)

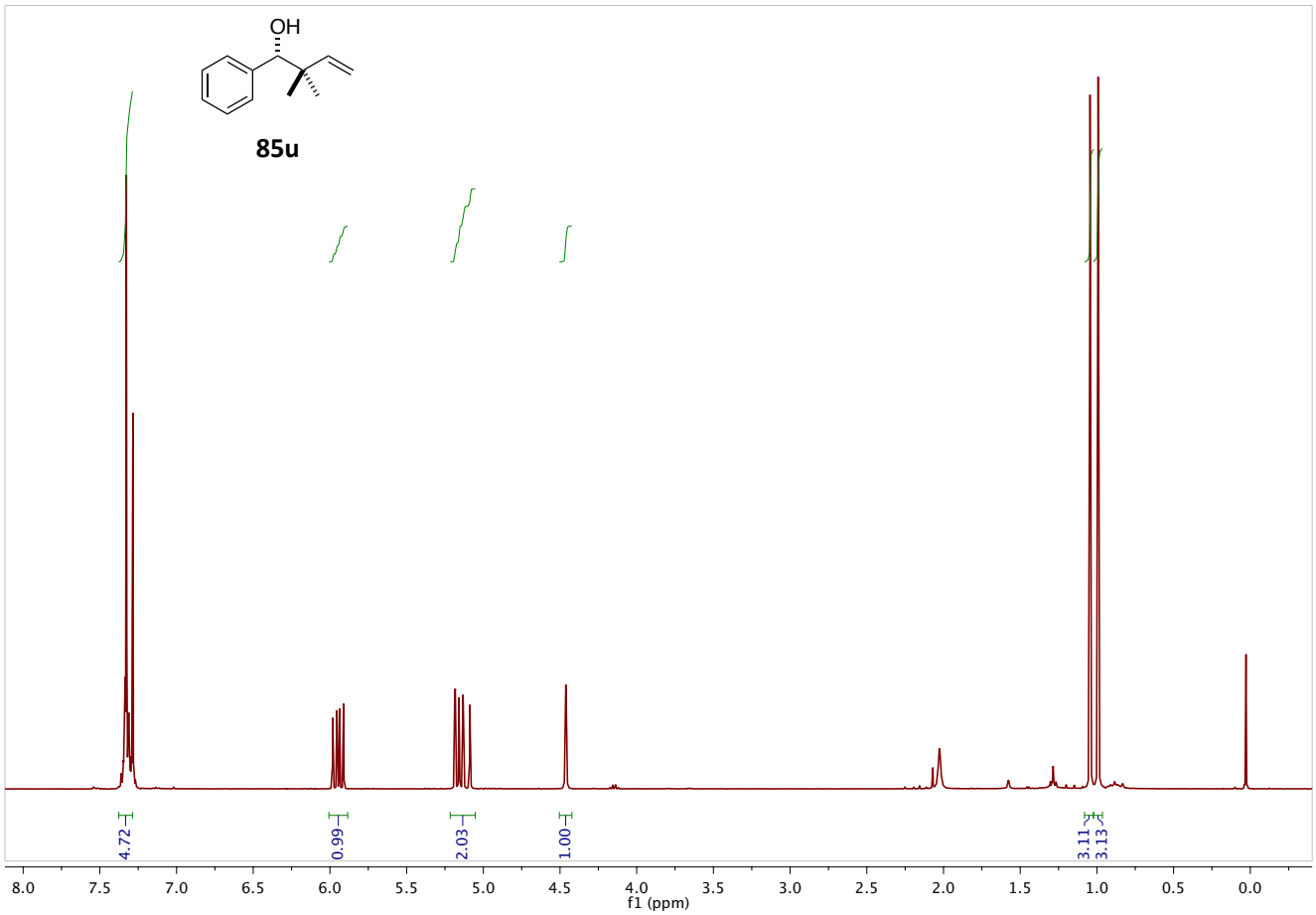
OH
85u
4.72
0.99
2.03
1.00
3.11
3.13
8.0
7.5
7.0
6.5
6.0
5.5
5.0
4.5
4.0
3.5
3.0
2.5
2.0
1.5
1.0
0.5
0.0
f1 (ppm)

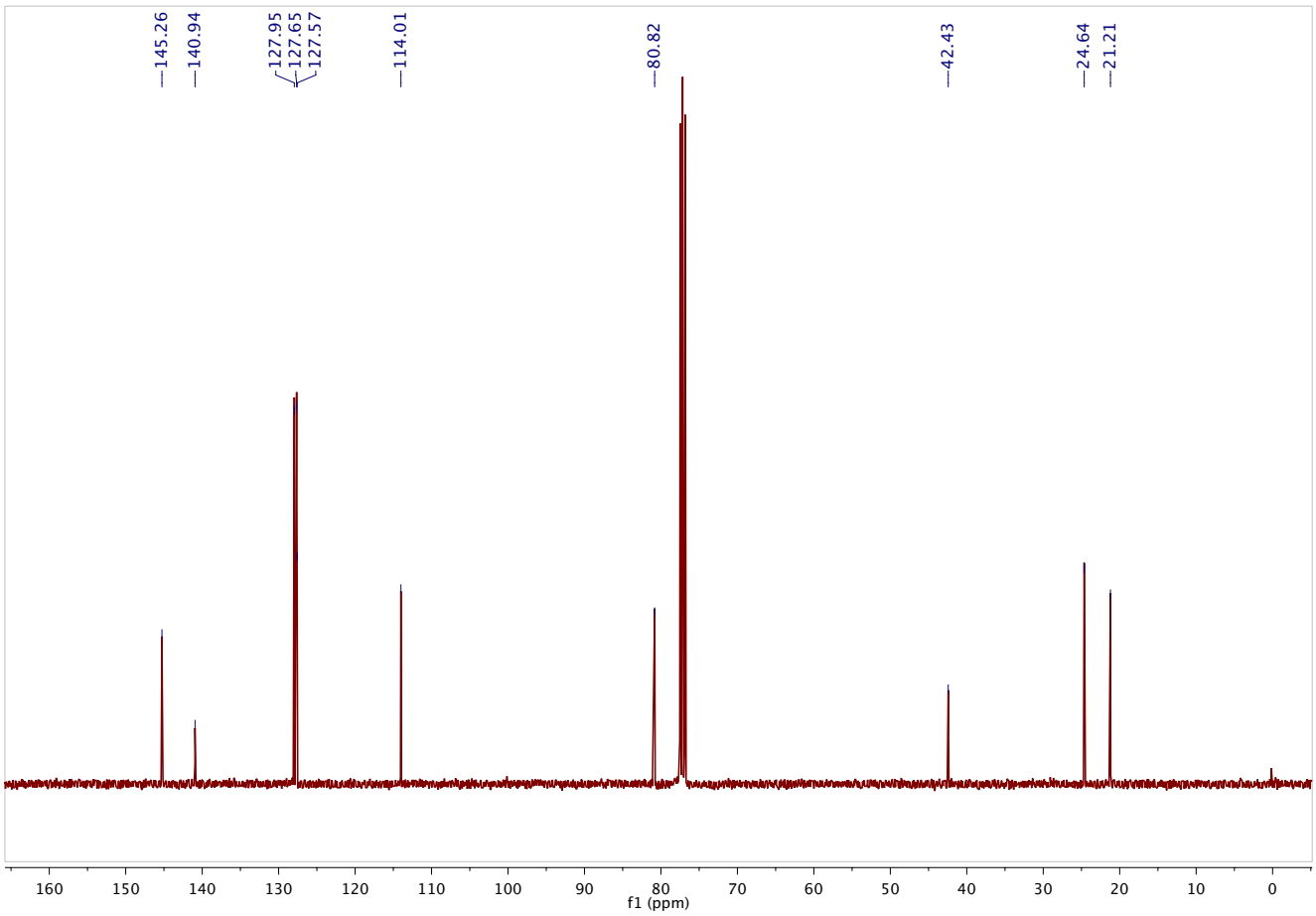
145.26
140.94
127.95
127.65
127.57
114.01
80.82
42.43
24.64
21.21
160
150
140
130
120
110
100
90
80
70
60
50
40
30
20
10
0
f1 (ppm)

3.8. HPLC, GC and SFC Chromatograms

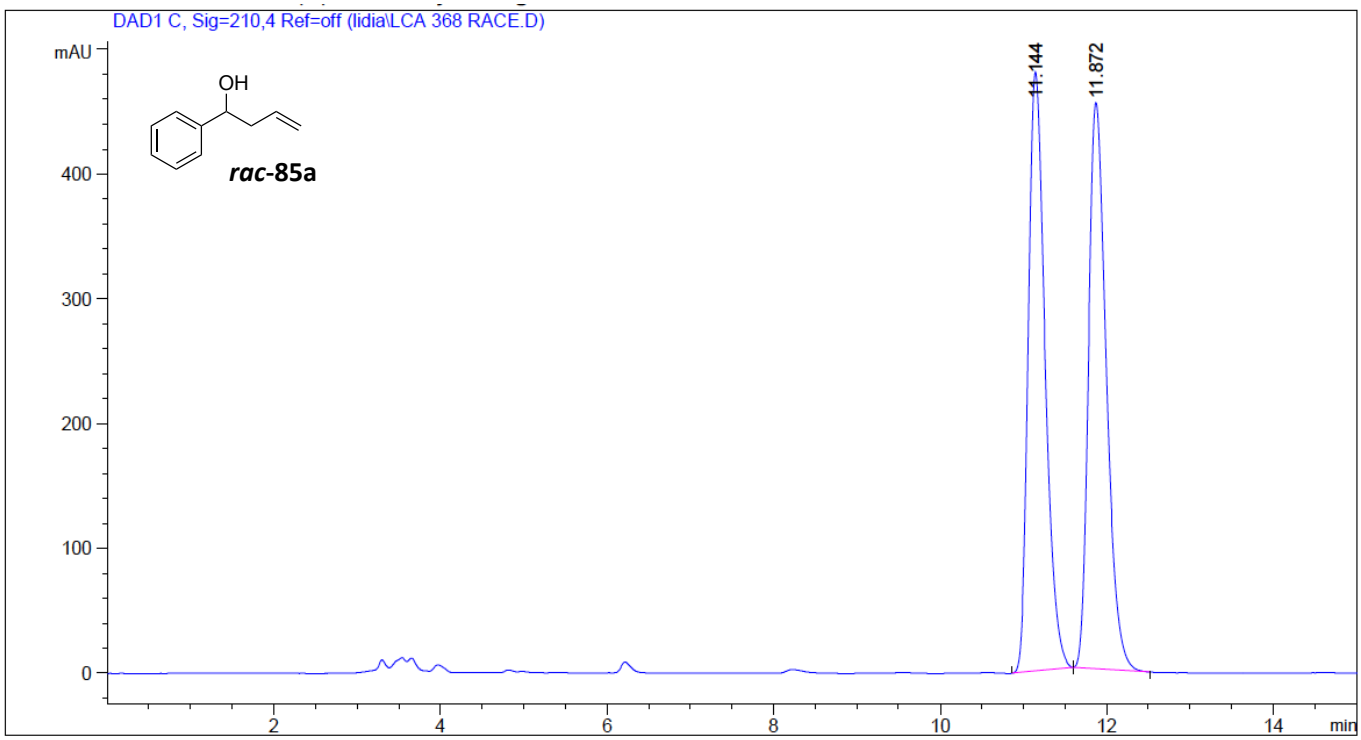

Peak #	RetTime [min]	Type	Width [min]	Area [mAU*s]	Height [mAU]	Area %
1	11.144	BB	0.2151	6710.13086	479.98883	49.9610
2	11.872	BB	0.2267	6720.61523	454.01169	50.0390

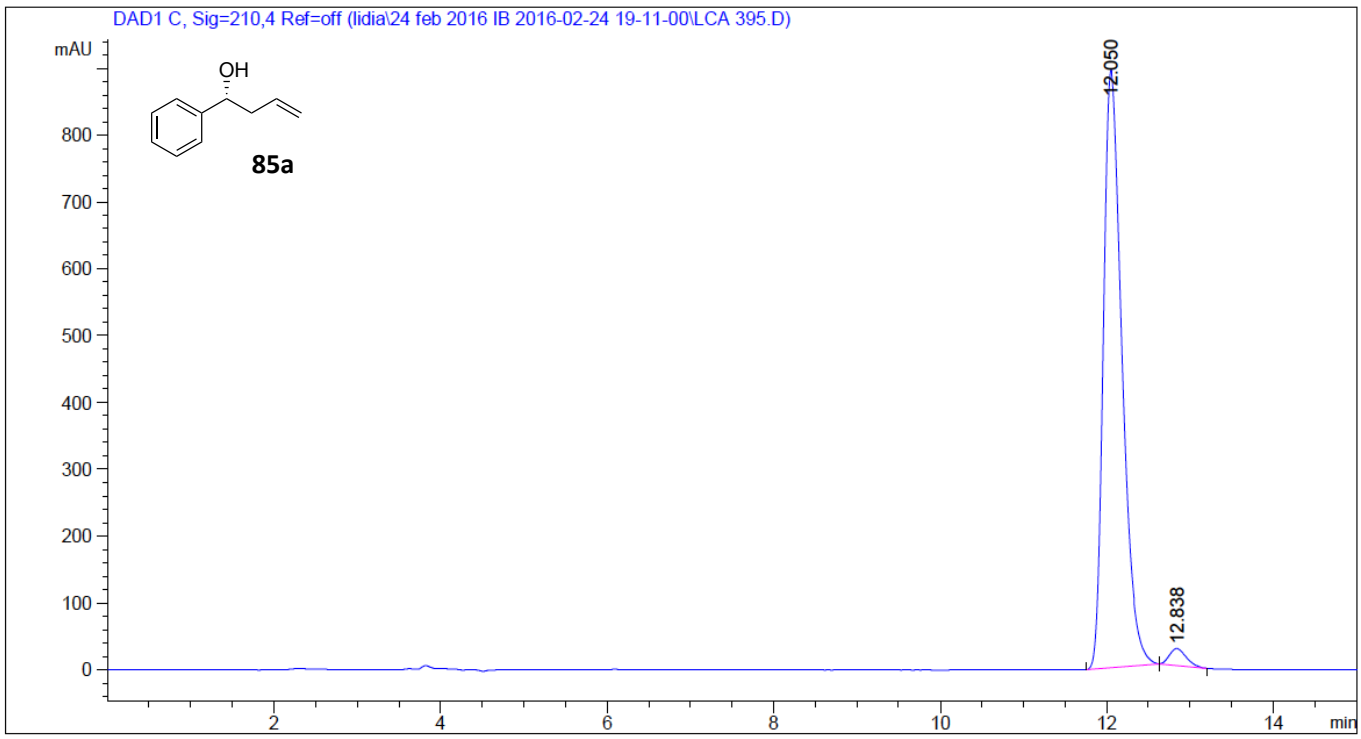

Peak #	RetTime [min]	Type	Width [min]	Area [mAU*s]	Height [mAU]	Area %
1	12.050	BB	0.2408	1.38702e4	894.83777	97.5061
2	12.838	BB	0.2179	354.76062	25.25859	2.4939

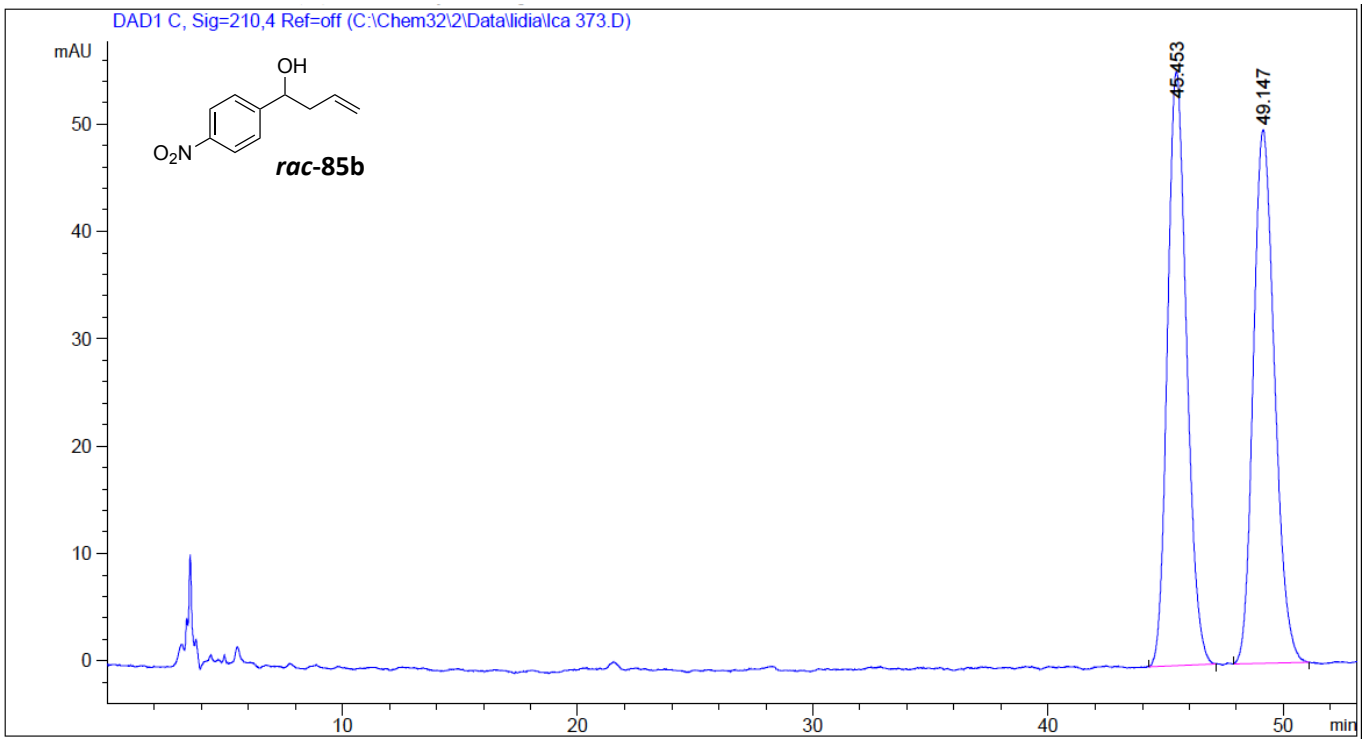

Peak #	RetTime [min]	Type	Width [min]	Area [mAU*s]	Height [mAU]	Area %
1	45.453	BB	0.7880	3131.64502	55.35711	50.0279
2	49.147	BB	0.8338	3128.15161	49.73304	49.9721

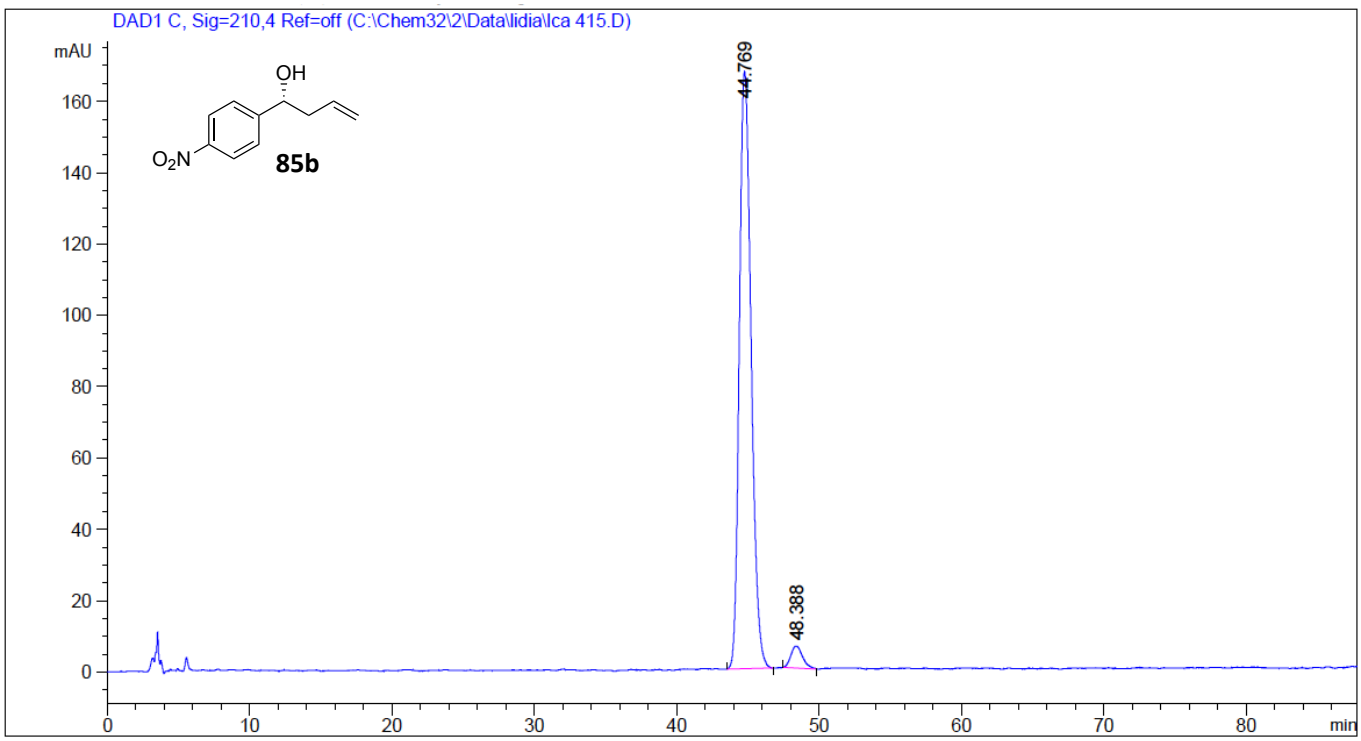

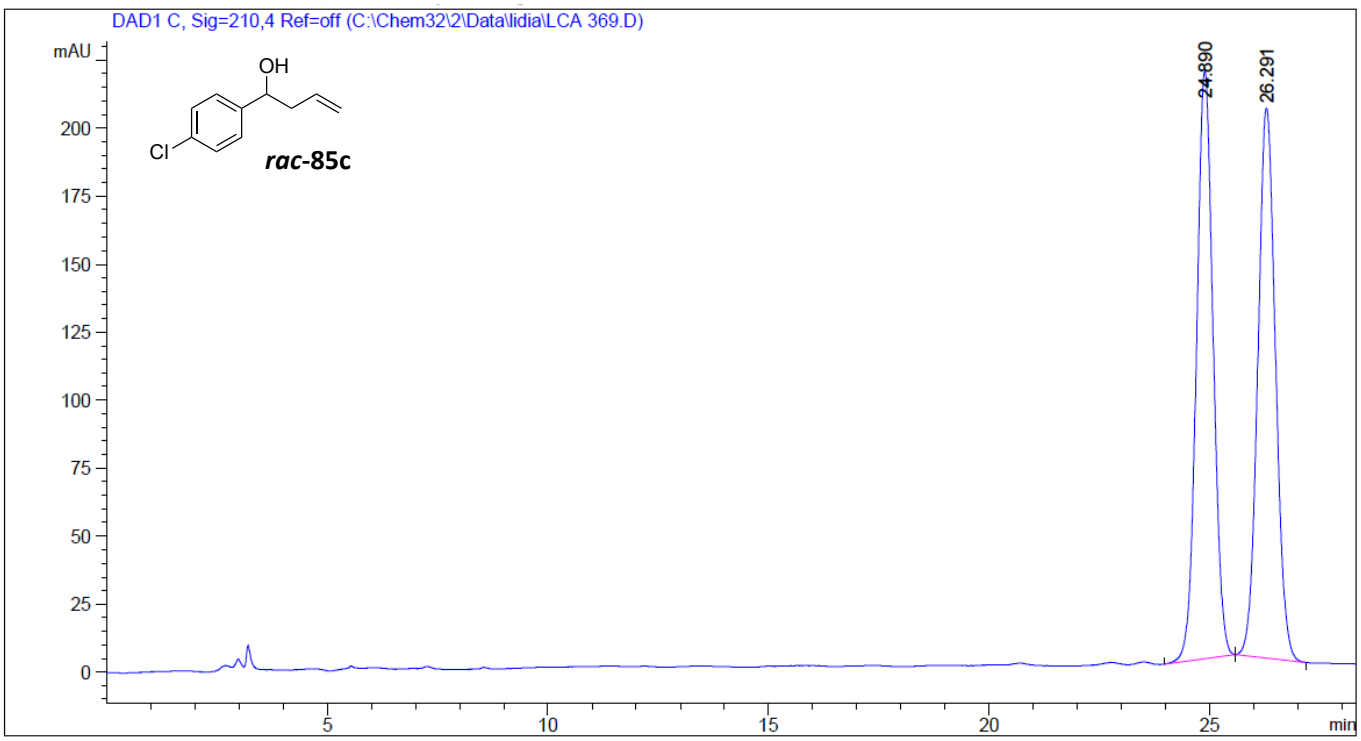

Peak #	RetTime [min]	Type	Width [min]	Area [mAU*s]	Height [mAU]	Area %
1	24.890	BB	0.4052	5649.41699	215.98663	50.1113
2	26.291	BB	0.4284	5624.31201	202.25497	49.8887

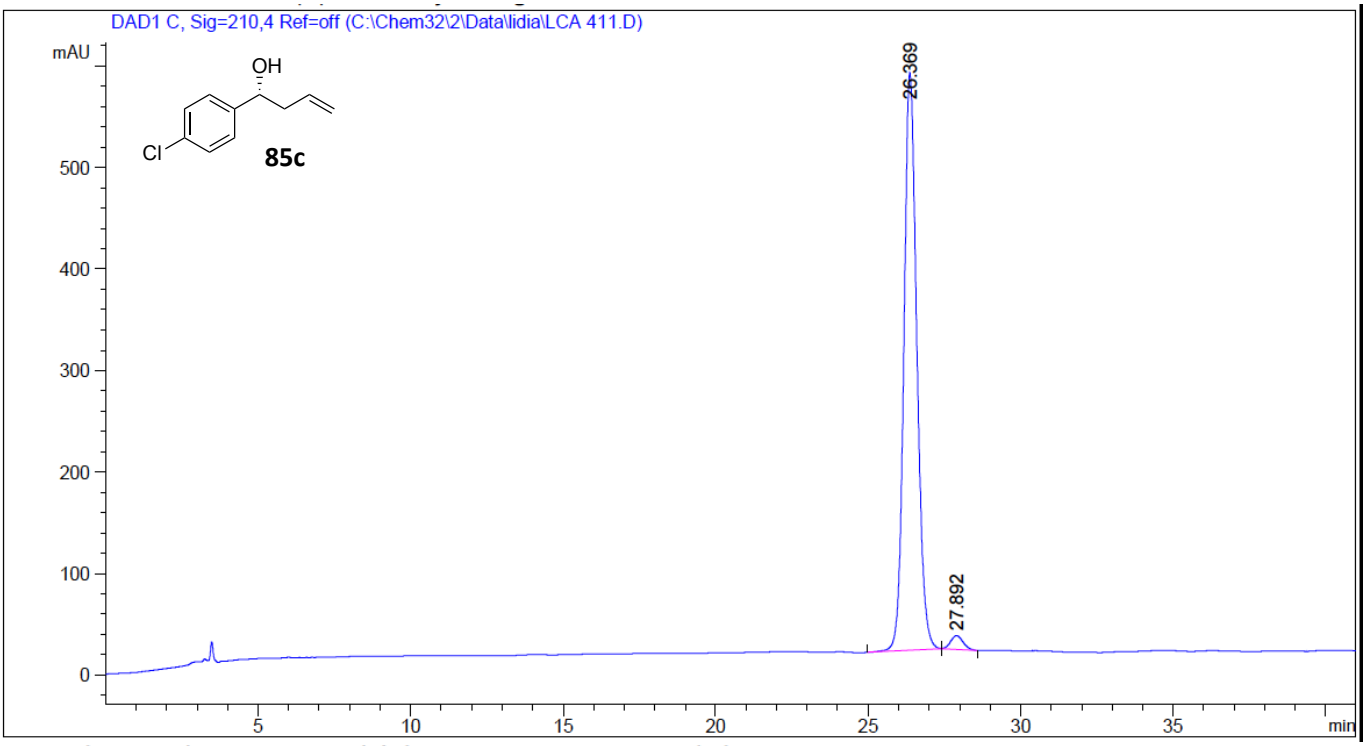

Peak #	RetTime [min]	Type	Width [min]	Area [mAU*s]	Height [mAU]	Area %
1	26.369	BB	0.4541	1.67834e4	568.96979	97.7878
2	27.892	BB	0.4258	379.67606	13.51272	2.2122

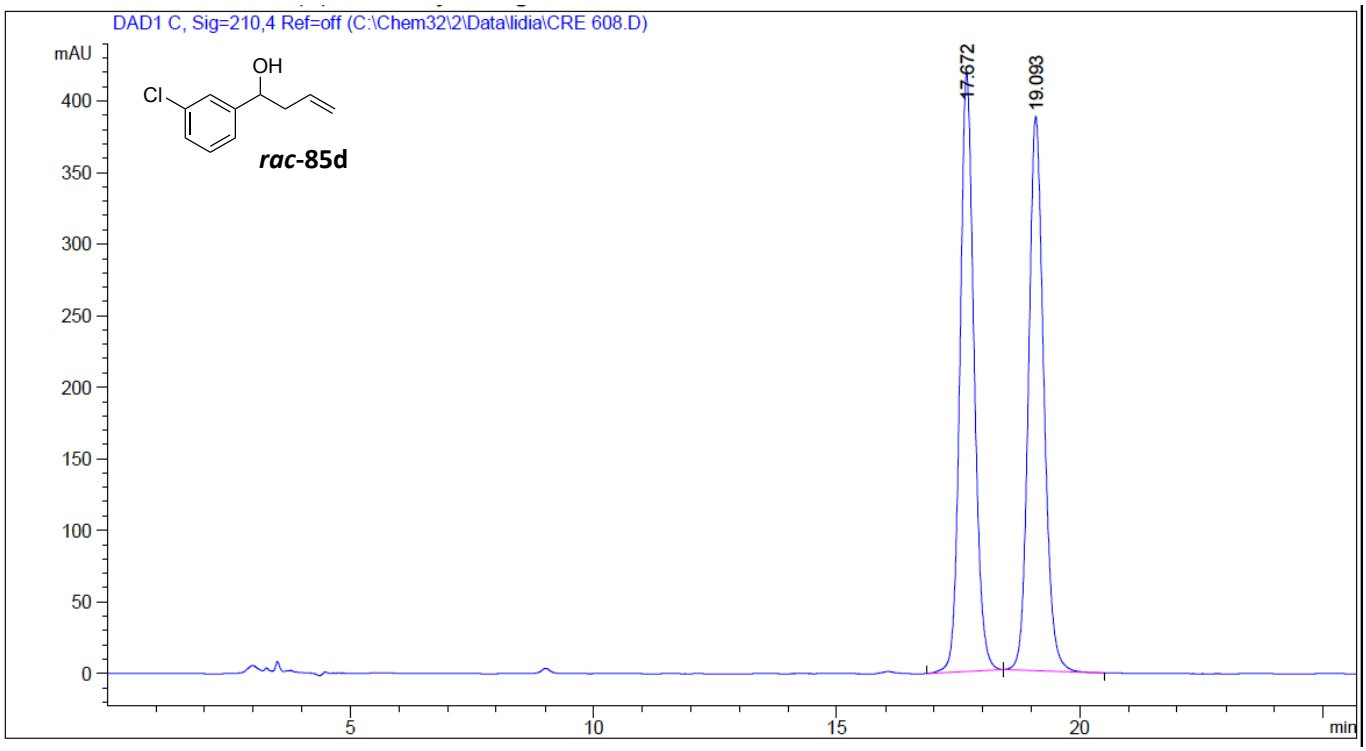

Peak #	RetTime [min]	Type	Width [min]	Area [mAU*s]	Height [mAU]	Area %
1	17.672	BB	0.3104	8466.20117	417.76270	49.9980
2	19.093	BB	0.3349	8466.87402	387.51147	50.0020

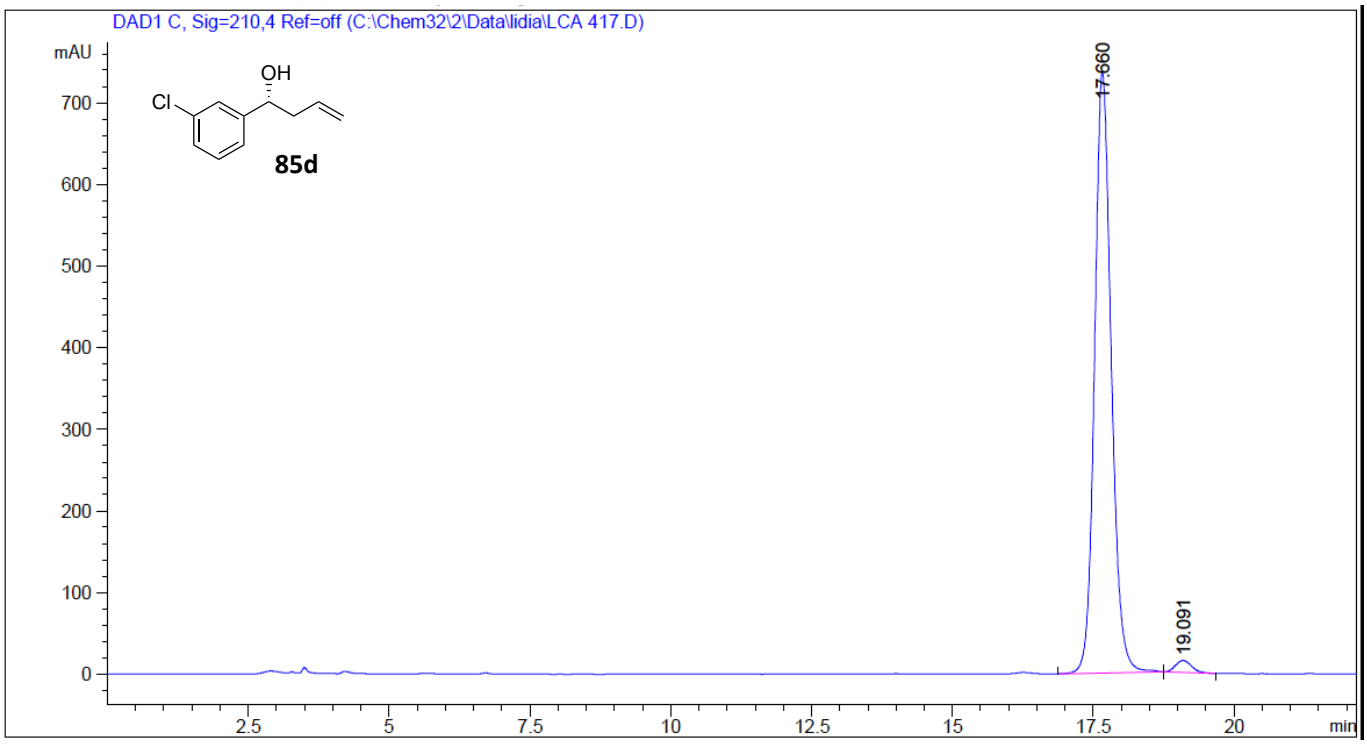

Peak #	RetTime [min]	Type	Width [min]	Area [mAU*s]	Height [mAU]	Area %
1	17.660	BB	0.3137	1.51179e4	735.85345	98.1234
2	19.091	BB	0.3063	289.12277	14.52187	1.8766

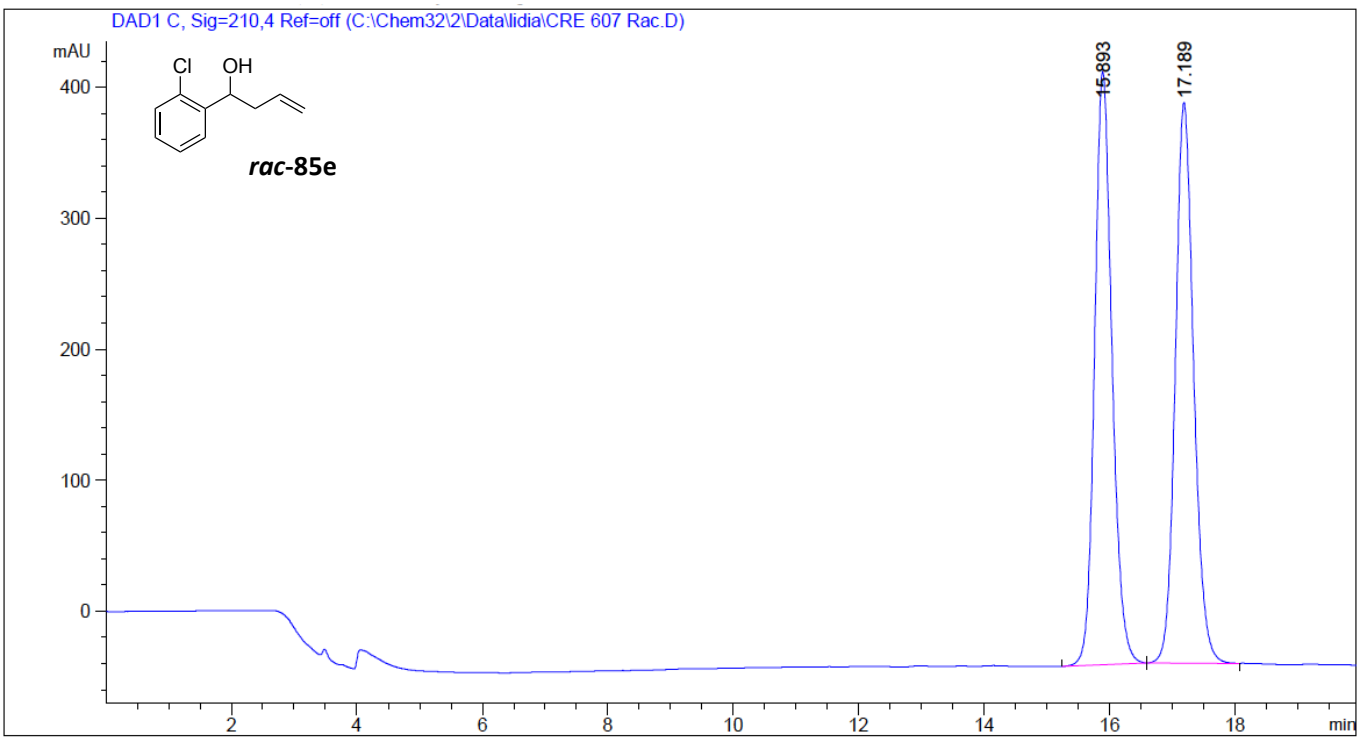

Peak #	RetTime [min]	Type	Width [min]	Area [mAU*s]	Height [mAU]	Area %
1	15.893	BB	0.2921	8698.63379	452.93420	50.0256
2	17.189	BB	0.3109	8689.74219	427.87265	49.9744

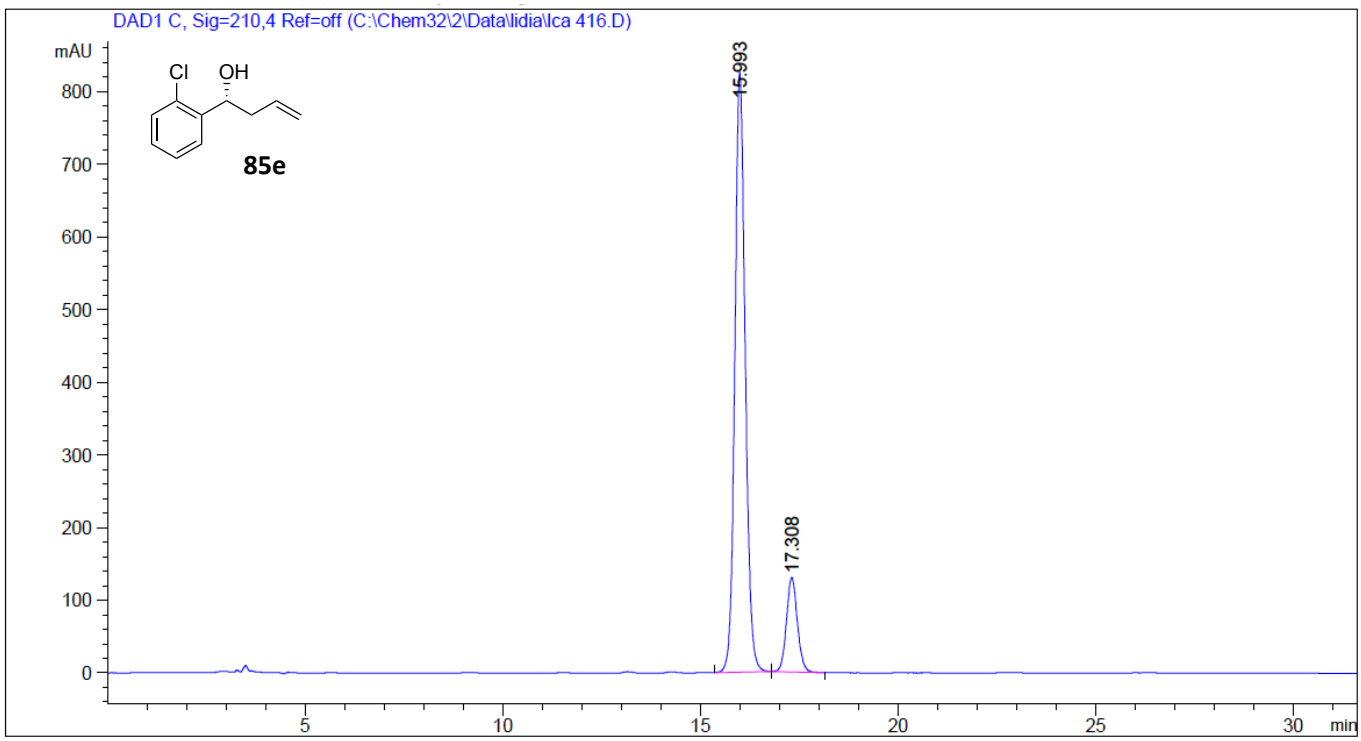

Peak #	RetTime [min]	Type	Width [min]	Area [mAU*s]	Height [mAU]	Area %
1	15.993	BB	0.2815	1.51343e4	827.07751	85.7971
2	17.308	BB	0.2967	2505.34888	130.06413	14.2029

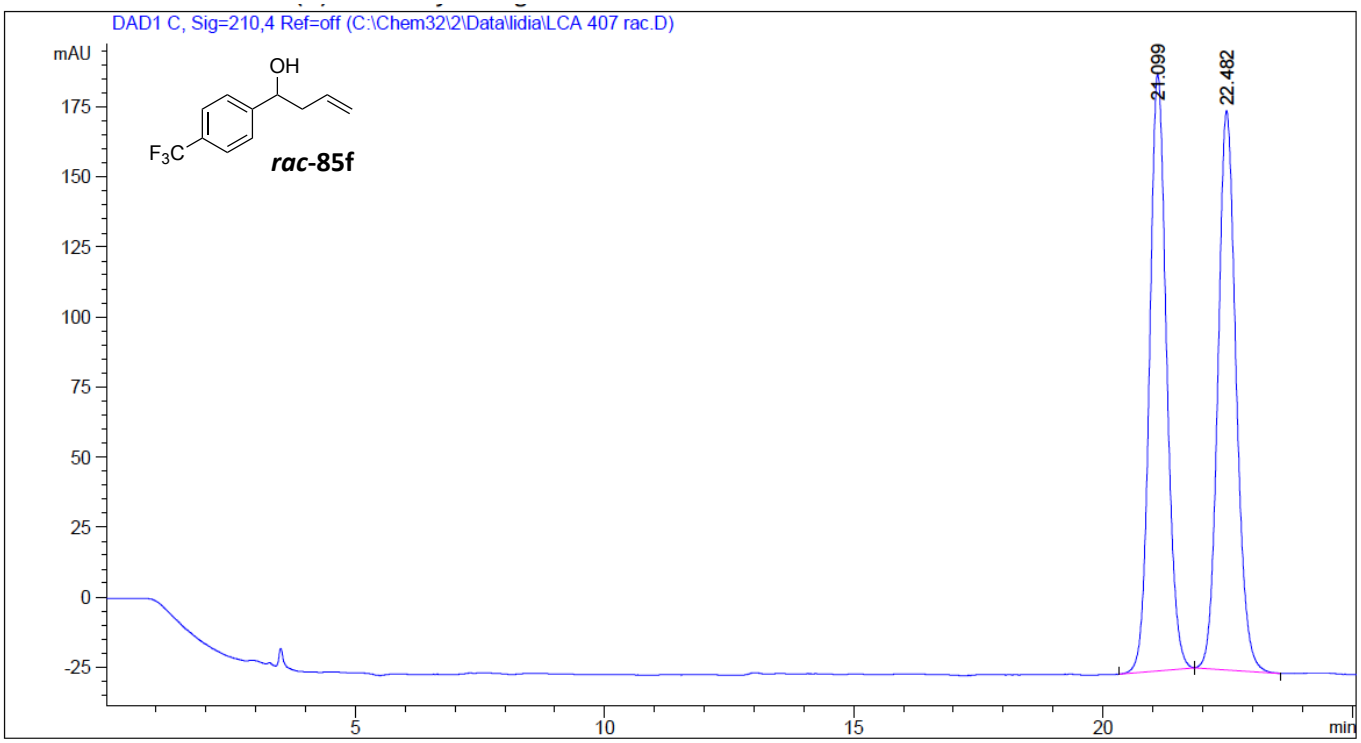

Peak #	RetTime [min]	Type	Width [min]	Area [mAU*s]	Height [mAU]	Area %
1	21.099	BB	0.3622	5044.47021	213.10628	49.9318
2	22.482	BB	0.3898	5058.24902	199.51920	50.0682

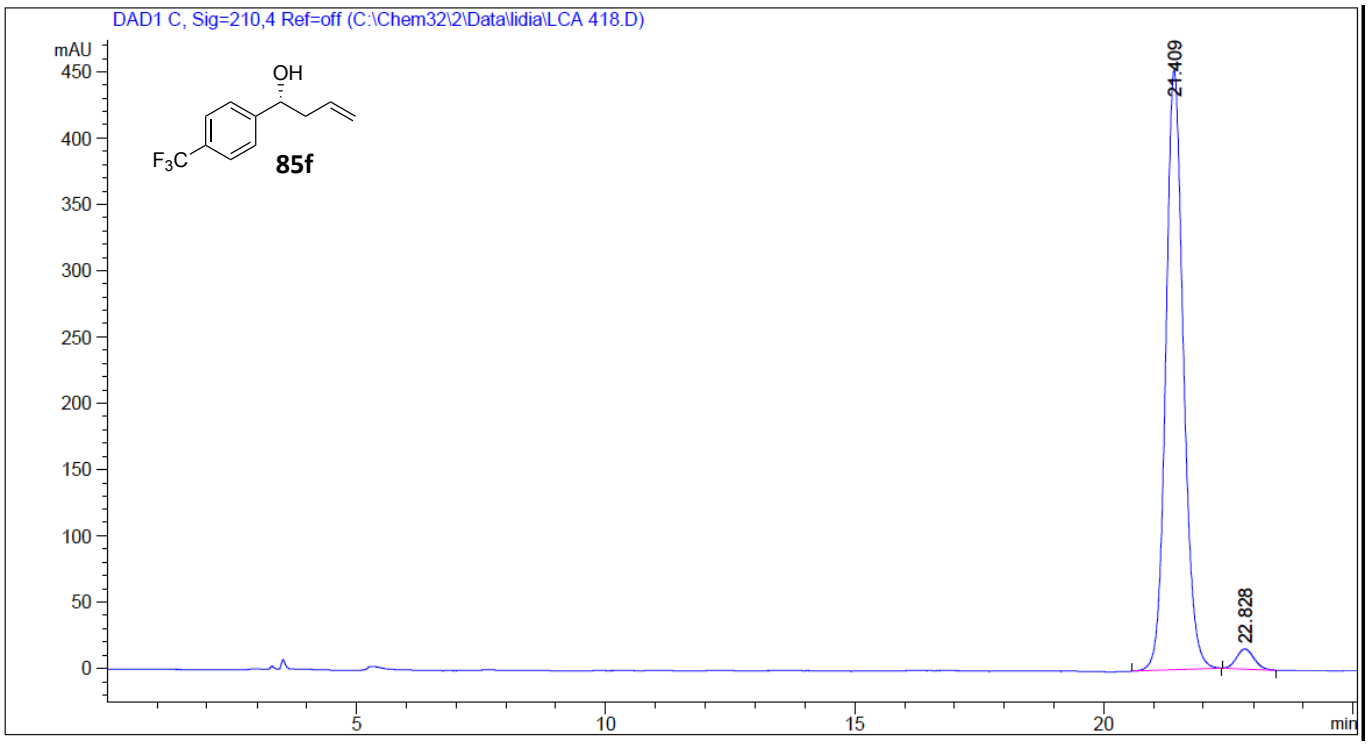

Peak #	RetTime [min]	Type	Width [min]	Area [mAU*s]	Height [mAU]	Area %
1	21.409	BB	0.3769	1.11213e4	452.25684	96.8037
2	22.828	BB	0.3615	367.21362	15.11143	3.1963

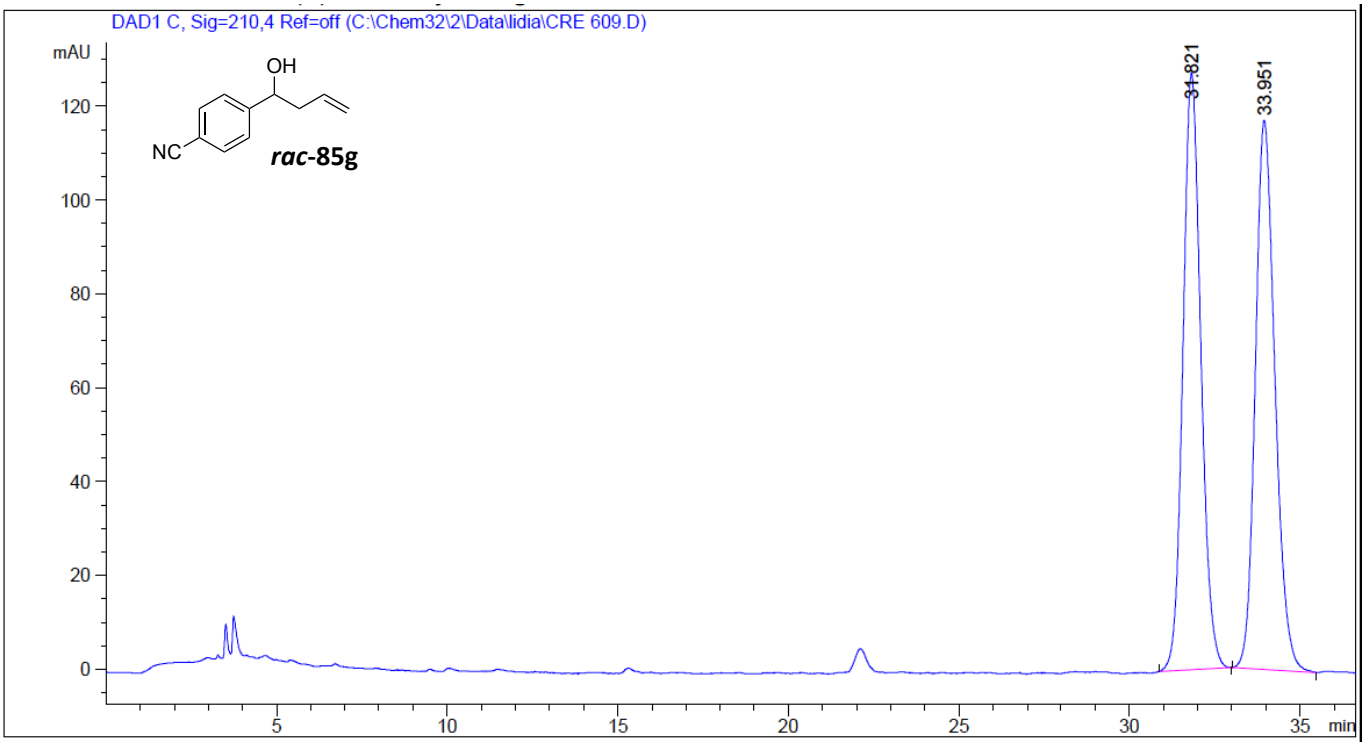

Peak #	RetTime [min]	Type	Width [min]	Area [mAU*s]	Height [mAU]	Area %
1	31.821	BB	0.5567	4633.33887	127.26745	49.8050
2	33.951	BB	0.6015	4669.61865	117.04390	50.1950

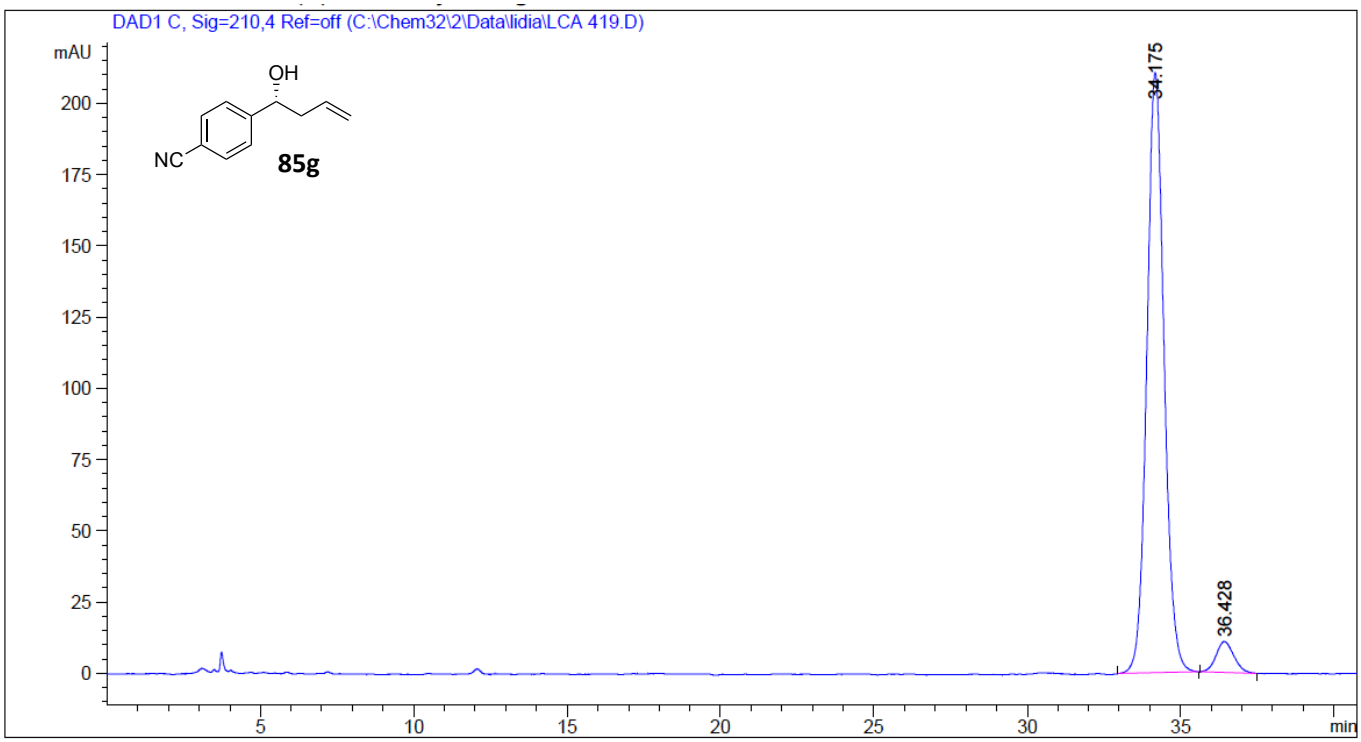

Peak #	RetTime [min]	Type	Width [min]	Area [mAU*s]	Height [mAU]	Area %
1	34.175	BB	0.5950	8214.65527	210.64412	94.9776
2	36.428	BB	0.4997	434.38824	10.79056	5.0224

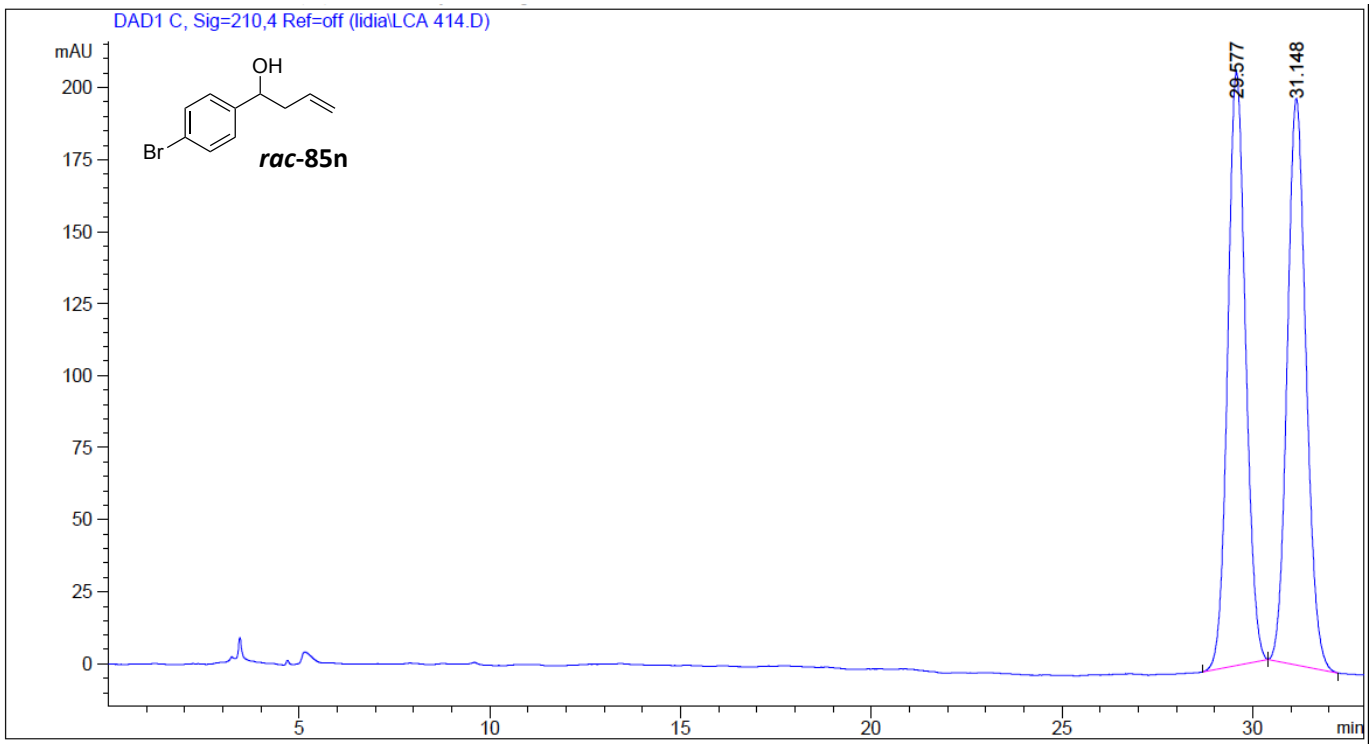

Peak #	RetTime [min]	Type	Width [min]	Area [mAU*s]	Height [mAU]	Area %
1	29.577	BB	0.5059	6708.92285	206.04655	49.8493
2	31.148	BB	0.5326	6749.47998	196.55547	50.1507

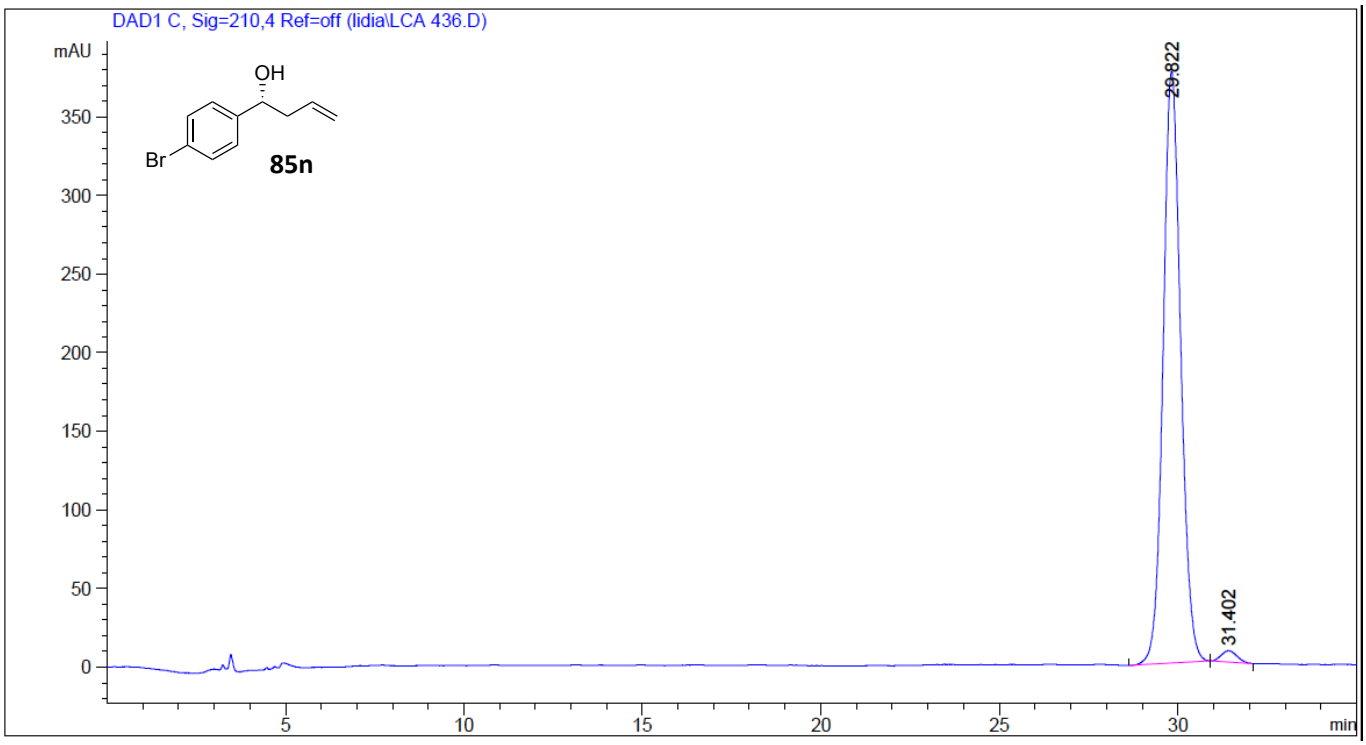

Peak #	RetTime [min]	Type	Width [min]	Area [mAU*s]	Height [mAU]	Area %
1	29.822	BB	0.5235	1.28911e4	376.49277	98.2924
2	31.402	BB	0.3784	223.95363	7.20911	1.7076

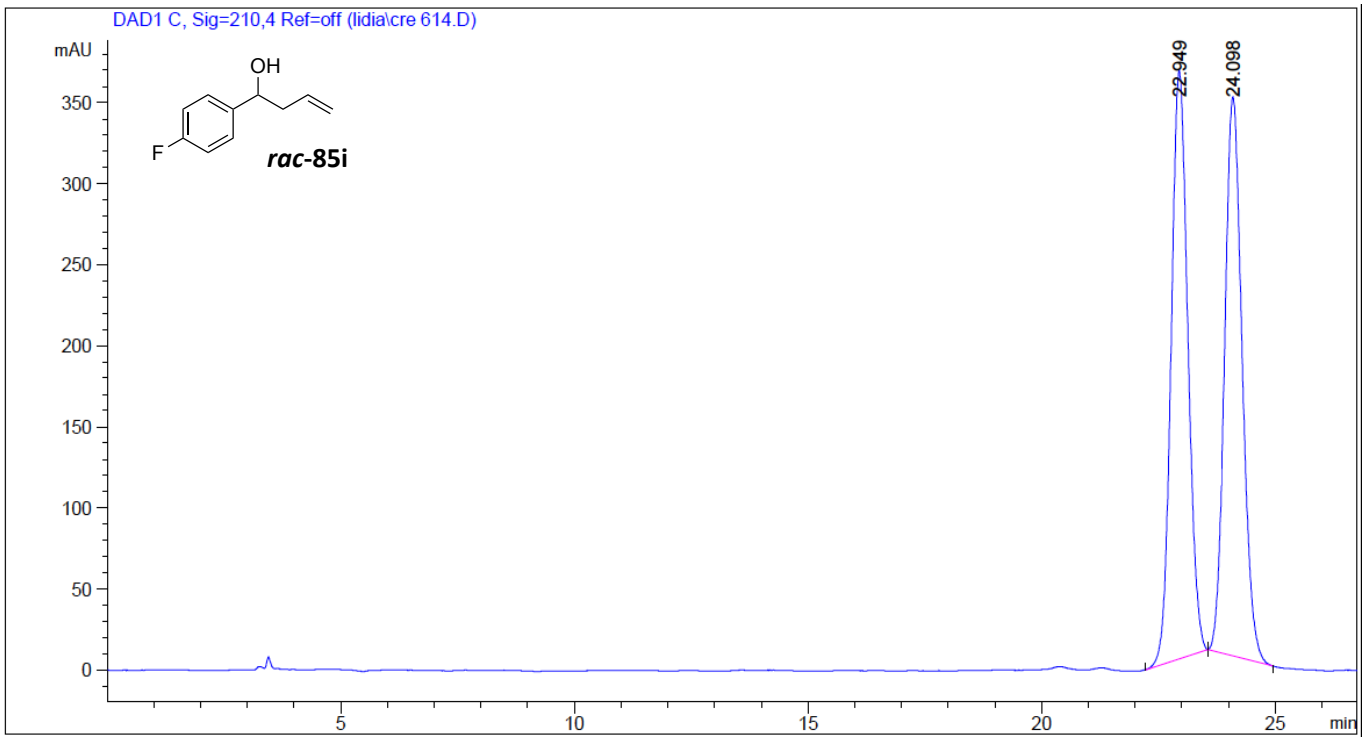

Peak #	RetTime [min]	Type	Width [min]	Area [mAU*s]	Height [mAU]	Area %
1	22.949	BB	0.3838	9019.67676	363.13745	50.0948
2	24.098	BB	0.4020	8985.55176	344.87231	49.9052

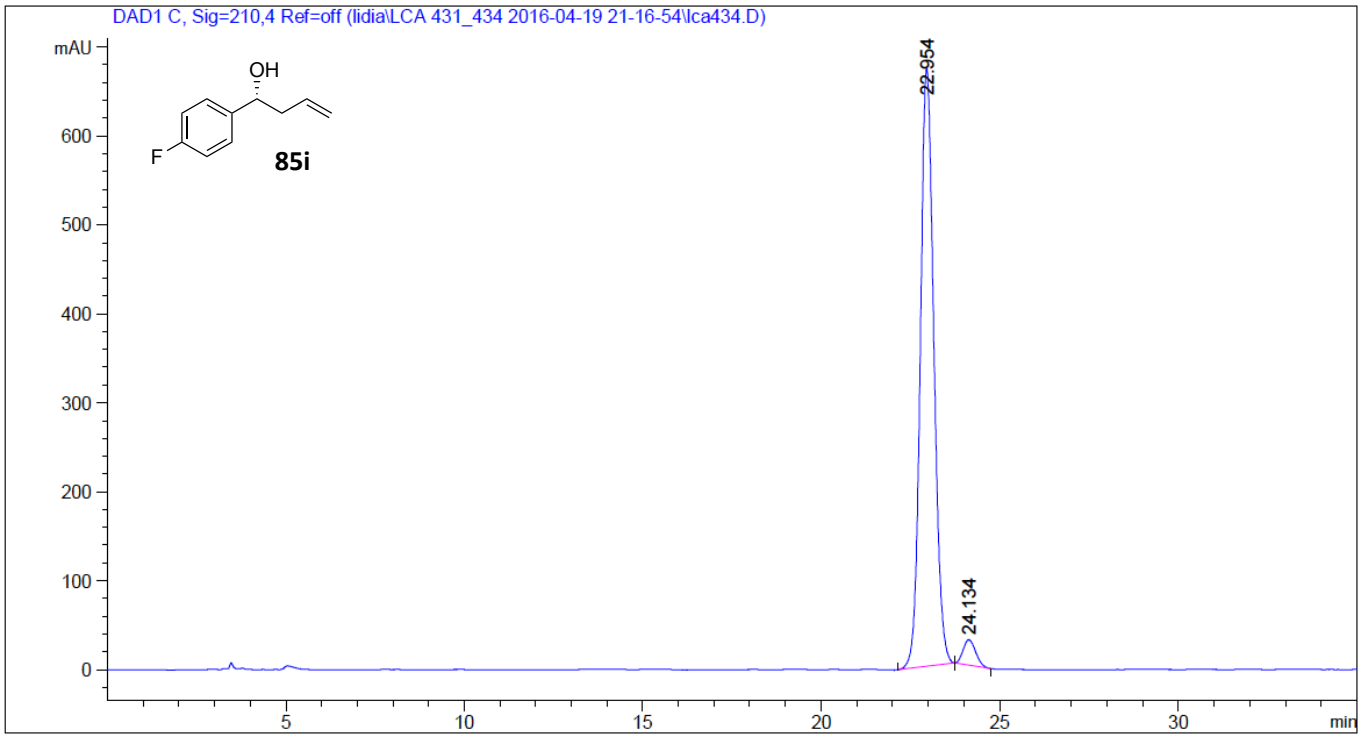

Peak #	RetTime [min]	Type	Width [min]	Area [mAU*s]	Height [mAU]	Area %
1	22.954	BB	0.4045	1.76700e4	672.56567	96.1928
2	24.134	BB	0.3805	699.36493	28.67926	3.8072

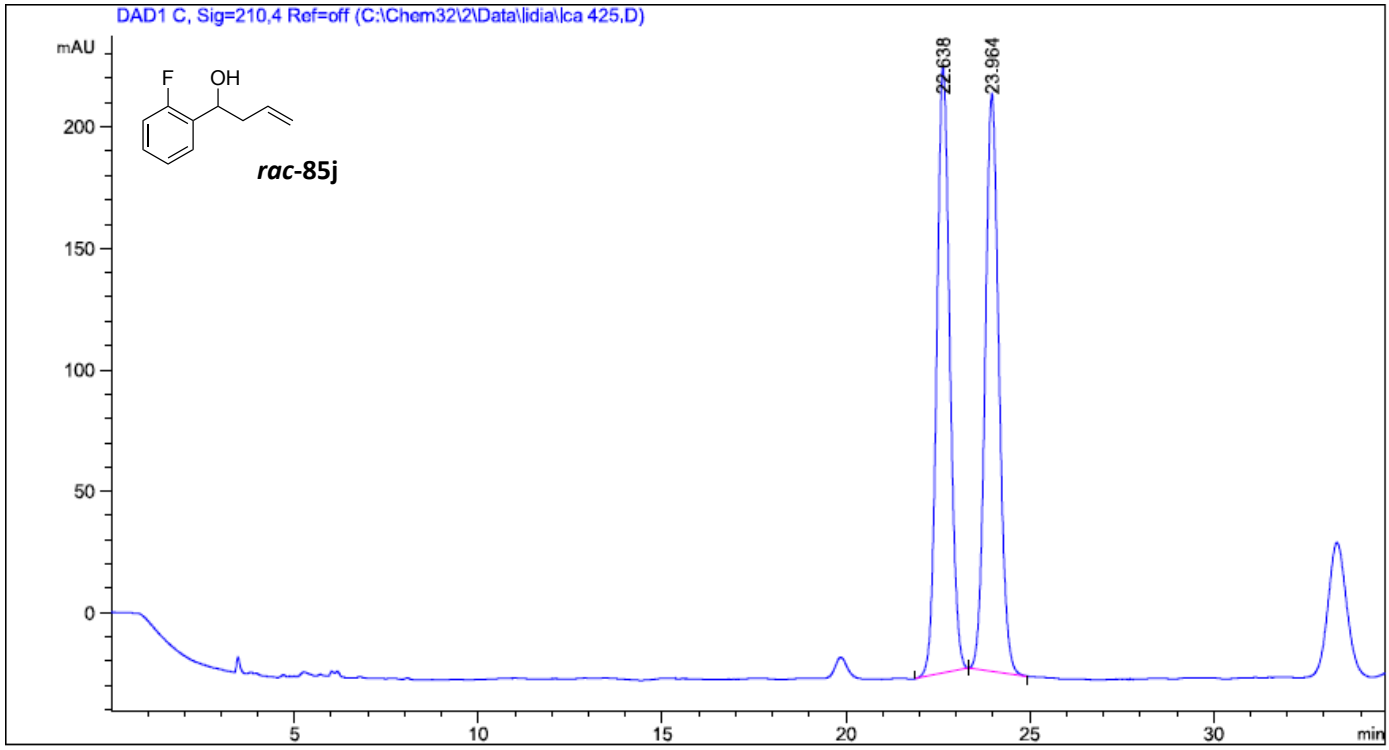

Peak #	RetTime [min]	Type	Width [min]	Area [mAU*s]	Height [mAU]	Area %
1	22.638	BB	0.3846	6167.79541	249.33110	49.8686
2	23.964	BB	0.4002	6200.30518	237.79550	50.1314

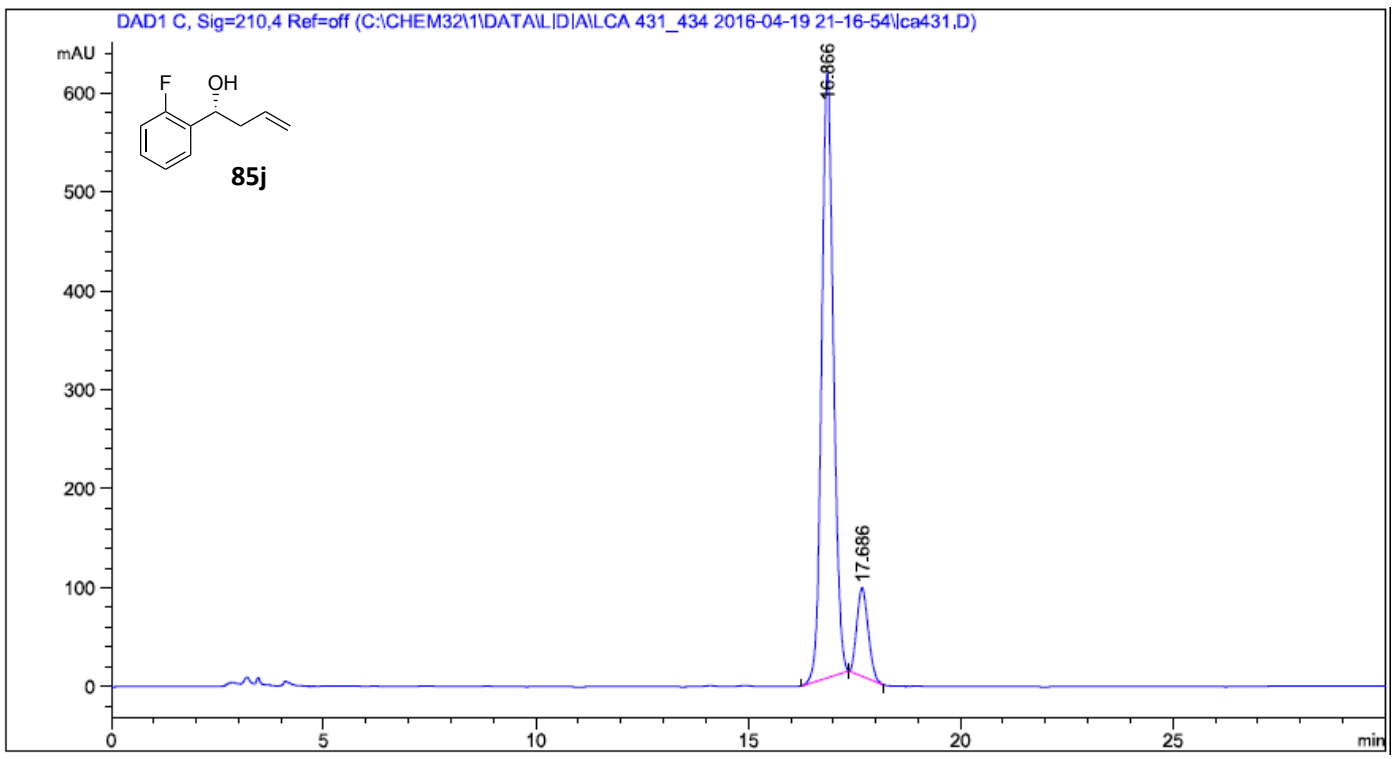

Peak #	RetTime [min]	Type	Width [min]	Area [mAU*s]	Height [mAU]	Area %
1	16.866	BB	0.2969	1.17790e4	610.91302	87.6886
2	17.686	BB	0.2901	1653.75342	89.29630	12.3114

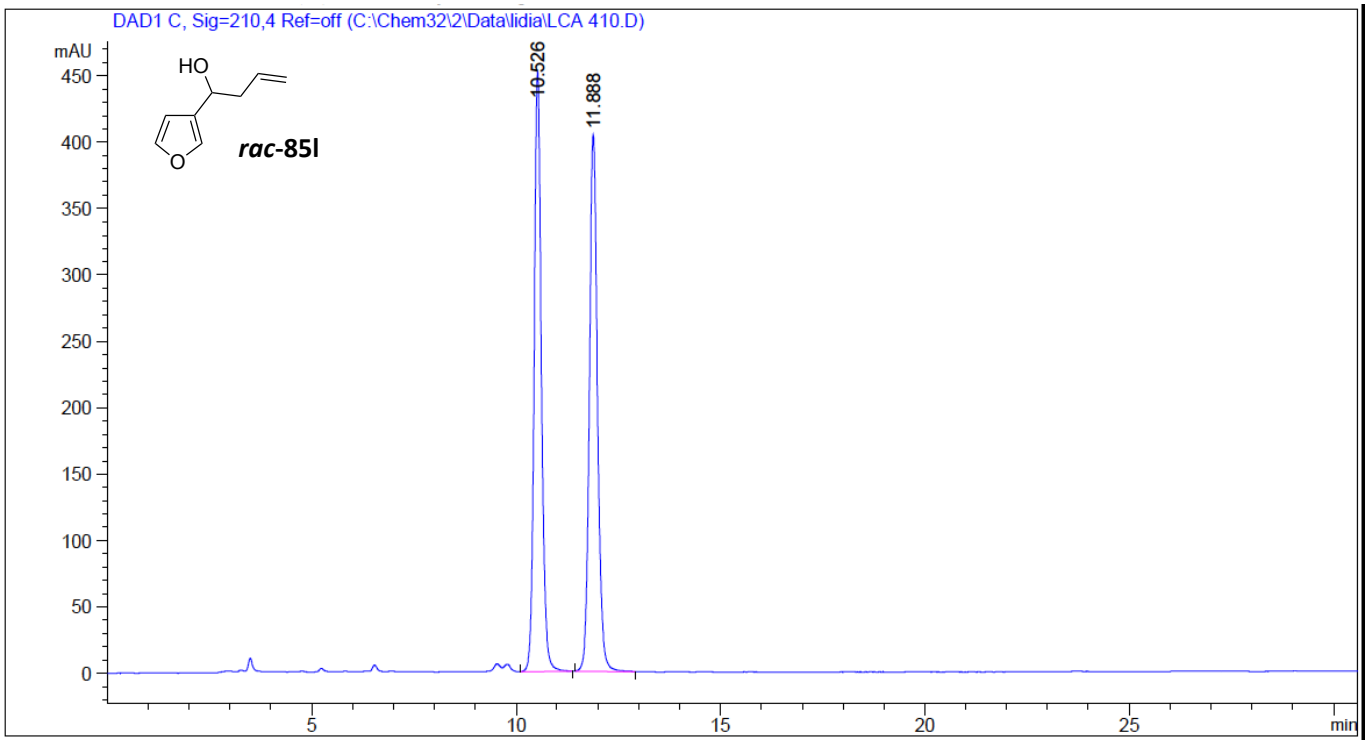

Peak #	RetTime [min]	Type	Width [min]	Area [mAU*s]	Height [mAU]	Area %
1	10.526	BB	0.1886	5604.95117	452.18607	49.9982
2	11.888	BB	0.2116	5605.35742	404.70920	50.0018

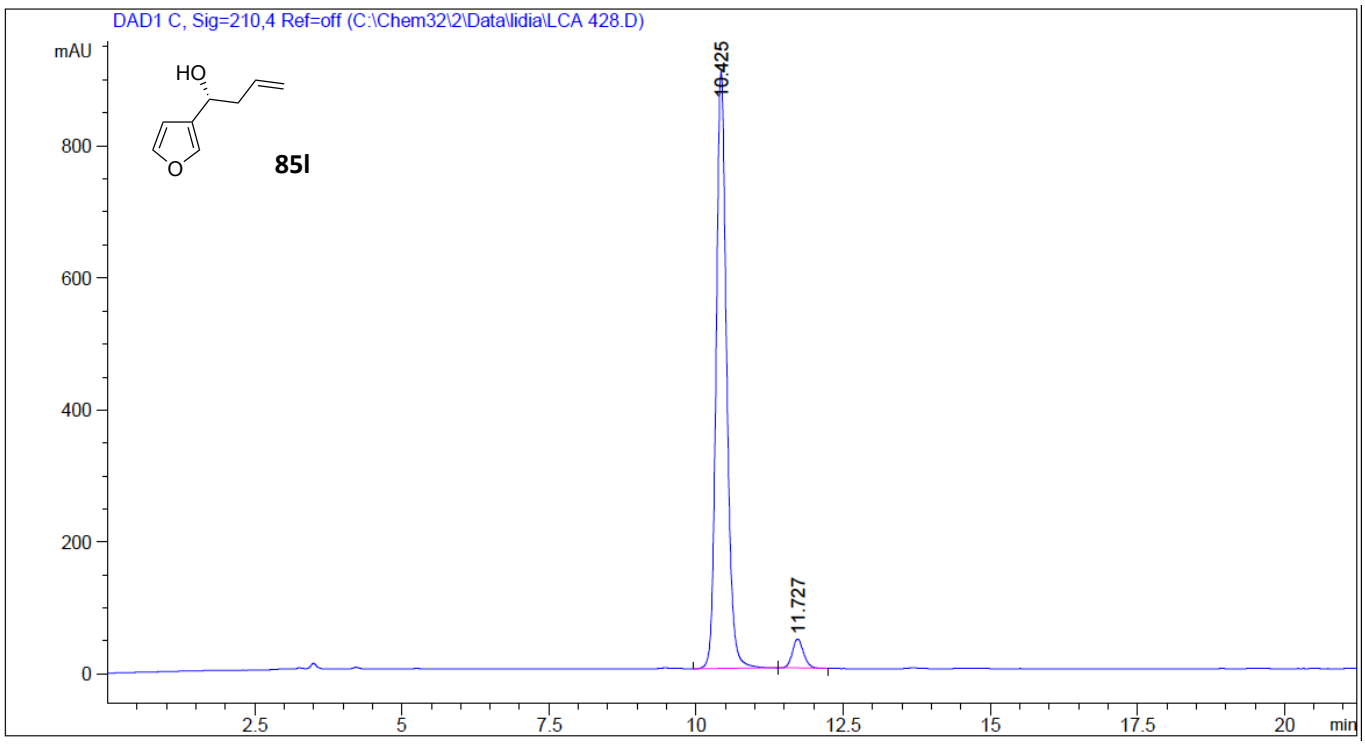

Peak #	RetTime [min]	Type	Width [min]	Area [mAU*s]	Height [mAU]	Area %
1	10.425	BB	0.1888	1.12268e4	904.58624	95.0118
2	11.727	BB	0.2014	589.41223	44.25939	4.9882

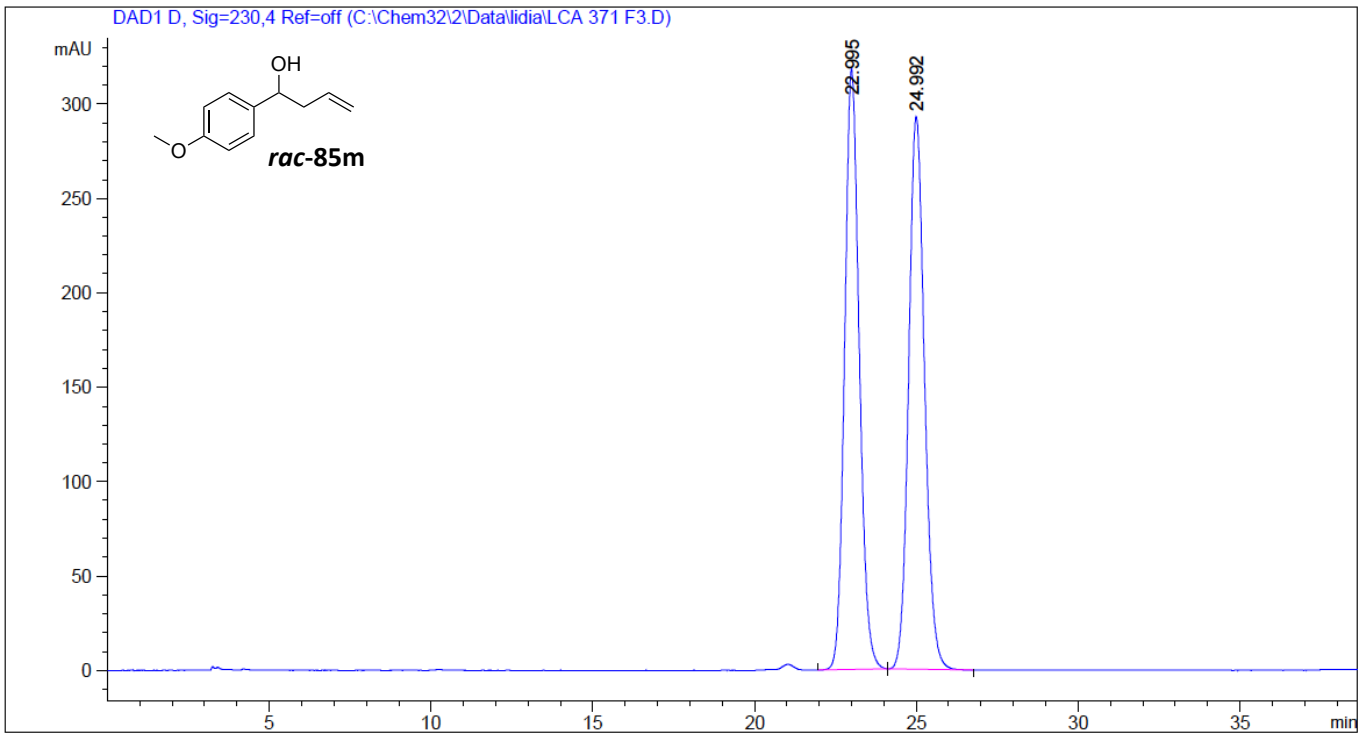

Peak #	RetTime [min]	Type	Width [min]	Area [mAU*s]	Height [mAU]	Area %
1	22.995	BB	0.4819	9979.35840	318.16644	49.9906
2	24.992	BB	0.5260	9983.11328	292.62802	50.0094

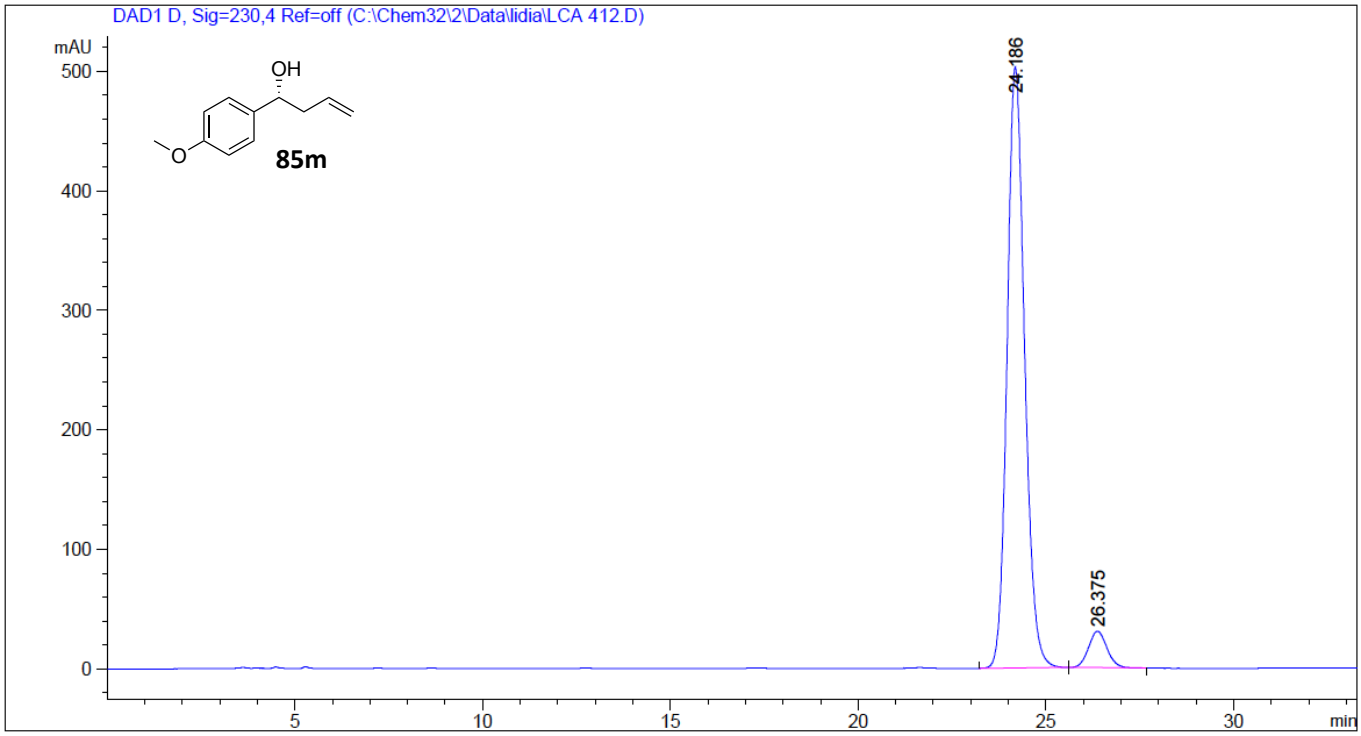

Peak #	RetTime [min]	Type	Width [min]	Area [mAU*s]	Height [mAU]	Area %
1	24.186	BB	0.4971	1.62545e4	502.83224	93.9680
2	26.375	BB	0.5288	1043.40552	30.52253	6.0320

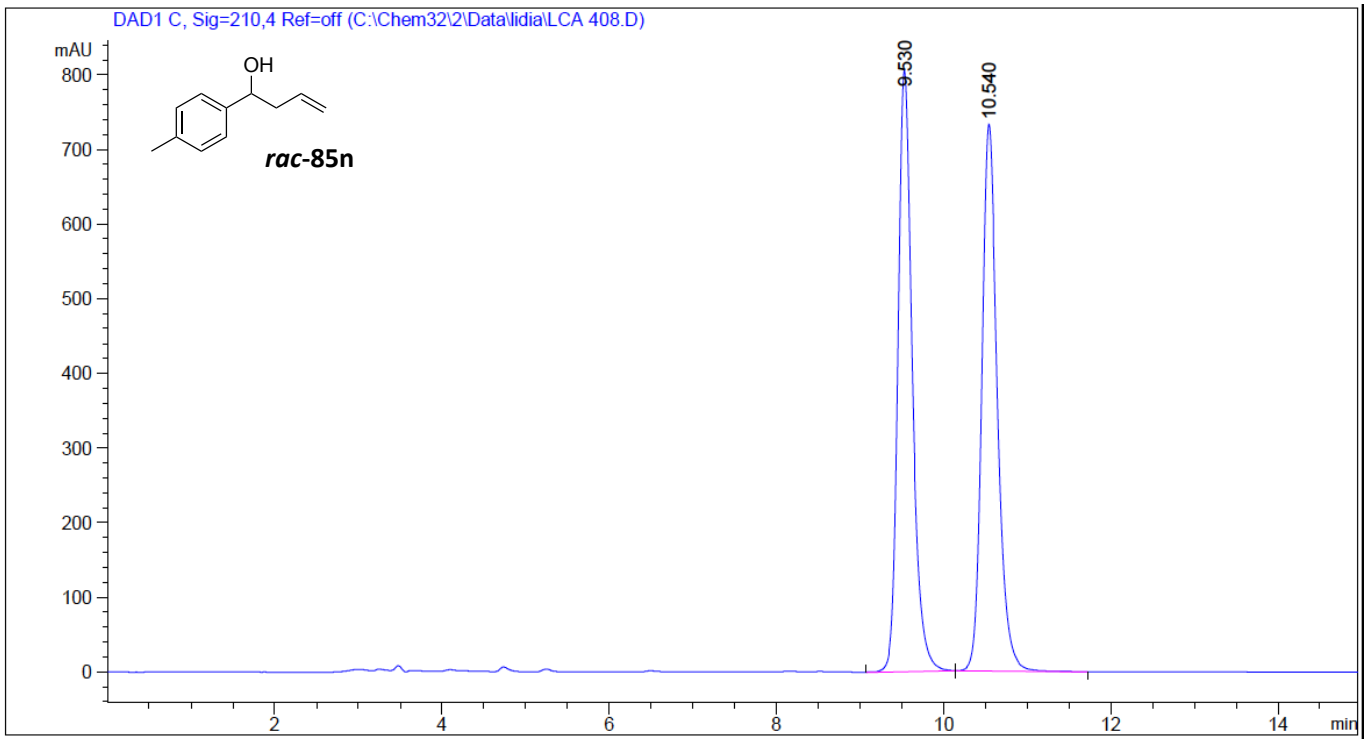

Peak #	RetTime [min]	Type	Width [min]	Area [mAU*s]	Height [mAU]	Area %
1	9.530	BB	0.1797	9505.90332	805.62811	50.1002
2	10.540	BB	0.1947	9467.86328	732.88647	49.8998

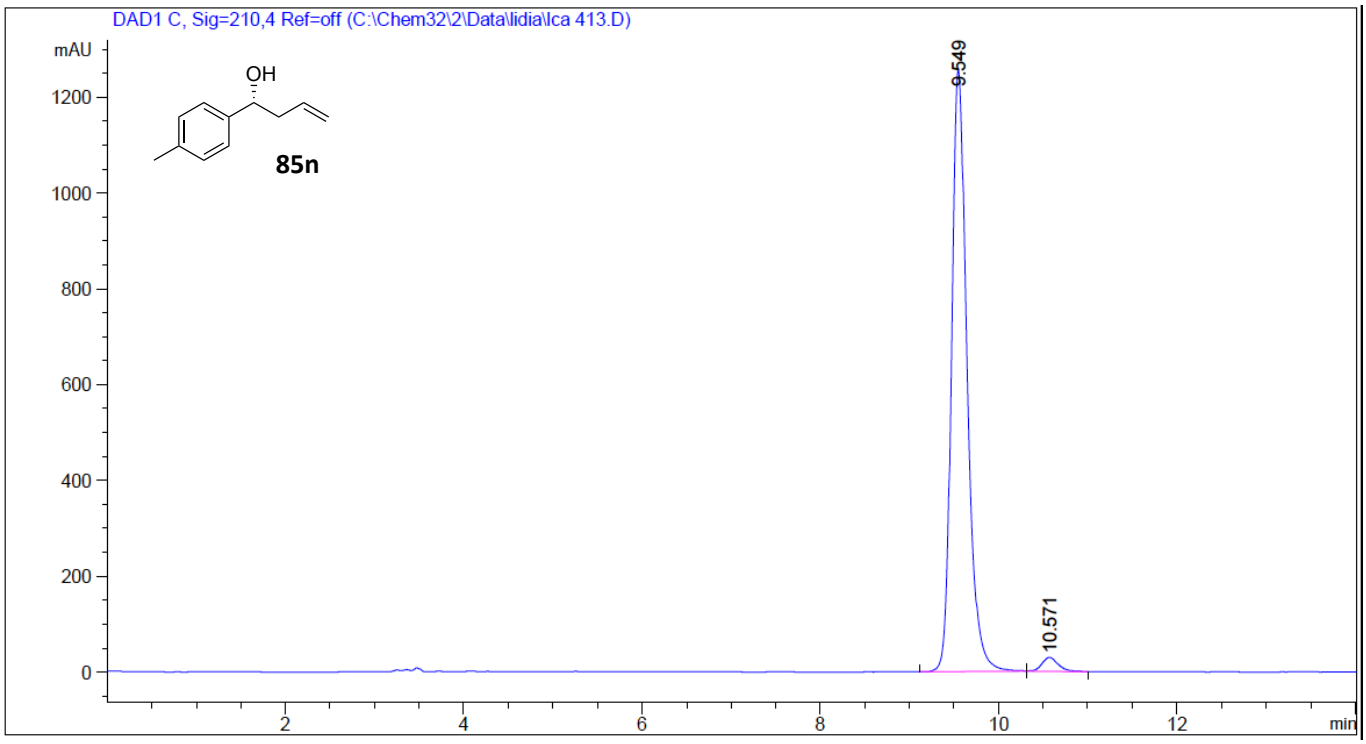

Peak #	RetTime [min]	Type	Width [min]	Area [mAU*s]	Height [mAU]	Area %
1	9.549	BB	0.1834	1.52254e4	1256.18140	97.7179
2	10.571	BB	0.1859	355.57843	28.82613	2.2821

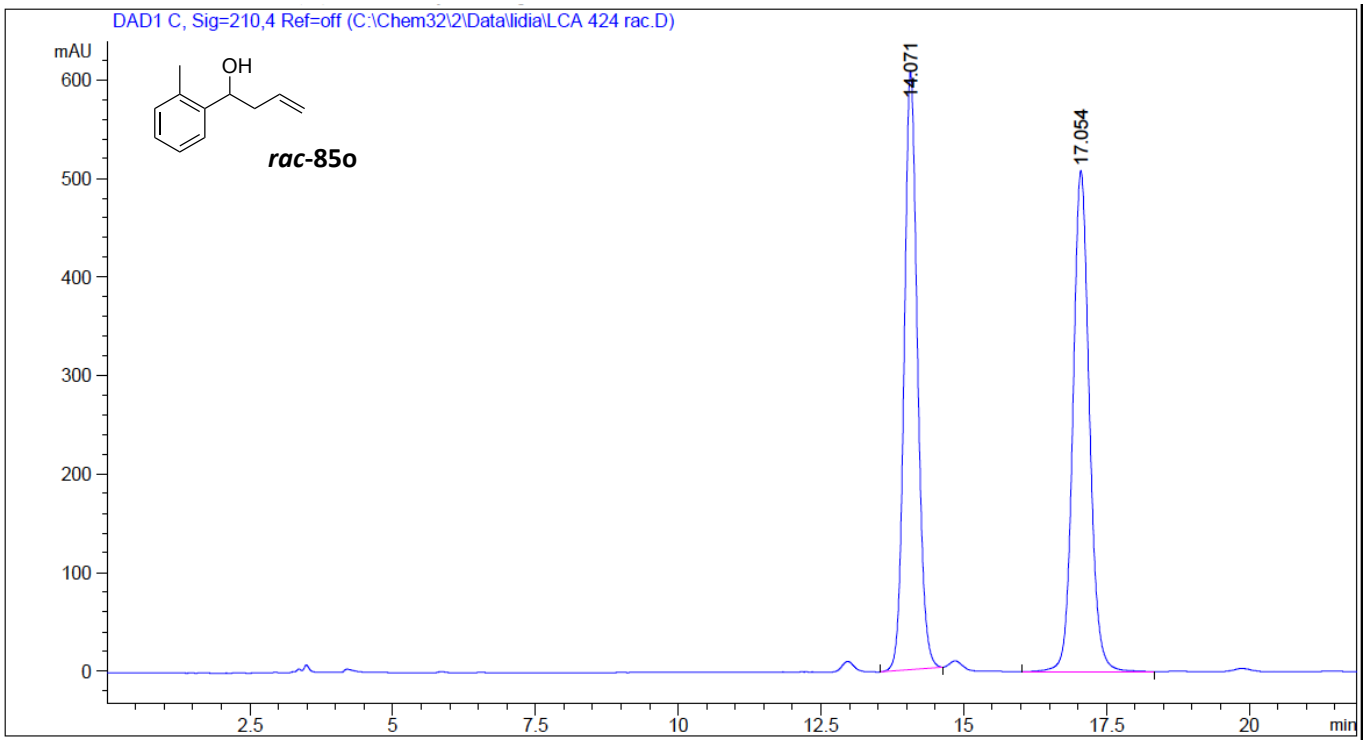

Peak #	RetTime [min]	Type	Width [min]	Area [mAU*s]	Height [mAU]	Area %
1	14.071	BB	0.2491	9838.40527	607.07391	49.2274
2	17.054	BB	0.3047	1.01472e4	508.79813	50.7726

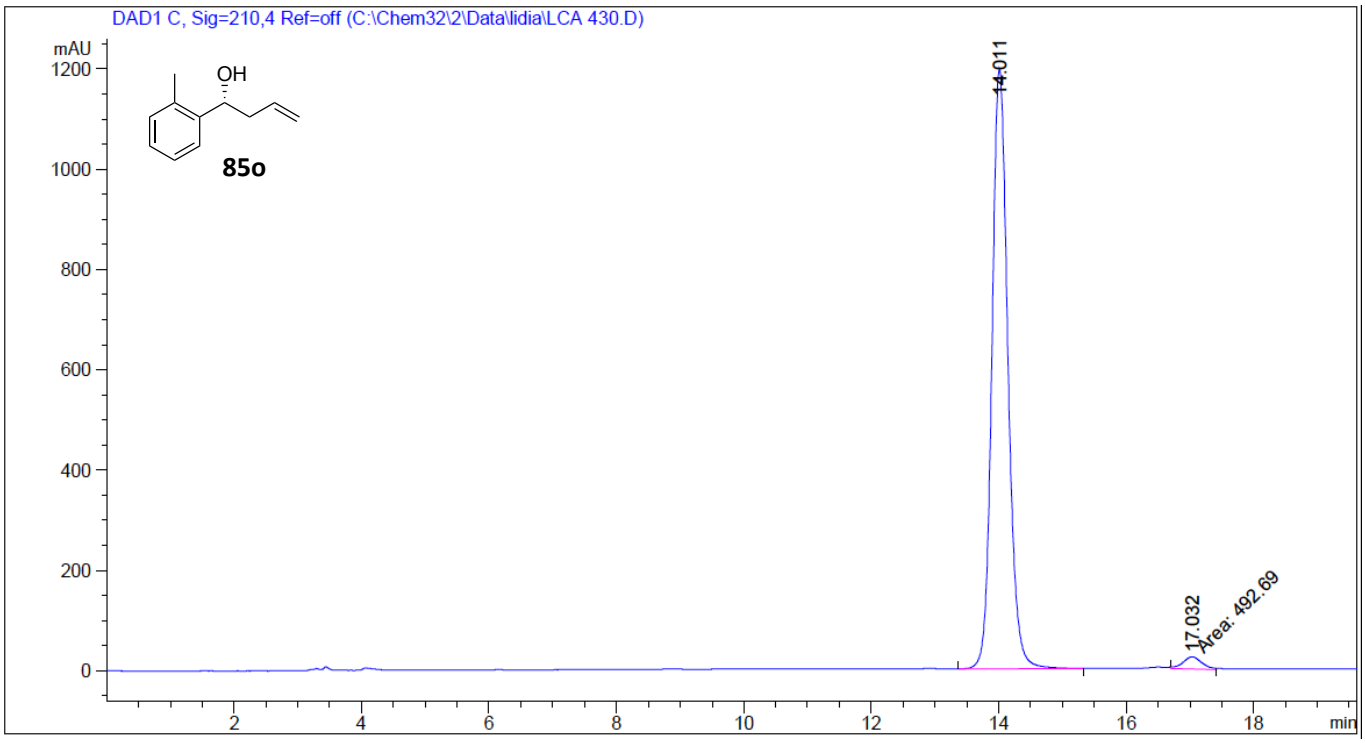

Peak #	RetTime [min]	Type	Width [min]	Area [mAU*s]	Height [mAU]	Area %
1	14.011	BB	0.2690	2.07906e4	1195.13416	97.6851
2	17.032	MM	0.3454	492.68970	23.77230	2.3149

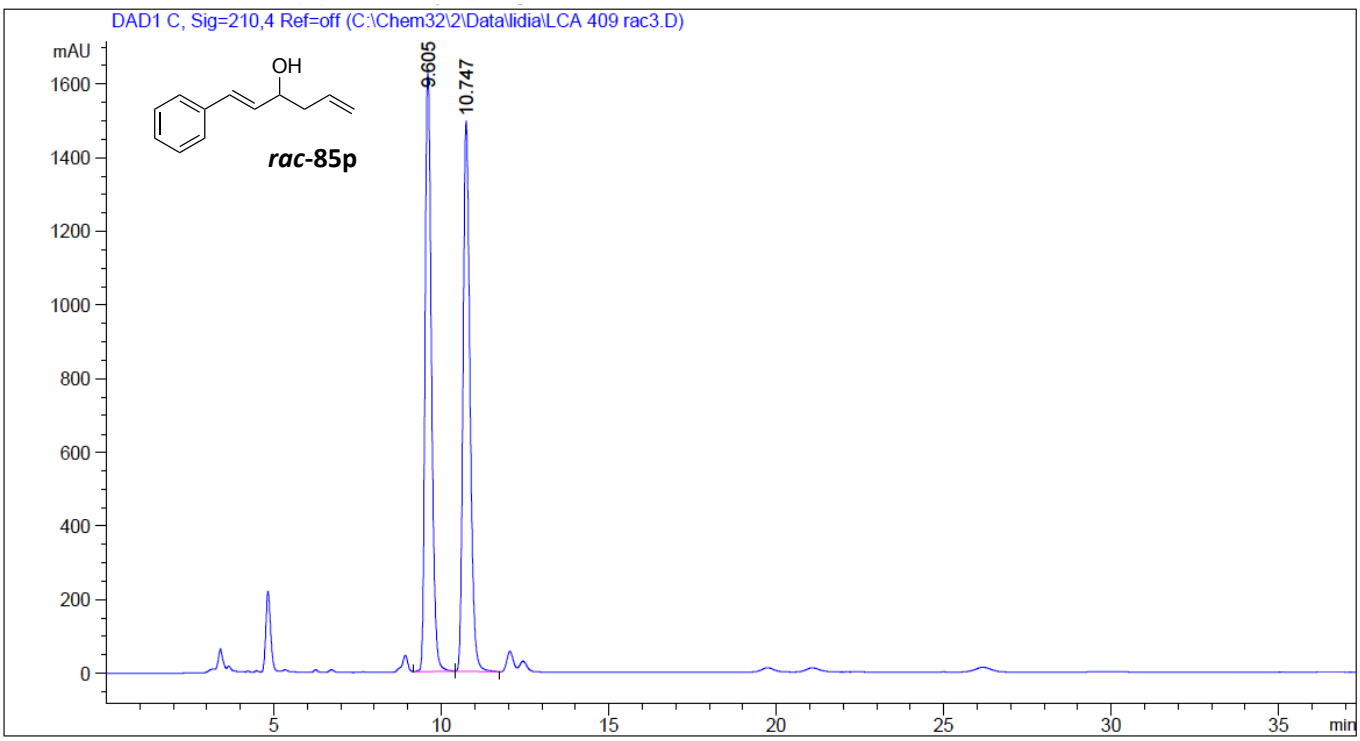

Peak #	RetTime [min]	Type	Width [min]	Area [mAU*s]	Height [mAU]	Area %
1	9.605	BB	0.2041	2.15292e4	1629.55493	49.6691
2	10.747	BB	0.2261	2.18161e4	1495.96765	50.3309

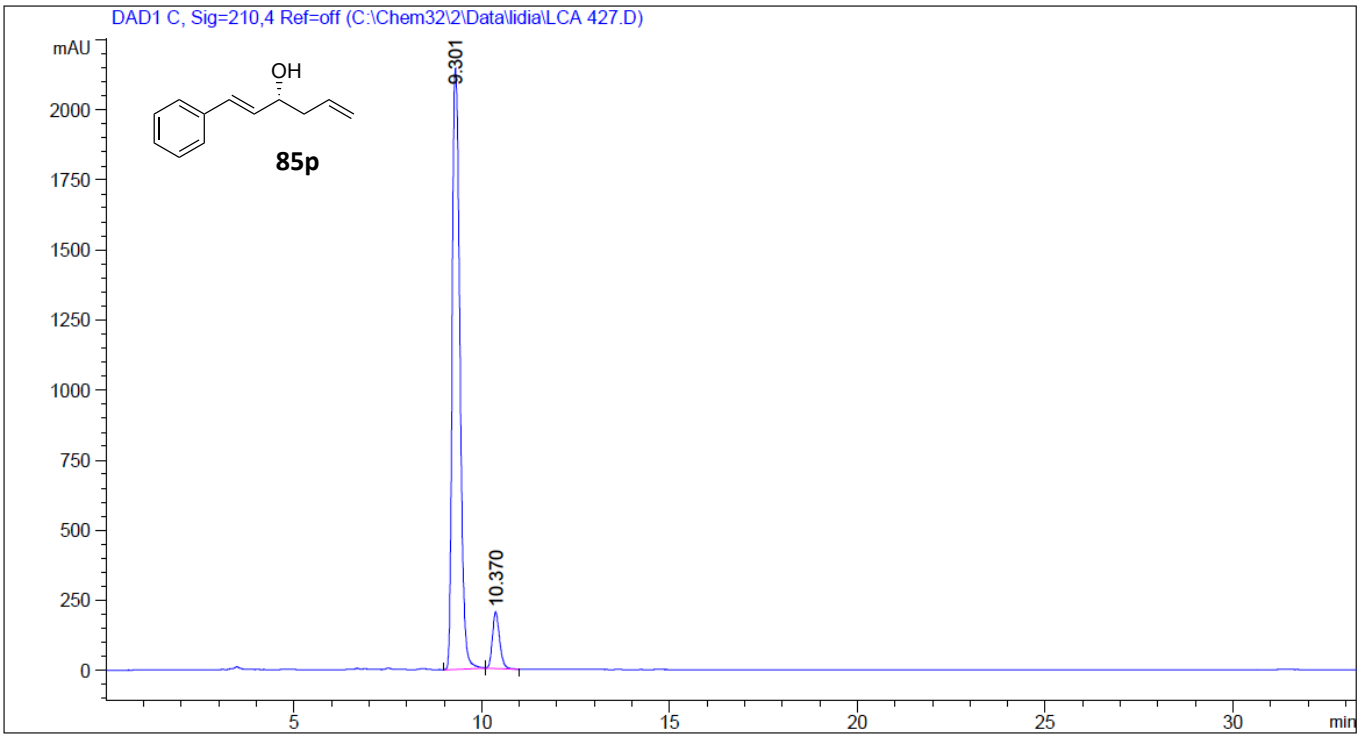

Peak #	RetTime [min]	Type	Width [min]	Area [mAU*s]	Height [mAU]	Area %
1	9.301	BB	0.2261	3.05356e4	2144.83716	91.9497
2	10.370	BB	0.2050	2673.43896	201.17265	8.0503

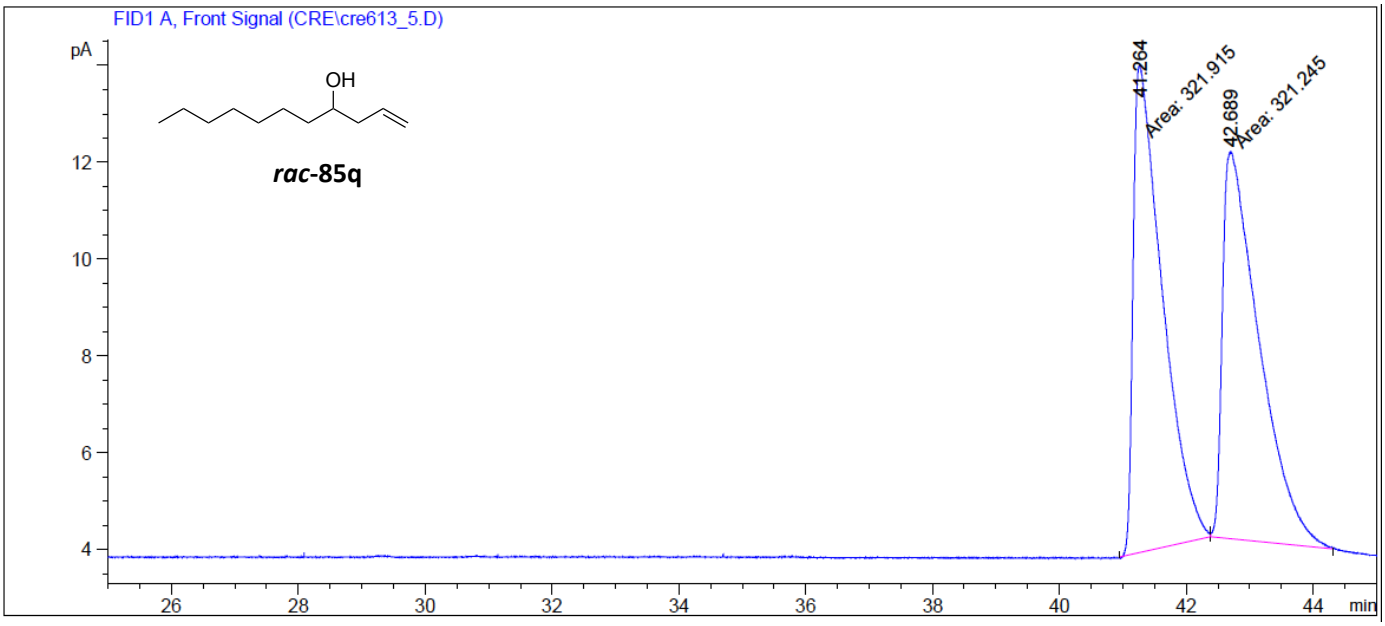

Peak #	RetTime [min]	Type	Width [min]	Area [pA*s]	Height [pA]	Area %
1	41.264	MM	0.5319	321.91458	10.08613	50.05204
2	42.689	MM	0.6700	321.24518	7.99135	49.94796

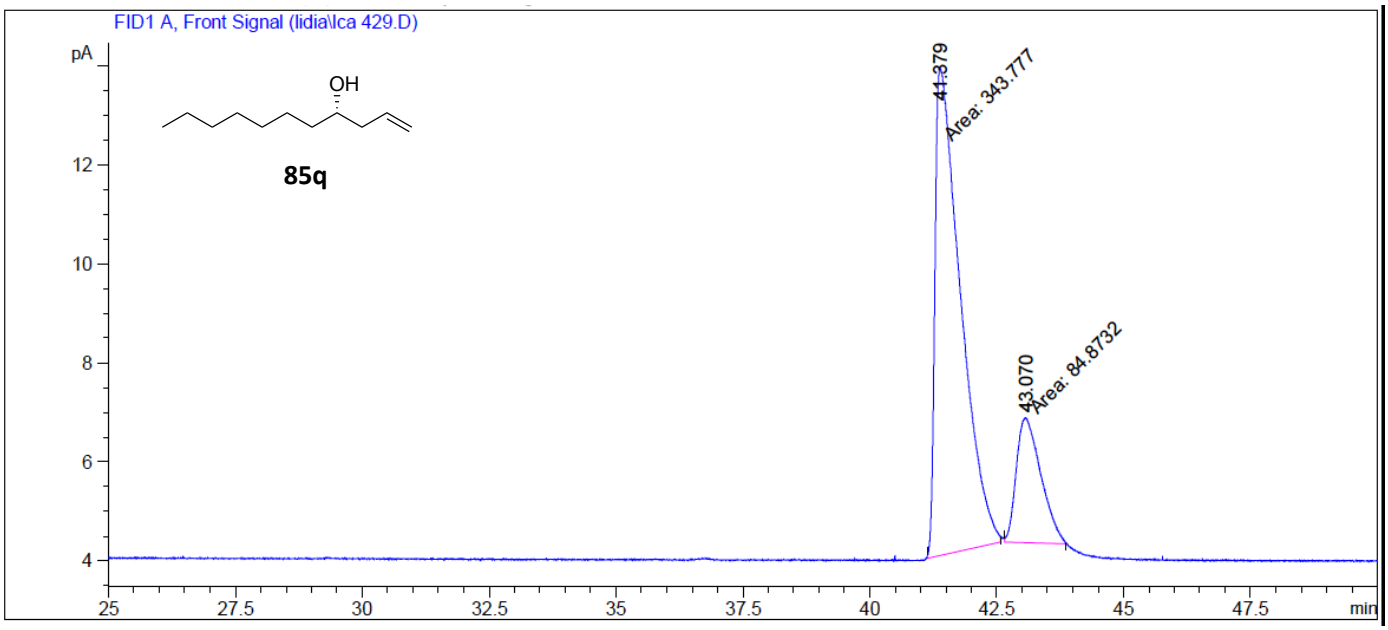

Peak #	RetTime [min]	Type	Width [min]	Area [pA*s]	Height [pA]	Area %
1	41.379	MM	0.5812	343.77670	9.85778	80.19989
2	43.070	MM	0.5590	84.87316	2.53058	19.80011

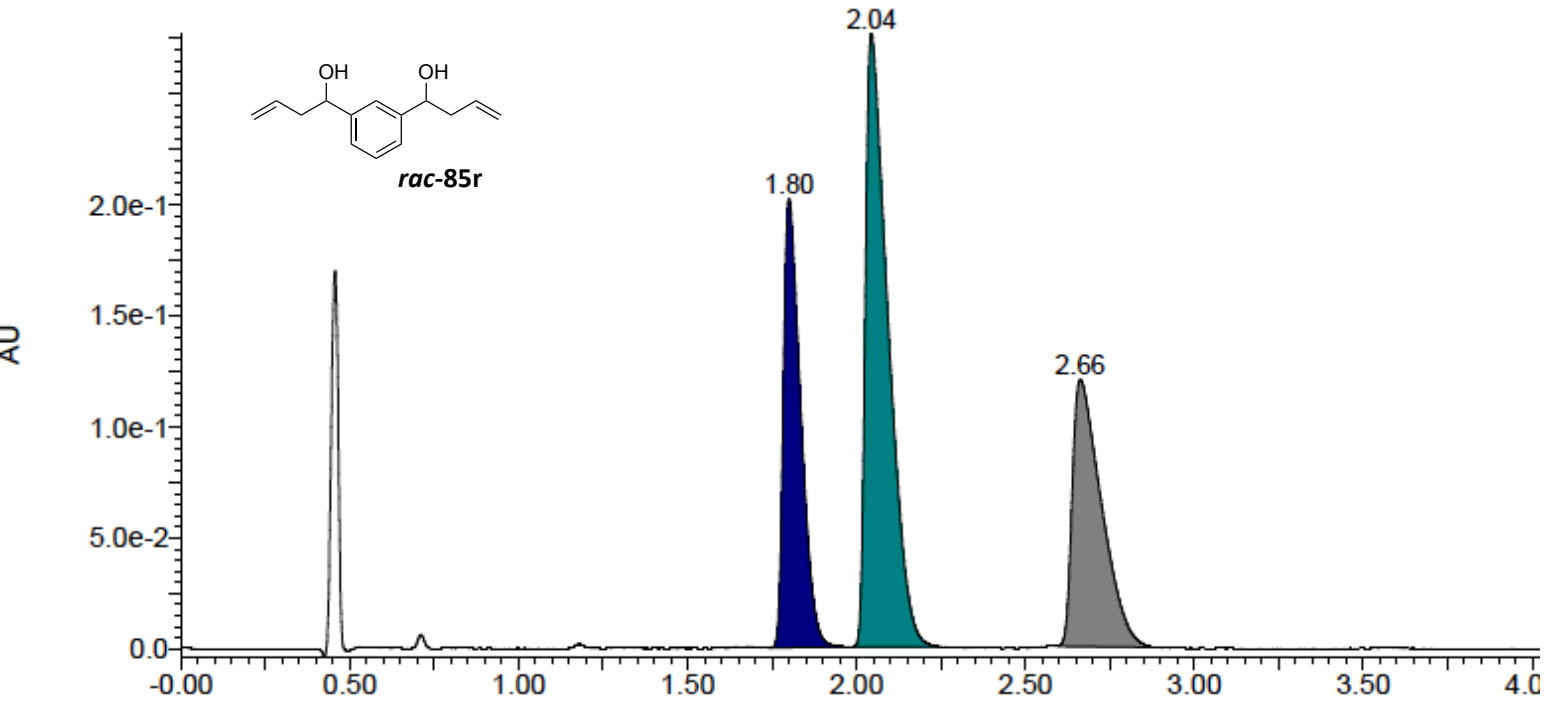

Time	Height	Area	Area%
1.80	202565	12011.77	26.44
2.04	276446	21437.24	47.18
2.66	120274	11987.12	26.38

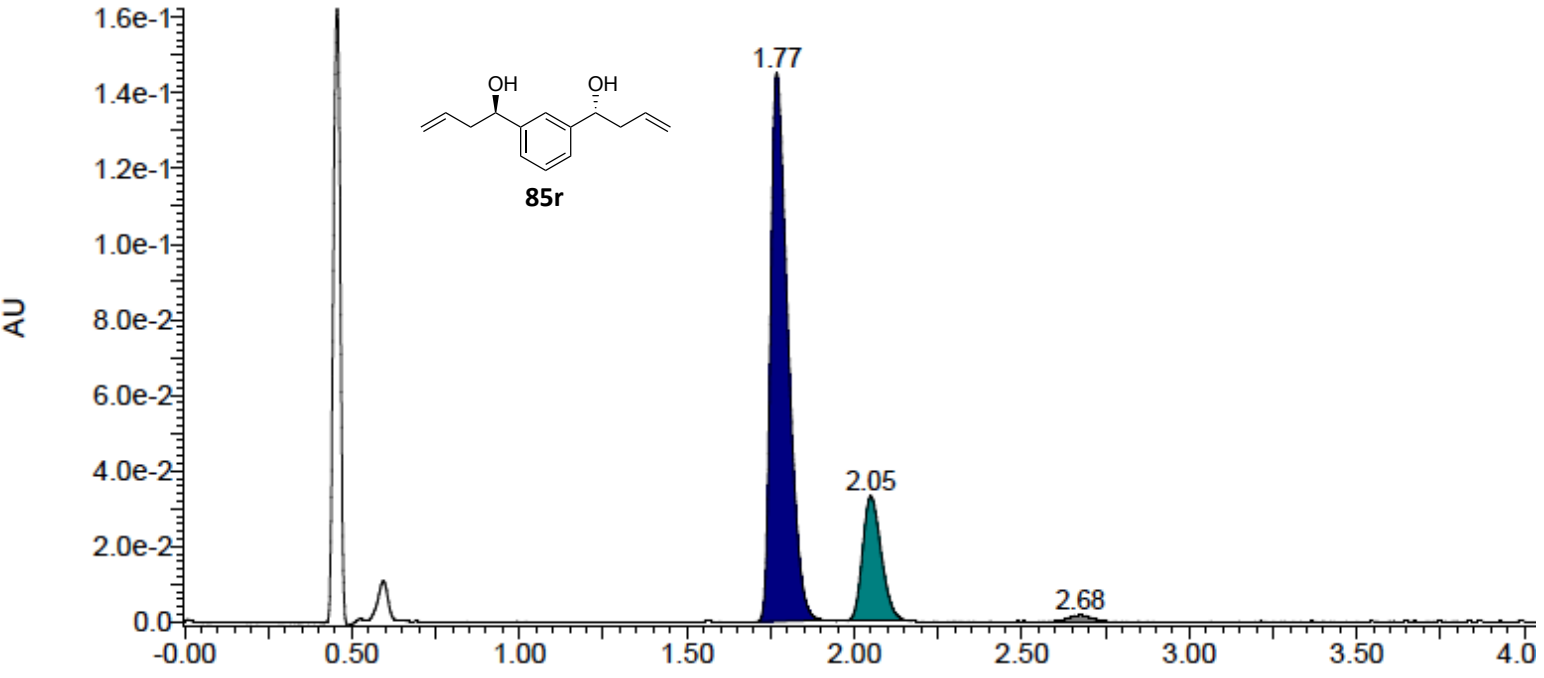

Time	Height	Area	Area%
1.77	145126	8618.26	78.83
2.05	33075	2162.91	19.78
2.68	1790	151.93	1.39

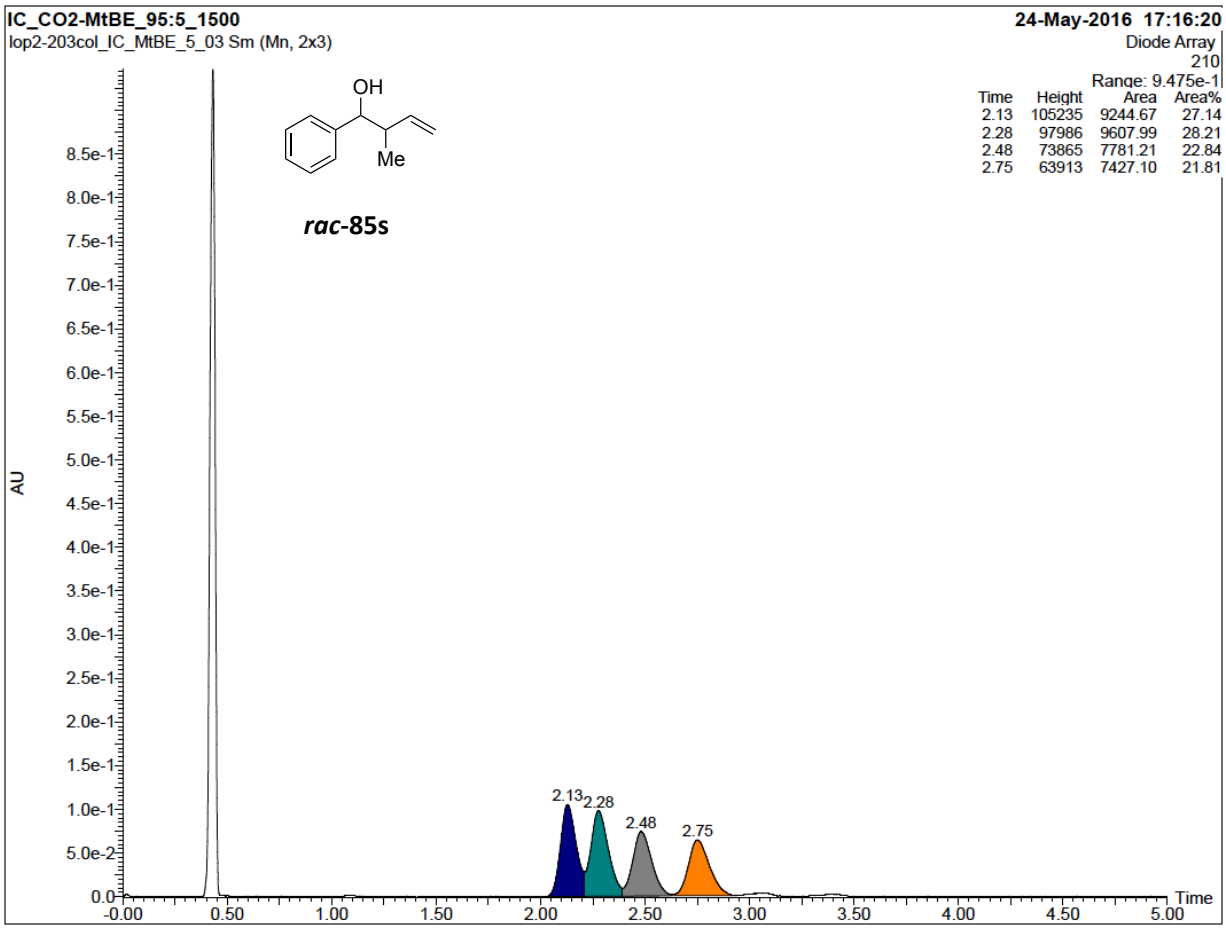
IC_CO2-MtBE_95:5_1500
lop2-203col_IC_MtBE_5_03 Sm (Mn, 2x3)
24-May-2016 17:16:20
Diode Array
210
Range: 9.475e-1
Time Height Area Area%
2.13 105235 9244.67 27.14
2.28 97986 9607.99 28.21
2.48 73865 7781.21 22.84
2.75 63913 7427.10 21.81
OH
Me
rac-85s
AU
Time
2.13
2.28
2.48
2.75

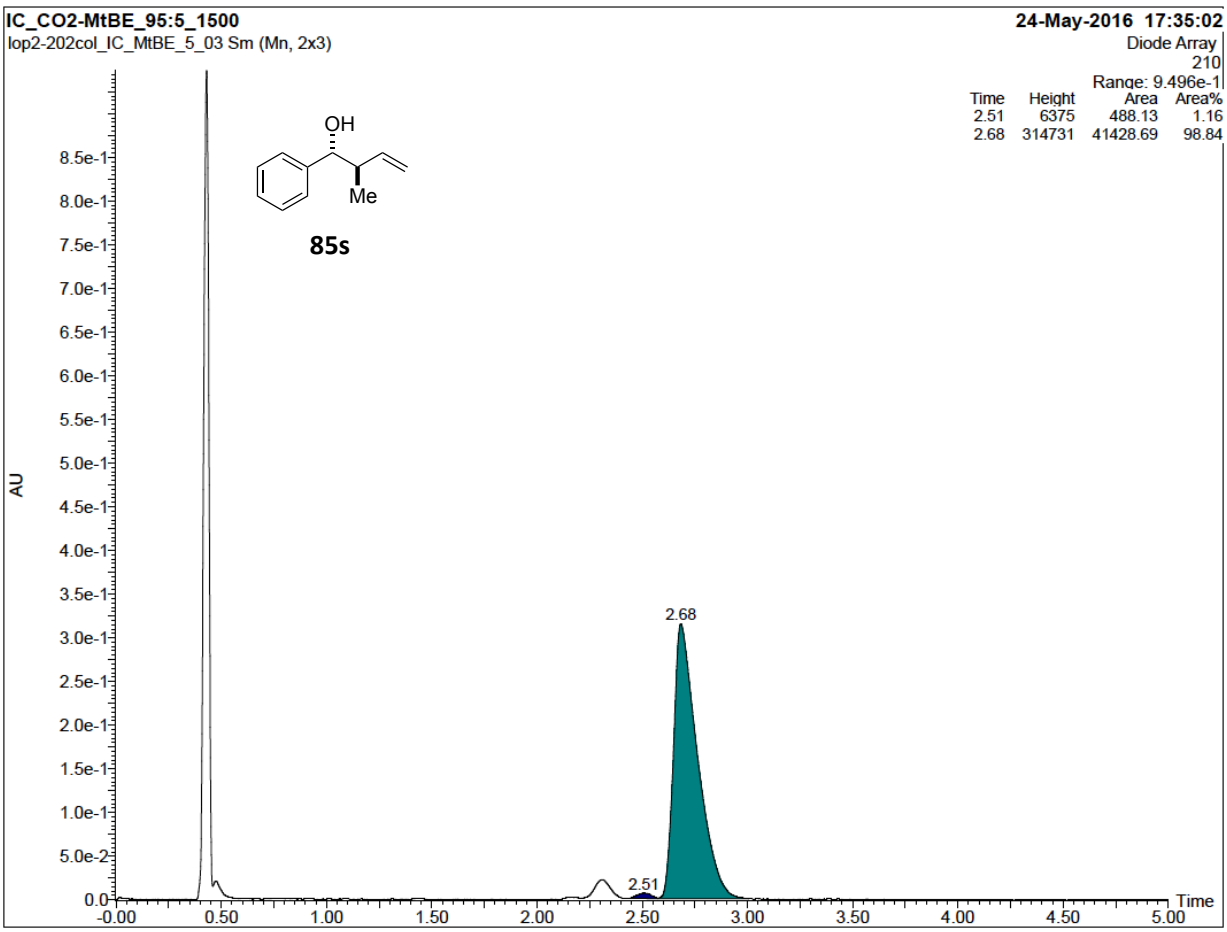
IC_CO2-MtBE_95:5_1500
lop2-202col_IC_MtBE_5_03 Sm (Mn, 2x3)
24-May-2016 17:35:02
Diode Array
210
Range: 9.496e-1
Time Height Area Area%
2.51 6375 488.13 1.16
2.68 314731 41428.69 98.84
OH
Me
85s
AU
Time
2.51
2.68

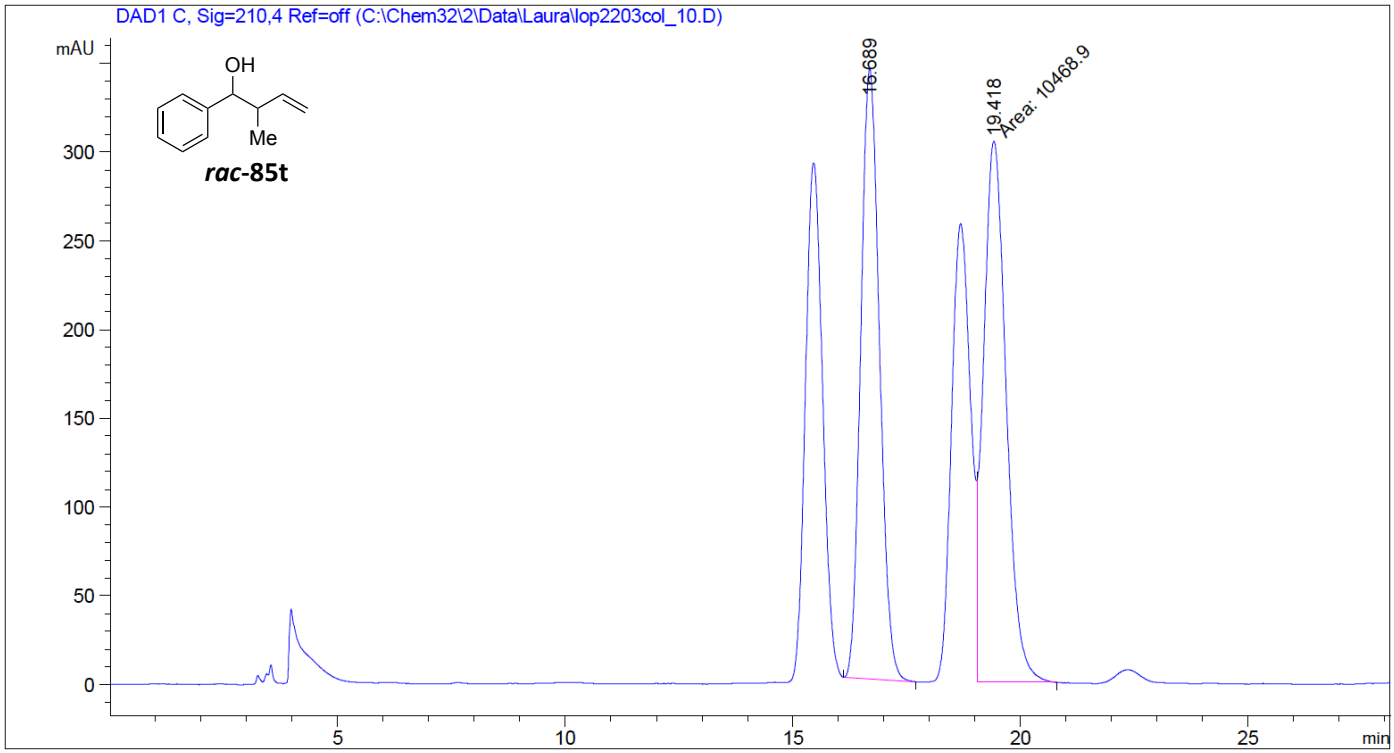

Peak #	RetTime [min]	Type	Width [min]	Area [mAU*s]	Height [mAU]	Area %
1	16.689	BB	0.4494	9823.20996	343.73239	48.4090
2	19.418	FM	0.5732	1.04689e4	304.38705	51.5910

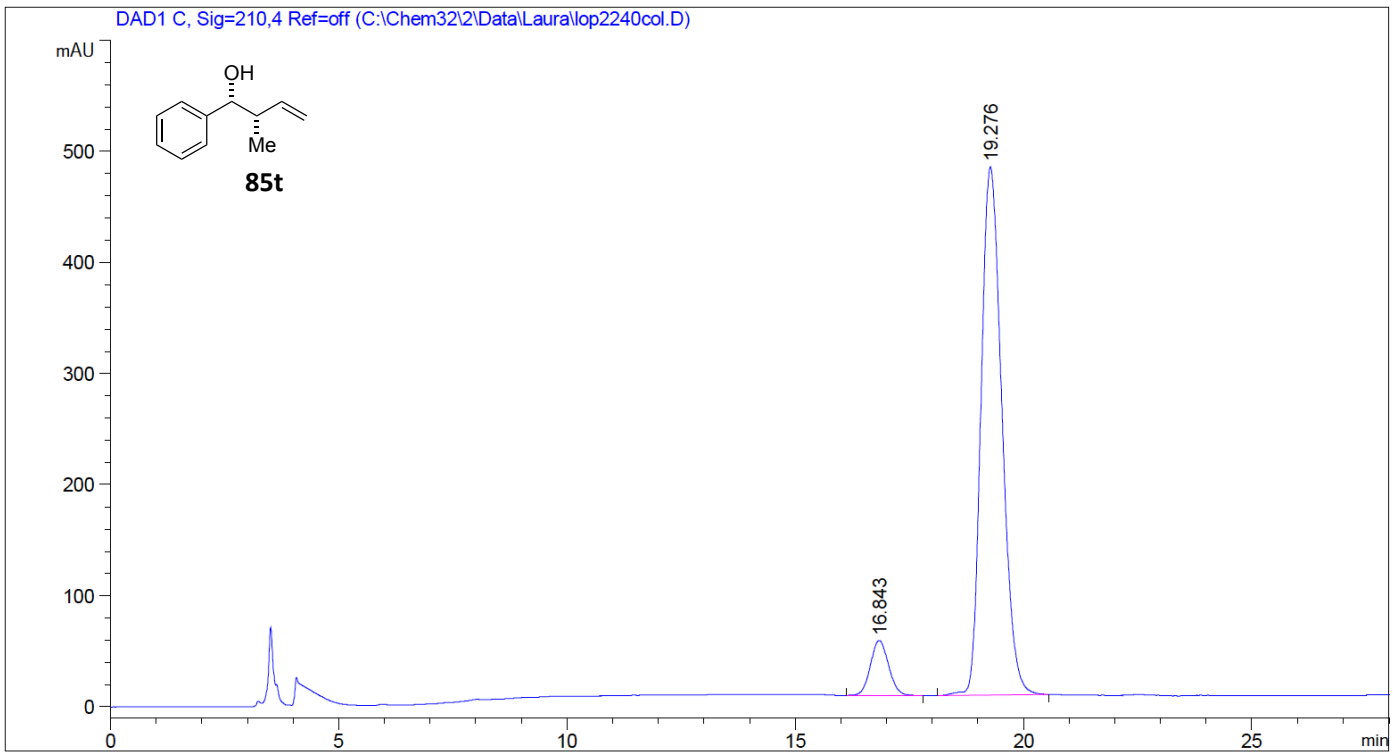

Peak #	RetTime [min]	Type	Width [min]	Area [mAU*s]	Height [mAU]	Area %
1	16.843	BB	0.4296	1384.54602	49.60903	8.4175
2	19.276	BB	0.4976	1.50639e4	475.46338	91.5825

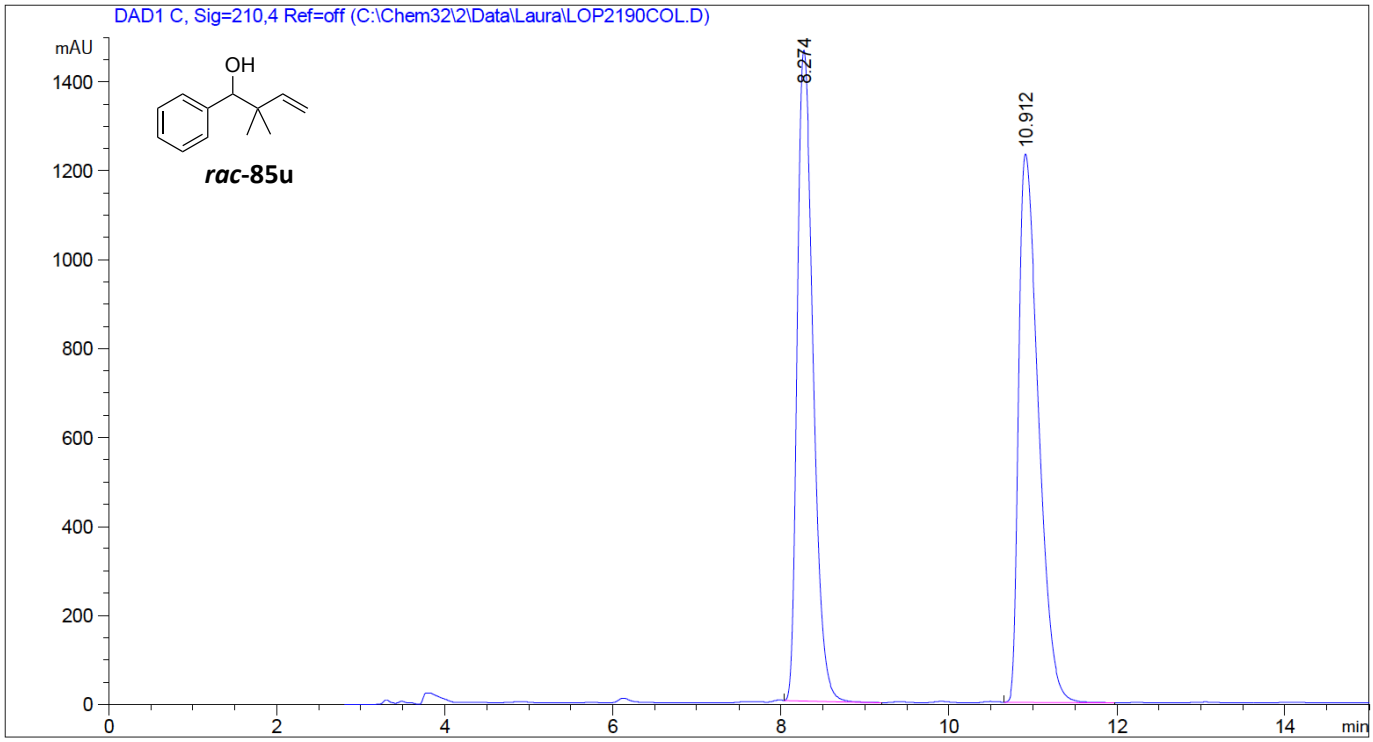

Peak #	RetTime [min]	Type	Width [min]	Area [mAU*s]	Height [mAU]	Area %
1	8.274	BB	0.2070	1.91911e4	1463.83154	48.9147
2	10.912	BB	0.2536	2.00427e4	1233.53503	51.0853

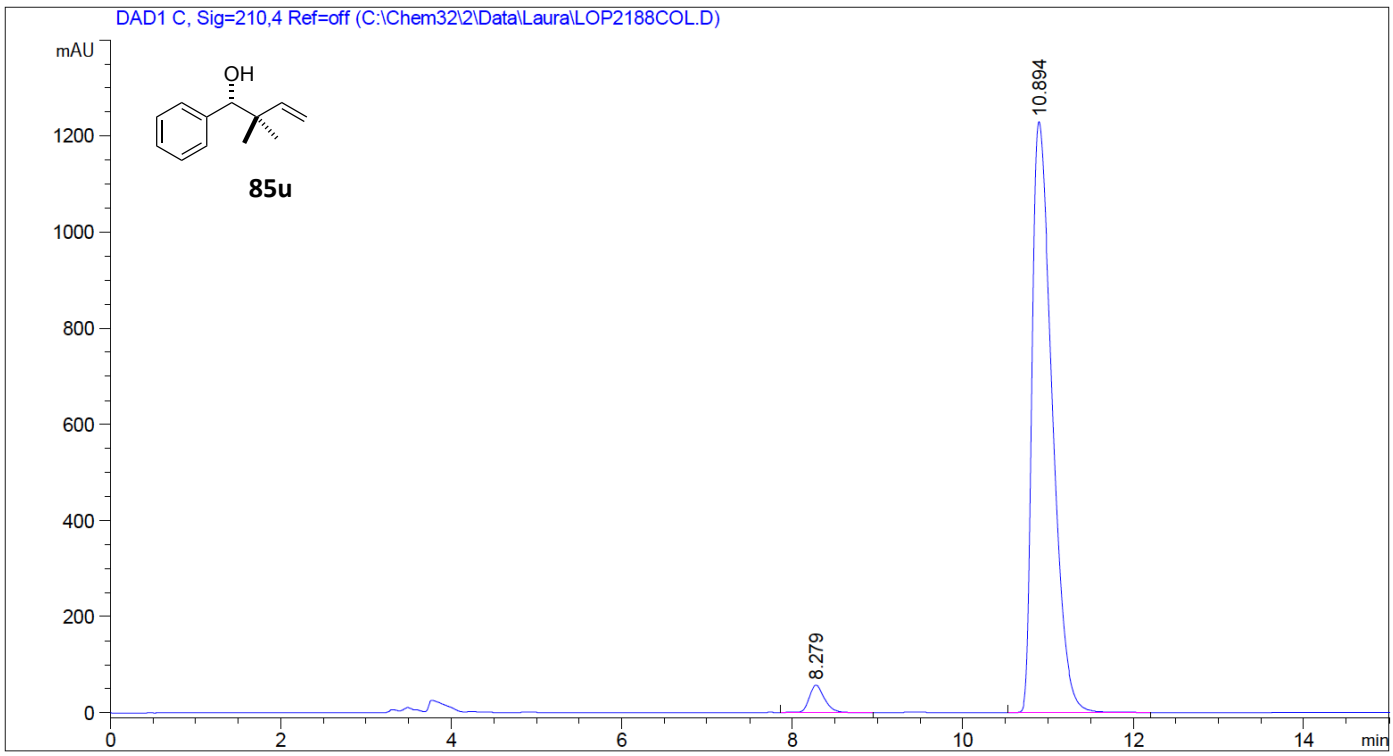

Peak #	RetTime [min]	Type	Width [min]	Area [mAU*s]	Height [mAU]	Area %
1	8.279	BB	0.1915	712.57343	57.13257	3.4409
2	10.894	BB	0.2538	1.99965e4	1229.20508	96.5591

UNIVERSITAT ROVIRA I VIRGILI
IMMOBILIZATION OF CHIRAL BRØNSTED ACIDS AND LEWIS BASES FOR BATCH AND FLOW ENANTIOSELECTIVE CATALYSIS
Lidia Clot Almenara

CHAPTER IV

UNIVERSITAT ROVIRA I VIRGILI
IMMOBILIZATION OF CHIRAL BRØNSTED ACIDS AND LEWIS BASES FOR BATCH AND FLOW ENANTIOSELECTIVE CATALYSIS
Lidia Clot Almenara

Chapter IV

Desymmetrization of *meso*-Diones

4.1. Introduction to Synthesis of Cyclohexenone Compounds

Cyclohexenone derivatives are versatile building blocks for the synthesis of natural products.[1] One of the most powerful synthetic strategies for their synthesis is the Robinson annulation[2] (Scheme 4.1), which involves a sequence of Michael addition followed by cyclization through aldol condensation.[3] The promising Michael products **86** and **88** intermediates obtained contain a prochiral center that allows the preparation of optically pure bicyclic **87** and **88** in the presence of the right chiral catalyst.

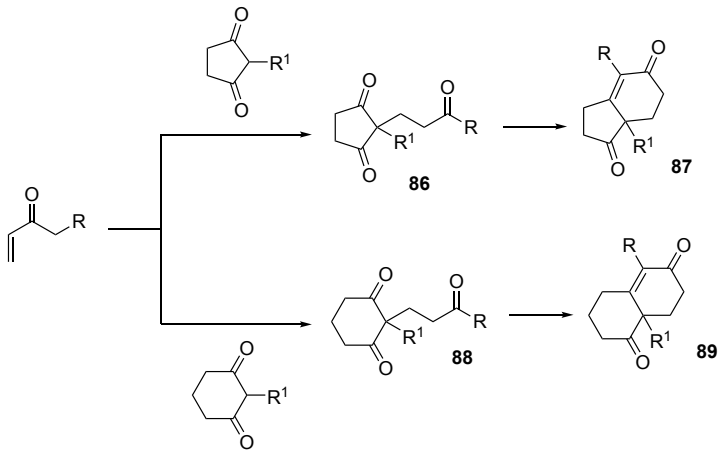

Scheme 4.1: Robinson annulation reaction.

The two major breakthroughs considered nowadays as the early stages of asymmetric organocatalysis, date back to 1971. Two industrial research groups, Hajos and Parrish (working at Hoffmann-La Roche)[4][5] and Eder, Sauer and Weichert (from Schering AG),[6][7] independently discovered an asymmetric

variant of the Robinson annulation; they reported that proline mediated an enantioselective aldol reaction that gives rise to chiral cyclic aldol products that are called Wieland-Miescher (WMK) and Hajos-Parrish ketones (HPK) (Scheme 4.2).

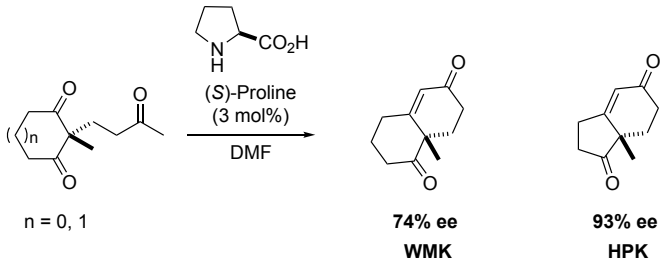

Scheme 4.2: Robinson annulation catalyzed by (*S*)-proline.

This transformation, commonly known as the Hajos-Parrish-Eder-Sauer-Wiechert reaction, has become a reference in asymmetric organocatalysis. In this process, proline fulfills the basic requirements of the ideal catalyst: it is inexpensive and readily available, low catalyst loading is used, and the products are obtained in a highly enantioselective manner.[8] In addition, the synthetic intermediates generated are powerful precursors for the total synthesis of natural products[4c, 9] and bioactive compounds,[10] the most remarkable being steroids, sesquiterpenoids,[11] terpene[12] and terpenoids,[13] which stand out for their antimicrobial, antiviral, anticancer and antineurodegenerative effects (Figure 4.1).[14]

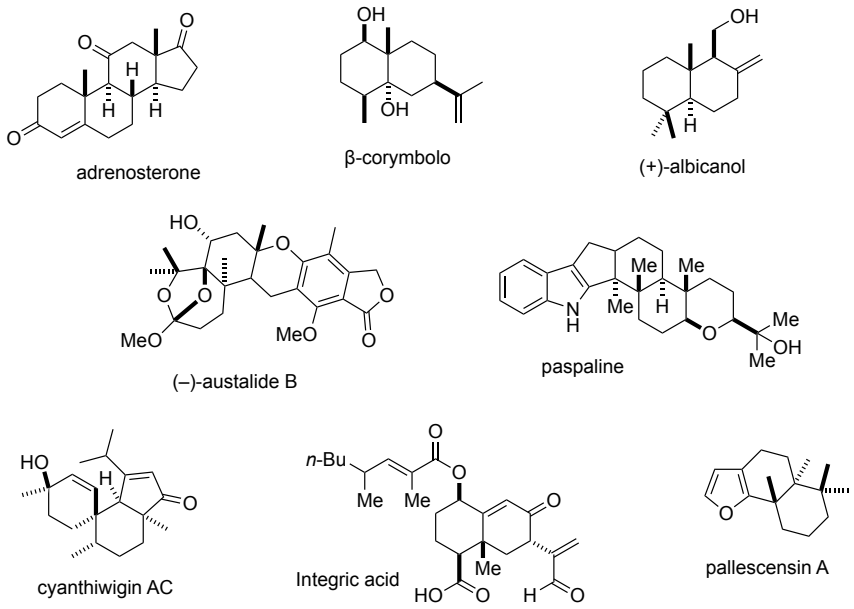

Figure 4.1: Natural products prepared using Wieland-Miescher and Hajos-Parrish ketones as intermediates.

4.1.1. Mechanistic Aspects to Prepare Wieland-Miescher and Hajos-Parrish ketones

Over the years, several mechanistic studies for the general understanding of Hajos-Parrish ketone formation have been carried out (Figure 4.2).[15][16][17] Initially, Hajos and Parrish[4a] tried to propose a reasonable mechanism that involve enamine formation. However, experiments with isotope-labeled water discarded this theory, because labeled oxygen was not incorporated in the final product. Then, they proposed a pathway that involves the addition of (*S*)-proline to one of the carbonyl groups present in the cyclopentanedione ring, thus forming a carbinolamine intermediate. Later in 1986, Agami[18] claimed the possibility that two proline subunits were involved in the mechanistic pathway. In this manner, the first proline reacted via an enamine formation and the second acted as proton-transfer mediator. Finally, the mechanism is now thought to proceed following the well-known model of Houk which involves an enamine intermediate and the establishment of a hydrogen bond

between the carboxylic acid and the acceptor carbonyl group.[15b, 15c, 19] However, this rationalization is relatively recent, and is precisely the lack of understanding of the mechanism which explains why this methodology remained in the shadow during the first 30 years.[20]

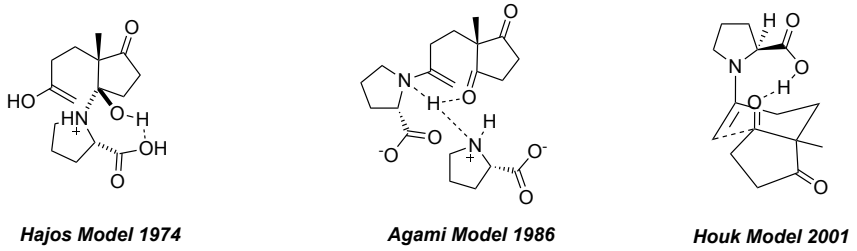

Figure 4.2: Activation modes proposed for the Hajos-Parrish-Eder-Sauer-Wiechert reaction.

4.1.2. Catalysts Able to Promote Cyclohexenone Formation

Remarkably, both industrial groups already observed that the reaction with the five-membered diketone gave moderate yield and ee; to date, it continues to be a challenge. Most of the strategies developed so far for the Hajos-Parrish-Eder-Sauer-Wiechert reaction involve the use of proline or some derivative as catalyst.[21] However, in search of higher enantiomeric excess and an effective route, many groups have tried to develop a straightforward pathway for the synthesis of WMK.[22] In fact, the most common procedure for the scale-up of the Robinson annulation was reported by Gutzwiller *et al*.[23] However, from a practical point of view, some issues need to be figured out in that process. For instance, the purification process, which involves difficult separation in the work-up due to the bad visualization because of the emulsion present, distillation and consecutive recrystallization in order to achieve enantiopure product. Furthermore, the use of high boiling points solvents (DMSO), time consuming synthesis, generation of waste and low yield have stressed the need

to improve the process by identifying an alternative organocatalyst able to promote the asymmetric Robinson annulation.

The first in developing an alternative to proline were Lerner, Barbas and Danishefsky in 1997. They proved that aldolase antibody Ab38C2 (**90**) could promote the Robinson annulation transformation to achieve WMK in 96% ee in 10 days.[24] This procedure involves expensive catalyst that has a high molecular weight. Later, the group of Davis proposed the use of β-amino acids instead of α-amino acids (**91**), because the additional carbon between the amino and carboxyl acid group can lead to greater conformational flexibility, but the long reaction times remained (5 d) and the ee's were slightly lower.[25] In 2007, Landais *et al*. found that a benzimidazole-pyrrolidine (**92**) in the presence of Brønsted acid catalyzed the aldol reaction and they decided to apply it to the Robinson annulation. The aldol reaction and the elimination process took place in one step thus giving the dehydrated product in less time.[26] Inomata,[27] in 2007, also developed a similar strategy; a pyrrolidine derived catalyst (**93**) was used for the WMK and the dehydration was accelerated by the addition of a Brønsted acid. Note that the presence of a Brønsted acid is required taking into account that Barbas previously also tried to apply these catalysts to the Robinson annulation, but the dehydration was too slow in basic media for the reaction to proceed.[28] Later, in 2008, Nájera and co-workers, studied in depth alternative families of catalysts which were able to increase considerably the yield and ee. They selected bifunctional a BINAM-L-prolinamide-derived catalyst (**94**) for solvent-free aldol reactions[29] and the same year also reported the use of prolinethioamdie (**95**).[30] Remarkably, prolinamide derivatives have shown to be one of the most efficient catalysts for aldol reactions.[31][32] In fact, Zhang[33] surveyed a broad number of simple prolinamide catalysts, differing in the commercially available prolinamide (**94**), which proceeded in moderate yield but good ee. Finally, more recently, Morán

published in 2010[34] a promising class of diamide derivatives (**97**), but their synthesis required 12 steps, which represents a major disadvantage (Figure 4.3).

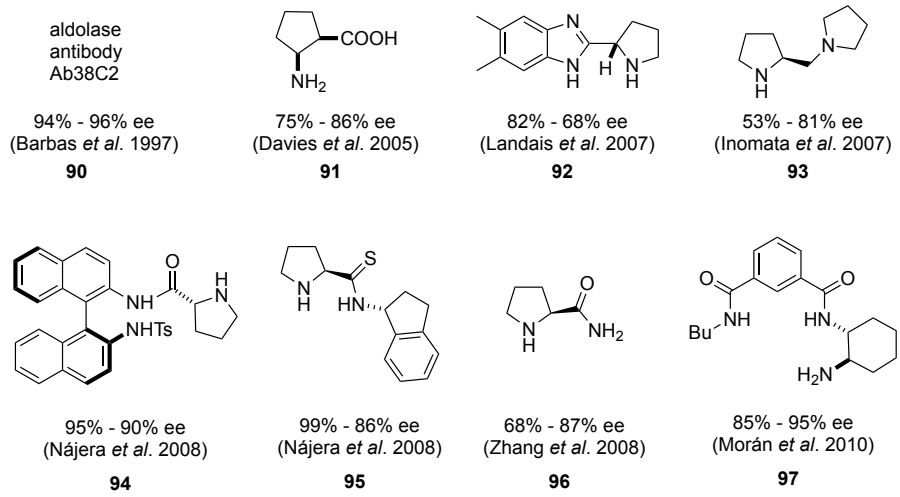

Figure 4.3: Overview of amino catalysts for the Wieland-Miescher ketone synthesis.

However, despite all the developments reported for the synthesis of cyclohexenones, the main challenge is to identify an effective catalyst that can carry out both reactions: the aldol and the consecutive dehydration.[35] To date, chiral secondary amines basically dominate this field and they are assumed to promote the reaction through the enamine activation mode. Taking into account the commonly accepted mechanistic, the presence of a base slows down the dehydration of the β-hydroxyketone intermediate. In fact, it has been demonstrated in several protocols the beneficial effect of adding acid after the starting material is consumed, due to the fact that in acidic media and in high temperatures, this step is accelerated. Actually, Brønsted acids alone are known to promote the Robinson annulation in an efficient manner.[36]

In 2009, Akiyama and co-workers, based on the previous results by Antilla in the asymmetric ring-opening of *meso*-aziridines by means of Brønsted acids,[37] showed that the desymmetrization of *meso*-1,3-diones can be promoted by chiral phosphoric acids in the absence of an acidic co-catalyst. The

stereoselectivity using CPAs, unlike in the aminocatalytic processes,[38] was controlled via non-covalent interactions and the catalyst in charge of the desymmetrization also promoted the final dehydration. In this manner, both reactions take place in the same conditions (Scheme 4.3). The desired chiral cyclohexenones were obtained in up to 94% yield and 94% ee.

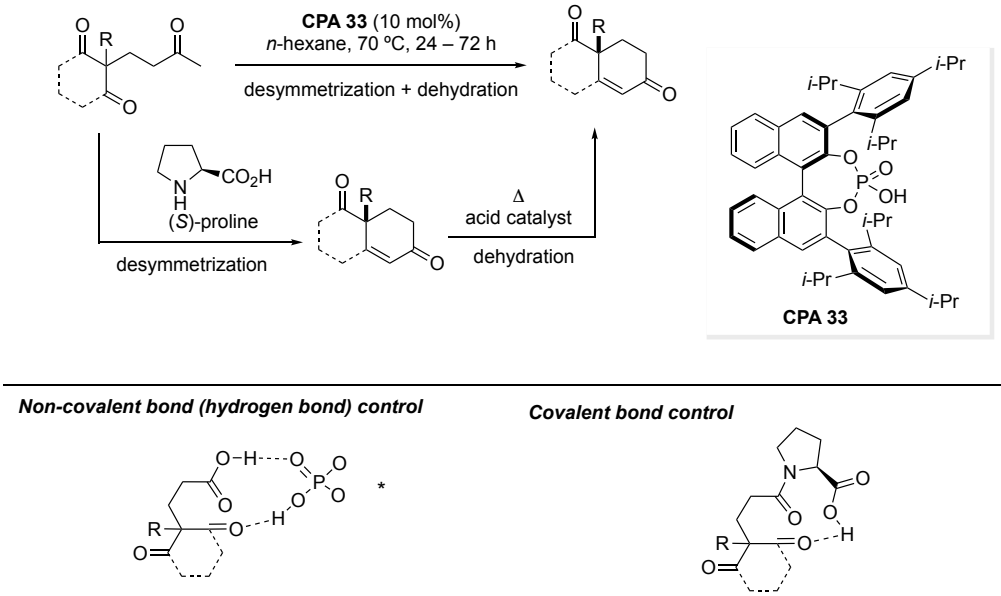

Scheme 4.3: CPA catalysis in contrast to proline strategy for cyclohexenone synthesis.

Significant contributions in the development of solid-supported catalysts for this reaction have been explored.[39] For instance as depicted in Figure 4.4, Benaglia and co-workers reported a Robinson annulation catalyzed by poly(ethyleneglycol)-supported proline. Under these conditions, the Wieland-Miescher ketone was isolated in 55% yield and 75 ee.[40] Alternative supports, like silica, are found in the precedents of Nájera and Vallribera *et al*.[41] Encouraged by the efficiency of BINAM-derived prolinamides for the aldol reaction,[29, 42] they decided to apply silica supported BINAM-prolinamides to the synthesis of both WMK (81% yield, 84% ee) and HPK (85% yield, 88% ee). The supported catalyst was able to promote the two-step Robinson annulation in one-pot in solvent-free conditions and it could be reused for nine cycles.

More recently, in our group, Luo's diamine catalyst[43] has been supported onto polystyrene, proving to be recyclable and allowing to carry out the asymmetric Robinson annulation in continuous flow systems. The chiral vicinal diamide showed high activity for enantioenriched bicyclic enones in very short reaction times (1-2 h).

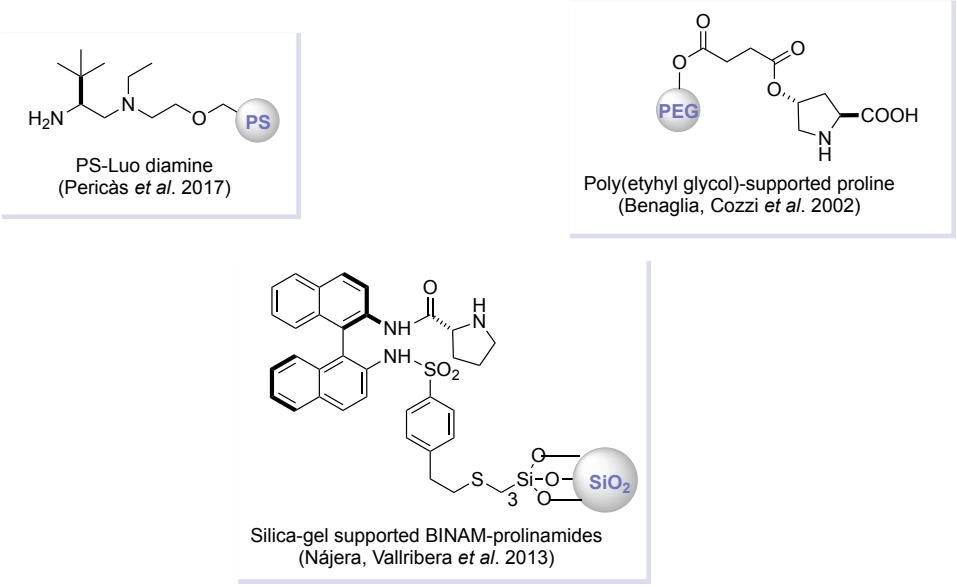

Figure 4.4: Previous supported catalysts for the desymmetrization of diketones.

4.2. Aims

Considering the results summarized in Chapter III, where we successfully applied our PS-TRIP catalyst in the allylation of aldehydes reaching up to 98% yield and 98% ee, we were encouraged to test our supported CPA in other reactions.

It is surprising that, although the acidic nature of the catalyst allows both processes (the aldol reaction and the dehydration) to take place in the same conditions, (without having to use any additive or modifying the temperature), the acid-catalyzed desymmetrization of *meso*-diones has not been sufficiently studied.

In view of these previous aspects, we decided to tackle the applicability of our PS-TRIP catalyst on the desymmetrization of *meso*-1,3-diones to produce chiral cyclohexenones.

Our main goal was to generate the cychlohexenone product in an efficient manner, by accelerating the dehydration of the intermediate aldol product. (Scheme 4.4) Furthermore, we have particular interest in the easy separation of the final product from the catalyst due to the heterogeneous nature of the supported catalyst. Finally, as we have proved in the previous chapter, our catalyst is easily recovered and recyclable, making it a convenient alternative for this transformation.

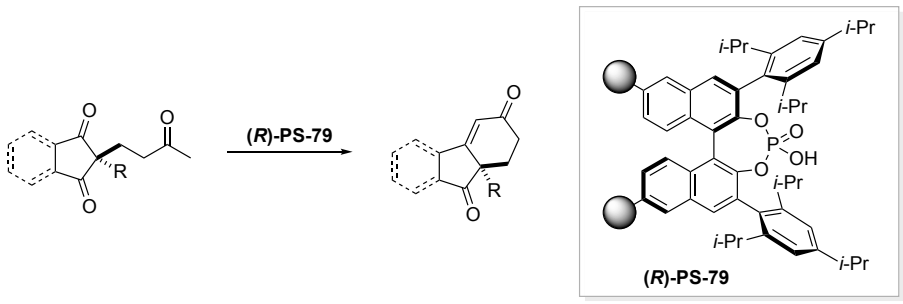

Scheme 4.4: Desymmetrization of *meso*-1,3-diones.

4.3. Results and Discussion

Akiyama *et al*. proved in 2009 the efficiency of CPAs for the synthesis of a broad range of cyclohexenones.[44] A possible way to improve this process would be to recover the catalyst, so we proceeded to examine our PS-TRIP in this powerful transformation. A detailed evaluation of our initial investigation is summarized in Table 4.1. Our first attempts at desymmetrization with PS-TRIP were carried out with triketone **98a** bearing a fused benzene ring as a model substrate. No reactivity was recorded at room temperature in different solvents (entries 1-5), with the exception of toluene, in which traces of the desired product were observed, and hexane. Even if the yield was low (35%) the high ee (90% ee) revealed the high selectivity of the catalyst. After that, a beneficial effect in yield was observed when heating up the reaction mixture to 70 ºC; to our delight , the high enantioselectivities were maintained (entry 6). Furthermore, increasing the catalyst loading to 10 mol% resulted in higher yields (entry 7). After these preliminary results, we decided to re-screen the solvent at 70 ºC (entries 8-9), however, both toluene and DCE did not provide further improvement. Finally, we increased the catalyst loading and extended the reaction time (entries 10-12), thus finding the optimal conditions under 20 mol% catalyst, 70 °C and 48 h (98% yield, 90% ee) to obtain the cyclohexenone product.

Table 4.1: Screening of reaction conditions for the desymmetrization of *meso*-diones [a].

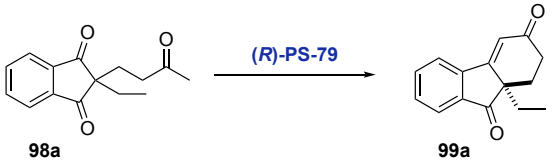

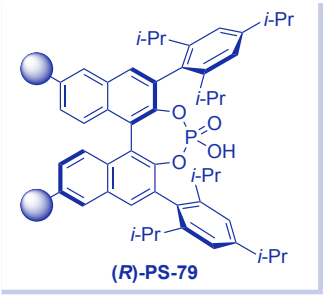

Entry	Solvent	Temp. [°C]	Cat. loading [%]	Time [h]	Yield [%][b]	ee [%][c]
1	Hexane	rt	5	32	35	90
2	EtOAc	rt	5	32	0	-
3	CH_2Cl_2	rt	5	32	0	-
4	THF	rt	5	32	0	-
5	Toluene	rt	5	32	traces	-
6	Hexane	70	5	48	50	91
7	Hexane	70	10	24	80	89
8	DCE	70	10	24	64	90
9	Toluene	70	10	24	75	88
10	Hexane	70	15	24	64	88
11	Hexane	70	20	24	69	88
12	Hexane	70	20	48	98	89

[a]Reactions were carried out with 0.2 mmol of **98a** in 2 mL of solvent. [b]Yield of isolated product. [c]Determined by HPLC on a chiral stationary phase.

With the optimized conditions in hand, we moved to explore the reaction scope. We first studied the generality of this method to benzo-fused *meso*-diones (Table 4.2). The methyl-substituted analogue **99b** was obtained in excellent yield and enantioselectivity (94%, 88% ee). For the analog bearing a phenyl group the yield was lower than 50%, which we attributed to the low solubility of the starting material. Indeed, when the reaction was carried out in toluene at 90 °C, **99c** was obtained in good yield. The related benzyl-substituted compound delivered cyclohexenone **99d** in considerably higher yields. Notably, the propargylic substrate displayed an excellent behavior, furnishing **99e** (which is an intermediate used in the synthesis of a gibbane framework[45]) in 96% yield and 92% ee, This kind of substrates generally

afford the desired cyclohexenones in very good yields and enantioselectivities, despite the somewhat elevated reaction temperatures employed.

Table 4.2: Scope of the desymmetrization reaction with benzene-fused *meso*-diones.

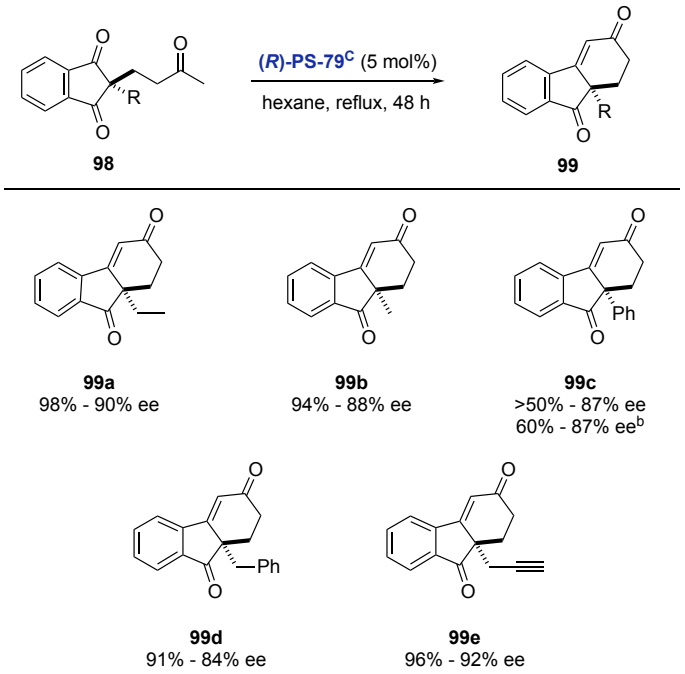

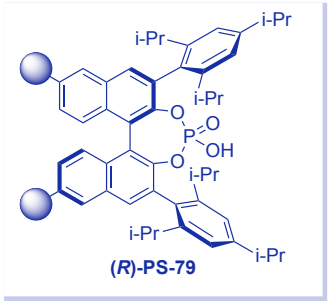

[a]Unless otherwise noted, the conditions are: starting material (0.12 mmol), PS-TRIP (**79**) (20 mol%), *n*-hexane (1.2 mL), reflux during 48 h. [b]In toluene at 90 °C for 48 h. [c]All reactions were carried out with the same sample of PS-TRIP.

Then, to expand the applicability of this method, we decided to explore substrates lacking the fused benzene ring and the results are summarized in Table 4.3. This kind of substrates, gave rise to the corresponding cyclohexenones in lower yields and ee's the ones shown in Table 4.2. For instance, the Hajos–Parrish **101a** and Wieland–Miescher **101c** ketones were produced under these conditions in decent yields but moderate ee's. Our PS-TRIP catalyst also enabled the formation of cyclohexenones bearing a tetrasubstituted alkene moiety (**101b**) in 68% yield, but unfortunately in low

enantioselectivity. Pleasingly, the Wieland-Miescher ketone derivative having a dimethylallyl group (**101d**) could be isolated in high yield.

Table 4.3: Scope of the desymmetrization reaction with cyclic *meso*-diones.[a]

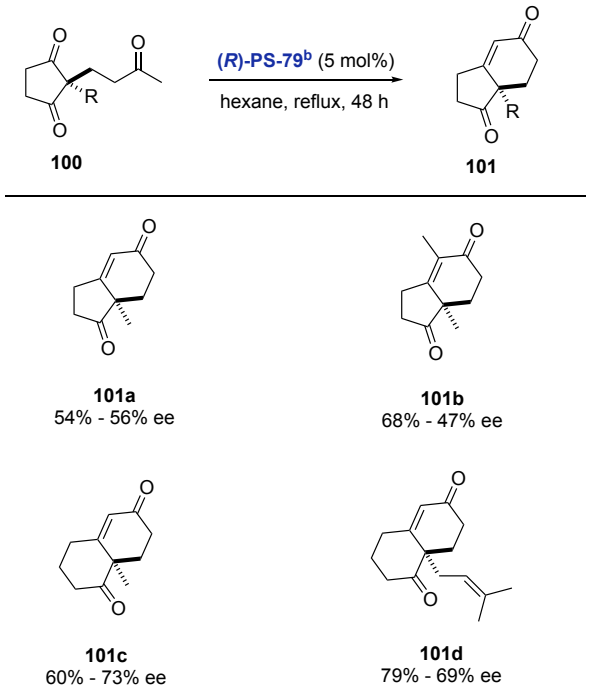

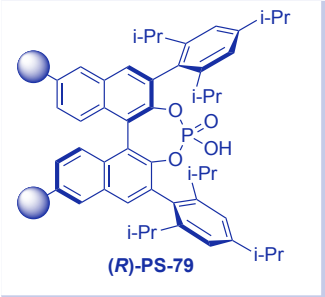

[a]Reaction conditions: starting material (0.12 mmol), PS-TRIP (20 mol%), hexane (1.2 mL), reflux during 48 h. [b]All reactions were carried out with the same sample of PS-TRIP.

It is worth highlighting that all substrates from the scope have been prepared with two samples of polymer, which were already employed in the screening table. Hence, our PS-TRIP **79** resin has not only shown to be highly active in a broad substrate scope but also to be highly recyclable. Indeed, each sample of polystyrene CPA has been recyclable in total 9 times without appreciable decay in activity. After each run, the catalyst was just washed with CH_2Cl_2 and dried in the vacuum line overnight. After that, the catalyst was operative and reused again without further reconditioning. Taking into account the multi-step and tedious preparation of the TRIP catalyst, the heterogeneous TRIP derivative represents an interesting alternative due to the fact that it can be re-used

several times. This has an associated advantage in terms of overall greenness of the process, as it saves huge amounts of solvent and reduces the production of chemical waste.

4.4. Conclusions

To sum up, we have established an alternative straightforward strategy for the desymmetrization of *meso*-1,3-diones catalyzed by a supported chiral TRIP phosphoric acid. This approach has been applied to a broad range of starting *meso*-diones, providing the corresponding cyclized products in up to 98% yield and 90% enantiomeric excess. In this work, we have also demonstrated that the catalyst can be easily recovered by simple filtration of the reaction mixture, thus facilitating the isolation of the final product. In contrast to the homogeneous version, our immobilized version of this CPA can be reused at least nine times. Once again, we can reaffirm that solid-supported CPAs turned out to be very active and robust.

4.5. Experimental Procedures and Characterization of Compounds

4.5.1. General Remarks

All reactions utilizing air- and moisture-sensitive reagents were carried out under a dry Argon atmosphere in oven-dried material. All solvents used in the reactions were dried using an SPS (Solvent Purification System) unless otherwise stated. Thin layer chromatography was performed on Merck TLC Silicagel 60 F254 aluminium sheets. Components were visualized by UV light (λ = 254 nm) and stained with *p*-anisaldehyde or phosphomolybdic dip. Flash column chromatography was carried out using Sigma-Aldrich 60 mesh silica gel and dry-packed columns. ^{1}H NMR and ^{13}C NMR spectra were recorded at 298 K on a Bruker Avance 500 or 400 Ultrashield apparatus. ^{1}H NMR spectroscopy chemical shifts are quoted in ppm relative to tetramethylsilane (TMS). $CDCl_3$ was used as internal standard for ^{13}C NMR spectra. Chemical shifts are given in δ and coupling constants in Hz. IR spectra were recorded on a Bruker Tensor 27 FT-IR spectrometer and are reported in wavenumbers (cm^{-1}). Elemental analyses were performed by MEDAC Ltd. (Surrey, UK) on a LECO CHNS 932 micro-analyzer. High performance liquid chromatography (HPLC) was performed on Agilent Technologies chromatographs (1100 and 1200 Series), using Chiralcel or Chiralpak columns and guard column. The column employed in each case is indicated. Racemic standard products were prepared according to the reported procedure using DL-Proline as catalyst[25b]. High resolution mass spectrometry analyses were performed in a Waters LCD Premier™ instrument operating in ESI (Electro-Spray Ionization) mode or APCI (Atmospheric-Pressure Chemical Ionization) mode. Specific optical rotation measurements were carried out on a Jasco P-1030 polarimeter.

4.5.2. General Procedure for desymmetrization of *meso*-1,3-dione.

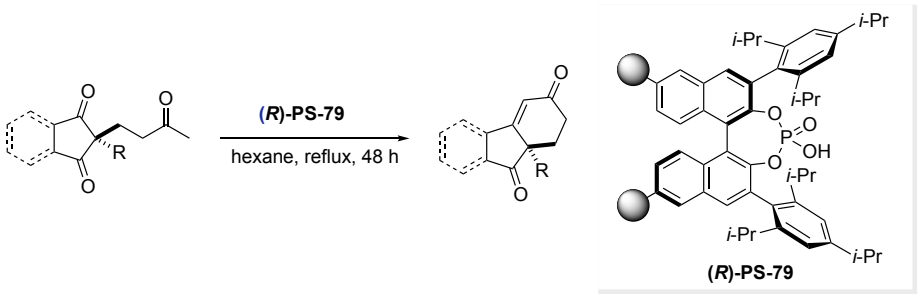

Supported (*R*)-TRIP **79** (20 mol%) was added at room temperature to a screw-cap reaction tube containing the triketone (0.12 mmol) in hexane (1.2 mL). Then, the reaction was heated at 70 °C, and monitored by TLC. After 48 h, the resin was filtered and rinsed with CH_2Cl_2. The filtrate was directly loaded on a silica gel column and the crude product was purified by flash chromatography using cyclohexane/EtOAc.

4.5.3. Characterization of the Chiral Cyclohexenone Products

(*R*)-9a-Ethyl-1,9a-dihydro-3*H*-fluorene-3,9(2*H*)-dione (99a)[44]

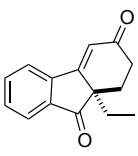

Compound **99a** was obtained in 98% yield and 90% ee as a slightly yellow solid. **^{1}H NMR** (400 MHz, CDCl3): δ 7.85 (dt, *J* = 7.6, 1.0 Hz, 1H), 7.80 (dt, *J* = 7.8, 1.0 Hz, 1H), 7.74 (td, *J* = 7.5, 1.2 Hz, 1H), 7.63 (td, *J* = 7.4, 1.1 Hz, 1H), 6.36 (s, 1H), 2.69 (ddd, *J* = 18.9, 13.5, 5.5 Hz, 1H), 2.61 – 2.52 (m, 1H), 2.42 (ddd, *J* = 13.5, 5.5, 1.8 Hz, 1H), 2.00 – 1.8 (m, 2H), 1.87-1.75 (m, 1H), 0.81 (t, *J* = 7.5 Hz, 3H). **^{13}C NMR** (101 MHz, CDCl3): δ 203.9, 198.8, 162.4, 145.3, 137.0, 135.5, 132.6, 124.3, 123.0, 118.6, 52.0, 33.6, 29.1, 25.6, 9.6. **HPLC** (Daicel Chiralpak IB column, hexane/*i*-PrOH 80:20, flow rate 1.0 mL/min, λ = 250 nm): t_{major} = 16.0 min.; t_{minor} = 15.1 min.

(*R*)-9a-Methyl-1,9a-dihydro-3*H*-fluorene-3,9(2*H*)-dione (99b)[44]

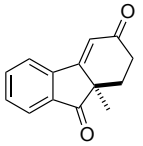

Compound **99b** was obtained in 94% yield and 88% ee as white solid. **^{1}H NMR** (400 MHz, $CDCl_3$): δ 7.87 (dt, *J* = 7.6, 1.1 Hz, 1H), 7.81 (dt, *J* = 7.7, 1.0 Hz, 1H), 7.75 (ddd, *J* = 7.8, 7.1, 1.1 Hz, 1H), 7.64 (td, *J* = 7.4, 1.1 Hz, 1H), 6.36 (s, 1H), 2.79 – 2.68 (m, 1H), 2.66 – 2.56 (m, 1H), 2.30 (ddd, *J* = 13.2, 5.3, 1.8 Hz, 1H), 2.01 (td, *J* = 13.4, 5.6 Hz, 1H), 1.42 (s, 3H). **^{13}C NMR** (126 MHz, $CDCl_3$): δ 204.2, 198.7, 162.3, 144.6, 135.9, 135.6, 132.6, 124.9, 123.5, 118.7, 48.4, 33.8, 27.7, 22.4. **HPLC** (Daicel Chiralpak OD-H column, hexane/*i*-PrOH 83:17, flow rate 0.5 mL/min, λ = 300 nm): t_{major} = 22.7 min.; t_{minor} = 20.3 min.

(*S*)-9a-Phenyl-1,9a-dihydro-3*H*-fluorene-3,9(2*H*)-dione (99c)[44]

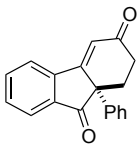

Compound **99c** was obtained in 60% yield and 87% ee as a white solid. **^{1}H NMR** (500 MHz, $CDCl_3$): δ 7.93 (dt, *J* = 7.7, 0.9 Hz, 1H), 7.83 – 7.72 (m, 2H), 7.61 (td, *J* = 7.5, 1.0 Hz, 1H), 7.55 – 7.47 (m, 2H), 7.35 – 7.22 (m, 3H), 6.67 (s, 1H), 2.82 (ddd, *J* = 12.7, 4.5, 2.2 Hz, 1H), 2.49 (m, 1H), 2.37 – 2.16 (m, 2H). **^{13}C NMR** (126 MHz, $CDCl_3$): δ 200.7, 199.2, 159.7, 145.5, 136.9, 136.2, 135.8, 132.9, 129.1 (×2), 128.2, 127.5 (×2), 125.2, 123.1, 120.9, 57.5, 34.4, 30.9. **HPLC** (Daicel Chiralpak AD-H column, hexane/*i*-PrOH 90:10, flow rate 0.6 mL/min, λ = 240 nm): t_{major} = 28.6 min.; t_{minor} = 27.3 min.

(*S*)-9a-Benzyl-1,9a-dihydro-3*H*-fluorene-3,9(2*H*)-dione (99d)[44]

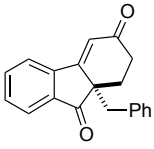

Compound **99d** was obtained in 91% yield and 84% ee as a slightly yellow solid. **^{1}H NMR** (400 MHz, $CDCl_3$): δ 7.63 (dt, *J* = 7.6, 1.0 Hz, 1H), 7.59 – 7.51 (m, 2H), 7.49 – 7.38 (m, 1H), 6.99 (dd, *J* = 5.0, 1.9 Hz, 3H), 6.92 – 6.82 (m, 2H), 6.43 (s, 1H), 3.20 (d, *J* = 13.0 Hz, 1H), 3.14 (d, *J* = 13.1 Hz, 1H), 2.83 (ddd, *J* = 19.1, 13.5, 5.7 Hz, 1H), 2.71 – 2.56

(m, 1H), 2.44 (ddd, *J* = 13.5, 5.8, 1.6 Hz, 1H), 2.05 (td, *J* = 13.6, 5.9 Hz, 1H). **^{13}C NMR** (101 MHz, $CDCl_3$): δ 203.7, 198.6, 161.3, 145.7, 137.3, 135.2, 135.2, 132.2, 129.7 (×2), 128.0 (×2), 127.0, 123.8, 122.6, 119.3, 53.7, 42.8, 33.8, 27.2. **HPLC** (Daicel Chiralpak AD-H column, hexane/*i*-PrOH 90:10, flow rate 0.5 mL/min, λ = 300 nm): t_{major} = 28.4 min.; t_{minor} = 25.4 min.

(*S*)-9a-(Prop-2-yn-1-yl)-1,9a-dihydro-3*H*-fluorene-3,9(2*H*)-dione (99e)[44]

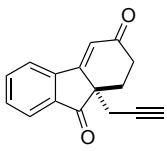

Compound **99e** was obtained in 96% yield and 92% ee as a slightly yellow solid. **^{1}H NMR** (500 MHz, $CDCl_3$): δ 7.88 (dt, *J* = 7.7, 1.0 Hz, 1H), 7.81 (dt, *J* = 7.7, 1.0 Hz, 1H), 7.75 (td, *J* = 7.5, 1.2 Hz, 1H), 7.64 (td, *J* = 7.4, 1.1 Hz, 1H), 6.42 (s, 1H), 2.82 – 2.74 (m, 1H), 2.72 (d, *J* = 2.8 Hz, 1H), 2.69 (d, *J* = 2.7 Hz, 1H), 2.67 – 2.62 (m, 1H), 2.61 – 2.53 (m, 1H), 2.03 (td, *J* = 13.6, 5.8 Hz, 1H), 1.96 (t, *J* = 2.7 Hz, 1H). **^{13}C NMR** (126 MHz, $CDCl_3$): δ 201.8, 198.1, 159.7, 145.2, 136.4, 135.8, 132.7, 124.7, 123.1, 119.6, 78.4, 73.5, 50.5, 33.6, 26.3, 25.9.

HPLC (Daicel Chiralpak AD-H column, hexane/*i*-PrOH 90:10, flow rate 1.0 mL/min, λ = 300 nm): t_{major} = 20.2 min.; t_{minor} = 18.9 min.

(*R*)-7a-Methyl-2,3,7,7a-tetrahydro-1*H*-indene-1,5(6*H*)-dione (101a)[44]

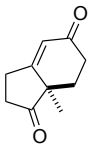

Compound **101a** was obtained in 54% yield and 56% ee as a slightly yellow oil. **^{1}H NMR** (500 MHz, $CDCl_3$): δ 5.97 (br d, *J* = 2.5 Hz, 1H), 3.06 – 2.90 (m, 1H), 2.84 – 2.70 (m, 2H), 2.58 – 2.38 (m, 3H), 2.11 (ddd, *J* = 13.6, 5.2, 2.2 Hz, 1H), 1.91 – 1.80 (m, 1H), 1.32 (s, 3H). **^{13}C NMR** (126 MHz, $CDCl_3$): δ 216.6, 198.3, 169.8, 124.1, 48.9, 36.0, 33.1, 29.4, 27.0, 20.7. **HPLC** (Daicel Chiralpak AD-H column, hexane/*i*-PrOH 95:5, flow rate 1.0 mL/min, λ = 240 nm): t_{major} = 18.2 min.; t_{minor} = 17.2 min.

(*R*)-4,7a-Dimethyl-2,3,7,7a-tetrahydro-1*H*-indene-1,5(6*H*)-dione (101b)[43]

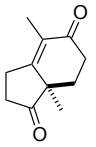

Compound **101b** was obtained in 68% yield and 47% ee as a pale yellow oil. **^{1}H NMR** (500 MHz, $CDCl_3$): δ 2.94 – 2.86 (m, 1H), 2.83 – 2.72 (m, 2H), 2.58 – 2.37 (m, 3H), 2.05 (ddd, *J* = 13.4, 5.3, 2.1 Hz, 1H), 1.83 (td, *J* = 13.7, 5.8 Hz, 1H), 1.76 (d, *J* = 1.5 Hz, 3H), 1.27 (s, 3H). **^{13}C NMR** (126 MHz, $CDCl_3$): δ 217.7, 197.9, 162.5, 129.8, 48.9, 35.5, 32.8, 28.9, 24.5, 21.3, 10.8. **HPLC** (Daicel Chiralpak AS-H column, hexane/*i*-PrOH 90:10, flow rate 1.0 mL/min, λ = 250 nm): t_{major} = 17.9 min.; t_{minor} = 23.5 min.

(*R*)-8a-Methyl-3,4,8,8a-tetrahydronaphthalene-1,6(2*H*,7*H*)-dione (101c)[44]

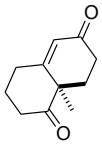

Compound **101c** was obtained in 60% yield and 73% ee as a colourless oil. **^{1}H NMR** (400 MHz, $CDCl_3$): δ 5.86 (d, *J* = 1.9 Hz, 1H), 2.78 – 2.66 (m, 2H), 2.54 – 2.37 (m, 4H), 2.20 – 2.07 (m, 3H), 1.78 – 1.68 (m, 1H), 1.45 (s, 3H). **^{13}C NMR** (126 MHz, $CDCl_3$): δ 126.0, 50.8, 37.8, 33.8, 31.9, 29.9 (×2), 23.4, 23.1, 1.2 (×2). **HPLC** (Daicel Chiralpak IC column, hexane/*i*-PrOH 80:20, flow rate 1.0 mL/min, λ = 250 nm): t_{major} = 29.0 min.; t_{minor} = 33.5 min.

(*S*)-8a-(3-Methylbut-2-en-1-yl)-3,4,8,8a-tetrahydronaphthalene-1,6(2*H*,7*H*)-dione (101d)[43]

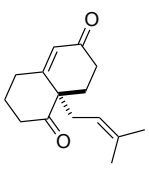

Compound **101d** was obtained in 79% yield and 69% ee as a colourless oil. **^{1}H NMR** (500 MHz, $CDCl_3$): δ 5.89 (d, *J* = 1.8 Hz, 1H), 4.93 – 4.88 (m, 1H), 2.83 – 2.75 (m, 1H), 2.71 – 2.59 (m, 2H), 2.54 – 2.45 (m, 3H), 2.41 – 2.37 (m, 2H), 2.19 – 2.12 (m, 2H), 2.08 – 2.00 (m, 1H), 1.69 (s, 3H), 1.75 – 1.64 (m, 1H), 1.61 (s, 3H). **^{13}C NMR** (126

MHz, $CDCl_3$): δ 210.1, 198.6, 165.7, 136.4, 126.6, 117.4, 55.3, 38.5, 34.6, 33.8, 32.3, 26.6, 26.1, 23.6, 18.2. **HPLC** (Daicel Chiralpak IC column, hexane/*i*-PrOH 80:20, flow rate 0.7 mL/min, λ = 254 nm): t_{major} = 35.9 min.; t_{minor} = 48.8 min.

4.6. References

[1] (a) X. Yang, J. Wang, P. Li, *Org. Biomol. Chem.* **2014**, *12*, 2499-2513; (b) D. Urabe, T. Asaba, M. Inoue, *Chem. Rev.* **2015**, *115*, 9207-9231.

[2] W. S. Rapson and R. Robinson, J. Chem. Soc. 1935, 1285-1288.

[3] (a) R. E. Gawley, *Synthesis* **1976**, 777-794; (b) B. List, *Acc. Chem. Res.* **2004**, *37*, 548-557; (c) B. List, R. A. Lerner, C. F. Barbas, *J. Am. Chem. Soc.* **2000**, *122*, 2395-2396.

[4] (a) Z. G. Hajos, D. R. Parrish, *J. Org. Chem.* **1974**, *39*, 1615-1621; (b) Z. G. Hajos, D. R. Parrish, *J. Org. Chem.* **1973**, *38*, 3239-3243; (c) A. Chanu, I. Safir, R. Basak, A. Chiaroni, S. Arseniyadis, *Org. Lett.* **2007**, *9*, 1351-1354; (d) R. A. Micheli, Z. G. Hojos, N. Cohen, D. R. Parrish, L. A. Portland, W. Sciamanna, M. A. Scott, P. A. Wehrli, *J. Org. Chem.* **1975**, *40*, 675-681.

[5] Z. G. Hajos and D. R. Parrish, German Patent DE 2102623, 1971

[6] U. Eder, G. Sauer, R. Wiechert, *Angew. Chem., Int. Ed.* **1971**, *10*, 496-497.

[7] U. Eder, G. R. Sauer and R. Wiechart, German Patent DE 2014757, 1971

[8] (a) B. Bradshaw, J. Bonjoch, *Synlett* **2012**, 337-356; (b) S. Afewerki, A. Córdova, *Chem. Rev.* **2016**, *116*, 13512-13570.

[9] (a) A. B. Smith, R. Mewshaw, *J. Org. Chem.* **1984**, *49*, 3685-3689; (b) P. A. Grieco, J. L. Collins, E. D. Moher, T. J. Fleck, R. S. Gross, *J. Am. Chem. Soc.* **1993**, *115*, 6078-6093; (c) R. C. A. Isaacs, M. J. Di Grandi, S. J. Danishefsky, *J. Org. Chem.* **1993**, *58*, 3938-3941; (d) L. A. Paquette, T.-Z. Wang, M. R. Sivik, *J. Am. Chem. Soc.* **1994**, *116*, 11323-11334; (e) T. J. Reddy, G. Bordeau, L. Trimble, *Org. Lett.* **2006**, *8*, 5585-5588; (f) S. Yamashita, K. Iso, M. Hirama, *Org. Lett.* **2008**, *10*, 3413-3415; (g) V. M. T. Carneiro, H. M. C. Ferraz, T. O. Vieira, E. E. Ishikawa, L. F. Silva, *J. Org. Chem.* **2010**, *75*, 2877-2882; (h) N. Harada, T. Sugioka, Y. Ando, H. Uda, T. Kuriki, *J. Am. Chem. Soc.* **1988**, *110*, 8483-8487.

[10] (a) E. J. Corey, M. Ohno, R. B. Mitra, P. A. Vatakencherry, *J. Am. Chem. Soc.* **1964**, *86*, 478-485; (b) J. E. McMurry, S. J. Isser, *J. Am. Chem. Soc.* **1972**, *94*, 7132-7137; (c) E. J. Cragoe, O. W. Woltersdorf, N. P. Gould, A. M. Pietruszkiewicz, C. Ziegler, Y. Sakurai, G. E. Stokker, P. S. Anderson, R. S. Bourke, *J. Med. Chem.* **1986**, *29*, 825-841; (d) C. D. Dzierba, K. S. Zandi, T. Möllers, K. J. Shea, *J. Am. Chem. Soc.* **1996**, *118*, 4711-4712; (e) D. C. J. Waalboer, H. A. van Kalkeren, M. C. Schaapman, F. L. van Delft, F. P. J. T. Rutjes, *J. Org. Chem.* **2009**, *74*, 8878-8881; (f) A. B. Smith, H. Cui, *Org. Lett.* **2003**, *5*, 587-590; (g) S. P. Waters, Y. Tian, Y.-M. Li, S. J. Danishefsky, *J. Am. Chem. Soc.* **2005**, *127*, 13514-13515; (h) W.-P. Deng, M. Zhong, X.-C. Guo, A. S. Kende, *J. Org. Chem.*

2003, *68*, 7422-7427; (i) G. Stork, F. West, H. Y. Lee, R. C. A. Isaacs, S. Manabe, *J. Am. Chem. Soc.* **1996**, *118*, 10660-10661.

[11] (a) H. M. C. Ferraz, A. J. C. Souza, B. S. M. Tenius, G. G. Bianco, *Tetrahedron* **2006**, *62*, 9232-9236; (b) K. Ma, C. Zhang, M. Liu, Y. Chu, L. Zhou, C. Hu, D. Ye, *Tetrahedron Lett.* **2010**, *51*, 1870-1872; (c) S. Karimi, P. Tavares, *J. Nat. Prod.* **2003**, *66*, 520-523; (d) C. H. Heathcock, E. G. DelMar, S. L. Graham, *J. Am. Chem. Soc.* **1982**, *104*, 1907-1917.

[12] A. B. Smith, T. Sunazuka, T. L. Leenay, J. Kingery-Wood, *J. Am. Chem. Soc.* **1990**, *112*, 8197-8198.

[13] (a) R. E. Mewshaw, M. D. Taylor, A. B. Smith, *J. Org. Chem.* **1989**, *54*, 3449-3462; (b) S. Hanessian, N. Boyer, G. J. Reddy, B. Deschênes-Simard, *Org. Lett.* **2009**, *11*, 4640-4643; (c) X.-S. Peng, H. N. C. Wong, *Chem. Asian J.* **2006**, *1*, 111-120; (d) L. A. Paquette, T.-Z. Wang, C. M. G. Philippo, S. Wang, *J. Am. Chem. Soc.* **1994**, *116*, 3367-3374.

[14] (a) F. E. Ziegler, O. B. Wallace, *J. Org. Chem.* **1995**, *60*, 3626-3636; (b) S. J. Danishefsky, J. J. Masters, W. B. Young, J. T. Link, L. B. Snyder, T. V. Magee, D. K. Jung, R. C. A. Isaacs, W. G. Bornmann, C. A. Alaimo, C. A. Coburn, M. J. Di Grandi, *J. Am. Chem. Soc.* **1996**, *118*, 2843-2859; (c) H. M. Lee, C. Nieto-Oberhuber, M. D. Shair, *J. Am. Chem. Soc.* **2008**, *130*, 16864-16866.

[15] (a) G. Stork, A. Brizzolara, H. Landesman, J. Szmuszkovicz, R. Terrell, *J. Am. Chem. Soc.* **1963**, *85*, 207-222; (b) S. Bahmanyar, K. N. Houk, *J. Am. Chem. Soc.* **2001**, *123*, 11273-11283; (c) S. Bahmanyar, K. N. Houk, *J. Am. Chem. Soc.* **2001**, *123*, 12911-12912; (d) C. Allemann, R. Gordillo, F. R. Clemente, P. H.-Y. Cheong, K. N. Houk, *Acc. Chem. Res.* **2004**, *37*, 558-569.

[16] The Chemistry of Enamines; Rappoport, Z., Ed.; Wiley: New Y ork, 1994.

[17] D. Rajagopal, M. S. Moni, S. Subramanian, S. Swaminathan, *Tetrahedron: Asymmetry* **1999**, *10*, 1631-1634.

[18] (a) C. Agami, F. Meynier, C. Puchot, J. Guilhem, C. Pascard, *Tetrahedron* **1984**, *40*, 1031-1038; (b) C. Agami, C. Puchot, H. Sevestre, *Tetrahedron Lett.* **1986**, *27*, 1501-1504.

[19] (a) S. Bahmanyar, K. N. Houk, H. J. Martin, B. List, *J. Am. Chem. Soc.* **2003**, *125*, 2475-2479; (b) L. Hoang, S. Bahmanyar, K. N. Houk, B. List, *J. Am. Chem. Soc.* **2003**, *125*, 16-17.

[20] The Chemistry of Enamines; Rappoport, Z., Ed.; Wiley: New York, 1994

[21] (a) C. M. R. Volla, I. Atodiresei, M. Rueping, *Chem. Rev.* **2014**, *114*, 2390-2431; (b) V. D'Elia, H. Zwicknagl, O. Reiser, *J. Org. Chem.* **2008**, *73*, 3262-3265; (c) T. Wakabayashi, K. Watanabe, Y. Kato, *Synth. Commun.* **1977**, *7*, 239-244; (d) P. H.-Y. Cheong, K. N. Houk, J. S.

Warrier, S. Hanessian, *Adv. Synth. Catal.* **2004**, *346*, 1111-1115; (e) P. H.-Y. Cheong, K. N. Houk, *Synthesis* **2005**, 1533-1537.

[22] (a) N. Harada, T. Sugioka, H. Uda, T. Kuriki, *Synthesis* **1990**, 53-56; (b) L. F. Tietze, J. Utecht, *Synthesis* **1993**, 957-958; (c) H. Hioki, T. Hashimoto, M. Kodama, *Tetrahedron: Asymmetry* **2000**, *11*, 829-834; (d) K.-i. Fuhshuku, N. Funa, T. Akeboshi, H. Ohta, H. Hosomi, S. Ohba, T. Sugai, *J. Org. Chem.* **2000**, *65*, 129-135; (e) K.-i. Fuhshuku, M. Tomita, T. Sugai, *Adv. Synth. Catal.* **2003**, *345*, 766-774; (f) Y. Kasai, K. Shimanuki, S. Kuwahara, M. Watanabe, N. Harada, *Chirality* **2006**, *18*, 177-187.

[23] J. Gutzwiller, P. Buchschacher, A. Fürst, *Synthesis* **1977**, 167-168.

[24] G. Zhong, T. Hoffmann, R. A. Lerner, S. Danishefsky, C. F. Barbas, *J. Am. Chem. Soc.* **1997**, *119*, 8131-8132.

[25] (a) S. G. Davies, R. L. Sheppard, A. D. Smith, J. E. Thomson, *Chem. Commun.* **2005**, 3802-3804; (b) S. G. Davies, A. J. Russell, R. L. Sheppard, A. D. Smith, J. E. Thomson, *Org. Biomol. Chem.* **2007**, *5*, 3190-3200.

[26] E. Lacoste, E. Vaique, M. Berlande, I. Pianet, J.-M. Vincent, Y. Landais, *Eur. J. Org. Chem.* **2007**, 167-177.

[27] Akahane, Y.; Inage, N.; Nagamine, T.; Inomata, K.; Endo, Y. Heterocycles 2007, 74, 637.

[28] T. Bui, C. F. Barbas, *Tetrahedron Lett.* **2000**, *41*, 6951-6954.

[29] G. Guillena, C. Nájera, S. F. Viózquez, *Synlett* **2008**, 3031-3035.

[30] D. Almaşi, D. A. Alonso, C. Nájera, *Adv. Synth. Catal.* **2008**, *350*, 2467-2472.

[31] Á. L. F. de Arriba, L. Simón, C. Raposo, V. Alcázar, J. R. Morán, *Tetrahedron* **2009**, *65*, 4841-4845.

[32] (a) Akahane, Y .; Inomata, K.; Endo, Y . Heterocycles 2009, 77, 1065. (b) Akahane, Y .; Inomata, K.; Endo, Y . Heterocycles 2011, 82, 1727.

[33] X.-M. Zhang, M. Wang, Y.-Q. Tu, C.-A. Fan, Y.-J. Jiang, S.-Y. Zhang, F.-M. Zhang, *Synlett* **2008**, 2831-2835.

[34] Á. L. Fuentes de Arriba, D. G. Seisdedos, L. Simón, V. Alcázar, C. Raposo, J. R. Morán, *J. Org. Chem.* **2010**, *75*, 8303-8306.

[35] X.-P. Zeng, Z.-Y. Cao, Y.-H. Wang, F. Zhou, J. Zhou, *Chem. Rev.* **2016**, *116*, 7330-7396.

[36] C. H. Heathcock, J. E. Ellis, J. E. McMurry, A. Coppolino, *Tetrahedron Lett.* **1971**, *12*, 4995-4996.

[37] E. B. Rowland, G. B. Rowland, E. Rivera-Otero, J. C. Antilla, *J. Am. Chem. Soc.* **2007**, *129*, 12084-12085.

[38] (a) T. Kanger, K. Kriis, M. Laars, T. Kailas, A.-M. Müürisepp, T. Pehk, M. Lopp, *J. Org. Chem.* **2007**, *72*, 5168-5173; (b) M. Laars, K. Kriis, T. Kailas, A.-M. Müürisepp, T. Pehk, T. Kanger, M. Lopp, *Tetrahedron: Asymmetry* **2008**, *19*, 641-645.

[39] (a) A. Monge-Marcet, R. Pleixats, X. Cattoen, M. W. C. Man, D. A. Alonso, C. Najerá, *New J. Chem.* **2011**, *35*, 2766-2772; (b) A. Monge-Marcet, X. Cattoen, D. A. Alonso, C. Najera, M. W. C. Man, R. Pleixats, *Green Chem.* **2012**, *14*, 1601-1610; (c) R. Pedrosa, J. M. Andrés, R. Manzano, C. Pérez-López, *Tetrahedron Lett.* **2013**, *54*, 3101-3104.

[40] M. Benaglia, M. Cinquini, F. Cozzi, A. Puglisi, G. Celentano, *Adv. Synth. Catal.* **2002**, *344*, 533-542.

[41] A. Bañón-Caballero, G. Guillena, C. Nájera, E. Faggi, R. M. Sebastián, A. Vallribera, *Tetrahedron* **2013**, *69*, 1307-1315.

[42] G. Guillena, M. d. C. Hita, C. Nájera, S. F. Viózquez, *J. Org. Chem.* **2008**, *73*, 5933-5943.

[43] S. Cañellas, C. Ayats, A. H. Henseler, M. A. Pericàs, *ACS Catalysis* **2017**, *7*, 1383-1391.

[44] K. Mori, T. Katoh, T. Suzuki, T. Noji, M. Yamanaka, T. Akiyama, *Angewandte Chemie International Edition* **2009**, *48*, 9652-9654.

[45] S. Takano, C. Kasahara, K. Ogasawara, *J. Chem. Soc., Chem. Commun.* **1981**, 635-637.

UNIVERSITAT ROVIRA I VIRGILI
IMMOBILIZATION OF CHIRAL BRØNSTED ACIDS AND LEWIS BASES FOR BATCH AND FLOW ENANTIOSELECTIVE CATALYSIS
Lidia Clot Almenara

4.7. ^{1}H and ^{13}C NMR Spectra

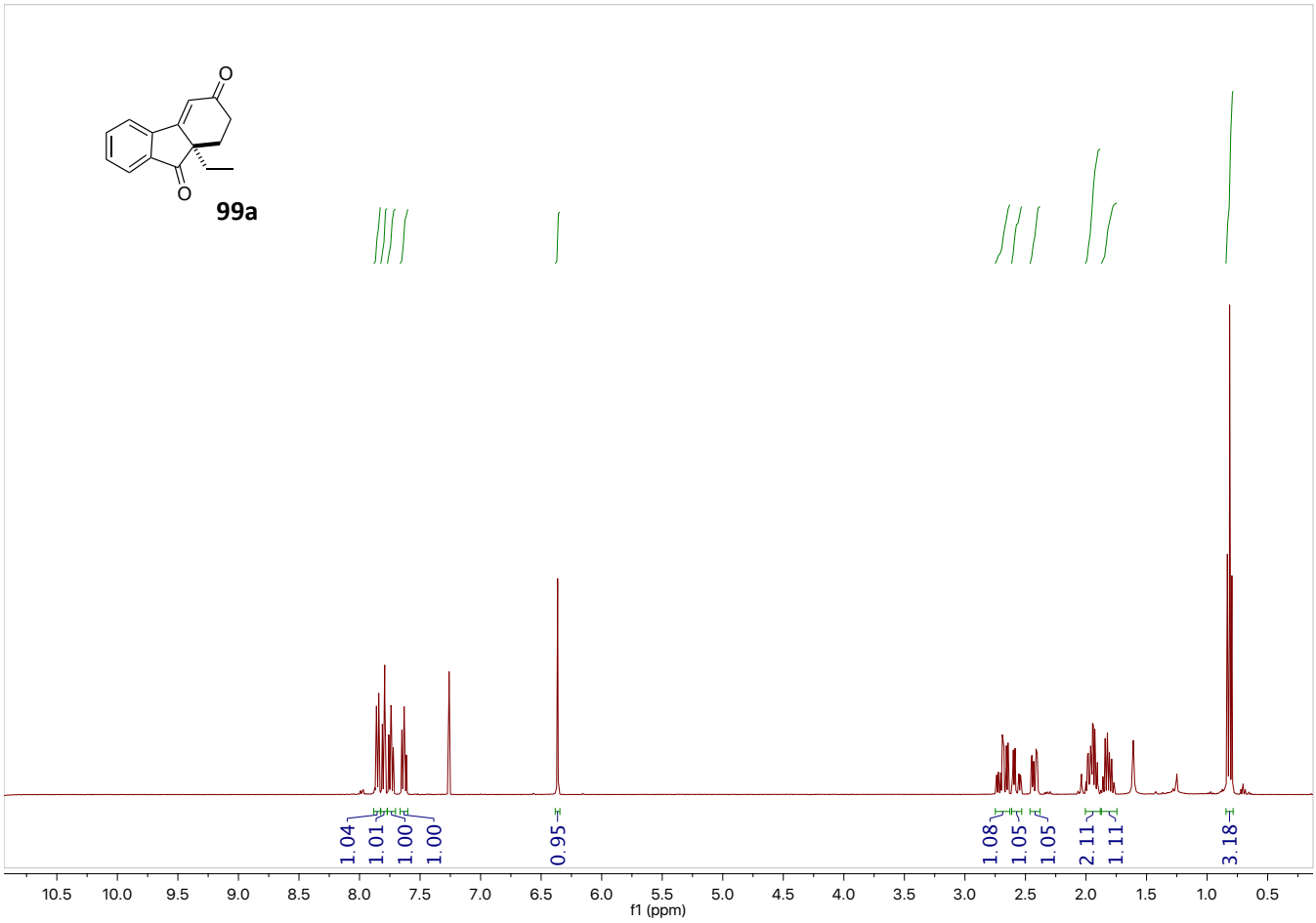

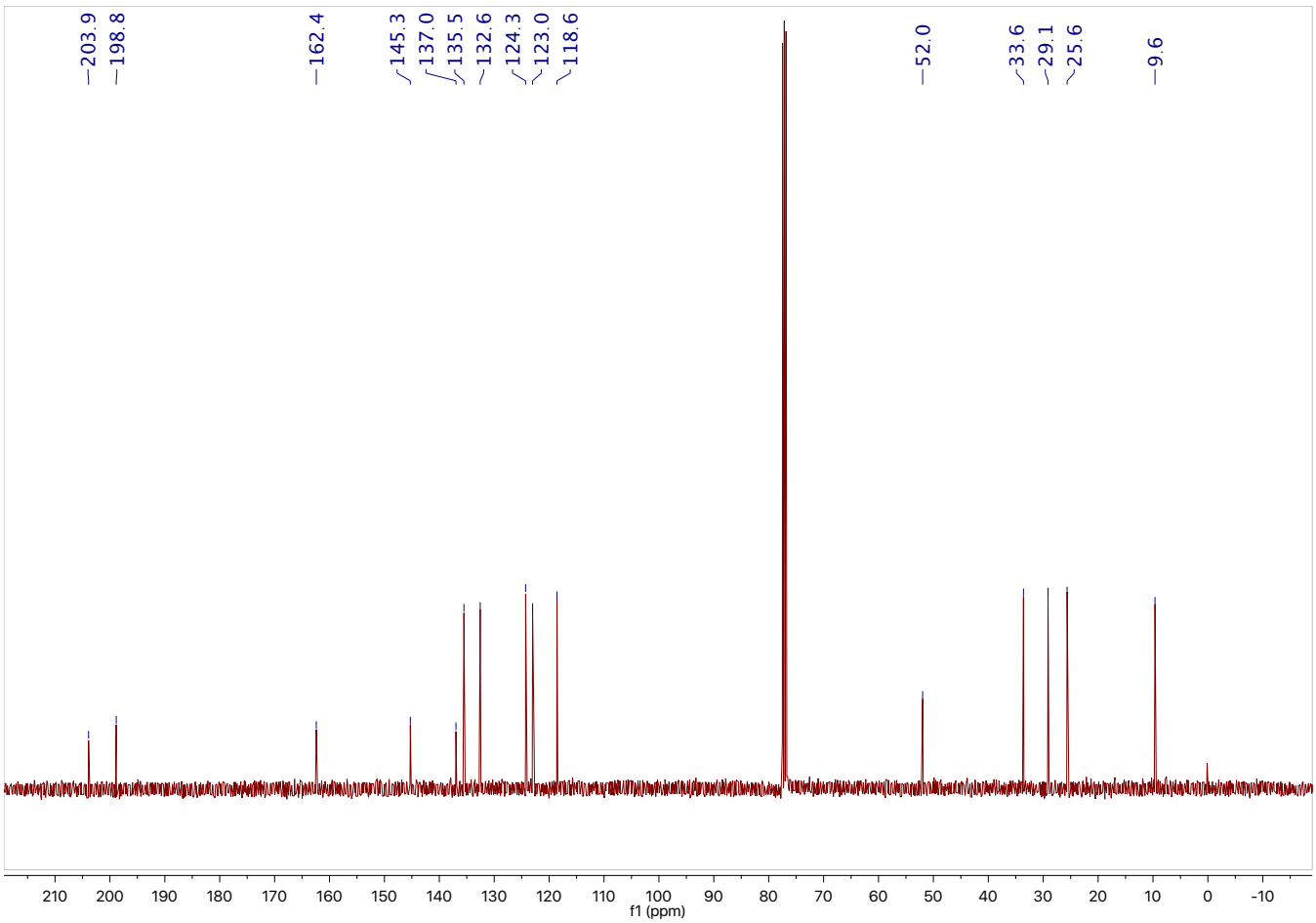

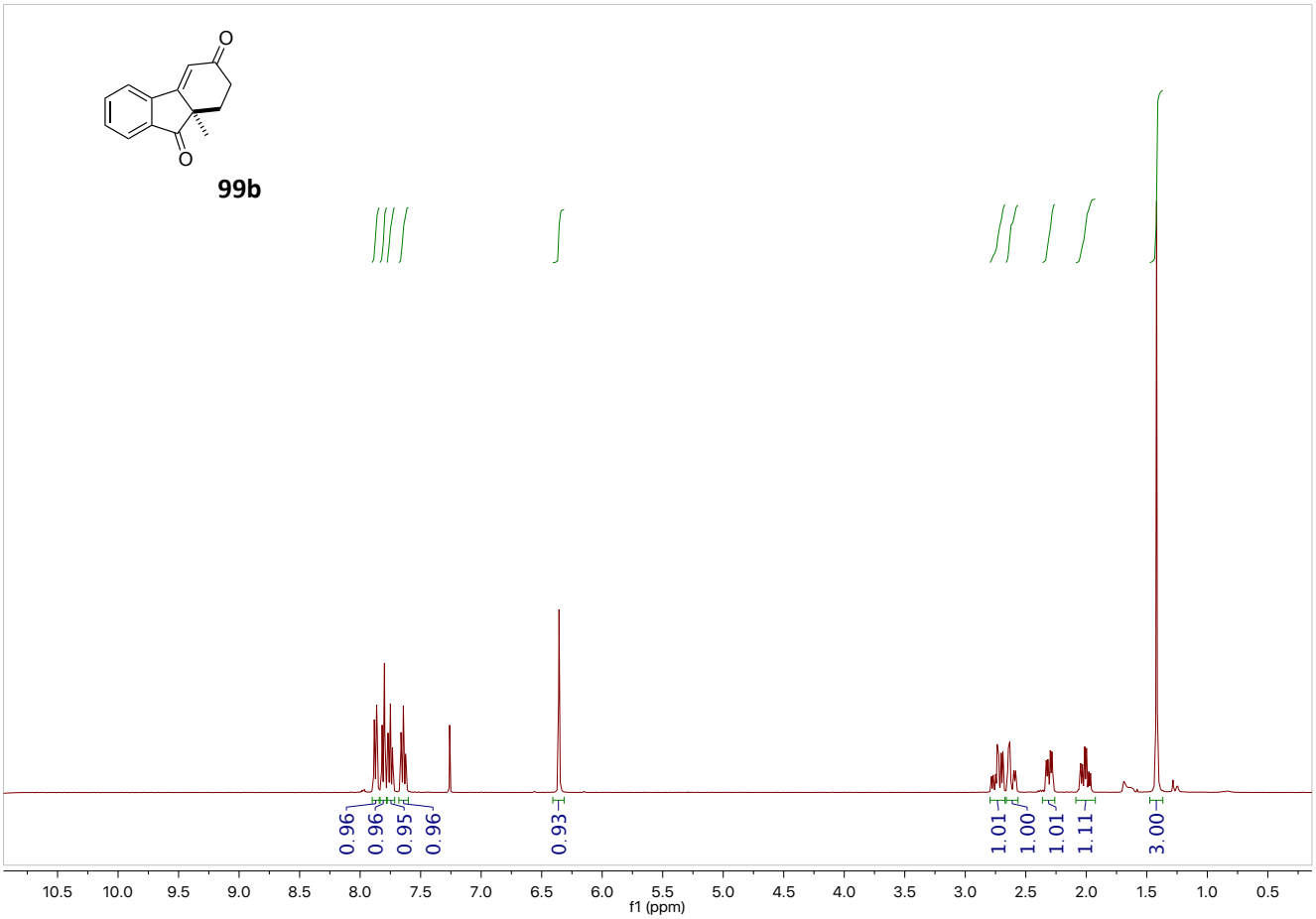
99b
0.96
0.96
0.95
0.96
0.93
1.01
1.00
1.01
1.11
3.00
f1 (ppm)

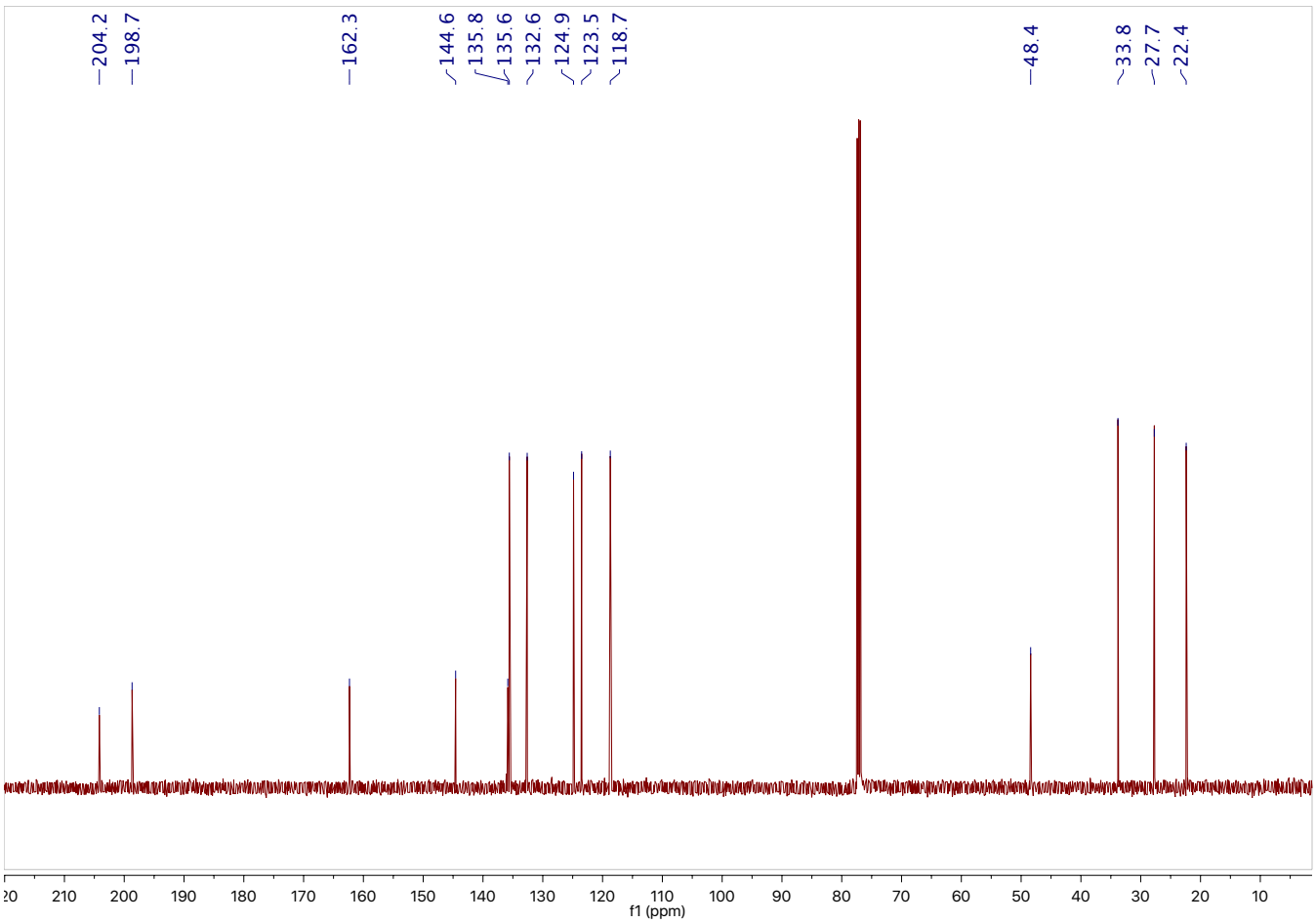
204.2
198.7
162.3
144.6
135.8
135.6
132.6
124.9
123.5
118.7
48.4
33.8
27.7
22.4
f1 (ppm)

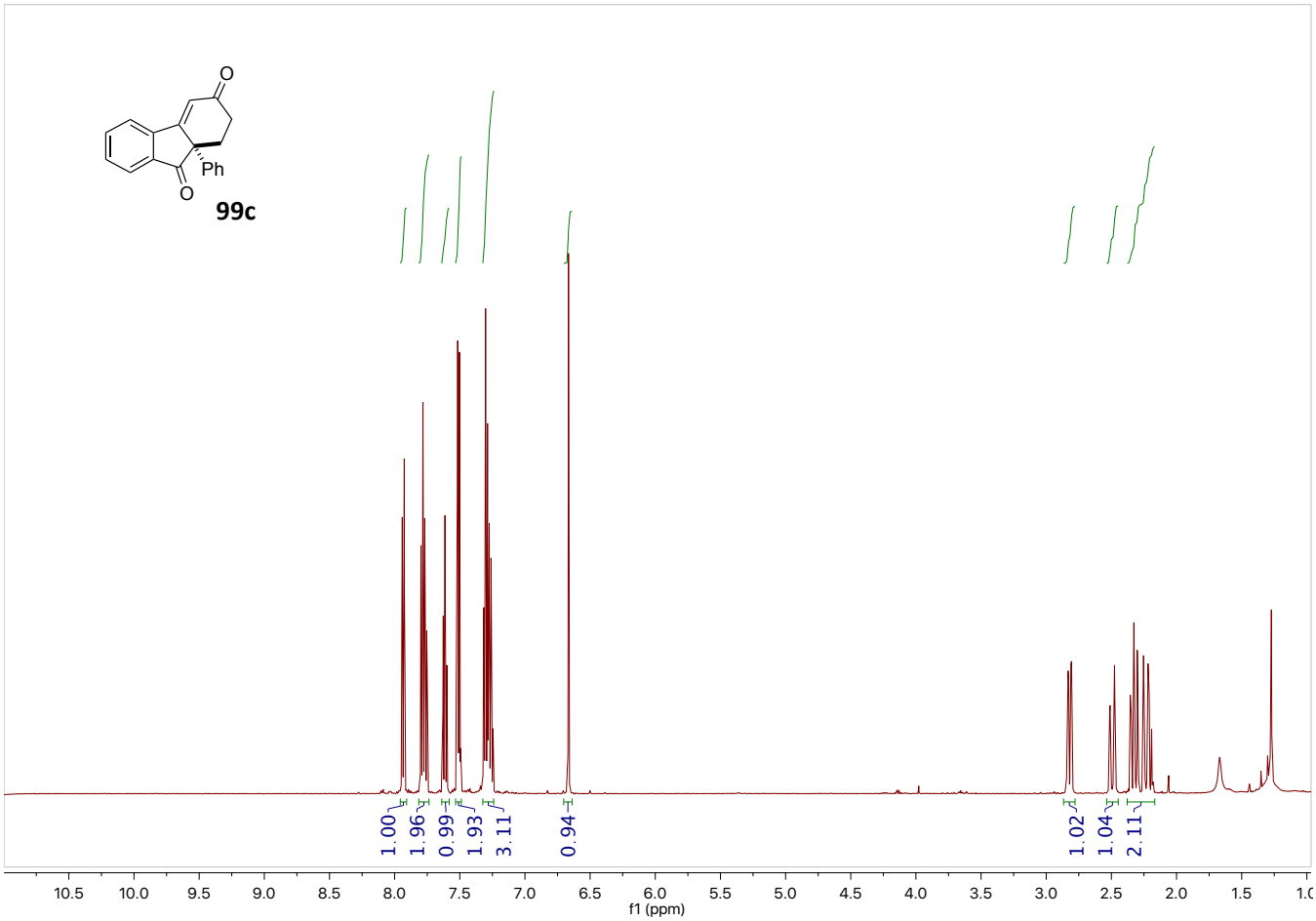
O
Ph
O
99c
1.00
1.96
0.99
1.93
3.11
0.94
1.02
1.04
2.11
f1 (ppm)

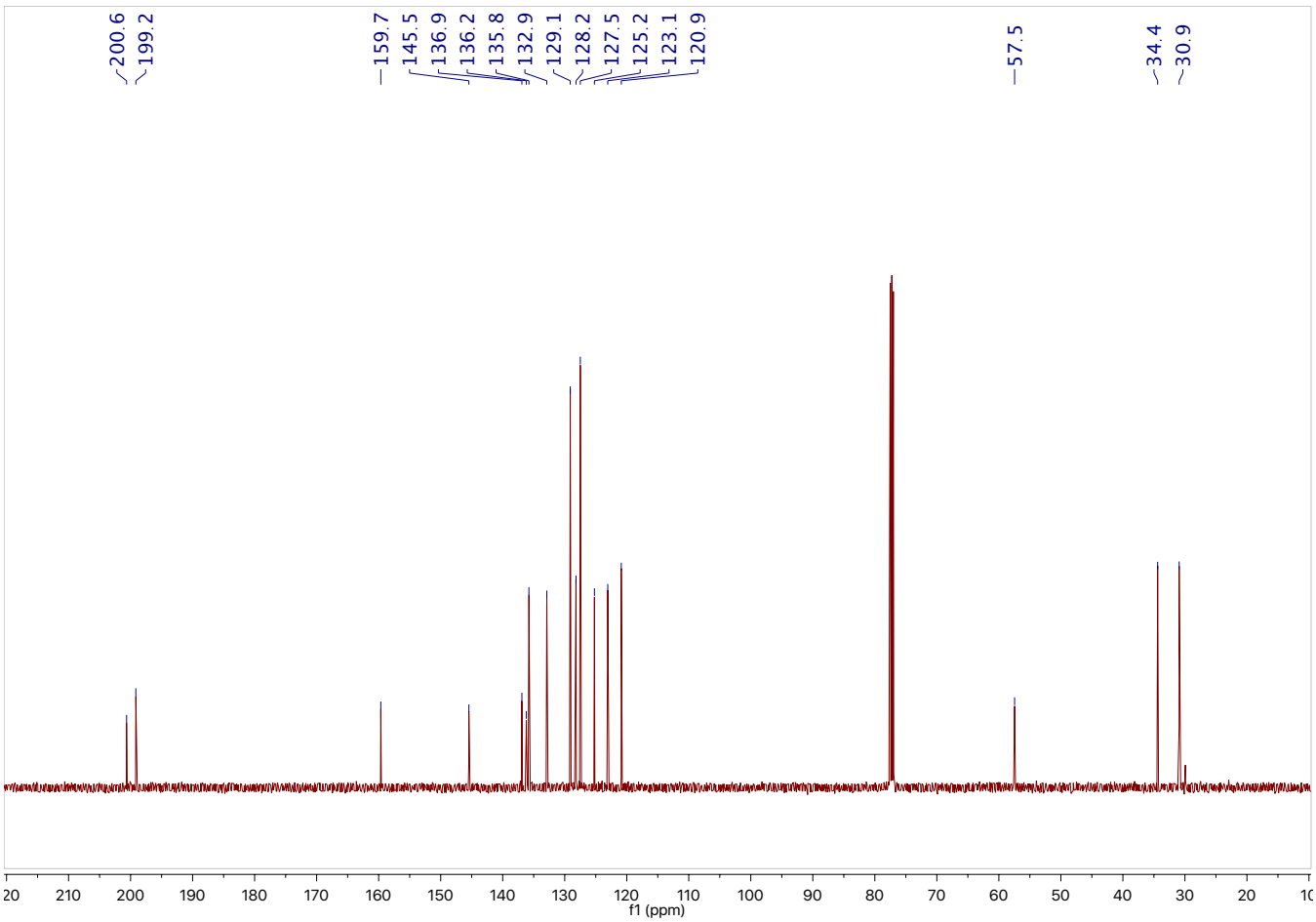
200.6
199.2
159.7
145.5
136.9
136.2
135.8
132.9
129.1
128.2
127.5
125.2
123.1
120.9
57.5
34.4
30.9
f1 (ppm)

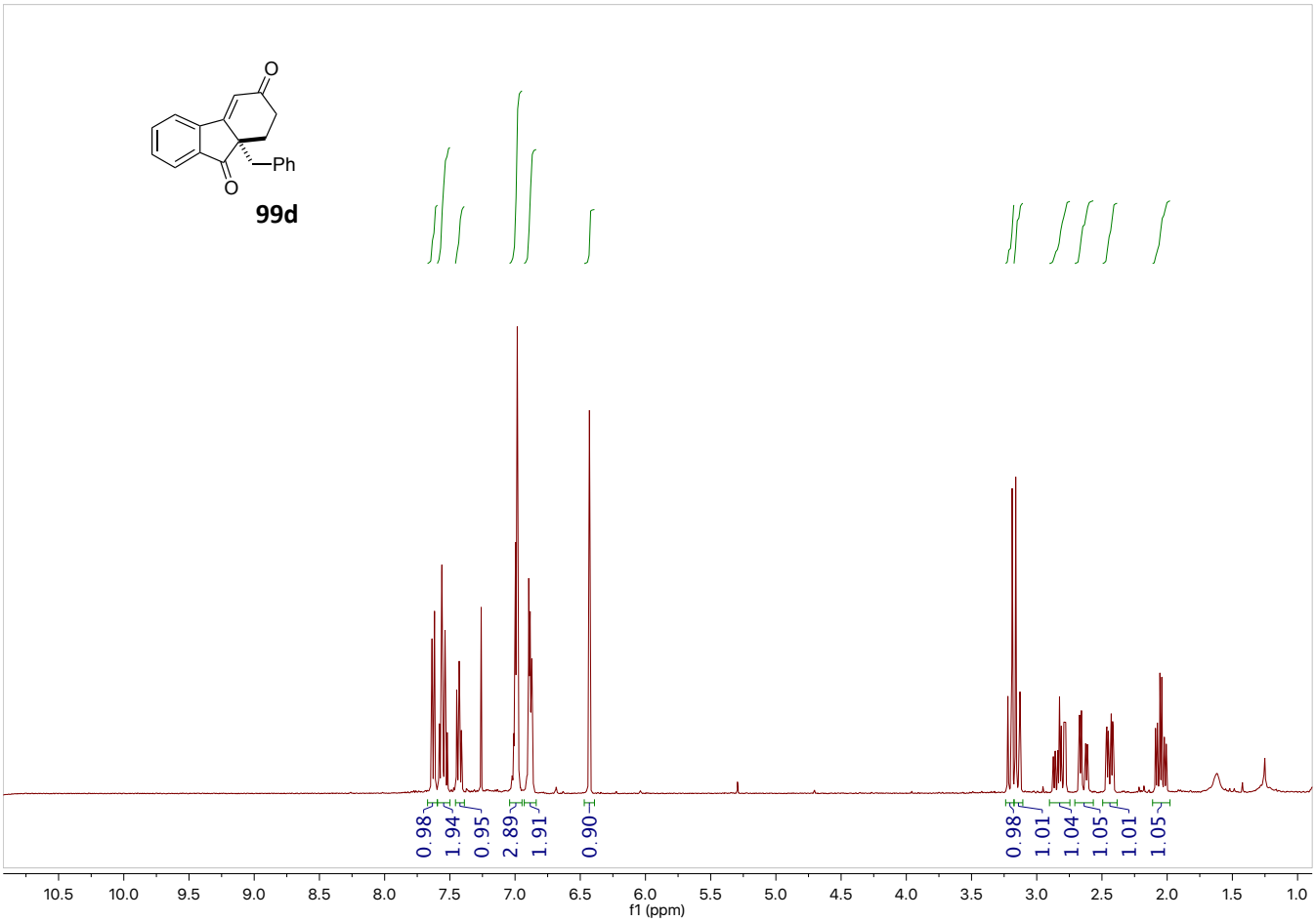
O
Ph
O
99d
0.98
1.94
0.95
2.89
1.91
0.90
0.98
1.01
1.04
1.05
1.01
1.05
f1 (ppm)

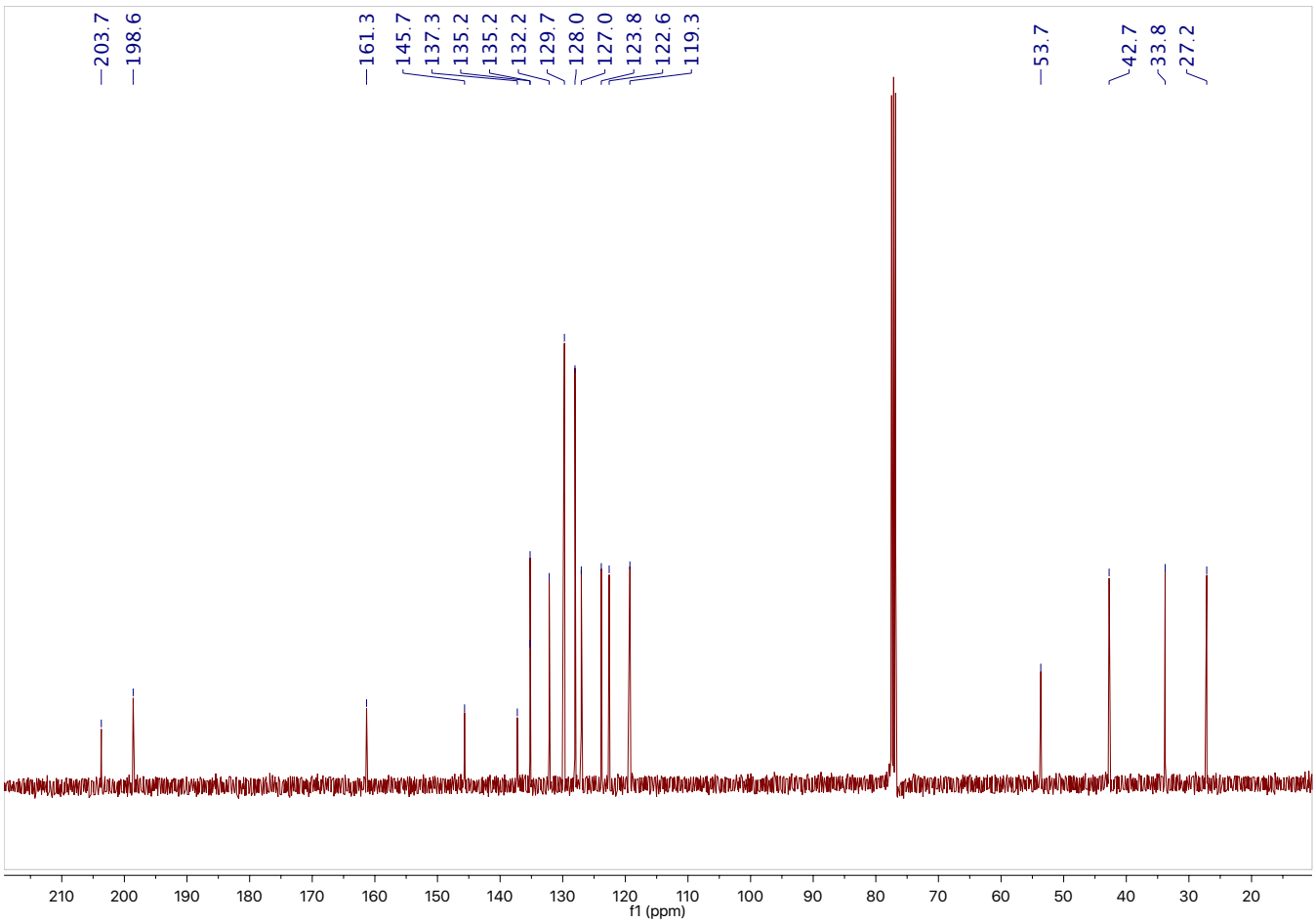
203.7
198.6
161.3
145.7
137.3
135.2
135.2
132.2
129.7
128.0
127.0
123.8
122.6
119.3
53.7
42.7
33.8
27.2
f1 (ppm)

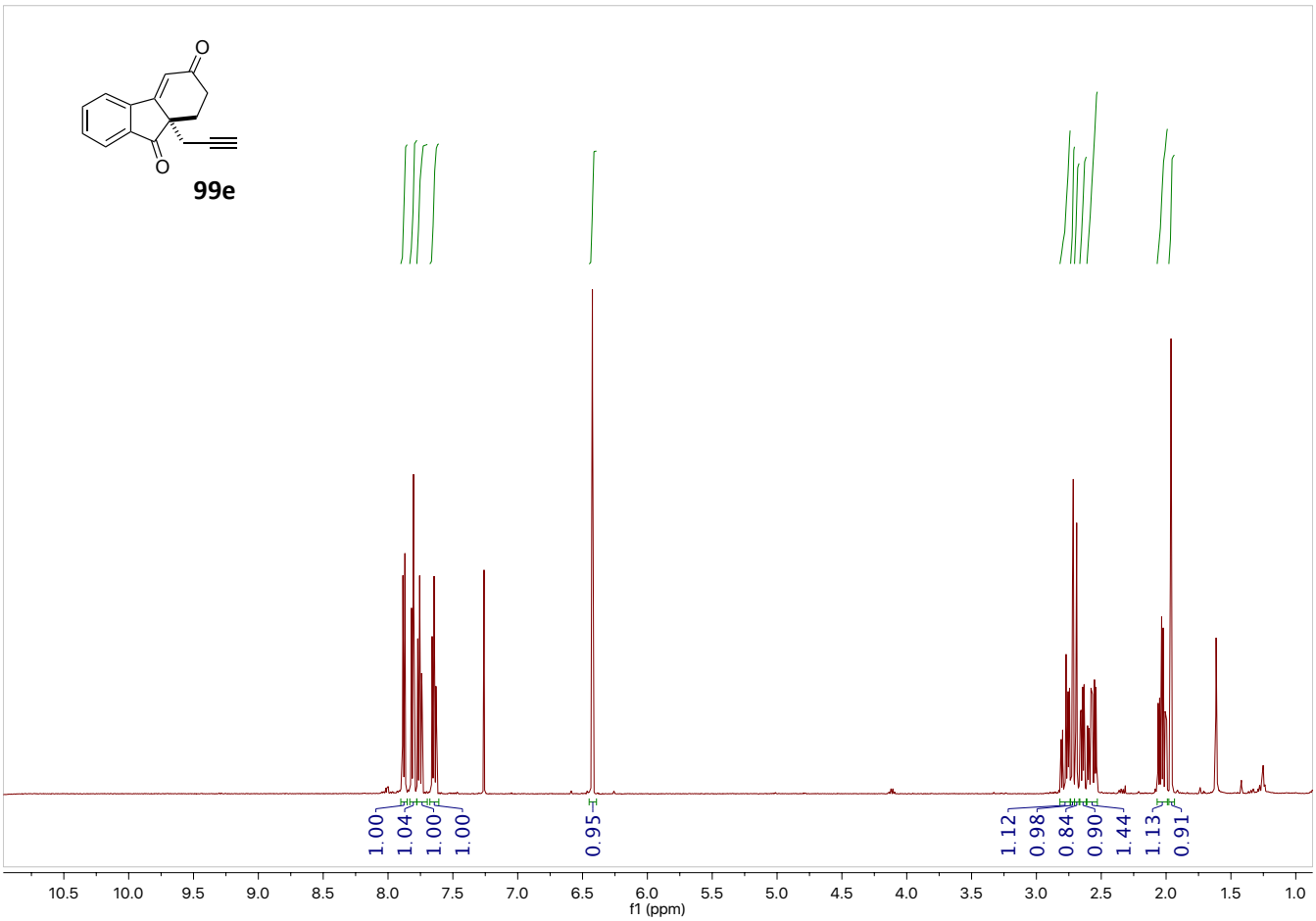
99e
1.00
1.04
1.00
1.00
0.95
1.12
0.98
0.84
0.90
1.44
1.13
0.91
f1 (ppm)

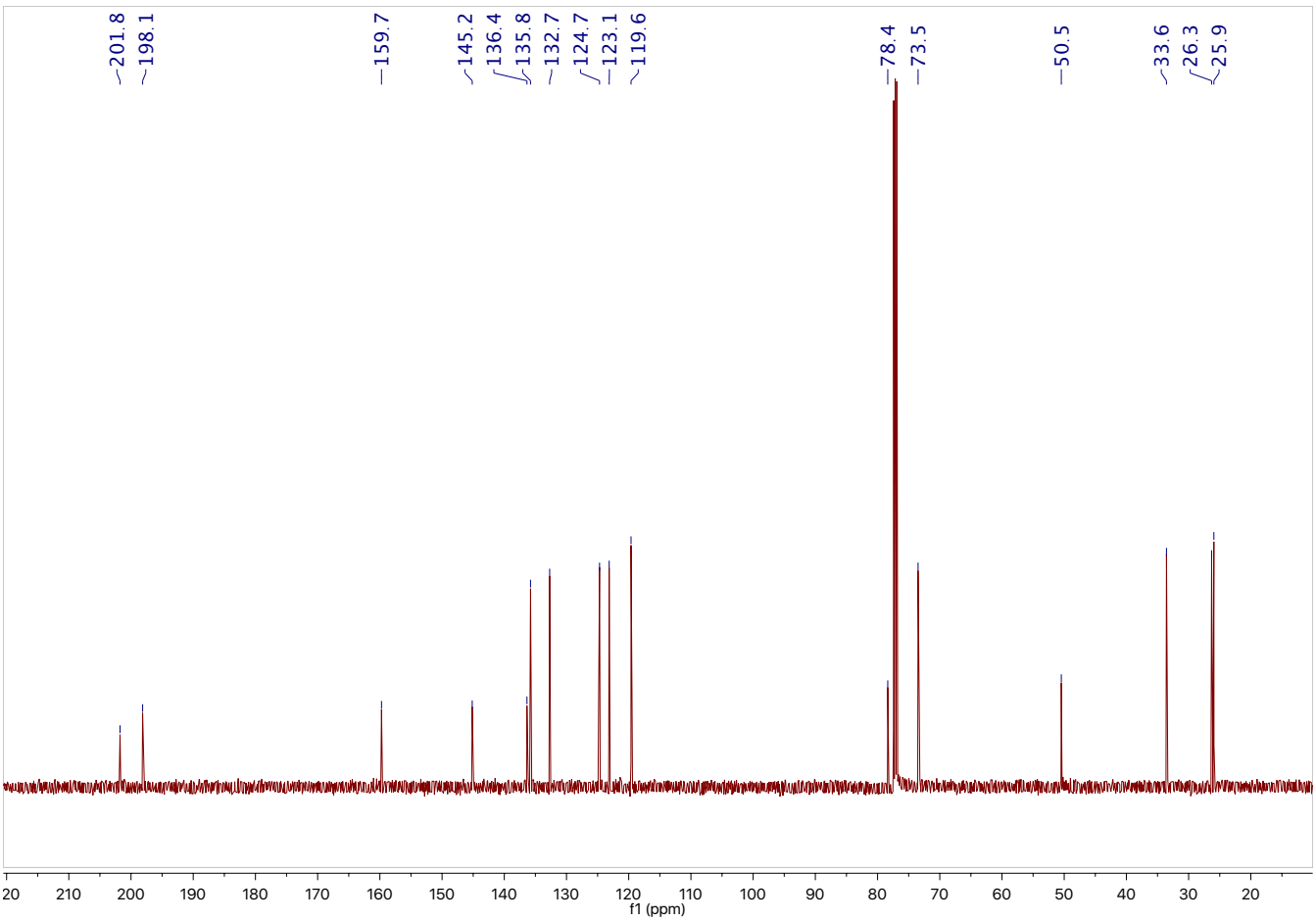
201.8
198.1
159.7
145.2
136.4
135.8
132.7
124.7
123.1
119.6
78.4
73.5
50.5
33.6
26.3
25.9
f1 (ppm)

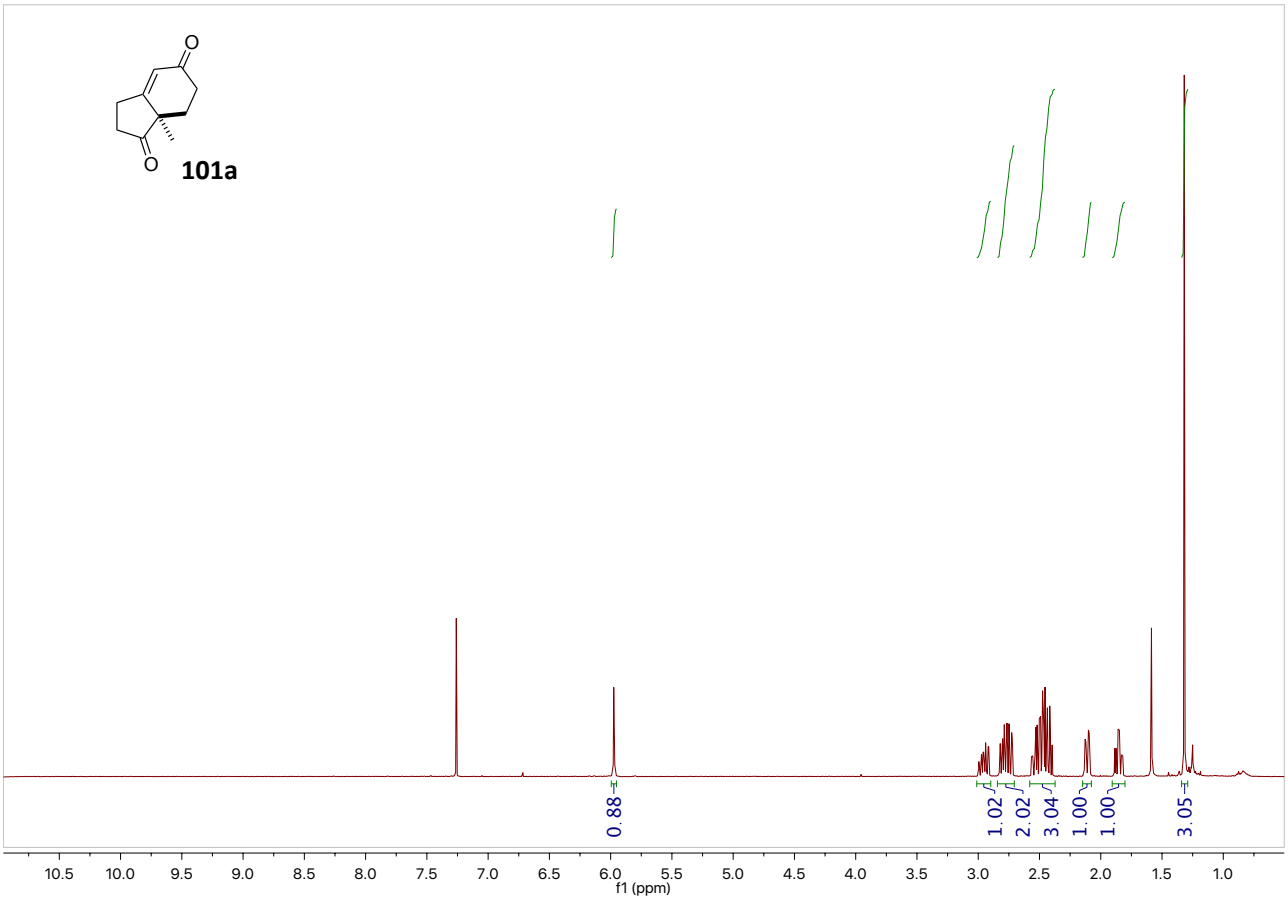
101a
0.88
1.02
2.02
3.04
1.00
1.00
3.05
f1 (ppm)

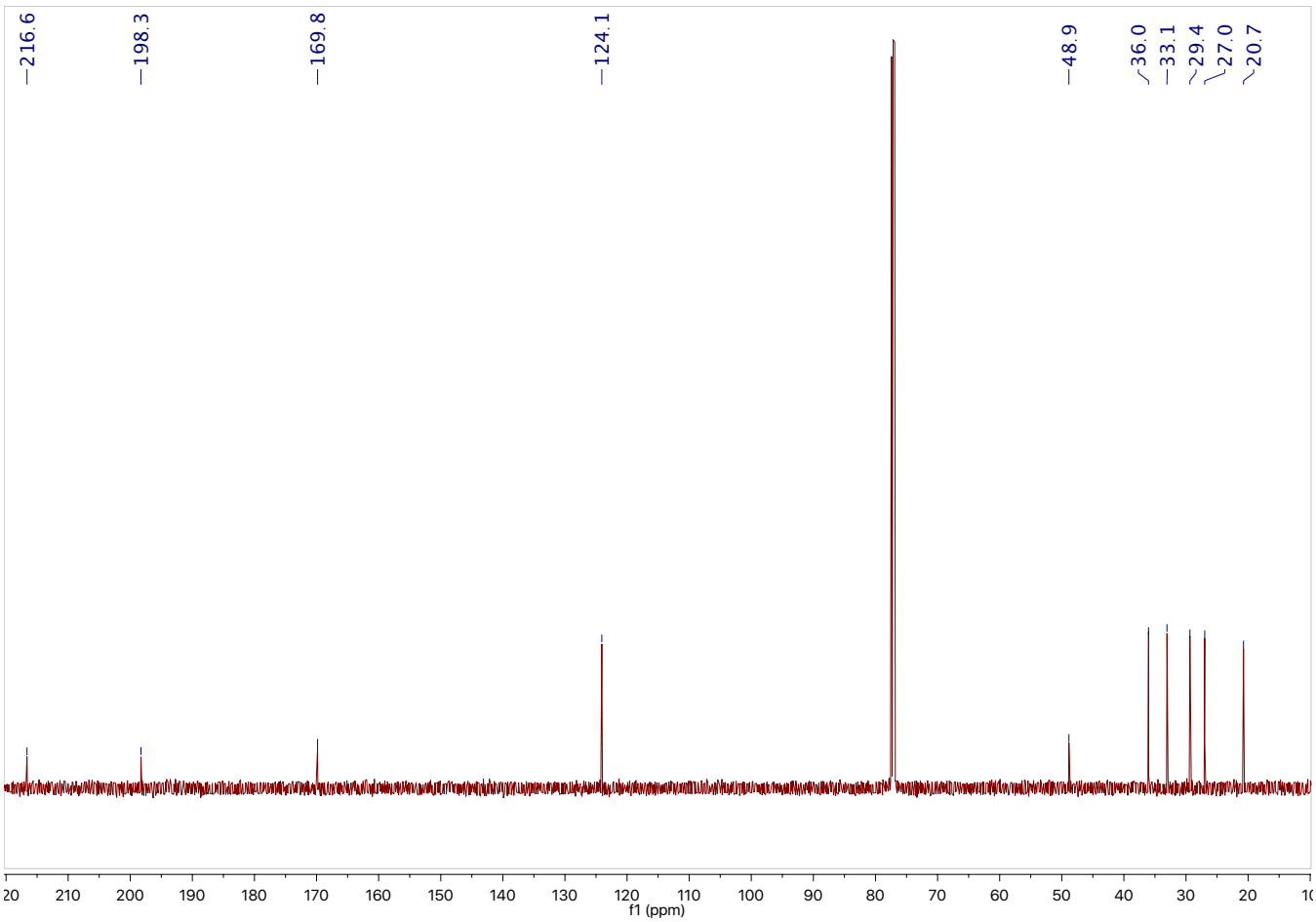
216.6
198.3
169.8
124.1
48.9
36.0
33.1
29.4
27.0
20.7
f1 (ppm)

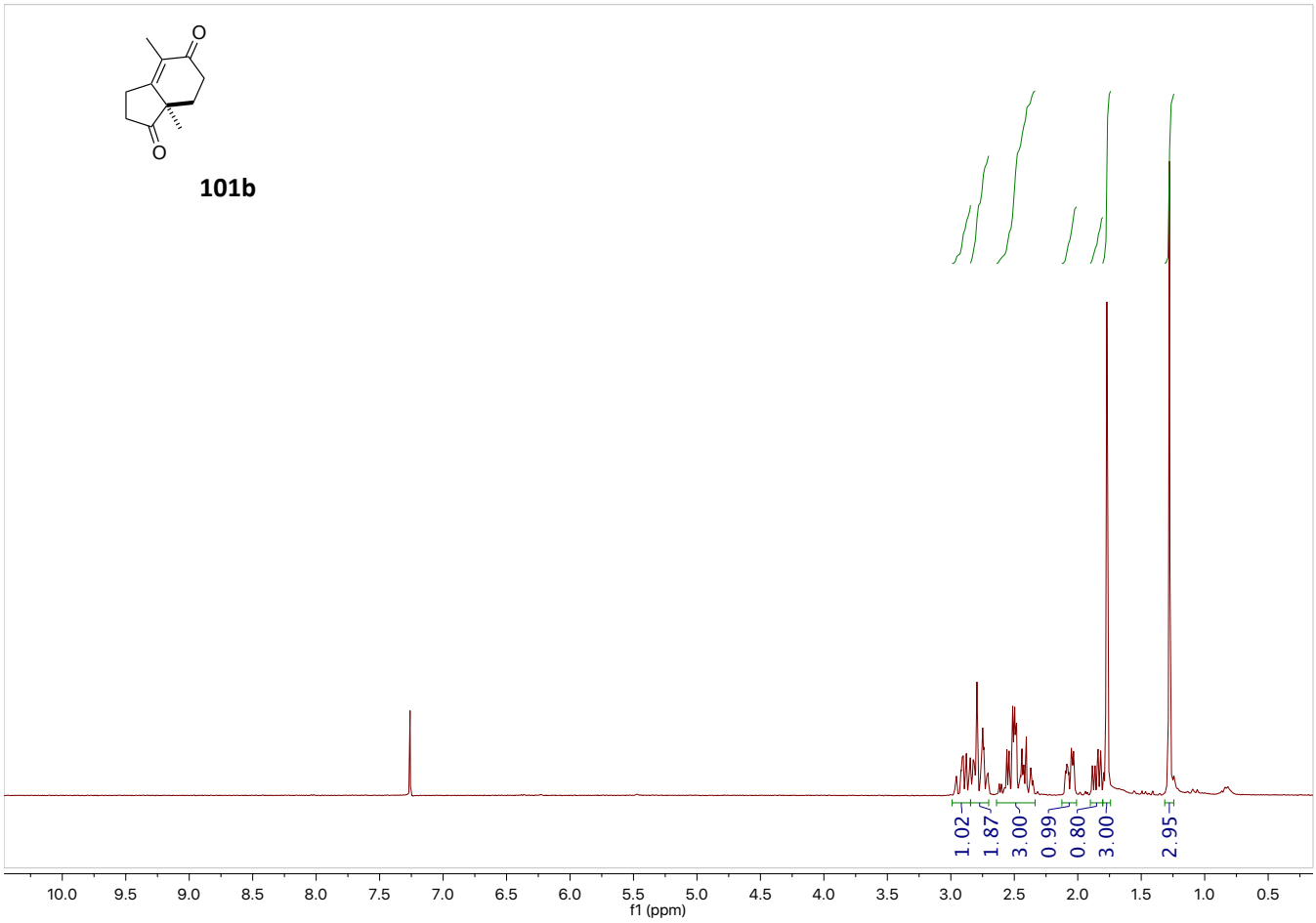
101b
1.02
1.87
3.00
0.99
0.80
3.00
2.95
f1 (ppm)

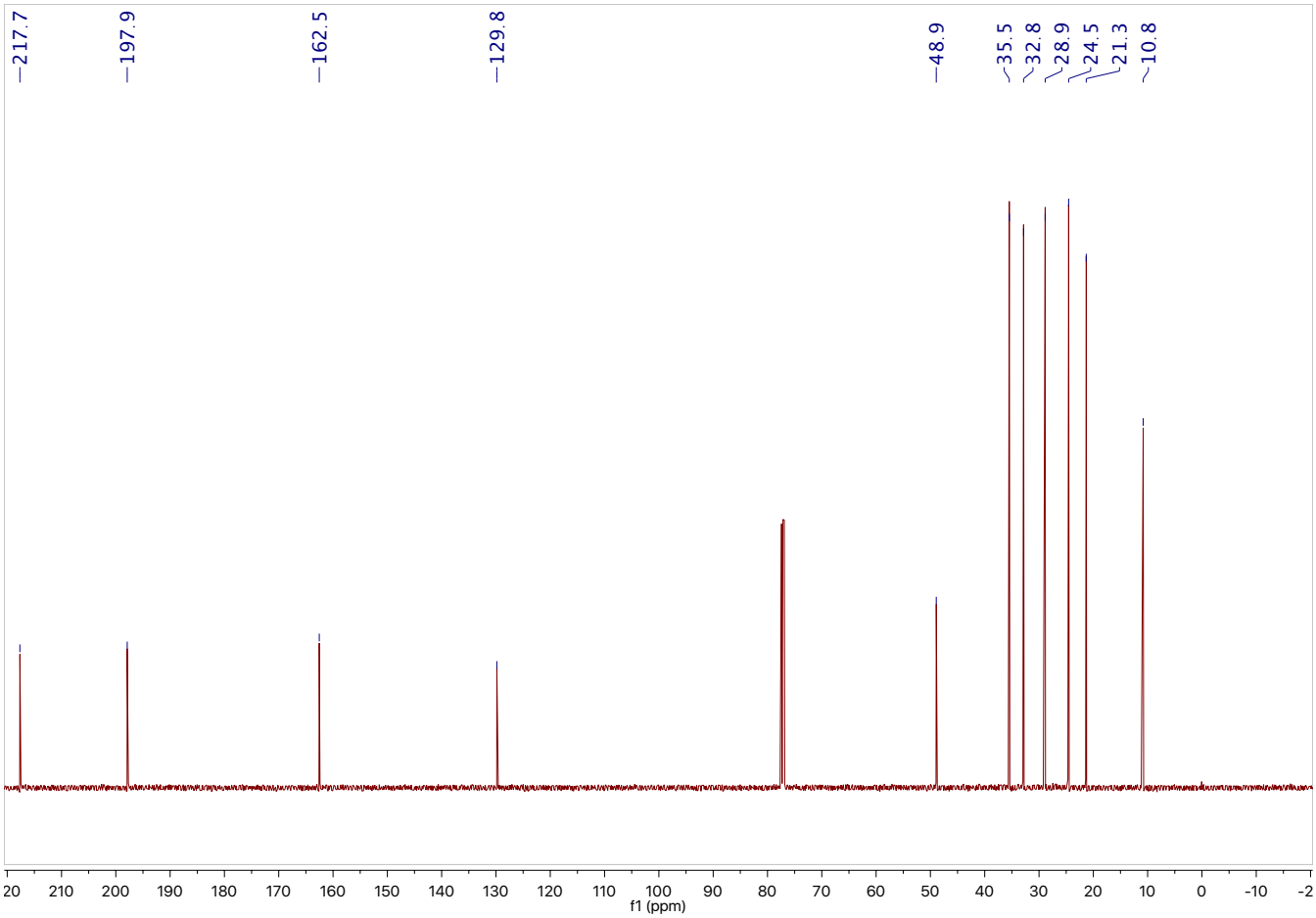
217.7
197.9
162.5
129.8
48.9
35.5
32.8
28.9
24.5
21.3
10.8
f1 (ppm)

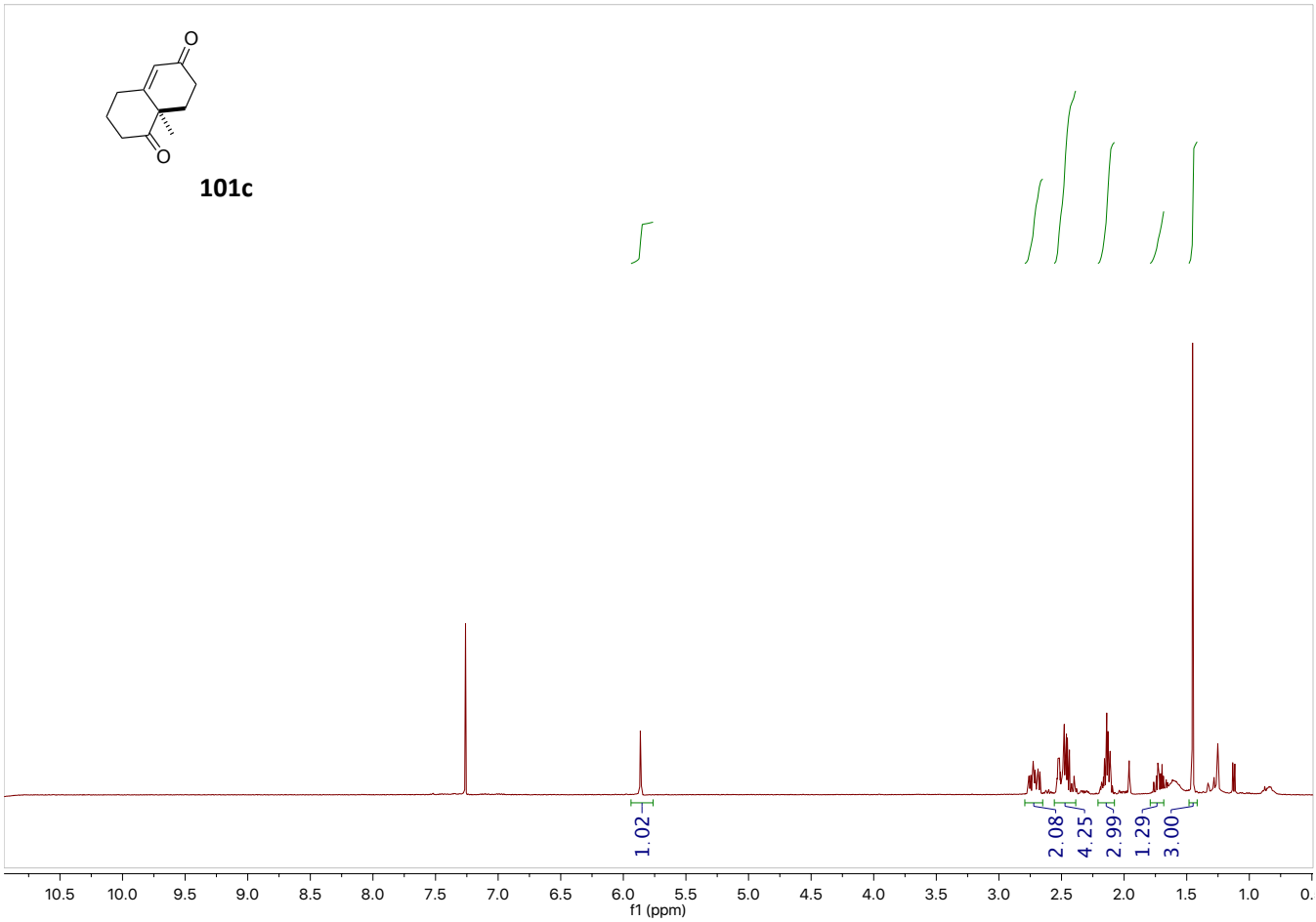
101c
1.02
2.08
4.25
2.99
1.29
3.00
f1 (ppm)

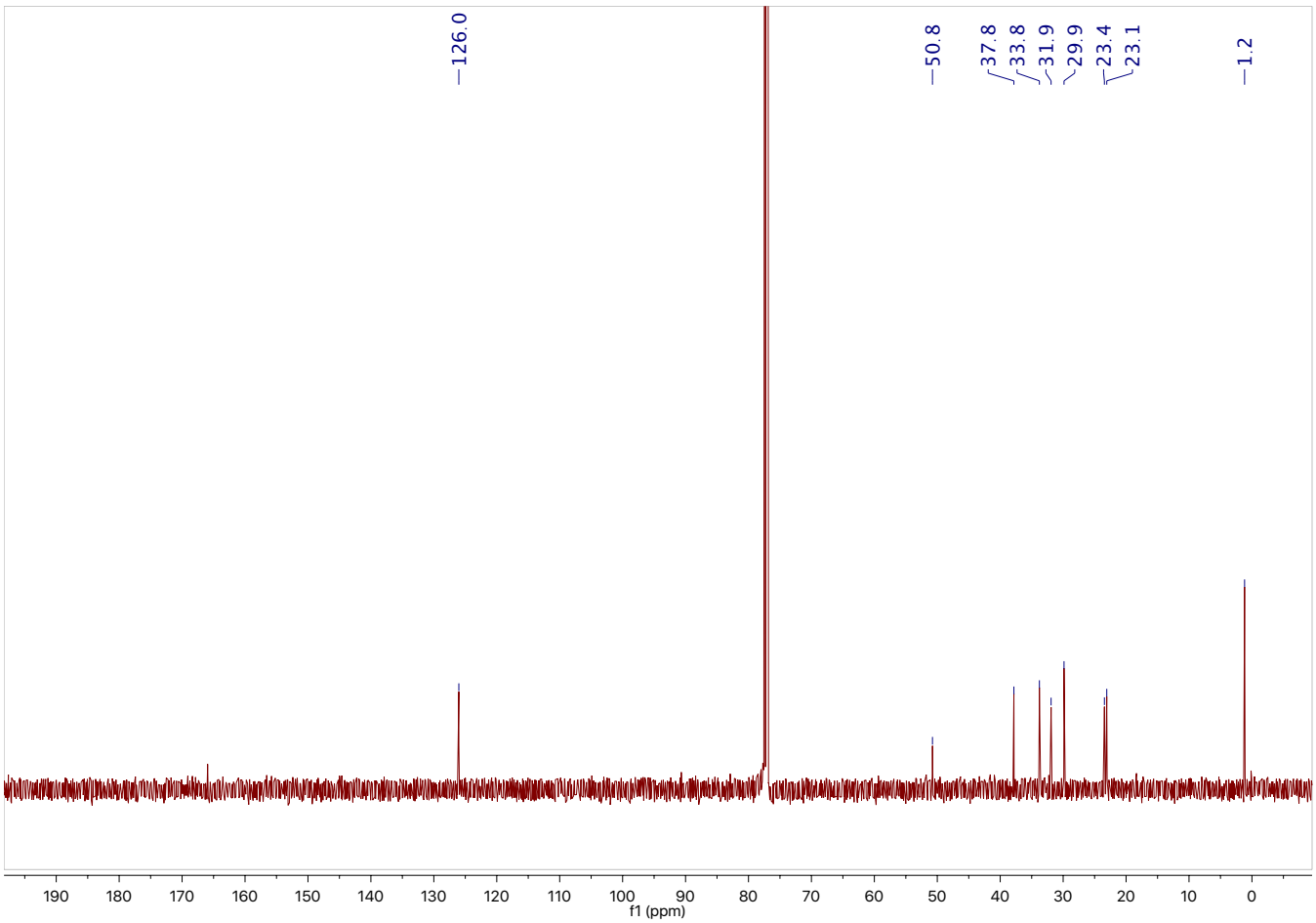
126.0
50.8
37.8
33.8
31.9
29.9
23.4
23.1
1.2
f1 (ppm)

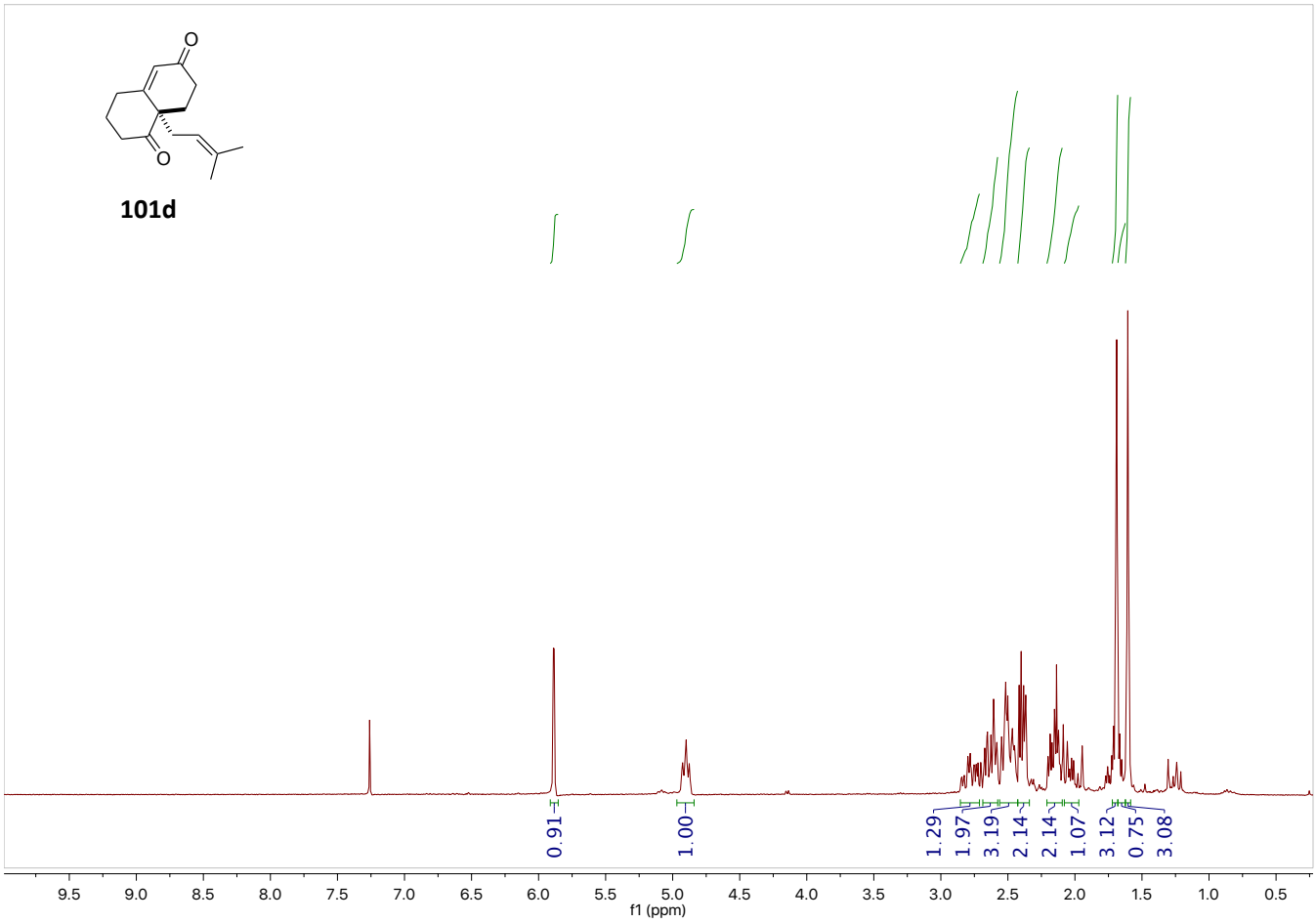
O
O
101d
0.91
1.00
1.29
1.97
3.19
2.14
2.14
1.07
3.12
0.75
3.08
f1 (ppm)

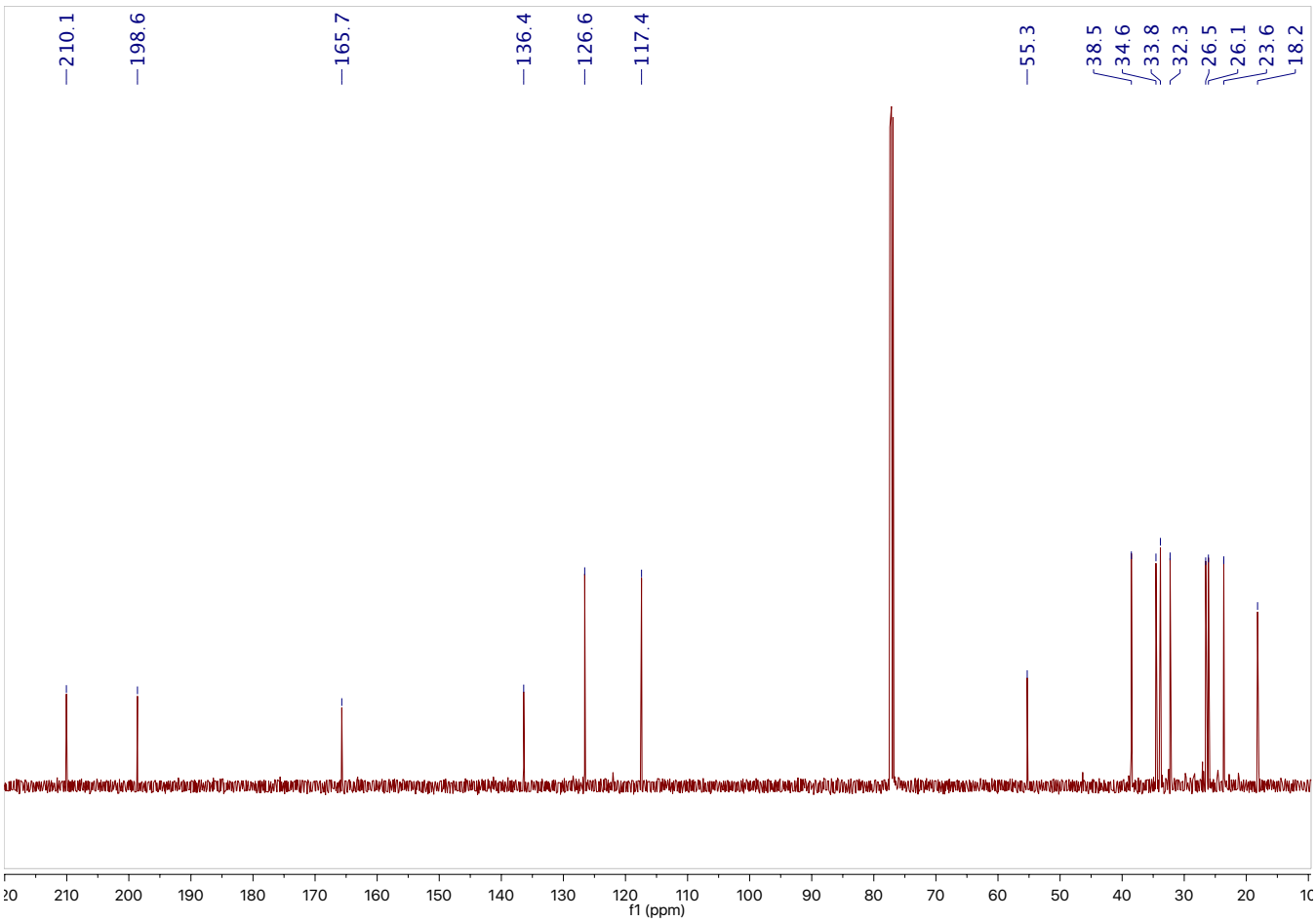
210.1
198.6
165.7
136.4
126.6
117.4
55.3
38.5
34.6
33.8
32.3
26.5
26.1
23.6
18.2
f1 (ppm)

4.8. HPLC, GC and SFC Chromatograms

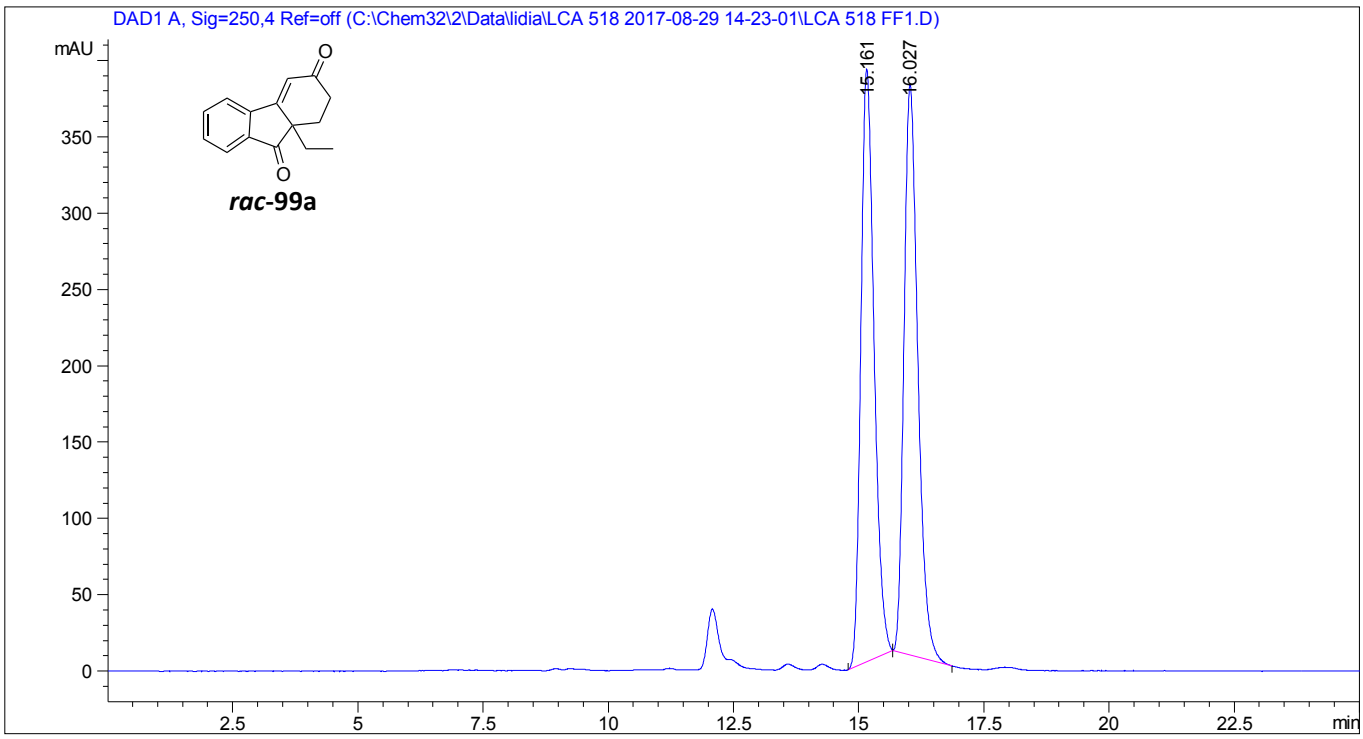

Peak #	Ret Time [min]	Type	Width [min]	Area [mAU*s]	Height [mAU]	Area %
1	15.161	BB	0.2818	7112.54199	388.14499	49.8096
2	16.027	BB	0.2960	7166.90527	373.32489	50.1904

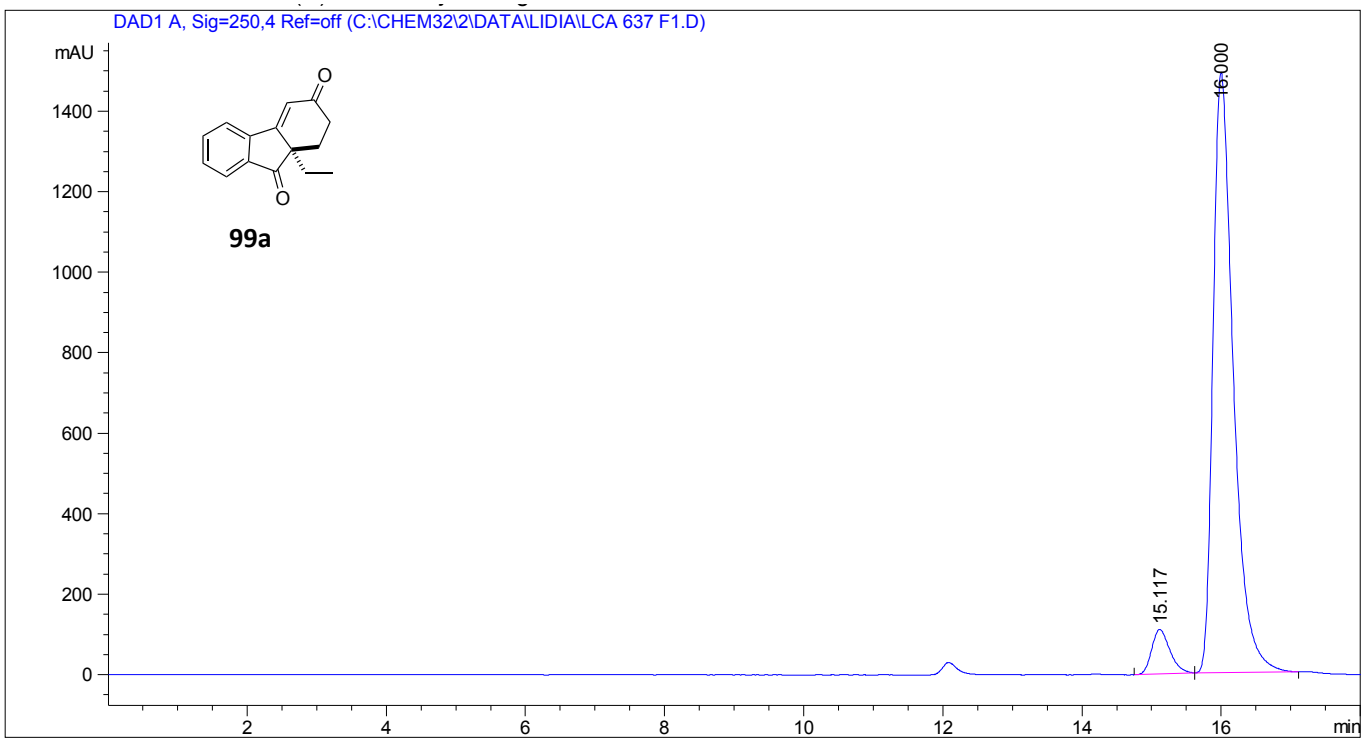

Peak #	Ret Time [min]	Type	Width [min]	Area [mAU*s]	Height [mAU]	Area %
1	15.117	BB	0.2758	2008.65942	110.65137	6.2453
2	16.000	BB	0.3059	3.01543e4	1491.04443	93.7547

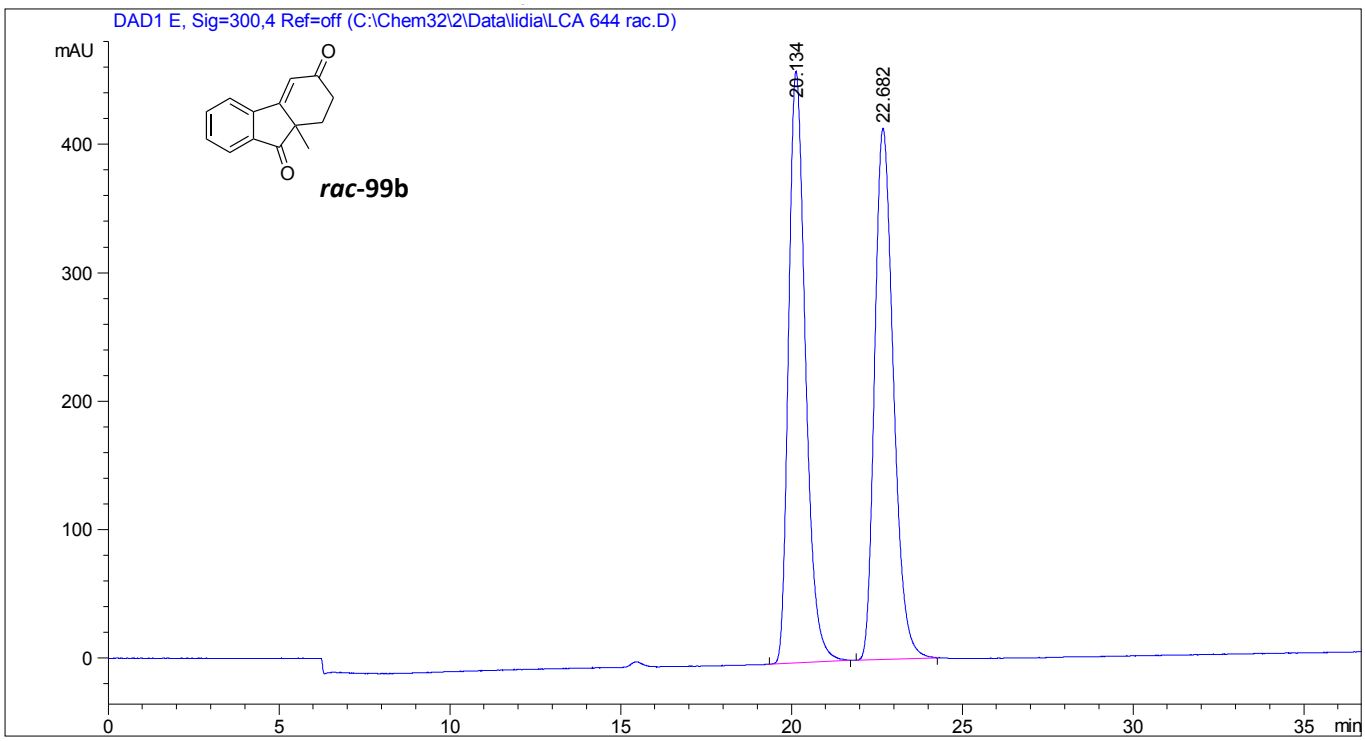

Peak #	Ret Time [min]	Type	Width [min]	Area [mAU*s]	Height [mAU]	Area %
1	20.134	BB	0.5327	1.58197e4	460.61551	50.0556
2	22.682	BB	0.5912	1.57846e4	413.63757	49.9444

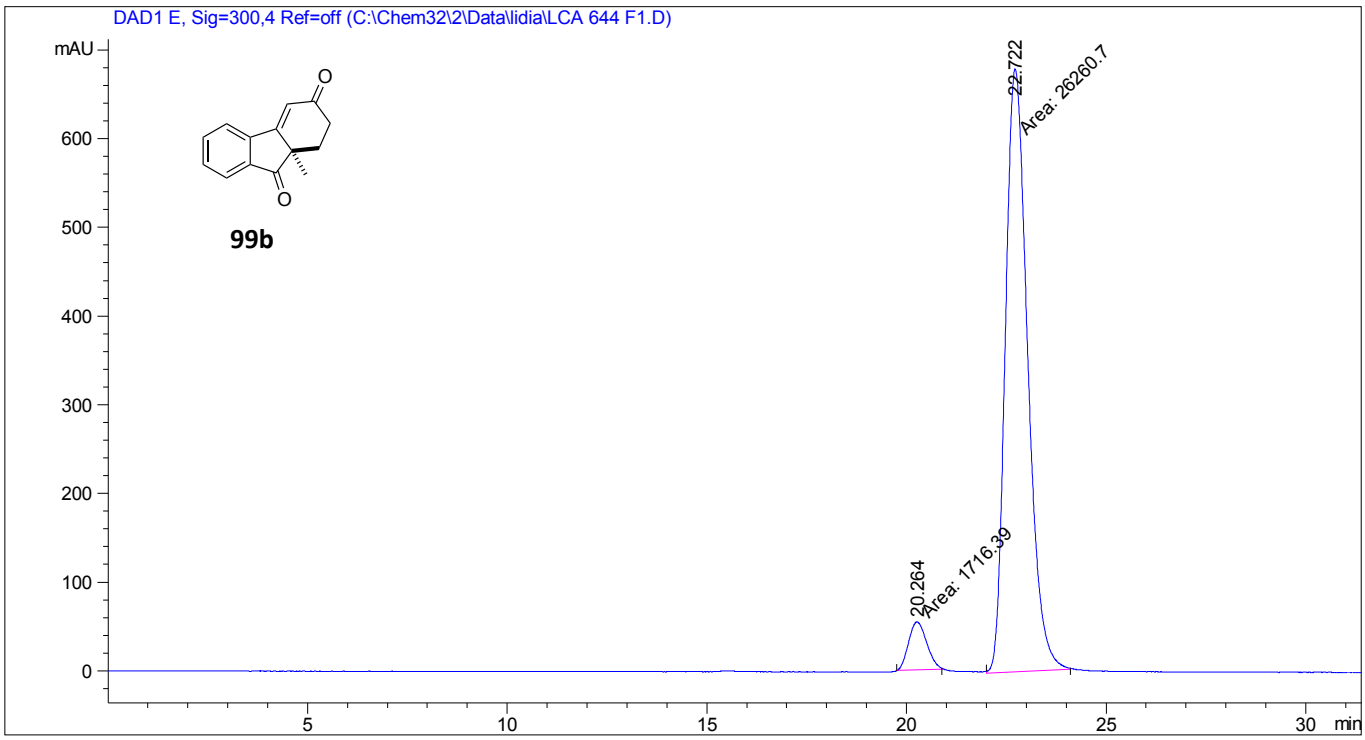

Peak #	Ret Time [min]	Type	Width [min]	Area [mAU*s]	Height [mAU]	Area %
1	20.264	MM	0.5270	1716.38916	54.28528	6.1350
2	22.722	MM	0.6441	2.62607e4	679.49506	93.8650

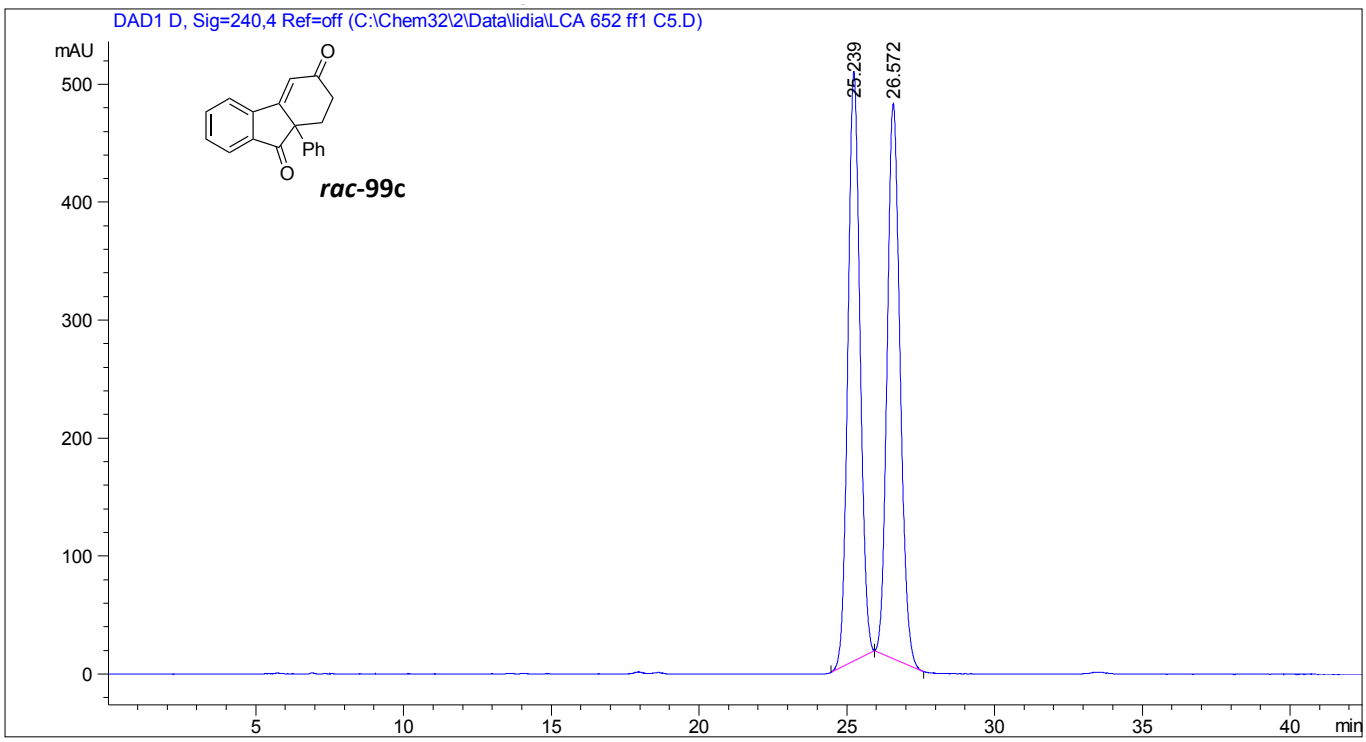

Peak #	Ret Time [min]	Type	Width [min]	Area [mAU*s]	Height [mAU]	Area %
1	25.239	BB	0.4475	1.42008e4	499.79587	49.8195
2	26.572	BB	0.4726	1.43037e4	470.60620	50.1805

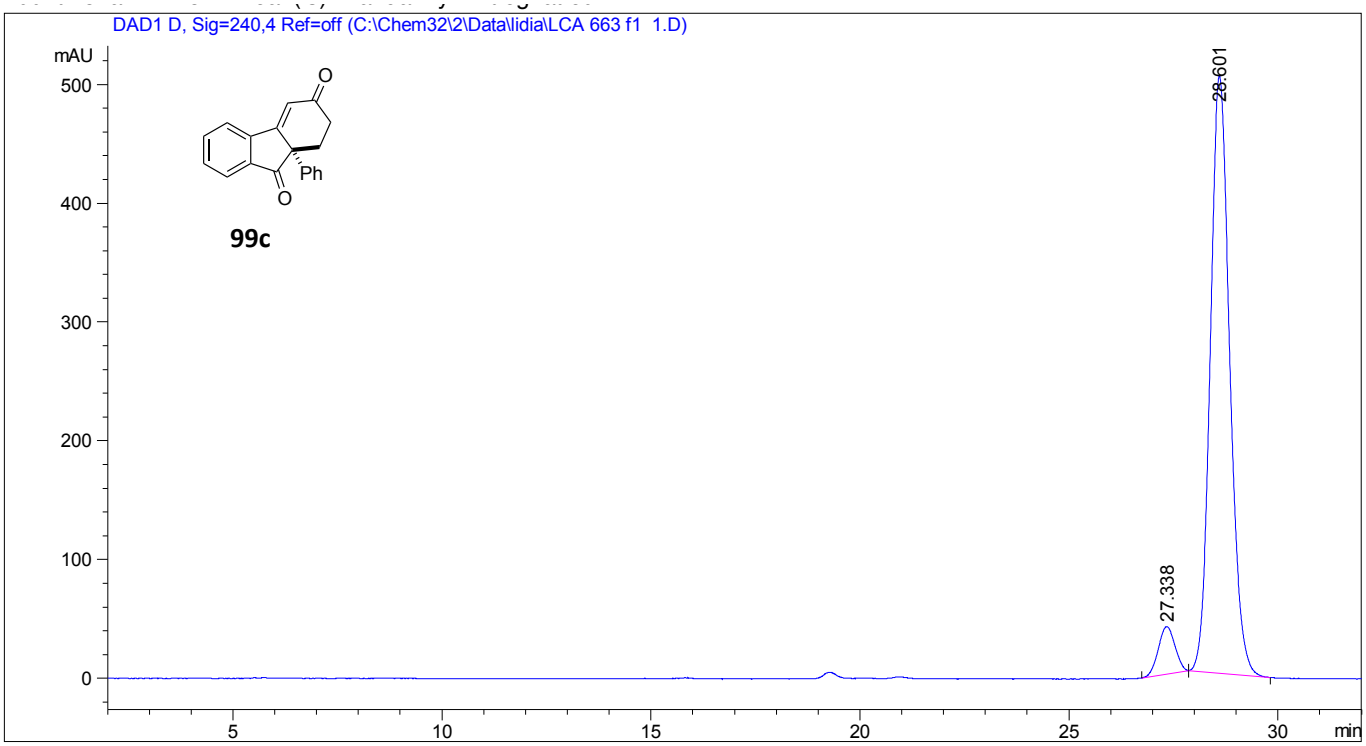

Peak #	Ret Time [min]	Type	Width [min]	Area [mAU*s]	Height [mAU]	Area %
1	27.338	BB	0.4087	1103.87598	39.91023	6.3822
2	28.601	BB	0.5035	1.61924e4	503.04770	93.6178

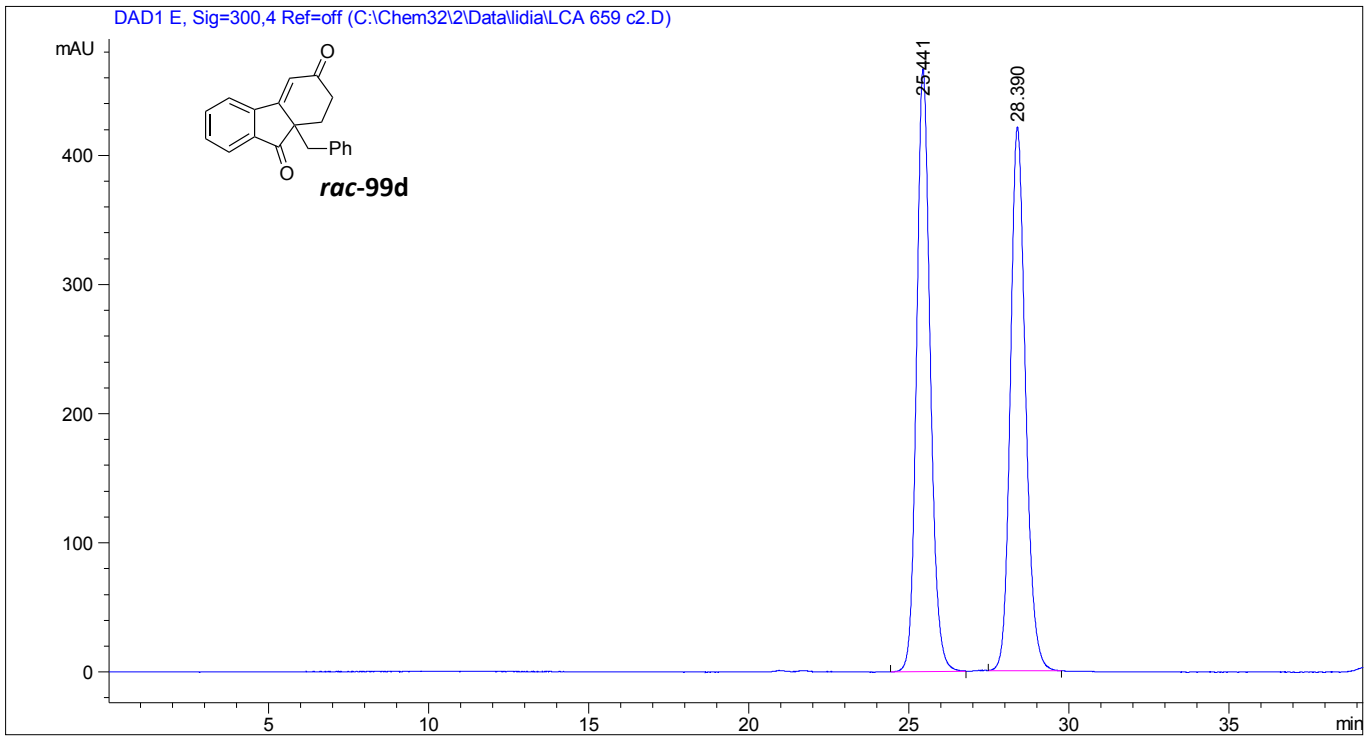

Peak #	Ret Time [min]	Type	Width [min]	Area [mAU*s]	Height [mAU]	Area %
1	25.441	BB	0.4513	1.38929e4	466.70422	50.1218
2	28.390	BB	0.5029	1.38253e4	421.21667	49.8782

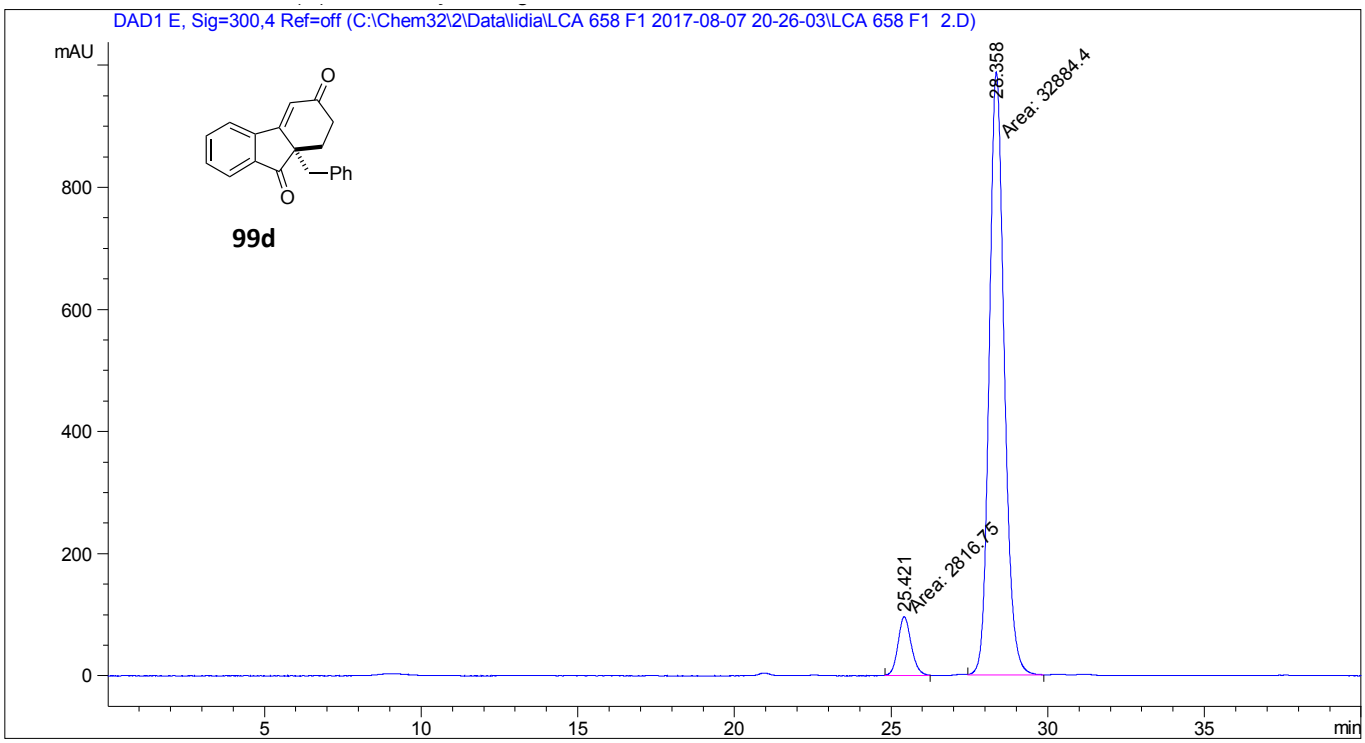

Peak #	Ret Time [min]	Type	Width [min]	Area [mAU*s]	Height [mAU]	Area %
1	25.421	MM	0.4892	2816.75000	95.96868	7.8898
2	28.358	MM	0.5551	3.28844e4	987.41382	92.1102

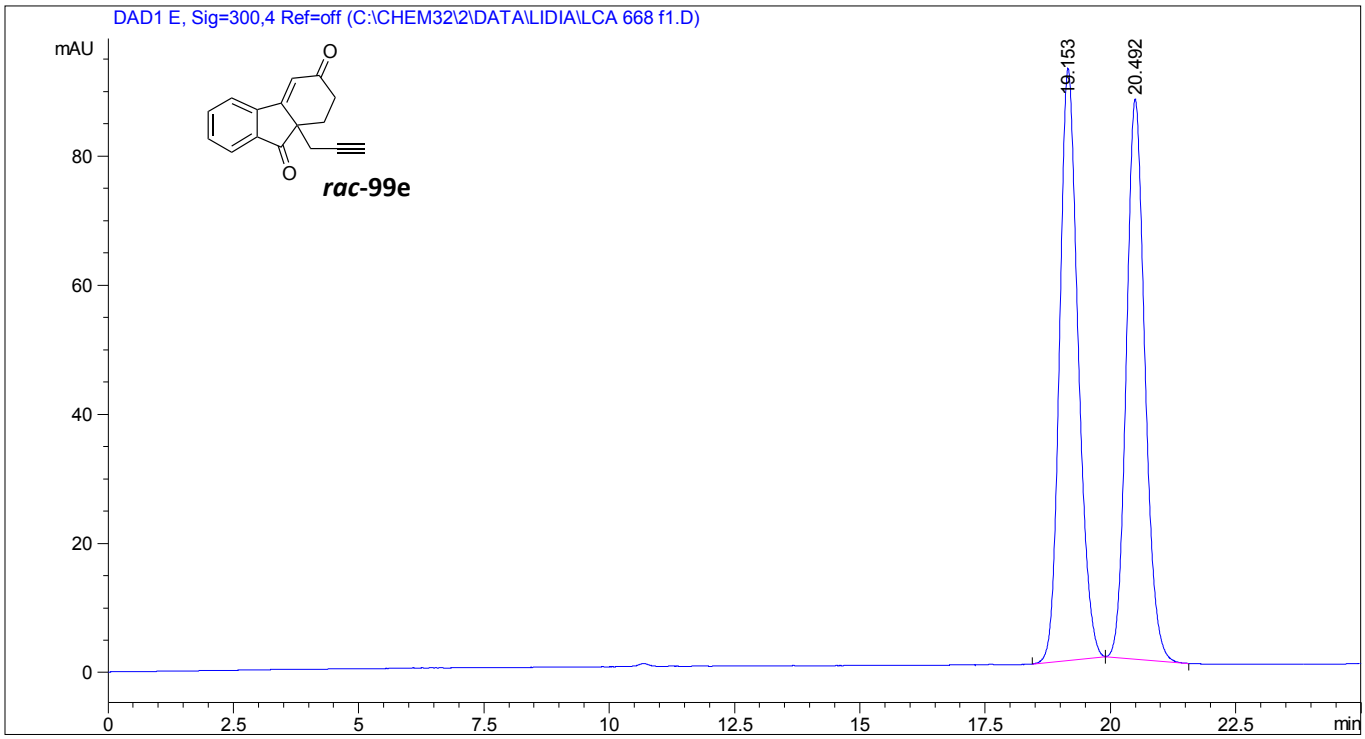

Peak #	Ret Time [min]	Type	Width [min]	Area [mAU*s]	Height [mAU]	Area %
1	19.153	BB	0.3948	2365.06958	91.71776	51.4605
2	20.492	BB	0.3940	2230.82324	86.75027	48.5395

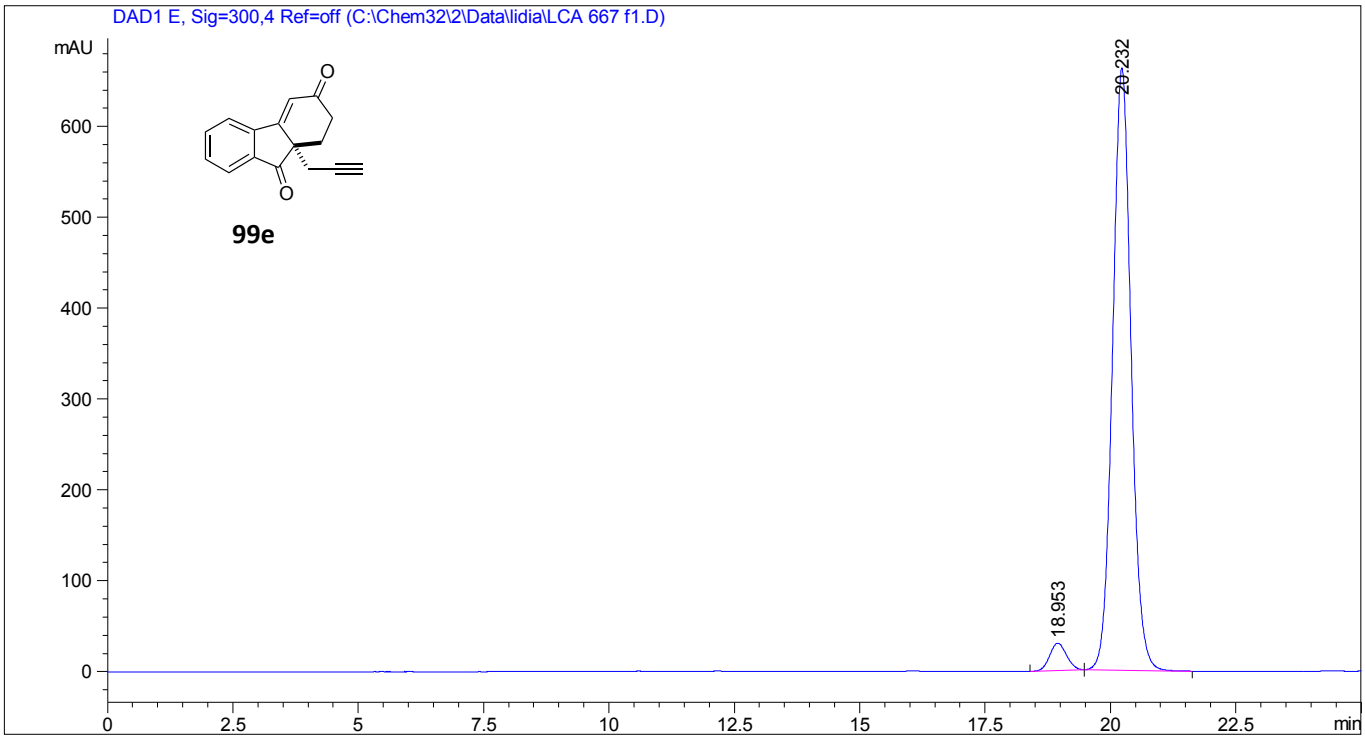

Peak #	Ret Time [min]	Type	Width [min]	Area [mAU*s]	Height [mAU]	Area %
1	18.953	BB	0.3649	706.74945	30.21742	3.9985
2	20.232	BB	0.3947	1.69686e4	662.71729	96.0015

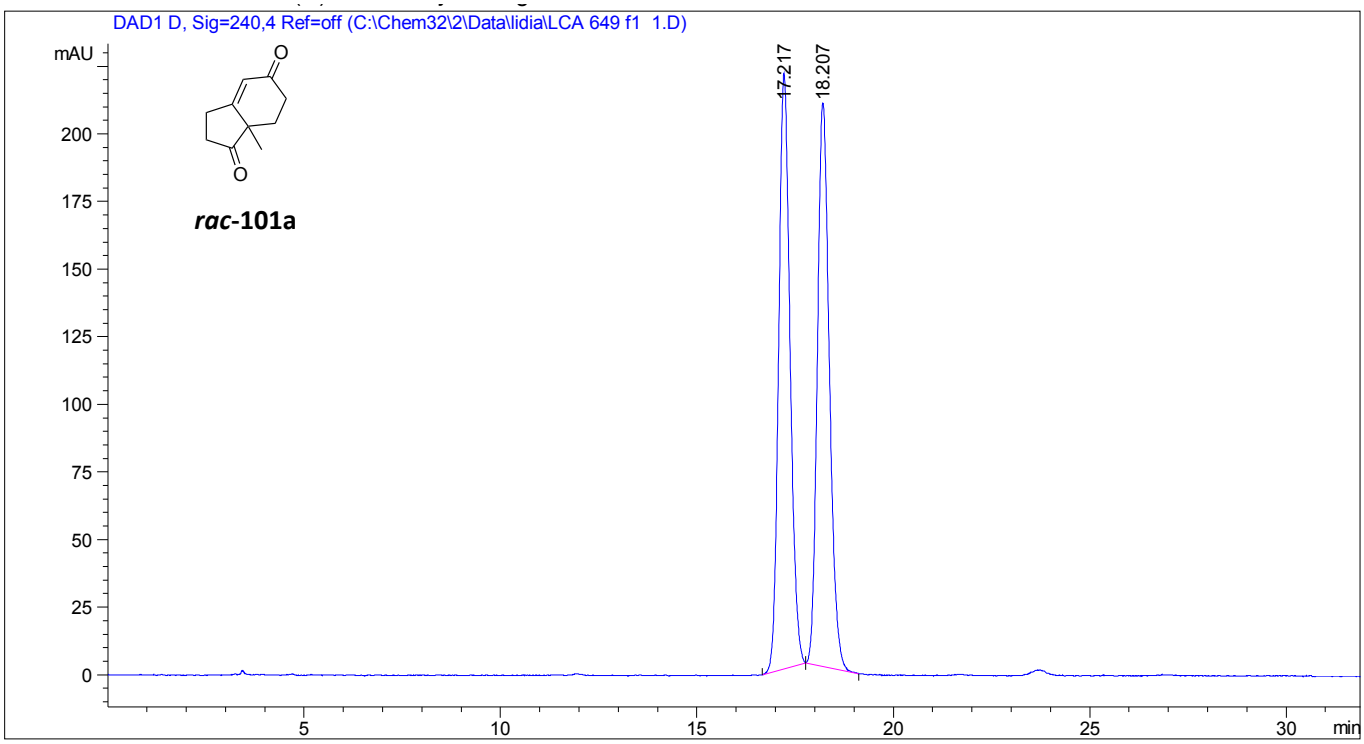

Peak #	Ret Time [min]	Type	Width [min]	Area [mAU*s]	Height [mAU]	Area %
1	17.217	BB	0.3074	4442.87939	220.18291	50.0327
2	18.207	BB	0.3304	4437.07813	208.39751	49.9673

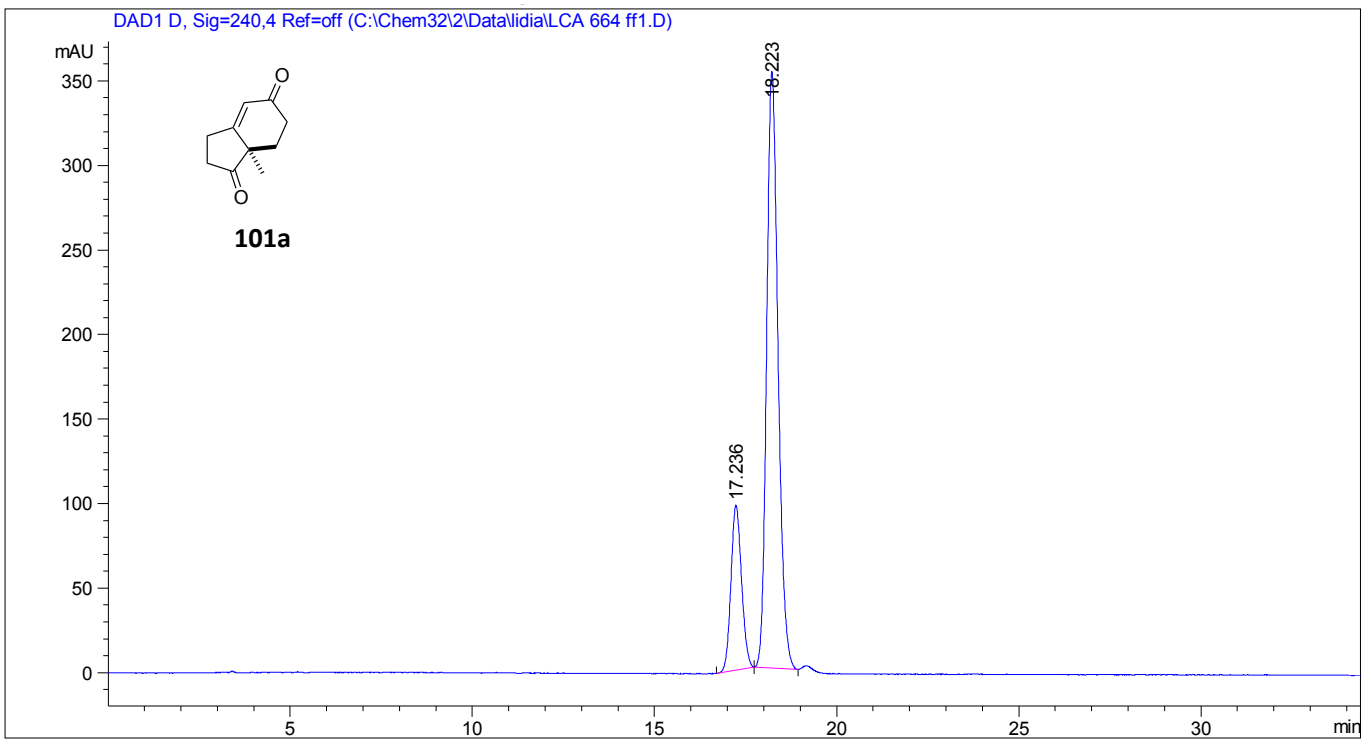

Peak #	Ret Time [min]	Type	Width [min]	Area [mAU*s]	Height [mAU]	Area %
1	17.236	BB	0.3059	1973.06824	97.57182	20.4902
2	18.223	BB	0.3331	7656.27148	352.92709	79.5098

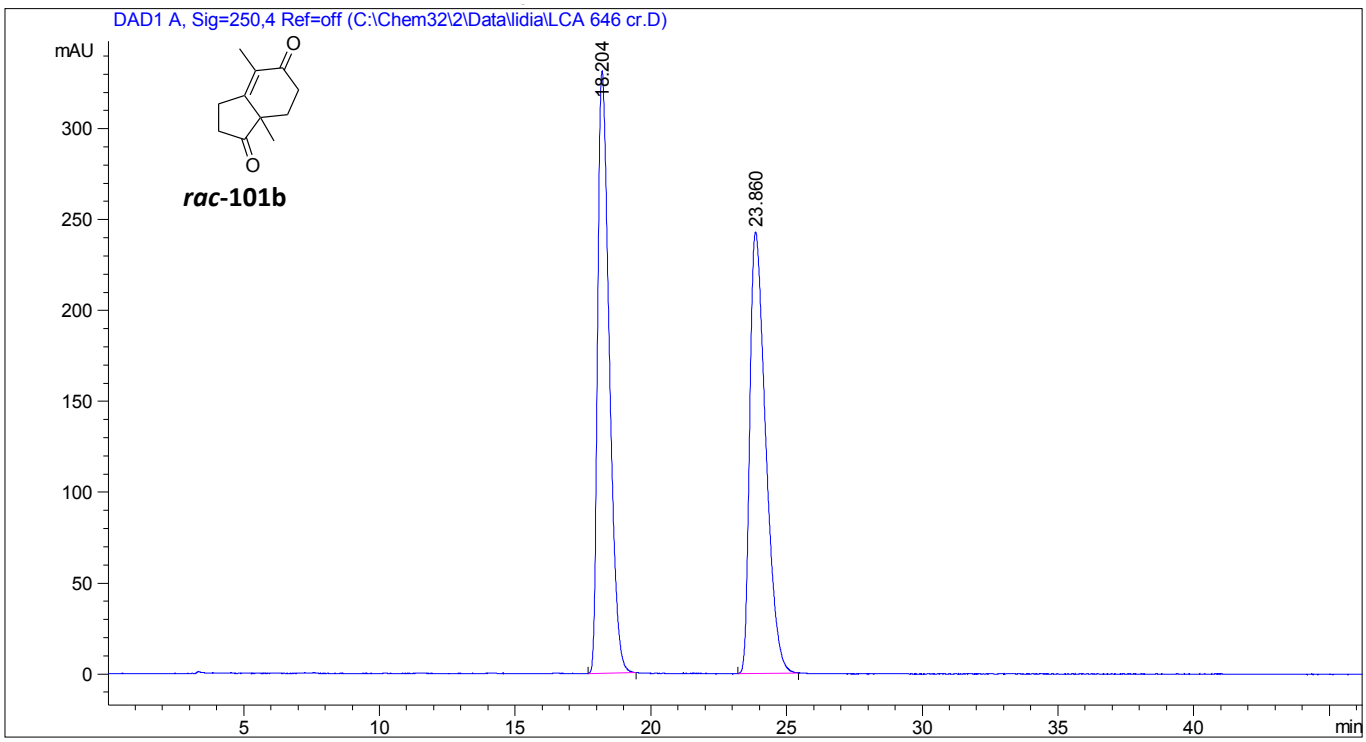

Peak #	Ret Time [min]	Type	Width [min]	Area [mAU*s]	Height [mAU]	Area %
1	18.204	BB	0.4599	9879.79688	331.32367	49.9872
2	23.860	BB	0.6086	9884.86523	243.00079	50.0128

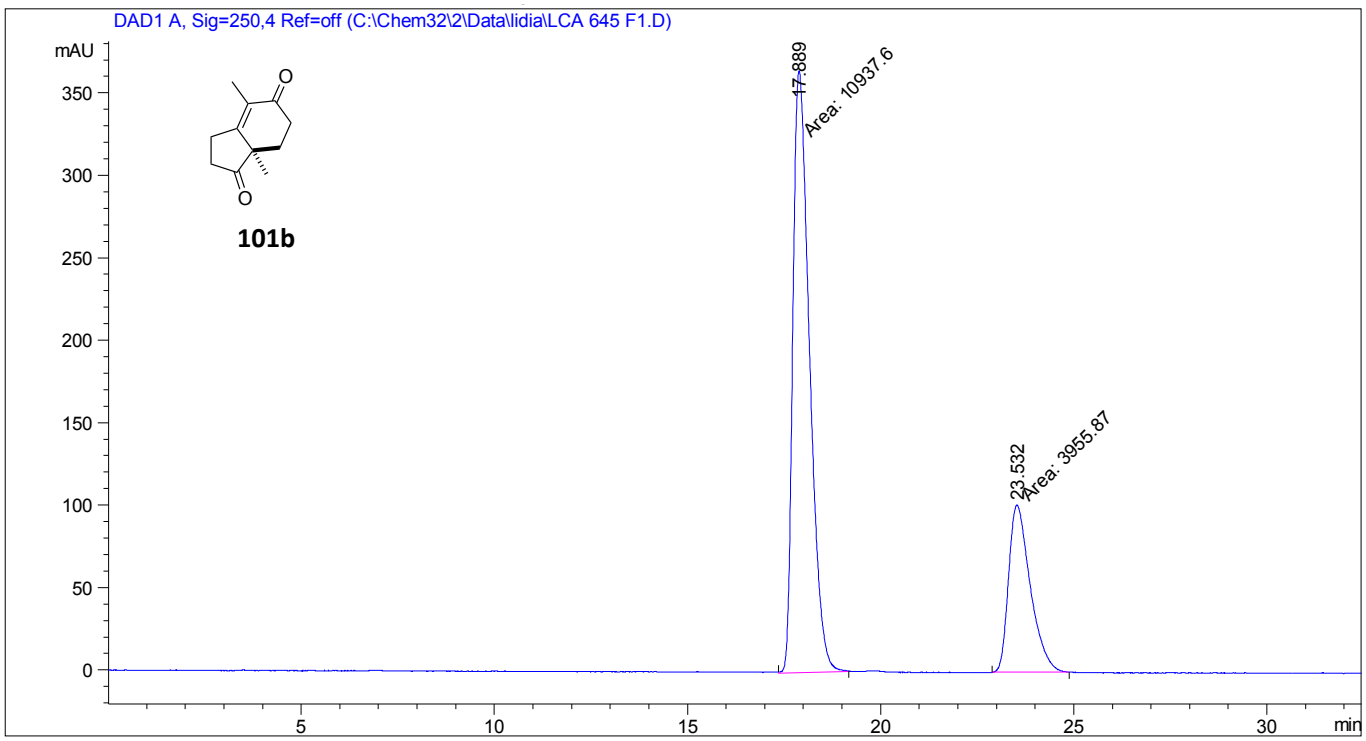

Peak #	Ret Time [min]	Type	Width [min]	Area [mAU*s]	Height [mAU]	Area %
1	17.889	MM	0.4996	1.09376e4	364.88327	73.4389
2	23.532	MM	0.6503	3955.86987	101.38622	26.5611

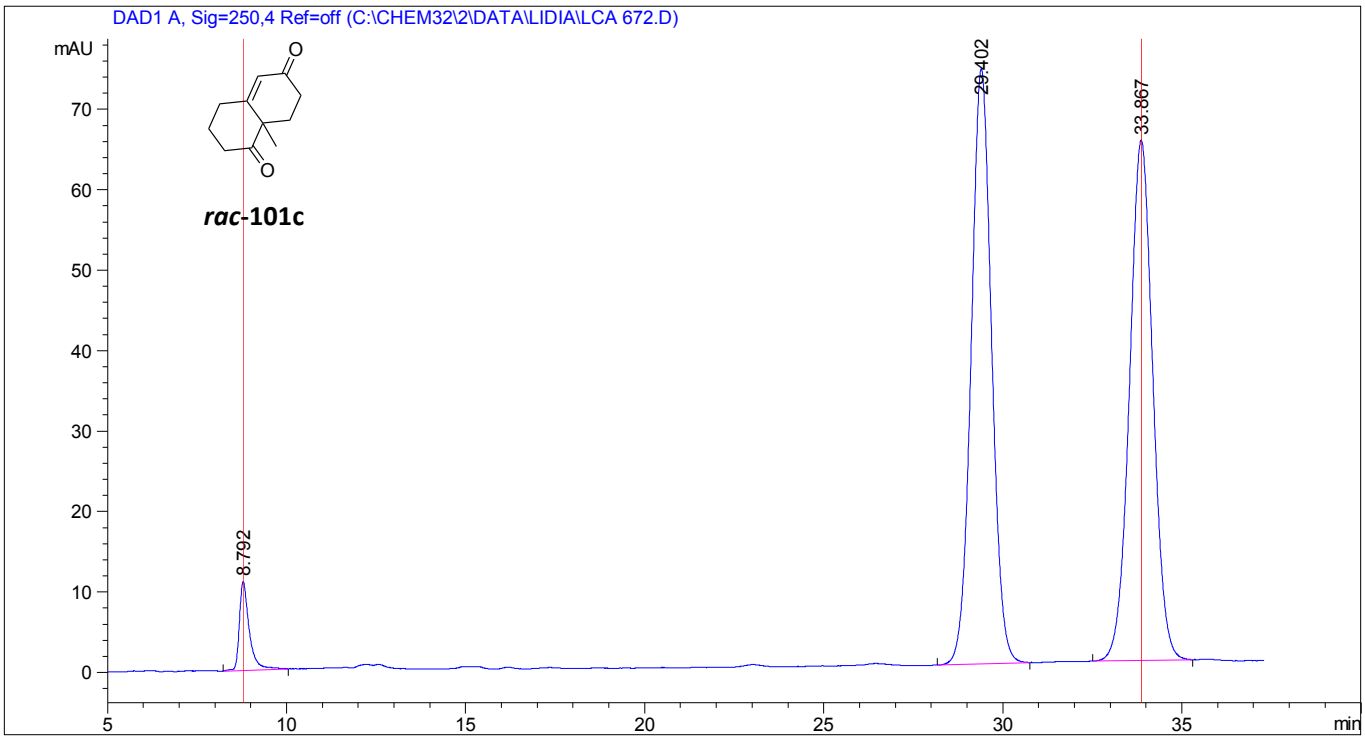

Peak #	Ret Time [min]	Type	Width [min]	Area [mAU*s]	Height [mAU]	Area %
1	8.792	BB	0.2838	211.11017	11.00668	3.4913
2	29.402	BB	0.6061	2917.20947	73.97626	48.2444
3	33.867	BB	0.6964	2918.41724	64.67725	48.2643

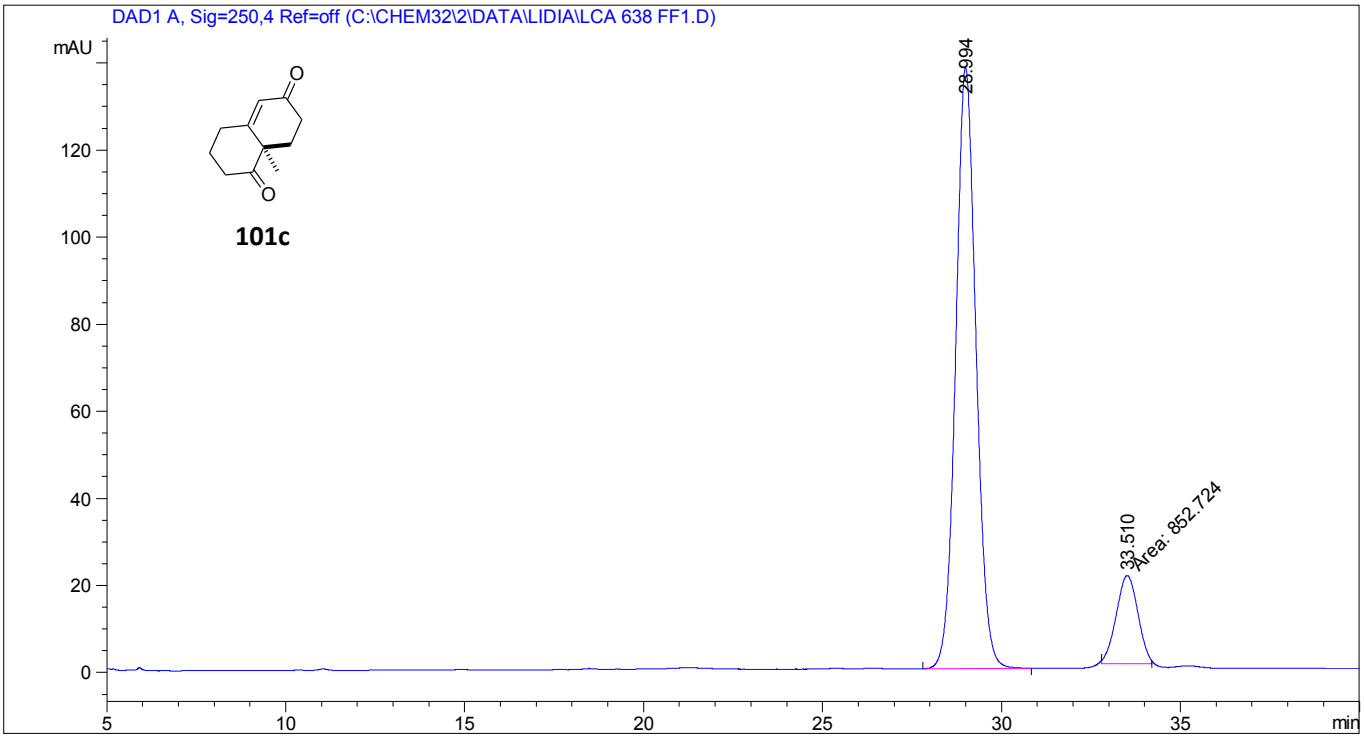

Peak #	Ret Time [min]	Type	Width [min]	Area [mAU*s]	Height [mAU]	Area %
1	28.994	BB	0.6037	5438.40967	138.01724	86.4456
2	33.510	MM	0.6994	852.72363	20.31983	13.5544

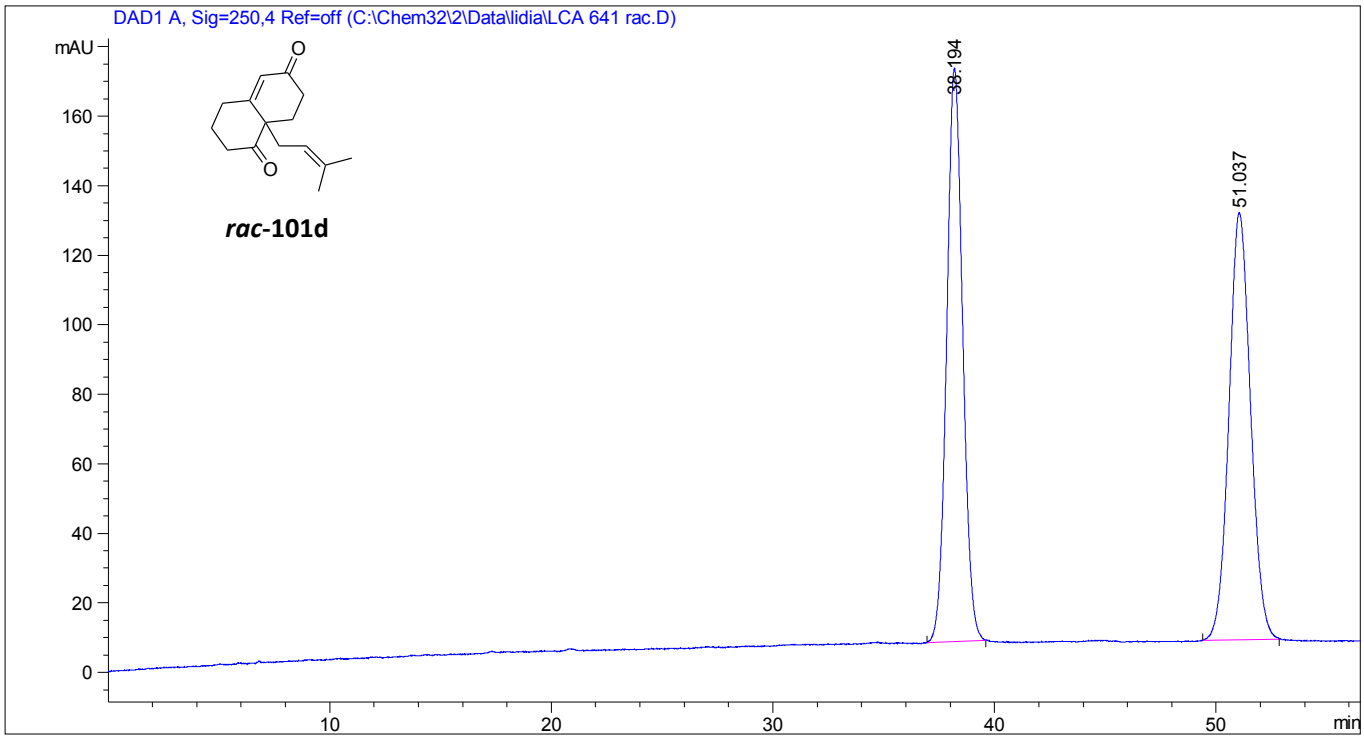

Peak #	Ret Time [min]	Type	Width [min]	Area [mAU*s]	Height [mAU]	Area %
1	38.194	BB	0.7513	8271.92578	164.88728	49.8589
2	51.037	BB	0.8747	8318.74512	122.74912	50.1411

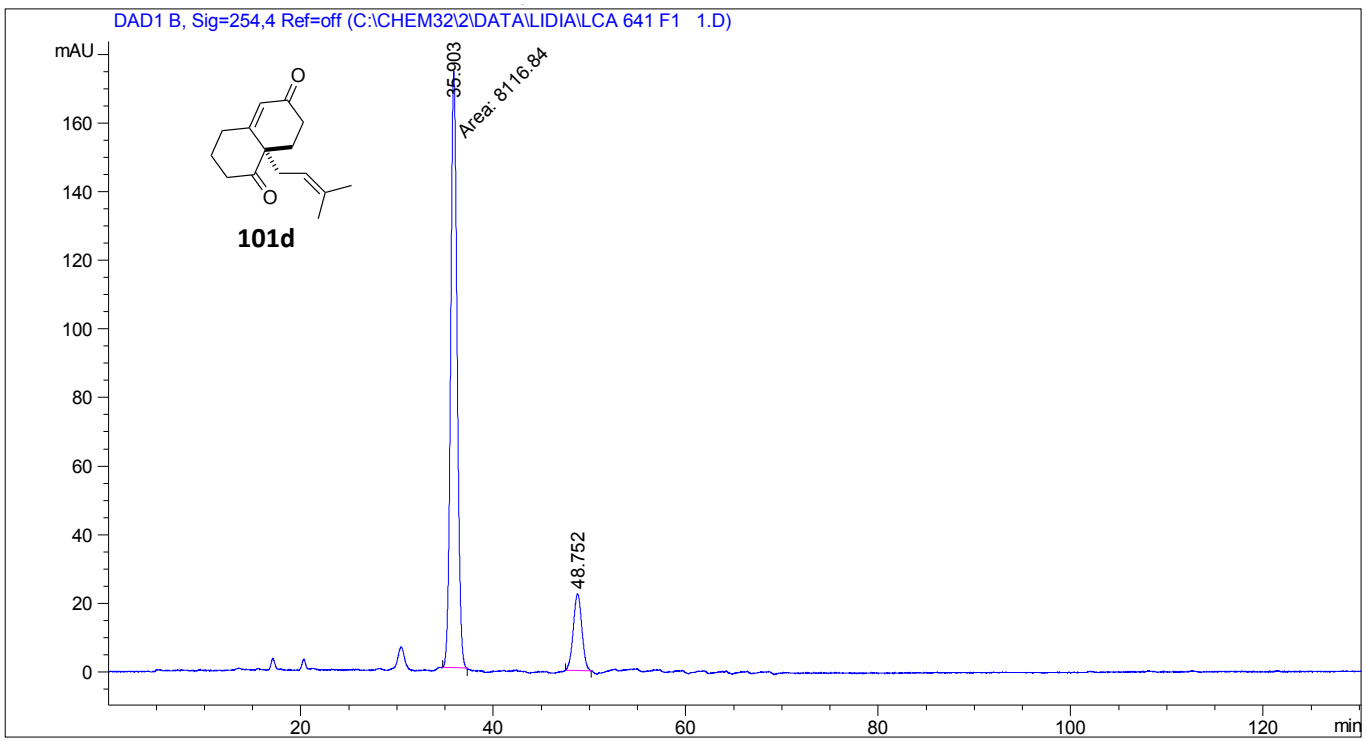

Peak #	Ret Time [min]	Type	Width [min]	Area [mAU*s]	Height [mAU]	Area %
1	35.903	MM	0.7780	8116.84424	173.88992	85.3737
2	48.752	BB	0.7335	1390.58728	22.42321	14.6263

CHAPTER V

UNIVERSITAT ROVIRA I VIRGILI
IMMOBILIZATION OF CHIRAL BRØNSTED ACIDS AND LEWIS BASES FOR BATCH AND FLOW ENANTIOSELECTIVE CATALYSIS
Lidia Clot Almenara

Chapter V

Chiral *N,N'*-Dioxide Amides: Ligands or Organocatalysts

5.1. Introduction to the use of *N,N'*-Dioxide Diamide Derivatives in Catalysis

One of the major challenges that chemists have to deal with is the design of the ideal catalyst able to induce chirality, which should be inexpensive, easy to synthesize, stable under moisture and air, and show high activity and selectivity.[1]

Catalysts or ligands that display C_2-symmetry are widespread in asymmetric transformations,[2][3] and constitute some of the most successful privileged chiral ligands: bis(phosphine) compounds (BINAP, DuPHOS, etc.),[4] spirobiindane based ligands[5] and bis(oxazolines).[6]

Early investigation documented that *N*-heteroaromatic *N*-oxides presented a powerful capacity as electron-pair donor catalysts, but this resulted in limited applications.[7] However, in the last decade, homochiral[8] C_2-symmetric *N*-oxide catalysts have had a remarkable impact in asymmetric catalysis.[9] The early synthesis of homochiral proline *N*-oxides dates back to 1993,[10] by the group of Ian A. O'Neil. They proved that the oxidation of the pyrrolidine in prolinamide derivatives using *m*-CPBA provided the desired *N*-oxide. Remarkably, the nitrogen becomes a stereocentre after quaternization, but the diastereoselectivity of the process is very high. Later on, the same group reported the synthesis of proline-derived homochiral amine oxides, which were stabilized by an intramolecular hydrogen bond. They attributed the complete

diastereoselectivity to hydrogen bond interaction between the peracid oxidant and the secondary amide. In order to examine the potential of these new catalysts, they were applied to the asymmetric Pauson-Khand reaction affording relatively high yields (Scheme 5.1).[11]

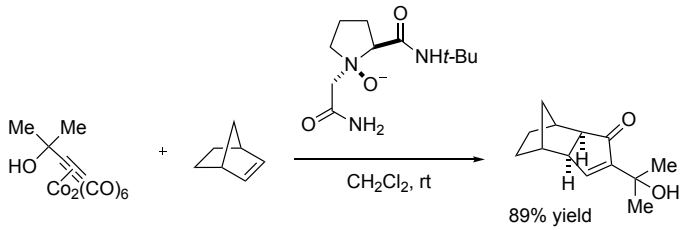

Scheme 5.1: Prolinamide-derived *N*-oxide proline derivative catalyzed Pauson-Khand reaction.

However, *N*-oxides display such a particular reactivity that they can even promote reactions in metal-free conditions. For instance, groundbreaking studies have been carried out with pyridine *N*-oxides, basically involving the formation of hypervalent silicate intermediates in the enantioselective allylation of aldehydes. *N*-Oxides display promising reactivity in the activation of organosilicon compounds[12] due to the highly nucleophilic character of the N-O bond toward silicon atoms,[13] similarly to what enables the formation of metal complexes.[14] Different precedents in the allylation of aldehydes catalyzed by Lewis bases have been reported.[15][16] For instance, Nakajima *et al.* showed the effectiveness of bisquinoline *N,N'*-dioxide (**(*S*)-102**) catalyst in the asymmetric addition of allyltrichlorosilanes to benzaldehydes (Scheme 5.2).[17]

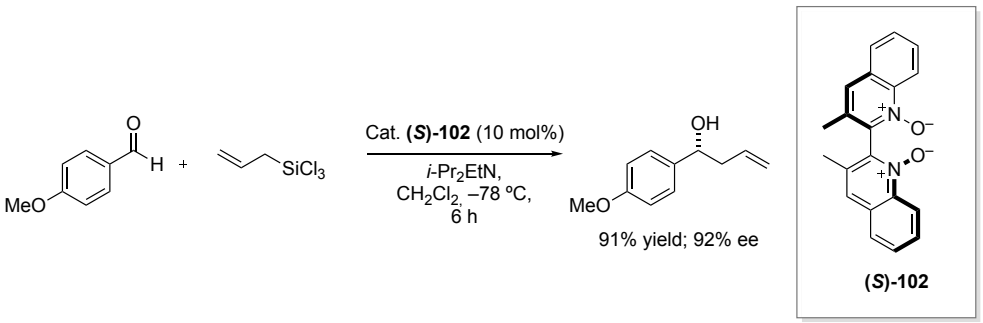

Scheme 5.2: Asymmetric allylation of aldehyde using allyltrichlorosilanes catalyzed by bisquinoline *N,N'*-dioxide.

The group of Xiaoming Feng has explored the synthesis of a homochiral ligand library based on *N,N'*-dioxide diamides. Feng designed this new family of ligands in an attempt to combine the benefits of the C_2-symmetry of the bisquinoline *N,N'*-dioxide framework[18] and the early success of O'Neil's L-prolinol-derived mono *N*-oxide as a bifunctional catalyst.[19] In this manner, they obtained multidentate *N,N'*-dioxide ligands for enantioselective catalysis as depicted in Figure 5.1.

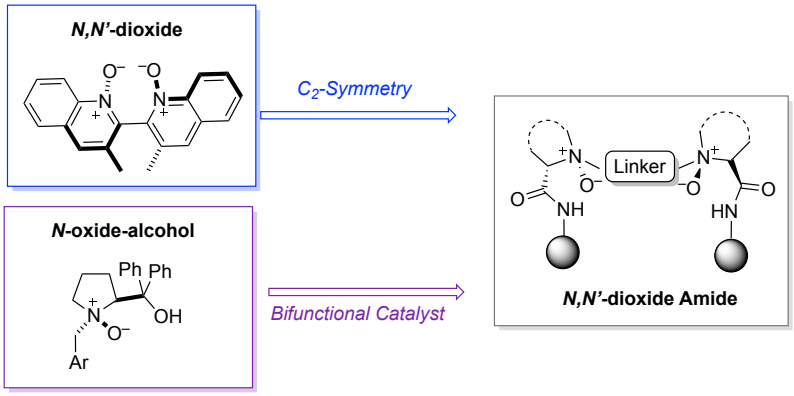

Figure 5.1: Feng's design of C_2-symmetric bifunctional *N,N'*-dioxide amide ligands.

These dimeric species are characterized for being very polar molecules, the catalytic center consists in a chiral quaternary nitrogen, with a stronger dipole in the *N*-oxide compared to common oxo-donors like alcohols, ethers or amides.[20] The electron-pair donor ability of the oxygen atoms promotes the coordination with protons, alcohols or Lewis acids.[21]

The ideal design of these catalysts opens up new possibilities to carry out asymmetric transformations. The application of chiral *N*-oxides can be divided in two groups. Firstly, they can be applied in metal-free catalytic reactions, as organocatalysts, because of the N-O affinity to silicon. On the other hand, they contain multiple O-donors with a certain electronic environment that allows them to act as tetradentate ligands for the coordination with a broad range of metal ions[14a] such as Cu(I), Cu(II), Ni(II), Cu(I), Mg(II), Fe(II), Co(II),

In(III), Sc(III), La(III), Y(III) and Nd(III), among others. This new family, emerged in the last decade, has been applied in several asymmetric reactions successfully (Scheme 5.3).[22]

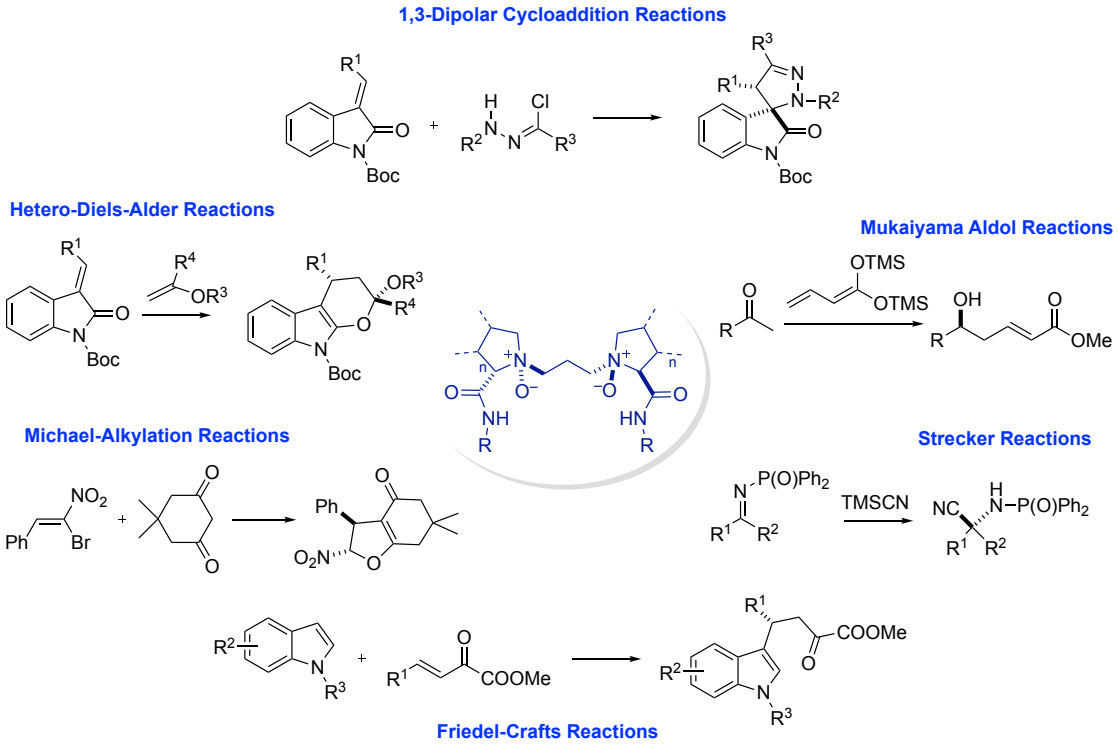

Scheme 5.3: Representative transformations catalyzed by *N,N'*-dioxide amides.

This is a very vast field, and a great number of *N*-oxides have been prepared and applied in catalysis. However, in the present thesis we will be more focused in C_2-symmetric *N*-oxides derived from a prolinamide dimer (Figure 5.2).

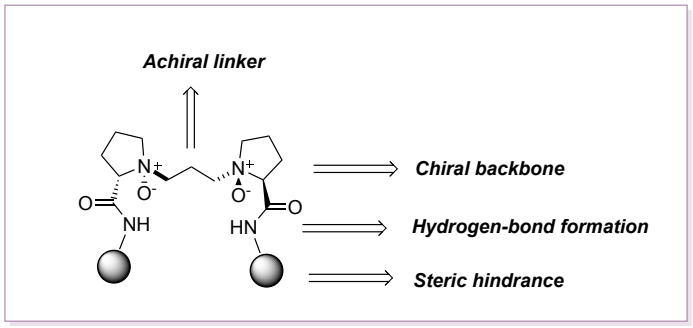

Figure 5.2: Framework of prolinamide dimer-derived *N,N'*-dioxides.

These compounds are characterized for being conformationally flexible ligands. The chirality is provided by tertiary amino oxide-amide backbone, whereas an achiral alkyl spacer connects the two amides units. They can be easily synthesized from cheap, optically pure amino acids.

5.1.1. Design and Synthesis of *N,N'*-Oxide Amides

N,N'-Dioxides can be divided in two main groups: (I) pyridine *N*-oxides,[23] and (II) tertiary amine-dimeric *N*-oxides (Figure 5.3). Within this second group we can distinguish two kinds of catalysts depending on the linker between the two catalytic subunits containing the N-O bond.[20, 24] This can either be more rigid, having the diamide as connector, usually involving an aryl chain (Figure 5.3, eq. 1) or a conformationally flexible alkyl chain formed through the nitrogen atom (Figure 5.3, eq. 2). In the first group, the *N*-heteroaromatic *N*-oxides, the $2p_{\pi}$ electrons of the oxygen are conjugated with the π-aromatic system. On the other hand, the amine-oxide of the second group presents a new stereocenter at nitrogen, which display a tetrahedral configuration.

- **Pyridine *N*-oxides:**

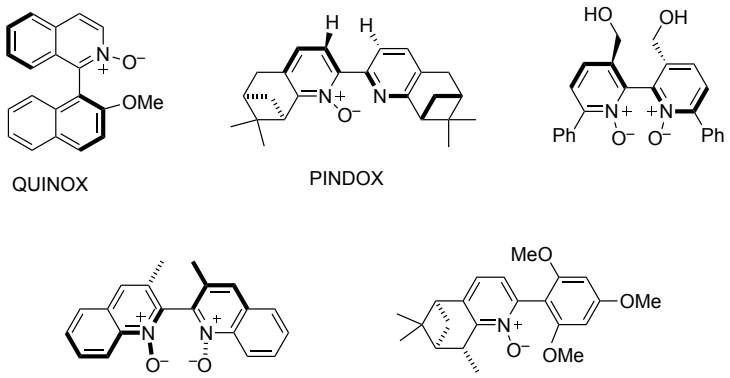

- **Tertiary amine-derived *N*-oxides:**

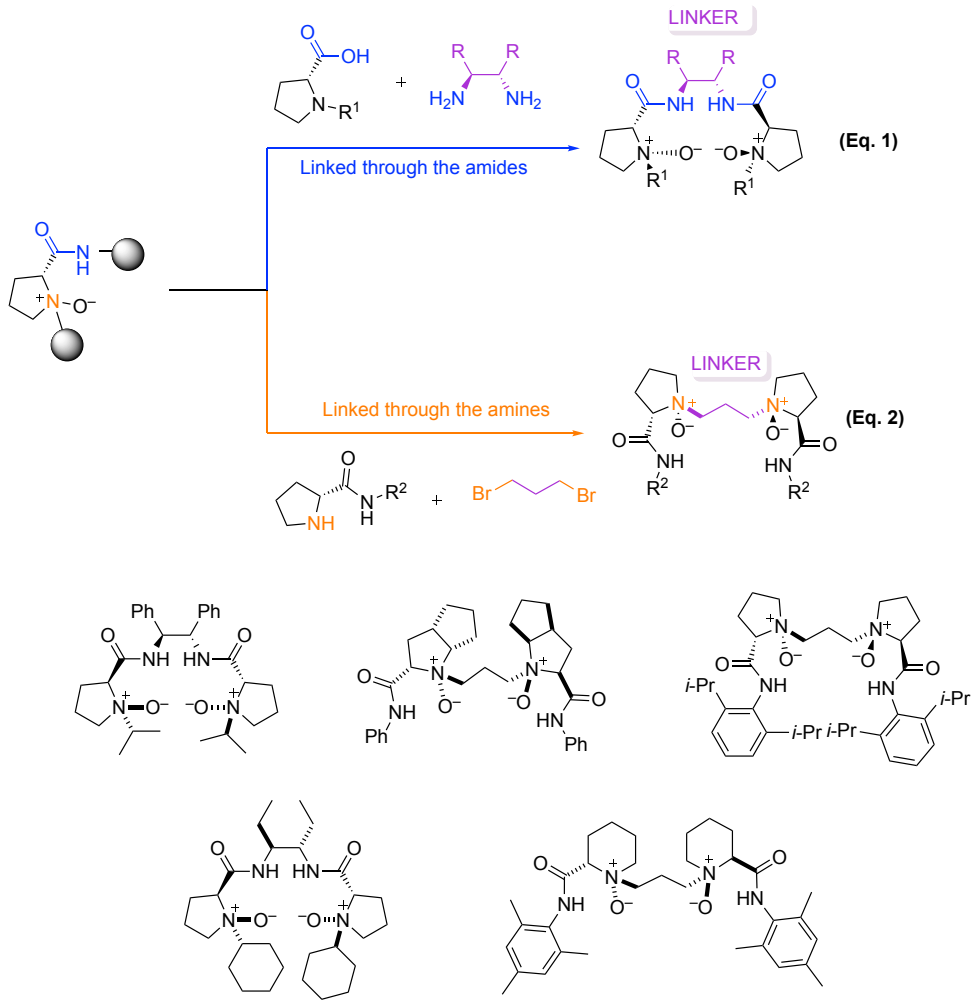

Figure 5.3: Most common *N*-oxide ligands and catalysts.

In Scheme 5.4 is depicted the straightforward and cost-effective synthesis of C_2-symmetric *N,N'*-dioxides. Following this route, it is possible to achieve a broad range of derivatives starting from chiral secondary amines derived from L-proline, L-pipecolic acid or L-ramipril. Firstly, formation of the amide takes place, followed by the deprotection of the amino group. Then, the corresponding linker is formed by double nucleophilic substitution using dibromo compounds. Finally, the desired *N,N'*-dioxide is generated as a single enantiomer after treatment of the corresponding pyridine or tertiary amines with peracids such as *m*-CPBA or hydrogen peroxides. This last step oxidizes the nitrogen, which becomes a stereocentre in a highly diastereoselective manner.

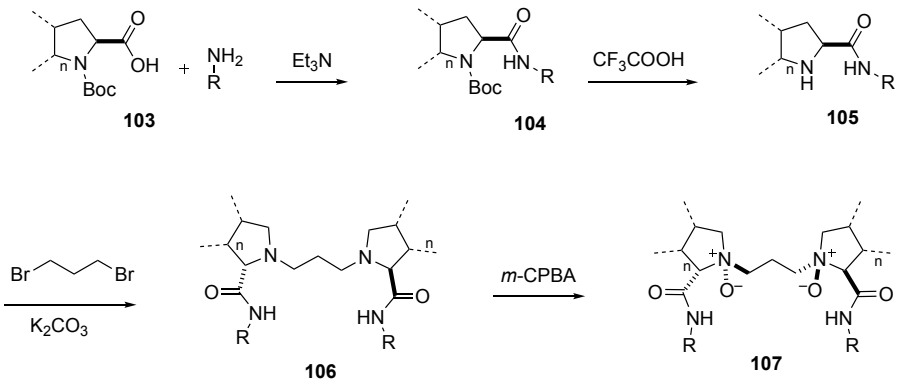

Scheme 5.4: General pathway for the synthesis of C_2-symmetric *N,N'*-dioxides.

The arrangement of the atoms, after the stereoselective oxidation, has been confirmed by ^{1}H NMR and X-ray analysis, showing the formation of six-membered hydrogen bonded rings (Scheme 5.5, a). The bidentate structure formed presents a chelate effect, which helps in the coordination to Lewis acids. In this manner, the four oxygen atoms are held close to one another, rendering a more compact structure. As expected, when *N,N'*-dioxides coordinate to a Lewis acid as a tetradentate ligand, the stabilized six-membered H-bond ring is disrupted (Scheme 5.5, b).[25]

a) Conformation of N,N'-dioxides as ligands, forming six-membered H-bonded rings

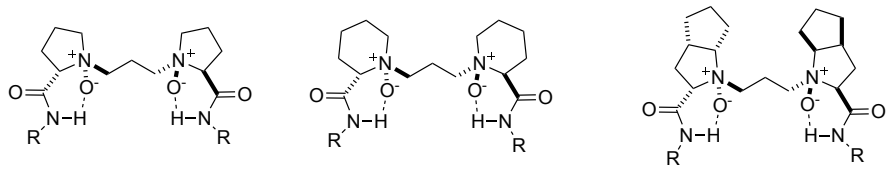

b) Conformation of N,N'-dioxides coordinated to metal centers

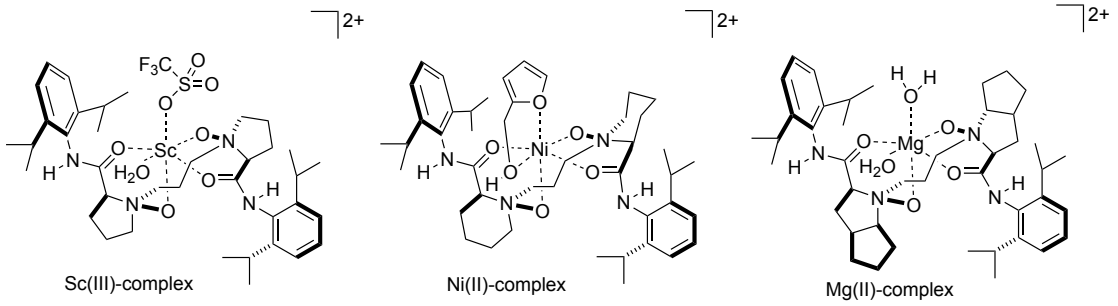

Scheme 5.5: Conformation of *N,N'*-dioxides and their metal complexes.

5.1.2. Application of *N,N'*-Dioxides as Chiral Organocatalysts

Due to the high nucleophilicity of the oxygen in *N*-oxides, these compounds have been most widely applied for organosilicon chemistry in asymmetric metal-free transformations.[26] The inherent affinity of silicon for oxygen, which is perfectly reflected in the strength of the Si-O bond in Me_3SiOMe (114 kcal mol^{-1}), allows carrying out processes that rely on the activation of organosilicon compounds forming hypervalent silicate intermediates.[15d, 27][28]

- **Activation of Organosilicon Compounds: Cyanation of Aldehydes, Ketones and Imines**

The cyanation of carbonyls and imine compounds is a straightforward strategy to synthesize for homochiral cyanohydrins and amino nitriles. Considering that a suitable nucleophile for silylcyanation is trimethylsilylcyanide (TMSCN),

which and it is activated by anionic or neutral Lewis bases, *N,N'*-dioxide catalysts facilitate this transformation because of a dual interaction: as Lewis bases to coordinate with TMSCN and as hydrogen bond donors with carbonyls or imines.

Xiaiming Feng *et al*. have demonstrated the efficiency of *N,N'*-dioxide diamides as organocatalysis for the activation of TMSCN in order to develop cyanosilylation of aldehydes, ketones and imines (Scheme 5.6). Remarkably, variation of the substituents in the amide has an impact over the ee and yield. After optimization, **108** showed to be optimal for cyanosilylation of aldehydes.[29] Later, they performed the **109**-catalyzed addition of TMSCN to more promising substrates as α,α-dialkoxy ketones.[30] Through NMR studies, they concluded that the mechanism proceeds through formation of a hypervalent silicon intermediate with TMSCN after this is attracted due to coordination with the oxygens of the N-O bonds. Afterwards, the carbonyl is activated via H-bonding with the N-H of the amide, which allows stereoselectice attack of the cyano group to the carbonyl to generate the desired compound. In order to improve the stereoselectivity, other bulky groups in the amide moiety were also designed (see **110**, Scheme 5.6), which promoted the Strecker reaction in highe enantioselectivity.[31]

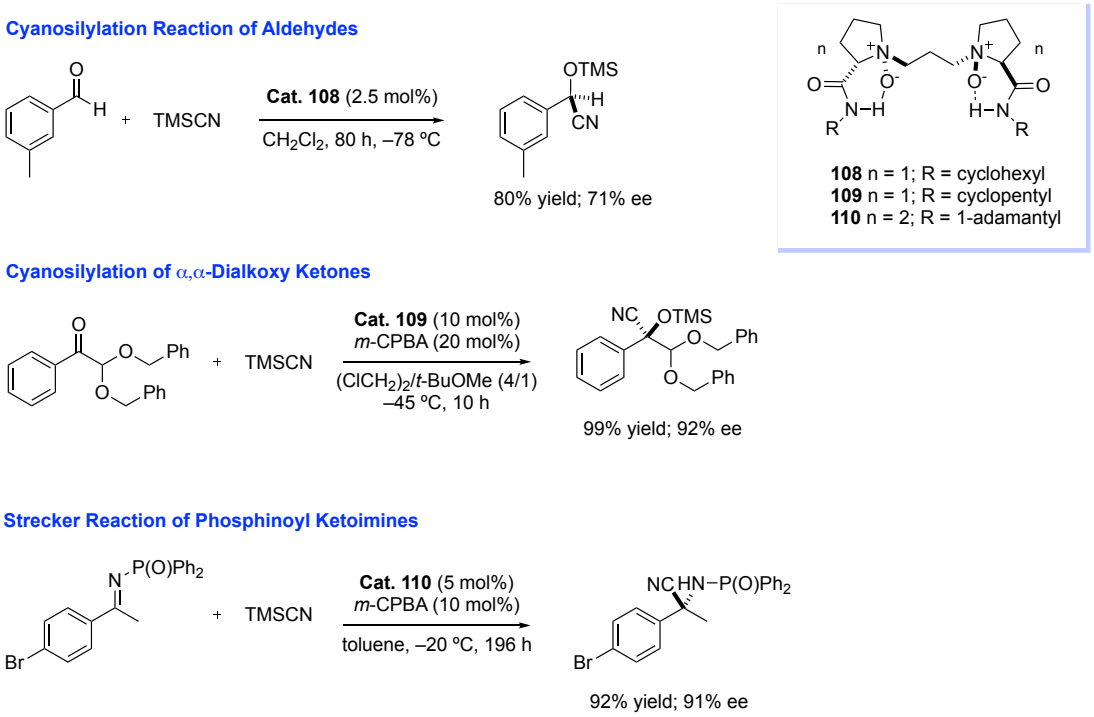

Scheme 5.6: Asymmetric silylcyanation reactions catalyzed by *N,N'*-dioxides.

- **α-Chlorination of Cyclic β-Ketoesters**

In addition to the use of *N,N'*-dioxides as organocatalysts involving silicon activation reaction, the chlorination of cyclic beta ketoesters opens new applications for these species. Catalyst **111** enables asymmetric halogenation in high yields and ee via simultaneous activation of cyclic β-ketoesters with electrophilic *N*-chlorosuccinimide (NCS).[32]

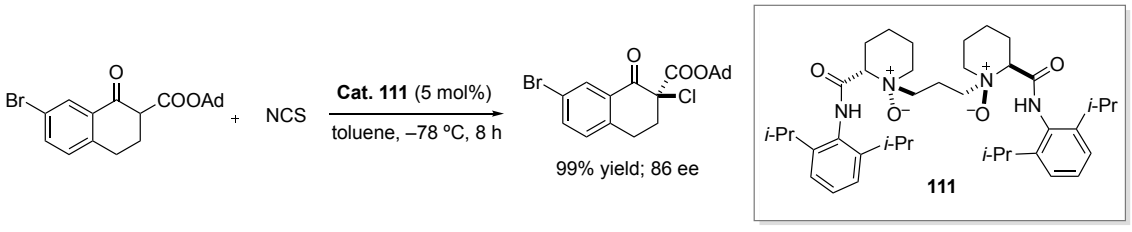

Scheme 5.7: Organocatalytic chlorination of β-ketoesters.

5.1.3. Application of *N,N'*-Dioxides as Chiral Metal–Ligand Complexes

Initially, *N,N'*-dioxides were employed basically as organocatalysts for Lewis base and H-bond assisted reactions. More recently, these catalysts have shown an enormous potential as ligands in asymmetric transformations, after their applicability is being extended to metal-catalyzed transformations.[33]

The bidentate nature of *N,N'*-dioxides allows a chelating effect in the presence of Lewis acids, in such a way that the metal center coordinates to the four oxygen atoms. In fact, Feng *et al*. who have explored the potential of these catalysts in depth, have found more applications where the *N,N'*-dioxides act as ligands than an organocatalysis. For instance, they have reported tandem Michael/ring-closure for the synthesis of a serotonin inhibitor((–)-Paroxetine),[34] Diels-Alder,[35] Friedel-Crafts alkylation,[36] Michael reactions,[37] 1,3-dipolar cycloaddition,[38] Mukaiyama aldol reaction,[39] Mannich reaction,[40] among others.[41]

The efficiency of *N,N'*-dioxides in challenging reactions can be demonstrated in the next example. A nickel/*N,N'*-dioxide complex has been used to promote the reaction of azaheptafulvene, an excellent 8π component, with alkylidene malonates to afford cycloheptatriene-fused pyrrole derivatives, an structural motif present in biologically active molecules.

Asymmetric [8+2] cycloadditions are a challenging class of reactions for the synthesis of important molecules. The higher-order cycloadditions afford medium-sized systems. The catalytic *N,N'*-dioxide nickel complex has shown to be versatile with a broad scope of substrates, bearing electron-donating or electron-withdrawing substituents on the *N*-aryl group. The mechanism of this process is proposed to start with the coordination of tetradenate *N,N'*-dioxide **112** (Scheme 5.8) and the bidentate alkylidene malonate to Ni^{II} to form an

octahedral geometry. The attack of azaheptafulvene is favored on the Si face due to the steric hindrance by the neighboring 2,6-diisopropylphenyl group on the ligand. Finally the ring closure occurs giving rise to the fused rings of the desired product.[42]

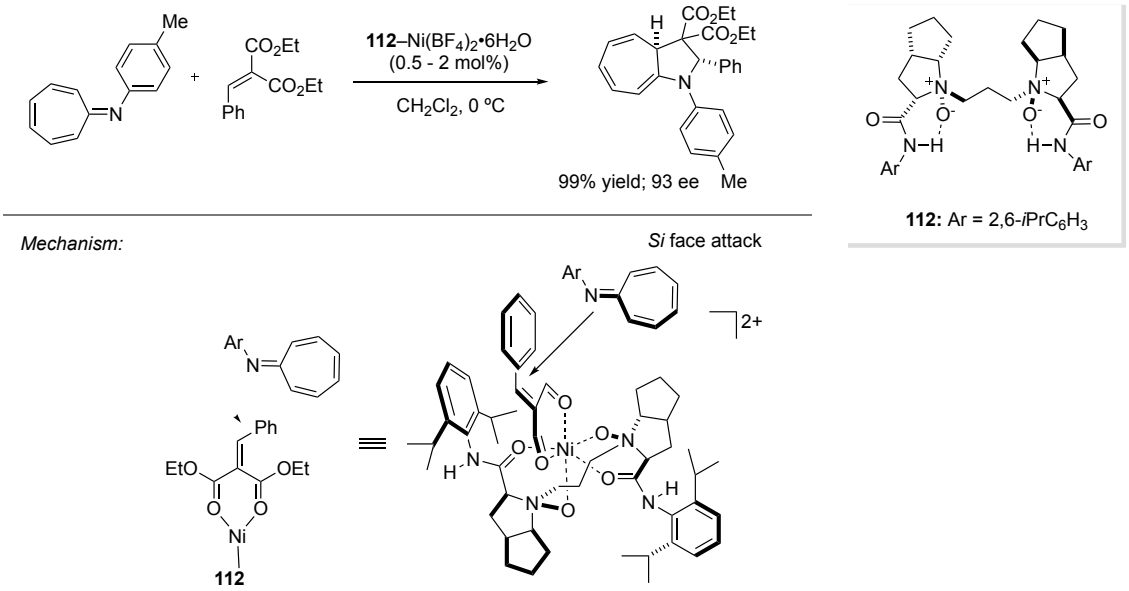

Scheme 5.8: [8+2] Cycloaddition between azaheptafulvene and alkylidene malonates.

5.2. Aims

The success of *N,N'*-dioxide amides, attributed to their structure that allows forming chiral ligand-metal complexes as well as being organocatalysts, makes them a perfect candidate to be immobilized onto a solid support.

Our main goal in this field, is to design an efficient and easy route to immobilize chiral *N,N'*-dioxides onto a polystyrene resin. According to the selected immobilization strategy (see Figure 5.4), we will focus on a dimeric structure that bears a linker between the two pyrrolidine nitrogen. The synthesis of C_2-symmetric *N,N'*-dioxides can be accomplished from readily available chiral amino acids; in this case we will use *N*-Boc-L-proline to build the chiral backbone, and we will employ 2,6-diisopropylanilinamides as bulky substituents that induce steric hindrance in order to create a perfect cavity. We chose this basic structure as a model because of the amount of applications reported with this scaffold in particular,[43] and the commercially availability of the starting materials. In addition, our goal is to create a general route that could be extended to all the supported derivatives.

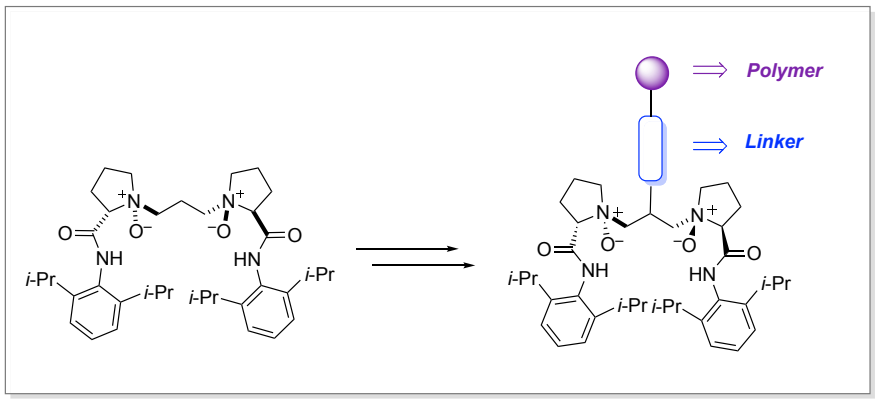

Figure 5.4: From homogeneous *N,N'*-dioxides to supported *N,N'*-dioxides.

5.3. Results and Discussion

The homogeneous *N,N'*-dioxide synthesis reported by Feng *et al.*, which is depicted in Scheme 5.9, began with the amide formation between the commercially available *N*-Boc-L-proline and 2,6-diisopropylaniline to obtain **113**. Subsequently, deprotection of the Boc group in acidic media afforded **114**, where two subunits of amide are joined via nucleophilic substitution with the appropriate 1,3-dibromopropane linker. In the last step, chiral compound **115** was oxidized using *m*-CPBA, giving rise to **116**. After analyzing the synthesis, we considered that an appropriate approach for the immobilization of this catalyst onto a solid support could be the use of a functionalized linker instead of 1,3-dibromopropane.[25a, 44]

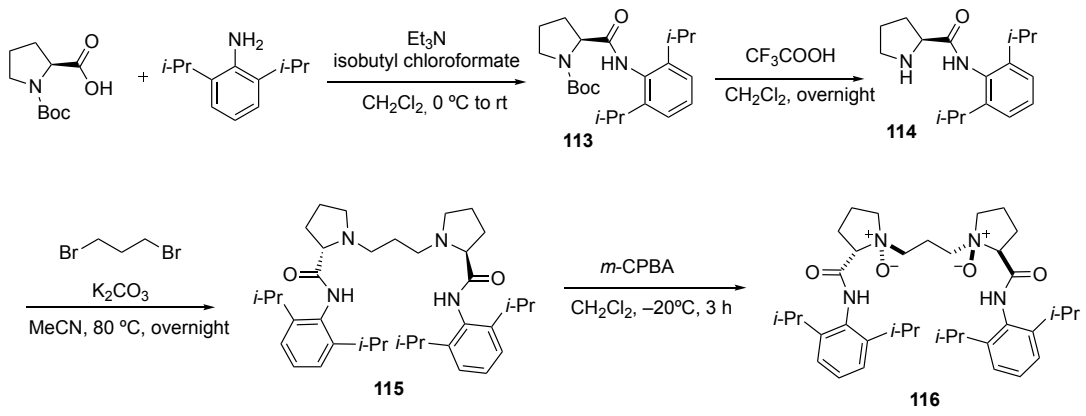

Scheme 5.9: General synthesis of homogeneous *N,N'*-dioxide **116** according to Feng.

With this idea in mind, we postulated the retrosynthetic analysis depicted in Scheme 5.10 that an ether could be an appropriate linker between the catalytic part and the polymer. In our first approach, we attempted to introduce a hydroxy group via hydroxyation of a double bond, which could be introduced in the linker between the two amide subunits (**118**).

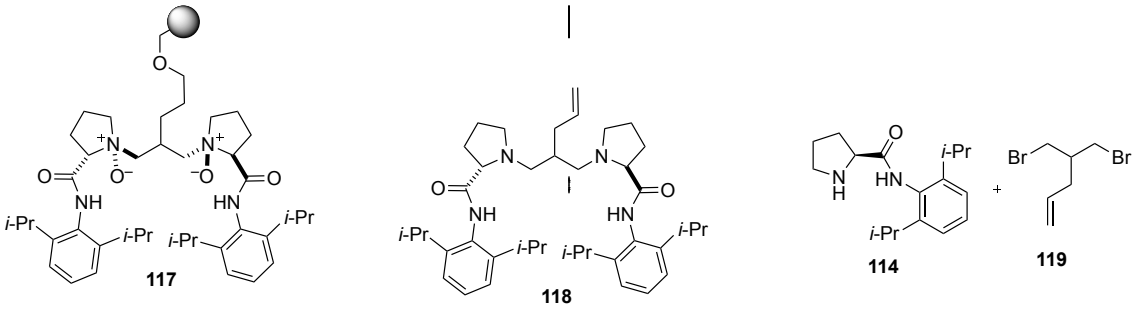

Scheme 5.10: Retrosynthetic analysis for the preparation of immobilized of amine *N,N'*-dioxides.

Our efforts to toward the synthesis of **117** are shown in Scheme 5.11. Reduction of commercially available diethyl allylmalonate with $LiAlH_4$ allowed rapid access to the corresponding diol **120**, which was subjected to Appel reaction to obtain the dibrominated compound **119**. However, under two different conditions using PBr_3 or CBr_4/PPh_3, the formation of compound **119** was not observed. Under conditions 1) the formation of an expected compound was observed, but GC-MS ruled out the formation of the desired product. In contrast, signals corresponding to monobrominated compound were recognized. Working with conditions 2) we recovered mostly starting material. Instead, an alternative was the incorporation of a good leaving group as mesylate to afford **121**. Then, we proceeded to integrate two units of **114**, and compound **118** was obtained with only 30% yield. At this point, the first strategy that we tried to functionalize the linker was the oxidative hydroboration of the alkene to give an alcohol. Unexpectedly, treatment with either 9-BBN or borane with H_2O_2 did not lead to **122**. In view of these results, we considered a second strategy, where 2-mercaptoethanol can be introduced as spacer via thiol-ene reaction, another example of click chemistry. This would leave a hydroxy group that could be used to anchor to the Merrifield resin via nucleophilic substitution. However, when we attempted this transformation (Scheme 5.11, 2nd strategy) a complex mixture was formed. Attempts to purify

via column chromatography resulted in an unidentified product by NMR and exhibited low yield.

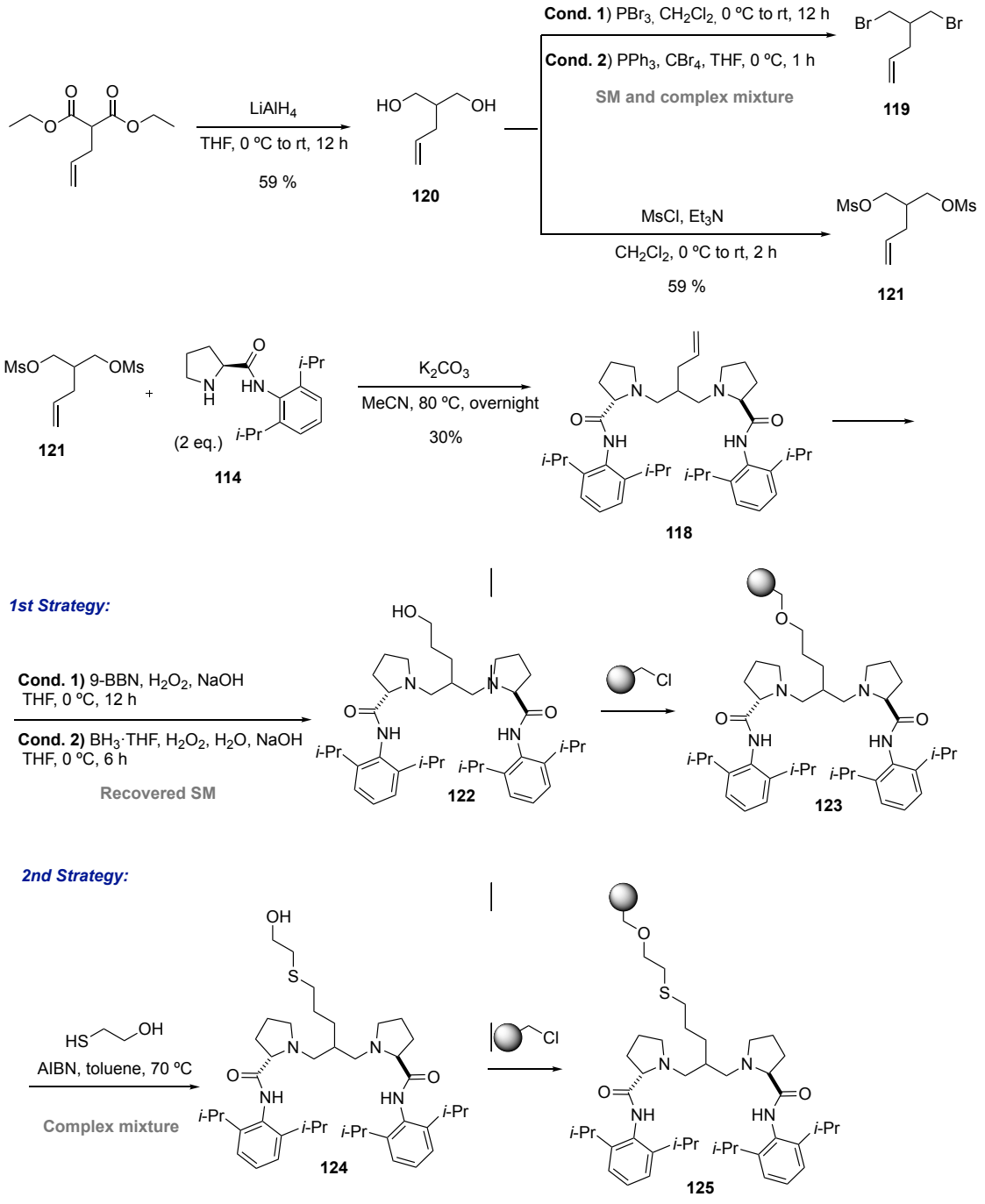

Scheme 5.11: Strategies for alkene functionalization and subsequent immobilization.

In a new modification of our initial strategy, commercially available 1,3-dibromopropan-2-ol was selected as the starting material (**126**, Scheme 5.12). Having a hydroxy group already present in the linker could significantly simplify our synthetic pathway. However, we envisioned the need of a spacer

between the linker and the resin, in order to separate the polystyrene resin from the catalytic center. In Scheme 5.12 the two possible strategies that we devised to immobilize the catalyst are depicted.

Thereby, we first proceeded with the double nucleophilic substitution to form diamide **127**, which was obtained in rather low yield (40%) in comparison of the route using 1,3-dibromopropane. Then, we moved to Path 1), we tried the introduction of 1,8-dichloro-3,6-dioxaoctane (**128**) in basic conditions, as a straightforward integration of the linker, even though double functionalization in the linker could be an issue. However, no reactivity was observed in strong basic conditions.

Next, in view of the difficulty of incorporating a proper functional group for anchoring the monomer to a readily available polymer, we postulated a co-polymerization based strategy analogous to the one followed in Chapter II for the immobilization of CPA. In this perspective, we planned Path 2), which involves the incorporation of a styrene motif in the linker promote the co-polymerization, but also acting as a spacer. Unfortunately, when diamide **127** was subjected to nucleophilic substitution in basic conditions with 4-vinylbenzyl chloride, once again, no reactivity was observed.

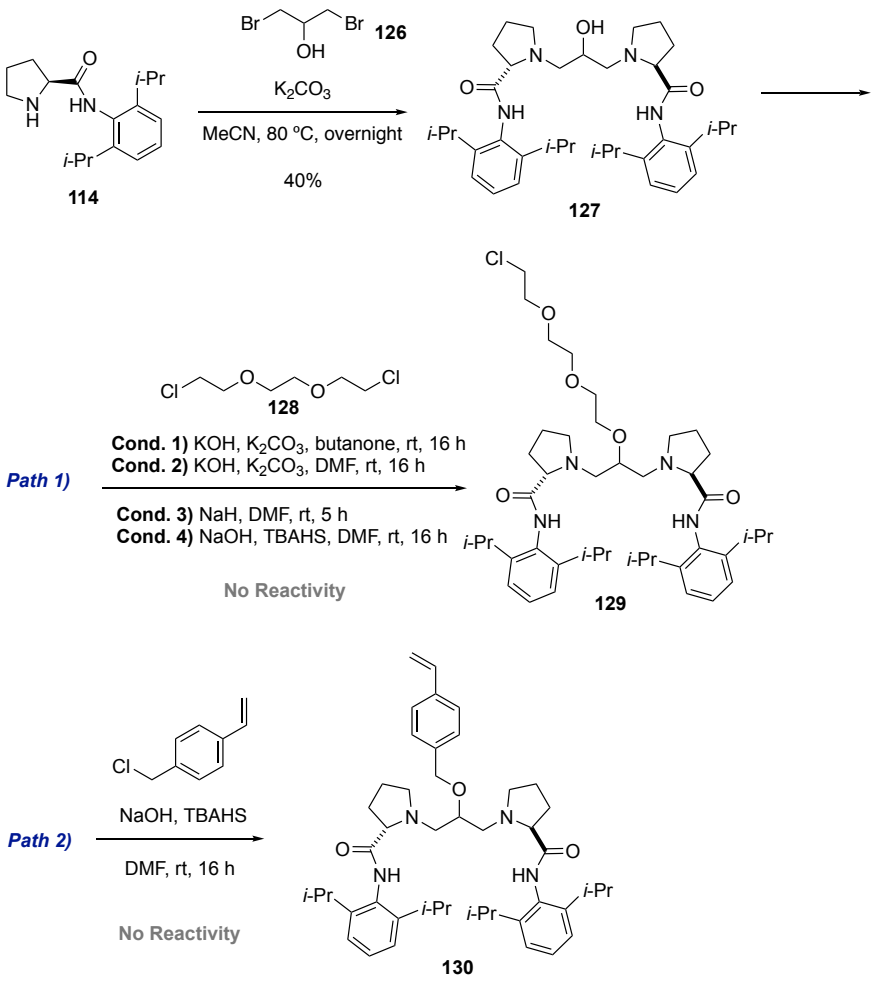

Scheme 5.12: Diamide formation using 1,3-dibromopropan-2-ol as linker.

At this point, we reasoned that the use of NaOH or other strong bases may not be compatible with the N-H amides, which would be a possible explanation to the lack of reactivity. Nevertheless, the last strategy inspired us to design a new synthesis in order to install a styrene moiety in the homogeneous counterpart allow co-polymerization. The new proposed sequence is shown in Scheme 5.13. We began with the esterification of readily available L-proline, which was then converted to **132** in a disappointing 20% yield. Unfortunately, the preparation of **133** could not be accomplished. By NMR analysis of the crude mixture, we could just identify the starting material 4-vinylbenzyl chloride. Under basic conditions, it is reasonable to expect the hydrolysis of

the ester group giving rise to the diacid, which should be soluble in the aqueous phase during the work-up.

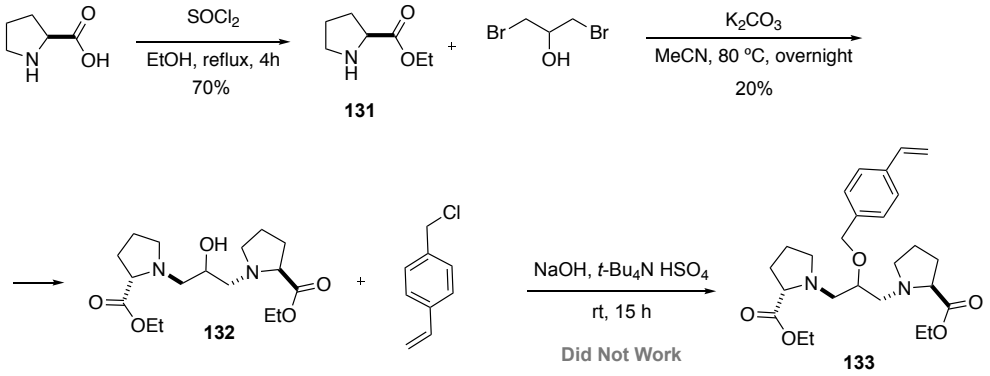

Scheme 5.13: Strategy for the incorporation of a styrene unit to be used in co-polymerization.

As a continuation of our efforts to establish a synthetic pathway involving co-polymerization of a styrene moiety in the linker, we believed that a practical solution could be the formation of a dibrominated linker containing a styrene moiety. Herein, we envisioned the use of a trichloroacetimidate **135** as a base-free alternative in order to develop the *O*-benzylaton leading to **136** (Scheme 5.14). However, efforts to obtain **136** ended up with the recovery of starting material.

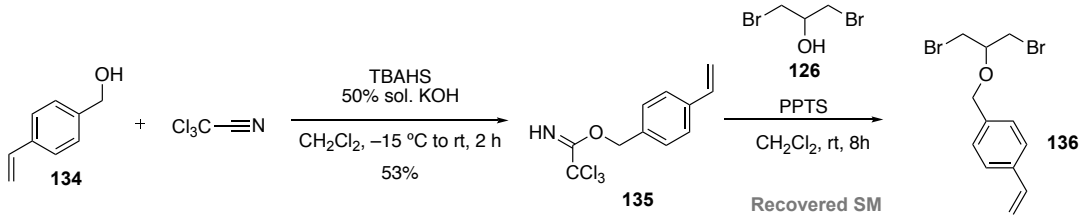

Scheme 5.14: *O*-Benzylation via trichloroacetimidate in acid media.

After these unsuccessful results, we were pleased to find that Kunishima's group reported a novel acid-catalyzed *O*-benzylating reagent, namely 2,4,6-tris(benzyloxy)-1,3,5-triazine (TriBOT) (Scheme 5.15).[45] They were able to convert different functionalized alcohols to the corresponding ether using this TriBOT reagent. The mechanism proceeds first with the protonation of TriBOT

with triflic acid in order to form the corresponding benzyl cation, which allows the formation of benzyl ether via S_N1 with the corresponding alcohol. This process can be repeated up to three times for each molecule of TriBOT. As a result of the absence of base, formation of the elimination product the epoxide or other side reactions, are not expected to take place.

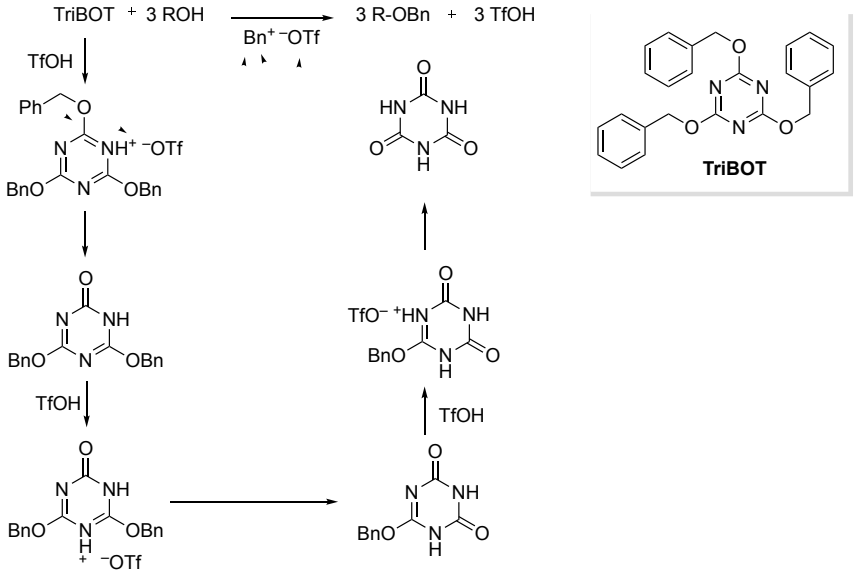

Scheme 5.15: Mechanism for *O*-benzylation using TriBOT.

With this idea in mind, we followed the synthesis in Scheme 5.16. First, we proceeded to prepare a TriBOT derivative from the corresponding 4-vinylbenzyl alcohol **134** (obtained from hydrolysis of 4-vinylbenzyl chloride). Treatment of **134** with cyanuric chloride in basic media resulted in the formation of **139** in 40% yield. Benzylation of 1,3-dibromopropanol using TriBOT analogue **139** in acidic media worked reasonably well. Subsequently, we envisioned that the desired diamide **140** could be generated by nucleophilic substitution of dibromide **136** with proline amide derivative **114**. With the styrene moiety incorporated on the diamide scaffold (**140**) and the previous experience in our group in the co-polymerization of homogeneous species, the plan was to use

the same conditions optimized in our group for the heterogenization of **140**. To this end, use of DVB, styrene and AIBN as radical initiator provided a polystyrene resin that was transformed in the supported *N,N'*-dioxide by oxidation of the tertiary amines of **141** using *m*-CPBA.

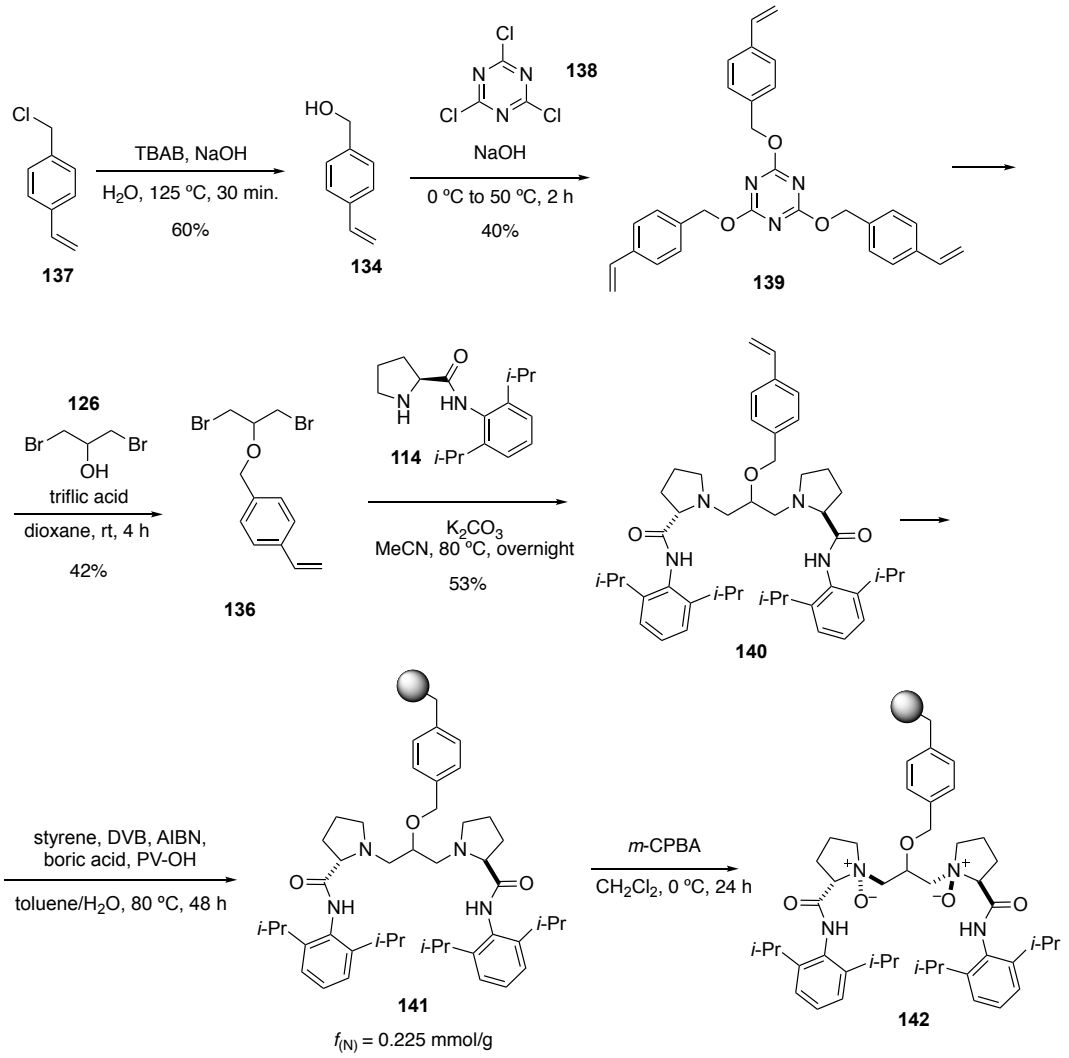

Scheme 5.16: TriBOT derivative for incorporation of a styrene moiety.

Once we achieved the immobilization of the desired *N,N'*-dioxide diamide (**142**), we proceeded to test it in catalysis. As a model reaction, we found a suitable choice could be the asymmetric aza-Friedel-Crafts reaction of sesamol with aldimines catalyzed by *N,N'*-dioxide-Sc(III), reported by the Feng group.[33f] This reaction was interesting due to the scarcity of reports dealing with the synthesis of enantioenriched α-amino-sesamol, which are present in a number of biologically active molecules. Unfortunately, no reactivity was observed, thus recovering starting material (Scheme 5.17). Based on the hypothesis that the problem could arise from the coordination of the metal, we decided to test the behaviour of our supported material as organocatalyst. To this end, we moved to the asymmetric domino Michael-alkylation reaction between (*Z*)-bromonitrostyrenes and dimedones reported by the same group.[43e] This strategy has been extensively applied for the synthesis of dihydrofurans; even 5-monosubstituted cyclohexane-1,3-diones have been examined, giving rise to bicyclic dihydrofurans with three stereocenters. Despite the increase in catalytic activity appreciated (up to 28% of yield of the desired product **144**). our endeavour was not successful in the formation of an optically active compound.

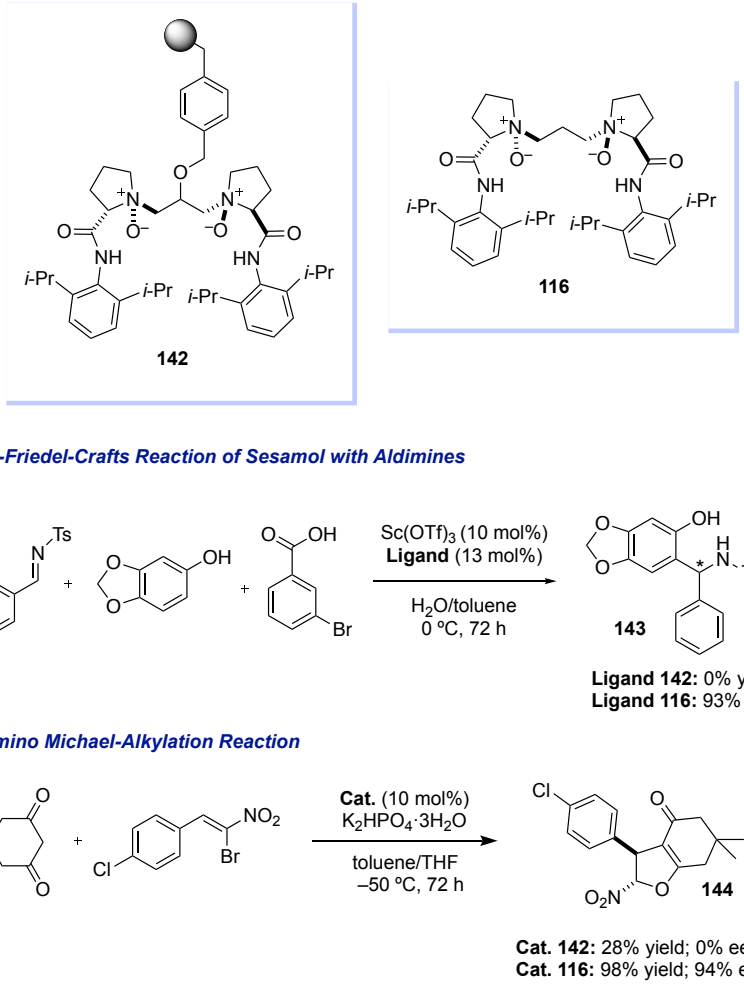

Scheme 5.17: Study of supported *N,N'*-dioxide **142** in the aza-Friedel-Crafts and Michael reactions.

We envisioned that the functionalization of the linker between the two subunits may somewhat influence the selectivity of the catalyst, thus distorting the appropriate chiral environment when the substrates are coordinated.

This results discussed encouraged us to look for a more appealing synthetic pathway, which involves anchoring the homogeneous catalyst onto an amine resin through amide formation.

In this way, we first planned to build up the linker between the two proline derivatives in order to form diacid **145**. For the subsequent amide formation step, two possible pathways were formulated. On the one hand, the amide can be formed directly from an amine-terminated resin (Scheme 5.18, Eq. 1). In

that case, we found convenient to employ benzylamine polystyrene resin (**147**), which can be easily synthesized by nucleophilic substitution of a Merrifield resin with commercially available 4-aminobenzoic acid.[46] Functional dilution in the polymer will ensure that only one of the two acids of the molecule reacts to give the amide, thus leaving one free carboxylic acid. Consequently, further treatments of the resin with 2,6-diisopropylphenyl group was required to get **148**. On the other hand, we speculated that an attractive route could involve the introduction of a spacer between the catalytically active unit and the resin. Thus, as shown in Scheme 5.18, Eq. 2, the first stage is the diamide formation using **146** which is smoothly prepared by bromination of 2,6-diisopropylphenyl with *n*-Bu_4NBr_3.[47] This latter path would allow us to install both 2,6-diisopropyl groups, which are known to be beneficial in terms of chirality induction, whereas the bromoarene could be used for anchoring via cross-coupling.

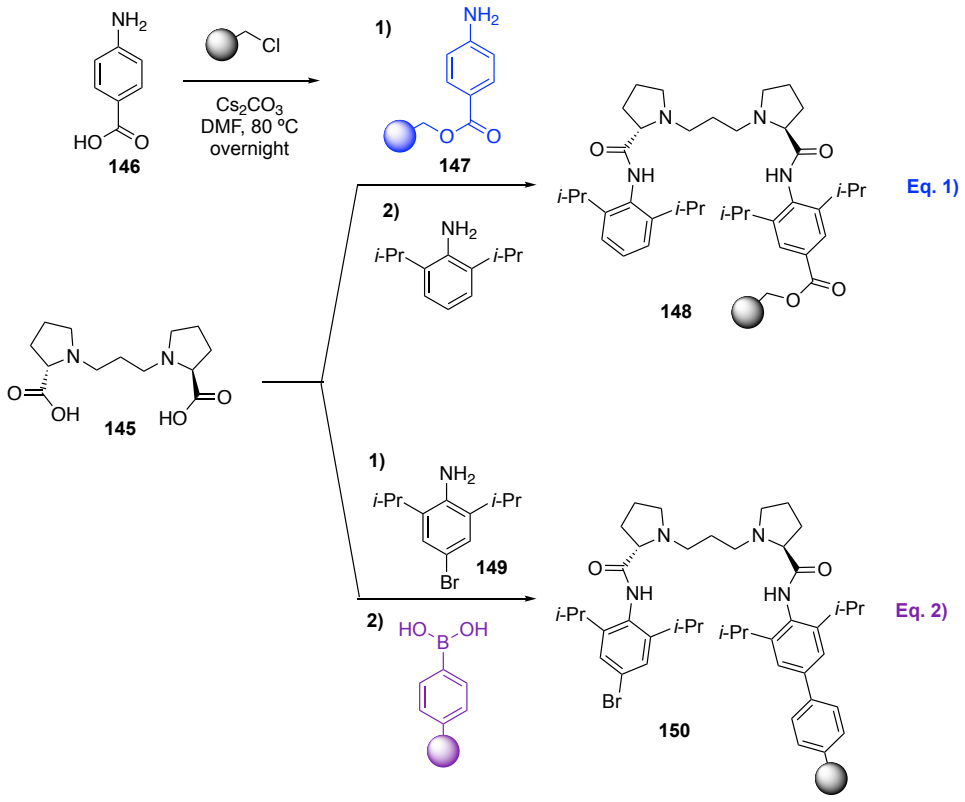

Scheme 5.18: Strategies for the immobilization onto polystyrene-supported aniline.

Our endeavour to implement this strategy started with the esterification of L-proline to furnish **153** in 92% yield as depicted in Scheme 5.19. Two molecules of benzyl prolinate were joined via nucleophilic substitution with 1,3-dibromopropane to generate **154** in moderate yield. This would later undergo hydrogenolysis of the benzyl ester using Pd/C. At this point, before anchoring to the resin, we decided to test the amide formation in homogeneous phase. Unexpectedly, under the typical conditions (Scheme 5.19, Cond. 1)[44] no reactivity was observed. Therefore, alterantive conditions were tested, but the target compound **156** was not obtained in any case.[48]

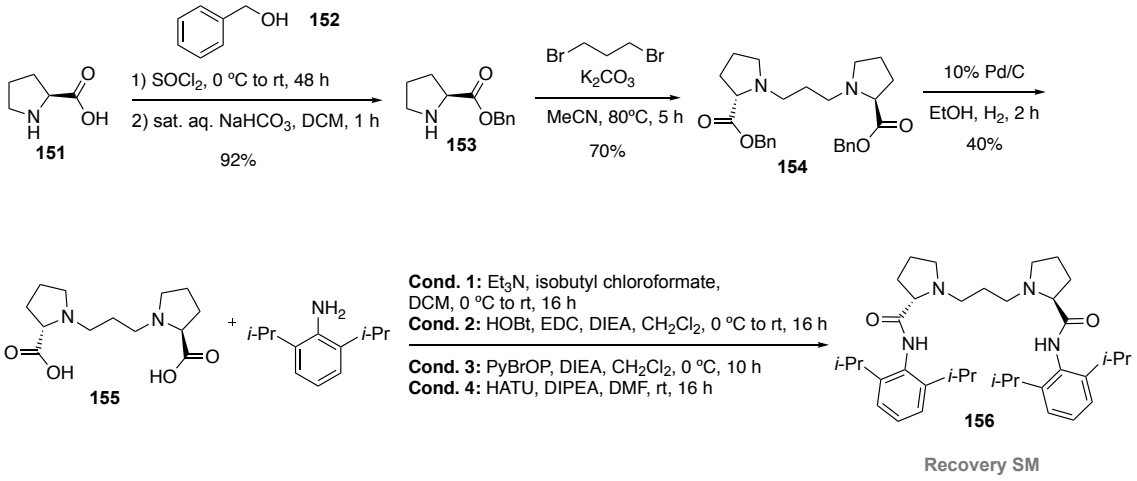

Scheme 5.19: Approach for formation of diamide **156.**

Interest in the strategy shown in Scheme 5.18 Eq. 2, which involves Suzuki coupling to anchor the monomer onto the resin, led us back to the general synthesis for the homogeneous *N,N'*-dioxide (Scheme 5.9). Having a bromine in the aniline moiety was not expected to influence the amide formation, so we thought this approach might lead to the desired diamide to be anchored onto the resin and oxidized.

As shown in Scheme 5.20, we began with the bromination of 2,6-diisopropylaniline in the presence of *n*-Bu_4NBr_3 to deliver **149**. Pleasingly,

intermediate **158** was established after two consecutive reactions, amide formation and deprotection of Boc group, without the need to purify.

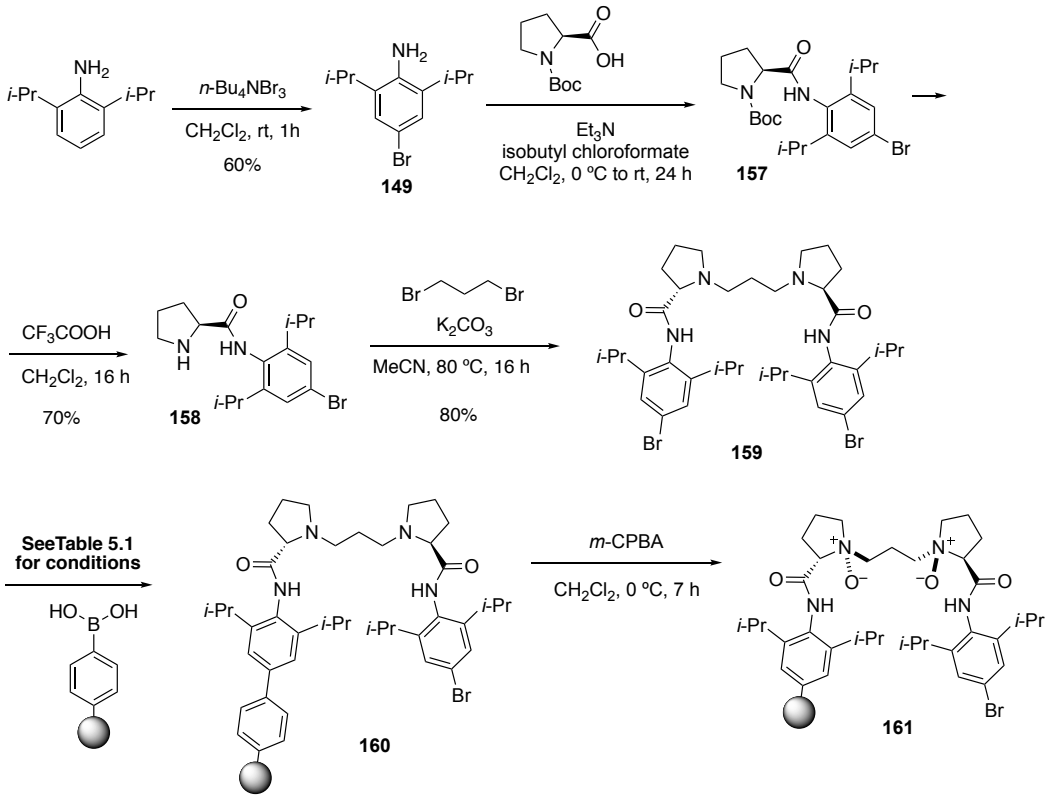

Scheme 5.20: Supported *N,N'*-dioxide amide synthesis via Suzuki coupling strategy.

Finally, to support **159** (Scheme5.20), we first proceeded with the conditions shown in entry 1, Table 5.1, which involve a solid-supported boronic acid. Unfortunately, elemental analysis of the resin showed no traces of nitrogen, thus proving that the reaction did not work. Other conditions, employing *tetrakis*-triphenylphosphine palladium as the catalyst and Na_2CO_3 as base in different solvents were also tested (Table 5.1). We were pleased to observe an improvement in the results under the conditions summarized in entry 6, using a mixture of solvents (toluene and EtOH), but maybe most significantly, the commercial resin employed was more functionalized than in the previous conditions. We were pleased to find that the functionalization of the resin increased up to 0.73 mmol/g_{resin}, being the maximum functionalization 0.87

mmol/g_{resin}. This results encouraged us to oxidize the amine groups in **160** in order to achieve the final supported catalyst **161**.

Table 5.1: Screening of conditions for the Suzuki coupling between diamide **159** and boronic acid resin.[a]

Entry	Catalyst	Reactants	Solvent	$f_{(N)}$	$f_{(Br)}$
1	$Pd(OAc)_2$	$(n\text{-Bu})_4NBr$ K_2CO_3	H_2O	<LOQ	n.d.
2	$Pd(PPh_3)_4$	$(n\text{-Bu})_4NBr$ 2 M aq. Na_2CO_3	toluene	0.39	n.d.
3	$Pd(PPh_3)_4$	0.5 M aq. Na_2CO_3	MeCN	0.18	n.d.
4	$Pd(PPh_3)_4$	0.5 M aq. Na_2CO_3	DMF	0.11	n.d.
5	$Pd(PPh_3)_4$	$(n\text{-Bu})_4NBr$ 2 M aq. Na_2CO_3	toluene	0.15	0.21
6[b]	**$Pd(PPh_3)_4$**	**2 M aq. Na_2CO_3**	**toluene/EtOH**	**0.73**	**0.38**

[a]Reaction conditions: diamide (1.3 eq.), boronic acid resin ($f_{(N)}$ = 1.1 mmol/g_{resin}; 1 eq.), $f_{(max.,\ 160)}$ = 0.65 mmol/g_{resin}, reaction time: 24 h. [b]boronic acid resin ($f_{(N)}$ = 1.9 mmol/g_{resin}; 1 eq.) $f_{(max.,\ 160)}$ = 0.87 mmol/g_{resin}. n.d. = not determined. LOQ = Limit of quantification

Assuming that complete oxidation of the tertiary amines to N-O oxides, with the desired supported PS-*N,N'*-dioxides diamides (**161**), we decided to test **161** as organocatalyst in the same Michael reaction mentioned before (Scheme 5.17). Even if the final product was obtained, **144** was isolated in a completely racemic manner (Scheme 5.21). Note that in the case of using **PS-161** catalyst the yield is much higher in comparison with **PS-142.** Further studies will be carried out in order to determine the best strategy for the immobilization or finding the suitable application for our immobilized Lewis base.

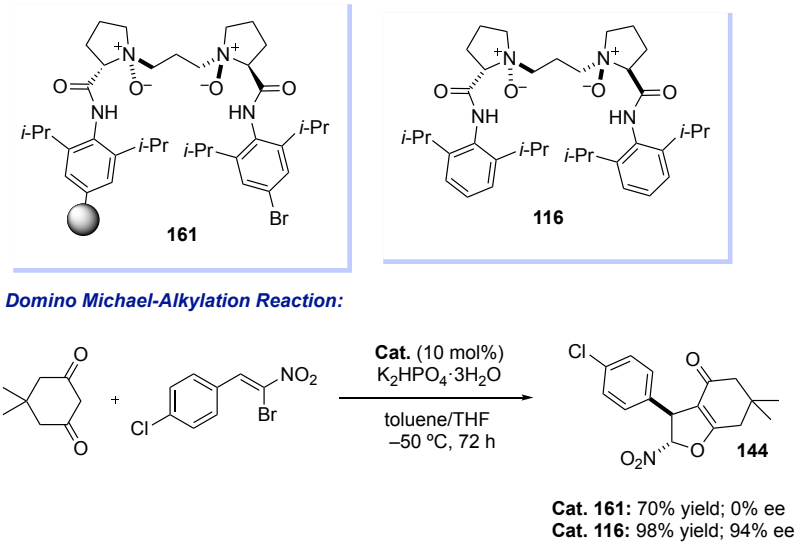

Scheme 5.21: Michael reaction catalyzed by *N,N'*-dioxides.

5.4. Conclusions

To sum up, concurrent with these studies, a proper modification of the precursor for a later immobilization of *N,N'*-dioxide has been designed, and we have been able to accomplish two synthetic pathways for the immobilization of C_2-symmetric *N,N'*-dioxide ligands onto polystyrene.

Unfortunately, both supported catalysts have proven inactive in the Michael reaction, showing low yield and giving rise to a racemic Michael product.

We have confidence that further studies to explore alternative immobilization strategies can lead to the identification of the appropriate supported catalysts.

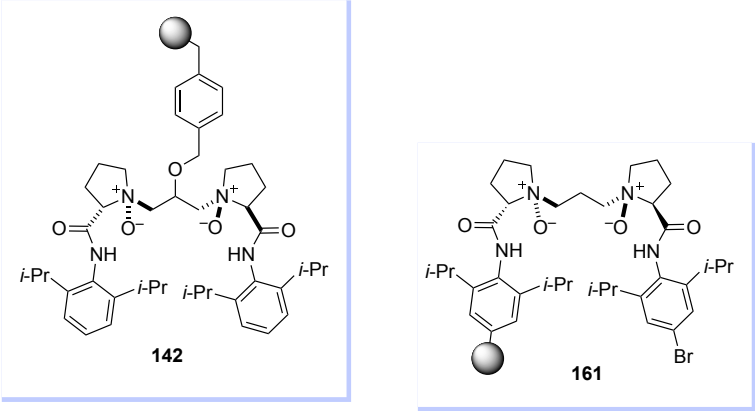

Figure 5.5: Immobilization of *N,N'*-dioxide diamides via two different strategies: **PS-142** via co-polymerization of styrene in the linker and **PS-161** via Suzuki cross coupling with the aryl halide of the amide.

5.5. Experimental Procedures and Characterization of Compounds

5.5.1. General Remarks

Thin layer chromatography was performed on Merck TLC Silicagel 60 F254 aluminum sheets. Components were visualized by UV light (λ = 254 nm) and stained with *p*-anisaldehyde or phosphomolybdic dip. Flash column chromatography was carried out using Sigma-Aldrich 60 mesh silica gel and dry-packed columns. ^{1}H NMR and ^{13}C NMR spectra were recorded at 298 K on a Bruker Avance 500 or 400 Ultrashield apparatus. ^{1}H NMR spectroscopy chemical shifts are quoted in ppm relative to tetramethylsilane (TMS). $CDCl_3$ was used as internal standard for ^{13}C NMR spectra. Chemical shifts are given in δ and coupling constants in Hz. IR spectra were recorded on a Bruker Tensor 27 FT-IR spectrometer and are reported in wavenumbers (cm^{-1}). Elemental analyses were performed by MEDAC Ltd. (Surrey, UK) on a LECO CHNS 932 micro-analyzer. High resolution mass spectrometry analyses were performed in a Waters LCD Premier™ instrument operating in ESI (Electro-Spray Ionization) mode or APCI (Atmospheric-Pressure Chemical Ionization) mode. Specific optical rotation measurements were carried out on a Jasco P-1030 polarimeter.

5.5.2. Characterization of the Intermediates Generated for the Synthesis of *N,N'*-Dioxide Diamides.

tert-Butyl (*S*)-2-((2,6-diisopropylphenyl)carbamoyl)pyrrolidine-1-carboxylate (113)[44]

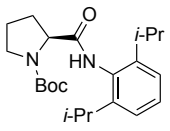

To a solution of Boc-Pro-OH (4 g, 18.60 mmol) in CH_2Cl_2 (37 mL) were added Et_3N (2.9 mL, 20.44 mmol) and isobutyl chloroformate (2.65 mL, 20.44 mmol) at 0 ºC under stirring. After 55 min., 2,6-diisopropylaniline (4.4 mL, 23.23 mmol) was added. The reaction mixture was allowed to warm to rt and monitored by TLC. After 24 h, the mixture was washed with 1 M $KHSO_4$, saturated $NaHCO_3$, brine, dried over anhydrous $MgSO_4$ and concentrated. The product **113** was used without further purification. **^{1}H NMR** (400 MHz, $CDCl_3$) δ 8.31 (br s, 1H), 7.31 – 7.27 (m, 1H), 7.16 (d, *J* = 7.7 Hz, 2H), 4.61 – 4.47 (m, 1H), 3.67 – 3.34 (m, 2H), 3.13 – 2.97 (m, 2H), 2.61 – 2.38 (m, 1H), 2.07 – 1.89 (m, 3H), 1.51 (s, 9H), 1.19 (dd, *J* = 11.8, 6.9 Hz, 12H).

(*S*)-*N*-(2,6-Diisopropylphenyl)pyrrolidine-2-carboxamide (114)[44]

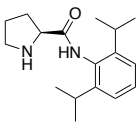

To a solution of **113** (3.3 g, 8.9 mmol) in CH_2Cl_2 (11.55 mL) was added trifluoroacetic acid (2.87 mL, 8.9 mmol) and the mixture was stirred for a further 10 h. Then, the solvent was evaporated and H_2O was added. The pH value of the mixture was brought into the range of 10 – 12 by addition of 2 M NaOH. The aqueous phase was extracted with CH_2Cl_2 (×5). The combined organic phase was washed with brine, dried over $MgSO_4$ and evaporated in vacuo. The residue was directly used in the next step without further purification. **^{1}H NMR** (500 MHz, $CDCl_3$) δ 9.17 (s, 1H), 7.29 – 7.24 (m, 1H), 7.16 (d, *J* = 7.7 Hz, 2H), 4.03 (dd, *J* = 9.2, 5.1 Hz, 1H), 3.20 – 3.11

(m, 1H), 3.11 – 2.95 (m, 3H), 2.32 – 2.20 (m, 1H), 2.17 – 2.06 (m, 1H), 1.92 – 1.77 (m, 2H), 1.20 (t, *J* = 6.7 Hz, 12H).

2-Allylpropane-1,3-diol (120)[49]

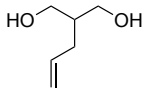

A 250 mL round-bottom flask flushed with argon was charged with a solution of $LiAlH_4$ 1.0 M in THF (36.7 mL, 36.7 mmol) and anhydrous THF (27 mL). Then, to the mixture was added via a cannula a solution of diethyl allylmalonate (3.45 ml, 17.48 mmol) in anhydrous THF (27 mL) at 0 ºC. The reaction was allowed to warm up to rt and stirred for 12 h. TLC analysis indicated the disappearance of the starting material and the reaction was quenched by adding dropwise water in an ice bath. The precipitated white aluminum salt was filtered off and washed thoroughly with ether (×3). The filtrate was washed with sat. aq. NaCl, dried over Na_2SO_4, and concentrated *in vacuo*. The crude product was purified by flash column chromatography eluting with cyclohexane/EtOAc (80:20) to afford the desired **120** as a colourless oil in 59% yield. **^{1}H NMR** (500 MHz, $CDCl_3$) δ 5.79 (ddt, *J* = 17.2, 10.1, 7.1 Hz, 1H), 5.10 – 5.00 (m, 2H), 3.80 (dd, *J* = 10.7, 4.0 Hz, 2H), 3.67 (dd, *J* = 10.7, 7.2 Hz, 2H), 2.45 (br s, 2H), 2.06 (tt, *J* = 7.1, 1.3 Hz, 2H), 1.92 – 1.81 (m, 1H). **^{13}C NMR** (126 MHz, $CDCl_3$) δ 136.4, 116.8, 65.9 (×2), 41.9, 32.7.

2-Allylpropane-1,3-diyl dimethanesulfonate (121)[50]

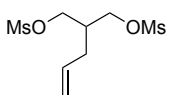

To a chilled solution of **120** (150 mg, 1.29 mmol), Et_3N (396 μL, 2.84 mmol) in dry DCM (4 mL) was added dropwise MsCl (220 μL, 2.84 mmol). The resulting suspension was stirred at 0 ºC for two hours. Then, it was quenched with water, acidified with 2 M HCl and extracted with DCM (×3). The combined organic phases were dried over Na_2SO_4 and

concentrated *in vacuo*. The crude product was purified using flash column chromatography with CH_2Cl_2/EtOAc (90:10) to afford the desired **121** as a colourless oil in 59% yield. **^{1}H NMR** (400 MHz, $CDCl_3$) δ 5.83 – 5.65 (m, 1H), 5.21 – 5.10 (m, 2H), 4.28 (dd, *J* = 10.1, 4.2 Hz, 2H), 4.19 (dd, *J* = 10.1, 6.0 Hz, 2H), 3.03 (s, 6H), 2.32 – 2.15 (m, 3H).

(2*S*,2'*S*)-1,1'-(2-Allylpropane-1,3-diyl)bis(*N*-(2,6-diisopropylphenyl) pyrrolidine-2-carboxamide) (118)

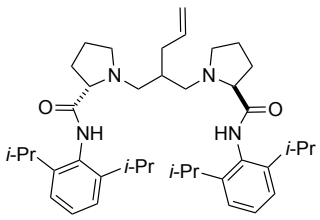

To a solution of the carboxamide **114** (242 mg, 0.881 mmol) in MeCN (1.3 μL) was added K_2CO_3 (268 mg, 1.94 mmol) and **121** (120 mg, 0,441 mmol) under stirring. The reaction mixture was kept at 80 °C overnight. Then, K_2CO_3 was removed by filtration and washed with CH_2Cl_2. The crude product was purified by flash column chromatography on silica gel using CH_2Cl_2/EtOAc (70:30) as the eluent to give compound **118** in 30% yield. **^{1}H NMR** (400 MHz, $CDCl_3$) δ 7.33 – 7.22 (m, 2H), 7.21 – 7.10 (m, 4H), 5.89 – 5.70 (m, 1H), 5.19 – 4.92 (m, 2H), 4.70 – 4.42 (m, 1H), 4.41 – 4.17 (m, 1H), 3.66 – 3.14 (m, 4H), 3.13 – 2.92 (m, 5H), 2.90 – 2.72 (m, 1H), 2.69 – 2.58 (m, 1H), 2.58 – 2.46 (m, 1H), 2.46 – 2.18 (m, 4H), 2.16 – 2.06 (m, 2H), 2.02 – 1.83 (m, 4H), 1.79 – 1.62 (m, 1H), 1.33 – 1.07 (m, 24H). **^{13}C NMR** (126 MHz, $CDCl_3$) δ 174.0 (×2), 146.1 (×2), 145.9 (×2), 135.8, 131.1 (×2), 128.2 (×2), 123.5 (×4), 117.2, 69.0 (×2), 60.9 (×2), 59.0 (×2), 54.3 (×2), 37.6, 30.7, 28.9 (×2), 28.8 (×2), 24.9 (×2), 23.8 (×4), 23.7 (×4). **HRMS** (ESI+): *m/z* calcd. for $C_{40}H_{61}N_4O_2$ $[M+H]^+$: 629.4789, found: 629.4760. **mp**: 88 – 92 °C. **$[\alpha]_D$**: +97.8 (*c* 1.00, CH_2Cl_2).

(2*S*,2'*S*)-1,1'-(2-Hydroxypropane-1,3-diyl)bis(*N*-(2,6-diisopropylphenyl)pyrrolidine -2-carboxamide) (117)

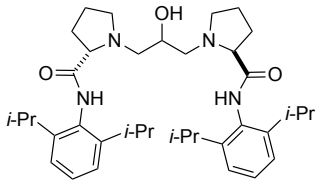

To a solution of carboxamide **114** (150 mg, 0.7 mmol) in MeCN (2 mL) was added K_2CO_3 (419 mg, 3.0 mmol) and 1,3-dibromopropan-2-ol (150 mg, 0.69 mmol) under stirring. The reaction mixture was kept at 80 ºC overnight. Then, K_2CO_3 was removed by filtration and washed with CH_2Cl_2. The crude product was purified by flash column chromatography on silica gel using CH_2Cl_2/EtOAc (90:10) as the eluent to give compound **117** in 40% yield. **^{1}H NMR** (400 MHz, $CDCl_3$) δ 8.70 (br s, 2H), 7.33 – 7.22 (m, 2H), 7.19 – 7.12 (m, 4H), 4.05 – 3.94 (m, 1H), 3.47 – 3.26 (m, 4H), 3.12 – 2.94 (m, 4H), 2.88 – 2.77 (m, 2H), 2.68 – 2.54 (m, 4H), 2.45 – 2.19 (m, 2H), 2.15 – 2.05 (m, 2H), 1.99 – 1.80 (m, 4H), 1.68 (br s, 1H), 1.23 – 1.17 (m, 24H). ^{13}C NMR (126 MHz, $CDCl_3$) δ 174.2, 173.5, 146.1, 145.8, 145.8, 131.4, 131.2, 128.3, 128.2, 128.0, 123.5 (×2), 123.4 (×2), 68.9, 68.8, 68.5, 61.5, 60.9, 60.4, 56.4, 53.6, 47.6, 31.0, 30.9, 30.5, 29.0, 29.0, 28.9, 28.8, 26.5, 25.3, 24.6, 23.9, 23.7, 23.6, 23.6. **HRMS** (ESI-): *m/z* calcd. for $C_{37}H_{55}N_4O_3$ $[M-H]^-$: 603.4280, found: 603.4268. **mp**: 95–100 °C. **$[\alpha]_D$**: –77.9 (*c* 1.00, CH_2Cl_2).

Ethyl *L*-prolinate (131)[51]

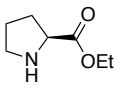

To a solution of L-proline (2 g, 17.4 mmol) in dry EtOH (39.9 mL) was added dropwise $SOCl_2$ (2.5 ml, 34.7 mmol) at rt. Then, the reaction mixture was refluxed for 4 h. After that time, the reaction mixture was concentrated under reduced pressure, neutralized with 4 N NaOH at 0 ºC and then successively extracted with CH_2Cl_2. The combined organic phases were washed with brine and dried over $MgSO_4$. The product was further purified by recrystallization using Et_2O to obtain **131** in 70% yield as a colourless oil. **^{1}H**

NMR (400 MHz, $CDCl_3$) δ 4.10 – 3.91 (m, 2H), 3.68 – 3.50 (m, 1H), 2.97 – 2.82 (m, 1H), 2.81 – 2.65 (m, 1H), 2.39 (s, 1H), 2.08 – 1.88 (m, 1H), 1.74 – 1.63 (m, 1H), 1.64 – 1.53 (m, 2H), 1.17 – 1.05 (m, 3H). **^{13}C NMR** (126 MHz, $CDCl_3$) δ 175.5, 61.1, 59.7, 47.0, 30.4, 25.5, 14.3.

Diethyl (2-hydroxypropane-1,3-diyl)(*S*)-di-L-prolinate (132)

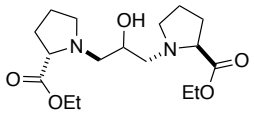

To a solution of ethyl L-prolinate (79 mg, 0.55 mmol) in MeCN (834 μl) was added K_2CO_3 (167 mg, 1.2 mmol) and 1,3-dibromopropan-2-ol (28.1 μL, 0,28 mmol) under stirring. The reaction mixture was kept at 80 °C and monitored by TLC. Then, K_2CO_3 was removed by filtration and washed with CH_2Cl_2. The crude product was purified by flash column chromatography on silica gel using CH_2Cl_2/EtOAc (90:10) as the eluent to give compound **132** in 20% yield as a slightly yellow solid. **^{1}H NMR** (500 MHz, $CDCl_3$) δ 4.13 (qt, *J* = 7.1, 1.5 Hz, 4H), 3.83 (br s, 1H), 3.76 – 3.67 (m, 1H), 3.35 – 3.24 (m, 1H), 3.24 – 3.11 (m, 3H), 2.67 – 2.47 (m, 5H), 2.44 – 2.36 (m, 1H), 2.17 – 2.03 (m, 2H), 1.94 – 1.72 (m, 6H), 1.23 (t, *J* = 7.1 Hz, 6H). **^{13}C NMR** (126 MHz, $CDCl_3$) δ 174.7, 174.7, 67.7, 66.3, 66.0, 60.7, 60.6, 59.4, 59.2, 54.5, 54.0, 29.7, 29.6, 23.8, 23.6, 14.3 (×2). **HRMS** (ESI+): *m/z* calcd. for $C_{17}H_{31}N_2O_5$ $[M+H]^+$: 343.2227, found: 343.2222. **mp**: 115 – 117 °C.

(4-Vinylphenyl)metanol (134)[52]

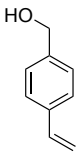

To a solution of NaOH (5.24 mg, 0.31 mmol) and tetrabutylammonium bromide (422 mg, 1.31 mmol) in water (6 mL) was added 4-vinylbenzyl chloride (185 μL, 1.31 mmol). The mixture was heated at 125 °C for 20 min. and subsequently cooled in an ice bath. Upon cooling, the mixture was extracted with EtOAc (×3), the combined organic layers were dried over $MgSO_4$ and the solvent was evaporated under reduced

pressure. The cude mixture was subjected to column chromatography eluting with cyclohexane/EtOAc (80:20). Compound **134** was obtained in 60% yield as a colourless oil. **^{1}H NMR** (500 MHz, $CDCl_3$) δ 7.40 (d, *J* = 8.2 Hz, 2H), 7.31 (d, *J* = 8.0 Hz, 2H), 6.72 (dd, *J* = 17.6, 10.9 Hz, 1H), 5.76 (dd, *J* = 17.6, 0.9 Hz, 1H), 5.25 (dd, *J* = 10.9, 0.9 Hz, 1H), 4.65 (s, 2H), 2.03 (br s, 1H). **^{13}C NMR** (126 MHz, $CDCl_3$) δ 140.5, 137.1, 136.6, 127.3 (×2), 126.5 (×2), 114.0, 65.1.

4-Vinylbenzyl 2,2,2-trichloroacetimidate (135)

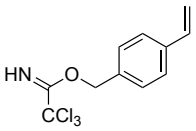

Into a mixed solution of **134** (1.0 g, 7.45 mmol) and CH_2Cl_2 (8 mL) was added a solution of 50% aq. KOH (8.10 mL, 7.45 mmol) and tetrabutylammonium hydrogensulfate (1.3 mg, 3.7 μmol). Then, the resulting mixture was vigorously stirred at –10 °C for 5 min and consequently 2,2,2-trichloroacetonitrile (0.9 mL, 8.94 mmol) was added dropwise. Finally, the reaction mixture was stirred for a further 30 min. and then allowed to warm to rt for 30 min. The organic layer was separated, and the aqueous layer was further extracted with CH_2Cl_2 (×3). Finally, the collected organic layers were dried with anhydrous Na_2SO_4. The concentrated residue was purified via column chromatography eluting with cyclohexane/CH_2Cl_2 (7:1). Compound **135** was obtained in 53% yield as a colourless oil. **^{1}H NMR** (300 MHz, $CDCl_3$) δ 8.40 (s, 1H), 7.50 – 7.33 (m, 4H), 6.73 (dd, *J* = 17.6, 10.9 Hz, 1H), 5.77 (dd, *J* = 17.6, 1.0 Hz, 1H), 5.34 (s, 2H), 5.28 (dd, *J* = 10.9, 0.9 Hz, 1H). **^{13}C NMR** (126 MHz, $CDCl_3$) δ 162.0, 138.5, 136.3, 133.2, 128.8 (×2), 126.7 (×2), 115.1, 70.6. **$[\alpha]_D$**: –3.1 (*c* 1.00, CH_2Cl_2).

2,4,6-tris((4-Vinylbenzyl)oxy)-1,3,5-triazine (139)

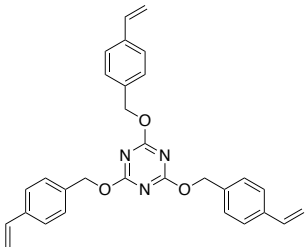

To a suspension of powdered sodium hydroxide (0.08 g, 2.0 mmol) in **134** (0.73 g, 5.46 mmol) was added cyanuric chloride (0.11 g, 0.6 mmol) portionwise at 0 °C. After stirring for 30 min, the reaction mixture was heated at 50 °C and stirred for additional 2 h. Then, the reaction mixture was cooled to rt, and the precipitate was filtered off through a silica pad. Excess benzyl alcohol was evaporated under reduced pressure, and the residue was purified by flash column chromatography eluting with cyclohexane/EtOAc (95:5) to give triazine **139** in 40% yield as a slightly yellow solid. **^{1}H NMR** (400 MHz, $CDCl_3$) δ 7.48 – 7.35 (m, 12H), 6.72 (dd, *J* = 17.6, 10.9 Hz, 3H), 5.76 (dd, *J* = 17.6, 0.9 Hz, 3H), 5.43 (s, 6H), 5.27 (dd, *J* = 10.8, 0.9 Hz, 3H). **^{13}C NMR** (101 MHz, $CDCl_3$) δ 173.1 (×3), 137.8 (×3), 136.4 (×3), 134.9 (×3), 128.6 (×6), 126.5 (×6), 114.5 (×3), 69.7 (×3). **HRMS** (ESI+): *m/z* calcd. for $C_{30}H_{28}N_3O_3$ $[M+H]^+$: 478.2125, found: 478.2112. **mp**: 95 – 97 °C.

1-(((1,3-Dibromopropan-2-yl)oxy)methyl)-4-vinylbenzene (136)

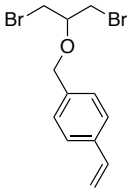

To a mixture of **139** (1.27 g, 2,66 mmol),1,3-dibromopropan-2-ol (0.68 mL, 6.65 mmol) and 5 Å MS (1.7 g, 25 mg/mL) in 1,4-dioxane (67 mL) was added triflic acid (0.12 mL, 1.33 mmol) at rt under N_2 atmosphere. The reaction mixture was stirred for 4 hours. After that time, the reaction mixture was neutralized with solid $NaHCO_3$, filtered through silica gel and concentrated under reduced pressure. The residue was purified by flash column chromatography on silica gel using cyclohexane/CH_2Cl_2 (90:10) as eluent to afford the dibromoalkene **136** as a pale oil in 42% yield. **^{1}H NMR** (400 MHz, $CDCl_3$) δ 7.42 (d, *J* = 8.1 Hz, 2H),

7.34 (d, *J* = 8.1 Hz, 2H), 6.72 (dd, *J* = 17.6, 10.9 Hz, 1H), 5.76 (dd, *J* = 17.6, 0.9 Hz, 1H), 5.27 (dd, *J* = 10.9, 0.9 Hz, 1H), 4.65 (s, 2H), 3.93 – 3.70 (m, 1H), 3.57 (d, *J* = 5.2 Hz, 4H). **^{13}C NMR** (101 MHz, $CDCl_3$) δ 137.7, 136.9, 136.5, 128.3 (×2), 126.5 (×2), 114.3, 77.2, 72.2, 32.7 (×2). **HRMS** (ESI+): *m/z* calcd. for $C_{12}H_{14}Br_2NaO$ $[M+Na]^+$: 354.9304, found: 354.9308.

(2*S*,2'*S*)-1,1'-(2-((4-Vinylbenzyl)oxy)propane-1,3-diyl)bis(*N*-(2,6-diisopropylphenyl)pyrrolidine-2-carboxamide) (140)

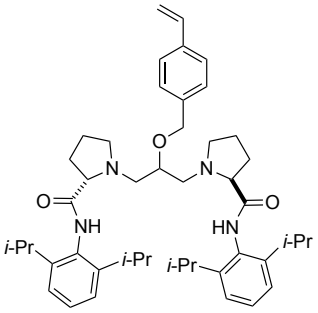

To a solution of **114** (232 mg, 0.84 mmol) in MeCN (1.3 mL) was added K_2CO_3 (257 mg, 1.86 mmol) and **136** (141 mg, 0,42 mmol) under stirring. The reaction mixture was kept at 80 ºC overnight. Then, K_2CO_3 was removed by filtration and washed with CH_2Cl_2. The crude was subjected to flash column chromatography on silicagel with 2.5% Et_3N, eluting with cyclohexane/EtOAc (80:20) to give diamide **140** in 53% yield as a slightly yellow solid. **^{1}H NMR** (400 MHz, $CDCl_3$) δ 9.11 (br s, 1H), 8.58 (br s, 1H), 7.33 – 7.24 (m, 3H), 7.21 – 7.10 (m, 4H), 7.03 (s, 3H), 6.57 (dd, *J* = 17.6, 10.9 Hz, 1H), 5.61 (dd, *J* = 17.6, 1.0 Hz, 1H), 5.20 (dd, *J* = 10.9, 0.9 Hz, 1H), 4.72 – 4.52 (m, 2H), 3.85 – 3.73 (m, 1H), 3.39 – 3.22 (m, 3H), 3.19 – 2.79 (m, 9H), 2.57 – 2.41 (m, 1H), 2.40 – 2.17 (m, 3H), 2.12 – 2.05 (m, 1H), 2.00 – 1.75 (m, 4H), 1.63 (s, 1H), 1.25 – 1.04 (m, 24H). **^{13}C NMR** (101 MHz, $CDCl_3$) δ 173.7, 173.7, 145.8 (×4), 137.2, 137.1, 136.4, 131.7, 131.0, 128.4, 128.1, 127.6 (×2), 126.2 (×2), 123.7 (×2), 123.4 (×2), 114.1, 75.7, 72.1, 69.6, 68.0, 59.7, 58.8, 54.9, 54.1, 30.6, 30.5, 29.0 (×2), 28.8 (×2), 25.2, 24.9, 23.8 (×4), 23.6 (×4). **HRMS** (ESI+): *m/z* calcd. for $C_{46}H_{65}N_4O_3$ $[M+H]^+$: 721.5051, found: 721.5077. **mp**: 70–77 °C. **$[\alpha]_D$**: +76.4 (*c* 1.00, CH_2Cl_2).

Polystyrene supported diamide (141)

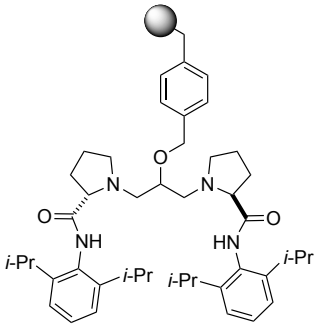

A 100 mL reactor was charged with a suspension of polyvinyl alcohol (PV-OH) (54.3 mg, 0.52 μmol) in 51 mL of deionized and degassed water. The solution was heated at 90 ºC until PV-OH was dissolved. Then, it was cooled to rt and a solution under N_2, containing divinylbenzene (DVB; 80%, 620 μL, 3.56 mmol; filtered on a short pad of silica immediately before use), diamide **140** (250 mg, 0.35 mmol), styrene (1.6 mL, 14.25 mmol), boric acid (251 mg, 4.06 mmol) and AIBN (16.4 mg, 0.1 mmol) in toluene (1.47 mL) was transferred to the reactor. After that, the system was heated at 80 ºC and mechanically stirred at 440 rpm. After two days, the aqueous solution was decanted off and the resin was washed with water (50 °C) several times, followed by MeOH and CH_2Cl_2. Finally, it was dried overnight in a vacuum oven at 40 °C to afford a colourless to pale yellow resin (1.22 g). **N elemental analysis** (%): 1.26. $f_{(N)}$: 0.225 mmol/$g_{resin.}$

Polystyrene supported *N,N'*-dioxide diamide (142)

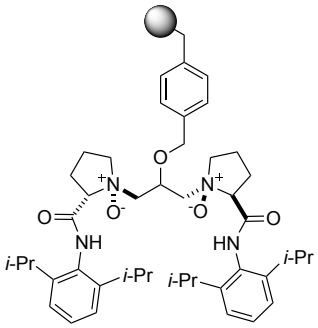

To a solution of diamide **141** (400 mg, 0.09 mmol) in CH_2Cl_2 (0.45 mL) was added *m*-CPBA (0.04 g, 0.18 mmol) at 0 ºC. The reaction mixture was stirred for 24 h at 0 °C. After that time, the resin was filtered and washed with MeOH and CH_2Cl_2. Finally, it was dried overnight in a vacuum oven at 40 °C to afford a colourless to pale yellow resin (400 mg).

Benzyl *L*-prolinate (153)[53]

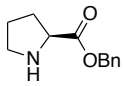

A 250 mL round bottom flask was charged with benzyl alcohol (67 ml, 651 mmol) and a magnetic stiring bar under nitrogen atmosphere. Then, it was cooled to 0 °C and $SOCl_2$ (6.7 mL, 91 mmol) was added slowly followed by L-proline (5.0 g, 87 mmol). The reaction mixture was stirred at 0 °C under nitrogen for 2 h. After that time, the solution was warmed to room temperature and stirring was maintained for a further 48 h. The solution was poured into 300 mL Et_2O and stored at –26 °C for one week. The precipitate was collected by vacuum filtration, rinsed with diethyl ether, and dried in vacuo to afford a white solid in 93% yield. The product obtained was treated in basic media. A solution of saturated bicarbonate (36 mL) was added dropwise over 20 min. at rt to a suspension of benzyl *L*-prolinate·HCl (4.65 g, 19.2 mmol) in CH_2Cl_2 (45 mL) under vigorous stirring. After stirring for 1 h the organic phase was extracted and dried over $MgSO_4$, filtered and concentrated in vacuo. **^{1}H NMR** (500 MHz, $CDCl_3$) δ 7.39 – 7.30 (m, 5H), 5.15 (s, 2H), 3.79 (dd, J = 8.7, 5.7 Hz, 1H), 3.10 – 3.02 (m, 1H), 2.95 – 2.83 (m, 1H), 2.44 (br s, 1H), 2.18 – 2.06 (m, 1H), 1.90 – 1.81 (m, 1H), 1.81 – 1.67 (m, 2H). **^{13}C NMR** (126 MHz, $CDCl_3$) δ 175.4, 135.9, 128.7, 128.5, 128.4, 128.2, 126.9, 66.7, 59.8, 47.1, 30.3, 25.5.

Dibenzyl propane-1,3-diyl(*S*)-di-*L*-prolinate (154)[48]

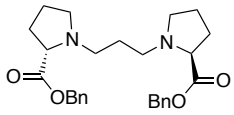

To a solution **153** (8.4 g, 41.1 mmol) in MeCN (51.4 ml) were added K_2CO_3 (13.4 g, 97 mmol) and 1,3-dibromopropane (2.1 mL, 20.6 mmol) under stirring. Then, the reaction was kept at 80 °C, and monitored by TLC. Once the reaction was completed, K_2CO_3 was removed by filtration and washed with CH_2Cl_2. The crude product was purified by flash column chromatography on silica gel using CH_2Cl_2/EtOAc

(90:10) as the eluent to give compound **154** in 70% yield as a slightly yellow oil with some impurities. **^{1}H NMR** (300 MHz, $CDCl_3$) δ 7.35 – 7.26 (m, 10H), 5.21 – 5.04 (m, 4H), 3.20 – 3.07 (m, 4H), 2.72 – 2.59 (m, 2H), 2.45 – 2.23 (m, 4H), 2.16 – 2.03 (m, 2H), 1.97 – 1.73 (m, 6H), 1.73 – 1.59 (m, 2H). **^{13}C NMR** (126 MHz, $CDCl_3$) δ 173.9, 141.2, 136.0, 128.6, 128.5, 128.3, 128.2, 127.5, 127.0, 66.3, 66.0, 65.1, 53.4, 53.1, 29.3, 23.1.

(2'*S*)-Propane-1,3-diyldi-*L*-proline (155)[48]

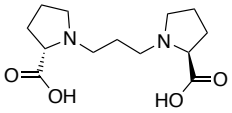

A 100 mL round bottom flask was charged with 10% Pd/C (1.05 g, 9.9 mmol) and degassed EtOH (35 mL) under H_2. To the suspension, **154** (5.1 g, 11.3 mmol) was added and the mixture was stirred at rt for 2 h. Once the reaction was completed, the solution was filtered through Celite to remove the Pd/C and the filtrate was evaporated to afford a white solid. This crude product was used in the next step without further purification. **^{1}H NMR** (500 MHz, D_2O) δ 4.00 (dd, J = 9.5, 6.5 Hz, 2H), 3.85 – 3.77 (m, 2H), 3.43 – 3.34 (m, 2H), 3.34 – 3.26 (m, 2H), 3.25 – 3.16 (m, 2H), 2.53 – 2.44 (m, 2H), 2.23 – 2.08 (m, 6H), 2.05 – 1.93 (m, 2H). **^{13}C NMR** (126 MHz, D_2O) δ 173.7 (×2), 69.3 (×2), 55.3 (×2), 51.0 (×2), 28.9 (×2), 23.0 (×2), 22.3.

4-Bromo-2,6-diisopropylaniline (149)[47, 54]

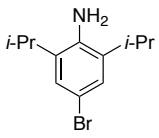

To a solution of 2,6-diisopropylaniline (0.23 mL, 2.5 mmol) in CH_2Cl_2 (24 mL) was rapidly added a solution of *n*-Bu_4NBr_3 (1.21 g, 2,5 mmol) in CH_2Cl_2 (24 mL). The reaction was stirred at rt for 1 h. After completion of the reaction, the solvent was evaporated to dryness and Et_2O (100 mL) was added to the residue. The organic layer was extracted with an aq. solution of 0.5 M NaOH and H_2O (×2), then dried with $MgSO_4$ and

concentrated in vacuo. The brominated compound **149** was obtained as a colourless oil (60%) and was used without further purification. **^{1}H NMR** (400 MHz, $CDCl_3$) δ 7.13 (s, 2H), 2.95 (hept, J = 6.7 Hz, 2H), 1.26 (d, J = 6.8 Hz, 12H). **^{13}C NMR** (126 MHz, $CDCl_3$) δ 139.4, 134.7 (×2), 125.9 (×2), 111.26, 28.15 (×2), 22.37 (×4).

tert-Butyl (*S*)-2-((4-bromo-2,6-diisopropylphenyl)carbamoyl)pyrrolidine-1-carboxylate (157)

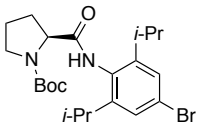

To a solution of Boc-Pro-OH (1 g, 4.65 mmol) in CH_2Cl_2 (7.37 mL) were added Et_3N (0.71 mL, 5.1 mmol) and isobutyl chloroformate (0.66 mL, 5.1 mmol) at 0ºC under stirring. After 55 min. 4-bromo-2,6-diisopropylaniline (1.5 g, 5.8 mmol) was added to the reaction mixture. Then, it was allowed to warm to rt and monitored by TLC. After 16 h, the mixture was washed with 1 M $KHSO_4$, saturated $NaHCO_3$, brine, dried over anhydrous $MgSO_4$ and concentrated under reduced pressure. The crude product **157** was obtained as a slightly yellow solid and it was used without further purification. **^{1}H NMR** (300 MHz, $CDCl_3$) δ 4.53 (d, J = 6.5 Hz, 1H), 3.46 (br s, 2H), 3.11 – 2.87 (m, 2H), 2.47 (br s, 1H), 2.14 – 1.82 (m, 3H), 1.50 (s, 9H), 1.16 (dd, J = 9.6, 6.8 Hz, 12H).

(*S*)-*N*-(4-Bromo-2,6-diisopropylphenyl)pyrrolidine-2-carboxamide (158)

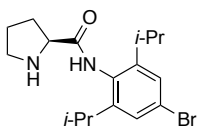

In a 25 mL round bottom flask containing a solution of **157** (2.1 g, 4.64 mmol) in CH_2Cl_2 (6 mL) was added dropwise at 0 ºC TFA (2.5 mL, 32.6 mmol). Then, the solution was warmed to rt and stirred until the reaction was finished (16 h). After that, the solvent was evaporated and H_2O was added. The pH value of the mixture was brought into the range of 10–12 by addition of aq. NaOH (2 M). The aqueous phase was extracted with

DCM (×5) and the combined organic phase were washed with brine and dried over $MgSO_4$ and evaporated in vacuo. The residue was directly used in the next step. **^{1}H NMR** (300 MHz, $CDCl_3$) δ 9.11 (br s, 1H), 7.26 (d, *J* = 0.9 Hz, 2H), 3.94 (dd, *J* = 9.2, 5.0 Hz, 1H), 3.20 – 2.89 (m, 4H), 2.31 – 2.14 (m, 1H), 2.14 – 1.97 (m, 1H), 1.89 – 1.74 (m, 2H), 1.18 (dd, *J* = 6.9, 3.7 Hz, 12H). **^{13}C NMR** (101 MHz, $CDCl_3$) δ 174.5, 148.1 (×2), 130.8, 126.8 (×2), 122.0, 60.8, 47.6, 30.9, 29.0 (×2), 26.4, 23.4 (×2), 23.3 (×2).

(2*S*,2'*S*)-1,1'-(Propane-1,3-diyl)bis(*N*-(4-bromo-2,6-diisopropylphenyl) pyrrolidine-2-carboxamide) (159)

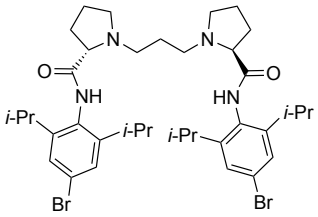

To a solution of **158** (600 mg, 1.7 mmol) in MeCN (2.7 mL) were added K_2CO_3 (517 mg, 3.74 mmol) and 1,3-dibromopropane (86 μL, 0.85 mmol) under stirring and it was stirred at 80 ºC overnight. Then, K_2CO_3 was removed by filtration and washed with DCM. The crude product was purified by flash column chromatography on silica gel using cyclohexane/EtOAc (50:50) as the eluent to give compound **159** in 80% yield as a slightly yellow solid. **^{1}H NMR** (400 MHz, $CDCl_3$) δ 8.72 (s, 1H), 7.28 (s, 4H), 3.35 – 3.22 (m, 4H), 2.97 (hept, *J* = 6.8 Hz, 4H), 2.86 – 2.74 (m, 2H), 2.67 – 2.57 (m, 2H), 2.44 – 2.36 (m, 2H), 2.34 – 2.22 (m, 2H), 2.10 – 1.98 (m, 2H), 1.99 – 1.76 (m, 6H), 1.19 (dd, *J* = 8.1, 6.9 Hz, 24H). **^{13}C NMR** (101 MHz, $CDCl_3$) δ 174.1 (×2), 148.2 (×4), 130.5 (×2), 127.0 (×4), 122.5 (×2), 68.3 (×2), 54.6 (×2), 54.4 (×2), 30.8 (×2), 29.9 (×2), 29.1 (×2), 25.0 (×2), 23.6 (×4), 23.5(×4). **HRMS** (ESI+): *m/z* calcd. for $C_{37}H_{55}Br_2N_4O_2$ $[M+H]^+$: 745.2686, found: 745.2706. **mp**: >200 ºC decompose. **$[\alpha]_D$**: +70.1 (*c* 1.00, CH_2Cl_2).

Polystyrene supported diamide (160)

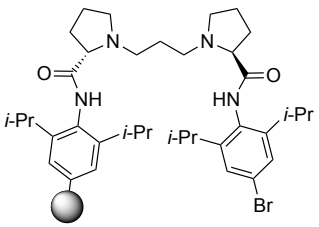

In a round bottom flask, **159** (0.18 g, 0,25 mmol) was suspended in degassed toluene (3.5 mL) and EtOH (0.7 mL). Then, $Pd(PPh_3)_4$ (0.02 g, 0.02 mmol) was added and the mixture was stirred for 10 min. After that time, 2 M Na_2CO_3 aqueous solution (0.57 mL, 1.14 mmol) and boronic acid polymer-bound (0.10 g, 0.19 mmol) were added, the mixture was degassed under Ar for 1 min and subsequently shaken for 24 h at 90 °C. Finally, the resin was filtered, washed with DMF, DCM, and MeOH, and it was dried overnight in a vacuum oven at 40 °C to afford a brownish resin (140 mg).

N elemental analysis (%): 4.06. $f_{(P)}$: 0.73 mmol/$g_{resin.}$ **Br elemental analysis** (%): 3.02. $f_{(P)}$: 0.38 mmol/$g_{resin.}$

Polystyrene supported *N,N'*-dioxide diamide (161)

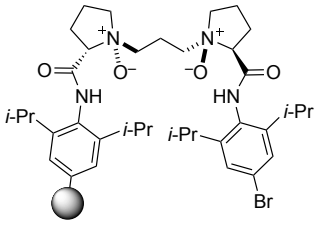

To a solution of diamide **160** (88 mg, 0.08 mmol) in CH_2Cl_2 (0.8 mL) was added *m*-CPBA (0.044 g, 0.20 mmol) at 0 °C. The reaction mixture was stirred for a further 24 h at 0 °C. After that time, the resin was filtered and washed with MeOH and CH_2Cl_2. Finally, it was dried overnight in a vacuum oven at 40 °C to afford a pale yellow resin (93 mg).

3-(4-Chlorophenyl)-6,6-dimethyl-2-nitro-3,5,6,7-tetrahydrobenzofuran-4(2*H*)-one (144)[43e]

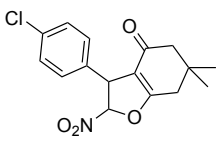

(*Z*)-1-(2-Bromo-2-nitrovinyl)-4-chlorobenzene (31 mg, 0.12 mmol), 5,5-dimethylcyclohexane-1,3-dione (14 mg, 0.1 mmol), catalyst (10.0 μmol; **142** $f_{(N)}$: 0.225 mmol/$g_{resin.}$, 44 mg,) or **161**

$f_{(N)}$: 0.73 mmol/$g_{resin.}$, 14 mg, 10.0 μmol), and $K_2HPO_4 \cdot 3H_2O$ (27 mg, 0.12 mmol) were dissolved in THF (0.2 mL) and toluene (0.8 mL) at –50 °C. The mixture was stirred for 72 hours in a test tube under air. Then, the crude product was purified directly by column chromatography on silica gel (cyclohexane/ethyl acetate = 10:1 to 5:1) to afford **144** (28% using **142** and 70% using **161**). **^{1}H NMR** (400 MHz, $CDCl_3$) δ 7.42 – 7.31 (m, 2H), 7.20 – 7.10 (m, 2H), 5.92 (d, *J* = 2.1 Hz, 1H), 4.65 – 4.52 (m, 1H), 2.77 – 2.50 (m, 2H), 2.41 – 2.20 (m, 2H), 1.20 (s, 6H). **^{13}C NMR** (101 MHz, $CDCl_3$) δ 193.0, 175.4, 135.6, 134.6, 129.7 (×2), 128.5 (×2), 115.0, 111.1, 52.7, 51.4, 37.4, 34.8, 28.9, 28.7. **HPLC** (Daicel Chiralpak AD-H column, hexane/*i*-PrOH 90:10, flow rate 1.0 mL/min, λ = 254 nm): t_{major} = 11.0 min; t_{minor} = 23.0 min.

5.6. References

[1] (a) J. A. Cowan, *Synth. React. Inorg. Met.-Org. Chem.* **1994**, *24*, 1239-1240; (b) S. E. Denmark, G. L. Beutner, *Angew. Chem. Int. Ed.* **2008**, *47*, 1560-1638.

[2] (a) J. K. Whitesell, *Chem. Rev.* **1989**, *89*, 1581-1590; (b) K. Ding, Z. Han, Z. Wang, *Chem. Asian J.* **2009**, *4*, 32-41.

[3] Privileged chiral ligands and catalysts, ed. Q.-L. Zhou, Wiley- VCH, Weinheim, 2011.

[4] T. Clark, C. Landis, *Tetrahedron: Asymmetry* **2004**, *15*, 2123-2137.

[5] S.-F. Zhu, Y. Fu, J.-H. Xie, B. Liu, L. Xing, Q.-L. Zhou, *Tetrahedron: Asymmetry* **2003**, *14*, 3219-3224.

[6] G. Desimoni, G. Faita, K. A. Jørgensen, *Chem. Rev.* **2006**, *106*, 3561-3651.

[7] (a) G. Chelucci, G. Murineddu, G. A. Pinna, *Tetrahedron: Asymmetry* **2004**, *15*, 1373-1389; (b) R. N. Butler, F. L. Scott, T. A. F. O'Mahony, *Chem. Rev.* **1973**, *73*, 93-112; (c) A. Albini, *Synthesis* **1993**, *1993*, 263-277; (d) T. Petrowitsch, P. Eilbracht, *Synlett* **1997**, 287-288.

[8] Homochiral catalyst for asymmetric synthesis: Ojiama, I. Catalytic Asymmetric synthesis; VCH: Weinheim, 1993; Noyori, R. Asymmetric Catalysis in Organic Synthesis; John Wiley: New York, 1994. Kagan, H. B. Chiral ligands for Asymmetric Catalysis. In Asymmetric Synthesis; Morrison, J. D., Ed.; Academic: London, 1985; Vol. 5, pp 1–39.

[9] (a) W. J. Kerr, G. G. Kirk, D. Middlemiss, *Synlett* **1995**, 1085-1086; (b) I. A. O'Neil, C. D. Turner, S. B. Kalindjian, *Synlett* **1997**, 777-780.

[10] I. A. O'Neil, N. D. Miller, J. Peake, J. V. Barkley, C. M. R. Low, S. B. Kalindjian, *Synlett* **1993**, 515-518.

[11] I. A. O'Neil, N. D. Miller, J. V. Barkley, C. M. R. Low, S. B. Kalindjian, *Synlett* **1995**, 617-618.

[12] M. A. Brooks, Silicon, in: Organic, Organometallic and Polymer Chemistry, Wiley & Sons, New York, 1999.

[13] K. Sato, M. Kira, H. Sakurai, *Tetrahedron Lett.* **1989**, *30*, 4375-4378.

[14] (a) N. M. Karayannis, L. L. Pytlewski, C. M. Mikulski, *Coord. Chem. Rev.* **1973**, *11*, 93-159; (b) M. Nakajima, H. Iwamoto, S.-i. Hashimoto, *Tetrahedron Lett.* **1998**, *39*, 87-88.

[15] (a) S. Kobayashi, K. Nishio, *Tetrahedron Lett.* **1993**, *34*, 3453-3456; (b) S. E. Denmark, D. M. Coe, N. E. Pratt, B. D. Griedel, *J. Org. Chem.* **1994**, *59*, 6161-6163; (c) S. Kobayashi, K. Nishio, *J. Org. Chem.* **1994**, *59*, 6620-6628; (d) S. E. Denmark, J. Fu, *Chem. Rev.* **2003**, *103*, 2763-2794.

[16] For Lewis base promoted reactions based on hypervalent silicates other than allylation, see: (a) Denmark, S. E.; Barsanti, P. A.; Wong, K.-T.; Stavenger, R. A. *J. Org. Chem.* **1998**, *63*, 2428-2429. (b) Denmark, S. E.;

Wong, K.-T.; Stavenger, R. A. *J. Am. Chem. Soc.* **1997**, *119*, 2333-2334. (c) Denmark, S. E.; Winter, S. B. D.; Su, X.; Wong, K.-T. *J. Am. Chem. Soc.* **1996,** *118*, 7404-7405. (d) Kobayashi, S.; Nishio, K. *J. Am. Chem. Soc.* **1995,** *117*, 6392-6393. (e) Kobayashi, S.; Yasuda, M.; Hachiya, I. *Chem. Lett.* **1996**, 407-408. (f) Kobayashi, S.; Tsuchiya, Y.; Mukaiyama, T. *Chem. Lett.* **1991**, 537-540.

[17] M. Nakajima, M. Saito, M. Shiro, S.-i. Hashimoto, *J. Am. Chem. Soc.* **1998**, *120*, 6419-6420.

[18] B. Liu, X. Feng, F. Chen, G. Zhang, X. Cui, Y. Jiang, *Synlett* **2001**, 1551-1554.

[19] Y. Shen, X. Feng, G. Zhang, Y. Jiang, *Synlett* **2002**, 1353-1355.

[20] X. Liu, L. Lin, X. Feng, *Acc. Chem. Res.* **2011**, *44*, 574-587.

[21] M. B. Diana, M. Marchetti, G. Melloni, *Tetrahedron: Asymmetry* **1995**, *6*, 1175-1179.

[22] A. V. Malkov, P. Kočovský, *Eur. J. Org. Chem.* **2007**, *2007*, 29-36.

[23] M. Nakajima, Y. Sasaki, M. Shiro, S.-i. Hashimoto, *Tetrahedron: Asymmetry* **1997**, *8*, 341-344.

[24] Y. Wen, B. Gao, Y. Fu, S. Dong, X. Liu, X. Feng, *Chem. Eur. J.* **2008**, *14*, 6789-6795.

[25] (a) Y. Liu, D. Shang, X. Zhou, X. Liu, X. Feng, *Chem. Eur. J.* **2009**, *15*, 2055-2058; (b) K. Zheng, X. Liu, J. Zhao, Y. Yang, L. Lin, X. Feng, *Chem. Commun.* **2010**, *46*, 3771-3773; (c) M. North, *Sustainable Catalysis: With Non-endangered Metals*, Royal Society of Chemistry, **2015**.

[26] (a) Z. Jiao, X. Feng, B. Liu, F. Chen, G. Zhang, Y. Jiang, *Eur. J. Org. Chem.* **2003**, *2003*, 3818-3826; (b) X. Huang, J. Huang, Y. Wen, X. Feng, *Adv. Synth. Catal.* **2006**, *348*, 2579-2584.

[27] (a) S. E. Denmark, R. A. Stavenger, *Acc. Chem. Res.* **2000**, *33*, 432-440; (b) S. E. Denmark, J. Fu, *Chem. Commun.* **2003**, 167-170; (c) S. Rendler, M. Oestreich, *Synthesis* **2005**, 1727-1747; (d) Y. Orito, M. Nakajima, *Synthesis* **2006**, 1391-1401.

[28] For recent reviews on hypervalent silicates, see: (a) Sakurai, H. Synlett 1989, 1-8. (b) Chuit, C.; Corriu, R. J. P.; Reye, C.; Young, J. C. Chem. ReV. 1993, 93, 1371-1448.

[29] Y. Wen, X. Huang, J. Huang, Y. Xiong, B. Qin, X. Feng, *Synlett* **2005**, 2445-2448.

[30] B. Qin, X. Liu, J. Shi, K. Zheng, H. Zhao, X. Feng, *J. Org. Chem.* **2007**, *72*, 2374-2378.

[31] J. Huang, X. Liu, Y. Wen, B. Qin, X. Feng, *J. Org. Chem.* **2007**, *72*, 204-208.

[32] Y. Cai, W. Wang, K. Shen, J. Wang, X. Hu, L. Lin, X. Liu, X. Feng, *Chem. Commun.* **2010**, *46*, 1250-1252.

[33] (a) Y. Xia, X. Liu, H. Zheng, L. Lin, X. Feng, *Angew. Chem. Int. Ed.* **2015**, *54*, 227-230; (b) Y. Liu, X. Liu, H. Hu, J. Guo, Y. Xia, L. Lin, X. Feng, *Angew. Chem. Int. Ed.* **2016**, *55*, 4054-4058; (c) Q. Yao, Y. Liao, L. Lin, X. Lin, J. Ji, X. Liu, X. Feng, *Angew. Chem. Int. Ed.* **2016**, *55*, 1859-1863; (d) J. Li, L. Lin, B. Hu, P. Zhou, T. Huang, X. Liu, X. Feng, *Angew. Chem. Int. Ed.* **2017**, *56*, 885-888; (e) X. Liu, L. Lin, X. Feng, *Org. Chem. Front.* **2014**, *1*, 298-302; (f) S. Bai, Y. Liao, L. Lin, W. Luo, X. Liu, X. Feng, *J. Org. Chem.* **2014**, *79*, 10662-10668.

[34] Y. Zhang, Y. Liao, X. Liu, Q. Yao, Y. Zhou, L. Lin, X. Feng, *Chem. Eur. J.* **2016**, n/a-n/a.

[35] (a) J. Zhang, L. Lin, C. He, Q. Xiong, X. Liu, X. Feng, *Chem. Commun.* **2017**; (b) Y. Zhou, L. Lin, C. Yin, Z. Wang, X. Liu, X. Feng, *Chem. Commun.* **2015**, *51*, 11689-11692.

[36] Y. Liu, D. Shang, X. Zhou, Y. Zhu, L. Lin, X. Liu, X. Feng, *Org. Lett.* **2010**, *12*, 180-183.

[37] Z. Wang, Z. Yang, D. Chen, X. Liu, L. Lin, X. Feng, *Angew. Chem. Int. Ed.* **2011**, *50*, 4928-4932.

[38] G. Wang, X. Liu, T. Huang, Y. Kuang, L. Lin, X. Feng, *Org. Lett.* **2013**, *15*, 76-79.

[39] K. Fu, J. Zheng, L. Lin, X. Liu, X. Feng, *Chem. Commun.* **2015**, *51*, 3106-3108.

[40] J. Zhao, B. Fang, W. Luo, X. Hao, X. Liu, L. Lin, X. Feng, *Angew. Chem. Int. Ed.* **2015**, *54*, 241-244.

[41] C. Wang, H. Yamamoto, *Angew. Chem. Int. Ed.* **2015**, *54*, 8760-8763.

[42] M. Xie, X. Liu, X. Wu, Y. Cai, L. Lin, X. Feng, *Angew. Chem. Int. Ed.* **2013**, *52*, 5604-5607.

[43] (a) Y. Hui, J. Jiang, W. Wang, W. Chen, Y. Cai, L. Lin, X. Liu, X. Feng, *Angew. Chem. Int. Ed.* **2010**, *49*, 4290-4293; (b) X. Zhao, X. Liu, H. Mei, J. Guo, L. Lin, X. Feng, *Angew. Chem. Int. Ed.* **2015**, *54*, 4032-4035; (c) X. Zhao, X. Liu, Q. Xiong, H. Mei, B. Ma, L. Lin, X. Feng, *Chem. Commun.* **2015**, *51*, 16076-16079; (d) K. Fu, J. Zhang, L. Lin, J. Li, X. Liu, X. Feng, *Org. Lett.* **2017**, *19*, 332-335; (e) J. Feng, L. Lin, K. Yu, X. Liu, X. Feng, *Adv. Synth. Catal.* **2015**, *357*, 1305-1310.

[44] Z. Yu, X. Liu, Z. Dong, M. Xie, X. Feng, *Angew. Chem. Int. Ed.* **2008**, *47*, 1308-1311.

[45] K. Yamada, H. Fujita, M. Kunishima, *Org. Lett.* **2012**, *14*, 5026-5029.

[46] L. Osorio-Planes, C. Rodriguez-Escrich, M. A. Pericas, *Catal. Sci. Technol.* **2016**, *6*, 4686-4689.

[47] V. Diemer, H. Chaumeil, A. Defoin, A. Fort, A. Boeglin, C. Carré, *Eur. J. Org. Chem.* **2006**, *2006*, 2727-2738.

[48] T. Kitanosono, S. Kobayashi, *Chem. Asian J.* **2015**, *10*, 133-138.

[49] J. Wang, R. P. Hsung, S. K. Ghosh, *Org. Lett.* **2004**, *6*, 1939-1942.

[50] J. Poldy, R. Peakall, R. A. Barrow, *Eur. J. Org. Chem.* **2012**, *2012*, 5818-5827.

[51] M. Abe, T. Imai, N. Ishii, M. Usui, *Biosci., Biotechnol., Biochem.* **2006**, *70*, 303-306.

[52] R. He, P. H. Toy, Y. Lam, *Adv. Synth. Catal.* **2008**, *350*, 54-60.

[53] S. M. Voshell, S. J. Lee, M. R. Gagné, *J. Am. Chem. Soc.* **2006**, *128*, 12422-12423.

[54] I. Koehne, N. Graw, T. Teuteberg, R. Herbst-Irmer, D. Stalke, *Inorg. Chem.* **2017**, *56*, 14968-14978.

UNIVERSITAT ROVIRA I VIRGILI
IMMOBILIZATION OF CHIRAL BRØNSTED ACIDS AND LEWIS BASES FOR BATCH AND FLOW ENANTIOSELECTIVE CATALYSIS
Lidia Clot Almenara

5.7. ^{1}H and ^{13}C NMR Spectra

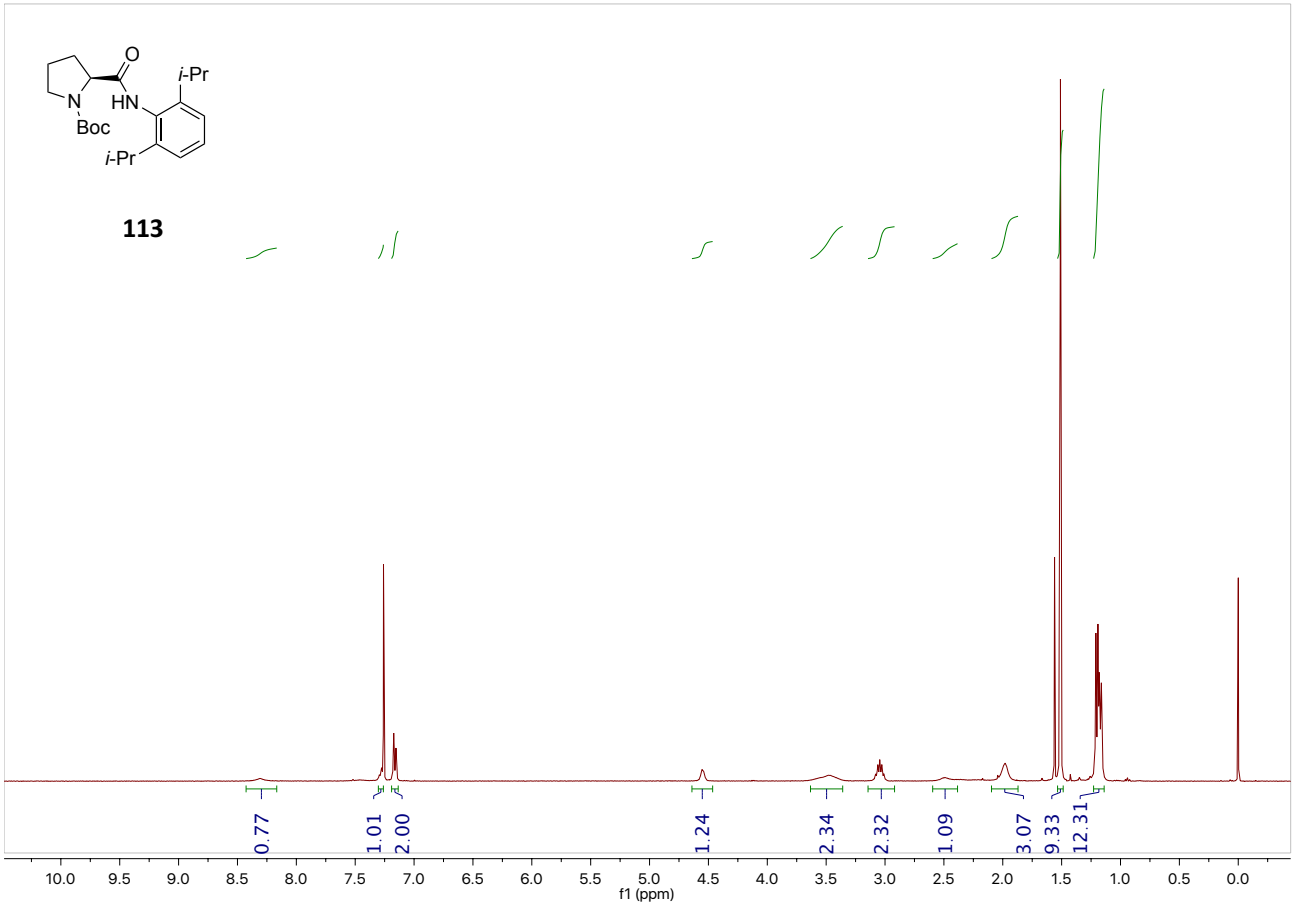

113

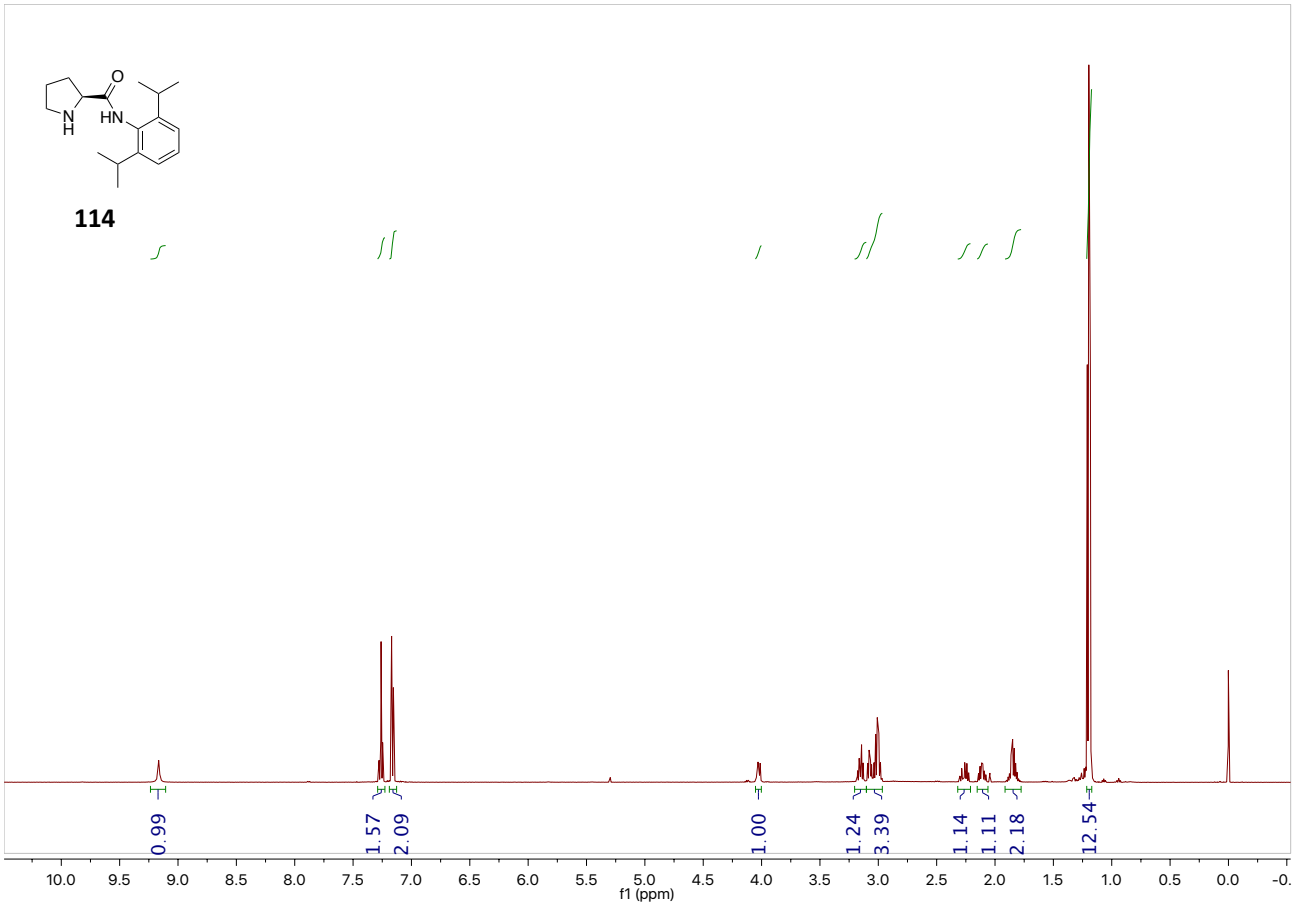

114

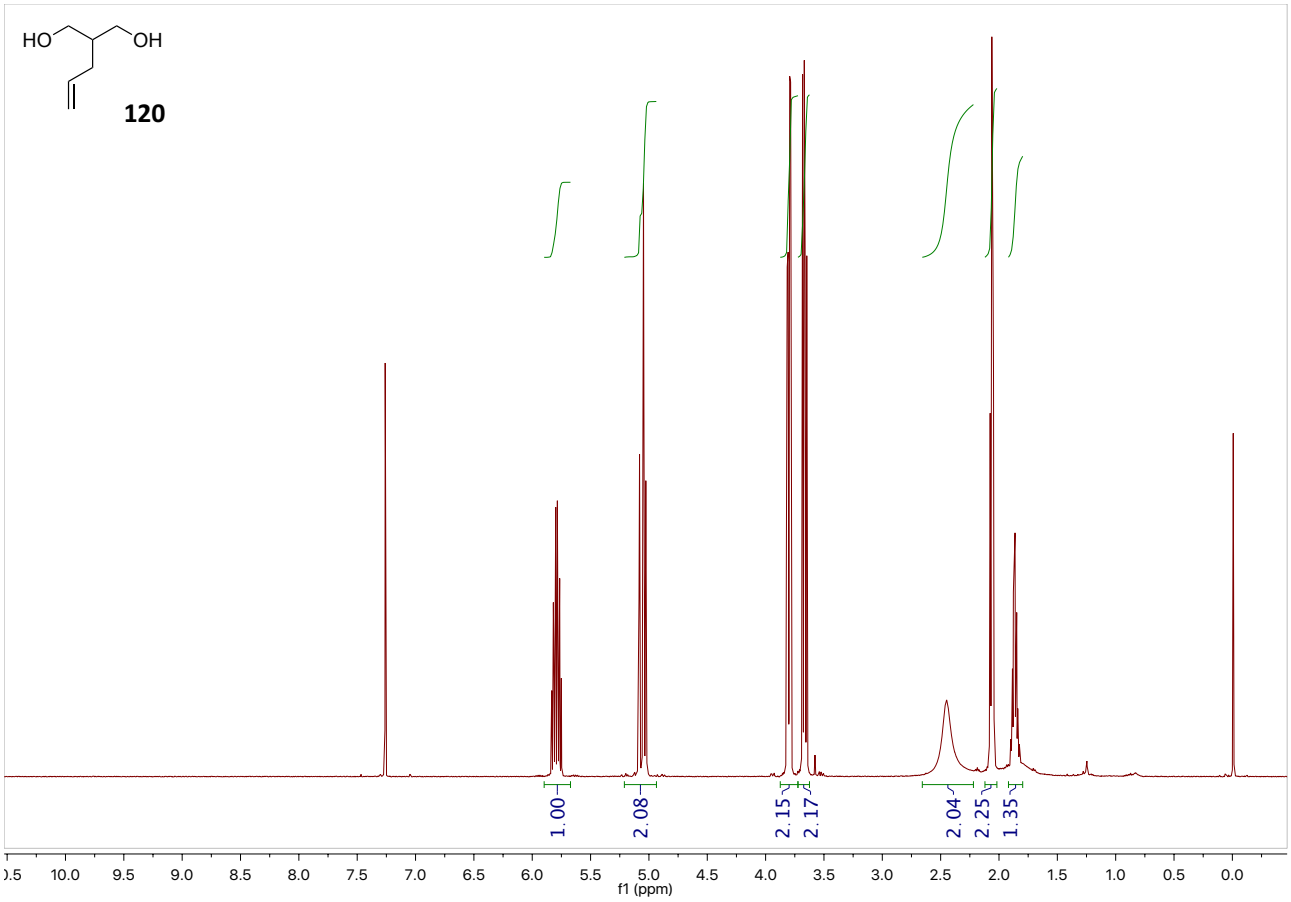
HO
OH
120
1.00
2.08
2.15
2.17
2.04
2.25
1.35
f1 (ppm)

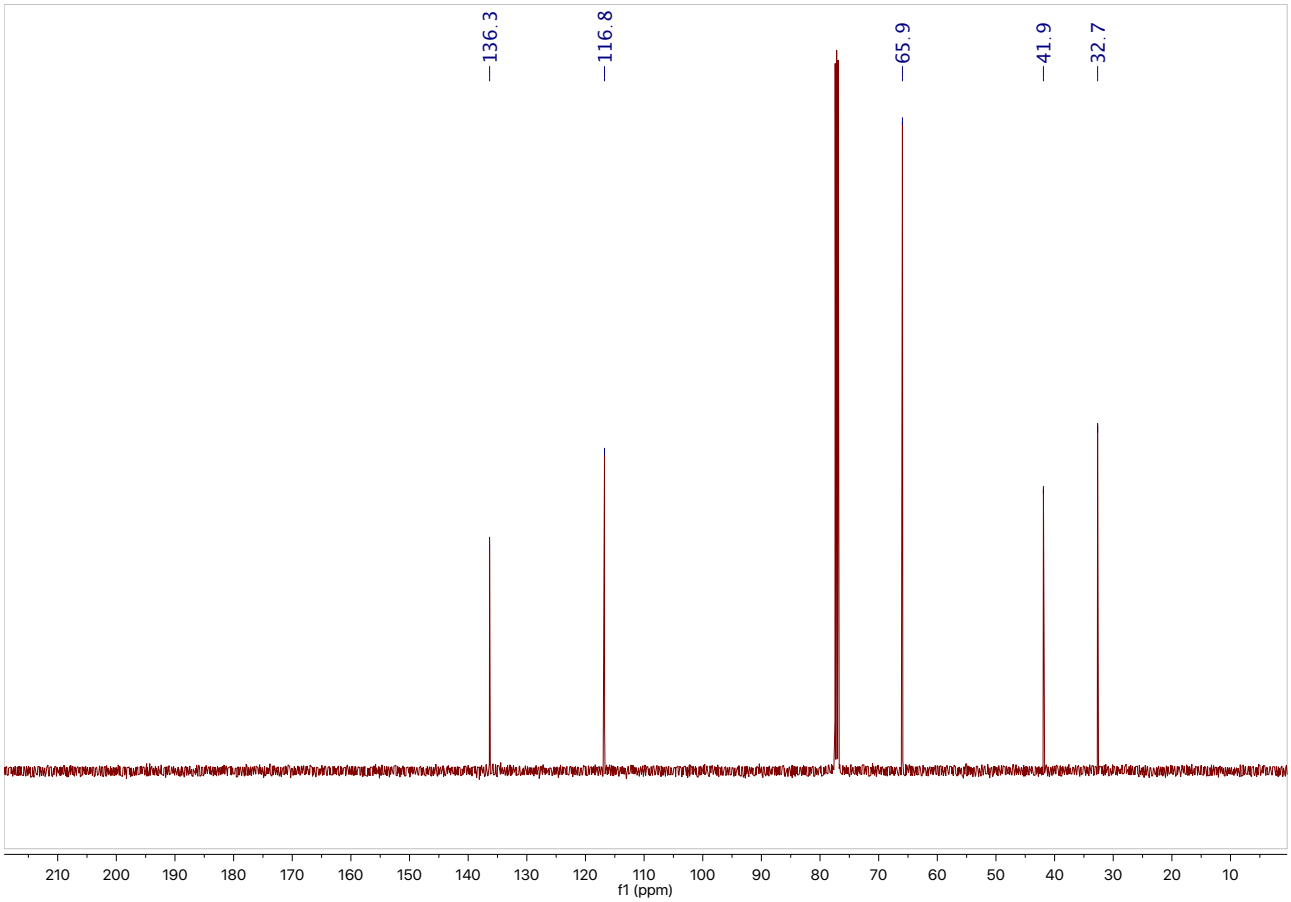
136.3
116.8
65.9
41.9
32.7
f1 (ppm)

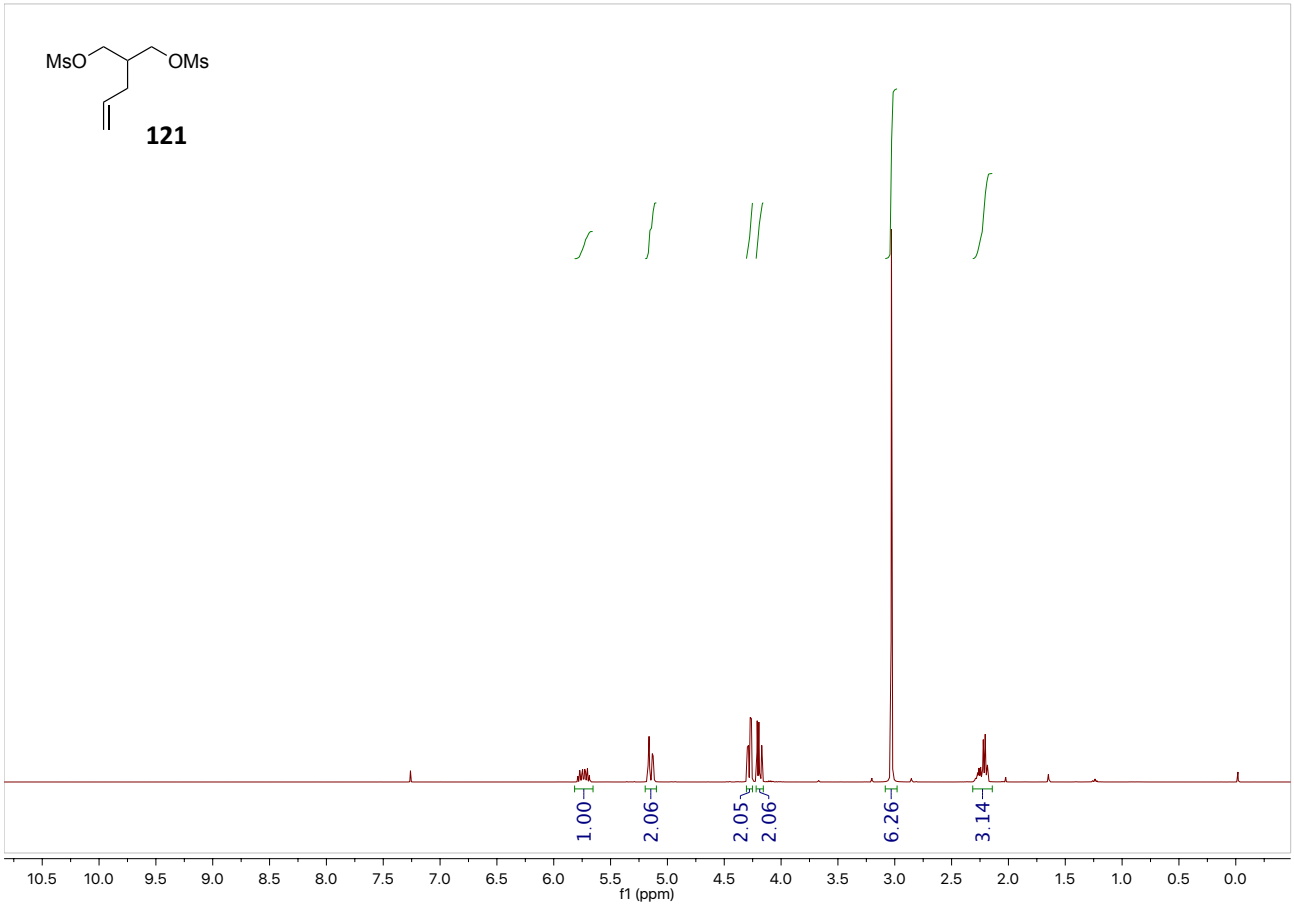
MsO
OMs
121
1.00
2.06
2.05
2.06
6.26
3.14
10.5 10.0 9.5 9.0 8.5 8.0 7.5 7.0 6.5 6.0 5.5 5.0 4.5 4.0 3.5 3.0 2.5 2.0 1.5 1.0 0.5 0.0
f1 (ppm)

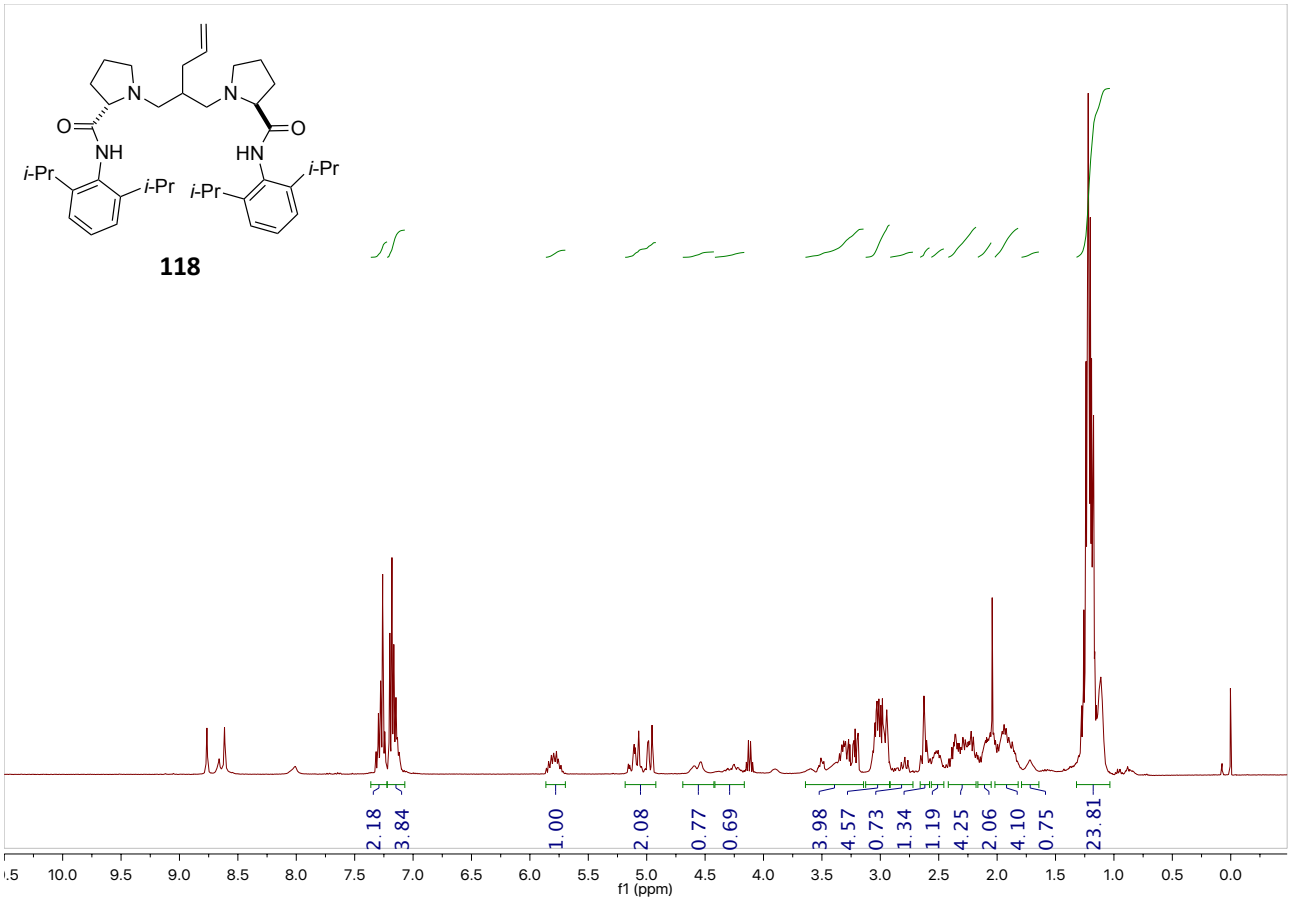
118
2.18
3.84
1.00
2.08
0.77
0.69
3.98
4.57
0.73
1.34
1.19
4.25
2.06
4.10
0.75
23.81
f1 (ppm)

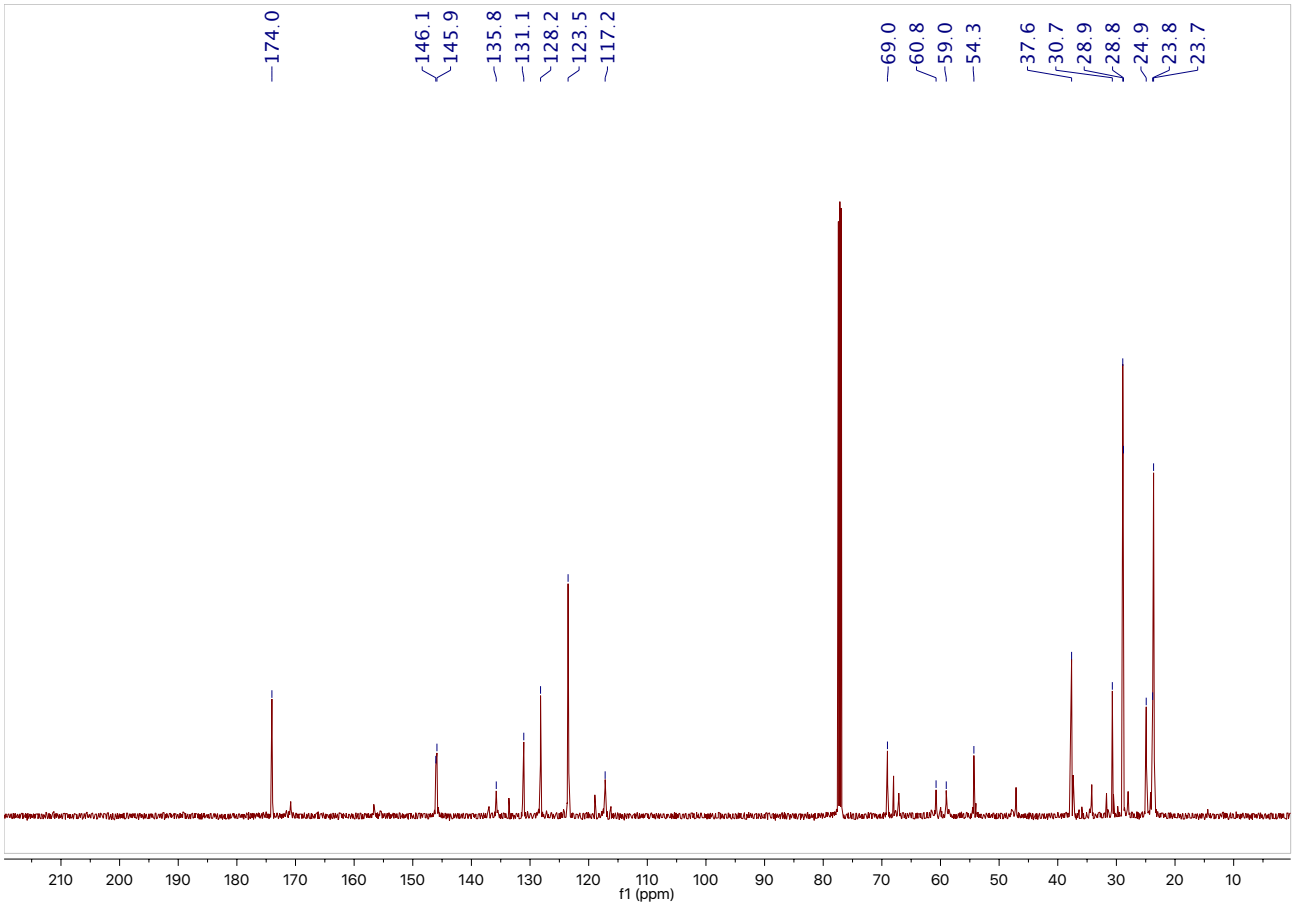
174.0
146.1
145.9
135.8
131.1
128.2
123.5
117.2
69.0
60.8
59.0
54.3
37.6
30.7
28.9
28.8
24.9
23.8
23.7
f1 (ppm)

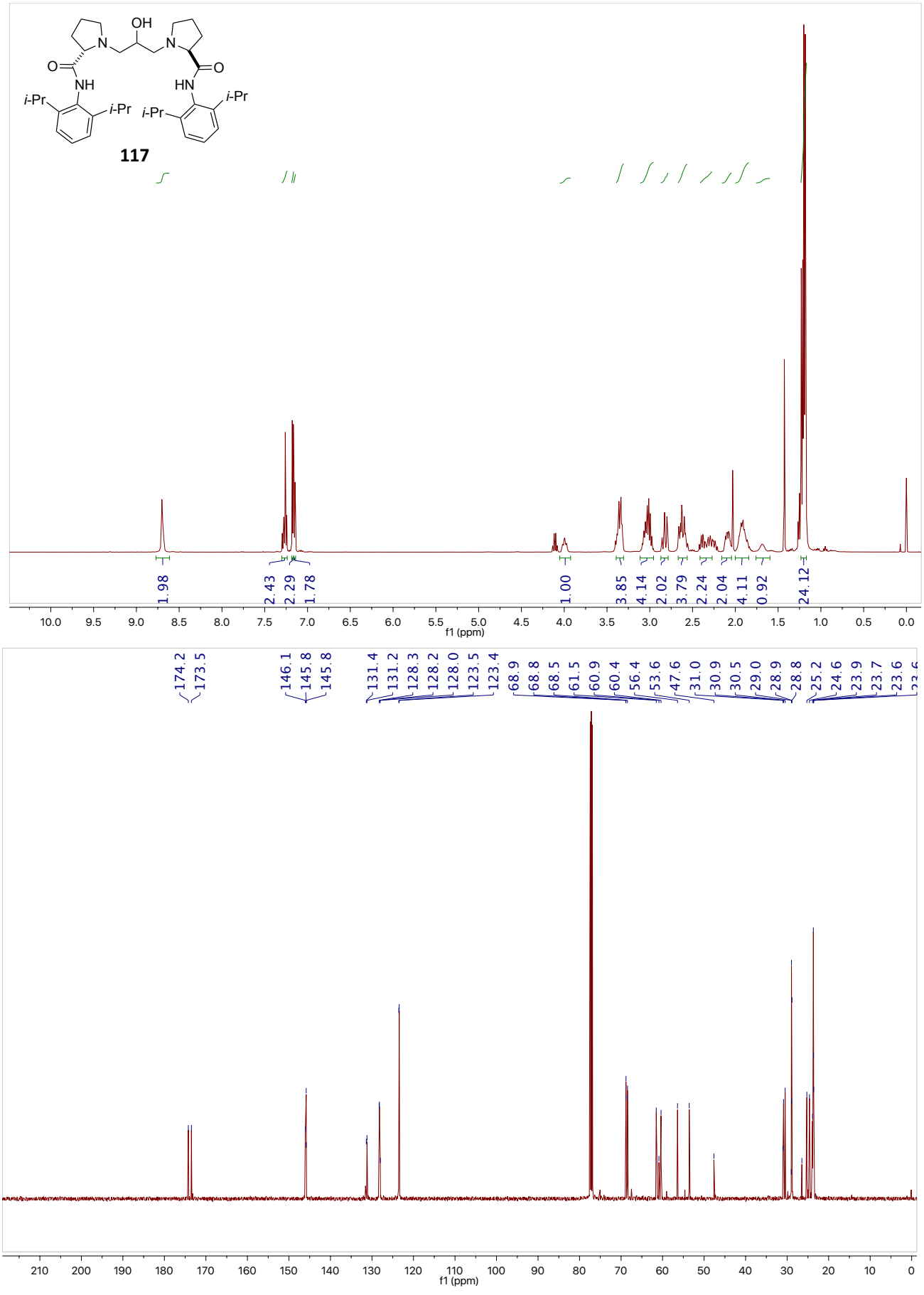
OH
N
N
O
NH
HN
O
i-Pr
i-Pr
i-Pr
i-Pr
117
1.98
2.43
2.29
1.78
1.00
3.85
4.14
2.02
3.79
2.24
2.04
4.11
0.92
24.12
f1 (ppm)
174.2
173.5
146.1
145.8
145.8
131.4
131.2
128.3
128.2
128.0
123.5
123.4
68.9
68.8
68.5
61.5
60.9
60.4
56.4
53.6
47.6
31.0
30.9
30.5
29.0
28.9
28.8
25.2
24.6
23.9
23.7
23.6
f1 (ppm)

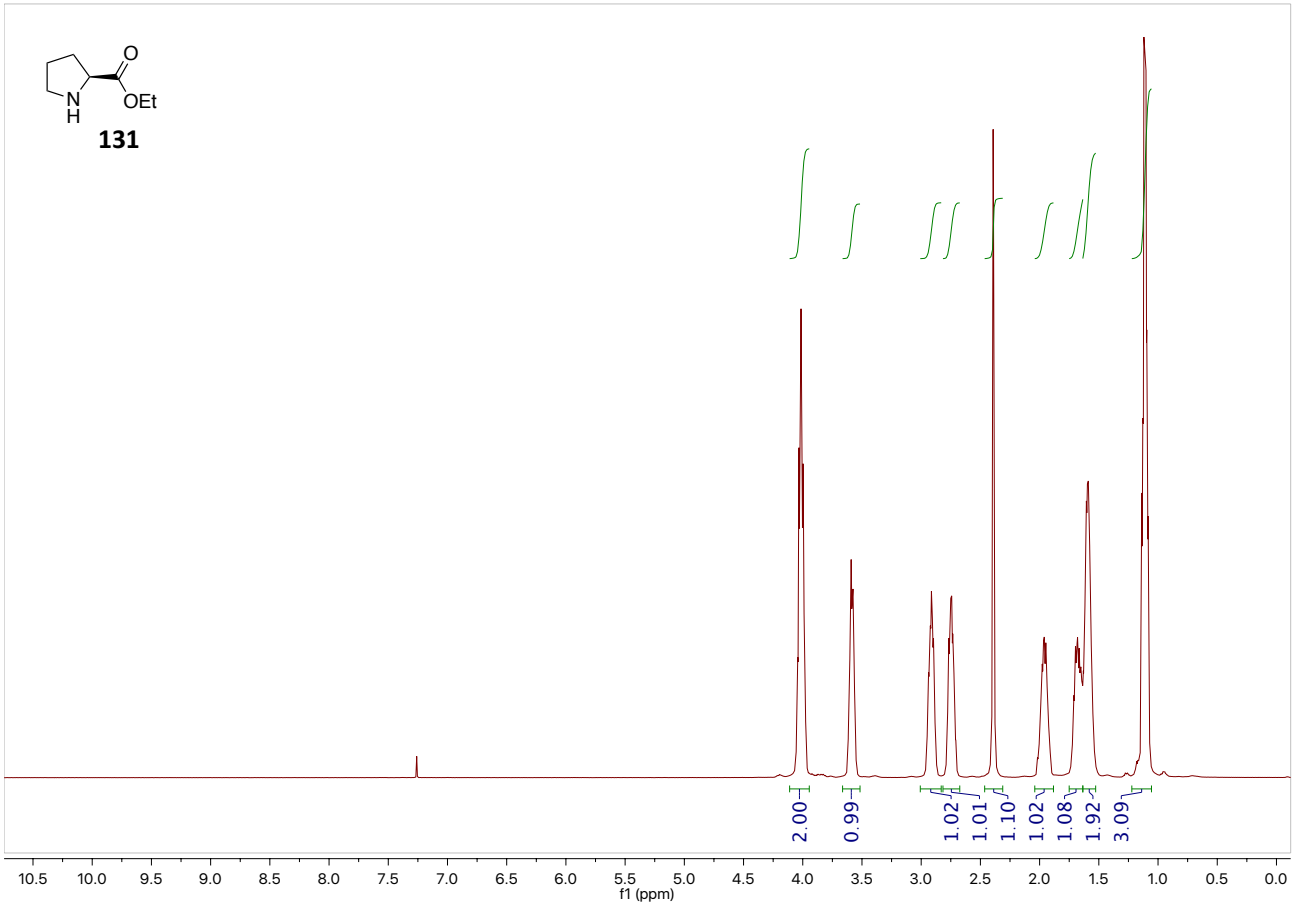
O
N
H
OEt
131
2.00
0.99
1.02
1.01
1.10
1.02
1.08
1.92
3.09
f1 (ppm)

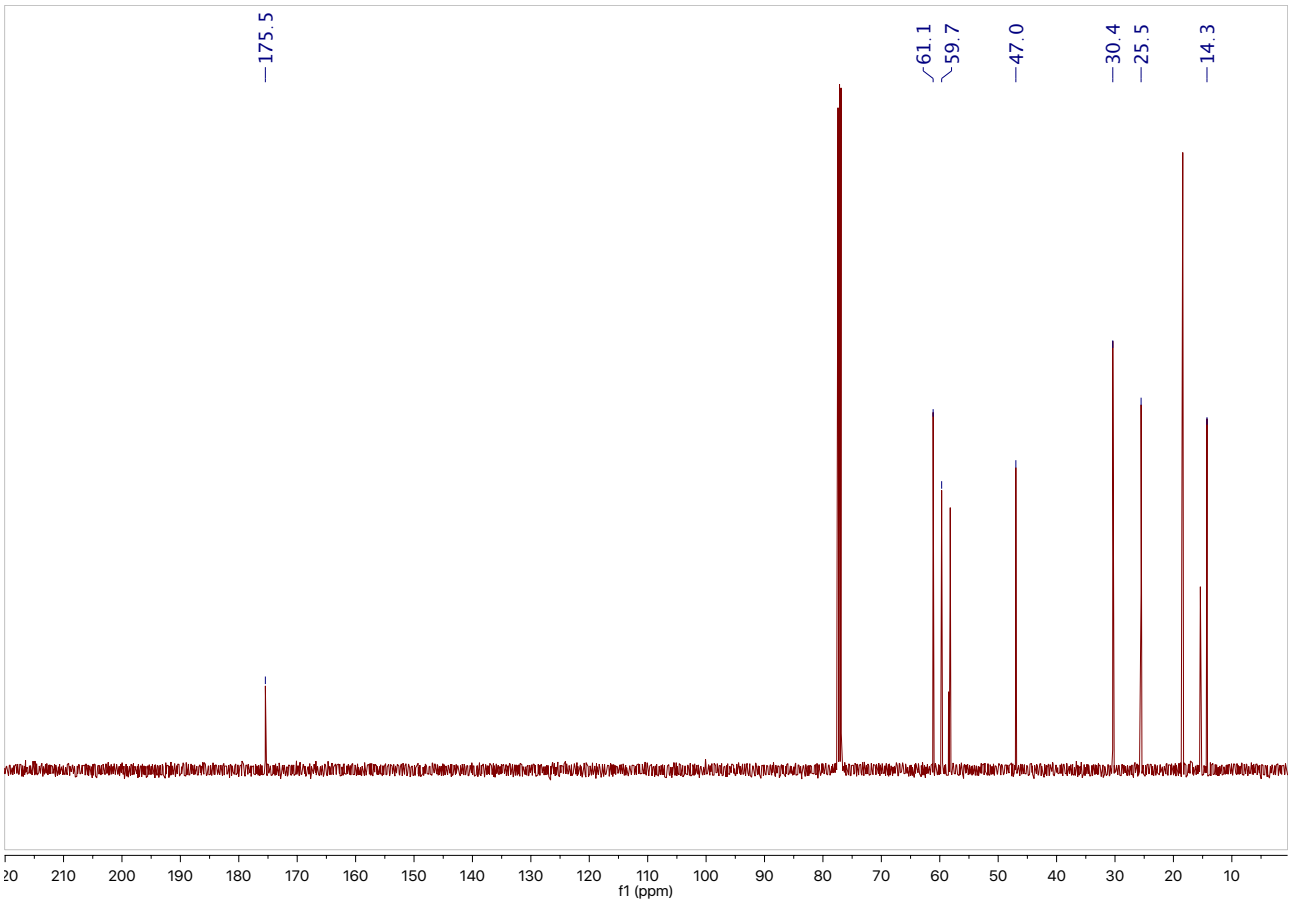
175.5
61.1
59.7
47.0
30.4
25.5
14.3
f1 (ppm)

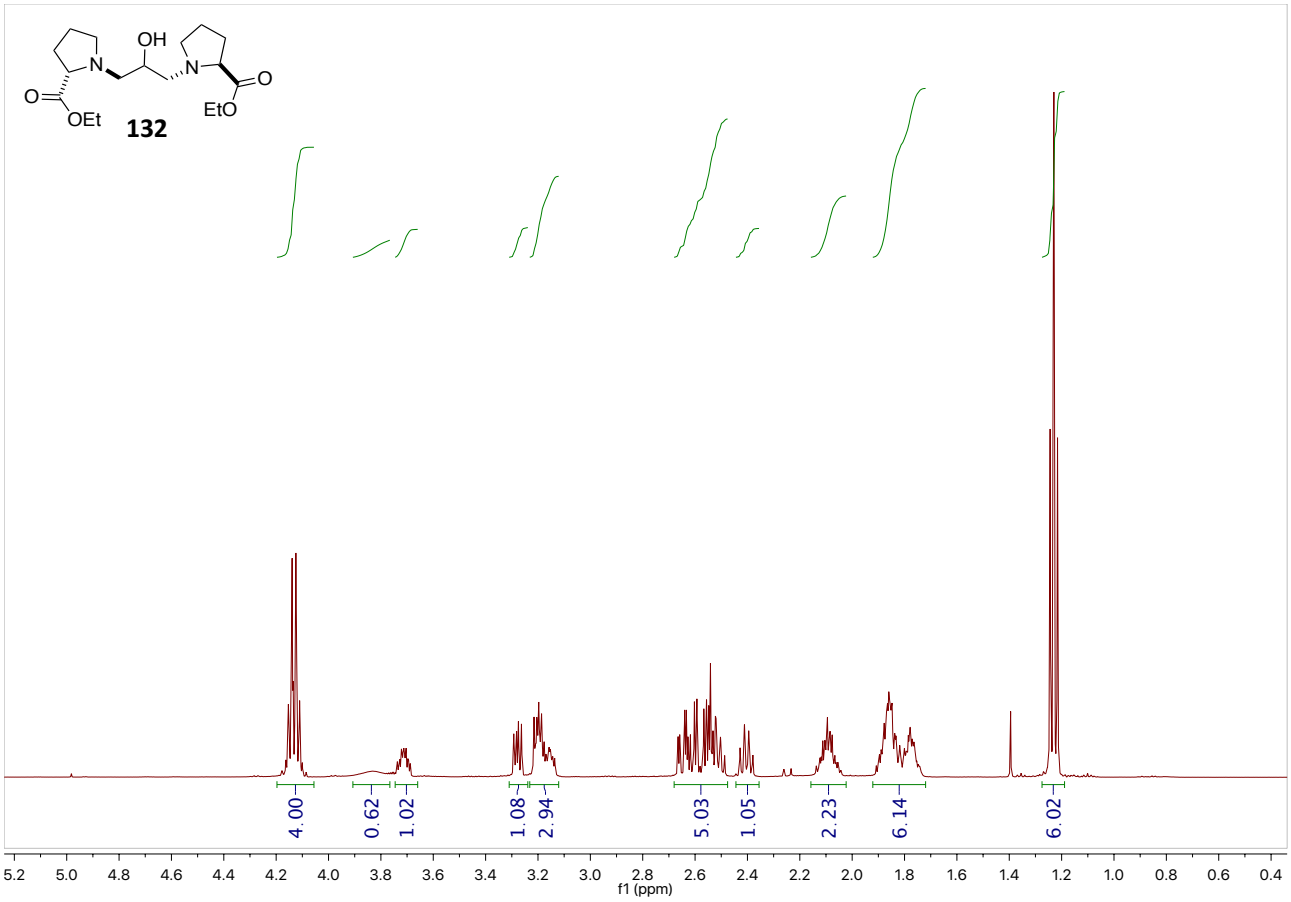
OH
N
N
O
OEt
EtO
O
132
4.00
0.62
1.02
1.08
2.94
5.03
1.05
2.23
6.14
6.02
f1 (ppm)

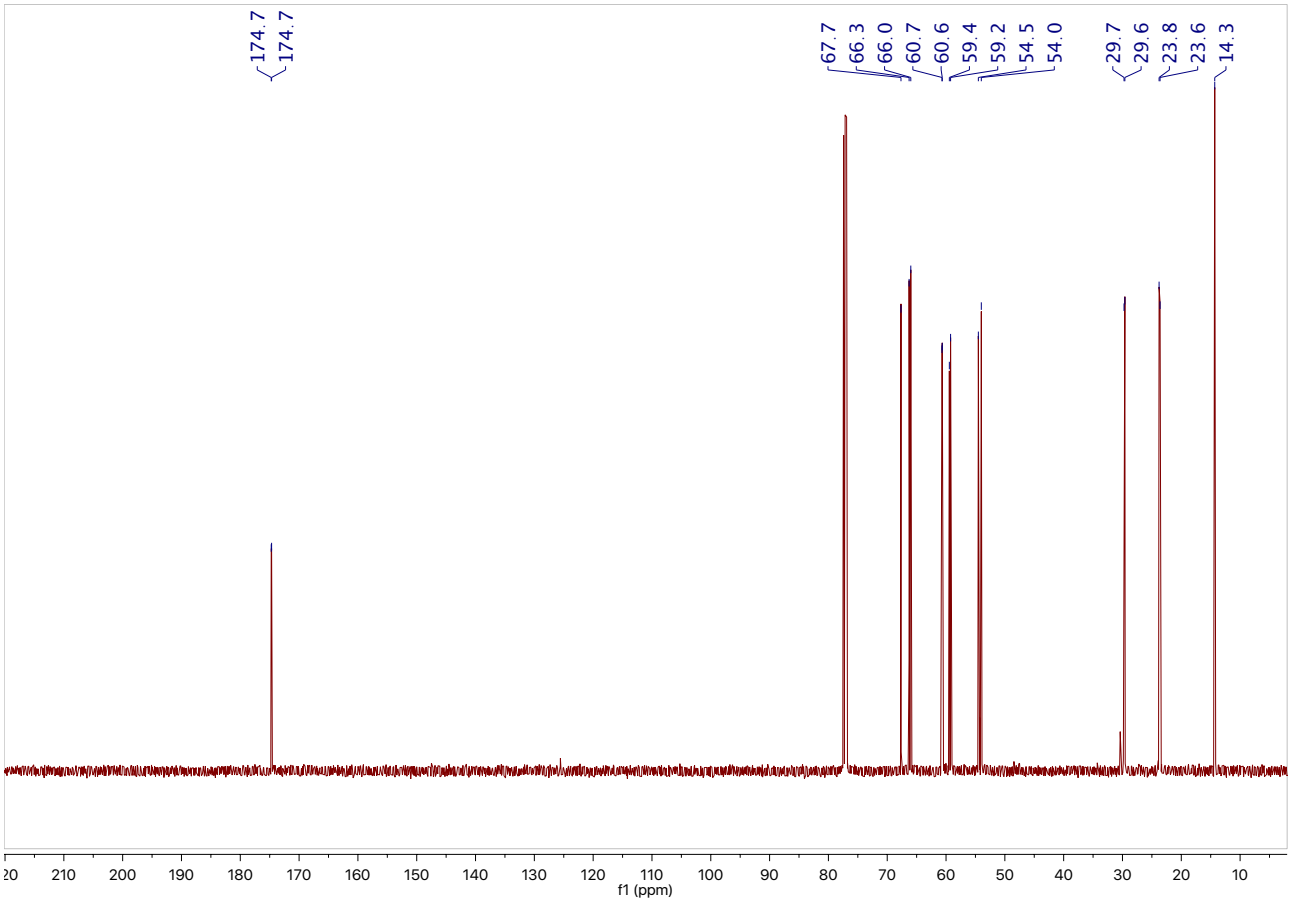
174.7
174.7
67.7
66.3
66.0
60.7
60.6
59.4
59.2
54.5
54.0
29.7
29.6
23.8
23.6
14.3
f1 (ppm)

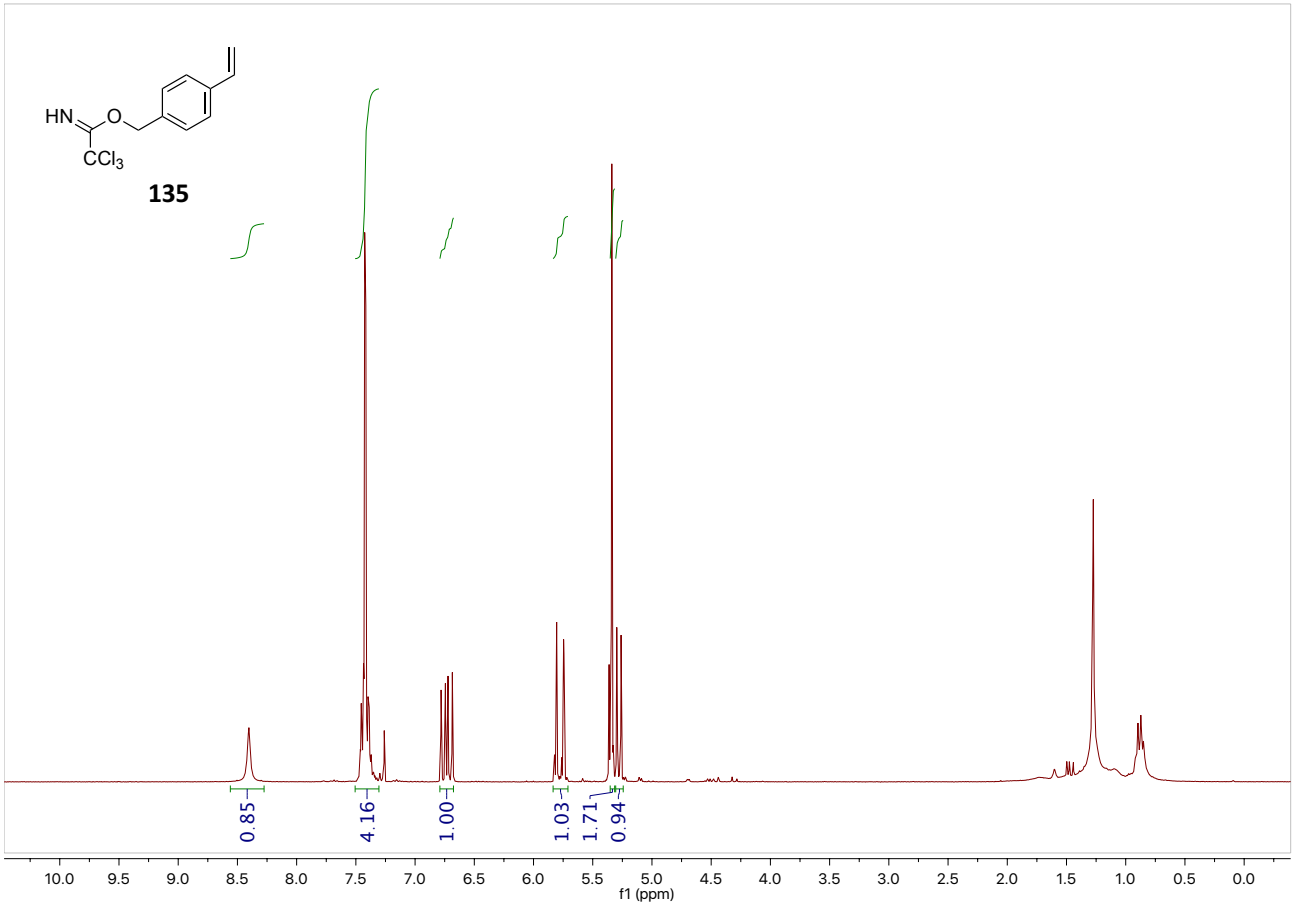
HN
O
CCl3
135
0.85
4.16
1.00
1.03
1.71
0.94
10.0 9.5 9.0 8.5 8.0 7.5 7.0 6.5 6.0 5.5 5.0 4.5 4.0 3.5 3.0 2.5 2.0 1.5 1.0 0.5 0.0
f1 (ppm)

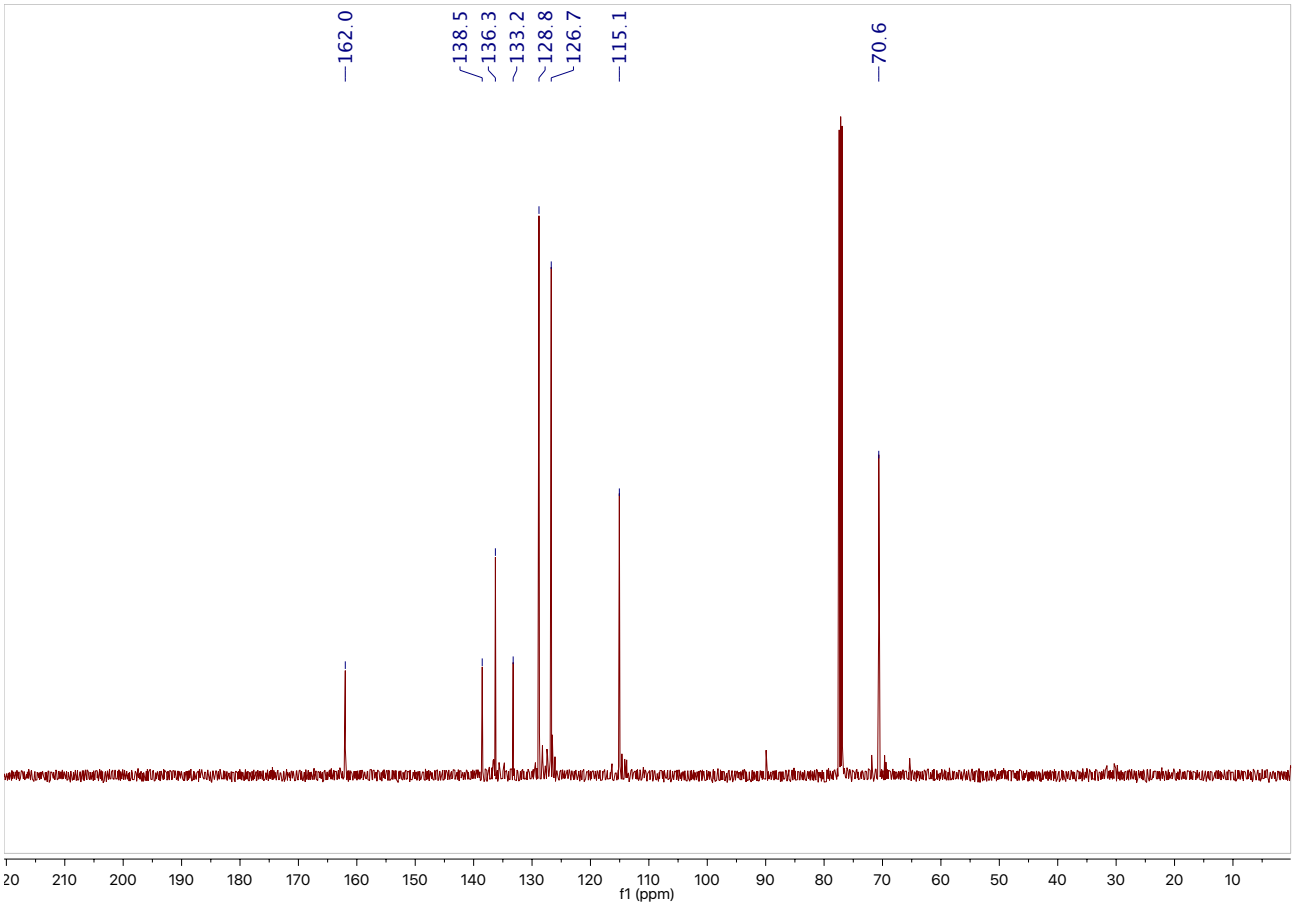
162.0
138.5
136.3
133.2
128.8
126.7
115.1
70.6
220 210 200 190 180 170 160 150 140 130 120 110 100 90 80 70 60 50 40 30 20 10
f1 (ppm)

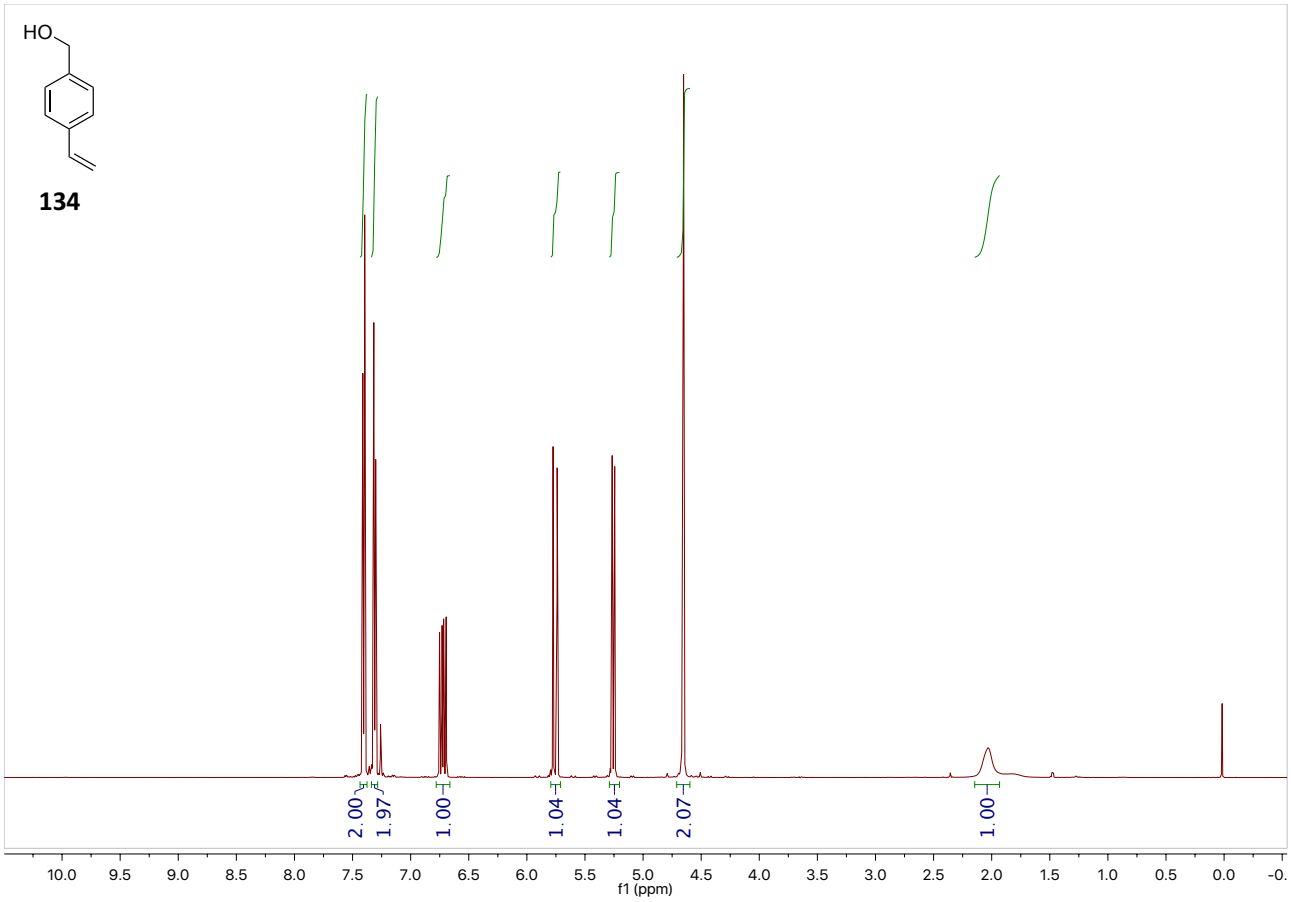
HO
134
2.00
1.97
1.00
1.04
1.04
2.07
1.00
f1 (ppm)

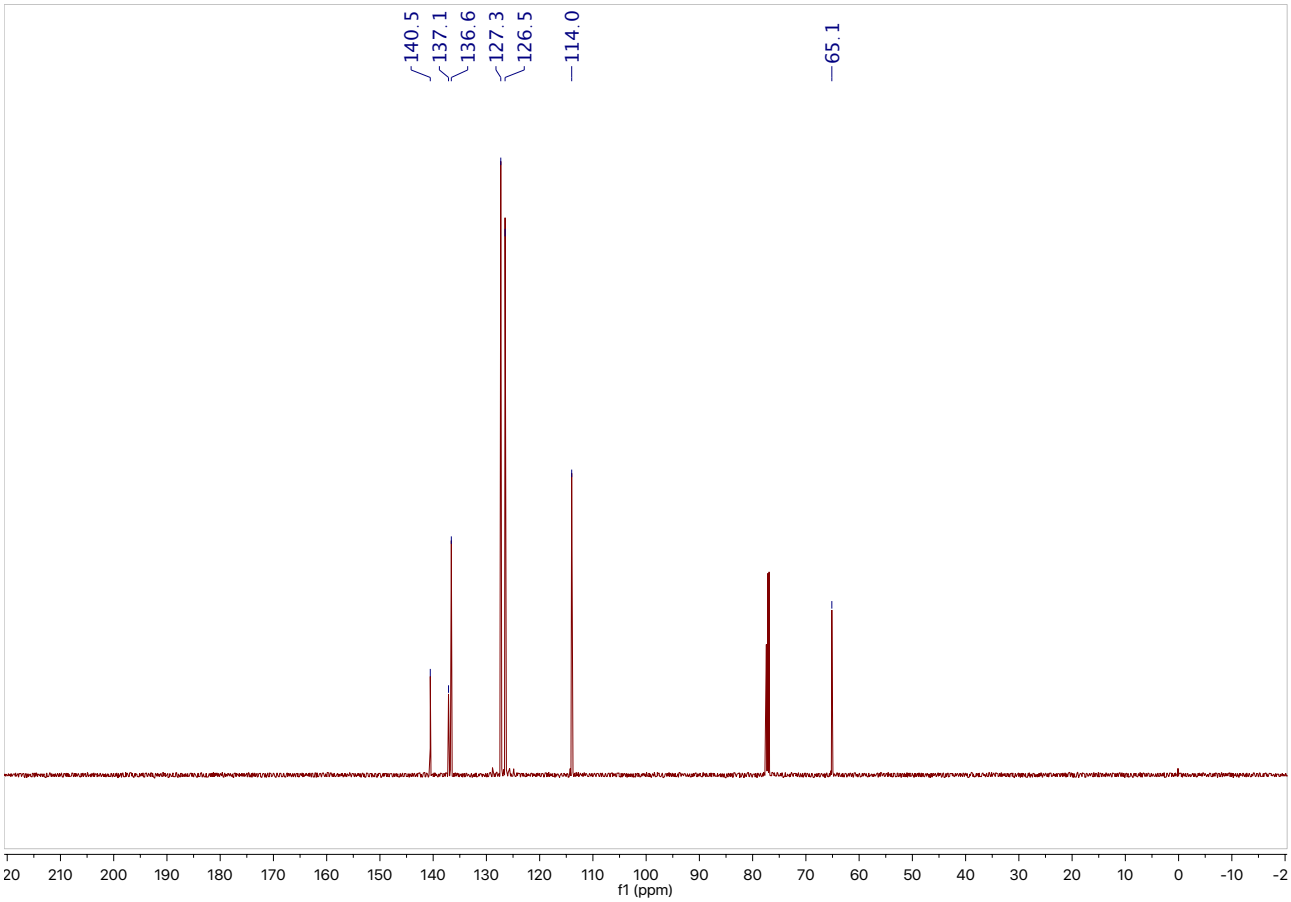
140.5
137.1
136.6
127.3
126.5
114.0
65.1
f1 (ppm)

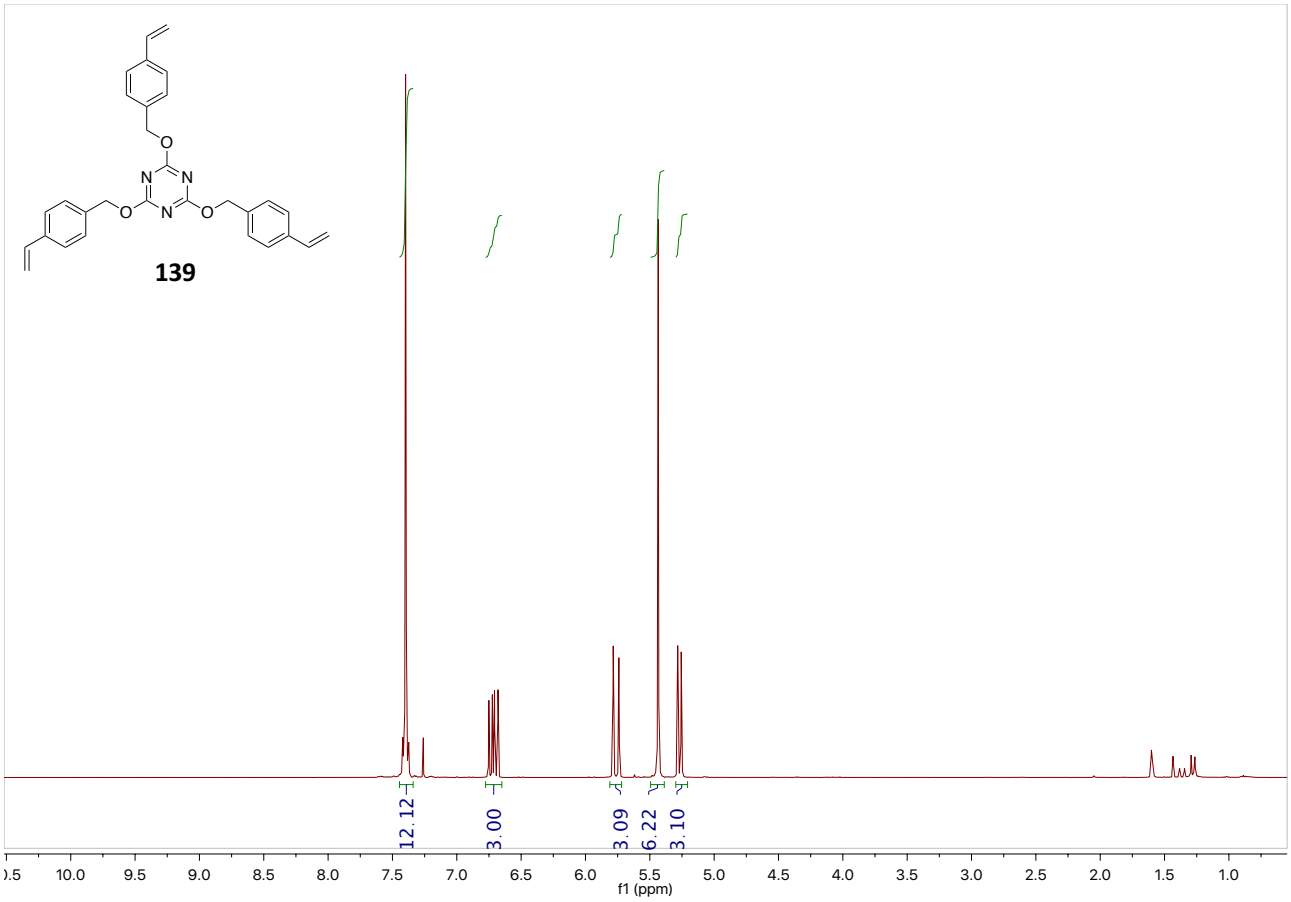
139
12.12
3.00
3.09
6.22
3.10
f1 (ppm)

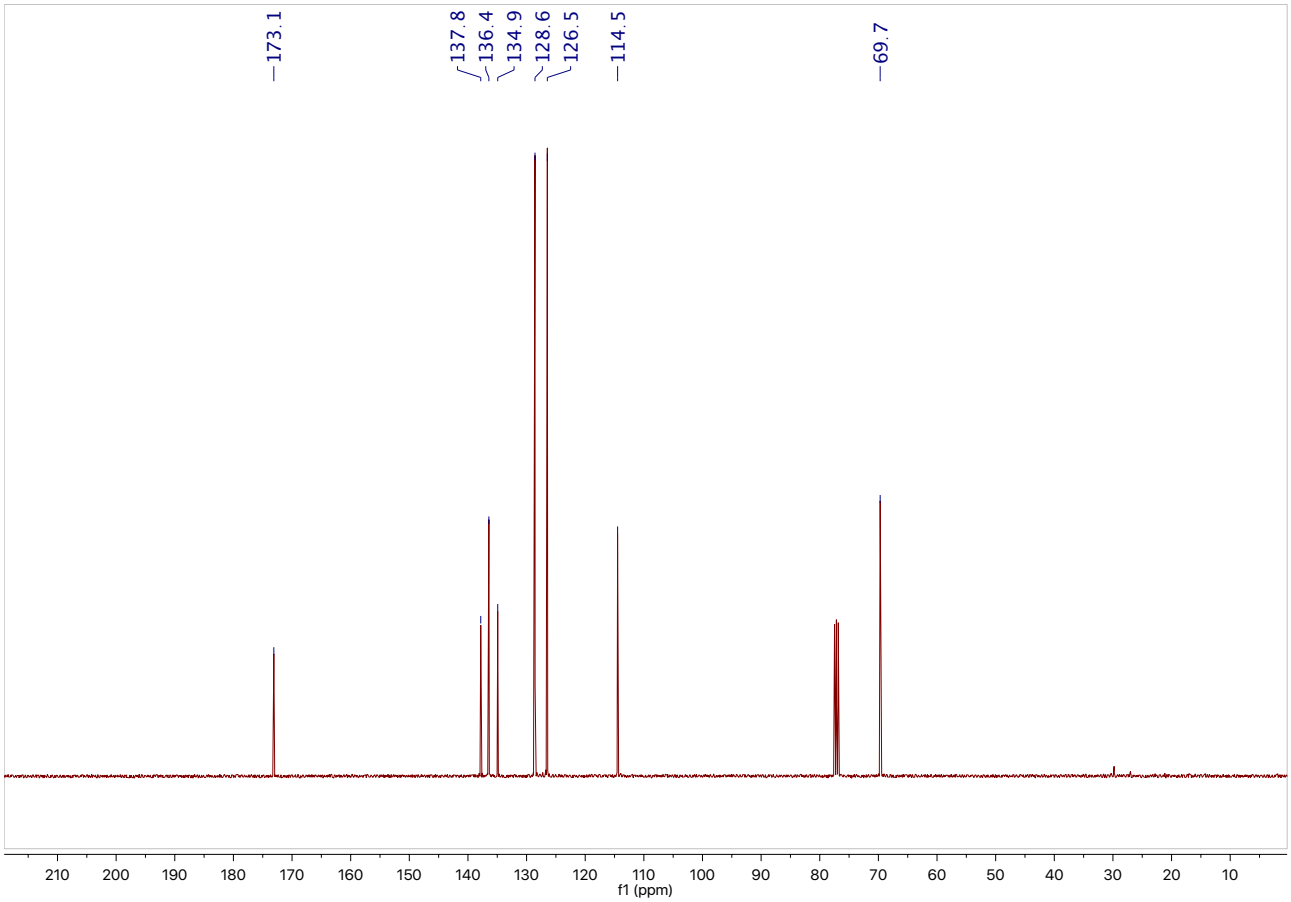
173.1
137.8
136.4
134.9
128.6
126.5
114.5
69.7
f1 (ppm)

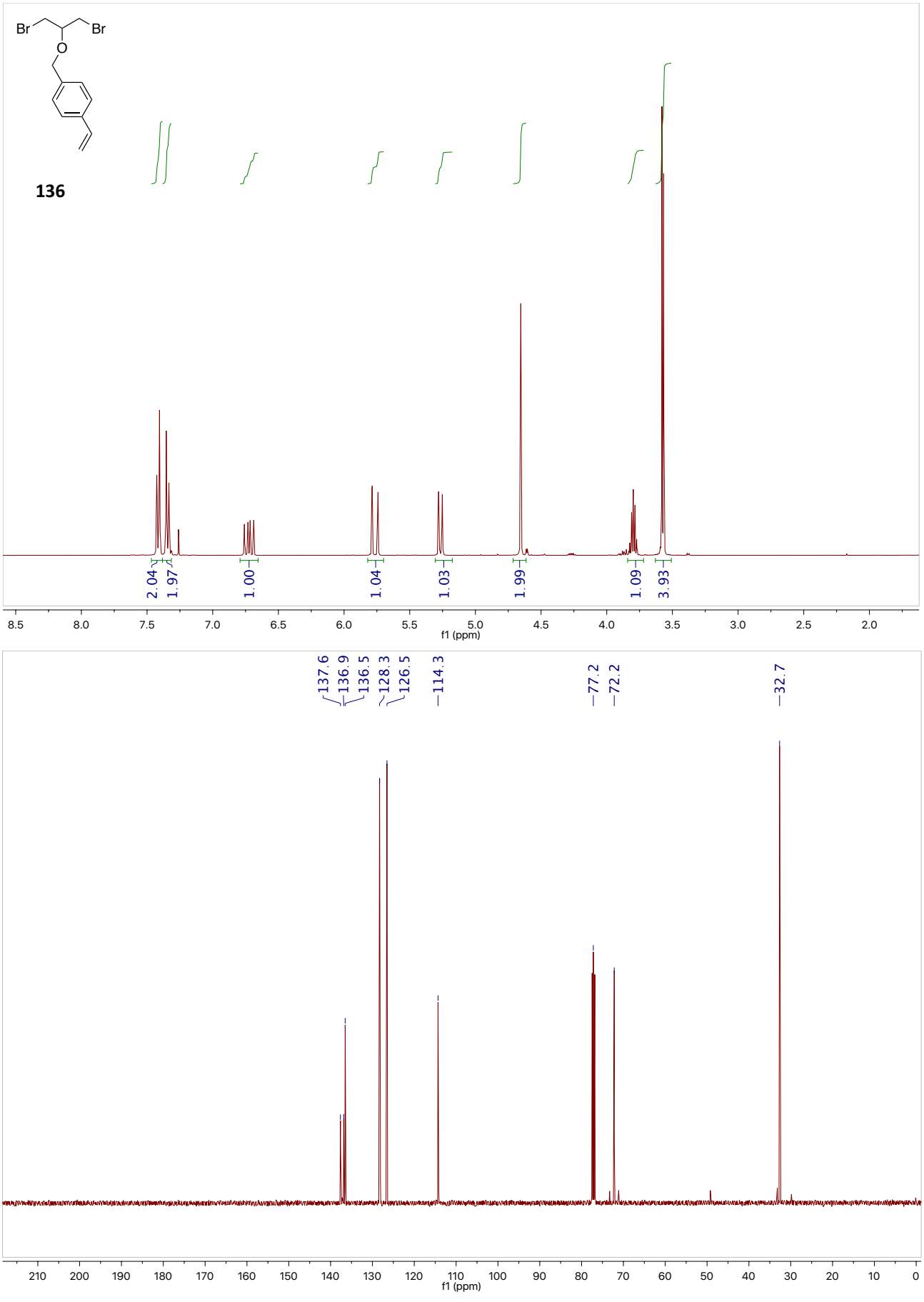
Br
Br
O
136
2.04
1.97
1.00
1.04
1.03
1.99
1.09
3.93
f1 (ppm)
137.6
136.9
136.5
128.3
126.5
114.3
77.2
72.2
32.7
f1 (ppm)

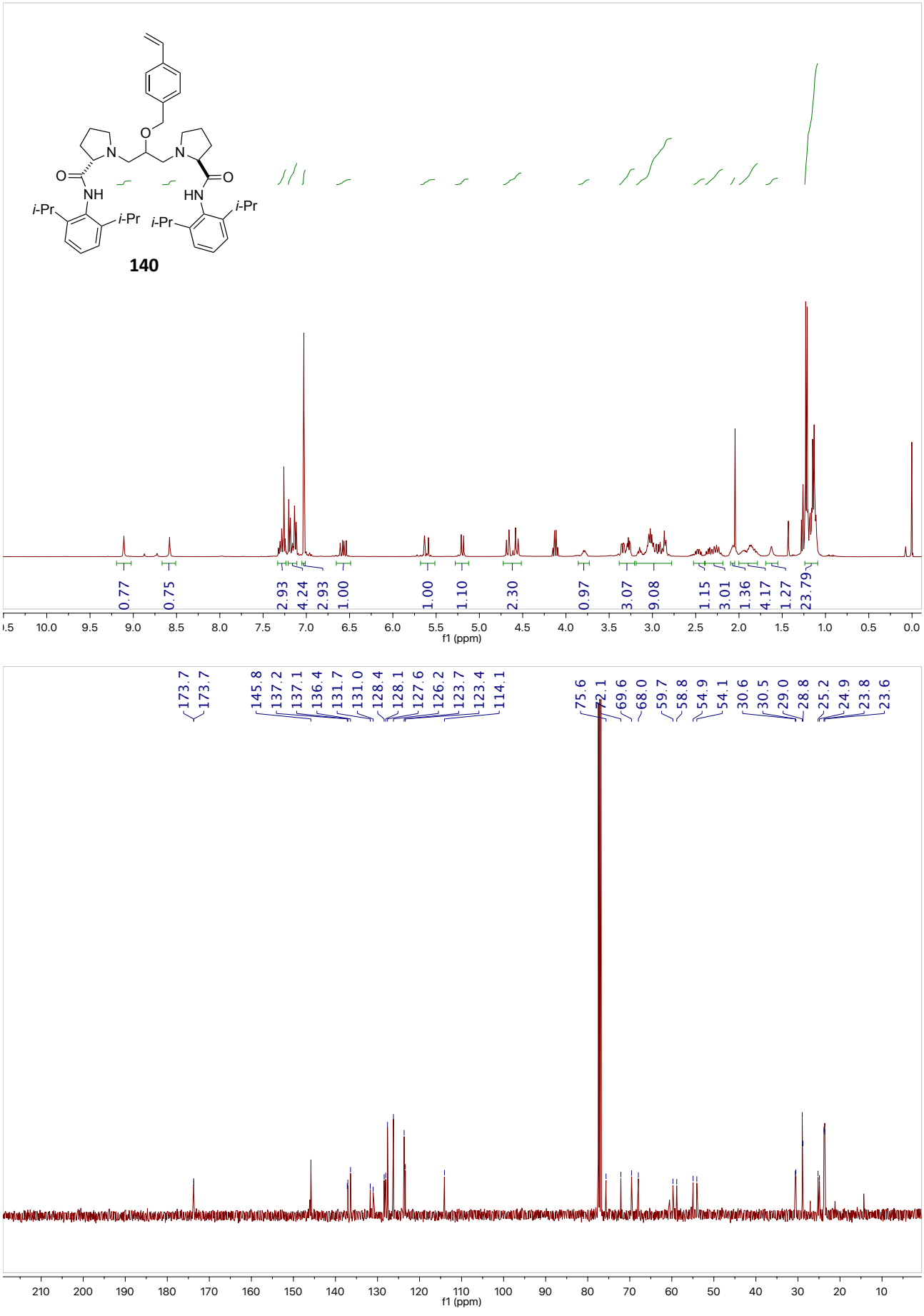
O
N
N
O
NH
HN
O
i-Pr
i-Pr
i-Pr
i-Pr
140
0.77
0.75
2.93
4.24
2.93
1.00
1.00
1.10
2.30
0.97
3.07
9.08
1.15
3.01
1.36
4.17
1.27
23.79
f1 (ppm)
173.7
173.7
145.8
137.2
137.1
136.4
131.7
131.0
128.4
128.1
127.6
126.2
123.7
123.4
114.1
75.6
72.1
69.6
68.0
59.7
58.8
54.9
54.1
30.6
30.5
29.0
28.8
25.2
24.9
23.8
23.6
f1 (ppm)

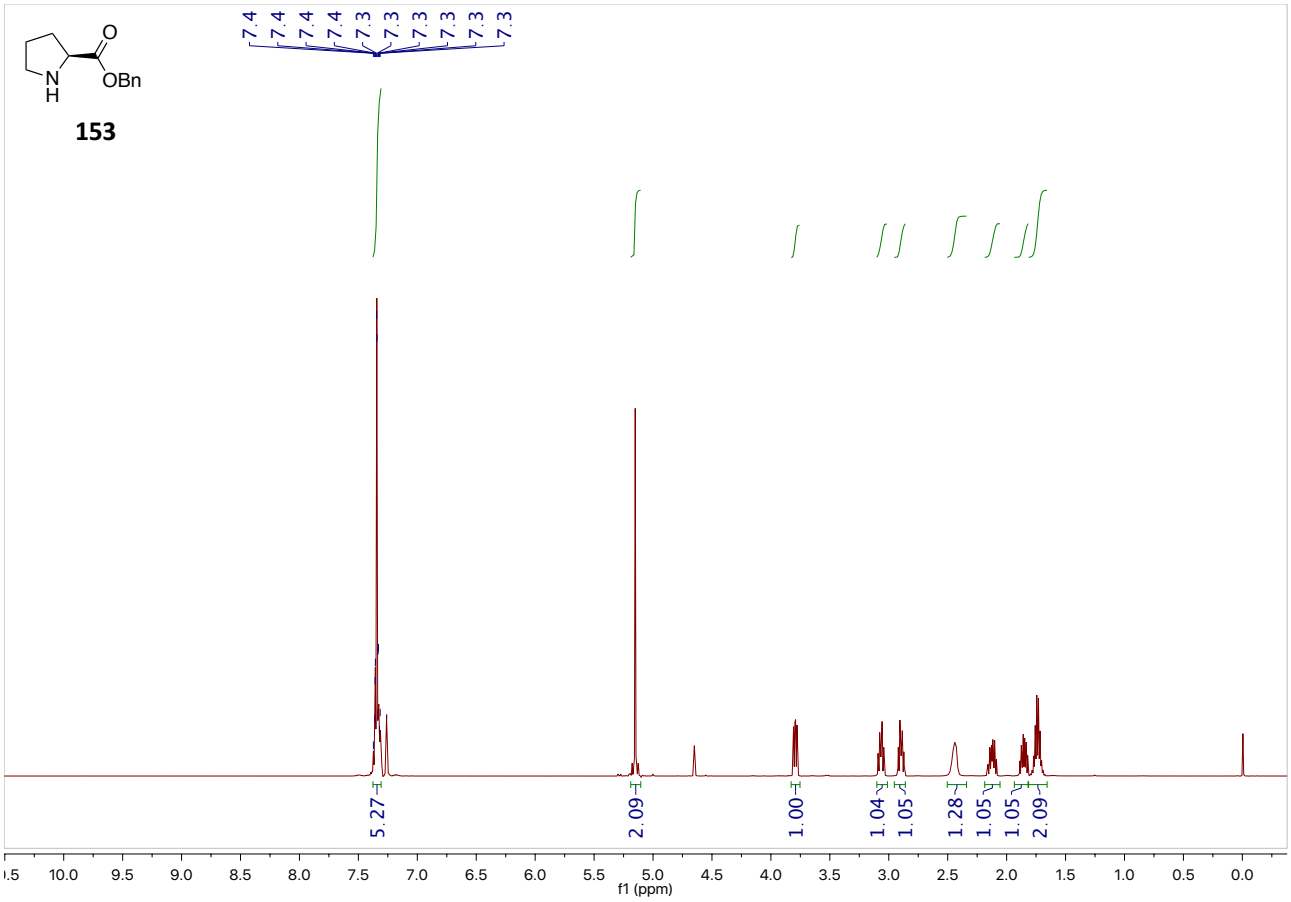
153
7.4
7.4
7.4
7.4
7.3
7.3
7.3
7.3
7.3
5.27
2.09
1.00
1.04
1.05
1.28
1.05
1.05
2.09
f1 (ppm)

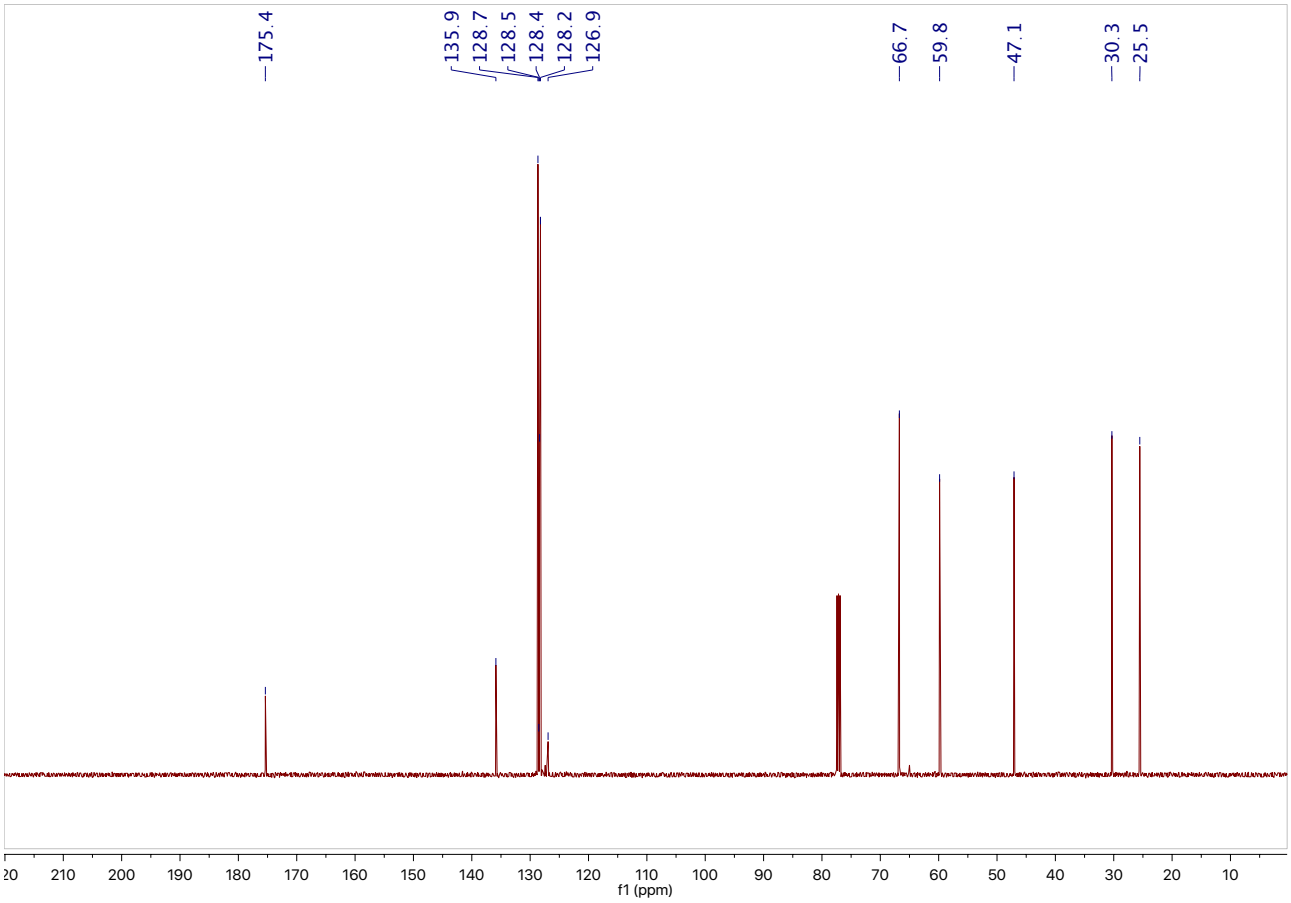
175.4
135.9
128.7
128.5
128.4
128.2
126.9
66.7
59.8
47.1
30.3
25.5
f1 (ppm)

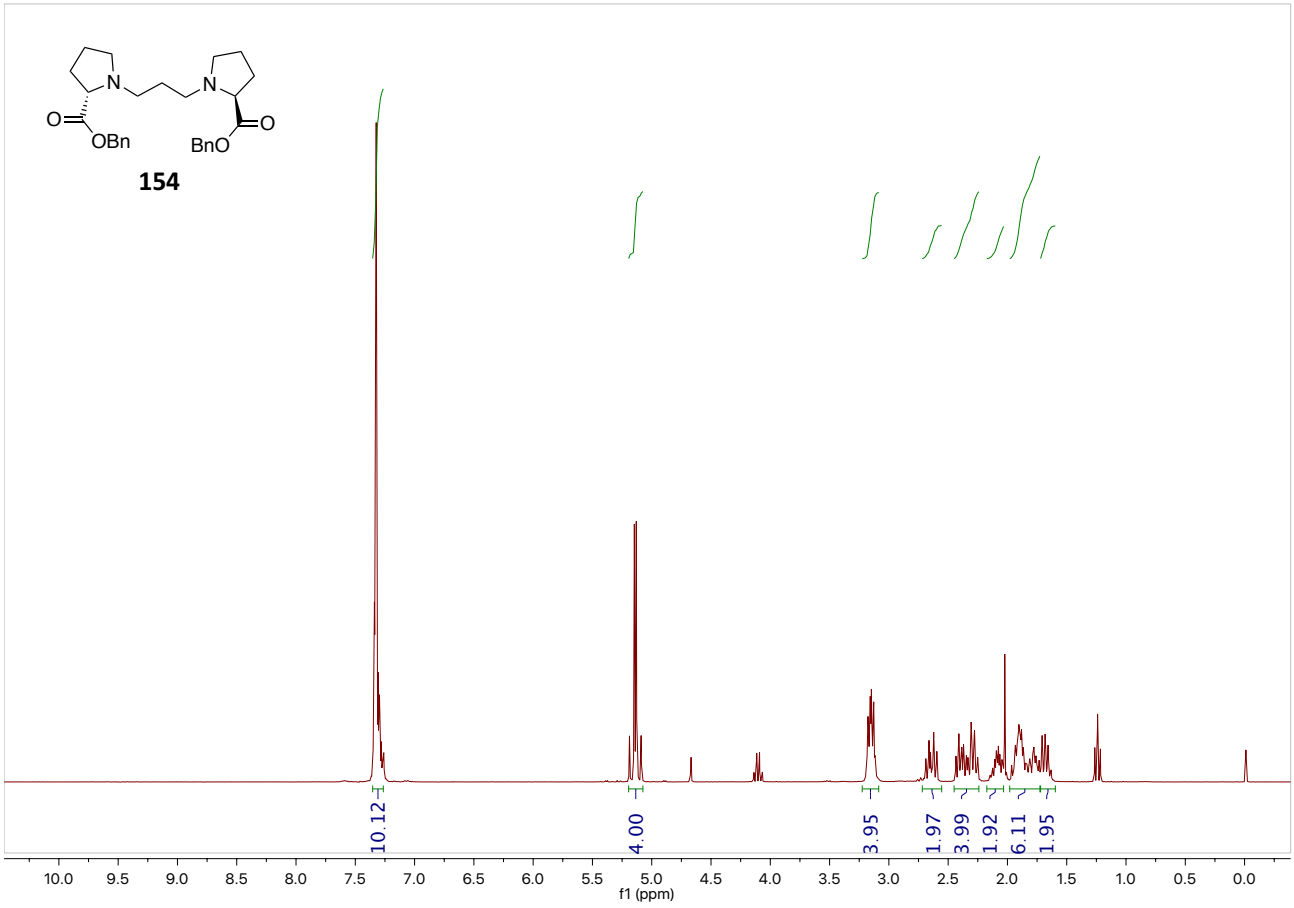
N
N
O
OBn
BnO
O
154
10.12
4.00
3.95
1.97
3.99
1.92
6.11
1.95
f1 (ppm)

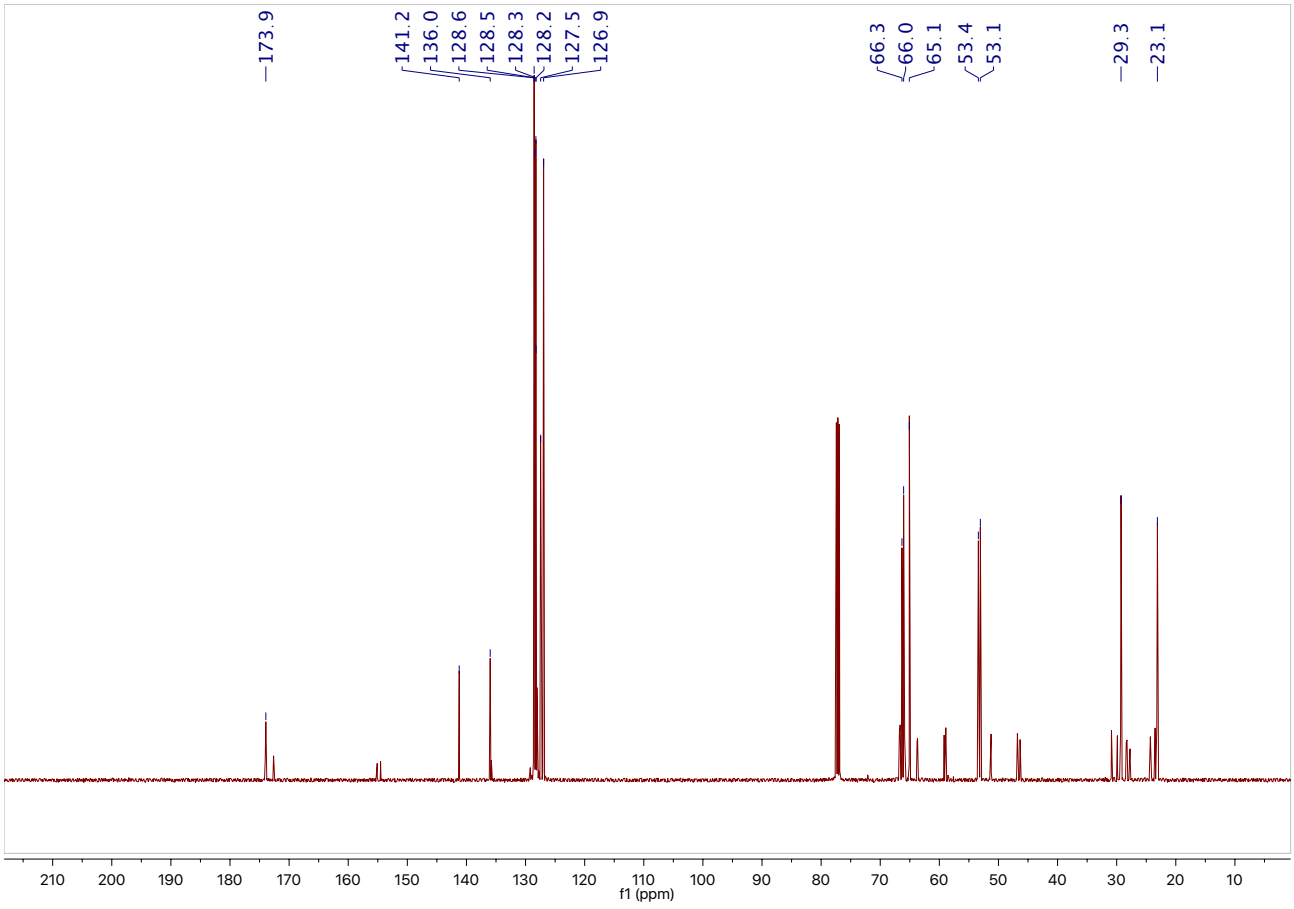
173.9
141.2
136.0
128.6
128.5
128.3
128.2
127.5
126.9
66.3
66.0
65.1
53.4
53.1
29.3
23.1
f1 (ppm)

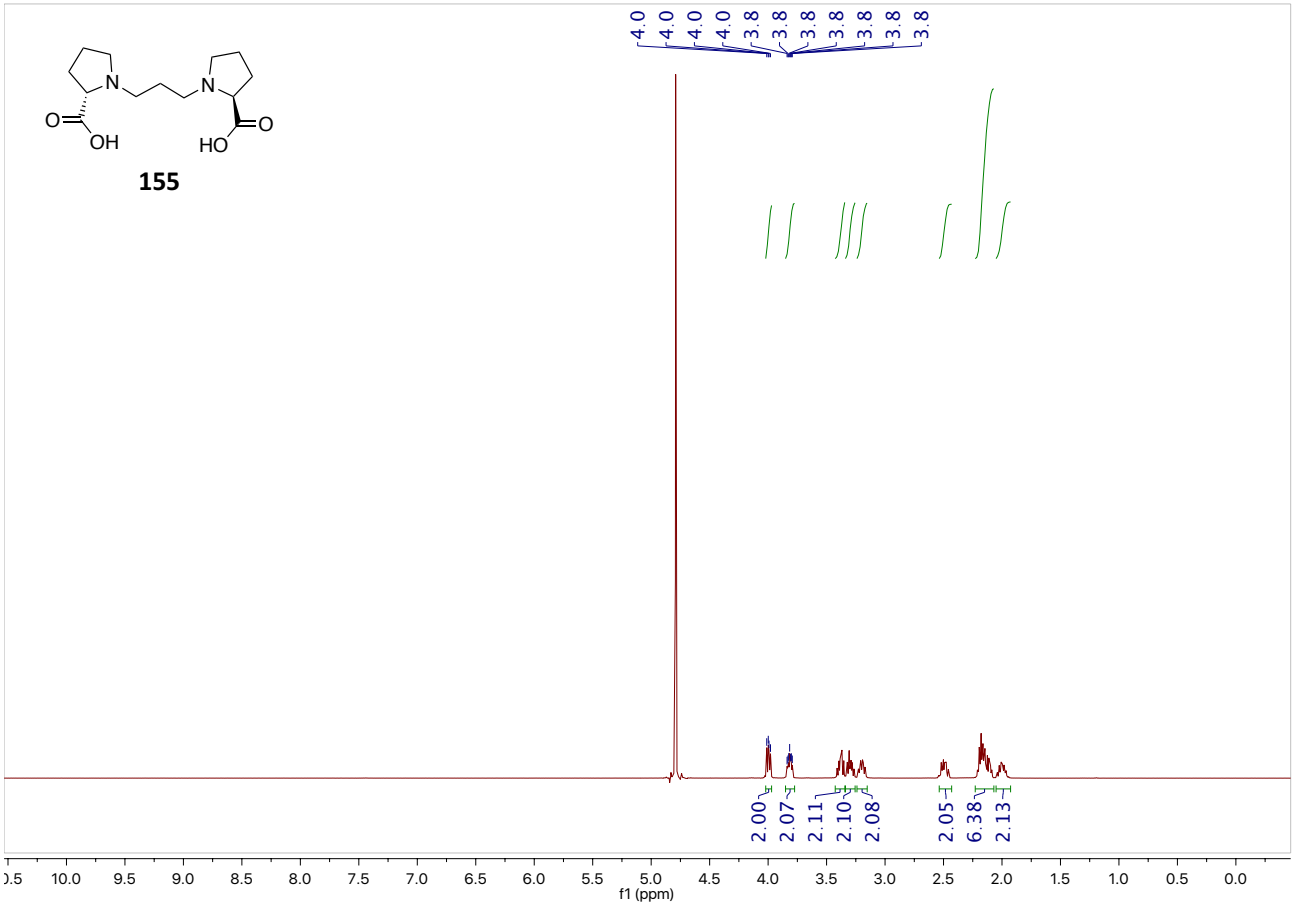
155
f1 (ppm)

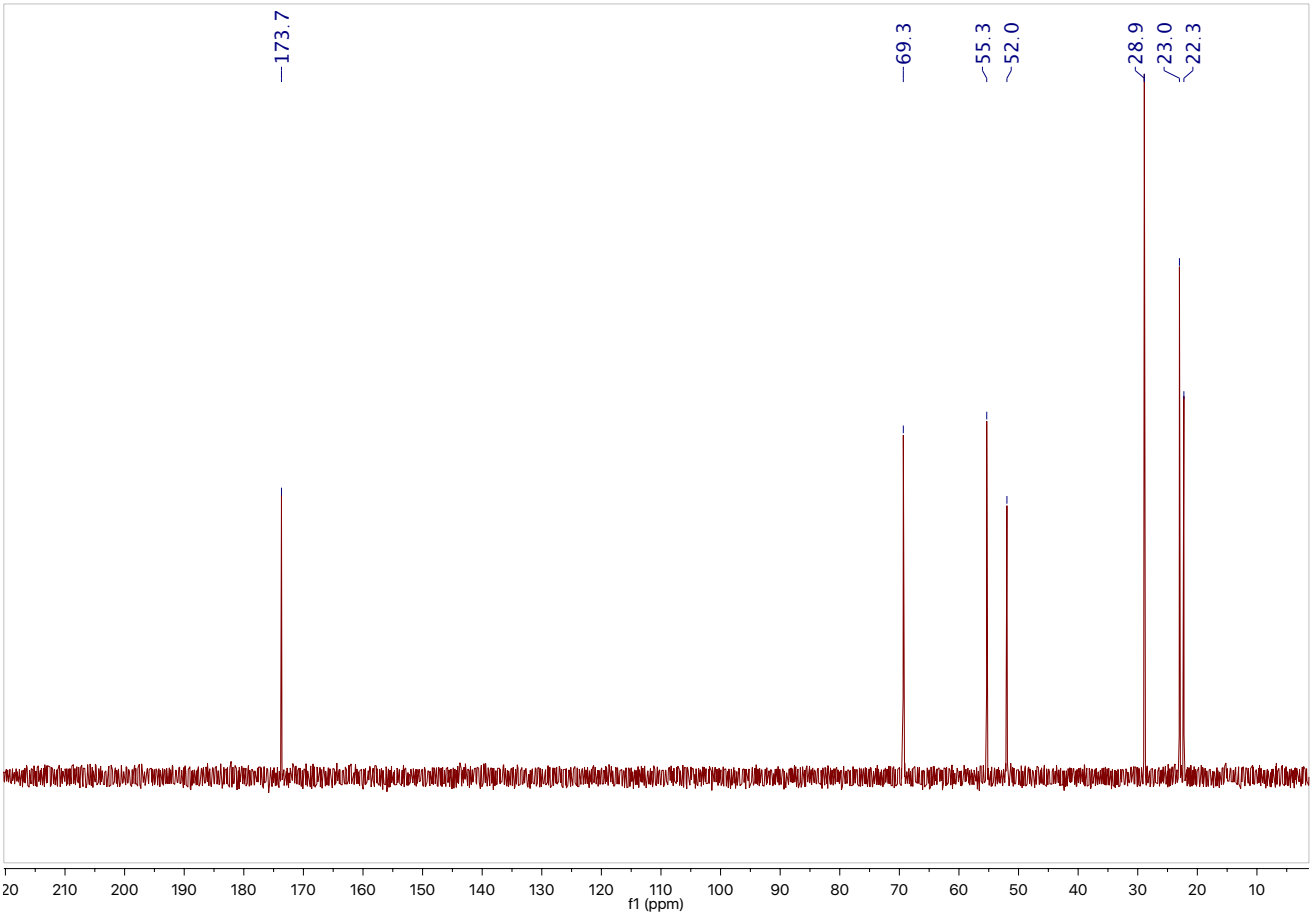
173.7
69.3
55.3
52.0
28.9
23.0
22.3
f1 (ppm)

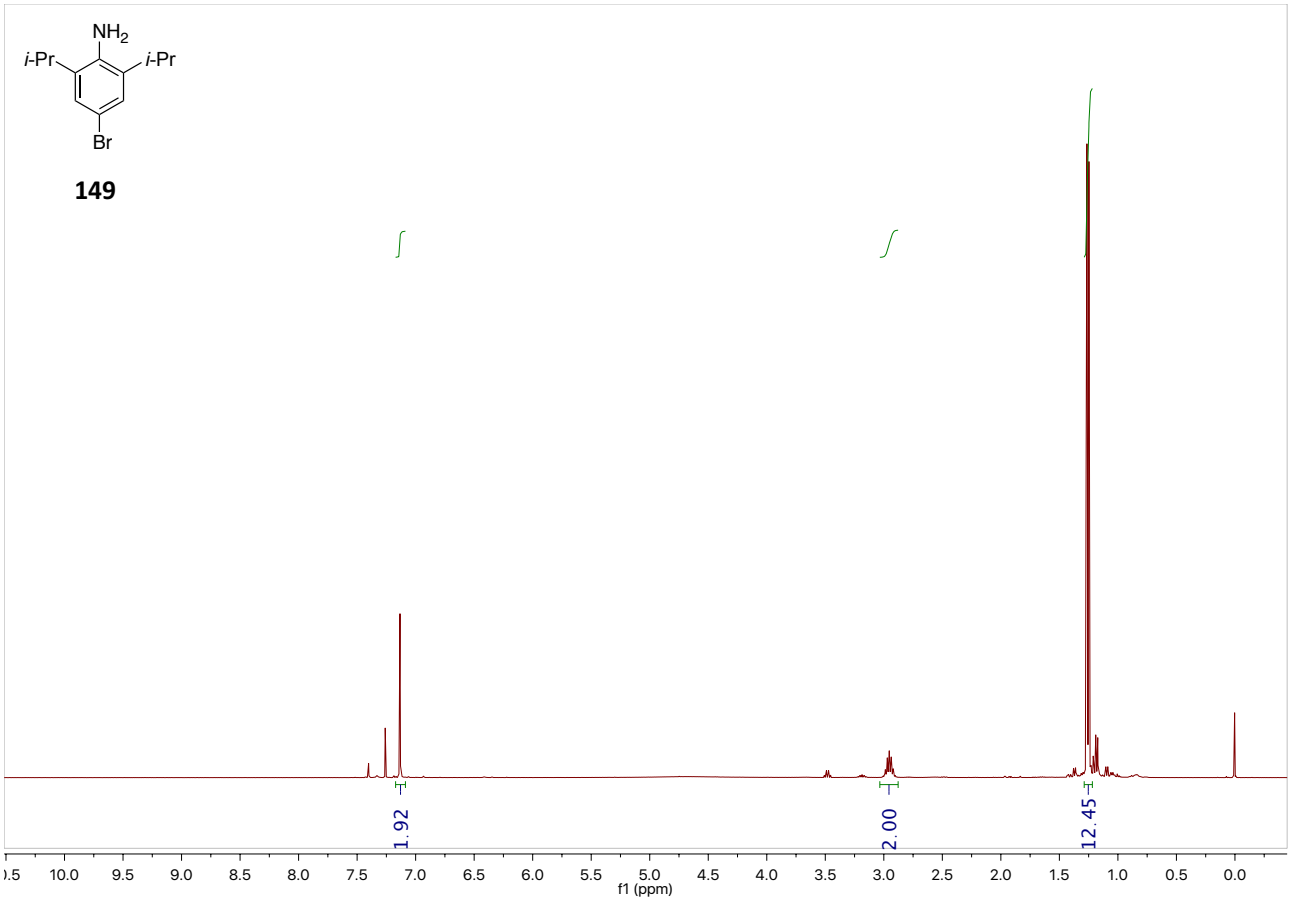
NH2
i-Pr
i-Pr
Br
149
1.92
2.00
12.45
f1 (ppm)

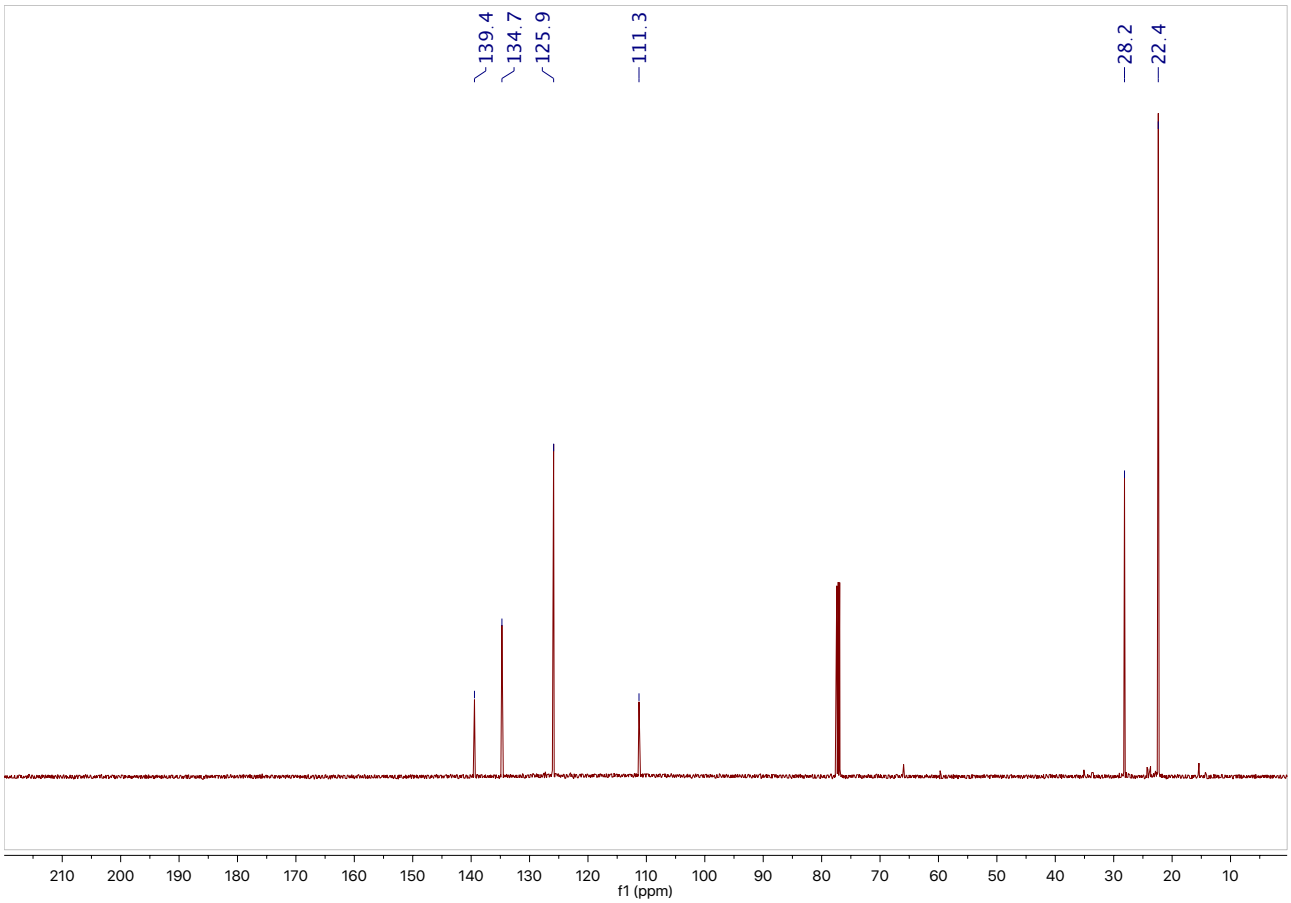
139.4
134.7
125.9
111.3
28.2
22.4
f1 (ppm)

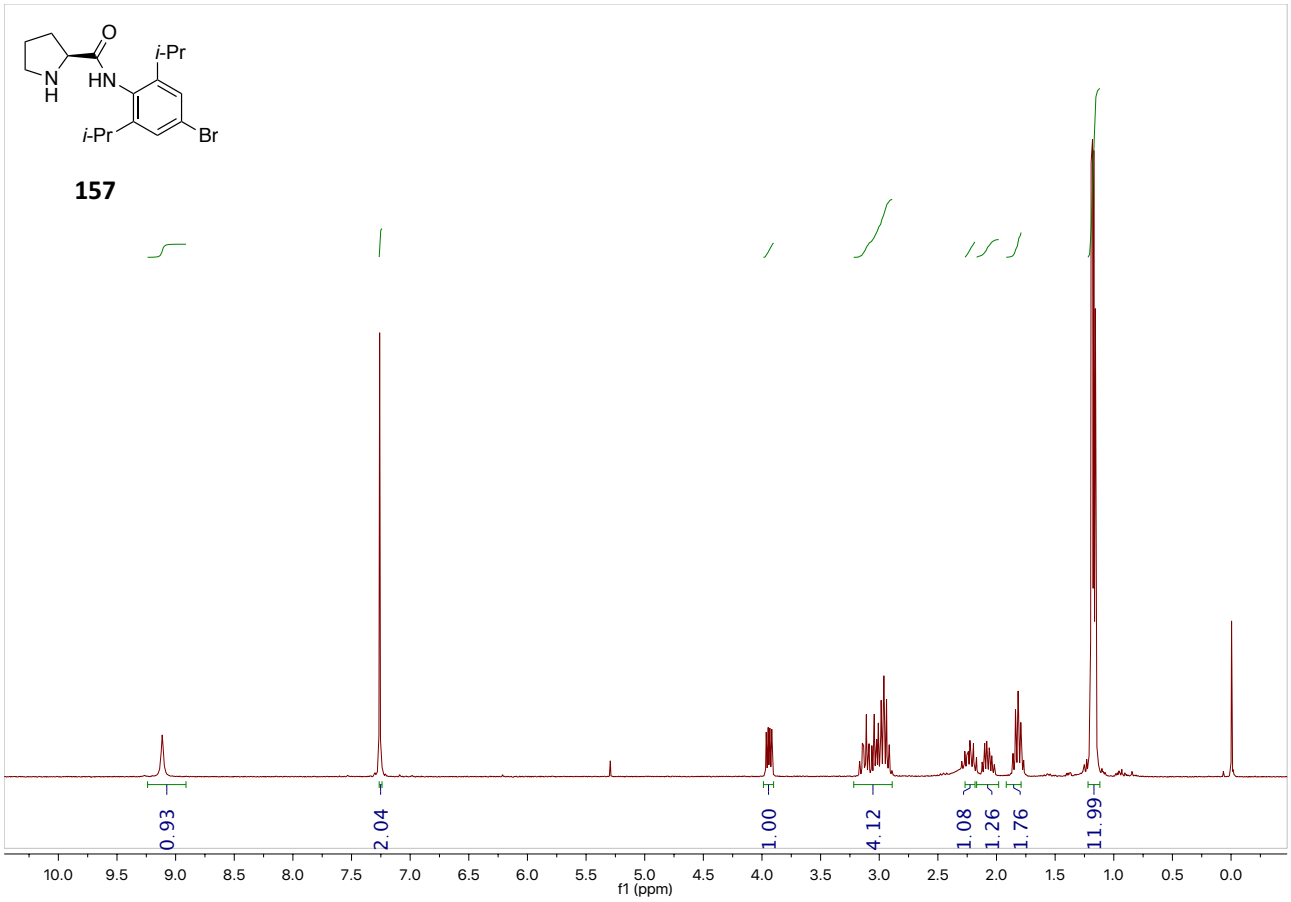
O
N
H
HN
i-Pr
i-Pr
Br
157
0.93
2.04
1.00
4.12
1.08
1.26
1.76
11.99
f1 (ppm)

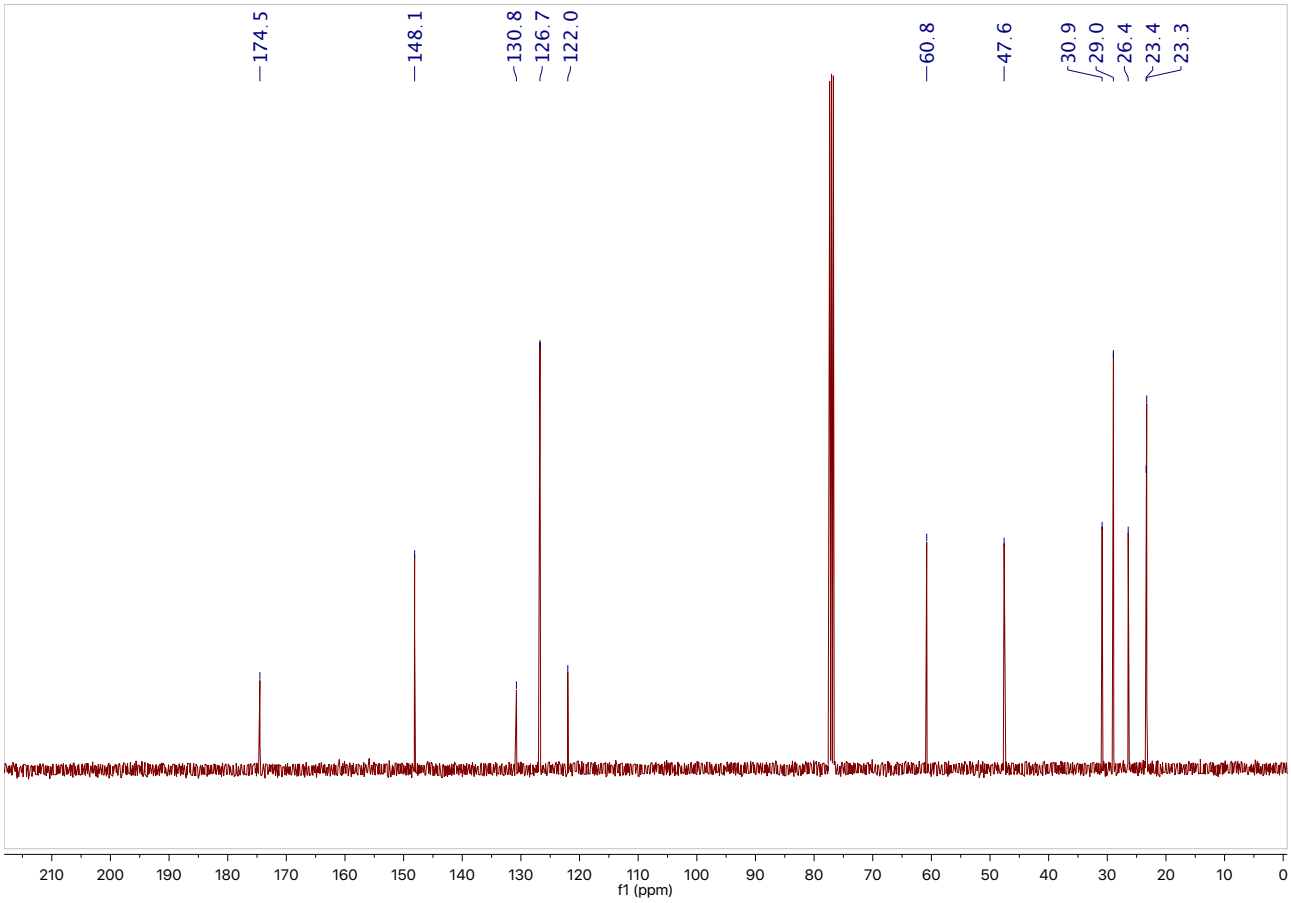
174.5
148.1
130.8
126.7
122.0
60.8
47.6
30.9
29.0
26.4
23.4
23.3
f1 (ppm)

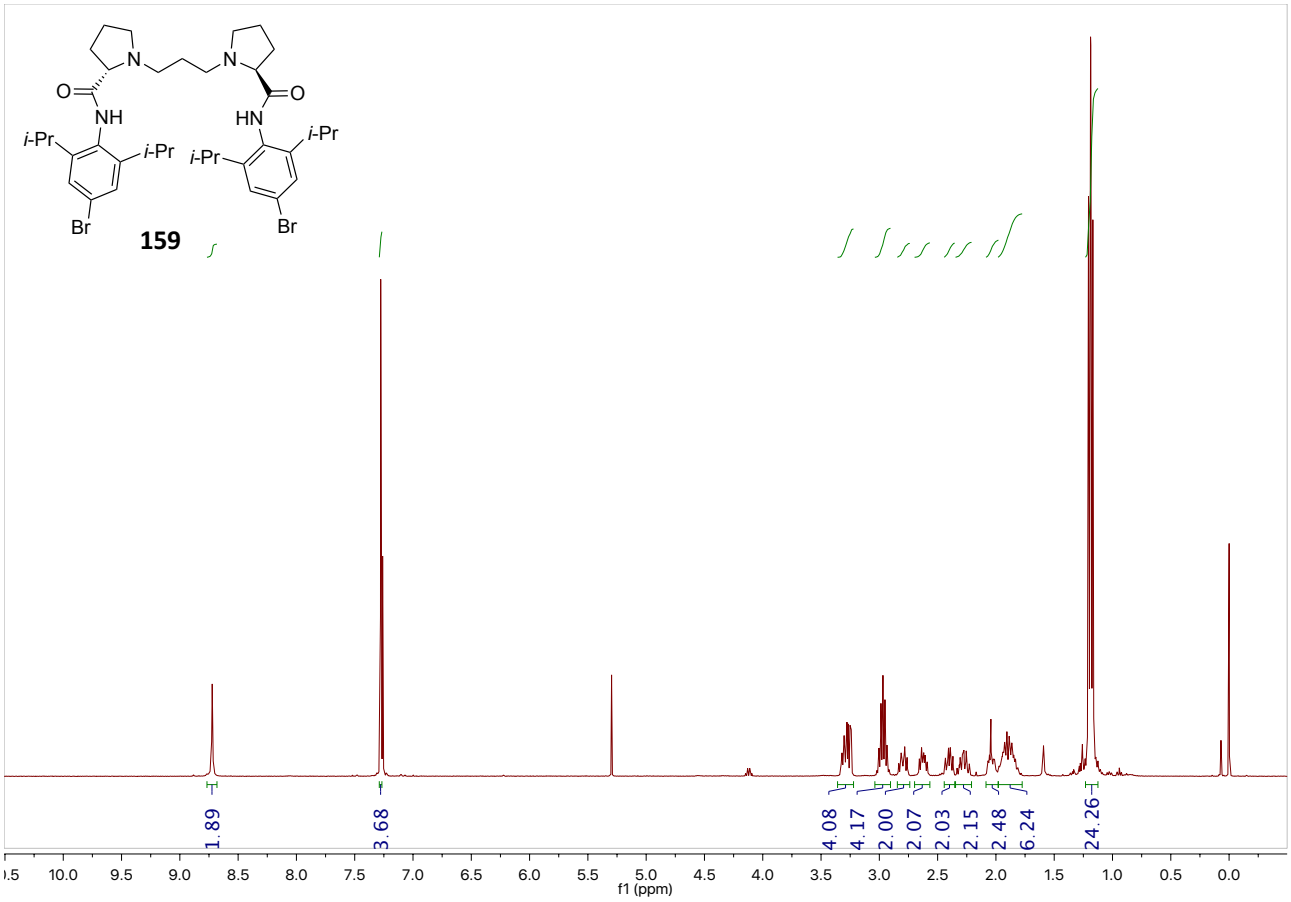
159
1.89
3.68
4.08
4.17
2.00
2.07
2.03
2.15
2.48
6.24
24.26
f1 (ppm)

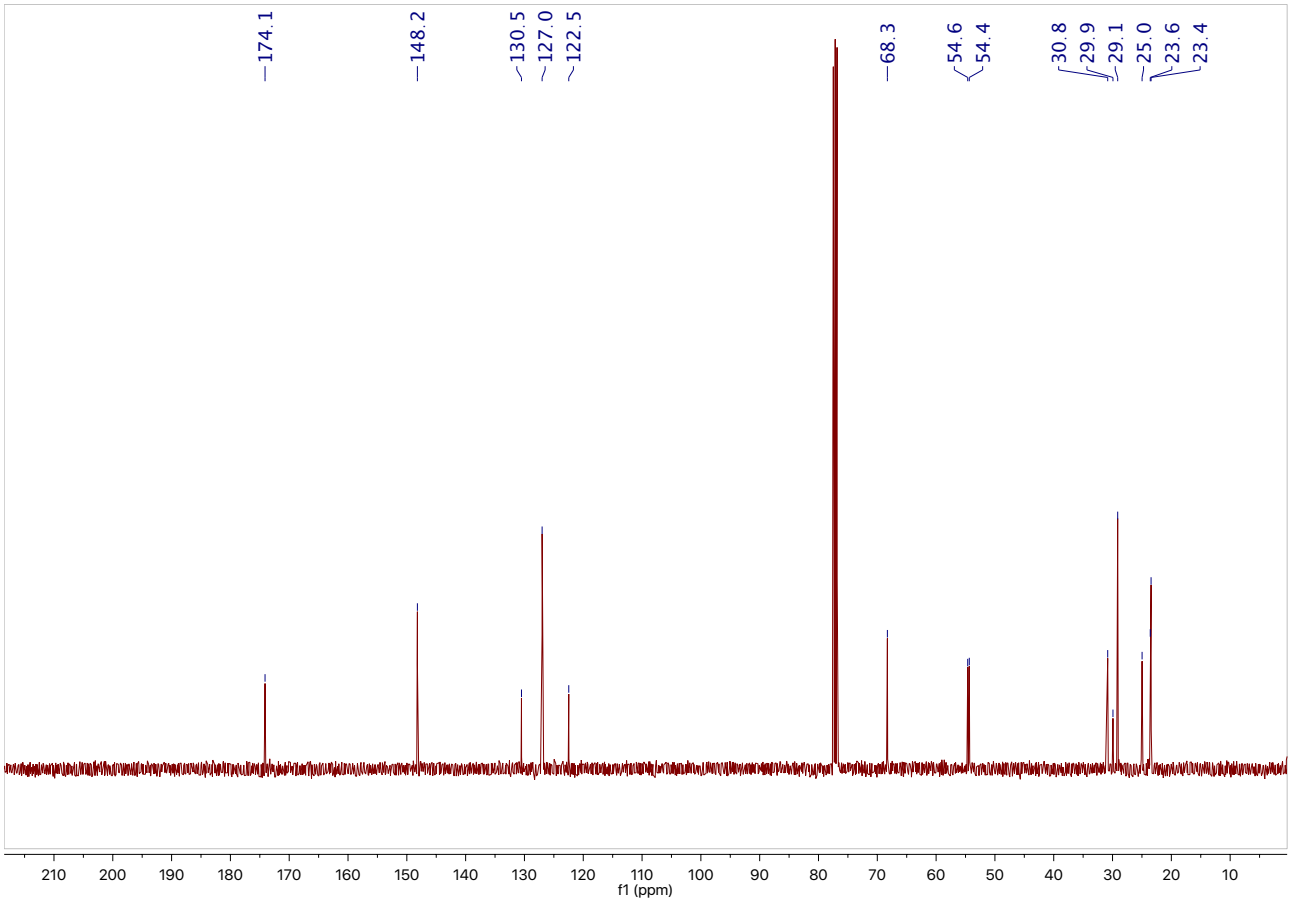
174.1
148.2
130.5
127.0
122.5
68.3
54.6
54.4
30.8
29.9
29.1
25.0
23.6
23.4
f1 (ppm)

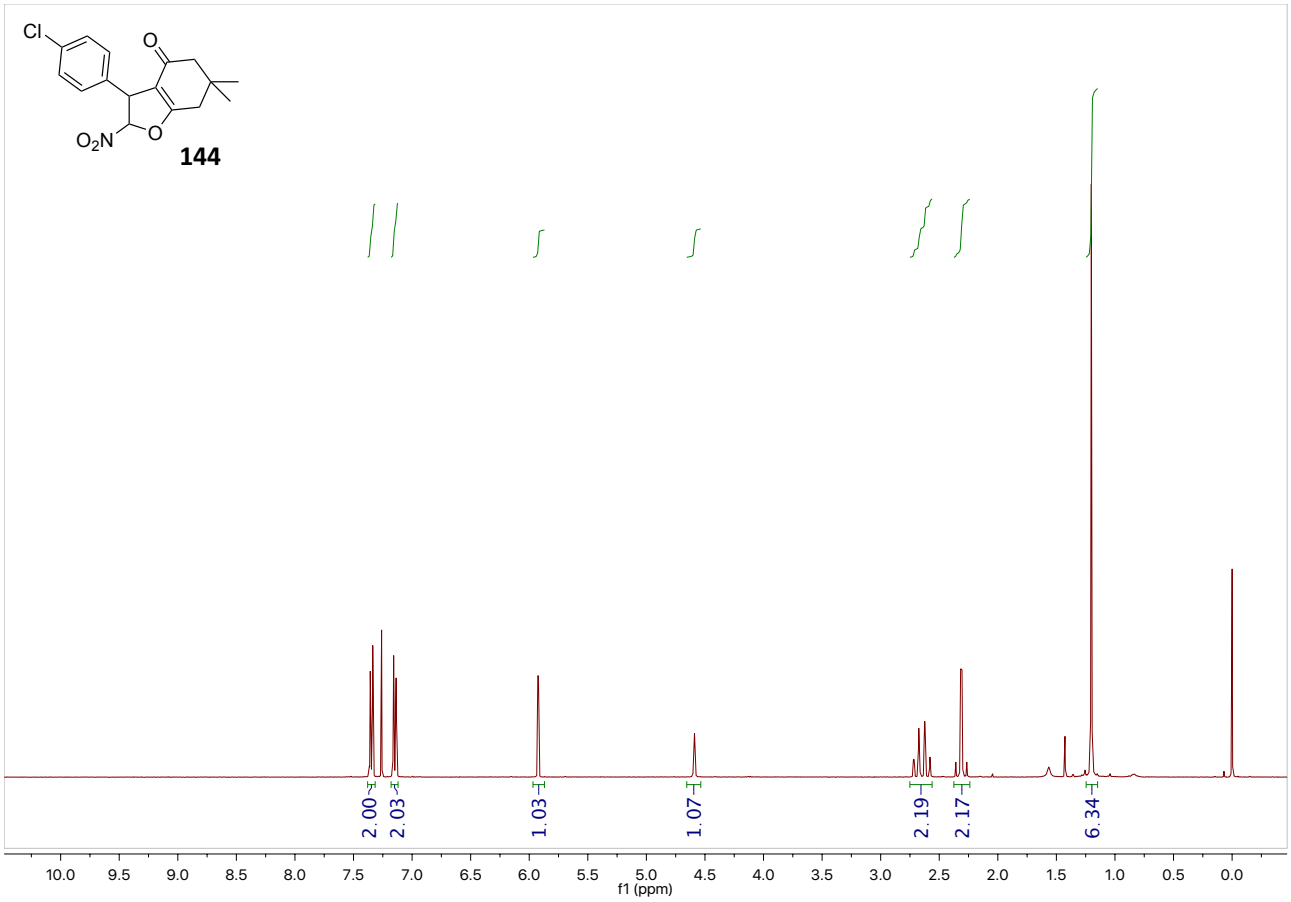
Cl
O
O_2N
O
144
2.00
2.03
1.03
1.07
2.19
2.17
6.34
f1 (ppm)

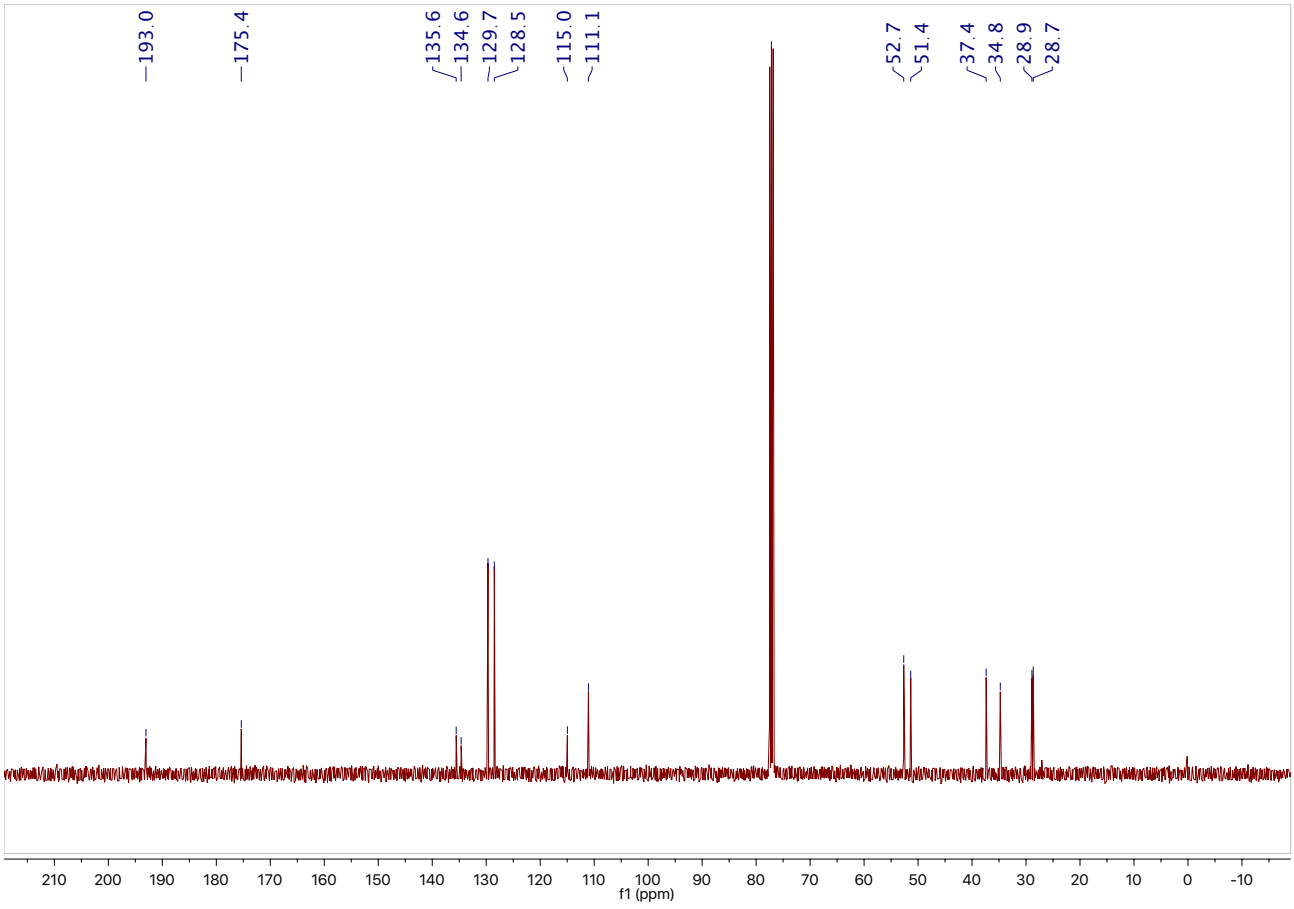
193.0
175.4
135.6
134.6
129.7
128.5
115.0
111.1
52.7
51.4
37.4
34.8
28.9
28.7
f1 (ppm)

UNIVERSITAT ROVIRA I VIRGILI
IMMOBILIZATION OF CHIRAL BRØNSTED ACIDS AND LEWIS BASES FOR BATCH AND FLOW ENANTIOSELECTIVE CATALYSIS
Lidia Clot Almenara

GENERAL CONCLUSIONS

UNIVERSITAT ROVIRA I VIRGILI
IMMOBILIZATION OF CHIRAL BRØNSTED ACIDS AND LEWIS BASES FOR BATCH AND FLOW ENANTIOSELECTIVE CATALYSIS
Lidia Clot Almenara

Concluding Remarks

In the present work we have explored the heterogenization of homogenous organocatalysts for batch and flow applications.

From the results summarized in this thesis, we can conclude that catalyst immobilization is an attractive strategy to improve some drawbacks inherent to homogenous catalysts. From the perspective of a practical use, reduction of chemical waste, mild conditions usually employed and extended life of the catalytic system of polymer-supported CPA has been corroborated by recycling them, running all the substrates from the scope with a single sample of catalyst.

We have satisfactorily achieved the resulting polystyrene-supported CPA and *N,N'*-dioxide, which were evaluated in enantioselective transformations.

As for the CPAs work, the concluding remarks shown that supported Brønsted acids performed both the allylation of aldehydes and the desymmetrization of *meso*-1,3-diones in high yields and enantioselectivities. PS-TRIP has been adapted to continuous flow operation. Furthermore, in case the catalyst is deactivated, it can be regenerated by washing with HCl/EtOAc.

Although we have designed a simple route to supported *N,N'*-dioxides diamides, unfortunately the behaviour of this material in the Michael reaction has not been as we expected, and further experiments need to be carried out.

UNIVERSITAT ROVIRA I VIRGILI
IMMOBILIZATION OF CHIRAL BRØNSTED ACIDS AND LEWIS BASES FOR BATCH AND FLOW ENANTIOSELECTIVE CATALYSIS
Lidia Clot Almenara

UNIVERSITAT ROVIRA I VIRGILI
IMMOBILIZATION OF CHIRAL BRØNSTED ACIDS AND LEWIS BASES FOR BATCH AND FLOW ENANTIOSELECTIVE CATALYSIS
Lidia Clot Almenara

UNIVERSITAT ROVIRA I VIRGILI
IMMOBILIZATION OF CHIRAL BRØNSTED ACIDS AND LEWIS BASES FOR BATCH AND FLOW ENANTIOSELECTIVE CATALYSIS
Lidia Clot Almenara